DISS. ETH NO. 25266

Optimal Control Strategies for Maximizing the Link Velocity of Elastic Joints with Nonlinear Impedance

A thesis submitted to attain the degree of

DOCTOR OF SCIENCES of ETH ZURICH

(Dr. sc. ETH Zurich)

presented by

Mehmet Can Özparpucu

M.Sc. in Mechanical and Process Engineering,
Technische Universität Darmstadt

born on *03.06.1985*

citizen of

Turkey and France

accepted on the recommendation of

Prof. Dr. Jonas Buchli, examiner

Dr. Christian Ott, co-examiner

Prof. Dr. Geir E. Dullerud, co-examiner

2018

Contents

Nomenclature

DTF	Dimensionless Time Function
EJ	Elastic Joint
EJR	Elastic Joint Robot
EMP	Energy Maximization Problem
FSJ	Floating Spring Joint
GOCP	General Optimal Control Problem
GTCP	General Terminal Cost Problem
LSEA	Linear Series Elastic Actuator
LTCP	Linear Terminal Cost Problem
LVMP	Link Velocity Maximization Problem
MSS	Mass Spring System
NPP	Nonlinear Programming Problem
NSEA	Nonlinear Series Elastic Actuator
OC	Optimal Control
PMP	Pontryagin's Minimum Principle
RJ	Rigid Joint
SDP	Stiffness-Deflection Profile
SEA	Series Elastic Actuator
SMP	Second Order Minimum Principle
TDP	Torque-Deflection Profile
VDA	Variable Damping Actuator
VGF	Velocity Gain Function
VSA	Variable Stiffness Actuator

List of Figures

List of Tables

Abstract

In this thesis, we investigate the problem of maximizing the link velocity of elastic joints using velocity-sourced elastic actuators. More specifically, focusing on joints with nonlinear series elastic actuators we derive motor control strategies such that the link velocity is maximized at a given time instant when the joint is initially at rest. Furthermore, we provide a physical interpretation for the derived strategies by exploiting their time optimality. The interpretation reveals the dependence of these strategies on periods of mass-spring systems which in turn explains how nonlinear torque-deflection profiles influence the maximal link velocity. In order to clearly illustrate this influence, we analyse in detail three different elastic joints with softening, linear and hardening springs. In particular, we compare their maximal link velocities as well as the corresponding control strategies and elaborate on the observed differences. Our theoretical results are experimentally validated on the DLR Floating Spring Joint where link velocities at least more than three times the maximally applied motor velocity are attained in less than a second. Several extensions are also provided which reveal the influence of damping and stiffness actuation on optimal control strategies. Finally, we give a proof of Pontryagin's Minimum Principle, the main theorem used in the thesis, by exploiting the properties of transition maps. Assuming an additional degree in the smoothness of the system dynamics and the cost functional, this leads to an extension of the principle, namely the Second Order Minimum Principle.

Zusammenfassung

In dieser Arbeit untersuchen wir das Problem der Maximierung der Ausgangsgeschwindigkeit von elastischen Gelenken mit geschwindigkeitsgesteuerten elastischen Aktuatoren. Wir konzentrieren uns dabei auf Gelenke mit nichtlinearen seriell elastischen Aktuatoren und leiten Motorsteuerungsstrategien ab, so dass die Ausgangsgeschwindigkeit zu einem gegebenen Zeitpunkt maximiert wird wenn das Gelenk anfänglich in Ruhe ist. Darüber hinaus liefern wir eine physikalische Interpretation für die abgeleiteten Strategien, indem wir deren Zeitoptimalität nutzen. Die Interpretation zeigt die Abhängigkeit dieser Strategien von Perioden von Masse-Feder-Systemen, die wiederum erklären wie nichtlineare Kennlinien für den Drehmoment die maximale Geschwindigkeit beeinflussen. Um diesen Einfluss deutlich zu veranschaulichen, analysieren wir im Detail drei verschiedene elastische Gelenke mit degressiven, linearen und progressiven Federkennlinien. Insbesondere vergleichen wir die maximal erreichbaren Geschwindigkeiten sowie die entsprechenden Steuerungsstrategien und erarbeiten die beobachteten Unterschiede. Unsere theoretischen Ergebnisse werden experimentell an dem DLR Floating Spring Joint validiert, wo Ausgangsgeschwindigkeiten von mehr als dem Dreifachen der maximal kommandierten Motorgeschwindigkeit in weniger als einer Sekunde erreicht werden. Es werden auch Erweiterungen hergeleitet, die den Einfluss einer aktiven Steifigkeits- und Dämpfungssteuerung auf optimale Steuerstrategien aufzeigen. Schließlich geben wir einen Beweis für das Minimumprinzip von Pontryagin, der Hauptsatz aus dem die Ergebnisse der Arbeit hervorgehen, indem wir die Eigenschaften von Flüssen von Differentialgleichungen nutzen. Unter der Annahme eines zusätzlichen Grads in der Differenzierbarkeit der Systemdynamik und des Kostenfunktionals führt dies zu einer erweiterten Version des Prinzips, nämlich zu dem Minimumprinzip zweiter Ordnung.

Acknowledgments

This thesis includes some of the main results of the research I conducted in German Aerospace Center (DLR) in the Institute of Robotics and Mechatronics. There are many people who have had an influence on this work and I want to use this part of the thesis to express my deepest gratitude to them.

First of all, I would like to thank Alin-Albu Schäffer and Christian Ott for giving me the opportunity to follow my own research interests. In particular, being interested in both control theory and mechanics they have allowed me to work on a basic problem which is related to both of these fields. In addition, I would like to thank Jonas Buchli for accepting me to be a part of his group in ETH Zurich and especially his suggestions regarding the organization of the thesis.

The current work can be regarded as a product of self study. Therefore, I want to also thank some of my former professors whose lectures and supervision during my earlier studies have had a great impact on the approach I followed when conducting my research. In particular, I would like to thank Lawrence A. Bergman and Alexander Vakakis whose research on nonlinear mechanical systems has undoubtedly affected the direction of my research. Moreover, I would like to thank William D. O'Brien, Jr. for allowing me to work in the Bioacoustics Research Lab and enabling me to look at problems in science from an experimental point of view. Finally, I would like to thank Geir E. Dullerud for introducing me to control theory from a mathematical perspective and accepting to be a co-examiner of my thesis.

Similarly, I would like to also thank several professors whose books have greatly contributed to my understanding of mathematics and optimal control theory, and also influenced my style of writing. More specifically, regarding my knowledge on mathematical analysis I would like to thank Vladimir A. Zorich, on ordinary differential equations Hartmut Logemann and Eugene P. Ryan, and finally on optimal control theory Heinz Schättler and Urszula Ledzewicz.

Finally, I would like to thank my loving wife Merve, with whom I luckily share my life, for her endless support, love and patience. In addition, I would like to thank members of the Özparpucu and Yaygıngöl family, i.e. Beatrice, Temel, Yasemin, Emre, Barış, Sevil, Beyhan, Hasan and Elif, again for their endless support, love and patience. Furthermore, I would also like to thank my colleagues Korbinian Nottensteiner, Juan Carlos Ramirez de la Cruz, Christian Gentner and Utku Gulan for their valuable friendship.

Chapter 1

Introduction

Robots are complex mechatronic systems whose performance limits largely depend on the properties of their actuators. Different actuation technologies exist each of which can, depending on the application, be more beneficial in terms of execution speed, energy efficiency, accuracy, etc [26]. One such technology, namely *Elastic Actuation Technology*, has attracted increasingly more attention over the last two decades [56, 20]. Many researchers regard this technology as the key in enabling humanoid robots to achieve human-like performances. This view is particularly supported by the mechanical robustness of systems with *elastic actuators* and by the possibility of using the elastic elements in these actuators as a potential energy source [60, 23].

Numerous elastic actuator designs with constant and variable impedance exist by now as well as studies which, for certain tasks, demonstrate their benefits. In particular, being hit with a baseball bat the DLR Floating Spring Joint (FSJ) [59], an *Elastic Joint* (EJ) with a variable stiffness actuator, has been shown to handle impacts which can not be handled by traditional rigid actuators currently found in industrial robots. Moreover, the DLR Hand Arm System [18], which is designed to mimic the behaviour of a human's arm and which consists of several FSJ's, has been shown to reach throwing velocities which are not achievable with a rigid actuator using the same maximal motor velocity and gear reduction as used during the experiments [22]. In other words, for an explosive throwing motion it has been experimentally shown that elastic actuators can increase the performance of a robot. Other similar explosive motion tasks, such as hammering and kicking, as well as periodic motion tasks, such as walking and hopping, have been also succesfully performed by robotic systems with elastic actuators [17, 16, 46, 48, 33].

The main advantages of incorporating an elastic element into an actuator are thus well understood and also validated at several EJ's and *Elastic Joint Robots* (EJR's). One mathematical tool, which is commonly used in these validations, is Optimal Control (OC) Theory [44] as it allows to find control strategies which can fully exploit the elasticity in elastic actuators. Consequently, several frameworks have been proposed to systematically apply this theory such that a given

task is efficiently accomplished by an EJ or an EJR, see for instance [7] and [25]. Nevertheless, being mainly based on numerical solution procedures these frameworks do not provide a general understanding for the computed control strategies and can also lead to suboptimal strategies.

Considering the lack of knowledge on the optimal control of even the simplest EJR's, the primary goal of this thesis has been to find physical principles for control strategies which maximize the performance of EJ's with nonlinear impedance. More specifically, a very basic EJ model has been investigated using OC Theory which takes account for the nonlinear torque-deflection profiles (TDP's) as they commonly occur in existing designs [20]. Making use of some simplifying assumptions, analytical solutions have been obtained which describe, in terms of physical quantities, the optimal way to transfer the energy generated by elastic actuators to the link of an EJ. Moreover, by studying the resulting motion, a quantitative analysis has been conducted in order to reveal the dependence of the attained performance on joint and task parameters. The second goal of the thesis was to extend the obtained results to more complex EJ models with variable impedance [56]. Focus was always given to explosive motion tasks as they clearly demonstrate the capability limits of these joints. The following papers have been published during the conducted research:

- Optimal Control for Maximizing Link Velocity of Visco-elastic joints.
  Mehmet Can Özparpucu and Sami Haddadin. Conference on Intelligent Robots and Systems (IROS), 2013.

- Optimal Control of Elastic Joints with Variable Damping.
  Mehmet Can Özparpucu and Sami Haddadin. 13th European Control Conference (ECC), 2014.

- Optimal Control of Variable Stiffness Actuators with Nonlinear Springs.
  Mehmet Can Özparpucu, Sami Haddadin and Alin Albu-Schäffer. IFAC World Congress (IFAC), 2014.

- Optimal Control Strategies for Maximizing the Performance of Variable Stiffness Joints with Nonlinear Springs.
  Mehmet Can Özparpucu and Alin Albu-Schäffer. Proc. 53st IEEE Conf. Decision and Control (CDC), 2014.

The purpose of this introductory chapter is to clarify the need for the undertaken line of research and to emphasize the significance of the attained results. To achieve this, we will first start with a motivation for the use of elastic actuators in robotic systems and discuss its main advantages. Moreover, taking an energy point of view we will underline two basic control and design questions for EJ's which constitute the main focus of this thesis. Then, we will elaborate on the approach we followed to tackle with these questions. Afterwards, an overview of the existing results on the OC of EJ's is given together with a classification of different EJ models. Finally, we conclude this chapter by briefly discussing the contents of the following chapters.

1.1 Motivation and Challenges

Today, robotic applications exist in diverse areas such as manufacturing, healthcare, agriculture, space, etc [54]. The advances in actuator, sensor and computing technology have played a crucial role in the vast increase of these applications as well as in their improvement. Conversely, the desire to use robots in different fields has stimulated the further development of these technologies as well. In particular, with the growing interest in making robots a part of our daily life providing robots with human-like abilities have become a major goal in robotics research. Motivated by the adjustable elasticity present in the musculoskeletal systems of humans, this interest has then resulted in the current Elastic Actuation Technology.

The musculoskeletal system of a human consists of elastic elements such as ligaments and tendons [58]. Taking a closer look at the actuators of this system, i.e. at the muscles, one can see that the forces generated there are transmitted to various joints not directly but rather by tendons which connect the muscles to the bones. Following the same principle, elastic actuators are characterized by the presence of elastic elements which can be modeled, similar to a tendon, as an elastic spring attached to a torque generating actuator. Compared to their rigid counterparts, the existence of such a spring leads to significant changes in the properties of elastic actuators as well as to challenges in their control when used in a robotic system. We want to next discuss these properties and challenges.

The series elastic actuator (SEA), one of the first elastic actuators, has been proposed more than two decades ago by Pratt and Williamson and consists simply of a DC Motor, a planetary gearbox and a steel torsion spring that is attached to the output shaft of the gearbox [45]. As discussed there, one of the main advantages of the spring in this design is the increase in the shock tolerance. This increase follows from the fact that the spring acts as a low-pass filter in case of collisions so that the corresponding peak forces at the gears are reduced. Consequently, the mechanical robustness of robotic systems can be significantly increased when equipped with elastic actuators. It is interesting to note here that current biomechanical studies similarly indicate that tendons protect the muscles by acting as a mechanical buffer during rapid motions [19, 50, 51].

A second advantage of using an elastic element in an actuator is the possibility to store potential energy in that element. This property can allow robots to accomplish periodic tasks, such as walking and hopping, with less energy expenditure [57]. Moreover, as already mentioned using a proper control strategy this additional source of energy can also be used to realize explosive motion tasks. Both of these aspects are also encountered in humans and animals [10, 4, 49].

Being mechanically robust, energy efficient and able to achieve energy intensive tasks in a short duration are clearly all important properties for robots, especially if they are to achieve human-like performances. Based on our discussion so far, we can clearly see that EJ's, i.e. joints with elastic actuators, can provide robots with such properties. Nevertheless, there are still many open questions on how to best control the actuators in these joints to accomplish

particular tasks. For instance, even for the simplest EJ models, which consist only of a motor, a nonlinear spring and a link, it is not fully understood how to control the motor in order to maximize the link velocity if all motor constraints are taken into account. Similarly, for this case it is also not known how to control the motor such that the link stops moving in the least possible amount of time in case of a collision. Such strategies are important to evaluate the capabilities and thus the safety of EJ's, especially if they are to be used in proximity to humans.

The reason for the deficiency in our understanding of the control strategies for EJ's follows mainly from the nontrivial relation between the motion of the actuator and the link. In a *Rigid Joint* (RJ), the link motion is uniquely determined by the motion of the rigid actuator and probably some kinematic relations present due to the gear mechanism. In an EJ, on the other hand, the motion of the link is infuenced only dynamically by the elastic forces present in the joint. This nontrivial relation results in at least doubling the number of the states which are required to analyse the dynamic behaviour of an EJ when compared to a RJ. Moreover, this dynamic behaviour gets more complicated if the elastic actuator can additionally adjust the impedance of the joint. Finally, the way how constraints for the elastic actuator infuence the possible link motions becomes also nontrivial as it can not be directly derived from kinematic considerations as done in a RJ.

In order to gain a better understanding on how to best make use of the relation between the actuator and the link motion, one possible way is to look at EJ's from an energy point of view. In particular, focusing on explosive motion tasks one can try to first find control strategies which, in a given time interval, maximize the energy that is transfered from the actuator to the link. As the corresponding maximal energy will in general depend on the system parameters, one can then try to analyse this dependence. This leads to the following two basic questions for EJ's:

- How can we maximize the link velocity of an elastic joint?

- How does the maximal link velocity depend on joint parameters?

It is important to realize here that finding an answer to the first question can provide a physical insight for how to optimally transfer the energy from the actuator to the link by using the inherent elasticity in EJ's. Understanding the dependence of the resulting maximal energies on the joint and in particular on the actuator parameters, the answer to the second question can be used to derive design guidelines for elastic actuators especially if these actuators are to be used for energy intensive tasks. In this thesis, we will apply OC Theory to find complete answers to both of these questions under practically relevant assumptions.

1.2 Approach

OC Theory is a mathematical tool which can be used to analyse the maximum performance of a system if there exists a *mathematical model* describing this system's dynamics in terms of first-order differential equations [44, 11]. More specifically, given such a model and a *cost functional*, which is expressed in terms of this model's states and which describes a performance criteria, OC Theory can be used to determine the control strategies which minimize this functional. Considering now the two control and design questions from the previous section, it is clear that by choosing an appropriate model for an EJ and cost functionals related to the joint's terminal link velocity, OC Theory can be directly used to address these questions. For deriving control strategies for EJ's and analyse the resulting performance we will, therefore, also make use of this theory.

It is important to realize here that the two questions, as we have stated in the previous section, are very basic but also very broad questions whose answers will in general depend, besides the initial conditions of the EJ and the given time interval, also on the chosen mathematical model. This model choice is, however, not unique as there exist numerous elastic actuator designs with different actuation possibilities. Even for the same design, different models can be chosen which, for instance, differ on how detailed they consider the motor dynamics. As we will see in Section 1.3, in contrary to the large number of existing designs, only a few number of EJ models have been analyzed so far using OC Theory. Moreover, these studies concentrate mostly on models with linear impedance, constant or adjustable, which allows them to obtain analytical solutions. Studies investigating models with nonlinear impedance also exist, but they rely on numerical methods and focus only on a particular design without a detailed analysis on how a different choice for actuator parameters might influence the system's performance. Noting that the output torque of existing elastic actuators with variable impedance are mostly described by a set of nonlinear functions [56, 20], the contributions of the existing studies to the control and design of EJ's are therefore limited.

In order to derive general physical principles for EJ's, we have analysed in this thesis simplified models of these joints such that the corresponding OC strategies could be expressed analytically. In particular, we have applied OC Theory to three such models and used them to investigate the influence of actuator parameters, such as spring nonlinearity and maximal motor velocity, and actuation possibilities, such as variable damping and variable stiffness. Our primary focus was given to a basic model consisting of a motor, a link and a nonlinear spring for which the analytical derivation turned out to be very complex due to the nontrivial relation between OC strategies and spring characteristics. The obtained results have been then extended to the other two models.
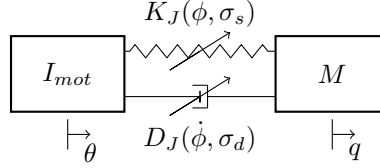
Figure 1.3.1: EJ with Variable Impedance

1.3 State of the Art

In this section, we want to give an overview of the existing results on OC strategies for EJ's. Moreover, we want to clarify how this thesis and our publications on the subject extend these results. As already mentioned, there are different design approaches for elastic actuators leading to different models for EJ's. To be able to clearly distinguish between the various results in literature, we will first introduce a classification for EJ models of different complexity.

1.3.1 Elastic Joint Models

From a mechanical perspective, an EJ can be regarded as a system consisting of two rigid bodies, namely a motor and a link, which are attached to each other by a torsional elastic spring and damper. The motor together with the spring and the damper constitute the elastic actuator of that system and the motion of the link is determined by this actuator through the torques acting at the spring and damper. Figure 1.3.1 graphically illustrates this system in its most general form, where I_{mot} denotes the motor's mass of inertia and θ its position. Similarly, M denotes the link's mass of intertia and q its position. Moreover, K_J stands for the stiffness of the spring and D_J for the damping coefficient of the damper. It is important to recall here that depending on their designs elastic actuators can control the torque acting between the motor and the link through different mechanisms [56]. This is accounted for in Fig. 1.3.1 by letting K_J to be a function of both the spring deflection $\phi = \theta - q$ and a *stiffness variable* σ_s. Similarly, D_J is defined as a function of the time-derivative[1] of the deflection $\dot{\phi}$ and a *damper variable* σ_d.

The dynamic behaviour of the system depicted in Fig. 1.3.1 can be mathematically described once we are given the function $\tau_{J,S}$, which describes the torque in the spring as a function of ϕ and σ_s, and the function $\tau_{J,D}$, which describes the torque in the damper as a function of $\dot{\phi}$ and σ_d. These functions influence the way how the energy of an EJ can in general be changed and also distributed along the motor, spring and link. As already mentioned, depending on the elastic actuator, the total torque τ_J between the motor and the link of an EJ, i.e. the sum of $\tau_{J,S}$ and $\tau_{J,D}$, may or may not be adjustable through a stiffness and/or damper variable. This, however, has a direct influence on the

---

[1]We use dots to indicate derivatives with respect to time t.

i	σ_s	σ_d
MC	$\sigma_s = \text{const.}$	$\sigma_d = \text{const.}$
MSC	-	$\sigma_d = \text{const.}$
MDC	$\sigma_s = \text{const.}$	-
MIC	-	-

(a) Assumptions for σ_s and σ_d
($i \in \{MC, MSC, MDC, MIC\}$)

j	$\tau_{J,S}$
LS	$\tau_{J,S}(\phi, \sigma_s) = \sigma_s \phi$
NS	-

(b) Assumptions for $\tau_{J,S}$
($j \in \{LS, NS\}$)

k	$\tau_{J,D}$
UD	$\tau_{J,D} \equiv 0$
LD	$\tau_{J,D}(\dot{\phi}, \sigma_d) = \sigma_d \dot{\phi}$
ND	-

(c) Assumptions for $\tau_{J,D}$
($k \in \{UD, LD, ND\}$)

Table 1.1: Classification of EJ Models ($\mathcal{EJ}_{i,j,k}$)

corresponding OC strategies. Moreover, the way how the two functions $\tau_{J,S}$ and $\tau_{J,D}$ are related to their arguments, i.e. whether this relation is linear or nonlinear, also has an effect on these strategies.

In order to be able to distinguish between the different actuation possibilities for EJ's we propose in Fig. 1.3.2 a classification of EJ models. As indicated there, we first have a general class of models $\mathcal{EJ}_{MIC}$ which is based on the system depicted in Fig. 1.3.1 and for which both σ_s and σ_d are adjustable. Three subclasses are then derived from this class which are denoted by $\mathcal{EJ}_{MC}, \mathcal{EJ}_{MSC}$ and $\mathcal{EJ}_{MDC}$. They only differ in the adjustability of σ_s and σ_d. More specifically, for models in the subclass $\mathcal{EJ}_{MC}$ both σ_s and σ_d are constrained to take constant values. This is indicated in Fig. 1.3.2 by representing K_J and D_J as a function of only ϕ and $\dot{\phi}$, respectively. Similarly, for models in $\mathcal{EJ}_{MSC}$ and $\mathcal{EJ}_{MDC}$ the damping variable σ_d and the stiffness variable σ_s are assumed to remain constant, respectively. In other words, models in $\mathcal{EJ}_{MSC}$ consist of a variable stiffness actuator (VSA) [60] and models in $\mathcal{EJ}_{MDC}$ a variable damping actuator (VDA) [56]. Finally, two additional subscripts are used to specify whether the two functions $\tau_{J,S}$ and $\tau_{J,D}$ are linear in their arguments and whether damping is present in the system. Table 1.1 gives a summary of the different assumptions for the proposed classes for EJ's.
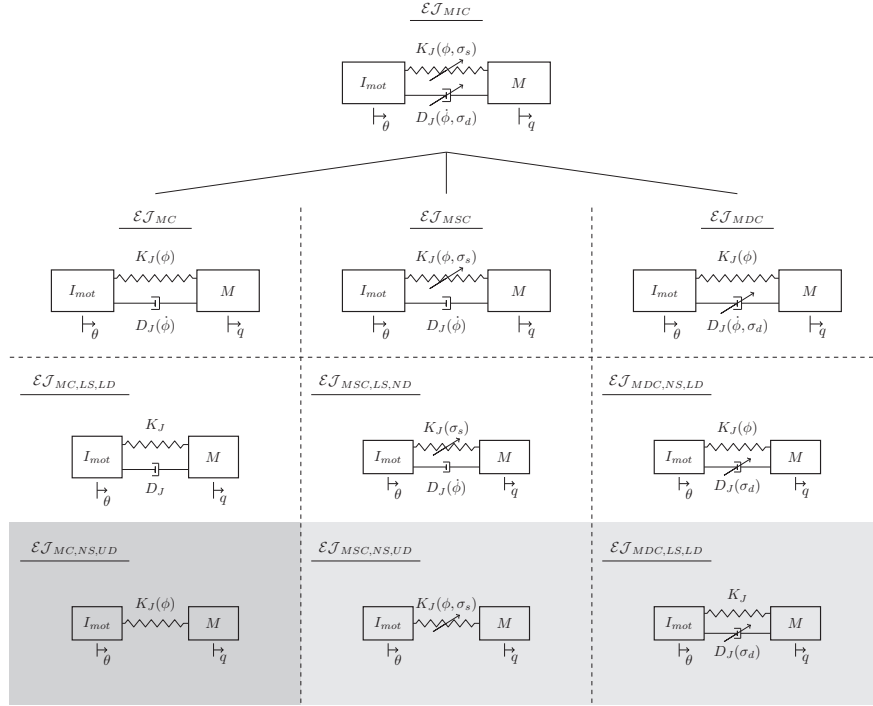
Figure 1.3.2: Classification of EJ Models
(In this thesis, the models in the gray area are investigated. The main focus is given to the model on the lower left corner.)

1.3.2   Optimal Control Strategies

Based on the classification we introduced in the previous subsection, Table 1.2 gives an overview of the EJ models which are investigated in the literature using OC Theory. As shown there, most existing works deal with joints having either a SEA, i.e. models in the class $\mathcal{EJ}_{MC}$, or a VSA, i.e. models in the class $\mathcal{EJ}_{MSC}$ [24, 16, 17, 39, 21]. Making use of different motor models, they all investigate motor control strategies which either maximize the terminal link velocity of EJ's or the stored potential energy. Similarly, in [47] EJ models in the classes $\mathcal{EJ}_{MDC}$ and $\mathcal{EJ}_{MIC}$ have been investigated to realize a reaching task. We will next summarize some of the main findings of these works and clarify how the results of this thesis extend them.

1.3.2.1   Elastic Joints with SEA's ($\mathcal{EJ}_{MC}$)

In the literature, studies following an approach similar to the one we pursue in this thesis mostly exist for undamped EJ's with linear SEA's (LSEA's) [17, 24, 16, 39, 21]. In these actuators, the TDP describing the output torque as a

	$\mathcal{EJ}_{MC,j,k}$		$\mathcal{EJ}_{MSC,j,k}$		$\mathcal{EJ}_{MDC,j,k}$	
	$j = LS$	$j = NS$	$j = LS$	$j = NS$	$k = LD$	$k = ND$
Analytical	[24, 17, 16] [39, 21, 40]	[43]	[17, 16] [39, 21]	[42, 43]	[41]	-
Numerical	-	[24]	-	[24]	-	[47]

Table 1.2: Investigated EJ Models in Literature (The publications [40, 41, 42] and [43] resulted from the research conducted by the author during the thesis period.)

function of the spring deflection is linear. Consequently, when the position of the motor is fixed the dynamics of an EJ with such an actuator corresponds exactly to the dynamics of a conservative and linear mass-spring system (MSS) [35]. In particular, the link will oscillate in this case with the corresponding MSS's eigenfrequency whenever the joint has a positive energy.

Existing studies on EJ's with LSEA's reveal a close relation between the oscillatory nature of MSS's and optimal control strategies maximizing the joint's terminal link velocity as well as the joint's potential energy. In particular, modeling the motor as a velocity source it has been shown in [24], using Pontryagin's Minimum Principle (PMP) [44], that in order to maximize the link velocity of an EJ with a LSEA at a given time instant, the motor velocity needs to periodically switch between its minimum and maximum value provided the given time is sufficiently high. Furthermore, the frequency of this switching has been shown to correspond to the eigenfrequency of the corresponding MSS while its phase has been shown to be uniquely determined by the final time. Similarly, in [39, 21] it has been shown that the same principle also applies when maximizing the potential energy at a given terminal time.

In [17], the problem of maximizing the link velocity is discussed as well. Nevertheless, in contrary to [24] the final time has been left free and constraints have been included on the switching number of the controls and on the final link position. Based on the conducted analysis, it can be observed that for this particular problem the optimal motor velocity simply changes its sign whenever the torque in the spring changes its sign. Moreover, the maximal link velocity is always attained at zero spring deflection. In this thesis, we will show how these problems are all closely related. More importantly, we will introduce the concept of resonance energies which extend existing results on joints with LSEA's to joints with nonlinear SEA's (NSEA's).

1.3.2.2 Elastic Joints with VSA's ($\mathcal{EJ}_{MSC}$)

VSA's enable EJ's to actively change their TDP. This change in turn influences both the potential energy stored in these joints and their oscillatory behaviour. In order to understand how to best exploit this additional degree of freedom in the control, research has been mainly directed towards EJ models in which an instantaneous change between two linear TDP's, a minimal and maximal TDP,

was allowed. In other words, the eigenfrequency of the corresponding MSS's was assumed to be directly controllable. Under this assumption, control strategies have been proposed in [17] for a position-sourced motor to attain high terminal link velocities at a given position. These strategies satisfy the necessary conditions provided by PMP for the task of maximizing the terminal link velocity and are determined under the assumption that the Hamiltonian is zero. A physical principle has been also found describing these strategies. According to this principle the motor position switches between its minimum and maximum value depending on the sign of the link velocity. Similarly, the VSA switches the controllable eigenfrequency between its minimum and maximum value, and the switchings occur whenever the product of the link velocity with the spring torque changes its sign [54].

In [39, 21], focus was given to an EJ model with a velocity-sourced motor. Under the simplifying assumption of directly controlling the eigenfrequency, the problem of maximizing the potential energy of an EJ at a given terminal time has been investigated there. The obtained analytical expressions for the control strategies show the existence of a physical principle closely related to the one found in [17] for EJ's with position-sourced motors. In particular, for control strategies leading to a zero Hamiltonian the motor velocity switches between its minimum and maximum value depending on the sign of the spring torque. The VSA, on the other hand, switches in this case the eigenfrequency between its minimum and maximum value depending on the sign of the product of this torque with its time-derivative. For control strategies leading to a non-zero Hamiltonian the principle is more complex, but can be described in terms of the potential energy of the joint and the kinetic energy of the link. In this thesis, we will show the existence of similar physical principles for the case when the VSA is allowed to instantaneously change the TDP by switching between two nonlinear functions of the deflection, see also [42, 43]. Considering the currently existing VSA designs, this is a practically more relevant scenario.

1.3.2.3 Elastic Joints with VDA's ($\mathcal{EJ}_{MDC}$)

Regarding the OC of EJ's with VDA's, a reaching task has been analysed in [47] such that a desired link position is reached while minimizing a cost functional that accounts for the deviation of the link trajectory from the given target. More specifically, setting the motor position to the desired link position and fixing the TDP of an EJ optimal control strategies have been found for the adjustable damping in a VDA. Numerical results obtained using the ILQR method [31] show that for this particular task the damping in the system needs to switch between its minimum and maximum value. In this thesis, OC strategies are investigated for a more simplified EJ model for which analytical solutions could be obtained. The existence of switching strategies as observed in [47] have been then shown to be necessary whenever a linear cost functional is to be minimized, see also [41].

1.4 Thesis Organization

In this thesis, we have mainly investigated optimal control strategies for an undamped EJ with a NSEA, see Fig. 1.3.2. In particular, treating the motor of the actuator as a velocity source and assuming that the joint is initially at rest we have fully solved the problem of maximizing the link velocity of such EJ's at a given terminal time. The main body of the thesis is devoted to deriving the solution to this problem. Furthermore, we also investigate optimal control strategies for more complex EJ models and more general cost functionals. The thesis is organized as follows:

- Chapter 2 formulates the problem of maximizing the link velocity of an EJ with a velocity-sourced NSEA in the context of OC theory.

- Chapter 3 provides several preliminary results on mass-spring systems as well as a novel result on their periods.

- Chapter 4 discusses switching control strategies maximizing the energy of EJ's.

- Chapter 5 introduces an iterative construction method to determine optimal control strategies maximizing the link velocity of EJ's.

- Chapter 6 discusses the maximal link velocity of EJ's by making use of the proposed method. Furthermore, the applicability of the obtained results is experimentally verified using the DLR FSJ.

- Chapter 7 extends the obtained results on optimal control strategies to EJ's with VDA's and VSA's.

- Chapter 8 concludes the thesis by summarizing the main results, discussing their implications and giving an outlook for future research directions.

There are also two appendices in the thesis. The first appendix, that is Appendix A, provides a proof of PMP for a fairly general OC problem and also shows how to further extend this principle under appropriate assumptions on the system dynamics and cost functional. Appendix B contains the proofs for the various propositions stated in the thesis.

Chapter 2

Problem Formulation

In this thesis, we will make use of OC Theory to mostly determine control strategies which maximize the link velocity of EJ's at a given time instant. Focusing on the case where the joints are initially at rest and controlled by velocity-sourced SEA's, the main purpose of the current chapter is to formulate this velocity maximization problem as an OC problem. This requires us to first find the control system that mathematically describes the dynamics of an EJ and then to express the cost functional describing our problem as a function of this system's states. In the following section, we focus on determining the required control system[1].

2.1 Control System Σ

The control system corresponding to a given OC problem is a 4-tuple consisting of the *state-space* $\mathbb{X}$, the *state dynamics* $\boldsymbol{f}$, the *control set* $\mathbb{U}$ and finally the *class of admissible controls* $\mathcal{U}$ [53]. In order to determine these four quantities and thus the control system Σ for our problem, we will first describe the dynamics of an EJ with a velocity sourced SEA. Moreover, we will also clarify several properties of TDP's of SEA's that are common in most existing designs and that we will take as granted.

As already discused in Sec. 1.3.1 and also illustrated in Figure 2.1.1, an EJ with a SEA can simply be regarded as a mechanical system which consists of a motor and a link that are attached to each other by a possibly nonlinear spring. Consequently, using q to denote the link position and θ for the motor position the dynamics of such a joint is given by the following two differential equations

---

[1]The introduced control system will be used in Chapters 4-6, i.e. the main body of the thesis, where we analyse EJ's with velocity-sourced SEA's. In Chapter 7, we will slightly adjust this system to be able to account for the additional parameters and control variables in the more complex EJ models. Similarly, we will also formulate there different OC problems dealing with more general cost functionals.
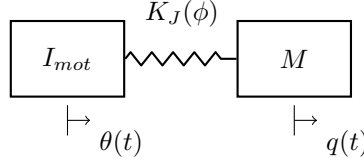
Figure 2.1.1: EJ Model with a SEA

[35]:

$$M\ddot{q} = \tau_J(\phi), \qquad (2.1.1)$$
$$\dot{\theta} = u \in [-\dot{\theta}_{max}, \dot{\theta}_{max}], \qquad (2.1.2)$$

where $M > 0$ stands for the link's mass of inertia with respect to its rotation axis, $\tau_J : \mathbb{R} \to \mathbb{R}$ for the TDP[2] describing the output torque as a function of the deflection in the spring $\phi = \theta - q$ and finally u for the controlled motor velocity whose magnitude is bounded by the maximum motor velocity $\dot{\theta}_{max} > 0$. Based on the TDP's present in most existing SEA designs, we will have the following three standing assumptions for τ_J:

(A1) $\tau_J : \mathbb{R} \to \mathbb{R}$ is symmetric with respect to the origin.

(A2) $\tau_J : \mathbb{R} \to \mathbb{R}$ is a continuously differentiable function of the deflection.

(A3) The stiffness-deflection profile (SDP) $K_J : \mathbb{R} \to \mathbb{R}$, i.e. the first derivative of τ_J, is positive at each deflection value.

Having described the dynamics of EJ's with SEA's and also clarified the general properties of their TDP's, we next find the state-space $\mathbb{X}$ and the state dynamics $\boldsymbol{f}$ for our problem.

Both $\mathbb{X}$ and $\boldsymbol{f}$ can be determined by the differential equations (2.1.1)-(2.1.2) and the mathematical states we choose to describe our problem. We take these states as the spring deflection and the link velocity, i.e. $\boldsymbol{x} = \begin{pmatrix} x_1 & x_2 \end{pmatrix}^T = \begin{pmatrix} \phi & \dot{q} \end{pmatrix}^T$, due to their direct relation to the potential energy stored in the SEA and to the kinetic energy of the link. With this choice, our state-space becomes simply the two-dimensional space $\mathbb{R}^2$, i.e.

$$\mathbb{X} = \mathbb{R}^2. \qquad (2.1.3)$$

Moreover, by differentiating $\boldsymbol{x}$ with respect to time we get using the differential equations (2.1.1)-(2.1.2) the state dynamics $\boldsymbol{f} : \mathbb{R}^2 \times \mathbb{R} \to \mathbb{R}^2$ with

$$\dot{\boldsymbol{x}} = \boldsymbol{f}(\boldsymbol{x}, u) = \begin{pmatrix} u - x_2 \\ \frac{\tau_J(x_1)}{M} \end{pmatrix}. \qquad (2.1.4)$$

---

[2]For an undamped EJ, we simply have $\tau_J = \tau_{J,S}$.

To determine our control system Σ, we now need to find its control set and further choose the class of admissible controls over which we will search for the optimal control strategy. The control set of a control system describes the constraints on the values of the control. For our problem, the control u in (2.1.4) corresponds to the motor velocity and according to (2.1.2) the control set is then given by

$$\mathbb{U} = [-\dot{\theta}_{max}, \dot{\theta}_{max}]. \tag{2.1.5}$$

Similar to the control set, the class of admissible controls $\mathcal{U}$ describes the function space to which the controlled motor velocity belongs. We will take this class to be the practically relevant set of piecewise continuous functions[3] which are defined on a compact interval $D = [t_0, t_f] \subset \mathbb{R}$ with $t_f > t_0$ and which take values in $\mathbb{U}$. Denoting this set by $\mathcal{PC}_{\mathbb{U}}$, we thus have

$$\mathcal{U} = \mathcal{PC}_{\mathbb{U}}. \tag{2.1.6}$$

In order to ease our analysis, we will assume that all the functions in $\mathcal{U}$ are left-continuous at $t \in [t_0, t_f)$ and continuous at t_f.

Equations (2.1.3)-(2.1.6) fully describe the control system $\Sigma = (\mathbb{X}, \boldsymbol{f}, \mathbb{U}, \mathcal{U})$ which we will use to formulate our OC problem in Section 2.3. It is important to remark here that in this description we do not specify particular values for M or $\dot{\theta}_{max}$. Similarly, we do not provide the exact expression for the TDP. This is justified by the fact that the solution method we propose in this thesis can be applied for any admissible choice for these three parameters. Nevertheless, we will also see that OC strategies and the resulting maximal link velocities do depend on these parameters. In order to be able to easily distinguish between control systems with different parameters and also to rigorously formulate our OC problem, we require some basic definitions which we provide next.

2.2 Basic Definitions

In this section, we present definitions and notations which we will use in the formulation of our OC problem and which will simplify our discussions in the later chapters where we derive and analyse the solution to the formulated problem.

Following [53], we call any control u in the set of admissible controls $\mathcal{U}$ an *admissible control*. A piecewise continuously differentiable function $\boldsymbol{x} : D = [t_0, t_f] \rightarrow \mathbb{X}$ is then said to be a *trajectory* of Σ if there exists an admissible control u sharing the same domain as $\boldsymbol{x}$ such that $\dot{\boldsymbol{x}}(t) = \boldsymbol{f}(\boldsymbol{x}(t), u(t))$ holds at each $t \in D$ where this derivative exists. Moreover, in this case we will call the pair $(\boldsymbol{x}, u)$ an *admissible controlled trajectory* of Σ and refer to $\boldsymbol{x}$ as the trajectory corresponding to u. Since $\Sigma = (\mathbb{X}, \boldsymbol{f}, \mathbb{U}, \mathcal{U})$ is a time-invariant system, without loss of generality we always choose the *initial time* t_0 of $\boldsymbol{x}$ and u as 0, i.e. $D = [t_0, t_f] = [0, t_f]$. Consequently, their domains of definition depend only on their *final time* $t_f > 0$.

---

[3]In the thesis, we will adopt the definition of piecewise continuous functions and piecewise continuously differentiable functions from [34].

Let us consider now the set of all trajectories of Σ. Following this time [55], we will denote this set by $\mathrm{Traj}(\Sigma)$. For each $\boldsymbol{x} \in \mathrm{Traj}(\Sigma)$, we use $\boldsymbol{x}_0 = \begin{pmatrix} x_{10} & x_{20} \end{pmatrix}^T := \boldsymbol{x}(0)$ to denote its *initial state* and $\boldsymbol{x}_f = \begin{pmatrix} x_{1f} & x_{2f} \end{pmatrix}^T := \boldsymbol{x}(t_f)$ to denote its *terminal state*. Moreover, we use $T(\boldsymbol{x}) := t_f$ to denote the final time of $\boldsymbol{x}$ and refer to this time also as the *time along* $\boldsymbol{x}$. The trajectory $\boldsymbol{x}^* \in \mathrm{Traj}(\Sigma)$ will then be called a *time-optimal trajectory* of Σ, if $T(\boldsymbol{x}^*)$ is less then or equal to $T(\boldsymbol{x})$ for any $\boldsymbol{x} \in \mathrm{Traj}(\Sigma)$ with $\boldsymbol{x}_0 = \boldsymbol{x}_0^*$ and $\boldsymbol{x}_f = \boldsymbol{x}_f^*$. Finally, an admissible control u^* is called a *time-optimal control* of Σ if there exists a time-optimal trajectory $\boldsymbol{x}^*$ of Σ such that $(\boldsymbol{x}^*, u^*)$ is an admissible controlled trajectory.

As we will see in Chapter 5, the notion of time-optimality we have just introduced plays an important role in understanding how to maximize the link velocity of series elastic actuators in a limited time. In particular, we will show that control strategies maximizing the link velocity at a given time are always time-optimal in case the joint is initially at rest. In that chapter, we will also show that these particular strategies are always piecewise-constant. We want to next introduce the definitions and notations used in the thesis to discuss different possibilities for piecewise-constant control strategies and the trajectories corresponding to them.

We call a control described by a piecewise-constant function of time simply a *switching control* and denote the set of all admissible switching controls by $\mathcal{S}_{\mathbb{U}}$. Note that a control in $\mathcal{S}_{\mathbb{U}} \subset \mathcal{PC}_{\mathbb{U}}$ is uniquely described by its final time t_f, its *switching times* in $(0, t_f)$ at which it changes its value and finally the control values at the initial time and at the switching times. We define the *switching number* of such a control as the number of its switching times, which is always non-negative and finite. Moreover, if $i \geq 0$ is the switching number of a control $u \in \mathcal{S}_{\mathbb{U}}$ we will refer to this control also as an *admissible switching control with i switchings*.

Given an admissible switching control $u : D \to \mathbb{U}$ with i switchings, we use $t_{S,0} := 0$ and $t_{S,i+1} := t_f$ to denote its initial and final time, respectively. Moreover, if $i > 0$ we use $t_{S,k}$ to denote the switching times of that control with $k \in \{1, \ldots, i\}$ and $t_{S,0} < t_{S,1} < \ldots < t_{S,i+1}$. Regardless of the value of i, we also introduce a finite partition of the domain D using the times $t_{S,0}, \ldots, t_{S,i+1}$ such that the control takes the same value in each element of this partition. This partition consists of $i + 1$ subsets of D defined by

$$D_k := \begin{cases} [t_{S,k}, t_{S,k+1}) & k \neq i \\ [t_{S,k}, t_{S,k+1}] & k = i \end{cases}, \tag{2.2.1}$$

where $k \in S_i := \{0, \ldots, i\}$.

Finally, for any time-dependent variable related to a switching control u with $i \geq 0$ switchings we indicate the value of that variable at $t_{S,k} \in \{t_{S,0}, \ldots, t_{S,i+1}\}$ by putting the upper left superscript k to that variable. For instance, ${}^k u$ denotes for each $k \in S_{i+1}$ the value of the control u at $t_{S,k}$. Similarly, if $\boldsymbol{x}$ is a trajectory corresponding to u, ${}^k \boldsymbol{x}$ denotes the value of that trajectory at $t_{S,k}$.

The definitions we have so far provided for Σ are valid regardless of our choice for the *control system parameter*, i.e. for the three-tuple $\boldsymbol{p} := (M, \tau_J, \dot{\theta}_{max}) \in P_\Sigma$ with

$$P_\Sigma := (0, \infty) \times \mathcal{C}_{\tau_J}^1 \times (0, \infty), \qquad (2.2.2)$$

where $C_{\tau_J}^1$ denotes the set of all TDP's satisfying $(A1)-(A3)$. Note that for each possible choice of $\boldsymbol{p}$, equations (2.1.3)-(2.1.6) describe a unique control system $\Sigma = (\mathbb{X}, \boldsymbol{f}, \mathbb{U}, \mathcal{U})$. More specifically, there exists a one-to-one correspondence between the *parameter set* P_Σ and the set of control systems satisfying the assumptions from Sec. 2.1. To emphasize this bijective relation between $\boldsymbol{p}$ and Σ, we will occasionally call Σ as *the control system corresponding to the parameter $\boldsymbol{p}$*. Similarly, for the functions which we will define in the following chapters for the control system Σ, we will either expand their domains using the set P_Σ or call them the *function corresponding to $\boldsymbol{p}$*, if we want to explicitly state their dependence on the elements of $\boldsymbol{p}$. This will especially be done in Chapter 6 where we analyse the influence of the control system parameters on the maximal link velocity of EJ's.

2.3 Optimal Control Problem

Based on the control system Σ described in Section 2.1, we introduce the following cost functional $J : \mathcal{U} \to \mathbb{R}$, with

$$J(u) = -x_{2f}, \qquad (2.3.1)$$

where x_{2f} denotes the terminal link velocity of the trajectory $\boldsymbol{x}$ which starts from the initial state $\boldsymbol{x}_0 = \boldsymbol{0}$ and which corresponds to the control u. Our OC problem on maximizing the link velocity of an EJ with a SEA can then be formulated as follows.

Link Velocity Maximization Problem (LVMP): Given a final time $t_f > 0$, find the control u^{opt} which minimizes $J(u)$ over all admissible controls $u \in \mathcal{U}$ defined on $D = [0, t_f]$.

Having mathematically formulated our OC problem, we want to use OC Theory to find its solution. As we show in Chapter 5, the control strategies solving the introduced LVMP, i.e. the *optimal controls* for the LVMP, can be derived using mainly PMP [44]. Nevertheless, in order to simplify the derivation of these controls and the computation of the corresponding *optimal trajectories* for the LVMP we will first provide some preliminary discussions on the properties of Σ. More specifically, in the following chapter we will have a detailed look at the trajectories of MSS's, i.e. trajectories of Σ corresponding to $u \equiv 0$, and at the time properties of these systems. In Chapter 4, we then turn our attention to trajectories of Σ corresponding to switching control strategies and discuss how to maximize the energy stored along these trajectories.

Chapter 3

Mass-Spring Systems

In this chapter, we will discuss trajectories and time properties of MSS's and investigate how they are influenced by the energy and TDP of such systems. Our results on trajectories will be used for constructing candidates for optimal control strategies solving the LVMP and for determining the resulting link velocities. Our results on time properties will, on the other hand, help in determining the optimality of the constructed strategies as well as in finding a physical interpretation for the optimal strategies.

3.1 Trajectories

A MSS consists simply of a mass that is attached to a wall by a spring. Consequently, such a system can be thought of as an EJ with a fixed motor position. Making use of (2.1.1) and the notations we have previously introduced for EJ's, the dynamics of a MSS can then be described by the second-order differential equation

$$M\ddot{\phi} + \tau_J(\phi) = 0, \tag{3.1.1}$$

where ϕ denotes as before the deflection in the spring. It is important to note here that given an initial deflection $\phi_0 := \phi(0)$ and an initial velocity $\dot{\phi}_0 := \dot{\phi}(0)$, a two-times continuously differentiable function $\phi : [0, t_f] \rightarrow \mathbb{R}$ solving (3.1.1) exists for each value of $t_f > 0$ due to our assumptions on τ_J. Moreover, this solution is unique [52]. Based on the definitions we have introduced in Section 2.2, we will call a pair $(\phi, \dot{\phi})$ that consists of a solution of (3.1.1) and its time-derivative a trajectory of a MSS. Our aim is now to first elaborate on the energy stored along trajectories of MSS's.

The energy of a MSS consists of the kinetic energy of its mass and the potential energy stored in its spring. The potential energy $E_{pot} : \mathbb{R} \rightarrow [0, \infty)$ is a function of only the deflection and is given by the integral

$$E_{pot}(\phi) = \int_0^{\phi} \tau_J(s)\mathrm{d}s. \tag{3.1.2}$$

26

Similarly, the kinetic energy $E_{kin} : \mathbb{R} \to [0, \infty)$ of a MSS depends only on its velocity $\dot{\phi}$:

$$E_{kin}(\dot{\phi}) = \frac{1}{2}M\dot{\phi}^2. \tag{3.1.3}$$

Multiplying now both sides of (3.1.1) with $\dot{\phi}$, integrating with respect to time and using our assumptions on τ_J, it can be observed that along a trajectory of a MSS the system's energy $E_{MSS} : \mathbb{R}^2 \to [0, \infty)$ with $E_{MSS}(\phi, \dot{\phi}) = E_{pot}(\phi) + E_{kin}(\dot{\phi})$ is constant and given by

$$
\begin{aligned}
E_{MSS}(\phi, \dot{\phi}) &= \int_0^{\phi_0} \tau_J(s)\mathrm{d}s + \frac{1}{2}M\dot{\phi}_0^2 \tag{3.1.4} \\
&= \int_0^{\phi_{max}} \tau_J(s)\mathrm{d}s = \frac{1}{2}M\dot{\phi}_{max}^2. \tag{3.1.5}
\end{aligned}
$$

Notice that in (3.1.5) we use $\phi_{max} \geq 0$ to denote the maximum deflection which the system can obtain at $\dot{\phi} = 0$, and similarly $\dot{\phi}_{max} \geq 0$ to denote the system's maximum velocity attainable at $\phi = 0$.

According to (3.1.4), the energy along a trajectory of a MSS is uniquely determined by the initial values ϕ_0 and $\dot{\phi}_0$. Moreover, this energy can only be equal to zero if both ϕ_0 and $\dot{\phi}_0$ are zero. In this case the MSS is simply in static equilibrium and does not move, i.e. $\phi \equiv 0$. In all other cases, the system's energy and thus ϕ_{max} and $\dot{\phi}_{max}$ are positive. Moreover, for a sufficiently high final time the system will periodically oscillate between $-\phi_{max}$ and ϕ_{max} [36, 52]. We want to next take a closer look at the trajectories of MSS's with positive energy.

It is important to first realize that for any given $\phi_{max} > 0$, the equality $E_{MSS}(\phi, \dot{\phi}) = \int_0^{\phi_{max}} \tau_J(s)\mathrm{d}s$ describes a closed curve in the phase plane. Indeed, this equality can be solved for the magnitude of the velocity as follows:

$$|\dot{\phi}|(\phi, \phi_{max}) = \sqrt{\frac{2\int_\phi^{\phi_{max}} \tau_J(s)\mathrm{d}s}{M}}, \tag{3.1.6}$$

where we have $|\dot{\phi}| : [-\phi_{max}, \phi_{max}] \times (0, \infty) \to [0, \infty)$. The values $|\dot{\phi}|(\phi, \phi_{max})$ takes at $\phi \in (-\phi_{max}, \phi_{max})$ provides then the upper half of the aforementioned curve in the phase plane while the negative of these values will give the lower half. Both parts will join at the minimum and maximum deflection values.

It now follows from (3.1.4)-(3.1.5) that in a phase plane trajectories of MSS's move on closed curves when their energies are positive. Figure 3.1.1 illustrates these curves as well as several trajectories moving on them for three different TDP's and various values of ϕ_{max} ($\tau_J \in \{\tau_{J,1}, \tau_{J,2}, \tau_{J,3}\}$, $M = 1[\mathrm{kgm}^2]$). More specifically, in Fig. 3.1.1 (Top) three TDP's are plotted for $\phi[\mathrm{rad}] \in [-\frac{4\pi}{45}, \frac{4\pi}{45}]$ together with the corresponding SDP's and potential energy functions. The TDP's are chosen such that each of them shows a different spring characteristic but attains the same potential energy of 5J at the deflection $\phi_c = \frac{\pi}{15}\mathrm{rad}$. For each of these TDP's, the corresponding closed curves are then plotted in Fig. 3.1.1 (Bottom) for four different values of ϕ_{max}. On each of these curves, a
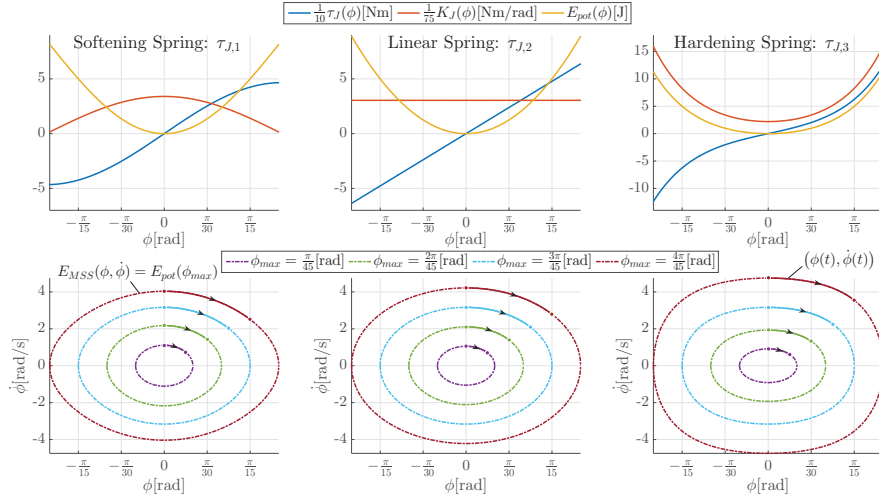
Figure 3.1.1: Trajectories of MSS's with different Spring Characteristics $\left(\tau_{J,1}(\phi) = \frac{875}{32\left(1-\cos\left(\frac{35\pi}{96}\right)\right)} \sin\left(\frac{175}{32}\phi\right), \tau_{J,2}(\phi) = \frac{2250}{\pi^2}\phi, \tau_{J,3}(\phi) = \frac{150}{\pi(\cosh(2)-1)} \sinh\left(\frac{30}{\pi}\phi\right), M = 1[\text{kgm}^2]\right)$

trajectory is also depicted which starts from zero deflection with the maximal velocity and terminates at $\phi = \frac{3\phi_{max}}{4}$. Notice that on the upper half of the phase planes where $\dot{\phi}$ is positive, the deflection increases, while on the lower part it decreases. Consequently, all the depicted trajectories rotate clockwise as they move on the closed curves in Fig. 3.1.1.

A closer look at Fig. 3.1.1 (Top) shows now how different spring characteristics can influence the values of τ_J, K_J and E_{pot} at various deflections. As illustrated there, for the third TDP $\tau_{J,3}$ which is depicted on the right and which shows a progressive spring characteristic, the torque at $\phi = \phi_c$ is greater than the torque values attained by the other two TDP's at this deflection. Similarly, the stiffness value at this deflection, i.e. $K_J(\phi_c)$, takes the highest value for $\tau_{J,3}$. These two observations are merely a consequence of the condition on the stored potential energy E_{pot} according to which the chosen TDP's need to store the exact same energy at this deflection. Another consequence of that condition is that for each $\phi > \phi_c$ the potential energy $E_{pot}(\phi)$ that is stored using $\tau_{J,3}$ is greater than the energy stored using the other two TDP's while for each ϕ in $(0, \phi_c)$ the potential energy stored using $\tau_{J,1}$, which shows a degressive spring characteristic, is the greatest. This also results in the stiffness value at zero deflection, i.e. $K_J(0)$, being the greatest for $\tau_{J,1}$.

As shown in Fig. 3.1.1 (Bottom), choosing different TDP's does not only influence the stiffness, torque and potential energy values at various deflections but also the curves on which the trajectories of MSS's move. In the following, we want to briefly discuss several properties of these curves which will explain

the similarities as well as the differences observed in Fig. 3.1.1 (Bottom) and show, in particular, how the differences are related to the previously discussed values of τ_J, K_J and E_{pot}.

Note that regardless of the TDP, the closed curves described by the equality $E_{MSS}(\phi, \dot{\phi}) = \int_0^{\phi_{max}} \tau_J(s)\mathrm{d}s$ enclose a greater area as ϕ_{max} and thus the system's energy increases. This follows from the partial derivative $\frac{\partial |\dot{\phi}|}{\partial \phi_{max}}$ being positive everywhere it is defined, see (3.1.6). Moreover, all these closed curves are symmetrical not only with respect to the horizontal axis, as expected from (3.1.6), but with respect to both axes. This property is due to the two energy functions (3.1.2) and (3.1.3) being both even functions and allows us to define similar to (3.1.6) the magnitude of the deflection $|\phi| : [-\dot{\phi}_{max}, \dot{\phi}_{max}] \times (0, \infty) \rightarrow [0, \infty)$ as a function of $\dot{\phi}$ and $\dot{\phi}_{max}$ with

$$|\phi|(\dot{\phi}, \dot{\phi}_{max}) = E_{pot}^{-1} \left(\frac{1}{2} M(\dot{\phi}_{max}^2 - \dot{\phi}^2) \right), \tag{3.1.7}$$

where E_{pot}^{-1} denotes the inverse of the potential energy function restricted to non-negative deflection values, i.e. of $E_{pot}|_{[0,\infty)}$. This symmetry property also allows us to concentrate only on the part of the phase plane where both ϕ and $\dot{\phi}$ are non-negative when analysing the properties of these curves. Consequently, all the properties of the curves can be found by simply analysing the two functions (3.1.6) and (3.1.7).

Focusing now on the differences in the curves in Fig. 3.1.1 (Bottom), one important difference exists in the values of the maximum velocity $\dot{\phi}_{max}$. As shown there, given the same maximum deflection value the maximum velocity the three MSS's attain are not necessarily equal to each other. The reason for this can be found by looking at the equality (3.1.5) which relates ϕ_{max} and $\dot{\phi}_{max}$. According to this equality, for any given MSS the value of $\dot{\phi}_{max}$ is directly related to the potential energy stored at the deflection ϕ_{max}. As already discussed, by our choice of the TDP's all the three MSS's analysed in Fig. 3.1.1 have the same potential energy for $\phi_{max} = \phi_c$ and since the masses of MSS's are also equal to each other so are their maximum velocities in this case. For $\phi_{max} < \phi_c$, however, $E_{pot}(\phi_{max})$ takes its maximum value for $\tau_{J,1}$ and similarly for $\phi_{max} > \phi_c$, $E_{pot}(\phi_{max})$ is maximal for $\tau_{J,3}$. Consequently, for $\phi_{max} < \phi_c$ the maximum velocity $\dot{\phi}_{max}$ is greatest for $\tau_{J,1}$ and for $\phi_{max} > \phi_c$ it is greatest for $\tau_{J,3}$.

Another important difference between the illustrated curves are their curvatures at zero deflection and at the maximal deflection. These curvatures can be quantitatively analysed by evaluating the partial derivatives $\frac{\partial^2 |\phi|}{\partial \phi^2}(\phi, \phi_{max})$ and $\frac{\partial^2 |\phi|}{\partial \dot{\phi}^2}(\dot{\phi}, \dot{\phi}_{max})$ at $\phi = 0$ and at $\dot{\phi} = 0$, respectively. Using equations (3.1.6)-

(3.1.7), it can be shown that these derivatives take the values

$$\frac{\partial^2 |\dot{\phi}|}{\partial \phi^2}(0, \phi_{max}) = -\frac{\omega_0^2}{\dot{\phi}_{max}}, \qquad (3.1.8)$$

$$\frac{\partial^2 |\phi|}{\partial \dot{\phi}^2}(0, \dot{\phi}_{max}) = -\frac{M}{\tau_J(\dot{\phi}_{max})}, \qquad (3.1.9)$$

where $\omega_0 := \sqrt{\frac{K_J(0)}{M}}$ denotes the eigenfrequency of MSS's when linearized around their equilibrium. Notice that equations (3.1.8)-(3.1.9) and the previously discussed values of τ_J, K_J and E_{pot} explain now why in Fig. 3.1.1 (Bottom) the curvatures of the light blue and dark red dashed lines ($\phi_{max} \geq \frac{3\pi}{45}$ rad) at the two deflection values $\phi = 0$ and $\phi = \phi_{max}$ are highest for $\tau_{J,1}$ and smallest for $\tau_{J,3}$.

For brevity, we will not go into a more detailed discussion on the properties of the illustrated curves, but summarize all the equations required for their analysis in Table 3.1. More specifically, we introduce in Table 3.1a the TDP types $\tau_{J,s}, \tau_{J,l}$ and $\tau_{J,sh}$ which respectively generalize the TDP's $\tau_{J,1}, \tau_{J,2}$ and $\tau_{J,3}$ from Fig. 3.1.1, and provide the corresponding SDP's and potential energy functions. Moreover, we give in Table 3.1b the expressions for the functions $|\dot{\phi}|$ and $|\phi|$ together with the equations for $\dot{\phi}_{max}$ and ω_0 which clarify the relation between the domains of these two functions[1].

Our discussion on the trajectories of MSS's so far elucidates their dependence on the system's energy and on the TDP. We have, however, not yet discussed the times these trajectories need to move from one state to another. In the following section, we show how to explicitly compute these times.

3.2 Time Properties

Based on our discussion on the trajectories of MSS's, we can see that for each initial state $(\phi_0, \dot{\phi}_0)$ with $E_{MSS}(\phi_0, \dot{\phi}_0) > 0$ there exists a unique periodic solution $\phi : [0, \infty) \to \mathbb{R}$ of (3.1.1) such that the corresponding trajectory constantly rotates on a closed curve when illustrated in a phase plane. Choosing an arbitrary state $(\phi_s, \dot{\phi}_s)$ on that curve, which is not equal to the given initial state, we are now interested in finding the times $t \in (0, \infty)$ at which this trajectory $(\phi, \dot{\phi})$ reaches this second state, i.e. for which we will have

$$\left(\phi(t), \dot{\phi}(t) \right) = (\phi_s, \dot{\phi}_s). \qquad (3.2.1)$$

---

[1]Notice that when using the expressions in Table 3.1 for the TDP $\tau_{J,s}$, ϕ and ϕ_{max} are allowed to take values only in the intervals $(-\frac{\pi}{2k_e}, \frac{\pi}{2k_e})$ and $(0, \frac{\pi}{2k_e})$, respectively. This is done in order to ensure that assumption $(A3)$ is satisfied, see Section 2.1. Moreover, in the definition of the TDP $\tau_{J,l}$ we use two parameters, K_e and k_e, instead of only one. This choice better indicates the similarities and differences between the different expressions for the three TDP's. In addition, it will also be useful in Sec. 6.2, where we analyse the dependence of the maximal link velocity on system parameters using dimensionless parameters.

(a) τ_J, K_J and E_{pot}

	Softening Spring: $\tau_{J,s}$	Linear Spring: $\tau_{J,l}$	Hardening Spring: $\tau_{J,sh}$
$\tau_J(\phi)$	$\phi \in \left(-\frac{\pi}{2k_e}, \frac{\pi}{2k_e}\right)$ $\tau_{J,s}(\phi) = K_e \sin(k_e\phi)$	$\phi \in \mathbb{R}$ $\tau_{J,l}(\phi) = K_e k_e \phi$	$\phi \in \mathbb{R}$ $\tau_{J,sh}(\phi) = K_e \sinh(k_e\phi)$
$K_J(\phi)$	$K_e k_e \cos(k_e\phi)$	$K_e k_e$	$K_e k_e \cosh(k_e\phi)$
$E_{pot}(\phi)$	$\frac{K_e}{k_e}(1 - \cos(k_e\phi))$	$\frac{1}{2}K_e k_e \phi^2$	$\frac{K_e}{k_e}(\cosh(k_e\phi) - 1)$

(b) $|\dot\phi|$, $|\phi|$, $\dot\phi_{max}$ and ω_0

	Softening Spring: $\tau_{J,s}$	Linear Spring: $\tau_{J,l}$	Hardening Spring: $\tau_{J,sh}$
	$\phi_{max} \in \left(0, \frac{\pi}{2k_e}\right)$	$\phi_{max} \in (0, \infty)$	$\phi_{max} \in (0, \infty)$
$|\dot\phi|(\phi, \phi_{max})$	$\omega_0 \frac{\sqrt{2(\cos(k_e\phi) - \cos(k_e\phi_{max}))}}{k_e}$	$\omega_0 \sqrt{\phi_{max}^2 - \phi^2}$	$\omega_0 \frac{\sqrt{2(\cosh(k_e\phi_{max}) - \cosh(k_e\phi))}}{k_e}$
$|\phi|(\dot\phi, \phi_{max})$	$\frac{\arccos\left(1 - \frac{k_e^2}{2\omega_0^2}(\phi_{max}^2 - \dot\phi^2)\right)}{k_e}$	$\frac{\sqrt{\phi_{max}^2 - \frac{\dot\phi^2}{\omega_0^2}}}{}$	$\frac{\cosh^{-1}\left(1 + \frac{k_e^2}{2\omega_0^2}(\phi_{max}^2 - \dot\phi^2)\right)}{k_e}$
$\dot\phi_{max}$	$\frac{2\omega_0}{k_e} \sin\left(\frac{k_e\phi_{max}}{2}\right)$	$\omega_0 \phi_{max}$	$\frac{2\omega_0}{k_e} \sinh\left(\frac{k_e\phi_{max}}{2}\right)$
$\omega_0 = \sqrt{\frac{K_J(0)}{M}}$	$\sqrt{\frac{K_e k_e}{M}}$	$\sqrt{\frac{K_e k_e}{M}}$	$\sqrt{\frac{K_e k_e}{M}}$

$F(z,k) : (-1,1)^2 \to \mathbb{R}, (z,k) \to F(z,k) = \int_0^z \frac{ds}{\sqrt{1-s^2}\sqrt{1-k^2 s^2}}, K(k) : (-1,1) \to \mathbb{R}, k \to K(k) = \lim_{z\to 1^-} F(z,k)$

(c) T_ϕ and $T_{\dot\phi}$

	Softening Spring: $\tau_{J,s}$	Linear Spring: $\tau_{J,l}$	Hardening Spring: $\tau_{J,sh}$
$T_\phi(\phi, \phi_{max})$	$\frac{1}{\omega_0} F\left(\frac{\sin(\frac{k_e\phi}{2})}{\sin(\frac{k_e\phi_{max}}{2})}, \sin\left(\frac{k_e\phi_{max}}{2}\right)\right)$	$\frac{\arcsin\left(\frac{\phi}{\phi_{max}}\right)}{\omega_0}$	$\frac{\text{sgn}(\phi)\left[K\left(\tanh(\frac{k_e\phi_{max}}{2}), \tanh(\frac{k_e\phi_{max}}{2})\right) - F\left(\frac{|\phi|(\phi,\phi_{max})}{2}, \tanh(\frac{k_e\phi_{max}}{2})\right)\right]}{\omega_0 \cosh\left(\frac{k_e\phi_{max}}{2}\right)}$
$T_{\dot\phi}(\dot\phi, \phi_{max})$	$\frac{\text{sgn}(\dot\phi)\left[K\left(\frac{k_e\phi_{max}}{2\omega_0}\right) - F\left(\frac{\sqrt{\phi_{max}^2 - \frac{\dot\phi^2}{\phi_{max}}}}{\phi_{max}}, \frac{k_e\phi_{max}}{2\omega_0}\right)\right]}{\omega_0}$	$\frac{\arcsin\left(\frac{\dot\phi}{\phi_{max}}\right)}{\omega_0}$	$\frac{1}{\sqrt{4\omega_0^2 + k_e^2\phi_{max}^2}} 2F\left(\frac{\dot\phi}{\phi_{max}}, \frac{k_e\phi_{max}}{\sqrt{4\omega_0^2 + k_e^2\phi_{max}^2}}\right)$

$F(z,k) : (-1,1)^2 \to \mathbb{R}, (z,k) \to F(z,k) = \int_0^z \frac{ds}{\sqrt{1-s^2}\sqrt{1-k^2 s^2}}, K(k) : (-1,1) \to \mathbb{R}, k \to K(k) = \lim_{z\to 1^-} F(z,k)$

(d) T_p and $\frac{dT_p}{d\phi_{max}}$

	Softening Spring: $\tau_{J,s}$	Linear Spring: $\tau_{J,l}$	Hardening Spring: $\tau_{J,sh}$
$T_p(\phi_{max})$	$\frac{4}{\omega_0} K(\sin(\Phi_{max}))$	$\frac{2\pi}{\omega_0}$	$\frac{4K(\tanh(\Phi_{max}))}{\omega_0 \cosh(\Phi_{max})}$
$\frac{dT_p}{d\phi_{max}}$	$\frac{2k_e[2E(\sin(\Phi_{max})) - (1+\cos(2\Phi_{max}))K(\sin(\Phi_{max}))]}{\omega_0 \sin(2\Phi_{max})}$	0	$\frac{2k_e[E(\tanh(\Phi_{max})) - K(\tanh(\Phi_{max}))]}{\omega_0 \sinh(\Phi_{max})}$

$\Phi_{max} = \frac{k_e\phi_{max}}{2}, E(k) : (-1,1) \to \mathbb{R}, k \to E(k) = \lim_{z\to 1^-} \int_0^z \frac{\sqrt{1-k^2 s^2}}{\sqrt{1-s^2}} ds$ and $\frac{dT_p}{d\phi_{max}}$

Table 3.1: Equations for MSS's with different Spring Characteristics ($K_e > 0, k_e > 0, M > 0$)

Moreover, we want to understand the influence a MSS's energy and TDP have on these times.

It is important to notice here that there exist infinitely many times for which (3.2.1) will hold. Indeed, as $(\phi, \dot\phi)$ rotates clockwise in the phase plane the state $(\phi_s, \dot\phi_s)$ will be reached for the first time at a positive time t_s and keep reaching this point after every oscillation period T_p. Consequently, t_s and T_p are sufficient to describe the set of all possible times at which (3.2.1) will hold. We will next show how to compute the minimum time t_s that is required to reach the state $(\phi_s, \dot\phi_s)$ from $(\phi_0, \dot\phi_0)$ and discuss some of its main properties.

3.2.1 Minimum Time t_s

There are different possibilities for computing the minimum time t_s. In the following, we will show how to compute t_s using (3.1.6) and (3.1.7).

Let us first assume that the trajectory starts from zero deflection with a positive velocity, as is the case for the trajectories illustrated in Fig. 3.1.1. Moreover, assume that the state $(\phi_s, \dot\phi_s)$ lies in the first quadrant of the phase plane. The velocity $\dot\phi$ will then remain positive and the deflection ϕ will strictly increase until $(\phi_s, \dot\phi_s)$ is reached for the first time. Consequently, for each $t \in [0, t_s]$ we will have $|\dot\phi|(\phi(t), \phi_{max}) = \frac{\mathrm{d}\phi}{\mathrm{d}t}(t)$. Dividing now this relation by its left hand side and integrating with respect to time, the minimum time t_s will, for positive values of ϕ_s, be given by the function $T_\phi : (-\phi_{max}, \phi_{max}) \times (0, \infty) \to \mathbb{R}$ with

$$T_\phi(\phi_s, \phi_{max}) = \int_0^{\phi_s} \frac{\mathrm{d}\phi}{|\dot\phi|(\phi, \phi_{max})}. \tag{3.2.2}$$

If we now look at the more general case with[2] $\mathrm{sgn}(\dot\phi_0) = \mathrm{sgn}(\dot\phi_s) = \mathrm{sgn}(\phi_s - \phi_0)$, the function T_ϕ can still be used to compute t_s. Indeed, in this case the velocity $\dot\phi$ will again not change its sign in the time interval $[0, t_s]$ and depending on this sign the deflection ϕ will either strictly increase or decrease until $(\phi_s, \dot\phi_s)$ is reached. Consequently, for each $t \in [0, t_s]$ we will now have $|\dot\phi|(\phi(t), \phi_{max}) = \mathrm{sgn}(\phi_s - \phi_0)\frac{\mathrm{d}\phi}{\mathrm{d}t}(t)$. Dividing again this relation by its left hand side, noting that both sides are positive and integrating with respect to time, t_s can be computed using now the function $t_{s,\phi} : (-\phi_{max}, \phi_{max})^2 \times (0, \infty) \to [0, \infty)$ with

$$t_{s,\phi}(\phi_0, \phi_s, \phi_{max}) = |T_\phi(\phi_s, \phi_{max}) - T_\phi(\phi_0, \phi_{max})|. \tag{3.2.3}$$

Equation (3.2.3) provides us a possible way to compute the minimum time t_s assuming that the sign of $\dot\phi$ remains constant. As we will next show, we can similarly find a function which can be used to compute t_s in case the deflection ϕ and thus the acceleration do not change their signs.

---

[2]The sign function is defined as follows:

$$\mathrm{sgn} : \mathbb{R} \to \{-1, 0, 1\}, x \to \mathrm{sgn}(x) = \begin{cases} -1 & x < 0 \\ 0 & x = 0 \\ 1 & x > 0 \end{cases}.$$

Assuming now that the initial state $(\phi_0, \dot{\phi}_0)$ lies in the first quadrant of the phase plane and that ϕ_s equals to the maximal deflection ϕ_{max}, ϕ and $\ddot{\phi}$ will not change their signs and the velocity will strictly decrease until $\dot{\phi}$ equals to $\dot{\phi}_s = 0$ for the first time. According to (3.1.1), the equality $\frac{\tau_J\left(|\phi|(\dot{\phi}(t), \dot{\phi}_{max})\right)}{M} = -\frac{\mathrm{d}\dot{\phi}}{\mathrm{d}t}(t)$ will hold in this case for each $t \in [0, t_s]$ leading to the function $T_{\dot{\phi}} : (-\dot{\phi}_{max}, \dot{\phi}_{max}) \times (0, \infty) \to \mathbb{R}$ with

$$T_{\dot{\phi}}(\dot{\phi}_0, \dot{\phi}_{max}) = \int_0^{\dot{\phi}_0} \frac{M \mathrm{d}\dot{\phi}}{\tau_J\left(|\phi|(\dot{\phi}, \dot{\phi}_{max})\right)}. \tag{3.2.4}$$

The function (3.2.4) gives the minimum time t_s which is required by a MSS starting from a positive deflection ϕ_0 and a positive velocity $\dot{\phi}_0$ to reach the maximum deflection ϕ_{max}. Similar to T_ϕ, the same function can also be used for the computation of t_s in the more general case in which we have $\mathrm{sgn}(\phi_0) = \mathrm{sgn}(\phi_s) = \mathrm{sgn}(\dot{\phi}_0 - \dot{\phi}_s)$. In this case, ϕ and $\ddot{\phi}$ will not change their signs in the interval $[0, t_s]$ either. Moreover, for each t in this time interval they will be related to the velocity $\dot{\phi}$ through the equality $\frac{\tau_J\left(|\phi|(\dot{\phi}(t), \dot{\phi}_{max})\right)}{M} = \mathrm{sgn}(\dot{\phi}_s - \dot{\phi}_0)\frac{\mathrm{d}\dot{\phi}}{\mathrm{d}t}(t)$ which in turn leads to the function $t_{s,\dot{\phi}} : (-\dot{\phi}_{max}, \dot{\phi}_{max})^2 \times (0, \infty) \to [0, \infty)$ with

$$t_{s,\dot{\phi}}(\dot{\phi}_0, \dot{\phi}_s, \dot{\phi}_{max}) = \left| T_{\dot{\phi}}(\dot{\phi}_s, \dot{\phi}_{max}) - T_{\dot{\phi}}(\dot{\phi}_0, \dot{\phi}_{max}) \right|. \tag{3.2.5}$$

Notice that (3.2.5) can be used to compute t_s whenever the sign of the deflection ϕ remains constant.

In general, both ϕ and $\dot{\phi}$ can change their signs in the time interval $[0, t_s]$. Nevertheless, these changes can never occur simultaneously. Therefore, it is always possible to divide the trajectory into a finite number of subtrajectories along which the sign of ϕ or $\dot{\phi}$ remains the same. Consequently, equations (3.2.2)-(3.2.5) provide all the necessary relations required to determine the time t_s for any state $(\phi_s, \dot{\phi}_s)$. As we will later show in Section 3.2.2, these equations can also be used to compute the period T_p of a MSS. Nevertheless, before showing how to compute the period of a MSS, we want to briefly discuss several properties of the functions T_ϕ and $T_{\dot{\phi}}$ which will clarify the influence of the system's energy and TDP on t_s and which will turn out to be useful in our analysis of T_p.

Looking first at T_ϕ, the properties of this function are according to (3.2.2) closely related to the properties of $|\dot{\phi}|$. Indeed, since for each given $\phi_{max} > 0$ the function $|\dot{\phi}|(., \phi_{max})$ is an even function of the deflection it follows from the definition of T_ϕ that we have for each $(\phi, \phi_{max}) \in D_{T_\phi} := (-\phi_{max}, \phi_{max}) \times (0, \infty)$

$$T_\phi(-\phi, \phi_{max}) = -T_\phi(\phi, \phi_{max}). \tag{3.2.6}$$

Moreover, since $|\dot{\phi}|$ is positive at each element of D_{T_ϕ} so is the partial derivative $\frac{\partial T_\phi}{\partial \phi}$. Consequently, for each given $\phi_{max} > 0$ $T_\phi(\phi, \phi_{max})$ will be a strictly
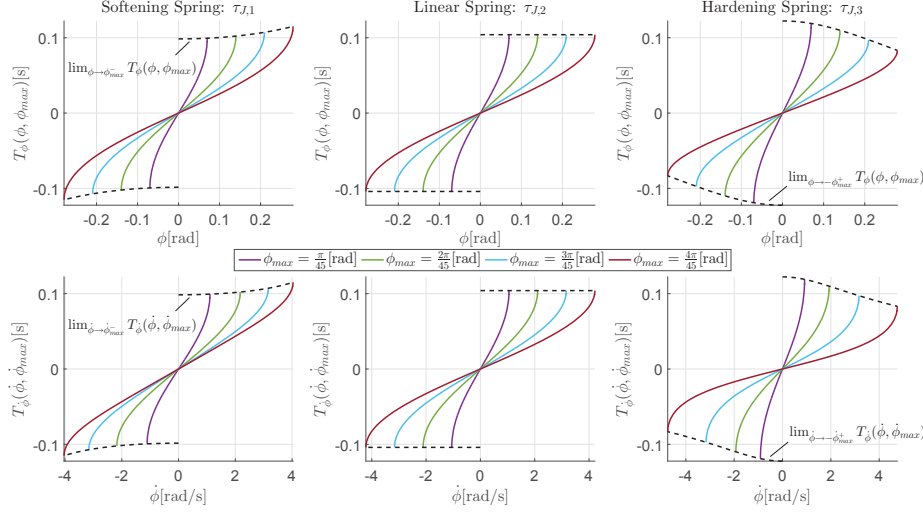
Figure 3.2.1: The Time Functions T_ϕ and $T_{\dot{\phi}}$ for MSS's with different Spring Characteristics

increasing function of ϕ. This simply means that the minimum time t_s a MSS with a given energy requires to reach a deflection $\phi_s \in (0, \phi_{max})$ from the state $(0, \dot{\phi}_{max})$ always increases as ϕ_s approaches the system's maximal deflection regardless of the system's TDP. Similarly, by looking at the partial derivative $\frac{\partial T_\phi}{\partial \phi_{max}}$ it can be shown that given a deflection $\phi_s > 0$ the minimum time required to reach ϕ_s by a MSS with a sufficiently high energy from the initial state $(\phi_0, \dot{\phi}_0) = (0, \dot{\phi}_{max})$, i.e. $T_\phi(\phi_s, \phi_{max})$, always decreases as $\phi_{max} > \phi_s$ and thus the system's energy increases. Indeed, by applying Leibniz rule [61] to (3.2.2) we first get $\frac{\partial T_\phi}{\partial \phi_{max}} : D_{T_\phi} \to \mathbb{R}$ with

$$\frac{\partial T_\phi}{\partial \phi_{max}}(\phi, \phi_{max}) = -\frac{\tau_J(\phi_{max})}{M} \int_0^\phi \frac{\mathrm{d}s}{\left(|\dot{\phi}|(s, \phi_{max})\right)^3}. \qquad (3.2.7)$$

The discussed decrease follows then from the partial derivative (3.2.7) being negative at each $(\phi, \phi_{max}) \in D_{T_\phi}$ with $\phi > 0$.

Figure 3.2.1 (Top) illustrates the function T_ϕ for the three MSS's whose trajectories have been depicted in Fig. 3.1.1. More specifically, for each of these MSS's T_ϕ is plotted as a function of the deflection ϕ for four different values[3] of ϕ_{max}. In addition, we have also plotted for the three MSS's the limits $\lim_{\phi \to \phi_{max}^-} T_\phi(\phi, \phi_{max})$ and $\lim_{\phi \to -\phi_{max}^+} T_\phi(\phi, \phi_{max})$ for $\phi_{max} \in (0, \frac{4\pi}{45})$, see the black dashed lines. According to (3.2.2) and (3.2.4), these limits provide the minimum time a MSS requires to reach the state $(\phi_{max}, 0)$ from $(0, \dot{\phi}_{max})$.

---

[3] The exact same values have been used in Section 3.1 when investigating the trajectories of these MSS's.

The illustrated graphs for the function T_ϕ verify all of its discussed properties. Moreover, as expected from the independence of these properties on the TDP, all the graphs for T_ϕ share a similar structure. Comparing the depicted limits, however, it can be observed that the dependence of these limits on ϕ_{max} is different for the three MSS's having different spring characteristics. We postpone a detailed analysis of this dependence to Section 3.2.2, where we will discuss oscillation periods of MSS's. Nevertheless, it is important to already note here how this observed difference is closely related to the difference in the SDP's of the three MSS's analysed, see Fig. 3.1.1.

If we now look at the properties of $T_{\dot\phi}$, we can see that they are similar to the properties of T_ϕ. Indeed, noting this time the close relation between $T_{\dot\phi}$ and $|\phi|$ it can be first shown using (3.2.4) that we have for each $(\dot\phi, \dot\phi_{max}) \in D_{T_{\dot\phi}} := (-\dot\phi_{max}, \dot\phi_{max}) \times (0, \infty)$

$$T_{\dot\phi}(-\dot\phi, \dot\phi_{max}) = -T_{\dot\phi}(\dot\phi, \dot\phi_{max}). \tag{3.2.8}$$

Moreover, since $|\phi|(\dot\phi, \dot\phi_{max}) > 0$ holds at each $(\dot\phi, \dot\phi_{max}) \in D_{T_{\dot\phi}}$ the partial derivative $\frac{\partial T_{\dot\phi}}{\partial \dot\phi}$ is positive at each element of $D_{T_{\dot\phi}}$. In addition, the partial derivative $\frac{\partial T_{\dot\phi}}{\partial \dot\phi_{max}} : D_{T_{\dot\phi}} \to \mathbb{R}$ which according to (3.2.4) equals to

$$\frac{\partial T_{\dot\phi}}{\partial \dot\phi_{max}}(\dot\phi, \dot\phi_{max}) = -M^2 \dot\phi_{max} \int_0^{\dot\phi} \frac{K_J\left(|\phi|(s, \dot\phi_{max})\right)}{\tau_J\left(|\phi|(s, \dot\phi_{max})\right)^3} \mathrm{d}s \tag{3.2.9}$$

takes always negative values. Finally, if we look at $\lim_{\dot\phi \to \dot\phi_{max}^-} T_{\dot\phi}(\dot\phi, \dot\phi_{max})$ for an arbitrary $\dot\phi_{max} > 0$ and note that this limit provides the minimum time a MSS requires to reach the state $(\phi_{max}, 0)$ from $(0, \dot\phi_{max})$, we can see that T_ϕ and $T_{\dot\phi}$ are related to each other as follows:

$$\lim_{\phi \to \phi_{max}^-} T_\phi(\phi, \phi_{max}) = \lim_{\dot\phi \to \dot\phi_{max}^-} T_{\dot\phi}(\dot\phi, \dot\phi_{max}). \tag{3.2.10}$$

Fig. 3.2.1 (Bottom) plots $T_{\dot\phi}$ as a function of $\dot\phi$ for four different values of $\dot\phi_{max}$ which correspond to the maximum deflection values used when plotting T_ϕ. Furthermore, $\lim_{\dot\phi \to \dot\phi_{max}^-} T_{\dot\phi}(\dot\phi, \dot\phi_{max})$ and $\lim_{\dot\phi \to -\dot\phi_{max}^+} T_{\dot\phi}(\dot\phi, \dot\phi_{max})$ are also depicted. Due to the close relation (3.1.5) between ϕ_{max} and $\dot\phi_{max}$ and the discussed similarities of the functions T_ϕ and $T_{\dot\phi}$ all the illustrated graphs share actually a similar structure. Table 3.1c provides analytical expressions of these two functions for the TDP's $\tau_{J,s}, \tau_{J,l}$ and $\tau_{J,sh}$ which have been used in creating Fig. 3.1.1. We will come back to these expressions again in Chapter 5 when we construct optimal control strategies solving the LVMP.

Having shown how to compute the minimum time t_s using mainly the two functions T_ϕ and $T_{\dot\phi}$ and having discussed their basic properties, we next turn our attention to the oscillation period T_p of MSS's.

3.2.2 Oscillation Period T_p

As already mentioned, functions $\phi : [0, \infty) \to \mathbb{R}$ solving (3.1.1) are periodic if $E_{MSS}(\phi_0, \dot{\phi}_0) > 0$. The oscillation period T_p of MSS's is given by the minimal period of these solutions and we want to next show how to compute this period.

Following our discussion in the beginning of Section 3.2, the oscillation period of a MSS is equal to the time required by its trajectory $(\phi, \dot{\phi})$ to reach the state $(\phi_s, \dot{\phi}_s)$ for the second time after t_s. Assuming that $(\phi_s, \dot{\phi}_s)$ is located in the first quadrant of the phase plane, i.e. $\phi_s > 0$ and $\dot{\phi}_s > 0$, let us introduce four trajectories, which respectively start from the states $(\phi_s, \dot{\phi}_s)$, $(\phi_s, -\dot{\phi}_s)$, $(-\phi_s, -\dot{\phi}_s)$, $(-\phi_s, \dot{\phi}_s)$ and terminate the first time they reach $(\phi_s, -\dot{\phi}_s)$, $(-\phi_s, -\dot{\phi}_s)$, $(-\phi_s, \dot{\phi}_s)$ and $(\phi_s, \dot{\phi}_s)$. Since along these trajectories the sign of either ϕ or $\dot{\phi}$ will not change, the time required by each of them to reach their final state can be determined using (3.2.3) and (3.2.5). Summing up these times leads us then to the function $T_p : (0, \infty) \to (0, \infty)$ with

$$T_p(\phi_{max}) = 4 \left[T_\phi(\phi_s, \phi_{max}) + T_{\dot{\phi}}(\dot{\phi}_s, \dot{\phi}_{max}) \right], \qquad (3.2.11)$$

where we have $E_{pot}(\phi_{max}) = E_{kin}(\dot{\phi}_{max}) = E_{MSS}(\phi_s, \dot{\phi}_s)$, $\dot{\phi}_{max} > 0$ and $(\phi_s, \dot{\phi}_s)^T \in (0, \phi_{max}) \times (0, \dot{\phi}_{max})$.

It is important to remark here that for deriving (3.2.11), we have made use of the symmetry properties (3.2.6) and (3.2.8) together with the fact that both T_ϕ and $T_{\dot{\phi}}$ take positive values in their domains of definition when their first arguments are positive. Moreover, notice that we have defined T_p as a function of only the maximum deflection corresponding to the system's energy. This follows from the fact that for any state $(\phi_s, \dot{\phi}_s)$ having the same positive energy the corresponding trajectories will move on the same closed curve and consequently the resulting oscillation period will be the same.

Using the fact that the oscillation period can be written as a function of only ϕ_{max}, the expression (3.2.11) for T_p can now be rewritten such that it only depends on T_ϕ or $T_{\dot{\phi}}$. To see this, let us substitute in the right-hand side of (3.2.11) the function $|\dot{\phi}|(\phi_s, \phi_{max})$ for the velocity $\dot{\phi}_s$. For each $\phi_{max} > 0$, the resulting expression will then be a constant function of ϕ_s. Taking the limit of this function as ϕ_s goes to 0^+ and to ϕ_{max}^- yields then the following two more common formulations for T_p:

$$
\begin{aligned}
T_p(\phi_{max}) &= 4 \lim_{\dot{\phi}_s \to \dot{\phi}_{max}^-} T_{\dot{\phi}}(\dot{\phi}_s, \dot{\phi}_{max}), & (3.2.12) \\
&= 4 \lim_{\phi_s \to \phi_{max}^-} T_\phi(\phi_s, \phi_{max}). & (3.2.13)
\end{aligned}
$$

Notice that the two equalities above clarify the well-known relation between the limits depicted in Fig. 3.2.1 and the oscillation period T_p of the corresponding MSS's.

Obviously, we could have directly defined the oscillation period using one of the two limits in (3.2.12)-(3.2.13). Nevertheless, for both of these limits an integral needs to be evaluated which has a singularity either at $\phi = \phi_{max}$ or at

$\dot{\phi} = \dot{\phi}_{max}$. Consequently, for TDP's for which no analytical expressions exist for T_ϕ or $T_{\dot{\phi}}$ approximating these integrals numerically is not straightforward. In order to have our method of finding the optimal control strategy being applicable for any TDP satisfying our assumptions we have decided to follow this current approach. Moreover, this approach enables us to analyse the dependence of T_p on ϕ_{max} for any MSS as we will shortly see.

Table 3.1d summarizes for the three TDP's $\tau_{J,s}, \tau_{J,l}$ and $\tau_{J,sh}$ analytical expressions for T_p which have been found using (3.2.13). Moreover, the derivatives $\frac{\mathrm{d}T_p}{\mathrm{d}\phi_{max}}$ of these expressions are provided in that table as well. Based on the sign of these derivatives, it can now be concluded that in accordance with the limits depicted in Fig. 3.2.1 the oscillation period T_p for the TDP $\tau_{J,s}$ is always a strictly increasing function of ϕ_{max} on $(0, \frac{\pi}{2k_e})$ regardless of the value of the parameters K_e, k_e and M. Similarly, for the linear TDP $\tau_{J,l}$ T_p is always constant while for $\tau_{J,sh}$ it is always strictly decreasing on $(0, \infty)$. In the remainder of this subsection, we will take a closer look at the derivative $\frac{\mathrm{d}T_p}{\mathrm{d}\phi_{max}}$ and show in particular how the observed monotonicity of T_p generalizes to MSS's with arbitrary softening and hardening springs[4].

A general expression for $\frac{\mathrm{d}T_p}{\mathrm{d}\phi_{max}}$ can be found by taking the derivative of (3.2.11) with respect to ϕ_{max}. When taking this derivative, however, it needs to be taken into account that in the right-hand side of (3.2.11) both ϕ_s and $\dot{\phi}_s$ are positive and lie on the closed curve described by $E_{MSS}(\phi_s, \dot{\phi}_s) = \int_0^{\phi_{max}} \tau_J(s)\mathrm{d}s$. This can be done by substituting, as before, the function $|\dot{\phi}|(\phi_s, \phi_{max})$ for the velocity $\dot{\phi}_s$. Taking the partial derivative of the resulting expression with respect to ϕ_{max} and using (3.1.5) together with (3.1.6) and (3.2.4) we can then conclude that $\frac{\mathrm{d}T_p}{\mathrm{d}\phi_{max}} : (0, \phi_{max}) \to \mathbb{R}$ is given by[5]

$$\frac{\mathrm{d}T_p}{\mathrm{d}\phi_{max}}(\phi_{max}) = 4\left[\frac{\partial T_\phi}{\partial \phi_{max}}(\phi_s, \phi_{max}) + \frac{\tau_J(\phi_{max})}{\tau_J(\phi_s)\dot{\phi}_s} + \frac{\tau_J(\phi_{max})}{M\dot{\phi}_{max}}\frac{\partial T_{\dot{\phi}}}{\partial \dot{\phi}_{max}}(\dot{\phi}_s, \dot{\phi}_{max})\right], \quad (3.2.14)$$

where we have the same conditions on $\dot{\phi}_{max}$ and $(\phi_s, \dot{\phi}_s)$ as in (3.2.11).

The dependence of the oscillation period of a MSS on its maximal deflection and thus on its energy can now be investigated by analysing the sign of (3.2.14). Based on our previous discussions, we already know that the first and third terms in the parenthesis are always negative. The second term, on the other hand, is always positive. Consequently, for a given MSS the sign of $\frac{\mathrm{d}T_p}{\mathrm{d}\phi_{max}}$ can take different values depending on ϕ_{max}. The following proposition gives

---

[4]We call a spring softening/hardening if the corresponding TDP satisfies assumptions $(A1) - (A3)$, is two-times continuously differentiable, and $\frac{\mathrm{d}^2\tau_J}{\mathrm{d}\phi^2}(\phi)$ is negative/positive for each $\phi > 0$.

[5]Notice that according to (3.1.5), (3.1.6) and (3.2.4), we have $\frac{\mathrm{d}\dot{\phi}_{max}}{\mathrm{d}\phi_{max}} = \frac{\tau_J(\phi_{max})}{M\dot{\phi}_{max}}$, $\frac{\partial|\dot{\phi}|}{\partial\phi_{max}}(\phi_s, \phi_{max}) = \frac{\tau_J(\phi_{max})}{M\dot{\phi}_s}$ and $\frac{\partial T_{\dot{\phi}}}{\partial\dot{\phi}}(\dot{\phi}_s, \dot{\phi}_{max}) = \frac{M}{\tau_J(\phi_s)}$.

sufficient conditions under which a sign change of $\frac{\mathrm{d}T_p}{\mathrm{d}\phi_{max}}$ can never occur in a given interval.

Proposition 1. *Let τ_J be a given TDP such that*

1. *τ_J satisfies assumptions $(A1) - (A3)$,*

2. *τ_J is two-times continously differentiable,*

3. *There exists a $\varphi_{max} > 0$ such that we have*

$$(\forall \phi \in (0, \varphi_{max})) \left(\mathrm{sgn}\left(\frac{\mathrm{d}^2 \tau_J}{\mathrm{d}\phi^2}(\phi) \right) = const. \right).$$

Then for any MSS with the TDP τ_J, we have

$$(\forall \phi \in (0, \varphi_{max})) \left[\mathrm{sgn}\left(\frac{\mathrm{d}T_p}{\mathrm{d}\phi_{max}}(\phi) \right) = -\mathrm{sgn}\left(\frac{\mathrm{d}^2 \tau_J}{\mathrm{d}\phi^2}(\phi) \right) \right].$$

Proof. See Appendix B.1. □

It is well known that the period of a MSS with a linear TDP is always constant and does not depend on the system's energy, see for instance [35]. Proposition 1 generalizes this property by providing a relation between the sign of the derivative $\frac{\mathrm{d}T_p}{\mathrm{d}\phi_{max}}$ and the sign of $\frac{\mathrm{d}^2 \tau_J}{\mathrm{d}\phi^2}$. More specifically, with this proposition we now see that the period of a MSS with a softening spring always increases if the system's energy is increased. Similarly, the period of a MSS always decreases with increased energy if the system has a hardening spring. In Chapter 5, we will see how different possibilities for the sign of $\frac{\mathrm{d}T_p}{\mathrm{d}\phi_{max}}$ influence the optimal control strategies solving the LVMP.

Chapter 4

Switching Control Strategies

As we will show in Chapter 5, optimal controls for the LVMP are all switching controls. In order to better understand the trajectories corresponding to these optimal controls, we derive in this chapter several properties of Σ for the case when the system is controlled by an element of $\mathcal{S}_\mathbb{U}$. In particular, we will first look at the trajectories corresponding to admissible switching controls and clarify their relation to trajectories of MSS's. Focusing on the energy stored along trajectories of Σ, we will then discuss the maximal energy which can be attained using admissible switching controls with a limited switching number.

4.1 Trajectories

Let us assume that $u : D \to \mathbb{U}$ is an admissible switching control with the switching number $i \geq 0$. By definition, we know that for any given $k \in S_i$ the value of the control u remains constant in the time interval D_k. Moreover, if i is positive and $k < i$ holds the control will instantaneously change its value at $t_{S,k+1}$. According to (2.1.4), along trajectories of the control system Σ which corresponds to u, the time-derivative of the deflection will then not be continuous at $t_{S,k+1}$. This is in clear contrast with trajectories of MSS's. Nevertheless, trajectories corresponding to u and trajectories of MSS's are both closely related and in this section we will elaborate on this relation. In particular, we will show how using this relation we can construct trajectories corresponding to any admissible switching control.

To see the above mentioned relation, let us first fix a $k \in S_i$ and focus on the time interval D_k where u is constant. Taking the time-derivative[1] of the first

---

[1]Strictly speaking, if $t_{S,k}$ is a switching time the time-derivative of x_1 does not exist at this time. Nevertheless, in such a case it follows from the continuity of the state $\boldsymbol{x}$ and the piecewise continuity of u that the two limits $\lim_{t \to t_{S,k}^-} \dot{x}_1(t)$ and $\lim_{t \to t_{S,k}^+} \dot{x}_1(t)$ exist, see (2.1.4). In accordance with our assumption on the control u being left-continuous, see the definition of $\mathcal{PC}_\mathbb{U}$ and $\mathcal{S}_\mathbb{U}$ in Sec. 2.2, we will use, with a slight abuse of notation, $\dot{x}_1(t_{S,k})$ to denote the limit $\lim_{t \to t_{S,k}^+} \dot{x}_1(t)$.

row of (2.1.4) and substituting the second row into the resulting expression, we arrive then at the following second-order differential equation for the dynamics of the deflection x_1:

$$M\ddot{x}_1 + \tau_J(x_1) = 0. \tag{4.1.1}$$

Clearly, (4.1.1) is the exact same differential equation that describes the dynamics of a MSS. Consequently, we can make use of all the functions introduced in the previous chapter to find and analyse the solution to this equation. In particular, using these functions with the mass and TDP of Σ we can uniquely compute x_1 and $\dot{x}_1$ at each $t \in D_k$, if we know the two boundary conditions ${}^k x_1 := x_1(t_{S,k})$ and ${}^k \dot{x}_1 := \dot{x}_1(t_{S,k})$. Moreover, using $x_2 = {}^k u - \dot{x}_1$ we can also determine the trajectory $\boldsymbol{x}$ corresponding to u for $t \in D_k$.

Depending on the values of ${}^k x_1$ and ${}^k \dot{x}_1$, it is important to distinguish here between two different cases as we have done for MSS's. First of all, from our discussions in Chapter 3 we know that in a phase plane the pair $(x_1, \dot{x}_1)$ will remain at the origin if both ${}^k x_1$ and ${}^k \dot{x}_1$ and thus $E_{MSS}({}^k x_1, {}^k \dot{x}_1)$ are equal to zero. In this case, the deflection in the spring remains at zero for each $t \in D_k$ while both the motor and the link rotate with the same velocity. In a phase plane, the trajectory $\boldsymbol{x}$ will then simply be described by a point on the vertical axis with its position depending only on the value of the control.

In the more general case where $({}^k x_1, {}^k \dot{x}_1) \neq \boldsymbol{0}$ holds, we know that in a phase plane the pair $(x_1, \dot{x}_1)$ will move on a closed curve described by $E_{MSS}(x_1, \dot{x}_1) = E_{MSS}({}^k x_1, {}^k \dot{x}_1)$. From the symmetry of this closed curve and the equality $x_2 = {}^k u - \dot{x}_1$ it follows that in a phase plane $\boldsymbol{x}$ will then also move on a closed curve. Moreover, this curve can be obtained from the closed curve for $(x_1, \dot{x}_1)$ by simply shifting it vertically by ${}^k u$. Finally, if the time interval D_k is sufficiently long x_1 will periodically oscillate between $-{}^k\phi_{max}$ and ${}^k\phi_{max}$ while x_2 will oscillate between ${}^k u - {}^k\dot{\phi}_{max}$ and ${}^k u + {}^k\dot{\phi}_{max}$.

It is important to remark here that for both cases discussed above, the constant value of $E_{MSS}(x_1, \dot{x}_1)$ in the time interval D_k corresponds physically to the energy of the EJ when computed relative to a frame that is rigidly attached to the motor. For that reason, we will call this value the system's *relative energy* along the trajectory $\boldsymbol{x}$ in D_k and denote it simply by ${}^k E_{rel}$. Since our choice for k was arbitrary, this energy is given for each $k \in S_i$ by

$$ {}^k E_{rel} := E_{pot}({}^k x_1) + E_{kin}({}^k \dot{x}_1). \tag{4.1.2}$$

So far we have shown how depending on ${}^k x_1, {}^k \dot{x}_1$ and ${}^k u$, we can compute and graphically illustrate $\boldsymbol{x}$ in D_k for any given $k \in S_i$. If the control u does not switch, i.e. $D = D_0$, the entire trajectory $\boldsymbol{x}$ can thus be found using merely the initial state $\boldsymbol{x}_0$ and the control $u \equiv {}^k u$. We show in the following how using $\boldsymbol{x}_0$ and u we can find the entire trajectory if the switching number is non-zero.

Assuming that $i > 0$ holds, we need to determine the values of x_1 and $\dot{x}_1$ at each $t_{S,k} \in \{t_{S,0}, \ldots, t_{S,i}\}$ in order to apply the results from our discussion above. It is important to realize here that these values are not independent of each other. Indeed, knowing the trajectory $\boldsymbol{x}$ in D_k with now $k \in S_{i-1}$ we can
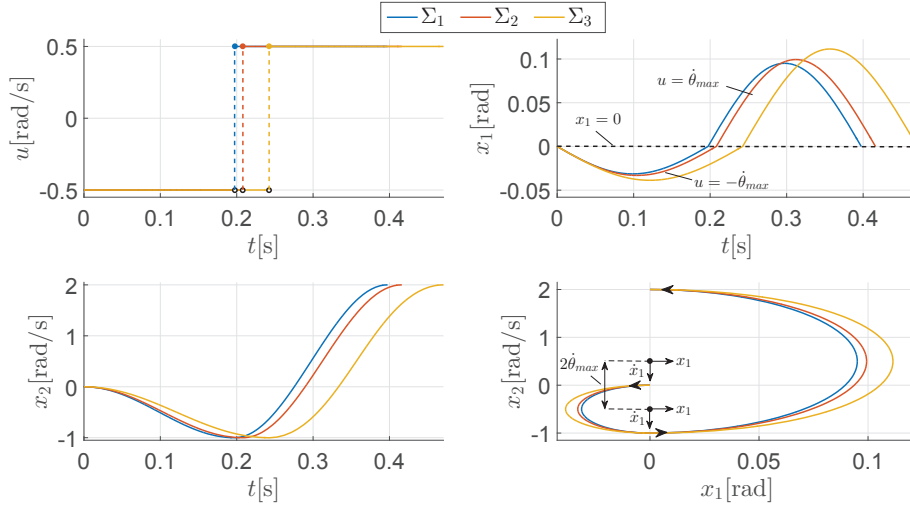
Figure 4.1.1: Trajectories of EJ's with velocity-sourced SEA's and different Spring Characteristics

uniquely determine the values of $^{k+1}x_1$ and $^{k+1}\dot{x}_1$ at the switching time $t_{S,k+1}$ using the continuity of $\boldsymbol{x}$:

$$
^{k+1}x_1 = \lim_{t \to t_{S,k+1}^-} x_1(t), \tag{4.1.3}
$$

$$
^{k+1}\dot{x}_1 = {}^{k+1}u - {}^{k}u + \lim_{t \to t_{S,k+1}^-} \dot{x}_1(t). \tag{4.1.4}
$$

With equations (4.1.3)-(4.1.4) we can now use the trajectory $\boldsymbol{x}$ in D_k and the change in the control at $t_{S,k+1}$ to find the values $^{k+1}x_1$ and $^{k+1}\dot{x}_1$. This also means that starting from $k = 0$ with the two values for $^0x_1$ and $^0\dot{x}_1$, we can iterarively construct the entire trajectory $\boldsymbol{x}$ by solving (4.1.1) to find $\boldsymbol{x}$ in D_k and using, if $k \neq i$, (4.1.3)-(4.1.4) to determine the required boundary conditions at the switching time $t_{S,k+1}$. Since the two values $^0x_1$ and $^0\dot{x}_1$ depend only on the initial state $\boldsymbol{x}_0$ and the control u, we have thus found our desired way of determining the trajectory $\boldsymbol{x}$ corresponding to u.

Note that our choice for the control u was arbitrary. Consequently, with our results obtained so far we can now uniquely construct trajectories of Σ which start from any given initial state $\boldsymbol{x}_0 \in \mathbb{R}^2$ and correspond to any $u \in \mathcal{S}_{\mathbb{U}}$. Moreover, having a means to construct these trajectories we can also analyse, as in Chapter 3, how different TDP's can influence trajectories of EJ's with velocity sourced SEA's. In the remainder of this section, we want to briefly conduct such an analysis by looking at the trajectories of three different control systems Σ_1, Σ_2 and Σ_3 which only differ in their TDP's[2], see Table 4.1a-4.1c. More specifically,

---

[2] The subscripts used for the control systems are in accordance with the functions describing their TDP's. That is, the TDP's in Σ_1, Σ_2 and Σ_3 are equal to $\tau_{J,1}, \tau_{J,2}$ and $\tau_{J,3}$, respectively.

	M	K_e	k_e	$\dot{\theta}_{max}$
Σ_{sin}	$M \in (0,\infty)$	$K_e \in (0,\infty)$	$k_e \in (0,\infty)$	$\dot{\theta}_{max} \in (0,\infty)$
Σ_1	$1[\mathrm{kgm}^2]$	$\frac{875}{32\left(1-\cos\left(\frac{35\pi}{96}\right)\right)}[\mathrm{Nm}]$	$\frac{175}{32}[1]$	$\frac{1}{2}\left[\frac{rad}{s}\right]$
$\tau_J(\phi) = \tau_{J,s}(\phi) = K_e \sin(k_e\phi), \phi \in \left(-\frac{\pi}{2k_e}, \frac{\pi}{2k_e}\right)$				

(a) Control Systems Σ_s and Σ_1

	M	K_e	k_e	$\dot{\theta}_{max}$
Σ_{id}	$M \in (0,\infty)$	$K_e \in (0,\infty)$	$k_e \in (0,\infty)$	$\dot{\theta}_{max} \in (0,\infty)$
Σ_2	$1[\mathrm{kgm}^2]$	$\frac{2250}{\pi^2}[\mathrm{Nm}]$	$1[1]$	$\frac{1}{2}\left[\frac{rad}{s}\right]$
$\tau_J(\phi) = \tau_{J,l}(\phi) = K_e k_e \phi, \phi \in \mathbb{R}$				

(b) Control Systems Σ_{id} and Σ_2

	M	K_e	k_e	$\dot{\theta}_{max}$
Σ_{sinh}	$M \in (0,\infty)$	$K_e \in (0,\infty)$	$k_e \in (0,\infty)$	$\dot{\theta}_{max} \in (0,\infty)$
Σ_3	$1[\mathrm{kgm}^2]$	$\frac{150}{\pi(\cosh(2)-1)}[\mathrm{Nm}]$	$\frac{30}{\pi}[1]$	$\frac{1}{2}\left[\frac{rad}{s}\right]$
$\Sigma_{FSJ,i}$	$2.251[\mathrm{kgm}^2]$	$135e^{-\frac{2\pi}{3}}[\mathrm{Nm}]$	$12[1]$	$i\left[\frac{rad}{s}\right]$
$\tau_J(\phi) = \tau_{J,sh}(\phi) = K_e \sinh(k_e\phi), \phi \in \mathbb{R}, i \in (0,\infty)$				

(c) Control Systems Σ_{sh}, Σ_3 and $\Sigma_{FSJ,i}$

Table 4.1: Parameters of the investigated Control Systems

we will apply to all these systems the same deflection dependent control strategy which is known to maximize the terminal link velocity of EJ's with LSEA's when they are initially at rest and when the control is constrained to have only one switching [17]. Comparing the resulting trajectories and refering to our results from the previous chapter, we will then see how with a NSEA we can reach the same terminal link velocity as with a LSEA using less spring deflection and a smaller amount of time.

Figure 4.1.1 illustrates for each of the three control systems the trajectory that starts from the origin and corresponds to the control strategy mentioned above. As shown there, all the applied controls start with their minimum motor velocity and switch once to their maximum value when the deflection in the spring equals to zero for the second time. Moreover, all trajectories terminate as soon as the deflection equals to zero for the third time.

A closer look at the phase plot in Fig. 4.1.1 shows that the applied control strategy results for each control system to the same values for x_1 and $\dot{x}_1$ at $t_{S,0}$ and $t_{S,1}$. Consequently, the relative energies ${}^0E_{rel}$ and ${}^1E_{rel}$ and thus the velocities ${}^0\dot{\phi}_{max}$ and ${}^1\dot{\phi}_{max}$ are not affected by the TDP. This then results not only in having a similar structure for the depicted trajectories but also in having the same terminal link velocity of $4\dot{\theta}_{max}$. Nevertheless, looking at the deflection values attained along the depicted trajectories we can observe that the values of ${}^0\phi_{max}$ and ${}^1\phi_{max}$ depend on the TDP of the system. More specifically, these two values are minimal for Σ_1 and maximal for Σ_3. This difference in the

deflection trajectories actually occurs since the TDP of each system requires different spring deflections to fully store the two relative energies $^0E_{rel}$ and $^1E_{rel}$ as potential energy, see Fig. 3.1.1. Note, in particular, that Σ_1 obtains the minimal values since the two relative energies $^0E_{rel}$ and $^1E_{rel}$ are less than 5J.

Comparing now the time along the depicted trajectories, it can be observed that similar to the maximal deflection values the final time also depends on the TDP of the systems. According to the relation between trajectories of EJ's and MSS's we have just shown, this final time will be equal to the sum $\frac{T_p(^0\phi_{max})}{2} + \frac{T_p(^1\phi_{max})}{2}$ for each system. Looking now at the limits depicted in Fig. 3.2.1 (Top), it can be seen that both of these terms in this sum take their minimal values for the control system Σ_1 and their maximal values for the control system Σ_3. Accordingly, we see in Fig. 4.1.1 that the terminal link velocity $4\dot{\theta}_{max}$ is reached by the control system Σ_1 using the least amount of time and by Σ_3 using the greatest amount.

Having introduced the concept of relative energy and shown how to construct trajectories of Σ corresponding to admissible switching controls, we next turn our attention to the maximal energy which can be stored along these trajectories. In particular, for a given switching number we provide switching strategies which maximize this energy in minimum time. With our results we will then see that the deflection dependent control strategy used in Fig. 4.1.1 actually maximize both the terminal link velocity and the terminal energy of all the three control systems over switching controls $u \in \mathcal{S}_{\mathbb{U}}$ with one switching.

4.2   Maximal Energy

As in a MSS, we define the energy of an EJ with a velocity sourced SEA as the sum of the potential energy stored in its elastic elements and the kinetic energy of its link. This energy is in general, in contrary to a MSS, not constant and depends on the motor velocity. To see this, let us first find a mathematical expression describing the energy stored along trajectories of Σ. These trajectories are uniquely determined by their initial state and by the control applied to them[3]. Taking also their time dependence into account leads us then to the energy function $E_{EJ} : \mathbb{R}^2 \times \mathcal{U} \times D \to \mathbb{R}$ with

$$E_{EJ}(\boldsymbol{x}_0, u, t) = E_{pot}(x_1(t)) + E_{kin}(x_2(t)), \qquad (4.2.1)$$

where $\boldsymbol{x}$ denotes the trajectory corresponding $u : D \to \mathbb{U}$. Equation (4.2.1) gives us the desired expression for the energy of Σ. The mentioned dependence of this energy on the applied control can now easily be seen by taking the time-derivative of this expression which leads to[4]

$$\frac{\partial E_{EJ}}{\partial t}(\boldsymbol{x}_0, u, t) \quad = \quad \tau_J(x_1(t))\, u(t). \qquad (4.2.2)$$

---

[3] See Appendix B.3.1.

[4] Notice that this time-derivative exists everywhere except at those points where u has a discontinuity and the deflection x_1 is non-zero.

Note that for deriving (4.2.2), we have simply used (2.1.4) together with the definitions (3.1.2)-(3.1.3).

According to (4.2.2) the influence of the control on the system's energy E_{EJ} is closely related to the torque in the spring. The aim of this section is to analyse this relation by discussing how to maximize E_{EJ} using admissible switching controls when the system is initially at rest. More specifically, we will deal with the problem of maximizing E_{EJ} using controls $u \in \mathcal{S}_\mathbb{U}$ with a limited number of switchings and focus in particular on the strategies which require the least amount of time to reach this maximal energy. In order to be more precise, let us now give here the mathematical formulation of this *Energy Maximization Problem* (EMP).

Energy Maximization Problem (EMP): For a given switching number $i \geq 0$, find the switching control u_S^* which maximizes $E_{EJ}(\mathbf{0}, u, t_f)$ over all admissible switching controls $u \in \mathcal{S}_\mathbb{U}$ with i switchings in minimum time.

To increase readability, we will from here on mostly omit the first argument of E_{EJ} whenever $\boldsymbol{x}_0$ equals to $\mathbf{0}$. Moreover, in the remainder of this section we will automatically assume that trajectories of a given control system start from the origin if we do not explicitly state their initial state.

In order to derive the solution to the EMP, we want to first take a closer look at the relative energy along a trajectory $\boldsymbol{x}$ which corresponds to a control $u \in \mathcal{S}_\mathbb{U}$ with $i \geq 0$ switchings. From our discussions in Section 4.1 we already know that this relative energy is going to take only a finite number of values, see (4.1.2). We will next show that these values are closely related to the system's energy. For this let us fix a $k \in S_i$ and compare the relative energy ${}^kE_{rel}$ with the energy $E_{EJ}(u,t)$ attained at a time $t \in D_k$. Using (4.1.2) and (4.2.1) we obtain the following relation between both energies:

$$E_{EJ}(u,t) \;=\; {}^kE_{rel} + M\left(\frac{{}^ku^2}{2} - {}^ku\dot{x}_1(t)\right) \tag{4.2.3}$$

$$\leq \; {}^kE_{rel} + M\left(\frac{\dot{\theta}_{max}^2}{2} + \dot{\theta}_{max}\,{}^k\dot{\phi}_{max}\right). \tag{4.2.4}$$

It is important to realize here that the inequality in (4.2.4) will hold with equality only if we have $|{}^ku| = \dot{\theta}_{max}$ for the magnitude of the control. Moreover, in case ${}^kE_{rel}$ is non-zero both $x_1(t) = 0$ and $\mathrm{sgn}\,(\dot{x}_1(t)) = -\mathrm{sgn}({}^ku)$ must hold at $t \in D_k$.

Equation (4.2.3) clarifies the relation between the system's relative and real energy while (4.2.4) uses this relation to provide an upper bound for the total energy along $\boldsymbol{x}$. Focusing on $E_{EJ}(u,t_f)$, we can see that the corresponding upper bound at the final time only depends on ${}^iE_{rel}$ and $\dot{\theta}_{max}$. Moreover, it follows from (4.2.3) that in case $|{}^iu| = \dot{\theta}_{max}$ holds we can always attain this upper bound by only adjusting, if necessary, the length of the time interval D_i. Based on these observations, it is tempting to assume that maximizing $E_{EJ}(u,t_f)$ requires us to first maximize the relative energy ${}^iE_{rel}$. This assumption can be verified using the following proposition which provides the maximal value for ${}^iE_{rel}$ as well as two sufficient conditions for a control to reach it.

Proposition 2. *Let $i \geq 0$ be a non-negative integer and $u \in \mathcal{S}_{\mathbb{U}}$ a control with the switching number i. Then, along the trajectory $\boldsymbol{x}$ which starts from $\boldsymbol{x}_0 = \boldsymbol{0}$ and corresponds to u we have for each $k \in S_i$ the following inequality for the relative energies:*

$$^{k}E_{rel} \leq E_{r,max}(k) := \frac{(2k+1)^2}{2} M\dot{\theta}_{max}^2. \tag{4.2.5}$$

Moreover, all the inequalities hold with equality in case we have

$$|u(0)| = \dot{\theta}_{max}, \tag{4.2.6}$$

and

$$(\forall t \in (0, t_f)) \, [x_1(t) \neq 0 \Rightarrow u(t) = \text{sgn}\,(x_1(t))\,\dot{\theta}_{max}]. \tag{4.2.7}$$

Proof. See Appendix B.2. $\square$

Proposition 2 tells us that along a trajectory $\boldsymbol{x}$ which corresponds to a control $u \in \mathcal{S}_{\mathbb{U}}$ with i switchings, $^{i}E_{rel}$ is always bounded above by $E_{r,max}(i)$. Moreover, this upper bound will be attained exactly if the control u satisfies the two conditions (4.2.6)-(4.2.7). Note that the magnitude of such a control will always remain at $\dot{\theta}_{max}$, since $\boldsymbol{x}$ can not remain at zero deflection when the relative energy remains positive.

We show in Appendix B.2 that an admissible switching control satisfying (4.2.6)-(4.2.7) always exists for any switching number[5]. Consequently, we can now conclude from (4.2.3)-(4.2.4) and from Proposition 2 that maximizing $E_{EJ}(u, t_f)$ using a control $u \in \mathcal{S}_{\mathbb{U}}$ with i switchings is indeed only possible by first maximizing $^{i}E_{rel}$ and then choosing the time interval D_i such that (4.2.4) holds with equality at t_f with $k = i$. The following proposition provides the corresponding maximum value of $E_{EJ}(u, t_f)$ and also clarifies how to reach it after maximizing the relative energy $^{i}E_{rel}$ using the control strategy described in Proposition 2.

Proposition 3. *Let $i \geq 0$ be a non-negative integer and $u \in \mathcal{S}_{\mathbb{U}}$ a control with the switching number i. Then we have the following inequality for the system's total energy:*

$$E_{EJ}(u, t_f) \leq E_{max}(i) := 2(i+1)^2 M\dot{\theta}_{max}^2. \tag{4.2.8}$$

Moreover, the inequality in (4.2.8) will hold with equality if along the controlled trajectory $(\boldsymbol{x}, u)$ with $\boldsymbol{x}_0 = \boldsymbol{0}$, (4.2.6)-(4.2.7) are satisfied together with

$$x_1(t_f) = 0. \tag{4.2.9}$$

---

[5]More specifically, we show in Lemma 41 that the two conditions (4.2.6)-(4.2.7) together with an initial control $u(0) \in \{-\dot{\theta}_{max}, \dot{\theta}_{max}\}$ and a final time t_f uniquely describe an admissible controlled trajectory $(\boldsymbol{x}, u)$ with $\boldsymbol{x}_0 = \boldsymbol{0}$. In addition, we show there that the control u will then always be an element of $\mathcal{S}_{\mathbb{U}}$ with its switching number depending on the final time t_f, see (B.2.5). It follows from this last relation between the switching number and the final time that for any given $i \geq 0$ we can find an admissible switching control satisfying the conditions (4.2.6)-(4.2.7) with i switchings.

Proof. Let u an admissible switching control with $i \geq 0$ switchings. The inequality (4.2.8) follows from the inequality (4.2.4) by noting that for $k = i$ and $t = t_f \in D_i$, the maximal value for ${}^iE_{rel}$ is given by $E_{r,max}(i)$ and the maximum value for ${}^i\dot{\phi}_{max}$ by $\sqrt{\frac{2E_{r,max}(i)}{M}} = (2i+1)\dot{\theta}_{max}$.

Let us now assume that along the controlled trajectory $(\boldsymbol{x}, u)$ with $\boldsymbol{x}_0 = \boldsymbol{0}$ the conditions (4.2.6), (4.2.7) and (4.2.9) are all satisfied. According to Proposition 2, for each $k \in S_i$ the relative energy ${}^kE_{rel}$ in D_k is then positive so that x_1 can never remain at zero in a finite time interval. This means that we have for each $k \in S_i$, ${}^kx_1 = 0$ and thus $|{}^k\dot{x}_1| = (2i+1)\dot{\theta}_{max} > 0$. Since u has i switchings, it follows from (4.2.6)-(4.2.7) and from the condition (4.2.9) that we must have $t_f = t_{S,i} + \frac{T_p({}^i\phi_{max})}{2}$ and thus $\dot{x}_1(t_f) = -{}^i\dot{x}_1$. The proof now follows from (4.2.3) with $k = i$ and $t = t_f$ if we also consider the equality $\text{sgn}({}^i\dot{x}_1) = \text{sgn}({}^iu)$ which holds due to Lemma 41. $\qquad\square$

According to Proposition 3, the maximal energy which can be transfered to an EJ with a velocity sourced SEA is given by $E_{max}(i)$ if we use an admissible switching control with $i \geq 0$ switchings and if the system is initially at rest. Moreover, this energy can be fully transfered to the system by using the deflection dependent control strategy from Proposition 2 if after the i'th switching the control remains constant until the deflection of the spring equals to zero for the first time after $t_{S,i}$. Note that there is a straightforward physical interpretation for this strategy. Indeed, according to (4.2.2) this strategy requires us simply to apply at each non-zero spring deflection the control input which maximizes the power that flows into the system until the maximum possible energy is transferred.

It is important to remark here that the three conditions (4.2.6)-(4.2.7) and (4.2.9) are only sufficient for maximizing the system's total energy using admissible switching controls and not necessary. This is most obvious for switching controls with 0 switchings where the corresponding trajectories are periodic. By applying the control $u \equiv \dot{\theta}_{max}$, for instance, the maximal energy for E_{EJ} can be attained periodically at multiple times if the final time is sufficiently high. Since, however, the deflection in the spring will then also change its sign periodically, we can see that E_{EJ} can be maximized without satisfying (4.2.7). Nevertheless, as the following proposition shows, in case the maximum value of E_{EJ} is to be attained in minimum time all the three conditions from Proposition 3 must be satisfied.

Proposition 4. *Let $i \geq 0$ be a non-negative integer and $u \in \mathcal{S}_{\mathbb{U}}$ a control with the switching number i such that $E_{EJ}(u, t_f) = E_{max}(i)$. Then, along the trajectory $\boldsymbol{x}$ which starts from $\boldsymbol{x}_0 = \boldsymbol{0}$ and corresponds to u we have for each $k \in S_i$*

$$
{}^kx_1 = 0 \wedge {}^kE_{rel} = E_{r,max}(k). \tag{4.2.10}
$$

In addition, for each $k \in S_{i+1} \backslash \{0\}$ the following inequality holds for the time

$t_{S,k}$:

$$t_{S,k} \geq t_{min}(k) := \frac{1}{2} \sum_{l=0}^{k-1} T_p({}^l\phi_{max}), \qquad (4.2.11)$$

with

$$E_{pot}({}^l\phi_{max}) = E_{r,max}(l). \qquad (4.2.12)$$

Finally, the inequality (4.2.11) will hold with equality for the final time t_f, i.e. for $k = i + 1$, if and only if both (4.2.6) and (4.2.7) hold along $(\boldsymbol{x}, u)$ together with (4.2.9). Moreover, in this case (4.2.11) will hold with equality also for each $k \in S_{i+1} \backslash \{0\}$.

Proof. See Appendix B.2. □

One important result we can immediately deduce from Proposition 4 is that using a control $u \in \mathcal{S}_\mathbb{U}$ with i switchings one can only reach the maximal value for $E_{EJ}(u, t_f)$, i.e. $E_{max}(i)$, if all the previously obtained relative energies are maximized by that control as well, see (4.2.10). Moreover, this will only be possible if switchings of the control occur at zero deflection and if the terminal deflection equals to zero. Looking at the minimum time required to maximize the system's energy, i.e. at $t_f = t_{min}(i + 1)$, the second important result of Proposition 4 is the direct relation between this time and the obtained relative energies in terms of the oscillation period T_p, see (4.2.11)-(4.2.12).

Propositions 3 and 4 provide now together the solution to the EMP. In particular, given a switching number $i \geq 0$ Proposition 3 establishes the existence of a maximum of $E_{EJ}(u, t_f)$ over controls in $\mathcal{S}_\mathbb{U}$ with i switchings. Proposition 4 provides then the final time as well as the switching times of the control which leads to this maximum value for E_{EJ} using the least amount of time, see (4.2.11). Since the magnitude of the control will remain at $\dot{\theta}_{max}$ due to (4.2.6)-(4.2.7), these times together with the initial value of the control $u(0) \in \{-\dot{\theta}_{max}, \dot{\theta}_{max}\}$ determine then uniquely the control strategy u_S^* which solves the EMP for the given switching number i. Note that this also means that for any switching number there exists exactly two different control strategies which will solve the EMP.

If we now look back at Fig. 4.1.1, it can be observed that the controlled trajectories there all satisfy the required conditions by Proposition 4 with $i = 1$. Consequently, the depicted controls solve the corresponding EMP. In other words, the maximum possible value for the total energy, which equals to $E_{max}(1)$ since the controls switch only once, is attained as fast as possible, i.e. $t_f = t_{min}(2)$. Moreover, since the terminal deflection is equal to zero and the final link velocity is positive we can also conclude that the depicted strategies actually maximize the terminal link velocity over the set of all admissible switching controls with one switching as well. It is important to realize here that given any switching number i, one can actually always find a control strategy that solves the EMP and simultaneously maximizes the terminal link velocity over

controls in $\mathcal{S}_{\mathbb{U}}$ with i switchings[6]. In the following two chapters, we will take a closer look at these control strategies solving the EMP and show in particular that these strategies satisfy all the necessary conditions from PMP to be a solution to the LVMP. Nevertheless, we will also see that for nonlinear TDP's they will not necessarily solve the LVMP.

---

[6]Note that for any given $i \geq 0$ the two control strategies solving the EMP only differ in their signs. Consequently, due to the symmetry of the TDP's the corresponding trajectories will be symmetric with respect to the origin when they are depicted in a phase plane. This means that one of the control strategies solving the EMP will always result to a positive terminal link velocity as $E_{max}(i) > 0$ and $^i x_1 = 0$.

Chapter 5

Optimal Control Strategies

In this chapter, we will first show that there always exists an admissible control strategy solving the LVMP regardless of the given final time $t_f > 0$. Then, in Sec. 5.2 we will derive several basic properties of these control strategies. In particular, making use of PMP [44] and the oscillation nature of both the state and costate dynamics we derive necessary conditions for these strategies in terms of the attained relative energies and spring deflections. Providing a construction method for extremals, i.e. controlled trajectories satisfying the conditions from PMP, and further introducing a parameterization to simultaneously account for their final times and terminal link velocities, Sec. 5.3 finally shows how to solve the LVMP. Noting the close relation between the time functions from Sec. 3.2 and the derived conditions for the solutions to the LVMP, we conclude the chapter by revealing a physical principle behind these solutions.

5.1 Existence

We have shown in Chapter 3 that the period of a MSS with a hardening spring strictly decreases as the system's energy increases. According to Table 3.1d, this period can even go to zero. For control strategies solving the EMP, this means that for a SEA with hardening springs the time between two switching times can go to zero as the number of switchings increase. Since by increasing the switching number we can always increase the terminal link velocity, it seems then reasonable to speculate that by using certain TDP's the link velocity of an EJ can be made arbitrarily large in a finite time. For such TDP's, however, the LVMP would not always have a solution. In this section, we will first show that the situation just described can never occur and then prove that a solution to the LVMP always exists.

We start our discussion by illustrating how for a given trajectory of Σ we can always build a compact subset of the state-space in which the trajectory remains. For this, we will take an energy based approach. More specifically, we will exploit (4.2.2) and show that the energy which can be transferred from or

to the system in a limited time must be bounded.

Let $(\boldsymbol{x}, u)$ be an arbitrary controlled trajectory of Σ defined on $D = [0, t_f]$. Looking at the right-hand side of (4.2.2), we can see that at each $t \in D$ the power input to the system can be bounded using the maximum motor velocity and the system's current energy E_{EJ}. Indeed, defining a maximal deflection function[1] $\psi_{max} : D \rightarrow [0, \infty)$ which corresponds to the energy stored along $(\boldsymbol{x}, u)$ with

$$\psi_{max}(t) = E_{pot}^{-1} \left(E_{EJ}(\boldsymbol{x}_0, u, t) \right), \tag{5.1.1}$$

we have the following inequality for E_{EJ} at each $t \in D$:

$$\left| \frac{\partial E_{EJ}}{\partial t} (\boldsymbol{x}_0, u, t) \right| \leq \dot{\theta}_{max} \tau_J \left(\psi_{max}(t) \right). \tag{5.1.2}$$

Using the fact that (5.1.2) can only hold with equality if the link velocity equals to zero, we arrive then at the following proposition leading to the desired compact set.

Proposition 5. *Let $(\boldsymbol{x}, u)$ be an admissible controlled trajectory defined on $D = [0, t_f]$. Then, the following inequality holds for the maximal deflection ψ_{max} given by (5.1.1):*

$$(\forall t \in (0, t_f]) \left[|\psi_{max}(t) - \psi_{max}(0)| < \dot{\theta}_{max} t \right]. \tag{5.1.3}$$

In particular, using the lower and upper bounds for ψ_{max} defined by

$$\psi_{lb} \quad := \quad \max \left\{ 0, \psi_{max}(0) - \dot{\theta}_{max} t_f \right\}, \tag{5.1.4}$$

$$\psi_{ub} \quad := \quad \psi_{max}(0) + \dot{\theta}_{max} t_f, \tag{5.1.5}$$

we can build a compact set S_{E_b} with

$$S_{E_b} := \left\{ \boldsymbol{y} \in \mathbb{R}^2 | E_{MSS}(y_1, y_2) \in [E_{pot}(\psi_{lb}), E_{pot}(\psi_{ub})] \right\} \tag{5.1.6}$$

such that the following relation holds along $\boldsymbol{x}$:

$$(\forall t \in [0, t_f]) \left[\boldsymbol{x}(t) \in S_{E_b} \right]. \tag{5.1.7}$$

Proof. See Appendix B.3.1. □

According to Proposition 5, we can now find for any trajectory of Σ a lower and an upper bound for the system's energy which in turn describe a compact set S_{E_b} to which the trajectory will belong. It is important to note here that these bounds depend only on $\boldsymbol{x}_0$ and t_f but not on the applied control, see (5.1.1) and (5.1.4)-(5.1.5). Consequently, any trajectory of Σ sharing the same initial state and final time will belong to the same compact set S_{E_b} described by (5.1.6). In particular, if we look at admissible trajectories starting from

---

[1]Note that for SEA's we have already reserved the symbol ϕ_{max} for the maximum deflection values corresponding to the system's relative energy.

the origin and terminating at the final time t_f, we can see that their energy is bounded above by $E_{pot}(\dot{\theta}_{max}t_f)$. This shows that their terminal link velocity can not grow unbounded in finite time as speculated.

With Proposition 5 we can now also solve the existence problem for the LVMP using mainly Filippov's Theorem [14]. Indeed, using the compact sets from that proposition together with the compactness of the control set $\mathbb{U}$ and the fact that the set $f_{\mathbb{U}}(\boldsymbol{x}) := \{\boldsymbol{f}(\boldsymbol{x}, u) \in \mathbb{R}^2 | u \in \mathbb{U}\}$ is convex for each $\boldsymbol{x} \in \mathbb{R}^2$, it can be seen that all the conditions required to apply this theorem are satisfied [11]. Taking also several properties of the optimal control strategies into account[2], we can then arrive at the main result of this section.

Proposition 6. *A solution to the LVMP exists for each final time $t_f > 0$.*

Proof. See Appendix B.3.1. □

Having established the existence of solutions to the LVMP, we next turn our attention to the necessary conditions which need to be satisfied by these solutions.

5.2 Basic Properties

In this section, we will derive several basic properties of control strategies solving the LVMP. More specifically, we will first apply PMP to find necessary conditions for these strategies in terms of costates. A first analysis of these conditions will show that optimal controls for the LVMP are always piecewise constant. Focusing on switching control strategies, we will then take a closer look at the time evolution of the costates. In particular, by analysing the differential equations describing the costate dynamics we will obtain mathematical expressions which clarify the relation between costates and trajectories corresponding to switching controls. Finally, we will use these expressions to find a relation between optimal control strategies and optimal trajectories.

5.2.1 Minimum Principle

Let us call an admissible controlled trajectory $(\boldsymbol{x}, u)$, which consists of an optimal control for the LVMP and the corresponding optimal trajectory with $\boldsymbol{x}_0 = \boldsymbol{0}$, an *optimally controlled trajectory*. According to PMP, we have then the following result for these trajectories.

Proposition 7. *Let $(\boldsymbol{x}, u)$ be an optimally controlled trajectory defined on the interval $D = [0, t_f]$. Then, there must exist a continuously differentiable costate[3] $\boldsymbol{\lambda} : D \to (\mathbb{R}^2)^*$ such that the following first three conditions hold at each $t \in D$ and the fourth condition at the final time t_f:*

---

[2]Filippov's Theorem can ensure for our OC problem only the existence of an OC strategy in the space of Lebesgue measurable functions taking values in $\mathbb{U}$ almost everywhere.

[3]As in [53], we use $(\mathbb{R}^n)^*$ to denote the set of all n-dimensional row vectors.

1. Costate Dynamics

$$\dot{\boldsymbol{\lambda}}(t) = \left(-\frac{K_J(x_1(t))}{M}\lambda_2(t) \quad \lambda_1(t) \right). \tag{5.2.1}$$

2. Minimum Condition

$$\mathbb{H}\left(\boldsymbol{x}(t), u(t), \boldsymbol{\lambda}(t)\right) = \min_{v \in \mathbb{U}} \mathbb{H}\left(\boldsymbol{x}(t), v, \boldsymbol{\lambda}(t)\right), \tag{5.2.2}$$

where $\mathbb{H} : \mathbb{R}^2 \times \mathbb{U} \times (\mathbb{R}^2)^* \to \mathbb{R}$ denotes the Hamiltonian function given by

$$\begin{aligned} \mathbb{H}(\boldsymbol{x}, u, \boldsymbol{\lambda}) &= \boldsymbol{\lambda} \boldsymbol{f}(\boldsymbol{x}, u) \\ &= \lambda_1(u - x_2) + \lambda_2 \frac{\tau_J(x_1)}{M}. \end{aligned} \tag{5.2.3}$$

3. Hamiltonian Condition

$$\mathbb{H}\left(\boldsymbol{x}(t), u(t), \boldsymbol{\lambda}(t)\right) = -\lambda_a, \tag{5.2.4}$$

where $\lambda_a \in \{0, 1\}$ is a constant scalar.

4. Transversality Condition

$$\boldsymbol{\lambda}(t_f) = \begin{pmatrix} 0 & -v \end{pmatrix}, \tag{5.2.5}$$

where v is a positive constant scalar.

Proof. The proof follows directly from applying PMP to the LVMP and is omitted for brevity. A proof of PMP is provided in Appendix A, see Theorem 37. □

Based on the definitions given in [53], we will call the 4−tuple $\Lambda = (\boldsymbol{x}, u, \boldsymbol{\lambda}, \lambda_a)$ consisting of an admissible controlled trajectory $(\boldsymbol{x}, u)$ with $\boldsymbol{x}_0 = \boldsymbol{0}$, a constant scalar $\lambda_a \in \{0, 1\}$ and a continuously differentiable costate $\boldsymbol{\lambda}$ such that the conditions (5.2.1)-(5.2.5) are satisfied an *extremal lift* for the LVMP. In addition, the admissible controlled trajectory $(\boldsymbol{x}, u)$ of such an extremal lift Λ will simply be called an *extremal* for the LVMP (corresponding to Λ). Moreover, if λ_a equals to zero we will call the extremal (lift) an *abnormal extremal (lift)* and otherwise a *normal extremal (lift)*. Finally, if an extremal is equal to an optimally controlled trajectory we will call this extremal an *optimal extremal* for the LVMP.

According to Prop. 7, we thus know that there exists an extremal lift for each optimally controlled trajectory. Moreover, using the condition (5.2.2) together with the Hamiltonian function in (5.2.3) we can see that given an extremal lift Λ the value of the control u in that lift always depends on the sign of the first costate λ_1 as follows:

$$u(t) = \begin{cases} -\dot{\theta}_{max} & \lambda_1(t) > 0 \\ \dot{\theta}_{max} & \lambda_1(t) < 0 \end{cases}, \tag{5.2.6}$$

where $t \in D$. In addition, notice that (5.2.1) and (5.2.5) imply that there always exists a sufficiently small time interval $(t_f - \varepsilon, t_f) \in D$ where λ_1 is negative. Consequently, using (5.2.6) we can also conclude that we have the following equality for the terminal value of u:

$$u(t_f) = \dot{\theta}_{max}. \tag{5.2.7}$$

It is important to remark here that (5.2.6) does not give any information on the control u if $\lambda_1(t) = 0$ holds in a finite time-interval. We have just seen that this can not happen in a sufficiently small neighborhood of the final time t_f. In the following proposition, we similarly show that whenever $\lambda_1(t)$ equals to zero in $t \in [0, t_f)$ its time-derivative will be non-zero so that the condition (5.2.6) actually uniquely determines the control u. Moreover, with this proposition we will also see that λ_1 can be equal to zero at most once in case the first state, i.e. the spring deflection, remains negative or positive.

Proposition 8. *Let $\Lambda = (\boldsymbol{x}, u, \boldsymbol{\lambda}, \lambda_a)$ be an extremal lift for the LVMP which is defined on the interval $D = [0, t_f]$. Then, u is a switching control with its initial value given by*

$$^0u = \begin{cases} -\dot{\theta}_{max} \operatorname{sgn}\left(\dot{\lambda}_1(0)\right) & \lambda_1(0) = 0 \\ -\dot{\theta}_{max} \operatorname{sgn}\left(\lambda_1(0)\right) & \lambda_1(0) \neq 0 \end{cases}, \tag{5.2.8}$$

where $\dot{\lambda}_1(0) \neq 0$ holds in case $\lambda_1(0)$ equals to zero. In addition, $t_S \in (0, t_f)$ is a switching time of u if and only if $\lambda_1(t_S)$ is equal to zero in which case we have

$$\frac{\tau_J\left(x_1(t_S)\right)}{K_J\left(x_1(t_S)\right)} \dot{\lambda}_1(t_S) = \lambda_a, \tag{5.2.9}$$

with $\dot{\lambda}_1(t_S) \neq 0$. Finally, if the control u has $i \geq 0$ switchings we have

$$\left(\forall k \in S_{i+1} \backslash \{0\}\right) \left[\operatorname{sgn}\left(^kx_1\right) = (-1)^{k+i+1}\lambda_a\right]. \tag{5.2.10}$$

Proof. See Appendix B.3.2. □

With (5.2.6) and Proposition 8, we can now conclude that optimal control strategies solving the LVMP will always be admissible switching controls which take values in the boundary of the control set $\mathbb{U}$. Moreover, if $(\boldsymbol{x}, u)$ is an optimally controlled trajectory corresponding to the extremal lift $\Lambda = (\boldsymbol{x}, u, \boldsymbol{\lambda}, \lambda_a)$, the initial value of the control u will depend according to (5.2.1) and (5.2.8) only on the *initial costate* $\boldsymbol{\lambda}_0 := \boldsymbol{\lambda}(0)$. Finally, the switching times of u will be uniquely given by the zeros of λ_1 in the interior of its domain.

Our analysis so far clearly demonstrates the close relation between the optimal control strategies and the costates. Since Σ represents a physical system, it is then natural to expect that we can find a description of these costates in terms of physical quantities. In the following subsection, we will see that this is indeed possible by studying the solutions to the differential equation (5.2.1) along trajectories corresponding to admissible switching controls.

5.2.2 Costates with $u \in \mathcal{S}_{\mathbb{U}}$

In Section 4.1, we have introduced an iterative procedure to construct a trajectory which starts from a given initial state and corresponds to a given admissible switching control. Note that for such a trajectory (5.2.1) describes a linear differential equation for the costate and has therefore a unique solution provided we know the initial costate. Our aim is now to introduce an iterative procedure which will enable us to construct this solution.

Let us assume that $(\boldsymbol{x}, u)$ is an admissible controlled trajectory with $u : D \to \mathbb{U}$ being a switching control with $i \geq 0$ switchings. As in Section 4.1, we will first focus on finding the solution $\boldsymbol{\lambda} : D \to (\mathbb{R}^2)^*$ of (5.2.1) in the time interval D_k where $k \in S_i$. In particular, we will show how to determine this particular part of the solution assuming we are given the boundary condition ${}^k\boldsymbol{\lambda} := \boldsymbol{\lambda}(t_{S,k})$.

Depending on the relative energy ${}^kE_{rel}$ stored along $\boldsymbol{x}$, we need to again distinguish between two cases. Assume first that ${}^kE_{rel}$ is zero. In this case, $x_1(t)$ will be equal to zero for each $t \in D_k$. Consequently, (5.2.1) becomes a linear differential equation with constant coefficients whose solution can be explicitly written as

$$\boldsymbol{\lambda}(t) = {}^k\boldsymbol{\lambda} \begin{pmatrix} \cos\left(\omega_0(t - t_{S,k})\right) & \frac{\sin(\omega_0(t-t_{S,k}))}{\omega_0} \\ -\omega_0 \sin\left(\omega_0(t - t_{S,k})\right) & \cos\left(\omega_0(t - t_{S,k})\right) \end{pmatrix}, \qquad (5.2.11)$$

where $t \in D_k$. Notice that (5.2.11) describes $\boldsymbol{\lambda}$ in terms of harmonic oscillations with the eigenfrequency $\omega_0 = \sqrt{\frac{K_J(0)}{M}}$.

Assuming now that ${}^kE_{rel}$ is non-zero, we already know from our previous discussions in Chapters 3-4 that x_1 will continuously increase and/or decrease over time. Moreover, x_1 will take values in the interval $[-{}^k\phi_{max}, {}^k\phi_{max}]$ and its time-derivative $\dot{x}_1$ will only change its sign whenever x_1 is at one of the boundaries of that interval. In order to find the solution of (5.2.1) for this case, one possible approach would be now to first make use of the relation (3.2.3) to express x_1 as a function of time. The resulting expression can then be substituted into (5.2.1) yielding a time-varying linear differential equation. Finally, the solution of that equation can be found, for instance, by computing the corresponding transition matrix function [34]. In this thesis, we will follow a more straightforward approach where the main idea is to use (3.2.3) to rewrite (5.2.1) such that the continuously changing deflection becomes the independent variable instead of the time. By exploiting the relation between the state and costate dynamics, this leads to a linear first-order partial differential equation whose solution can be directly related to the solution of (5.2.1) as shown in the following proposition.

Proposition 9. *Let $(\boldsymbol{x}, u)$ be an admissible controlled trajectory such that $u : D \to \mathbb{U}$ is a switching control with $i \geq 0$ switchings and let $\boldsymbol{\lambda} : D \to (\mathbb{R}^2)^*$ be a solution of (5.2.1) for this trajectory. Moreover, let $\eta : (-\phi_{max}, \phi_{max}) \times (0, \infty) \to \mathbb{R}, (x, \phi_{max}) \to \eta(x, \phi_{max})$ be a solution to the following partial differ-*

ential equation:

$$\left(|\dot{\phi}|(x,\phi_{max})\right)^2 \frac{\partial\eta}{\partial x} + \frac{\tau_J(x)}{M}\eta + \eta_c = 0, \qquad (5.2.12)$$

where η_c is a constant scalar. Finally, let k be an element of S_i and $\bar{D}_k \subset D_k$ a non-empty open interval with

$$\left(\forall t \in \bar{D}_k\right)\left[\mathrm{sgn}\left(\dot{x}_1(t)\right) = v_\phi\right], \qquad (5.2.13)$$

where $v_\phi \in \{-1,1\}$ is also a constant scalar. In this case, if there exists a $\bar{t} \in \bar{D}_k$ such that

$$\lambda_2(\bar{t}) = \eta(x_1(\bar{t}),{}^k\phi_{max}) \wedge \mathbb{H}\left(\boldsymbol{x}(\bar{t}),u(\bar{t}),\boldsymbol{\lambda}(\bar{t})\right) = -\eta_c, \qquad (5.2.14)$$

then for each $t \in \bar{D}_k$ we have

$$\boldsymbol{\lambda}(t) = \left(-\frac{\eta_c v_\phi}{|\dot{\phi}|(x_1(t),{}^k\phi_{max})} \quad 0\right)$$
$$+ \eta(x_1(t),{}^k\phi_{max})\left(-\frac{\tau_J(x_1(t))v_\phi}{M|\dot{\phi}|(x_1(t),{}^k\phi_{max})} \quad 1\right). \qquad (5.2.15)$$

Moreover, at each boundary point $\bar{t}_b$ of $\bar{D}_k$ the equality (5.2.15) still holds if $\lim_{\bar{D}_k \ni t \to \bar{t}_b} \dot{x}_1(t) \neq 0$ while if this limit is equal to zero we have

$$\boldsymbol{\lambda}(\bar{t}_b) = \left(-\frac{v_\phi \eta_c}{4}\frac{\mathrm{d}T_p}{\mathrm{d}\phi_{max}}({}^k\phi_{max}) \quad 0\right)$$
$$- \mathrm{sgn}\left(x_1(\bar{t}_b)\right)\left(\frac{v_\phi \eta(0,{}^k\phi_{max})}{\frac{M{}^k\dot{\phi}_{max}}{\tau_J({}^k\phi_{max})}} \quad \frac{M\eta_c}{\tau_J({}^k\phi_{max})}\right). \qquad (5.2.16)$$

Proof. See Appendix B.3.2.   □

With Prop. 9 we can now see that in an open interval $\bar{D}_k \subset D_k$, in which the deflection x_1 either increases or decreases, $\boldsymbol{\lambda}$ can always be described using $(\boldsymbol{x},u)$ and a solution of (5.2.12) provided the two conditions in (5.2.14) hold, see (5.2.15). One of the main advantages of this description is that solutions of (5.2.12) can be explicitly expressed in terms of physical quantities as we show Appendix B.3.2, see Lemma 45. Furthermore, taking a closer look at the corresponding expression, which we provide in Table 5.1a, we can conclude from (5.2.15) that the costate $\boldsymbol{\lambda}$ in $\bar{D}_k$ can be uniquely described as a function of the deflection if we know, in addition to $(\boldsymbol{x},u)$, the values of η_c and $\eta(0,{}^k\phi_{max})$. Moreover, with these values $\boldsymbol{\lambda}$ can also be determined at the boundaries of $\bar{D}_k$. It is important to remark here that the number of times, at which $\dot{x}_1$ changes its sign in the interval D_k, is always finite. Consequently, we can always find a finite number of open intervals satisfying the hypothesis of Prop. 9 such that D_k is contained in the closure of their union. To construct $\boldsymbol{\lambda}$ in D_k, it would then be sufficient to find for each of these intervals the values of η_c and $\eta(0,{}^k\phi_{max})$. We illustrate next how to systematically carry out this construction.

$\eta(x,\phi_{max})$	$\frac{\|\dot\phi\|(x,\phi_{max})}{\dot\phi_{max}}$	$\left[\eta(0,\phi_{max})+\eta_c\frac{M\dot\phi_{max}}{\tau_J(\phi_{max})}\frac{\partial T_\phi}{\partial\phi_{max}}(x,\phi_{max})\right]$

(a) Mathematical Expression for η

$\lim_{D_\phi\ni x\to\phi_b}\eta(x,\phi_{max})$	$-\operatorname{sgn}(\phi_b)\frac{M\eta_c}{\tau_J(\phi_{max})}$
$\lim_{D_\phi\ni x\to\phi_b}\frac{\frac{\partial\eta}{\partial x}(x,\phi_{max})}{\frac{1}{\|\dot\phi\|(x,\phi_{max})}}$	$-\frac{\eta_c}{4}\frac{\mathrm{d}T_p}{\mathrm{d}\phi_{max}}(\phi_{max})-\operatorname{sgn}(\phi_b)\frac{\tau_J(\phi_{max})}{M\dot\phi_{max}}\eta(0,\phi_{max})$
$\phi_{max}>0,\phi_b\in\{-\phi_{max},\phi_{max}\},D_\phi=(-\phi_{max},\phi_{max})$	

(b) Limits for $\eta(.,\phi_{max})$ and $\frac{\partial\eta}{\partial x}(.,\phi_{max})$

Table 5.1: The Function $\eta:D_{T_\phi}\to\mathbb{R}$

Computing η_c and $\eta(0,{}^k\phi_{max})$ in D_k Let $m_k\in\{0,1,\ldots\}$ denote the necessarily finite number of times at which $\dot x_1$ is equal to zero in $(t_{S,k},t_{S,k+1})$. Moreover, for each $j\in S_{m_k}\backslash\{0\}$ let t_{S,k_j} denote the j'th time at which $\dot x_1$ is equal to zero in this interval. In addition, let t_{S,k_0} be equal to the switching time $t_{S,k}$ and $t_{S,k_{m+1}}$ to $t_{S,k+1}$. Finally, for each $j\in S_{m_k}$ introduce the open interval $D_{k_j}:=(t_{S,k_j},t_{S,k_{j+1}})$ which always satisfies the hypothesis of Prop. 9 by construction. As already discussed above, for each $j\in S_{m_k}$ the values $\boldsymbol\lambda$ takes in D_{k_j} can be determined using (5.2.15) if we know the corresponding value of η and $\eta(0,{}^k\phi_{max})$. In addition, using (5.2.16) the values at the boundaries of D_{k_j} can be determined as well. To be able to distinguish between different intervals, we will from now on use ${}^k\eta_{c,j}$ and ${}^k\eta_{0,j}$ to denote, respectively, the value of η and $\eta(0,{}^k\phi_{max})$ in the interval D_{k_j}. Moreover, we will use ${}^kv_{\phi,j}:=(-1)^j\,{}^kv_{\phi,0}$ to denote the sign of $\dot x_1$ in D_{k_j}. We want to next show how to describe for each $j\in S_{m_k}$ the values of ${}^k\eta_{c,j}$ and ${}^k\eta_{0,j}$ in terms of ${}^k\boldsymbol\lambda$.

Let j be an arbitrary element of S_{m_k}. We want to first show how to determine the value of ${}^k\eta_{c,j}$. For this, let us note that the value of the Hamiltonian function $\mathbb{H}(\boldsymbol x(t),u(t),\boldsymbol\lambda(t))$ will always remain constant in D_k regardless of whether the pair $(\boldsymbol x,u)$ is an extremal or not, see the proof of Prop. 9. Consequently, when applying Prop. 9 to construct $\boldsymbol\lambda$ in D_{k_j} we can simply set ${}^k\eta_{c,j}$ to

$$
{}^k\eta_{c,j}={}^k\eta_c:=-\mathbb{H}\left({}^k\boldsymbol x,{}^ku,{}^k\boldsymbol\lambda\right). \tag{5.2.17}
$$

Finding an expression for ${}^k\eta_{0,j}$ in terms of ${}^k\boldsymbol\lambda$ is unfortunately more involved as it depends, in contrary to ${}^k\eta_{c,j}$, also on $\dot x_1|_{D_k}$. To see this dependence, let us first focus on the interval D_{k_0}. Noting that $t_{S,k}$ is a boundary point, it follows then from Prop. 9 that two different expressions will exist for ${}^k\eta_{0,0}$ depending on whether ${}^k\dot x_1$ is equal to 0 or not. Indeed, if ${}^k\dot x_1$ is not equal to zero it follows from evaluating (5.2.15) at $t=t_{S,k}$ und using (5.2.17) that we have

$$
{}^k\eta_{0,0}=\frac{{}^k\dot\phi_{max}\,{}^k\lambda_2}{\|\dot\phi\|({}^kx_1,{}^k\phi_{max})}-\frac{{}^k\eta_c\frac{\partial T_\phi}{\partial\phi_{max}}({}^kx_1,{}^k\phi_{max})}{\frac{\tau_J({}^k\phi_{max})}{M\,{}^k\dot\phi_{max}}}, \tag{5.2.18}
$$

where we have also made use of the expression for $\eta(x,\phi_{max})$ in Table 5.1a. If ${}^k\dot x_1(t_{S,k})=0$, on the other hand, it follows from (5.2.16) with $\bar t_b=t_{S,k}$ that

$^k\eta_{0,0}$ will be equal to

$$^k\eta_{0,0} = -\frac{M\,^k\dot{\phi}_{max}}{\tau_J(^k\phi_{max})}\frac{\left[^k v_{\phi,0}\,^k\lambda_1 + \frac{^k\eta_c}{4}\frac{\mathrm{d}T_p}{\mathrm{d}\phi_{max}}(^k\phi_{max})\right]}{\mathrm{sgn}(^k x_1)}. \tag{5.2.19}$$

Note that using (5.2.15)-(5.2.19), we can determine the costate $\boldsymbol{\lambda}$ in D_{k_0} and at t_{S,k_1}.

Focusing now on an interval[4] D_{k_j} with a positive $j \in S_{m_k}$, it can be shown that $^k\eta_{0,j}$ is closely related to $^k\eta_{0,j-1}$. Indeed, we know that the first costate is continuous at t_{S,k_j} and that t_{S,k_j} is a boundary point of both $D_{k_{j-1}}$ and D_{k_j}. Consequently, using (5.2.16) and the fact that $x_1(t_{S,k_j})$ has the same sign as $\dot{x}_1$ in $D_{k_{j-1}}$, we can see that $^k\eta_{0,j}$ is given by

$$^k\eta_{0,j} = -^k\eta_{0,j-1} + 2\,^k\eta_c\,^k v_{\phi,j-1}\Delta(^k\phi_{max}), \tag{5.2.20}$$

where $\Delta : (0,\infty) \to \mathbb{R}$ is the function defined by

$$\Delta(\phi_{max}) = -\frac{1}{4}\frac{M\dot{\phi}_{max}}{\tau_J(\phi_{max})}\frac{\mathrm{d}T_p}{\mathrm{d}\phi_{max}}(\phi_{max}). \tag{5.2.21}$$

With (5.2.18)-(5.2.20), we can now iteratively compute $^k\eta_{0,j}$ for each $j \in S_{m_k}\backslash\{0\}$ and thus determine $\boldsymbol{\lambda}$ in D_{k_j} as well as at $t_{S,k_{j+1}}$.

Our discussion above provides all the means to construct $\boldsymbol{\lambda}|_{D_k}$ along the admissible controlled trajectory $(\boldsymbol{x}, u)$ when $^k\phi_{max} > 0$. This construction is graphically illustrated in Figure 5.2.1 for the three control systems Σ_1, Σ_2 and Σ_3 from Table 4.1 by plotting for each system two different costate trajectories against the time varying deflection. More specifically, for each of these systems the costate trajectories are determined in $D = D_0$ using Prop. 9 and (5.2.17)-(5.2.20) for the controlled trajectory $(\boldsymbol{x}, u)$ with $\boldsymbol{x}_0 = \begin{pmatrix} 0 & -5\dot{\theta}_{max} \end{pmatrix}^T$, $u \equiv \dot{\theta}_{max}$ and $t_f = \frac{3}{4}T_p(^0\phi_{max})$. In addition, for the costates in Fig. 5.2.1 (Top) $\boldsymbol{\lambda}_0$ was set to $\begin{pmatrix} 0 & -\frac{1}{10} \end{pmatrix}^T$ and in Fig. 5.2.1 (Bottom) to $\begin{pmatrix} -\frac{1}{6\dot{\theta}_{max}} & -\frac{1}{10} \end{pmatrix}^T$. Notice that along each controlled trajectory, $\dot{x}_1$ always changes its sign once at $t_{S_{0_1}} = \frac{1}{2}T_p(^0\phi_{max})$. Moreover, depending on the chosen initial costate $^0\eta_c$ is either equal to 0 or to 1, see (5.2.17).

As one can see from the graphs in Fig. 5.2.1, when the initial first costate and thus $^0\eta_c$ is equal to zero the costates possess of symmetry properties shared by each control system. This directly follows from (5.2.15) and (5.2.20) according to which for $^0\eta_c = 0$ the first and second costates remain proportional to the torque in the spring and to the time-derivative of the deflection, respectively. Consequently, all the three curves representing the first costate in Fig. 5.2.1 (Top) can be directly expressed as a function of the deflection. For the second costate, on the other hand, the corresponding curves do not directly represent a function. Nevertheless, following our construction method described above one

---

[4]Clearly, such an interval only exists if $\dot{x}_1$ changes its sign in $(t_{S,k}, t_{S,k+1})$, i.e. $m_k \geq 1$.
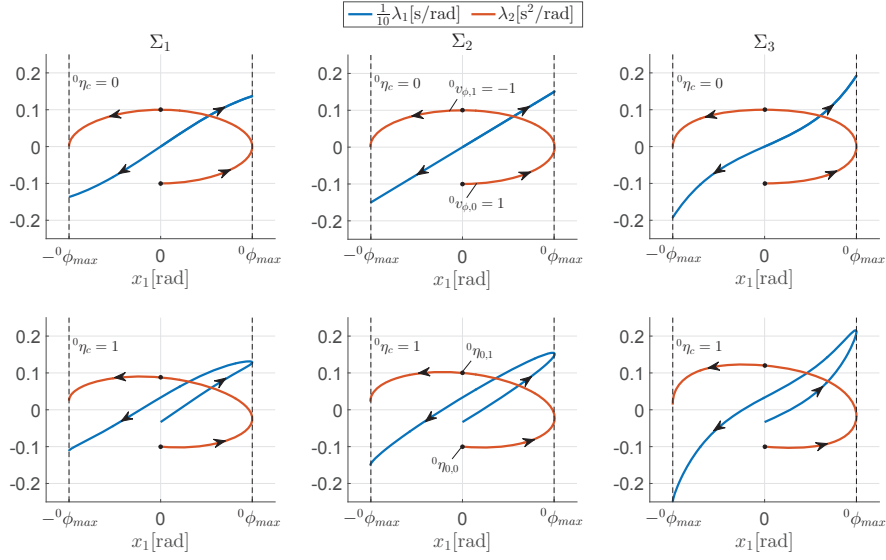
Figure 5.2.1: Costate Trajectories in $D = [0, \frac{3T_p(^0\phi_{max})}{4}]$
$(u \equiv \dot{\theta}_{max}, \boldsymbol{x}_0 = (0, -5\dot{\theta}_{max})^T, \boldsymbol{\lambda}_0 = (-\frac{^0\eta_c}{6\dot{\theta}_{max}}, -\frac{1}{10}))$

can divide each of these curves into two subcurves on which the deflection either increases or decreases. These two subcurves can then be described by a function of the deflection, namely the function $\eta(., {}^0\phi_{max})$ with $\eta_c = 0$ and $\eta(0, \phi_{max}) \in \{{}^0\eta_{0,0}, {}^0\eta_{0,1}\}$. Furthermore, they will join each other at the maximal deflection ${}^0\phi_{max}$.

If we now look at the graphs in Fig. 5.2.1 (Bottom), it can be observed that for all the three systems two different functions of the deflection are needed to fully describe the first as well as the second costate. In particular, both costates take two different values at zero deflection. For the first costate, these are given according to (5.2.17) by $-\frac{^0v_{\phi,j}}{6\dot{\theta}_{max}}$, with $j \in \{0, 1\}$, and thus only differ in their signs. For the second costate, they are given by ${}^0\eta_{0,j}$ with $j \in \{0, 1\}$, see (5.2.15). As shown in Fig. 5.2.1, for the systems Σ_1 and Σ_3 these values differ, consistent with (5.2.20), both in their signs and their magnitudes. Moreover, for Σ_1, i.e. the control system with the softening spring, there is a decrease in the magnitude, while for the system Σ_3 with the hardening spring there is an increase. For the system Σ_2 with the linear TDP, on the other hand, there is again only a change of sign. In Sec. 5.4, we will provide a physical interpretation which will explain why the value for $\eta(0, \phi_{max})$ in general changes with a sign change of $\dot{x}_1$ and clarify in particular how this change is related to the stiffness characteristics of TDP's. The interpretation will also explain the relation between the costates and the partial derivative $\frac{\partial T_\phi}{\partial \phi_{max}}$ which exists whenever the Hamiltonian function is not equal to zero, see Table 5.1a. Notice that, it is this

relation and the condition (5.2.20) which result in the more complex costate trajectories in Fig. 5.2.1 (Bottom) when compared to the trajectories in Fig. 5.2.1 (Top).

Our results so far show that we can always use (5.2.20) or Prop. 9 to construct the costate $\boldsymbol{\lambda}$ in the interval $D_k \subset D$ using ${}^k\boldsymbol{\lambda}$. Notice that in both cases, we can uniquely determine ${}^{k+1}\boldsymbol{\lambda}$ by making use of the continuity of $\boldsymbol{\lambda}$. Consequently, if the initial value of the costate $\boldsymbol{\lambda}_0 = {}^0\boldsymbol{\lambda}$ is given we can determine the costate $\boldsymbol{\lambda}$ in the whole interval D. Indeed, starting from $k = 0$ and using for each $k \in S_i$ the controlled trajectory $(\boldsymbol{x}, u)$ to determine whether ${}^kE_{rel}$ is zero or positive, we can iteratively apply our results to fully construct $\boldsymbol{\lambda}$ as desired.

5.2.3 Switching and Terminal State Conditions

Let $\Lambda = (\boldsymbol{x}, u, \boldsymbol{\lambda}, \lambda_a)$ be an extremal lift for the LVMP. We already know from Sec. 5.2.1 that the control u in this lift is a switching control which is uniquely determined by the sign of λ_1. From Sec. 5.2.2, we further know that for each $k \in S_i$, with $i \geq 0$ denoting the switching number of u, $\boldsymbol{\lambda}|_{D_k}$ can be expressed in terms of ${}^k\boldsymbol{\lambda}$, x_1 and $\dot{x}_1$ assuming that the relative energy ${}^kE_{rel}$ is positive. Under this assumption, the control $u|_{D_k}$ can therefore also be expressed in terms of these three terms. In the following, we will derive such an expression for the control and use it to derive various conditions for its switching times as well as the terminal time in terms of the attained deflection values. The assumption on the relative energy ${}^kE_{rel}$ being positive will be justified in Section 5.3, where we show that for each extremal lift for the LVMP the relative energy actually remains positive along the whole trajectory.

Let k be an element of S_i for which the relative energy ${}^kE_{rel}$ is positive and let m_k denote, as in Sec. 5.2.2, the number of times at which $\dot{x}_1$ equals to zero in the interior of D_k. Moreover, let j be an element of S_{m_k}. According to Prop. 7-8, we know that $u(t)$ is given by $-\dot{\theta}_{max} \operatorname{sgn}(\lambda_1(t))$ for each $t \in D_{k_j}$. If we now use Prop. 9 and in particular (5.2.15), we can rewrite this relation between u and λ_1 to obtain the following equality which holds for each $t \in D_{k_j}$ when $x_1(t) \neq 0$:

$$\frac{u(t)}{\dot{\theta}_{max}} = \frac{\operatorname{sgn}\left(\left[{}^k\eta_{0,j} - \lambda_a C(x_1(t), {}^k\phi_{max})\right] x_1(t)\right)}{{}^kv_{\phi,j}}, \tag{5.2.22}$$

where $C : D_C \to \mathbb{R}$ is the function defined by

$$C(x, \phi_{max}) = -\frac{\frac{\partial T_\phi}{\partial \phi_{max}}(x, \phi_{max}) + \frac{\tau_J(\phi_{max})}{\tau_J(x)|\dot{\phi}|(x, \phi_{max})}}{\frac{\tau_J(\phi_{max})}{M\dot{\phi}_{max}}}, \tag{5.2.23}$$

with $D_C := D_{T_\phi} \backslash \{0\} \times (0, \infty)$. It is important to remark here that in (5.2.22), ${}^k\eta_{0,j}$, ${}^kv_{\phi,j}$, ${}^k\phi_{max}$ and λ_a are all constant. Consequently, one can regard the right-hand side of (5.2.22) as a function of the deflection which is defined on $(-{}^k\phi_{max}, {}^k\phi_{max}) \backslash \{0\}$. If $x_1(t)$ is an element of this set, with $t \in D_{k_j}$, the value of this function at this deflection will be equal to the ratio $\frac{u(t)}{\dot{\theta}_{max}} = \frac{{}^ku}{\dot{\theta}_{max}}$ and thus

non-zero. Moreover, since both ${}^k v_{\phi,j}$ and u are constant in D_{k_j} the set $\{x_1(t) \in \mathbb{R} | t \in D_{k_j}\}$ will describe an open interval depending only on $x_1(t_{S,k_j})$ and $x_1(t_{S,k_{j+1}})$, and for each non-zero deflection value in this interval the function will take the exactly same value. Finally, even if there exists a time $t \in D_{k_j}$ with $x_1(t) = 0$ this function can still be used to determine $u(t)$ by taking its limit as the deflection goes to zero. This simply follows from the fact that there exists at most one zero of x_1 in D_{k_j} and that $u|_{D_{k_j}}$ is constant.

Our discussion above shows how the right-hand side of (5.2.22) can be used to determine the control in D_{k_j}. Based on the continuity properties of u, the value of u at t_{S,k_j} can be clearly obtained using this expression as well. More specifically, $u(t_{S,k_j})$ will be equal to the limit of the expression as $x_1(t)$ approaches $x_1(t_{S,k_j})$ from the right if ${}^k v_{\phi,j} > 0$ and from the left, otherwise. The value of the control u at $t_{S,k_{j+1}}$ can be similarly obtained by calculating the corresponding limit of the expression at $x_1(t_{S,k_{j+1}})$, if $t_{S,k_{j+1}}$ is not a switching time. Nevertheless, if $t_{S,k_{j+1}}$ is a switching time the jump in u must be accounted for as well. In order to find $u(t_{S,k_{j+1}})$, it is therefore crucial to determine whether $t_{S,k_{j+1}}$ is a switching time or not. The following proposition shows how this can be done by using the product at the numerator of the right-hand side of (5.2.22).

Proposition 10. *Let $\Lambda = (\boldsymbol{x}, u, \boldsymbol{\lambda}, \lambda_a)$ be an extremal lift for the LVMP and u a control with $i \geq 0$ switchings. Moreover, let $k \in S_i$ such that ${}^k E_{rel} > 0$, $j \in S_{m_k}, t \in D_{k_j}$ and $\phi = x_1(t)$. Finally, let S_{ϕ_b} the set of all deflections ϕ_b such that $|{}^b\phi| \leq {}^k\phi_{max}$ and*

$$\lim_{D_{k_\phi}\setminus\{0\}\ni x \to \phi_b} \left[{}^k\eta_{0,j} - \lambda_a C(x, {}^k\phi_{max}) \right] x = 0, \tag{5.2.24}$$

where D_{k_ϕ} denotes the open interval $(-{}^k\phi_{max}, {}^k\phi_{max})$. Then, t_{S,k_j} is the k'th switching time if and only if $k > 0$ and there exists an element $\phi_b \in S_{\phi_b}$ such that $\operatorname{sgn}(\phi - \phi_b) = {}^k v_{\phi,j}$. Moreover, in this case we have

$$x_1(t_{S,k_j}) = \begin{cases} \min\{\phi_b \in S_{\phi_b} | \phi_b > \phi\}, & {}^k v_{\phi,j} = -1 \\ \max\{\phi_b \in S_{\phi_b} | \phi_b < \phi\}, & {}^k v_{\phi,j} = 1 \end{cases}. \tag{5.2.25}$$

Similarly, $t_{S,k_{j+1}}$ is the $k+1$'th switching time (respectively, the final time) if and only if $k < i$ (respectively, $k = i$) and there exists an element $\phi_b \in S_{\phi_b}$ such that $\operatorname{sgn}(\phi_b - \phi) = {}^k v_{\phi,j}$. Finally, in this case we have

$$x_1(t_{S,k_{j+1}}) = \begin{cases} \max\{\phi_b \in S_{\phi_b} | \phi_b < \phi\}, & {}^k v_{\phi,j} = -1 \\ \min\{\phi_b \in S_{\phi_b} | \phi_b > \phi\}, & {}^k v_{\phi,j} = 1 \end{cases}. \tag{5.2.26}$$

Proof. See Appendix B.3.2. $\qquad\square$

Prop. 10 provides now for both t_{S,k_j} and $t_{S,k_{j+1}}$ a sufficient and necessary condition to be a switching time. Moreover, for each of these times the attained
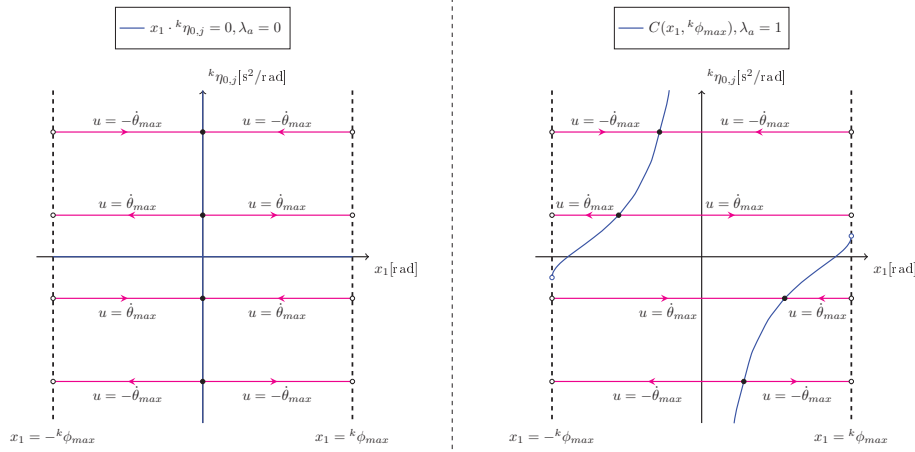
Figure 5.2.2: Controls along Extremal Lifts
$(t \in D_{k_j}, i \in \{0, 1, \ldots\}, k \in S_i, j \in S_{m_k}, {}^k\phi_{max} > 0)$

deflection is also provided if the control switches at this time, see (5.2.25)-(5.2.26). According to the definition of the set S_{ϕ_b} in the proposition, it is clear that the zeros of the limits of the product in (5.2.24) play an important role in determining the deflection values $x_1(t_{S,k_j})$ and $x_1(t_{S,k_{j+1}})$. Moreover, as we have already discussed the sign of this product, with $x = x_1(t)$, divided by ${}^k v_{\phi,j}$ uniquely determines the control in D_{k_j}, see (5.2.22). In order to better understand the dependence of the control on the time-varying deflection and the parameters ${}^k\eta_{0,j}$, ${}^k v_{\phi,j}$ and λ_a, we will next investigate in detail the different possibilities for the sign of this product along Λ, the zeros of its limits and the value of ${}^k v_{\phi,j}$. We start our investigation by distinguishing between two cases based on the value of λ_a.

Abnormal Extremal Lifts   Let us assume that Λ is an abnormal extremal lift so that $\lambda_a = 0$. According to (5.2.22), the value of u in D_{k_j} depends then directly on the sign of the product ${}^k\eta_{0,j} x_1$ in D_{k_j} and ${}^k v_{\phi,j}$. Clearly, ${}^k v_{\phi,j}$ is an element of $\{-1, 1\}$. Similarly, the sign of ${}^k\eta_{0,j}$ also belongs to this set. Indeed, according to (5.2.4) and Prop. 8 both ${}^k\lambda_1$ and ${}^k x_1$ must be equal to zero since λ_a is equal to zero and $\boldsymbol{x}_0 = \boldsymbol{0}$. Moreover, since ${}^k\eta_c = \lambda_a$ we know from (5.2.20) and Prop. 9 that $|{}^k\eta_{0,j}|$ will be equal to $|{}^k\eta_{0,0}| = |{}^k\lambda_2|$. It follows then from (5.2.5) that ${}^k\boldsymbol{\lambda} \neq \boldsymbol{0}$ holds implying that ${}^k\eta_{0,j}$ is non-zero. Finally, the sign of x_1 in D_{k_j} is constant and non-zero. To see this, let us first note that for a given time $t \in D_{k_j}$ it follows from (5.2.4) and the positiveness of the relative energy ${}^k E_{rel}$ that $\lambda_1(t)$ must be zero if $x_1(t) = 0$. According to Prop. 8, t would then be a switching time contradicting the fact that it is an element of $(t_{S,k}, t_{S,k+1})$. Since x_1 is continuous, we can finally conclude that its sign remains constant and belongs to $\{-1, 1\}$.

   With our discussion above, we now see that there are in total eight different

possibilities regarding the signs of $^k\eta_{0,j}$ and x_1 and the value of $^kv_{\phi,j}$. Each of these possibilities results according to (5.2.22) in the control u to attain either its minimum or maximum value. This is graphically illustrated in Fig. 5.2.2 (Left) by introducing a coordinate system in which the horizontal and vertical axis denote the values of x_1 and $^k\eta_{0,j}$, respectively. More specifically, for each of the eight possibilities a horizontal line segment has been drawn there with an arrow representing the value of $^kv_{\phi,j}$. These segments all correspond to a particular value of $^k\eta_{0,j}$ and either start from the vertical axis, i.e. at zero deflection, and terminate at $^kv_{\phi,j}{}^k\phi_{max}$ or vice versa. It is important to notice here that for $\lambda_a = 0$, the equality in (5.2.24) is satisfied, regardless of the particular values of $^k\eta_{0,j}$ and $^kv_{\phi,j}$, if and only if the deflection ϕ_b is zero. This is indicated in Fig. 5.2.2 (Left) by the black dots on the vertical axis and can be used with (5.2.22) and Prop. 10 to find explicit expressions for the deflections $x_1(t_{S,k_j}), x_1(t_{S,k_{j+1}})$ and the control $u(t_{S,k_j})$ depending on whether t_{S,k_j} is the initial time, a switching time or a time at which $\dot{x}_1$ changes its sign without a change in the control. Moreover, it can also be determined whether $t_{S,k_{j+1}}$ will be equal to the final time of D_{k_j}, i.e. to $t_{S,k+1}$, which in turn yields the value of $u(t_{S,k_{j+1}})$. The resulting expressions are provided[5] in Table 5.2a.

Normal Extremal Lifts   If Λ is a normal extremal lift, i.e. $\lambda_a = 1$, $^k\eta_{0,j}$ can this time take any real value without violating (5.2.4)-(5.2.5). Moreover, in this case the function C will influence the values which the product in (5.2.24) will take along Λ. In the following, we will first take a closer look at the properties of this function. Then, similar to the previous case we will introduce a graphical illustration which clarifies the dependence of the control on $^k\eta_{0,j}$, x_1 and $^kv_{\phi,j}$.

First of all, according to (5.2.23) and the symmetry properties of $\tau_J, |\dot{\phi}|$ and T_ϕ we have

$$C(-x, \phi_{max}) = -C(x, \phi_{max}), \tag{5.2.27}$$

for each $(x, \phi_{max}) \in D_C$. Moreover, at each such point C is differentiable with respect to x and the corresponding partial derivative is given by

$$\frac{\partial C}{\partial x}(x, \phi_{max}) = \frac{M\dot{\phi}_{max}K_J(x)}{\tau_J^2(x)|\dot{\phi}|(x, \phi_{max})}, \tag{5.2.28}$$

where we have made use of (3.1.6) and (3.2.7). Since (5.2.28) is positive for each $(x, \phi_{max}) \in D_C$, the function $C(., \phi_{max})$ is strictly increasing on $(-\phi_{max}, 0)$ and $(0, \phi_{max})$ for each $\phi_{max} > 0$. Finally, using (3.2.14) and (5.2.23) it can be shown that the limits of this function as x approaches zero from the right and as x approaches ϕ_{max} from the left are given by

$$\lim_{x \to 0^+} C(x, \phi_{max}) = -\infty, \tag{5.2.29}$$

---

[5]We use "$\lfloor . \rfloor$" to denote the floor function. Consequently, the value of $\left\lfloor \frac{t_{S,k_{j+1}}}{t_{S,k+1}} \right\rfloor$ determines whether $t_{S,k_{j+1}}$ is equal to $t_{S,k+1}$ or not.

	$\frac{t_{S,k_{j+1}}}{t_{S,k+1}}$	$x_1(t_{S,k_j})$	$u(t_{S,k_j})$	$x_1(t_{S,k_{j+1}})$	$u(t_{S,k_{j+1}})$
$t_{S,k_j} = t_{S,k}$	0	0	$\frac{\dot\theta_{max}}{\mathrm{sgn}(^k\eta_{0,j})}$	$\frac{^k\phi_{max}}{^kv_{\phi,j}}$	^ku
$t_{S,k_j} > t_{S,k}$	1	$-\frac{^k\phi_{max}}{^kv_{\phi,j}}$	^ku	0	$\begin{cases} -^ku & k<i \\ ^ku & k=i \end{cases}$

(a) Abnormal Extremal Lifts $(\lambda_a = 0, {}^k\eta_{0,j} \neq 0)$

		$\frac{t_{S,k_{j+1}}}{t_{S,k+1}}$	$x_1(t_{S,k_j})$	$u(t_{S,k_j})$	$x_1(t_{S,k_{j+1}})$	$u(t_{S,k_{j+1}})$
$t_{S,k_j} = 0$	$\frac{^k\eta_{0,j}}{^kv_{\phi,j}} \leq \Delta(^k\phi_{max})$	1	0	$\frac{\dot\theta_{max}}{^kv_{\phi,j}}$	$K_{\phi,1}$	$\begin{cases} -^ku & k<i \\ ^ku & k=i \end{cases}$
	$\frac{^k\eta_{0,j}}{^kv_{\phi,j}} > \Delta(^k\phi_{max})$	0	0	$\frac{\dot\theta_{max}}{^kv_{\phi,j}}$	$\frac{^k\phi_{max}}{^kv_{\phi,j}}$	^ku

(b) Normal Extremal Lifts $(\lambda_a = 1, k = j = 0, \Delta(^k\phi_{max}) \in \mathbb{R})$

		$\frac{t_{S,k_{j+1}}}{t_{S,k+1}}$	$x_1(t_{S,k_j})$	$u(t_{S,k_j})$	$x_1(t_{S,k_{j+1}})$	$u(t_{S,k_{j+1}})$
$t_{S,k_j} = t_{S,k}$, $k > 0$	$\frac{|^k\eta_{0,j}|}{|\Delta(^k\phi_{max})|} < 1$	–	–	–	–	–
	$\frac{|^k\eta_{0,j}|}{|\Delta(^k\phi_{max})|} \geq 1$	0	$K_{\phi,2}$	$\frac{\dot\theta_{max}}{\mathrm{sgn}(^k\eta_{0,j})}$	$\frac{^k\phi_{max}}{^kv_{\phi,j}}$	^ku
$t_{S,k_j} > t_{S,k}$, $k \geq 0$	$\frac{|^k\eta_{0,j}|}{|\Delta(^k\phi_{max})|} < 1$	0	$-\frac{^k\phi_{max}}{^kv_{\phi,j}}$	^ku	$\frac{^k\phi_{max}}{^kv_{\phi,j}}$	^ku
	$\frac{|^k\eta_{0,j}|}{|\Delta(^k\phi_{max})|} = 1$	–	–	–	–	–
	$\frac{|^k\eta_{0,j}|}{|\Delta(^k\phi_{max})|} > 1$	1	$-\frac{^k\phi_{max}}{^kv_{\phi,j}}$	^ku	$K_{\phi,2}$	$\begin{cases} -^ku & k<i \\ ^ku & k=i \end{cases}$

(c) Normal Extremal Lifts $(\lambda_a = 1, \Delta(^k\phi_{max}) < 0)$

		$\frac{t_{S,k_{j+1}}}{t_{S,k+1}}$	$x_1(t_{S,k_j})$	$u(t_{S,k_j})$	$x_1(t_{S,k_{j+1}})$	$u(t_{S,k_{j+1}})$
$t_{S,k_j} = t_{S,k}$, $k > 0$	$^k\eta_{0,j} = 0$	1	$-\frac{^k\phi_{max}}{^kv_{\phi,j}}$	$\frac{\dot\theta_{max}}{^kv_{\phi,j}}$	$\frac{^k\phi_{max}}{^kv_{\phi,j}}$	$\begin{cases} -^ku & k<i \\ ^ku & k=i \end{cases}$
	$|^k\eta_{0,j}| > 0$	0	$K_{\phi,2}$	$\frac{\dot\theta_{max}}{\mathrm{sgn}(^k\eta_{0,j})}$	$\frac{^k\phi_{max}}{^kv_{\phi,j}}$	^ku
$t_{S,k_j} > t_{S,k}$, $k \geq 0$	$^k\eta_{0,j} = 0$	–	–	–	–	–
	$|^k\eta_{0,j}| > 0$	1	$-\frac{^k\phi_{max}}{^kv_{\phi,j}}$	^ku	$K_{\phi,2}$	$\begin{cases} -^ku & k<i \\ ^ku & k=i \end{cases}$

(d) Normal Extremal Lifts $(\lambda_a = 1, \Delta(^k\phi_{max}) = 0)$

		$\frac{t_{S,k_{j+1}}}{t_{S,k+1}}$	$x_1(t_{S,k_j})$	$u(t_{S,k_j})$	$x_1(t_{S,k_{j+1}})$	$u(t_{S,k_{j+1}})$
$t_{S,k_j} = t_{S,k}$, $k > 0$	$\frac{|^k\eta_{0,j}|}{\Delta(^k\phi_{max})} \leq 1$	$\begin{cases} 1 & \frac{^kv_{\phi,j}}{\mathrm{sgn}(^kx_1)} < 0 \\ 0 & \frac{^kv_{\phi,j}}{\mathrm{sgn}(^kx_1)} > 0 \end{cases}$	$K_{\phi,3}$	$-\frac{\dot\theta_{max}}{\mathrm{sgn}(^kx_1)}$	$\begin{cases} K_{\phi,4} & \frac{^kv_{\phi,j}}{\mathrm{sgn}(^kx_1)} < 0 \\ \frac{^k\phi_{max}}{\mathrm{sgn}(^kx_1)} & \frac{^kv_{\phi,j}}{\mathrm{sgn}(^kx_1)} > 0 \end{cases}$	$\begin{cases} \frac{^kv_{\phi,j}\cdot{}^ku}{\mathrm{sgn}(^kx_1)} & k<i \\ ^ku & k=i \end{cases}$
	$\frac{|^k\eta_{0,j}|}{\Delta(^k\phi_{max})} > 1$	0	$K_{\phi,2}$	$\frac{\dot\theta_{max}}{\mathrm{sgn}(^k\eta_{0,j})}$	$\frac{^k\phi_{max}}{^kv_{\phi,j}}$	^ku
$t_{S,k_j} > t_{S,k}$, $k \geq 0$	$\frac{|^k\eta_{0,j}|}{\Delta(^k\phi_{max})} \leq 1$	1	$-\frac{^k\phi_{max}}{^kv_{\phi,j}}$	^ku	$K_{\phi,5}$	$\begin{cases} -^ku & k<i \\ ^ku & k=i \end{cases}$
	$\frac{|^k\eta_{0,j}|}{\Delta(^k\phi_{max})} > 1$	1	$-\frac{^k\phi_{max}}{^kv_{\phi,j}}$	^ku	$K_{\phi,2}$	$\begin{cases} -^ku & k<i \\ ^ku & k=i \end{cases}$

(e) Normal Extremal Lifts $(\lambda_a = 1, \Delta(^k\phi_{max}) > 0)$

$K_{\phi,1}$	$K_{\phi,2}$	$K_{\phi,3}$	$K_{\phi,4}$	$K_{\phi,5}$
$\frac{K_\phi\left(\frac{^k\eta_{0,j}}{^kv_{\phi,j}}, {}^k\phi_{max}\right)}{^kv_{\phi,j}}$	$\frac{K_\phi(-|^k\eta_{0,j}|, {}^k\phi_{max})}{-\mathrm{sgn}(^k\eta_{0,j})}$	$\frac{K_\phi\left(\frac{^k\eta_{0,j}}{\mathrm{sgn}(^kx_1)}, {}^k\phi_{max}\right)}{\mathrm{sgn}(^kx_1)}$	$\frac{K_\phi\left(-\frac{^k\eta_{0,j}}{\mathrm{sgn}(^kx_1)}, {}^k\phi_{max}\right)}{-\mathrm{sgn}(^kx_1)}$	$\frac{K_\phi\left(-\frac{^k\eta_{0,j}}{^kv_{\phi,j}}, {}^k\phi_{max}\right)}{-^kv_{\phi,j}}$

(f) Parameter Definitions

Table 5.2: Deflection Values and Controls at the Boundaries of D_{k_j} $(i \in \{0,1,\ldots\}, k \in S_i, j \in S_{m_k}, {}^k\phi_{max} > 0, {}^kv_{\phi,j} \in \{-1,1\}, {}^k\eta_{0,j} \in \mathbb{R})$

and

$$\lim_{x \to \phi_{max}^-} C(x, \phi_{max}) = \Delta(\phi_{max}), \qquad (5.2.30)$$

respectively. It is important to recall here that the function Δ in the second limit was introduced in Sec. 5.2.2 when we discussed how to use Prop. 9 to construct a costate trajectory and analysed the changes in $\eta(0, \phi_{max})$ which can occur at the minimal and/or maximal deflection values, see (5.2.20)-(5.2.21).

Based on the properties of C, we can now conclude that the graph of the function $C(., {}^k\phi_{max})$ divides the set $\{(x_1, {}^k\eta_{0,j}) \in \mathbb{R}^2 | |x_1| < {}^k\phi_{max}\}$ into three open regions as illustrated in Fig. 5.2.2 (Right). As indicated there by the horizontal line segments and arrows, for each of these regions the corresponding elements lead, according to (5.2.22), to the same control value when the sign of $\dot{x}_1$ is the same. In addition, regardless of the value of ${}^k\eta_{0,j}$ and ${}^kv_{\phi,j}$ there can exist at most two deflection values for ϕ_b for which the equality in (5.2.24) will hold. In other words, the set S_{ϕ_b} from Prop. 10 has at most two elements and it follows further from (5.2.27)-(5.2.30) that the number of elements depends on ${}^k\eta_{0,j}$ and $\Delta({}^k\phi_{max})$. Finally, these elements can all be graphically determined by finding the intersection points between a horizontal line, which corresponds to the value of ${}^k\eta_{0,j}$, and the two curves described by the closure of the graph of $C(., {}^k\phi_{max})$, see Fig. 5.2.2 (Right). As in the previous case, this can be used together with (5.2.22) and Prop. 10 to find expressions for the deflections and controls at the boundaries of D_{k_j} depending on the properties of t_{S,k_j}. These are provided in Table 5.2b-5.2e, where we use $K_\phi : (-\infty, \Delta(\phi_{max})] \times (0, \infty) \to (0, \phi_{max}], (\eta_0, \phi_{max}) \to K_\phi(\eta_0, \phi_{max})$ to denote the function which for each $\phi_{max} > 0$ equals to the continuously extended inverse of the function $C|_{(0,\phi_{max}) \times \{\phi_{max}\}}(., \phi_{max})$. Notice that each of these tables considers a different case which is characterized by whether t_{S,k_j} is equal to the initial time or not and by the sign of $\Delta({}^k\phi_{max})$. Moreover, for each of these cases the magnitude of ${}^k\eta_{0,j}$ and $\Delta({}^k\phi_{max})$ influence whether $t_{S,k_{j+1}}$ can be equal to a switching time or the terminal time.

It is important to remark here that knowing the deflection values at t_{S,k_j} and $t_{S,k_{j+1}}$, as provided in Table 5.2, we can directly determine the length of the interval D_{k_j} since ${}^kv_{\phi,j}$ is constant. Consequently, by combining all our results so far we can now uniquely construct the extremal lift Λ in the closure of D_{k_j} by knowing only t_{S,k_j}, $\boldsymbol{x}(t_{S,k_j}), \boldsymbol{\lambda}(t_{S,k_j})$ and the integers k and i. Indeed, based on our results from Sec. 5.2.1 we can first determine the control $u(t_{S,k_j})$ using $\boldsymbol{\lambda}(t_{S,k_j})$ and then ${}^k\phi_{max}$ and ${}^kv_{\phi,j}$ using this control and $\boldsymbol{x}(t_{S,k_j})$. In addition, depending on the value of t_{S,k_j} and $\lambda_1(t_{S,k_j})$ we can find out whether t_{S,k_j} is equal to $t_{S,k}$ or not. Furthermore, we can determine the value of λ_a using (5.2.4) and the value of ${}^k\eta_{0,j}$ using Prop. 9. Moreover, the expressions in Table 5.2 together with (3.2.3) will yield $t_{S,k_{j+1}}$ and $x_1(t_{S,k_{j+1}})$. Using the construction procedures for states and costates in Sec. 4.1 and Sec. 5.2.2, this will finally lead to the desired extremal lift Λ in the closure of D_{k_j}. In addition, using either the value of λ_1 at $t_{S,k_{j+1}}$ or again Table 5.2 we can additionally determine whether $t_{S,k_{j+1}}$ is equal to $t_{S,k+1}$ or not.

Our discussion so far is valid for any $j \in S_{m_k}$. Since both $\boldsymbol{x}$ and $\boldsymbol{\lambda}$ are

continuous, this means that starting from $j = 0$ we can actually iteratively apply the procedure described above to determine m_k and construct Λ in the closure of D_k by using the values of $t_{S,k}$, $^k\boldsymbol{x}$, $^k\boldsymbol{\lambda}$, k and i. Similarly, in our choice for $k \in S_i$ we only required $^kE_{rel}$ to be positive. Consequently, if this energy is known to be positive for each $k \in S_i$ our results actually provide an iterative procedure to fully construct the extremal lift Λ depending only[6] on its initial costate $\boldsymbol{\lambda}_0$ and the switching number of its control. In the following section, we will see that the relative energy is indeed always positive along trajectories in extremal lifts. Moreover, we will illustrate how to determine the set of all extremals by making use of the iterative procedures just described.

5.3   Extremals for the LVMP

Let $\Lambda = (\boldsymbol{x}, u, \boldsymbol{\lambda}, \lambda_a)$ be an extremal lift for the LVMP such that u is a switching control with $i \geq 0$ switchings. It follows then from the transversality condition (5.2.5) that the terminal costate is non-zero and this implies due to the linearity of the costate dynamics the following inequality for the initial costate:

$$\boldsymbol{\lambda}_0 = (\lambda_{10}, \lambda_{20}) \neq \boldsymbol{0}. \tag{5.3.1}$$

Moreover, by evaluating the Hamiltonian function $\mathbb{H}(\boldsymbol{x}(t), u(t), \boldsymbol{\lambda}(t))$ at the initial time using (5.2.3)-(5.2.4) and noting that $\boldsymbol{x}$ starts from the origin we can arrive at the following equality for λ_{10}:

$$\lambda_{10} = -\frac{\lambda_a}{^0u} \in \{-\frac{1}{\dot{\theta}_{max}}, 0, \frac{1}{\dot{\theta}_{max}}\}, \tag{5.3.2}$$

where we have also used the fact that $\lambda_a \in \{0, 1\}$ and $|^0u| = \dot{\theta}_{max}$, see Prop. 7-8. Finally, as already discussed in Sec. 5.2 the terminal control in an extremal lift is always positive which means that for each $k \in S_i$ the control must satisfy

$$^ku = (-1)^{i+k}\dot{\theta}_{max}. \tag{5.3.3}$$

Depending on whether $|\lambda_{10}|$ is zero or non-zero, or equivalently depending on whether Λ is an abnormal or a normal extremal lift, evaluating (5.3.3) at $k = 0$ leads then according to (5.2.1), (5.2.8) and (5.3.2) to two different conditions for the sign of the initial costate in terms of the switching number:

$$\lambda_{10} = 0 \Rightarrow \operatorname{sgn}(\lambda_{20}) = (-1)^i, \tag{5.3.4}$$

and

$$\lambda_{10} \neq 0 \Rightarrow \operatorname{sgn}(\lambda_{10}) = (-1)^{i-1}. \tag{5.3.5}$$

Clearly, there exists an infinite number of switching numbers $i \geq 0$ and initial costates $\boldsymbol{\lambda}_0 \in (\mathbb{R}^2)^*$ which satisfy (5.3.1)-(5.3.2) and (5.3.4)-(5.3.5). Moreover, it follows from the properties of the state and costate dynamics in (2.1.4) and

---

[6]Notice that $t_{S,0} = 0$ and $^0\boldsymbol{x} = \boldsymbol{x}_0 = \boldsymbol{0}$.

(5.2.1) that for each such $\boldsymbol{\lambda}_0$ and i there always exists a unique extremal lift. In this section, we will first show how to construct this extremal lift. More specifically, using mainly our results from Sec. 5.2 we will show in Sec. 5.3.1-5.3.2 how to uniquely construct abnormal and normal extremal lifts knowing only their initial costate and the switching number of their controls. Exploiting the properties of the extremals in these lifts, we will then show in Sec. 5.3.3 how the set of all extremals can be parameterized by using only a one-dimensional parameter. Since optimal extremals necessarily belong to this set, this will enable us to reformulate the LVMP as a nonlinear programming problem (NPP) [5] whose solution can be determined graphically or numerically.

5.3.1 Abnormal Extremal Lifts

Assuming that $\Lambda = (\boldsymbol{x}, u, \boldsymbol{\lambda}, \lambda_a)$ is an abnormal extremal lift, we know from (5.3.1)-(5.3.2) that λ_{10} is equal to zero and that λ_{20} is non-zero with its sign given by (5.3.4). Moreover, regardless of the sign of λ_{20}, or equivalently the switching number i of u, the magnitude of the initial control will be equal to the maximal motor velocity so that the relative energy ${}^0E_{rel}$ will according to (4.1.2) and (4.2.5) satisfy

$$ {}^0E_{rel} = E_{r,max}(0) = \frac{1}{2}M\dot{\theta}_{max}^2, \qquad (5.3.6) $$

since $\boldsymbol{x}_0 = \boldsymbol{0}$. Consequently, ${}^0E_{rel}$ is positive and we can use Table 5.2a, Prop. 9 and our results from Chapter 4 to show that the control u in Λ can be uniquely determined by its switching number i. Indeed, noting first that ${}^0\eta_{0,0} = \lambda_{20} \neq 0$ holds by Prop. 9, we can see from the first row of the table that $t_{S,0_1}$ is never a switching time or the final time. Moreover, the magnitude of the deflection at this time is equal to ${}^0\phi_{max} > 0$. Using then the second row of the table, we can see that $t_{S,0_2}$ is a switching time if $i > 0$ and the terminal time if $i = 0$, i.e. $t_{S,0_2} = t_{S,1}$. Furthermore, in both cases we have $x_1(t_{S,1}) = 0$. Consequently, the time $t_{S,1}$ is equal to $\frac{T_p({}^0\phi_{max})}{2}$ which together with (5.3.3) uniquely determines the control u in D_0. In addition, $m_0 = 1$ and for each $j \in S_{m_0}$ we have the equalities ${}^0v_{\phi,j} = (-1)^j \operatorname{sgn}({}^0\dot{x}_1) = (-1)^j \operatorname{sgn}(\lambda_{20})$ and, by (5.2.4), (5.2.17) and (5.2.20), ${}^0\eta_{0,j} = (-1)^j\lambda_{20}$. Using these expressions in (5.2.22), we can then directly relate the applied control u to the sign of the deflection x_1 as follows:

$$ [\forall t \in (t_{S,0}, t_{S,1})] \left(\frac{u(t)}{\dot{\theta}_{max}} = \operatorname{sgn}(x_1(t)) \neq 0 \right). \qquad (5.3.7) $$

It is important to realize here that the control strategy in (5.3.7) has already been encountered in Sec. 4.2 when discussing switching control strategies maximizing the energy of an EJ with a velocity-sourced SEA. In particular, if $i = 0$ it follows from Prop. 3-4 that u is a solution to the EMP since $x_1(t_f) = x_1(t_{S,1}) = 0$. As we show in the following proposition, if $i > 0$ the relation between u and x_1 in (5.3.7) still holds at each time in D at which the deflection is non-zero. Consequently, the control u always provides a solution to the EMP.

Proposition 11. *Let $(\boldsymbol{x}, u)$ be an admissible controlled trajectory defined on $D = [0, t_f]$ with $\boldsymbol{x}_0 = \boldsymbol{0}$. Then, $(\boldsymbol{x}, u)$ is an abnormal extremal if and only if there exists an integer $i \geq 0$ such that u is a switching control with i switchings and solves the EMP with ${}^0u = (-1)^i \dot{\theta}_{max}$. Moreover, in this case we have for each $k \in S_{i+1} \backslash \{0\}$*

$$t_{S,k} = t_{min}(k), \tag{5.3.8}$$

and

$$
{}^k\boldsymbol{x} = (-1)^{i+k-1} 2k \begin{pmatrix} 0 \\ \dot{\theta}_{max} \end{pmatrix}. \tag{5.3.9}
$$

Proof. See Appendix B.3.3. $\qquad\square$

With Prop. 11 we now see that the control u in Λ can indeed be uniquely determined by its switching number i, see (5.3.3) and (5.3.8). Moreover, knowing the value of i the corresponding trajectory $\boldsymbol{x}$ can also be uniquely constructed using our results from Sec. 4.1, see (5.3.9). Note that for the case when $i = 1$, this construction is already illustrated in Fig. 4.1.1 for the systems Σ_1, Σ_2 and Σ_3 since the control strategies depicted there solve the corresponding EMP with one switching and with ${}^0u = -\dot{\theta}_{max}$.

In order to now fully construct Λ, we need to determine the costate $\boldsymbol{\lambda}$ and for this it is sufficient to know the magnitude of λ_{20} in addition to i. This is shown in the following proposition, where we use our results from Sec. 5.2.2 to describe $\boldsymbol{\lambda}$ in terms of the extremal $(\boldsymbol{x}, u)$.

Proposition 12. *Let $\Lambda = (\boldsymbol{x}, u, \boldsymbol{\lambda}, \lambda_a)$ be an abnormal extremal such that u is a control with $i \geq 0$ switchings. Then, for each $k \in S_i$ and $t \in D_k$ we have*

$$
\boldsymbol{\lambda}(t) = \frac{|\lambda_{20}|}{k \dot{\phi}_{max}} \left(-\frac{\tau_J(x_1(t))}{M} \quad \dot{x}_1(t) \right). \tag{5.3.10}
$$

Proof. See Appendix B.3.3. $\qquad\square$

When discussing the costate trajectories depicted in Fig. 5.2.1 (Top), we had actually already noted the existence of a linear relation between the costate, the torque in the spring and the time-derivative of the deflection for the case when the Hamiltonian function is equal to zero. With Prop. 12, we now additionally see how for an abnormal extremal this relation depends on the relative energy. In the following we will see, as in Fig. 5.2.1 (Bottom), that the relation between costates and the extremals are more complex if the Hamiltonian function is non-zero.

5.3.2 Normal Extremal Lifts

If $\Lambda = (\boldsymbol{x}, u, \boldsymbol{\lambda}, \lambda_a)$ is a normal extremal lift, the conditions (5.3.2) and (5.3.5) uniquely determine λ_{10} in terms of the switching number i of the control u. Moreover, since the initial control is equal to the maximal motor velocity and since by Prop. 8 we have ${}^kx_1 \neq 0$ for each $k \in S_i \backslash \{0\}$ the relative energy

	$(-1)^i\lambda_{20} < \Delta(^0\phi_{max})$	$(-1)^i\lambda_{20} = \Delta(^0\phi_{max})$	$(-1)^i\lambda_{20} > \Delta(^0\phi_{max})$
m_0	0	0	1
$^1x_1$	$(-1)^iK_\phi\left((-1)^i\lambda_{20}, {}^0\phi_{max}\right)$	$(-1)^i \cdot {}^0\phi_{max}$	$(-1)^iK_\phi\left((-1)^i \cdot {}^0\eta_{0,1}, {}^0\phi_{max}\right)$
$t_{S,1}$	$T_\phi(|^1x_1|, {}^0\phi_{max})$	$\frac{T_p(^0\phi_{max})}{4}$	$\frac{T_p(^0\phi_{max})}{2} - T_\phi(|^1x_1|, {}^0\phi_{max})$
$^0\eta_{0,1} = (-1)^i2\Delta(^0\phi_{max}) - \lambda_{20},\ E_{pot}(^0\phi_{max}) = E_{r,max}(0),\ {}^0v_{\phi,0} = {}^0u = (-1)^i, i \in \{0,1,2,\ldots\}$			

Table 5.3: $m_0, {}^1x_1$ and $t_{S,1}$ along a Normal Extremal

will remain positive along $\boldsymbol{x}$. Consequently, Λ can be iteratively constructed if the values of $\lambda_{20} \in \mathbb{R}$ and $i \geq 0$ are known, see Sec. 5.2.3. In the following, we will illustrate how to carry out this construction and clarify how these two values influence the switching times of the control as well as the deflection values attained at these times. We start our discussion with the construction of Λ in the interval D_0. Focusing on the case when the control is not constant, i.e. $i > 0$, we then show how for each $k \in S_i\backslash\{0\}$ we can construct Λ in D_k using mainly the value of the deflection, the sign of its time-derivative and the relative energy at the k'th switching time.

Construction in D_0 $(i \geq 0)$ Let us first note that the sign of the control ^0u and thus $^0v_{\phi,0}$ directly depends on the value of i, see (5.3.3). Moreover, since the initial deflection is equal to zero we know by Prop. 9 that $^0\eta_{0,0} = \lambda_{20}$ will hold. Using Table 5.2b-5.2e, with $k = 0$ and $j \in S_{m_0} \subset \{0,1\}$, together with (5.2.20) we can then find different expressions for the values of $m_0, {}^1x_1$ and $t_{S,1}$ depending on $\lambda_{20}, \Delta(^0\phi_{max})$ and i. Table 5.3 provides these expressions while Fig. 5.3.1 (Top) graphically illustrates their derivation. More specifically, focusing on the case when i is an even integer the figure shows how we can determine them by using the graph of $C(., {}^0\phi_{max})$ and by plotting for each $j \in S_{m_0}$ the scalar $^0\eta_{0,j}$ as a constant function of the deflection, see Fig. 5.2.2 (Right). For the case when i is an odd integer, the expressions in Table 5.3 can be similarly derived using the graph of $C(., {}^0\phi_{max})$ and noting that $^0v_{\phi,0}$ will this time be negative. The dependence of the provided expressions on the switching number follows from the symmetry properties of C and from (5.2.20).

With the expressions in Table 5.3, we can now uniquely construct both the control u and the corresponding trajectory $\boldsymbol{x}$ in D_0 if we know the sign of the initial control and λ_{20}, see Fig. 5.3.1 (Bottom). Moreover, by using the resulting controlled trajectory and applying the construction procedure from Sec. 5.2.2 with $^0\eta_{0,0} = \lambda_{20}$ the costate $\boldsymbol{\lambda}$ can be determined, as well. This shows how to construct Λ in D_0 depending only on λ_{20} and i.

Construction in D_k $(k \geq 1, i \geq 1)$ Let us assume that $i \geq 1$ and $k \in S_i\backslash\{0\}$ so that $t_{S,k}$ is a switching time and $^k\eta_{0,0}$ is equal to $C(^kx_1, {}^k\phi_{max})$, see Prop. 10. According to the relations provided in Table 5.2b-5.2e, there exist then different possibilities for the variables $m_k, {}^{k+1}x_1$ and $t_{S,k+1}$ depending on the values of $^kx_1, {}^k\phi_{max}, {}^kv_{\phi,0}$ and $\Delta(^k\phi_{max})$. By successively applying the provided relations in the table, as discussed in Sec. 5.2.3, and making use of
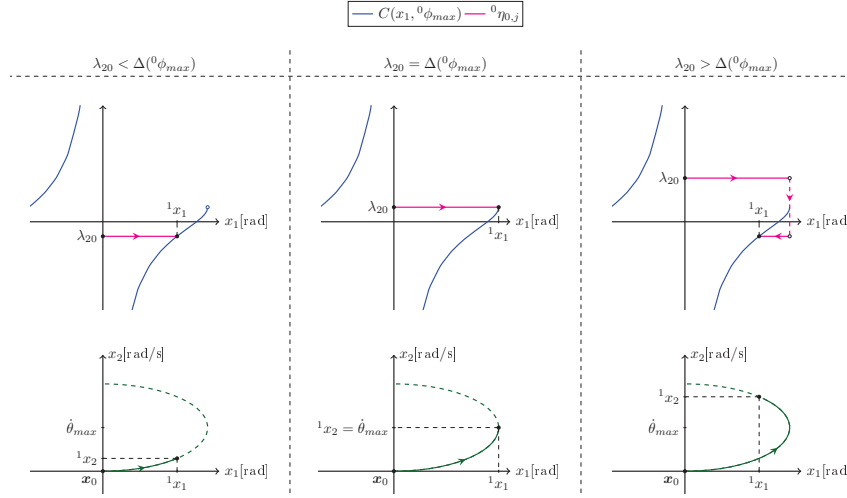
Figure 5.3.1: Construction of $\boldsymbol{x}$ in D_0 ($^0u = \dot{\theta}_{max}, i \in \{0, 2, \ldots\}, j \in S_{m_0}$)

the graphical illustration provided in Fig. 5.2.2 (Right) together with (5.2.20), these possibilities can all be described using four main *Switching Patterns* each of which provides a different relation for the desired variables, see Table 5.4a-5.4d. The derivations of these relations are depicted in Fig. 5.3.2 for the case when the deflection at $t_{S,k}$ is positive. As indicated there, a continuous change in the values of this deflection and its time-derivative can change the switching pattern followed by the control if $\Delta(^k\phi_{max})$ is fixed. This leads to five *Limiting Switching Patterns* clarifying the relation between the main switching patterns, see Table 5.4e.

Using the expressions in Table 5.4, it is now possible to uniquely determine the values of $m_k, {}^{k+1}x_1$ and $t_{S,k+1}$ using $^k\boldsymbol{x}, {}^ku$ and $t_{S,k}$. As in the previous case, these three terms can in turn be used to uniquely determine the extremal $(\boldsymbol{x}, u)$ in D_k, see Sec. 4.1. Moreover, with this extremal and the equality $^k\eta_{0,0} = C(^kx_1, {}^k\phi_{max})$ the costate $\boldsymbol{\lambda}|_{D_k}$ can be determined as well, see Sec. 5.2.2. In other words, Table 5.4 provides all the necessary information to construct Λ in D_k using the k'th switching time and the value of the extremal at this time.

It is important to remark here that knowing Λ in D_k, it is always possible to determine the value of the extremal at $t_{S,k+1}$. Since in our discussion above the value for $k \in S_i \backslash \{0\}$ was chosen arbitrarily, this means that Table 5.4 actually provides all the relations required to iteratively construct the extremal lift Λ in $D \backslash D_0$ if we know the values of $^1\boldsymbol{x}, {}^1u$ and $t_{S,1}$. Moreover, these three terms depend on λ_{20} and i as we have seen when discussing the construction of Λ in D_0. Combining our results on the construction of extremal lifts leads then to an iterative procedure with which we can uniquely construct Λ in D depending only on λ_{20} and i. This procedure is graphically illustrated in Fig. 5.3.3 for the systems Σ_1, Σ_2 and Σ_3 from Table 4.1, where we used the expressions in Table

m_k	$^{k+1}x_1$	$t_{S,k+1} - t_{S,k}$
1	$\frac{^k\eta_{0,0}+C(^{k+1}x_1,{}^k\phi_{max})}{2\,{}^kv_{\phi,0}} = \Delta(^k\phi_{max})$	$\frac{T_p(^k\phi_{max})}{2} - T_\phi(|^kx_1|,{}^k\phi_{max}) + T_\phi(|^{k+1}x_1|,{}^k\phi_{max})$

(a) Switching Pattern $S_{w_1} : {}^kx_1 \cdot {}^kv_{\phi,0} > 0 \wedge \frac{^k\eta_{0,0}}{^kv_{\phi,0}} \leq 3\Delta(^k\phi_{max})$

m_k	$^{k+1}x_1$	$t_{S,k+1} - t_{S,k}$
0	$^k\eta_{0,0} = C(^{k+1}x_1,{}^k\phi_{max})$	$T_\phi(|^kx_1|,{}^k\phi_{max}) + T_\phi(|^{k+1}x_1|,{}^k\phi_{max})$

(b) Switching Pattern $S_{w_2} : {}^kx_1 \cdot {}^kv_{\phi,0} < 0 \wedge \frac{^k\eta_{0,0}}{^kv_{\phi,0}} \leq \Delta(^k\phi_{max})$

m_k	$^{k+1}x_1$	$t_{S,k+1} - t_{S,k}$
1	$\frac{^k\eta_{0,0}+C(^{k+1}x_1,{}^k\phi_{max})}{2\,{}^kv_{\phi,0}} = \Delta(^k\phi_{max})$	$\frac{T_p(^k\phi_{max})}{2} + T_\phi(|^kx_1|,{}^k\phi_{max}) - T_\phi(|^{k+1}x_1|,{}^k\phi_{max})$

(c) Switching Pattern $S_{w_3} : {}^kx_1 \cdot {}^kv_{\phi,0} < 0 \wedge \frac{^k\eta_{0,0}}{^kv_{\phi,0}} > \Delta(^k\phi_{max})$

m_k	$^{k+1}x_1$	$t_{S,k+1} - t_{S,k}$
2	$\frac{^k\eta_{0,0}-C(^{k+1}x_1,{}^k\phi_{max})}{4\,{}^kv_{\phi,0}} = \Delta(^k\phi_{max})$	$T_p(^k\phi_{max}) - T_\phi(|^kx_1|,{}^k\phi_{max}) - T_\phi(|^{k+1}x_1|,{}^k\phi_{max})$

(d) Switching Pattern $S_{w_4} : {}^kx_1 \cdot {}^kv_{\phi,0} > 0 \wedge \frac{^k\eta_{0,0}}{^kv_{\phi,0}} > 3\Delta(^k\phi_{max})$

	m_k	$^{k+1}x_1$	$t_{S,k+1} - t_{S,k}$
$S_{w_{1,2}} : \Delta(^k\phi_{max}) = -\frac{^k\eta_{0,0}}{^kv_{\phi,0}} > 0$	0	$\frac{C(^{k+1}x_1,{}^k\phi_{max})}{^kv_{\phi,0}\Delta(^k\phi_{max})} = -1$	$\frac{T_p(^k\phi_{max})}{4} + T_\phi(|^{k+1}x_1|,{}^k\phi_{max})$
$S_{w_{2,3}} : \Delta(^k\phi_{max}) = \frac{^k\eta_{0,0}}{^kv_{\phi,0}} > 0$	0	$\frac{^k\phi_{max}}{^kv_{\phi,0}}$	$T_\phi(|^kx_1|,{}^k\phi_{max}) + \frac{T_p(^k\phi_{max})}{4}$
$S_{w_{1,4}} : \Delta(^k\phi_{max}) = \frac{^k\eta_{0,0}}{3\,{}^kv_{\phi,0}} < 0$	1	$\frac{^k\phi_{max}}{^kv_{\phi,0}}$	$\frac{3T_p(^k\phi_{max})}{4} - T_\phi(|^kx_1|,{}^k\phi_{max})$
$S_{w_{3,4}} : \Delta(^k\phi_{max}) = -\frac{^k\eta_{0,0}}{^kv_{\phi,0}} < 0$	1	$\frac{C(^{k+1}x_1,{}^k\phi_{max})}{3\,{}^kv_{\phi,0}\Delta(^k\phi_{max})} = 1$	$\frac{3T_p(^k\phi_{max})}{4} - T_\phi(|^{k+1}x_1|,{}^k\phi_{max})$
$S_{w_{1,2,3,4}} : \Delta(^k\phi_{max}) = {}^k\eta_{0,0} = 0$	0	$\frac{^k\phi_{max}}{^kv_{\phi,0}}$	$\frac{T_p(^k\phi_{max})}{2}$

(e) Limiting Switching Patterns $S_{w_{1,2}}, S_{w_{2,3}}, S_{w_{1,4}}, S_{w_{3,4}}, S_{w_{1,2,3,4}}$

Table 5.4: $m_k, {}^{k+1}x_1$ and $t_{S,k+1}$ along a Normal Extremal
$(i \geq 1, k \in S_i \backslash \{0\}, {}^k\phi_{max} > 0, {}^k\eta_{0,0} = C(^kx_1,{}^k\phi_{max}), \frac{\mathrm{sgn}(^{k+1}x_1)}{\mathrm{sgn}(^kx_1)} = -1)$
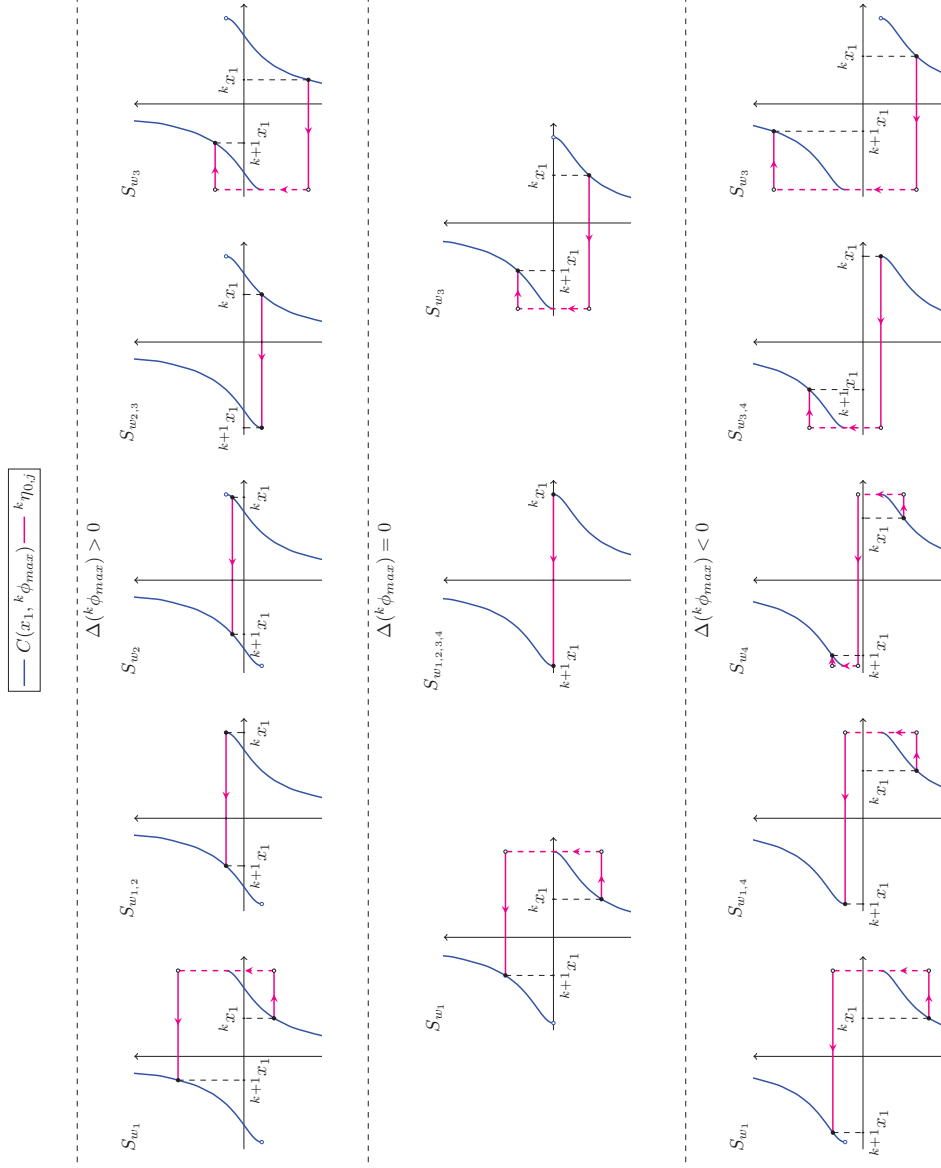
Figure 5.3.2: Switching Patterns in D_k ($i \in \{1, 2, \ldots\}, k \in S_i \setminus \{0\}, j \in S_{m_k}, {}^k x_1 > 0$)
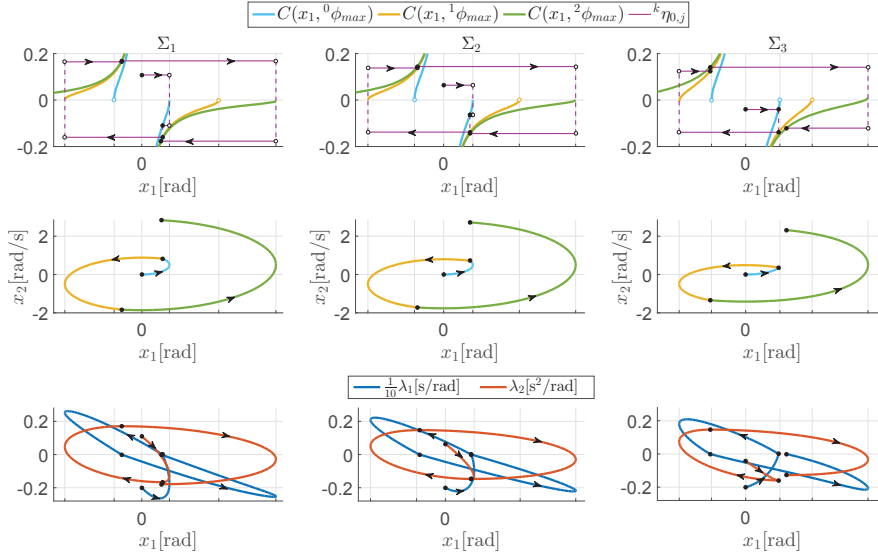
Figure 5.3.3: Normal Extremal Lift Construction for Σ_1, Σ_2 and Σ_3
$(i = 2, k \in S_i, j \in S_{m_k}, t_f = 0.55\mathrm{s})$

3.1 to construct for each system an extremal lift with a control switching two times, i.e. $i = 2$. Moreover, for each lift the initial costate λ_{20} is chosen such that the terminal time satisfies $t_f = t_{S,2} = 0.55[\mathrm{s}]$. Fig. 5.3.3 (Top) clarifies the changes of $^k\eta_{0,j}$ along the extremal lifts, with $k \in S_2$ and $j \in S_{m_k}$, as well as its relation to the deflection values at the switching times and terminal time. Fig. 5.3.3 (Middle) plots the trajectories corresponding to the applied controls, and finally Fig. 5.3.3 (Bottom) depicts the costate trajectories along the lifts.

5.3.3 Parameterization of Extremals

As we have already discussed, there exists a one-to-one correspondence between extremal lifts and the set of pairs $(\boldsymbol{\lambda}_0, i)$ satisying (5.3.1)-(5.3.2) and (5.3.4)-(5.3.5). Therefore, each solution to the LVMP can be referred to by at least one such pair. Note that our results from Sec. 5.3.1 and Sec. 5.3.2 show how to determine for each such pair the corresponding extremal. Consequently, with the construction procedures described there we can in principle solve the LVMP for any given terminal time t_f. Indeed, the desired solution can be found if we first determine the set of all pairs $(\boldsymbol{\lambda}_0, i)$, which lead to an extremal terminating at the given time, then compare the corresponding terminal link velocities and finally choose one pair resulting in the maximal terminal link velocity. In the following, we will show how to simplify this solution process by finding a parameterization for the family of all extremals [2]. This will lead to a reformulation of the LVMP as a NPP which can be efficiently solved.

We start our discussion by showing how to parameterize all the normal

extremals by exploiting their dependence on the initial costates. Focusing first on normal extremals $(\boldsymbol{x}, u)$ for which the initial control is positive, Fig. 5.3.1 already indicates that there exists a continuous relation between the initial costate λ_{20} and the state ${}^1\boldsymbol{x}$. More specifically, the figure suggests that as λ_{20} goes from minus infinity to positive infinity, the state ${}^1\boldsymbol{x}$ will continuously move from the origin to the state $(0, 2\dot{\theta}_{max})^T$ while remaining on the closed curve described by the relative energy ${}^0E_{rel} = \frac{1}{2}M\dot{\theta}_{max}^2$ and the control ${}^0u = \dot{\theta}_{max}$, see Sec. 4.1. Based on this observation and the dependence of ${}^1\boldsymbol{x}$ on the switching number, let us introduce the injective and continuous function ${}^1\boldsymbol{x}_S^{ext} : D_\alpha \to \mathbb{R}^2, \alpha \to {}^1\boldsymbol{x}_S^{ext}(\alpha) = \begin{pmatrix} {}^1x_{1S}^{ext}(\alpha) & {}^1x_{2S}^{ext}(\alpha) \end{pmatrix}^T$ with

$$
{}^1\boldsymbol{x}_S^{ext}(\alpha) = \begin{pmatrix} \frac{E_{pot}^{-1}\left(2M\dot{\theta}_{max}^2 |\alpha|(1-|\alpha|)\right)}{\operatorname{sgn}(\alpha)} \\ 2\alpha\dot{\theta}_{max} \end{pmatrix}, \tag{5.3.11}
$$

and $D_\alpha := (-1,1)\backslash\{0\}$. For $\alpha \in (0,1)$, the image of this function describes the set of all states which normal extremals can attain at $t_{S,1}$ if the control has an even number of switchings, see Table 5.3 and the green dashed curves in Fig. 5.3.1 (Bottom). Similarly, the image of ${}^1\boldsymbol{x}_S^{ext}|_{(-1,0)}$ is equal to the set of all states which normal extremals with ${}^0u = -\dot{\theta}_{max}$ can attain at $t_{S,1}$. Moreover, the union of these two images and the set of initial costates $\boldsymbol{\lambda}_0$ satisfying (5.3.1)-(5.3.2) with $\lambda_a = 1$ are homeomorphic. This can be shown using the homeomorphism $\boldsymbol{\lambda}_0^{ext}$ in Table 5.5a which is derived using (5.3.2),(5.3.5) and Table 5.3. Finally, notice that $\lim_{\alpha\to 1^-} {}^1\boldsymbol{x}_S^{ext}(\alpha)$ is equal to the value of ${}^1\boldsymbol{x}$ attained by an abnormal extremal $(\boldsymbol{x}, u)$ if λ_{20} is positive, and $\lim_{\alpha\to -1^+} {}^1\boldsymbol{x}_S^{ext}(\alpha)$ gives the value of the same state if λ_{20} is negative, see (5.3.4) and Prop. 11.

If we now take a closer look at our results from Sec. 5.3.2, we can observe that for normal extremal lifts sharing the same initial costate the switching number only influences the number of the switching times but not their values or the values of the states at these times. This simply follows from the properties of the state and costate dynamics in (2.1.4) and (5.2.1) according to which the condition (5.2.2) uniquely determines both the state and costate trajectories when the initial costate is non-trivial, see Appendix B.3.3. Since for any normal extremal lift, the first costate is zero not only at the switching times but also at the terminal time, based on Prop. 8 we can therefore conclude the following: If $\Lambda = (\boldsymbol{x}, u, \boldsymbol{\lambda}, \lambda_a)$ and $\tilde{\Lambda} = (\tilde{\boldsymbol{x}}, \tilde{u}, \tilde{\boldsymbol{\lambda}}, \lambda_a)$ are two extremal lifts with $\boldsymbol{\lambda}_0 = \tilde{\boldsymbol{\lambda}}_0$ and $i \geq \tilde{i} \geq 0$, where i and $\tilde{i}$ denote the switching numbers of u and $\tilde{u}$, respectively; then for each $k \in S_{\tilde{i}+1}$ we have $t_{S,k} = \tilde{t}_{S,k}$ and ${}^k\boldsymbol{x} = {}^k\tilde{\boldsymbol{x}}$. With the homeomorphism from Table 5.5a, this result shows us that for each non-negative integer k there must exist functions ${}^kt_S^{ext} : D_\alpha \to \mathbb{R}$ and ${}^k\boldsymbol{x}_S^{ext} : D_\alpha \to \mathbb{R}^2$ such that for any normal extremal Λ with $i \geq \max\{0, k-1\}$ switching times and

$$
\boldsymbol{\lambda}_0 = \boldsymbol{\lambda}_0^{ext}(\alpha), \tag{5.3.12}
$$

we have

$$
{}^kt_S^{ext}(\alpha) = t_{S,k} \wedge {}^k\boldsymbol{x}_S^{ext}(\alpha) = {}^k\boldsymbol{x}. \tag{5.3.13}
$$

α	$\boldsymbol{\lambda}_0^{ext}(\alpha)$
$0 < |\alpha| < \frac{1}{2}$	$\left(-\frac{\text{sgn}(\alpha)}{\dot\theta_{max}}, C\left({}^1x_{1S}^{ext}(\alpha), {}^0\phi_{max}\right)\right)$
$|\alpha| = \frac{1}{2}$	$\left(-\frac{\text{sgn}(\alpha)}{\dot\theta_{max}}, \frac{\Delta({}^0\phi_{max})}{\text{sgn}(\alpha)}\right)$
$\frac{1}{2} < |\alpha| < 1$	$\left(-\frac{\text{sgn}(\alpha)}{\dot\theta_{max}}, \frac{2\Delta({}^0\phi_{max})}{\text{sgn}(\alpha)} - C\left({}^1x_{1S}^{ext}(\alpha), {}^0\phi_{max}\right)\right)$
${}^0\phi_{max} = E_{pot}^{-1}(\frac{1}{2}M\dot\theta_{max}^2) > 0$	

(a) $\boldsymbol{\lambda}_0^{ext}: D_\alpha \to (\mathbb{R}^2)^*$

${}^k t_S^{ext}(\alpha)$	$\frac{(k-1)\pi + \arccos(1-2|\alpha|)}{\omega_0}$
${}^k \boldsymbol{x}_S^{ext}(\alpha)$	$(-1)^{k-1} 2\dot\theta_{max}\,\text{sgn}(\alpha) \begin{pmatrix} \frac{\sqrt{|\alpha|(1-|\alpha|)}}{\omega_0} \\ k-1+|\alpha| \end{pmatrix}$
$k \in \{1,2,\dots\},\, \alpha \in D_\alpha = (-1,1)\backslash\{0\}$	

(b) ${}^k t_S^{ext}$ and ${}^k \boldsymbol{x}_S^{ext}$ for Σ_{id}

$t_S^{ext}(\beta)$	$\begin{cases} {}^k t_S^{ext}(\beta - k + 1) & \beta \in (k-1, k) \\ t_{min}(k) & \beta = k \end{cases}$
$\boldsymbol{x}_S^{ext}(\beta)$	$\begin{cases} (-1)^{k-1} \cdot {}^k \boldsymbol{x}_S^{ext}(\beta - k + 1) & \beta \in (k-1, k) \\ 2k \begin{pmatrix} 0 & \dot\theta_{max} \end{pmatrix}^T & \beta = k \end{cases}$
$\beta \in (k-1, k],\, k \in \{1,2,\dots\}$	

(c) $t_S^{ext}: (0,\infty) \to \mathbb{R}$ and $\boldsymbol{x}_S^{ext}: (0,\infty) \to \mathbb{R}^2$

Table 5.5: Parameterization of Extremals

Notice that for $k = 0$, we simply have $^0 t_S^{ext} \equiv 0$ and $^0 \boldsymbol{x}_S^{ext} \equiv \boldsymbol{0}$. More importantly, for $k = 1$ this definition is in accordance with the previously introduced function in (5.3.11).

It is important to realize here that the values of the functions in (5.3.13) can be uniquely determined using the construction procedure from Sec. 5.3.2 and the function $\boldsymbol{\lambda}_0^{ext}$. Table 5.5b provides these functions for the linear control system Σ_{id}. By using elliptic integrals and their inverses [1], it is actually also possible to mathematically describe these functions for the nonlinear systems Σ_{sin} and Σ_{sinh}, see Table 3.1 and Table 5.3-5.4. Nevertheless, the resulting terms become very long due to the iterative nature of the proposed construction procedure and are therefore not given.

Turning back to our problem of solving the LVMP, let us assume that Λ is a normal extremal lift with a control u having $i \geq 0$ switchings. Our results so far show how instead of using the pair $(\boldsymbol{\lambda}_0, i)$ we can equivalently use the pair (α, i) to refer to this lift if (5.3.12) holds. Moreover, using the functions just introduced above we can also directly refer to the final time of u which will be given by $^{i+1} t_S^{ext}(\alpha)$. This means that the control u in this lift might be a solution to the LVMP for the final time $t_f = {}^{i+1} t_S^{ext}(\alpha)$. To definitely solve this particular LVMP, however, we need to find the set of all controls which are contained in an extremal, normal or abnormal, with the final time t_f. According to Prop. 11 and in particular (5.3.8), the question of whether there exists such a control in an abnormal extremal is equivalent to the question of whether there exists an integer $k \geq 1$ such that

$$t_{min}(k) = t_f. \tag{5.3.14}$$

Similarly, the existence question for controls belonging to a normal extremal and terminating at t_f can be investigated by making use of the time functions in (5.3.13). More specifically, based on the properties of $\boldsymbol{\lambda}_0^{ext}$ and the three conditions (5.3.1),(5.3.2) and (5.3.5) we can identify the set of all such controls by finding for each $k \geq 1$ the parameters β, which belong to the set $D_k^{ext} \subset D_\alpha$ defined by

$$D_k^{ext} := \left\{ \beta \in D_\alpha \,|\, \mathrm{sgn}(\beta) = (-1)^{k-1} \right\}, \tag{5.3.15}$$

and satisfy

$$^k t_S^{ext}(\beta) = t_f. \tag{5.3.16}$$

Note that equations (5.3.14) and (5.3.16) provide an infinite number of equality constraints for the integer $k \geq 1$ and the pair $(\beta, k) \in D_k^{ext} \times \{1, 2, \ldots\}$, respectively. In addition, based on our discussion above we can see that for any given final time $t_f > 0$, solving the LVMP requires us to first find the solution set for each of them and then to compare the corresponding terminal link velocities. We want to next show how by exploiting the properties of the functions in these equality constraints we can describe this whole process as a one-dimensional NPP. The following proposition will be essential in our discussion.

Proposition 13. *For any positive integer k, the functions $^k t_S^{ext} : D_\alpha \to \mathbb{R}$ and $^k \boldsymbol{x}_S^{ext} : D_\alpha \to \mathbb{R}^2$ are continuous. Moreover, if τ_J is two-times continuously*

differentiable they are continuously differentiable. In addition, in each case we have for each $\alpha \in D_\alpha$

$$^kt_S^{ext}(-\alpha) = {}^kt_S^{ext}(\alpha) > 0, \qquad (5.3.17)$$

and

$$^k\boldsymbol{x}_S^{ext}(-\alpha) = -{}^k\boldsymbol{x}_S^{ext}(\alpha). \qquad (5.3.18)$$

Finally, for t_S^{ext} we have

$$\lim_{\alpha \to 0} {}^kt_S^{ext}(\alpha) = \begin{cases} 0 & k = 1 \\ t_{min}(k-1) & k \geq 2 \end{cases}, \qquad (5.3.19)$$

and

$$\lim_{\alpha \to 1^-} {}^kt_S^{ext}(\alpha) = t_{min}(k), \qquad (5.3.20)$$

while for ${}^k\boldsymbol{x}_S^{ext}$ we have

$$\lim_{\alpha \to 0^+} {}^k\boldsymbol{x}_S^{ext}(\alpha) = (-1)^{k-1}2(k-1)\begin{pmatrix} 0 \\ \dot{\theta}_{max} \end{pmatrix}, \qquad (5.3.21)$$

and

$$\lim_{\alpha \to 1^-} {}^k\boldsymbol{x}_S^{ext}(\alpha) = (-1)^{k-1}2k\begin{pmatrix} 0 \\ \dot{\theta}_{max} \end{pmatrix}. \qquad (5.3.22)$$

Proof. See Appendix B.3.3. $\qquad\qquad\qquad\qquad\qquad\qquad\qquad\qquad\qquad\qquad$ □

We had already given an explicit expression for ${}^1\boldsymbol{x}_S^{ext}$ in (5.3.11) which shows that this function is continuous. Moreover, by the relations provided in Table 5.3 the same expression also implies that ${}^1t_S^{ext}$ is continuous. The main value of Prop. 13 is that it shows that the functions ${}^k\boldsymbol{x}_S^{ext}$ and ${}^kt_S^{ext}$ remain to be continuous for $k \geq 2$. In addition, it also states that for each $k \geq 1$ their limits at the boundaries of D_α are closely related to abnormal extremals as we have also previously observed when discussing the limits of ${}^1\boldsymbol{x}_S^{ext}$ at the non-zero boundaries of D_α.

Choosing an arbitrary $k \geq 1$ and concentrating at the restriction of the function ${}^kt_S^{ext}$ to the interval D_k^{ext}, we can now make use of the limits in (5.3.19)-(5.3.20) together with the symmetry property (5.3.17) to obtain the following relation:

$$\lim_{\mathcal{B}_{k,1}} {}^kt_S^{ext}(\beta) = \lim_{\mathcal{B}_{k+1,0}} {}^{k+1}t_S^{ext}(\beta) = t_{min}(k), \qquad (5.3.23)$$

where $\mathcal{B}_{k,1}$ denotes the base[7] $D_k^{ext} \ni \beta \to (-1)^{k-1}$ and $\mathcal{B}_{k+1,0}$ the base $D_{k+1}^{ext} \ni \beta \to 0$. According to (5.3.23), the two restricted functions ${}^kt_S^{ext}|_{D_k^{ext}}$ and ${}^{k+1}t_S^{ext}|_{D_{k+1}^{ext}}$ can be both continuously extended and, more importantly, simultaneously described using one continuous function with a suitable domain. More generally, since our choice for k was arbitrary it is possible to construct a continuous function whose graph contains, after a suitable transformation of the

---

[7]For notational simplicity, we use here the concept of the limit of a function over a base, see [62].
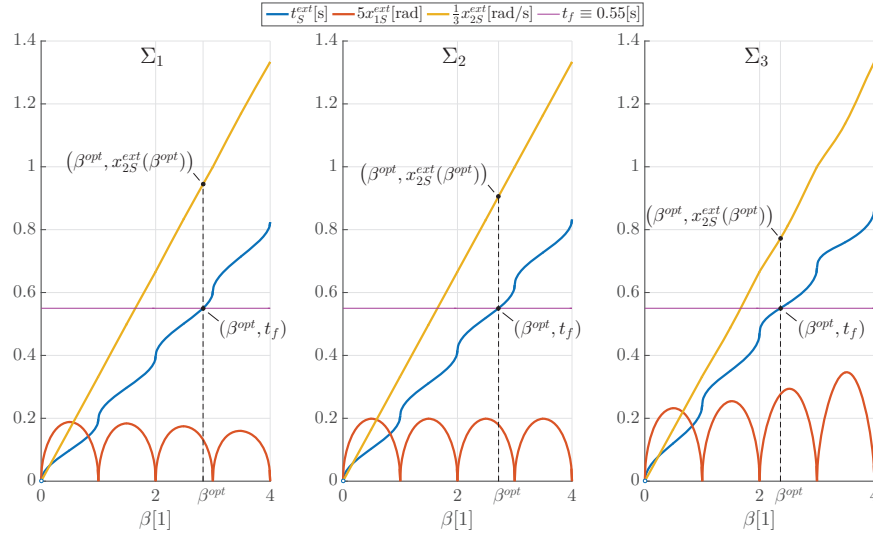
Figure 5.3.4: The Functions t_S^{ext} and $\boldsymbol{x}_S^{ext}$ for Σ_1, Σ_2 and Σ_3, and the Maximal Link Velocity $x_{2S}^{ext}(\beta_{opt})$ for $t_f = 0.55$[s].

domain, the graph of all the restricted functions ${}^k t_S^{ext}|_{D_k^{ext}}$ with $k \geq 1$. The function $t_S^{ext} : (0, \infty) \to \mathbb{R}$ provided in Table 5.5c is such a function. It is constructed by using for each $k \geq 1$ the mapping $\beta_k^{ext} : D_k^{ext} \to (k-1, k), \beta \to \beta_k^{ext}(\beta) = k-1+|\beta|$ and the condition that $t_S^{ext}\left(\beta_k^{ext}(\beta)\right) = {}^k t_S^{ext}(\beta)$ holds at each $\beta \in D_k^{ext}$. Fig. 5.3.4 depicts t_S^{ext} for the three control systems Σ_1, Σ_2 and Σ_3 in the interval $(0, 4]$. Moreover, for each system the figure also illustrates, in the same interval, the function $\boldsymbol{x}_S^{ext}$ defined in Table 5.5c. Similar to t_S^{ext}, this function is continuous and constructed using the condition[8] $\boldsymbol{x}_S^{ext}\left(\beta_k^{ext}(\beta)\right) = {}^k \boldsymbol{x}_S^{ext}(\beta)$ for each $k \geq 1$ and $\beta \in D_k^{ext}$.

As already mentioned, solving the LVMP for a given final time $t_f > 0$ requires us to find for each $k \geq 0$ the set of all solutions for the equality constraints (5.3.14) and (5.3.16). Based on its construction and its relation to abnormal extremals as described by (5.3.23), the function t_S^{ext} provides us a means to determine the union of all these sets by finding the set of all parameters $\beta \in (0, \infty)$ solving the equality $t_S^{ext}(\beta) = t_f$. Moreover, by evaluating $\boldsymbol{x}_S^{ext}$ at each such β we can also determine the final states reached by all the extremals corresponding to these parameters and thus also their final link velocity. Since the desired optimal control is known to maximize this velocity, this leads us directly to the following proposition[9] which shows how we can determine for any given final time the solution to the LVMP by solving a NPP.

---

[8]Notice that similar to (5.3.23), we have according to (5.3.18) and (5.3.21)-(5.3.22) $\lim_{\mathcal{B}_{k,1}} {}^k \boldsymbol{x}_S^{ext}(\beta) = \lim_{\mathcal{B}_{k+1,0}} {}^{k+1} \boldsymbol{x}_S^{ext}(\beta)$ for each $k \geq 1$.

[9]The proof of the proposition follows simply from Prop. 7 and the definition of the functions t_S^{ext} and $\boldsymbol{x}_S^{ext}$. It is omitted for brevity.

Proposition 14. *Let t_f be an arbitrary positive scalar. Then the nonlinear programming problem*

$$Maximize \ x_{2S}^{ext}(\beta) \tag{5.3.24}$$

$$subject \ to \ t_S^{ext}(\beta) = t_f, \tag{5.3.25}$$

$$\beta \in (0, \infty), \tag{5.3.26}$$

has at least one optimal solution. Moreover, the admissible switching control $u : [0, t_f] \to \mathbb{U}$ with $i \geq 0$ switchings and $|u| \equiv \dot{\theta}_{max}$ solves the LVMP if and only if there exists a solution $\beta^{opt} \in (i, i + 1]$ to the problem such that we have

$$^0u = (-1)^i \dot{\theta}_{max}, \tag{5.3.27}$$

for the initial value of that control and

$$(\forall k \in S_i)[t_{S,k+1} = t_S^{ext}(\beta^{opt} - i + k)], \tag{5.3.28}$$

for its switching times and final time. Finally, in this case we have

$$(\forall k \in S_i)[^{k+1}\boldsymbol{x} = (-1)^{i+k} \cdot \boldsymbol{x}_S^{ext}(\beta^{opt} - i + k)], \tag{5.3.29}$$

for the optimally controlled trajectory $(\boldsymbol{x}, u)$.

Given any final time $t_f > 0$, the optimal solution to the NPP in Prop. 14 can be searched for graphically since it is a one-dimensional problem. Fig. 5.3.4 illustrates this by showing how the graphs of t_S^{ext} and x_{2S}^{ext} can be used to determine, for the systems Σ_1, Σ_2 and Σ_3 and for $t_f = 0.55[\text{s}]$, the parameter β^{opt} solving the problem and the corresponding maximal link velocity $x_{2S}^{ext}(\beta^{opt})$. It is important to remark here that for all the three systems analysed in the figure, it is sufficient to restrict our search for a solution to the interval $(0, 4]$. This follows from the observation that the function $t_S^{ext}|_{(0,4]}$ is strictly increasing and from the fact that the value of $^k t_S^{ext}(\alpha)$, with $\alpha \in D_\alpha$, and of $t_{min}(k)$ always increase with increasing $k \geq 1$.

According to Fig. 5.3.4, for the systems Σ_1, Σ_2 and Σ_3 there exists only one solution to the NPP in Prop. 14 when $t_f = 0.55[\text{s}]$. This means that for all these three systems there can only exist one extremal terminating at this final time. Consequently, we can now conclude that each of the three extremal lifts constructed in Fig. 5.3.3 are actually optimal. Unfortunately, in general there might exist multiple extremals terminating at the same terminal time. We will see this in the next chapter, when we investigate the maximal link velocity of control systems sharing the same dynamics as the DLR FSJ [59]. Since our results only imply continuity of the function t_S^{ext} but not monotonicity, in such cases it is not straightforward to determine the solution set of the equality (5.3.25). We conclude this section with a proposition, which provides lower and upper bounds for this set as well as for the maximal value that can be attained by the objective function (5.3.24). The proposition is especially useful when the NPP in Prop. 14 is to be solved numerically.

Proposition 15. *Let $t_f > 0$ be an arbitrary scalar and $\beta^{ext} \in (0, \infty)$ a scalar for which the equality $t_f = t_S^{ext}(\beta^{ext})$ holds. Moreover, let*

$$\omega_{min} = \min_{\phi \in [0, \dot{\theta}_{max} t_f]} \sqrt{\frac{K_J(\phi)}{M}}, \tag{5.3.30}$$

and

$$\omega_{max} = \max_{\phi \in [0, \dot{\theta}_{max} t_f]} \sqrt{\frac{K_J(\phi)}{M}}, \tag{5.3.31}$$

denote the minimal and maximal eigenfrequency attainable at the final time t_f, respectively. Finally, let the integers i_{lb} and i_{ub} be given as follows[10]:

$$i_{lb} = \max\{0, \left\lceil \frac{\omega_{min} t_f}{\pi} \right\rceil - 2\}, \tag{5.3.32}$$

and

$$i_{ub} = \left\lceil \frac{\omega_{max} t_f}{\pi} \right\rceil + 1. \tag{5.3.33}$$

Then, we have

$$\beta^{ext} \in (i_{lb}, i_{ub} + 1]. \tag{5.3.34}$$

Moreover, if β^{ext} also solves the nonlinear programming problem described by (5.3.24)-(5.3.26), the following inequalities hold for the corresponding terminal link velocity $x_{2S}^{ext}(\beta^{ext})$:

$$0 < x_{2S}^{ext}(\beta^{ext}) < \sqrt{\frac{2E_{pot}(\dot{\theta}_{max} t_f)}{M}}. \tag{5.3.35}$$

Proof. See Appendix B.3.3. $\qquad \square$

5.4 Resonance Energies

The LVMP as formulated in Sec. 2.3 is actually a problem already studied in [24] for the case when the TDP is linear [53]. As already mentioned, for sufficiently large terminal times the corresponding OC strategies periodically switch between their minimum and maximum values with the EJ's eigenfrequency. From a mechanics point of view, OC Theory thus establishes the fact that an EJ with a linear spring must be excited with its resonance frequency when the terminal link velocity is to be maximized. The main aim of this section is to show how our results obtained so far extend this well-known concept of resonance frequency to a new concept which we will call *resonance energies.*

We will start our discussion by first clarifying the main properties of optimally controlled trajectories for the linear control system Σ_{id}, see Table 4.1b. These properties will directly follow from well-known results on the OC of linear

---

[10]We use "$\lceil . \rceil$" to denote the ceiling function.

systems [30]. Afterwards, we show that some of these properties remain also valid for systems with nonlinear TDP's. Focusing on the common properties, we then make use of Bellman's principle of optimality [9] together with the concept of parameterized families of extremals [37, 53] to find a physical interpretation for the costates as well as the optimal control strategies. Using this interpretation, we further explain the relation between costate trajectories and the time functions introduced in Sec. 3.2. Noting that this relation is valid for any TDP, linear and nonlinear, our discussion will finally lead to the concept of resonance energies.

The control system Σ_{id} is a completely controllable system with a compact and convex control set. Consequently, given a final time $t_f > 0$ the time-t_f-reachable set from the origin, which we will denote by $\text{Reach}_{\Sigma_{id},t_f}(\mathbf{0})$, is compact and convex [53]. Moreover, since the same system also satisfies the normality condition this set is actually strictly convex [30]. In addition, for each $t_f > 0$ there exists exactly one control strategy solving the LVMP. More generally, for any non-trivial linear combination of terminal states there exists exactly one control strategy minimizing this combination. The following proposition clarifies the relation between these strategies and also show that they all lead to time-optimal and boundary trajectories[11].

Proposition 16. *Let τ_J be a linear TDP and $\Lambda = (\mathbf{x}, u, \boldsymbol{\lambda}, \lambda_a)$ an extremal lift for the LVMP which is defined on $D = [0, t_f]$. Then, Λ is optimal, $\mathbf{x}$ is time-optimal and $(\mathbf{x}, u)$ is a boundary trajectory. Moreover, for each $\bar{t}_f \in (0, t_f]$ the admissible control $\bar{u} : [0, \bar{t}_f] \to \mathbb{U}$ defined by*

$$\forall t \in [0, \bar{t}_f] \, [\bar{u}(t) = u(t)], \tag{5.4.1}$$

is the unique control that minimizes the cost functional $\bar{J} : \mathcal{PC}_{\mathbb{U}} \to \mathbb{R}$ with[12]

$$\bar{J}(\tilde{u}) = \boldsymbol{\lambda}(\bar{t}_f)\tilde{\mathbf{x}}_f, \tag{5.4.2}$$

over all admissible controls $\tilde{u}$ defined on $[0, \bar{t}_f]$.

Proof. See Appendix B.3.4. □

In general, it is not possible to directly determine whether the time-t-reachable sets of Σ are convex or not if the TDP is nonlinear. Consequently, for such systems the conditions provided by PMP can only be regarded as necessary conditions. This also means that Prop. 16 can not be directly extended to extremal lifts for an arbitrary control system Σ. Nevertheless, applying first Filippov's Theorem [2] and then Sturm Comparison Theorem [3], as done in the proof of Prop. 6, it is possible to see that $\text{Reach}_{\Sigma,t_f}(\mathbf{0})$ will be compact for each $t_f > 0$. Moreover, an optimal extremal $(\mathbf{x}, u)$ for the LVMP, defined on $D = [0, t_f]$, will always terminate at the boundary this set. Finally, as we show in the following proposition $\mathbf{x}$ will in this case also be a time-optimal trajectory.

---

[11]See [53] for the definition of a boundary trajectory.

[12]Similar to (2.3.1), $\tilde{\mathbf{x}}_f$ denotes in (5.4.2) the terminal state to which the admissible control $\tilde{u}$ will steer the system Σ from the origin.

Proposition 17. *Let $(\boldsymbol{x}, u)$ be an optimally controlled trajectory. Then, $(\boldsymbol{x}, u)$ is a boundary trajectory and $\boldsymbol{x}$ is a time-optimal trajectory.*

Proof. See Appendix B.3.4. □

According to Prop. 17, time-optimality is a property shared by every optimally controlled trajectory regardless of the TDP. This is in accordance with the mathematical expressions we have found in Table 5.1a which describe the costates in terms of the time functions from Sec. 3.2, see Prop. 9. Similarly, for each control system Σ optimally controlled trajectories belong at each time to the boundaries of the systems time-t-reachable sets. In order to extend the concept of resonance frequency, we will next investigate these common properties in more detail and provide, in particular, a physical explanation for the costates.

When using Bellman's optimality principle to solve an OC problem, it is known that the costates of the problem will be given by the gradient of the value function if this function is continuously differentiable [15, 9]. To be able to physically interpret the costates, we will therefore search for a value function which can be used to distinguish between optimal and non-optimal trajectories for the LVMP. For this aim, we will make use of the parameterized family of extremals we introduced in Sec. 5.3.3.

Following [53], let us now introduce the continuous flow of extremals $\boldsymbol{x}^{ext}$: $D_\alpha \times [0, \infty) \to \mathbb{R}^2, (\alpha, t) \to \boldsymbol{x}^{ext}(\alpha, t)$ which for each $k \geq 0$ and $t \in D_k$ satisfies

$$\boldsymbol{x}^{ext}(\alpha, t) = {}^k\boldsymbol{x}_S^{ext}(\alpha) + \int_{{}^k t_S^{ext}(\alpha)}^t \boldsymbol{f}(\boldsymbol{x}^{ext}(\alpha, s), {}^k u) \mathrm{d}s. \qquad (5.4.3)$$

Similarly, let $\boldsymbol{\lambda}^{ext} : D_\alpha \times [0, \infty) \to \mathbb{R}^2, (\alpha, t) \to \boldsymbol{\lambda}^{ext}(\alpha, t)$ denote the continuous flow of costates defined by[13]

$$\boldsymbol{\lambda}^{ext}(\alpha, t) = \boldsymbol{\lambda}_0^{ext}(\alpha) - \int_0^t \boldsymbol{\lambda}^{ext}(\alpha, s) \frac{\partial \boldsymbol{f}}{\partial \boldsymbol{x}} \left(\boldsymbol{x}^{ext}(\alpha, s) \right) \mathrm{d}s. \qquad (5.4.4)$$

Moreover, let $\Lambda = (\boldsymbol{x}, u, \boldsymbol{\lambda}, \lambda_a)$ be a normal optimal extremal such that u is a switching control with the terminal time t_f and switching number $i^{opt} \geq 1$. Then, by our results from Sec. 5.3.3 we know that there must exist a parameter $\alpha^{opt} \in D_\alpha$ such that $\boldsymbol{x}$ is given by the restriction of $\boldsymbol{x}^{ext}(\alpha^{opt}, .)$ to the interval $[0, {}^{i^{opt}+1} t_{S,k}(\alpha^{opt})]$. Finally, assume that there exists an open interval $I_{\alpha^{opt}} \subset D_\alpha$ containing α^{opt} such that for each $\alpha \in I_{\alpha^{opt}}$ the restriction of $\boldsymbol{x}^{ext}(\alpha, .)$ to the interval $[0, {}^{i^{opt}+2} t_S^{ext}(\alpha)]$ is optimal with ${}^{i^{opt}+1} t_S^{ext}(\alpha) < {}^{i^{opt}+2} t_S^{ext}(\alpha^{opt})$. In this case, it follows from Prop. 17 that the set

$$S_f := \left\{ \boldsymbol{x}^{ext}(\alpha, t_f) \in \mathbb{R}^2 \,|\, \alpha \in I_{\alpha^{opt}} \right\}, \qquad (5.4.5)$$

defines a continuous curve on the boundary of $\mathrm{Reach}_{\Sigma, t_f}(\boldsymbol{0})$. This is graphically illustrated in Fig. 5.4.1 for the nonlinear control system Σ_3 with $i_{opt} = 2$,

---

[13] Noting that $\frac{\partial \boldsymbol{f}}{\partial \boldsymbol{x}}$ does not depend on the applied control strategy, we omit here, with a slight abuse of notation, the second argument of this derivative.
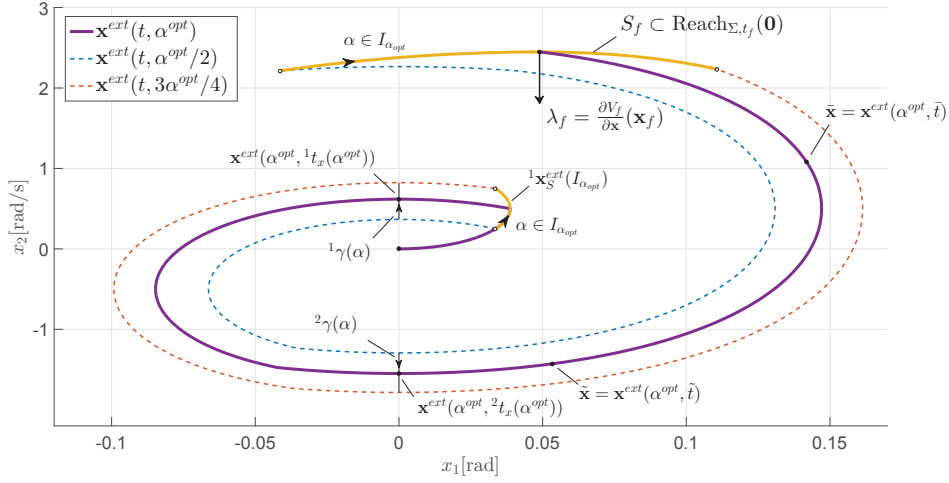
Figure 5.4.1: Physical Interpretation for the Costates
$(\Sigma = \Sigma_3, \alpha^{opt} = \frac{1}{2}, I_{\alpha^{opt}} = (\frac{1}{4}, \frac{3}{4}), i^{opt} = 2, t_f \approx 0.57[\text{s}])$

$\alpha^{opt} = \frac{1}{2}$ and $I_{\alpha^{opt}} = (\frac{1}{4}, \frac{3}{4})$. As shown there, the costate $\boldsymbol{\lambda}_f$ represents in this case a normal vector to S_f and thus also to $\text{Reach}_{\Sigma, t_f}(\mathbf{0})$. In the following, we will derive our desired physical interpretation for the costates which will reveal the reason behind this geometric property.

Making use of the set S_f, let us introduce the value function $V_f : D_{V_f} \to \mathbb{R}$ with

$$D_{\boldsymbol{x}^{opt}} := I_{\alpha^{opt}} \times [0, t_f], \tag{5.4.6}$$

$$D_{V_f} := \boldsymbol{x}^{ext}(D_{\boldsymbol{x}^{opt}}), \tag{5.4.7}$$

such that

$$V_f(\boldsymbol{y}) = 0, \tag{5.4.8}$$

if $\boldsymbol{y} \in S_f$ and[14]

$$V_f(\boldsymbol{y}) = \min \left\{ T(\boldsymbol{z}) \, | \, \boldsymbol{z} \in \text{Traj}(\Sigma) \wedge \boldsymbol{z}_0 = \boldsymbol{y} \wedge \boldsymbol{z}_f \in S_f \right\}, \tag{5.4.9}$$

if $\boldsymbol{y} \notin S_f$. According to its definition, $V_f(\boldsymbol{y})$ provides the minimum time[15] required by trajectories of Σ to terminate on the set S_f when they start from $\boldsymbol{y} \in D_{V_f} \backslash S_f$ and remain in D_{V_f}. Clearly, for trajectories starting from the origin we always have $V_f(\mathbf{0}) = t_f$. More generally, by the Bellman's principle of optimality [9] we have for each $\alpha \in I_{\alpha^{opt}}$ and $t \in [0, t_f]$

$$V_f\left(\boldsymbol{x}^{ext}(\alpha, t)\right) = t_f - t. \tag{5.4.10}$$

The equality in (5.4.10) simply shows that the value function V_f linearly decreases over time when evaluated along optimal trajectories. Assuming that

---

[14]Recall that for each trajectory $\boldsymbol{x}$ of Σ, $T(\boldsymbol{x})$ denotes the terminal time t_f.

[15]Notice that the existence of the minimum directly follows from our assumptions on the existence of optimal extremals corresponding to pairs $(\alpha, i^{opt} + 2)$ with $\alpha \in I_{\alpha^{opt}}$.

V_f is continuously differentiable, we can take the time-derivative of (5.4.10) everywhere except at the switching times. This leads, as expected from the Hamilton-Jacobi-Bellman equation, to the equality

$$\frac{\partial V_f}{\partial \boldsymbol{x}}\left(\boldsymbol{x}^{ext}(\alpha, t)\right)\frac{\partial \boldsymbol{x}^{ext}}{\partial t}(\alpha, t) = -1, \qquad (5.4.11)$$

which holds at each $(\alpha, t) \in \mathring{D}_{\boldsymbol{x}^{opt}} := D_{\boldsymbol{x}^{opt}} \backslash I_{\alpha^{opt}} \times \{^1t_S(\alpha), \ldots, {}^{i^{opt}}t_S(\alpha)\}$.

A comparison of the Hamiltonian function in Prop. 7 with (5.4.11) already suggests a close relation between $\boldsymbol{\lambda}$ and the gradient of V_f. Similarly, if we additionally assume that $\boldsymbol{x}^{ext}(\alpha, t)$ is differentiable with respect to α, we obtain the following equality from (5.4.10):

$$\frac{\partial V_f}{\partial \boldsymbol{x}}\left(\boldsymbol{x}^{ext}(\alpha, t)\right)\frac{\partial \boldsymbol{x}^{ext}}{\partial \alpha}(\alpha, t) = 0. \qquad (5.4.12)$$

Taking now a closer look at (5.4.11)-(5.4.12), one can see that knowing the derivatives of $\boldsymbol{x}^{ext}$ with respect to the time t and parameter α one can uniquely determine $\frac{\partial V_f}{\partial \boldsymbol{x}}\left(\boldsymbol{x}^{ext}(\alpha, t)\right)$ in $\mathring{D}_{\boldsymbol{x}^{opt}}$ provided that these derivatives exist and are linearly independent. The following proposition, which is closely related to the results from [53] such as the Shadow-Price Lemma[16], provides conditions under which this will be true for $\boldsymbol{x}^{ext}(\alpha, t)$ in a particular subset of $\mathring{D}_{\boldsymbol{x}^{opt}}$. Moreover, as shown there the provided conditions also ensure V_f to be continuously differentiable in this subset with a gradient which directly corresponds to the costates of optimal extremals corresponding to parameters in $I_{\alpha^{opt}}$.

Proposition 18. *Let $i \geq 1$ be a positive integer and $I_{\alpha^{ext}} \subset D_\alpha = (-1, 1)\backslash\{0\}$ a non-empty open interval. In addition, assume that for each $k \in S_i\backslash\{0\}$ the functions ${}^kt_S^{ext}$ and ${}^k\boldsymbol{x}_S^{ext}$ are continuously differentiable on $I_{\alpha^{ext}}$ and that for each $\alpha \in I_{\alpha^{ext}}$ we have*

$$\frac{\partial E_{MSS}}{\partial \boldsymbol{x}}\left({}^kx_{1S}^{ext}(\alpha), {}^kx_{2S}^{ext}(\alpha) - {}^ku\right)\frac{\mathrm{d}^kx_S^{ext}}{\mathrm{d}\alpha}(\alpha) > 0. \qquad (5.4.13)$$

Finally, let $\mathring{D}_{\boldsymbol{x}^{ext}}$, $D_{\boldsymbol{x}^{ext}}$ and $D_{t_f^{ext}}$ denote the sets

$$\mathring{D}_{\boldsymbol{x}^{ext}} := \left\{(\alpha, t)\,\big|\,\alpha \in I_{\alpha^{ext}} \wedge t \in \cup_{k=1}^i\left({}^kt_S^{ext}(\alpha), {}^{k+1}t_S^{ext}(\alpha)\right)\right\},$$

$$D_{\boldsymbol{x}^{ext}} := I_{\alpha^{ext}} \times \left({}^1t_S^{ext}(\alpha), {}^{i+1}t_S^{ext}(\alpha)\right),$$

and

$$D_{t_f^{ext}} := \boldsymbol{x}^{ext}(D_{\boldsymbol{x}^{ext}}),$$

and assume further that the restriction of $\boldsymbol{x}^{ext}$ to $D_{\boldsymbol{x}^{ext}}$ is an injective function. Then, the restriction of $\boldsymbol{x}^{ext}$ to $\mathring{D}_{\boldsymbol{x}^{ext}}$ is continuously differentiable and we have

$$det\left(\frac{\partial \boldsymbol{x}^{ext}}{\partial \alpha}(\alpha, t)\quad \frac{\partial \boldsymbol{x}^{ext}}{\partial t}(\alpha, t)\right) > 0, \qquad (5.4.14)$$

---

[16]The main contribution of the proposition is the interpretation of the time along trajectories as an additional parameter used to parameterize the extremals.

for each $(\alpha, t) \in \mathring{D}_{\boldsymbol{x}^{ext}}$. In addition, the unique function $t_f^{ext} : D_{t_f^{ext}} \to \mathbb{R}, \boldsymbol{x} \to t_f^{ext}$ which satisfies

$$(\forall (\alpha, t) \in D_{\boldsymbol{x}^{ext}}) \left[t_f^{ext}(\boldsymbol{x}^{ext}(\alpha, t)) = t \right], \tag{5.4.15}$$

is continuously differentiable and for each $(\alpha, t) \in \mathring{D}_{\boldsymbol{x}^{ext}}$ we have

$$\frac{\partial t_f^{ext}}{\partial \boldsymbol{x}} \left(\boldsymbol{x}^{ext}(\alpha, t) \right) = (0 \ 1) \left(\frac{\partial \boldsymbol{x}^{ext}}{\partial \alpha}(\alpha, t) \quad \frac{\partial \boldsymbol{x}^{ext}}{\partial t}(\alpha, t) \right)^{-1}, \tag{5.4.16}$$

while for each $(\alpha, t) \in D_{\boldsymbol{x}^{ext}}$ we have

$$\frac{\partial t_f^{ext}}{\partial \boldsymbol{x}} \left(\boldsymbol{x}^{ext}(\alpha, t) \right) = -\boldsymbol{\lambda}^{ext}(\alpha, t). \tag{5.4.17}$$

Proof. See Appendix B.3.4. □

By applying Prop. 18, with $I_{\alpha^{ext}} = I_{\alpha^{opt}}$ and $i = i^{opt} + 1$, we can see that for each point $\boldsymbol{y}$ in the set $D_{V_f} \backslash \boldsymbol{x}^{ext} \left(I_{\alpha^{opt}} \times [0, {}^1t_S^{ext}(\alpha)] \right)$ the function V_f will be exactly equal to the difference $t_f - t_f^{ext}(\boldsymbol{y})$ provided $\boldsymbol{x}^{ext}|_{I_{\alpha^{opt}} \times \left({}^1t_S^{ext}(\alpha), {}^{i^{opt}+2}t_S^{ext}(\alpha) \right)}$ is a surjection and (5.4.13) holds for each $k \in S_{i^{opt}+1}$. Moreover, in this case it follows from (5.4.16)-(5.4.17) that the gradient of the value function $\frac{\partial V_f}{\partial \boldsymbol{x}}$ will exist at each point in the set $D_{V_f} \backslash \boldsymbol{x}^{ext} \left(I_{\alpha^{opt}} \times [0, {}^1t_S(\alpha)] \right)$ and satisfy

$$\frac{\partial V_f}{\partial \boldsymbol{x}}(\boldsymbol{x}^{ext}(\alpha, t)) = \boldsymbol{\lambda}^{ext}(\alpha, t), \tag{5.4.18}$$

for each $(\alpha, t) \in I_{\alpha^{opt}} \times \left({}^1t_S^{ext}(\alpha), {}^{i^{opt}+1}t_S^{ext}(\alpha) \right)$. It is important to remark here that Prop. 18 can always be applied to analyse the extremals of systems with linear TDP's. Moreover, the differentiability condition on the functions ${}^kt_S^{ext}$ and ${}^k\boldsymbol{x}_S^{ext}$ can always be ensured when the TDP is two-times continuously differentiable, see Prop. 13. Finally, regardless of the TDP the proposition can always be applied if $i^{opt} = 1$. In deriving the concept of resonance energies we will take the conditions required to apply Prop. 18 as granted. Note that these conditions are also satisfied by the family of extremals analysed in Fig. 5.4.1.

Equation (5.4.18) provides us now the desired physical interpretation for the costates according to which the costates represent, after the first switching time of the control, the gradient of the minimum time required to reach the set S_f in (5.4.5). In particular, evaluating (5.4.18) along the optimal extremal Λ, by setting α to α^{opt}, and using (5.4.16) we can see that for each $t \in ({}^1t_S(\alpha^{opt}), t_f]$ $\boldsymbol{\lambda}(t)$ will satisfy

$$\boldsymbol{\lambda}(t) \cdot \lim_{\mathcal{B}_{V_f}(t)} \left(\frac{\partial \boldsymbol{x}^{ext}}{\partial \alpha}(\alpha, s) \quad \frac{\partial \boldsymbol{x}^{ext}}{\partial t}(\alpha, s) \right) = \left(0 \quad -1 \right), \tag{5.4.19}$$

with $\mathcal{B}_{V_f}(t) := \mathring{D}_{V_f} \ni (\alpha, s) \to (\alpha^{opt}, t)$. With (5.4.19), we can now also see that $\boldsymbol{\lambda}(t)$ will be a normal vector to the boundary of the reachable set $\text{Reach}_{\Sigma, t}(\boldsymbol{0})$

pointing inwards whenever $t > t_{S,1}$. Moreover, according to (5.4.19) we also see that at each such time the Minimum Condition in (5.2.2) simply requires the optimal control to adjust the time-derivative of the optimal trajectory such that the trajectory leaves the corresponding time-t-reachable set at its highest possible rate. Finally, evaluating (5.4.19) at $t = t_f$ one can observe, in accordance with Fig. 5.4.1, that the transversality condition requires the limit $\lim_{\mathcal{B}_{V_f}(t_f)} \frac{\partial \boldsymbol{x}^{ext}}{\partial \alpha}(\alpha, s)$ to be a horizontal vector ensuring that the terminal link velocity attained by the neighbouring extremals can not be greater then $x_2(t_f)$.

In our analysis above, we have used the parameterization from Sec. 5.3.3 to find an additional condition on optimally controlled trajectories, see (5.4.12). Using this condition together with (5.4.11), we could relate in Prop. 18 the gradient of V_f to the flow of costates. We want to next further exploit this condition to understand the meaning behind the analytical expressions we have found in Sec. 5.2.2 for the costates. For this aim, let us recall that for each $k \in S_{i^{opt}}$ and $j \in S_{m_k}$, the costate $\boldsymbol{\lambda}$ in D_{k_j} is uniquely determined by $(\boldsymbol{x}, u)$ if we additionally know the value of $^j\eta_{0,k}$ or equivalently the value of λ_2 when the deflection is equal to zero in D_{k_j}, see Sec. 5.2.2. Based on this property, let us introduce, as in Fig. 5.4.1, for each $k \in S_{i^{opt}} \backslash \{0\}$ the continuous curves $^k\boldsymbol{\gamma} : I_{\alpha^{opt}} \to \mathbb{R}^2$ with

$$^k\boldsymbol{\gamma}(\alpha) = \begin{pmatrix} 0 \\ x_2^{ext}\left(\alpha, {}^kt_x(\alpha)\right) \end{pmatrix},$$

where $^kt_x : I_{\alpha^{opt}} \to \left({}^kt_S(\alpha), {}^{k+1}t_S(\alpha)\right)$ is the unique continuously differentiable function satisfying the equality

$$(\forall \alpha \in I_{\alpha^{opt}}) \left[x_1^{ext}\left(\alpha, {}^kt_x(\alpha)\right) = 0 \right].$$

Moreover, let $^k\varphi_{max} : I_{\alpha^{opt}} \to [0, \infty)$ denote the maximal deflection function corresponding to the relative energies attained along these curves. That is

$$(\forall \alpha \in I_{\alpha^{opt}}) \left[{}^k\varphi_{max}(\alpha) = E_{pot}^{-1}\left(E_{kin}\left({}^ku - {}^k\gamma_2(\alpha)\right)\right) \right].$$

Without loss of generality, assume now that for a given $k \in S_{i^{opt}} \backslash \{0\}$ the derivative $\frac{\partial x_1^{ext}}{\partial t}(\alpha, t_x(\alpha))$ is positive for each $\alpha \in I_{\alpha^{opt}}$ and fix the integer $j \in S_{m_k - 1} = \{0, 1\}$ such that $t_x(\alpha^{opt}) \in D_{k_j}$. If we now choose a time $\tilde{t}$ from the same interval D_{k_j} and set $\tilde{\boldsymbol{x}} = \boldsymbol{x}(\tilde{t})$, there will exist a sufficiently small neighborhood $N_{\tilde{\boldsymbol{x}}}$ of $\tilde{\boldsymbol{x}}$ such that for each $\tilde{\boldsymbol{y}} \in N_{\tilde{\boldsymbol{x}}}$ we have

$$V_f(\tilde{\boldsymbol{y}}) = V_f\left({}^k\boldsymbol{\gamma}(\tilde{\alpha})\right) - T_\phi\left(\tilde{y}_1, {}^k\varphi_{max}(\tilde{\alpha})\right), \qquad (5.4.20)$$

with

$$E_{kin}\left({}^ku - {}^k\gamma_2(\tilde{\alpha})\right) = E_{MSS}\left(\tilde{y}_1, {}^ku - \tilde{y}_2\right). \qquad (5.4.21)$$

Similarly, if we choose a time $\bar{t}$ from the interval $D_{k_{j+1}}$ and set $\bar{\boldsymbol{x}} = \boldsymbol{x}(\bar{t})$ there will exist a sufficiently small neighborhood $N_{\bar{\boldsymbol{x}}}$ of $\bar{\boldsymbol{x}}$ such that for each $\bar{\boldsymbol{y}} \in N_{\bar{\boldsymbol{x}}}$ we have

$$V_f(\bar{\boldsymbol{y}}) = V_f({}^k\boldsymbol{\gamma}(\bar{\alpha})) - \frac{T_p\left({}^k\varphi_{max}(\bar{\alpha})\right)}{2} + T_\phi\left(\bar{y}_1, {}^k\varphi_{max}(\bar{\alpha})\right), \qquad (5.4.22)$$

with

$$E_{kin}\left({}^{k}u - {}^{k}\gamma_2(\bar{\alpha})\right) = E_{MSS}\left(\bar{y}_1, {}^{k}u - \bar{y}_2\right). \qquad (5.4.23)$$

Fig. 5.4.1 ilustrates two such possible choices for $\tilde{t}$ and $\bar{t}$.

As one can observe from Fig. 5.4.1, equations (5.4.20)-(5.4.21) simply illustrate the fact that using only the function T_ϕ we can relate the minimum time required to reach the set S_f from a given state $\tilde{\boldsymbol{y}}$ to the minimum time required to reach the same set from a state ${}^{k}\boldsymbol{\gamma}(\tilde{\alpha})$ at which the deflection is zero provided both states share the same relative energy and same sign of the velocity ${}^{k}v_{\phi,j}$. If, on the other hand, there is a change in the velocity, the oscillation period T_p must also be accounted for as shown by (5.4.22). Furthermore, by partially differentiating (5.4.20) and making use of the equalities in (5.4.18) and (5.4.21) we can now get the exact same expressions for the costates $\boldsymbol{\lambda}$ in D_{k_j} as provided in Prop. 9 and Table 5.1b. Similarly, by partially differentiating (5.4.22) we can also find the expressions describing $\boldsymbol{\lambda}$ in $D_{k_{j+1}}$ if we additionally use (5.2.20)-(5.2.21) to relate ${}^{j+1}\eta_{0,k}$ to ${}^{j}\eta_{0,k} = \frac{\partial V_f}{\partial x_2}\left({}^{k}\boldsymbol{\gamma}(\alpha^{opt})\right)$ and $\frac{\mathrm{d}T_p}{\mathrm{d}\phi_{max}}\left({}^{k}\varphi_{max}(\alpha^{opt})\right)$.

Focusing now on the optimal control u in the normal extremal lift Λ, we can see from (5.4.20)-(5.4.23) why for $k \geq 1$ knowing the relative energy ${}^{k}\phi_{max}$ and the boundary condition ${}^{j}\eta_{0,k}$ we can describe $u|_{D_{k_j}}$ as a function of the deflection using the function $C(., {}^{k}\phi_{max})$. In addition, the equations also clarify why this description of the control must be adjusted whenever there is a change in the sign of $\dot{x}_1$ and why this adjustment is related to the system's period T_p and thus TDP. Looking now back at the switching patterns illustrated in Fig. 5.3.2, one can observe that it is the period T_p, or more specifically its derivative $\frac{\mathrm{d}T_p}{\mathrm{d}\phi_{max}} = -\frac{4\Delta(\phi_{max})\tau_J(\phi_{max})}{M\phi_{max}}$, which complicates the description of optimal control strategies. For system's with linear TDP's, this derivative is equal to zero. Consequently, it follows from the symmetry properties of C, that the value of the deflection at two consecutive switching instants will share the same magnitude, see Fig 5.3.2 (Middle Row). That is at both these instants the same potential energy will be stored and this leads to the well-known harmonic oscillation of such systems. For systems with nonlinear TDP's, the same principle still holds regarding the influence of the function C on the potential energies at the switching instants. In particular, knowing the first switching instant one can uniquely determine all the other switching instants by making use of this dependence. Describing the resulting control as a function of time is, however, not straight-forward as for systems with linear TDP's. This follows from the energy-dependence of T_p. The potential energies at the switching times and the relative energies attained along the trajectories can, on the other hand, be more easily determined and they also better explain the switching structure of the optimal control. Since this is also true for controls in abnormal extremals and, more importantly, for any control system Σ, we regard optimal control strategies for the LVMP as excitation of the system with its resonance energies.

Chapter 6

Maximal Link Velocity

As stated in Prop. 6, a solution to the LVMP exists for each final time $t_f > 0$. Moreover, it follows from Prop. 15 that the terminal link velocity attained using this solution is always positive. Consequently, for EJ's with velocity-sourced SEA's we can always define a *maximal link velocity function* $\dot{q}_{max} : (0, \infty) \rightarrow (0, \infty)$ with

$$\dot{q}_{max}(t) = -J(u^*), \tag{6.0.1}$$

where u^* denotes the control strategy solving the LVMP for the final time $t_f = t$, see also (2.3.1). The purpose of the current chapter is to first study the properties of this maximal link velocity function. More specifically, we want to clarify how this function depends on the final time as well as the parameters of the control system Σ such as the maximal motor velocity and the TDP. Secondly, we want to experimentally illustrate how to attain this maximal link velocity with the DLR FSJ and thus validate our theoretical results. We will start our discussion by investigating the dependence of $\dot{q}_{max}$ on the final time.

6.1   Final Time Dependence

In this section, we will first prove that the function $\dot{q}_{max}$ is a continuous and strictly increasing function of the final time. This will require us to investigate in detail the relation between $\dot{q}_{max}$ and optimally controlled trajectories. Then, taking a geometrical approach and exploiting the derived properties of $\dot{q}_{max}$ we will discuss how to construct the graph of $\dot{q}_{max}$ in a given interval. Moreover, following the described procedure we will graphically illustrate $\dot{q}_{max}$ for several control systems.

6.1.1   Continuity and Monotonicity

Let us assume that $(\boldsymbol{x}, u)$ is an optimally controlled trajectory defined in the interval $D = [0, t_f]$. According to (6.0.1), the value of $\dot{q}_{max}$ at t_f will then be clearly equal to the terminal link velocity $x_2(t_f)$. Moreover, for final times

greater than t_f the values attained by $\dot{q}_{max}$ will be greater than or equal to $x_2(t_f)$. Indeed, for any $\bar{t}_f > t_f$ we can define an admissible control $\bar{u} : [0, \bar{t}_f] \rightarrow \mathbb{U}$ with

$$\bar{u}(t) = \begin{cases} 0 & t < \varepsilon \\ u(t - \varepsilon) & t \geq \varepsilon \end{cases}, \tag{6.1.1}$$

and $\varepsilon = \bar{t}_f - t_f$. Using (2.1.4) and noting in particular that the origin is an equilibrium point of Σ when the control equals to zero, we can then see that the pair $(\bar{\boldsymbol{x}}, \bar{u})$ defined in the interval $[0, \bar{t}_f]$ with

$$\bar{\boldsymbol{x}}(t) = \begin{cases} \boldsymbol{0} & t < \varepsilon \\ \boldsymbol{x}(t - \varepsilon) & t \geq \varepsilon \end{cases}, \tag{6.1.2}$$

is an admissible controlled trajectory. Moreover, this trajectory starts from the origin and terminates at $\bar{\boldsymbol{x}}_f = \boldsymbol{x}_f$ so that we have $x_2(t_f) \leq \dot{q}_{max}(\bar{t}_f)$. Since our choice for $\bar{t}_f$ was arbitrary, we finally arrive at the relation

$$(\forall t \in (t_f, \infty)) \left[x_2(t_f) = \dot{q}_{max}(t_f) \leq \dot{q}_{max}(t) \right]. \tag{6.1.3}$$

Our discussion above simply shows that the terminal link velocity of $(\boldsymbol{x}, u)$ is a lower bound of $\dot{q}_{max}$ in the interval $[t_f, \infty)$. Similarly, we can show that the trajectory of the link velocity, i.e. x_2, is a lower bound of $\dot{q}_{max}$ in the interval $(0, t_f]$. To see this, let us first note that the restriction of $\boldsymbol{x}$ to a closed interval $[0, t] \subset D$ will always be a trajectory of Σ if $t > 0$. Clearly, this trajectory will also start from the origin. Based on the definition of $\dot{q}_{max}$, we can then directly arrive at the following relation between x_2 and $\dot{q}_{max}$:

$$(\forall t \in (0, t_f]) \left[x_2(t) \leq \dot{q}_{max}(t) \right]. \tag{6.1.4}$$

It is important to note here that equations (6.1.3)-(6.1.4) can be combined to define a continuous function taking values always less than or equal to $\dot{q}_{max}$, i.e. a continuous lower bound of $\dot{q}_{max}$. Similarly, using the arguments above and additionally exploiting the limits on the system's maximal energy as discussed in Prop. 5, we can find a continuous upper bound of $\dot{q}_{max}$ which depends on the terminal link velocity $x_2(t_f)$ and the maximal motor velocity. The following proposition introduces these two functions and also clarifies their relation to $\dot{q}_{max}$.

Proposition 19. *Let $(\boldsymbol{x}, u)$ be an optimally controlled trajectory which is defined on the interval $D = [0, t_f]$. Moreover, let $\dot{q}_{lb} : (0, \infty) \rightarrow \mathbb{R}$ and $\dot{q}_{ub} : (0, \infty) \rightarrow \mathbb{R}$ be two functions with*

$$\dot{q}_{lb}(t) = \begin{cases} x_2(t) & t < t_f \\ x_2(t_f) & t \geq t_f \end{cases}, \tag{6.1.5}$$

and

$$\dot{q}_{ub}(t) = \begin{cases} x_2(t_f) & t < t_f \\ x_2(t_f) + \frac{E_{pot}(\dot{\theta}_{max}t) - E_{pot}(\dot{\theta}_{max}t_f)}{M\dot{\theta}_{max}} & t \geq t_f \end{cases}, \tag{6.1.6}$$

respectively. Then, both $\dot{q}_{lb}$ and $\dot{q}_{ub}$ are continuous functions and we have

$$(t \in (0, \infty)) \left[\dot{q}_{lb}(t) \leq \dot{q}_{max}(t) \leq \dot{q}_{ub}(t) \right]. \tag{6.1.7}$$

Moreover, all inequalities in (6.1.7) hold with equality at $t = t_f$.

Proof. See Appendix B.4.1. □

Given an optimally controlled trajectory, Prop. 19 provides now a means to construct a continuous lower and upper bound of $\dot{q}_{max}$ using this trajectory as well as the parameters describing Σ, see (6.1.5)-(6.1.7). Moreover, since these two bounds intersect each other as well as $\dot{q}_{max}$ at the final time of the given trajectory, Prop. 19 can be used together with Prop. 6, to show that $\dot{q}_{max}$ is continuous at every point of its domain. Using additionally our results on optimally controlled trajectories from Sec. 5.2 and 5.3, we can prove the following proposition which establishes the desired monotonicity and continuity properties[1] of $\dot{q}_{max}$.

Proposition 20. *The maximal link velocity $\dot{q}_{max} : (0, \infty) \to (0, \infty)$ is a continuous and strictly increasing function with the following limits:*

$$\lim_{t \to 0^+} \dot{q}_{max}(t) = 0 \wedge \lim_{t \to \infty} \dot{q}_{max}(t) = \infty. \tag{6.1.8}$$

Proof. See Appendix B.4.1. □

6.1.2 Graph Construction

As we have seen in the previous chapter, if $(\boldsymbol{x}, u)$ is an optimally controlled trajectory defined on $D = [0, t_f]$ there always exists a positive integer k and a parameter $\beta^{opt} \in (k - 1, k]$, such that the trajectory's final time and terminal link velocity are given by $t_S^{ext}(\beta^{opt})$ and $x_{2S}^{ext}(\beta^{opt})$, respectively. Consequently, the value of $\dot{q}_{max}$ at $t_S^{ext}(\beta^{opt})$ will in this case be given by $x_{2S}^{ext}(\beta^{opt})$. Moreover, following a geometric approach we can define[2] a continuous map $^k\boldsymbol{\gamma} : (k-1, k] \to \mathbb{R}^2$ with

$$^k\boldsymbol{\gamma}(\beta) = \begin{pmatrix} t_S^{ext}(\beta) \\ x_{2S}^{ext}(\beta) \end{pmatrix}. \tag{6.1.9}$$

The image of this map will then contain the set of all final times and terminal link velocities which can be attained by extremals when the control switches $k-1$ times. In addition, the map itself will describe a plane curve intersecting the graph of $\dot{q}_{max}$ at the point $(t_S^{ext}(\beta^{opt}), x_{2S}^{ext}(\beta^{opt}))^T$. Furthermore, if there exists a neighborhood $I_{\beta^{opt}}$ of β^{opt} in $(k - 1, k]$ such that extremals corresponding to parameters in this neighborhood are all optimal, the curve $^k\boldsymbol{\gamma}$ restricted to $I_{\beta^{opt}}$

---

[1] As we show in the proof of the proposition, Prop. 6 and Prop. 19 already imply that $\dot{q}_{max}$ is an increasing function. Nevertheless, in order to show that $\dot{q}_{max}$ is strictly increasing we also require some of the properties of optimally controlled trajectories which we derived in Sec. 5.2 and 5.3.

[2] with a slight abuse of notation, see Sec. 5.4.
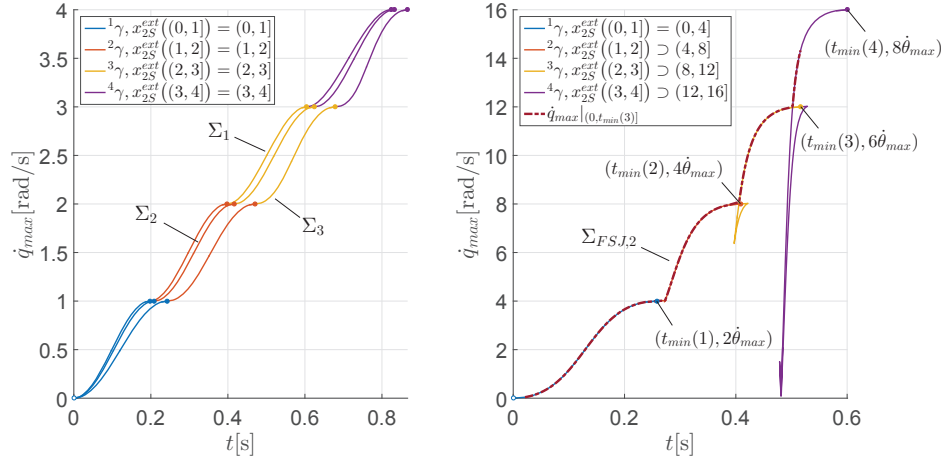
Figure 6.1.1: The Maximal Link Velocity Function $\dot{q}_{max}$
(Left: Σ_1, Σ_2 and Σ_3. Right: $\Sigma_{FSJ,2}$.)

will coincide with the graph of $\dot{q}_{max}$ for $t \in t_S^{ext}(I_{\beta^{opt}})$. We want to next describe how to exploit this relation between $^k\boldsymbol{\gamma}$ and $\dot{q}_{max}$ to construct the graph of $\dot{q}_{max}$ in a given time interval $I_{\dot{q}_{max}} := (0, t_{f,max}] \subset (0, \infty)$.

Let $t_{f,max} > 0$ be an arbitrary scalar. The values of $\dot{q}_{max}$ in the interval $I_{\dot{q}_{max}}$ can then be clearly determined by finding the set of all optimally controlled trajectories with a final time less than or equal to $t_{f,max}$. Note that by Prop. 7-8 and Prop. 14, each of these trajectories is necessarily equal to an extremal $(\boldsymbol{x}, u)$ which corresponds to a parameter $\beta \in (0, \infty)$ such that (5.3.28)-(5.3.29) hold. Moreover, by Prop. 15 there always exists a maximum switching number i_{max} which will be valid for all the controls of these trajectories[3]. Consequently, if we construct for each $k \in \{1, \ldots, i_{max} + 1\}$ the map $^k\boldsymbol{\gamma}$ according to (6.1.9), the union of the images of the resulting maps will contain the graph of $\dot{q}_{max}$ in $I_{\dot{q}_{max}}$. In addition, based on the way we defined the functions t_S^{ext} and $\boldsymbol{x}_S^{ext}$ in Sec. 5.3.3 this union can be represented as one possibly self-intersecting curve. Finally, it follows from Prop. 20 that we can always extract a continuous part of this curve which will correspond to the graph of $\dot{q}_{max}|_{I_{\dot{q}_{max}}}$.

Fig. 6.1.1 (Left) graphically illustrates the construction procedure described above for the three control systems Σ_1, Σ_2 and Σ_3 which have been already investigated in Chapters 4 and 5. For each of the constructed graphs, the maximal final time $t_{f,max}$ was set to $t_S^{ext}(4) = t_{min}(4)$ and the maximal switching number i_{max} was found to be equal to three. Consequently, twelve curves have been in total computed using (6.1.9). None of these curves intersect each other and they also do not have any self-intersections. Therefore, they all uniquely

---

[3]In particular, according to Prop. 15 we will have $i_{max} \leq \left\lceil \frac{\omega_{max} t_{f,max}}{\pi} \right\rceil + 1$ with $\omega_{max} = \max_{\phi \in [0, \dot{\theta}_{max} \cdot t_{f,max}]} \sqrt{\frac{K_J(\phi)}{M}}$.

represent one particular part of the graphs and can be directly combined as done in the figure. It is important to remark here that with the constructed graphs we can now conclude that abnormal extremals terminating at $t_{min}(i)$, with $i \in \{1, 2, 3, 4\}$, are all optimal for Σ_1, Σ_2 and Σ_3. Consequently, the control strategies depicted in Fig. 4.1.1 solve both the EMP and the LVMP. In addition, the graphs also indicate the optimality of the trajectories in Fig. 5.3.3 which we had previously established in Sec. 5.3.3 using Fig. 5.3.4.

Unfortunately, combining the curves ${}^k\boldsymbol{\gamma}$ with $k \in \{1, \ldots, i_{max} + 1\}$ does not always directly lead to the desired graph of $\dot{q}_{max}$ as in Fig. 6.1.1 (Left). This is exemplified in Fig. 6.1.1 (Right), where we illustrate the function $\dot{q}_{max}|_{I_{\dot{q}_{max}}}$ for the control system $\Sigma_{FSJ,2}$ which describes a DLR FSJ with the parameters given in Table 4.1c. The maximal time $t_{f,max}$ was set this time to $t_S^{ext}(3) = t_{min}(3)$ while the maximal switching number i_{max} was found to be again equal to three. Consequently, four curves were computed to determine the graph of $\dot{q}_{max}$ in the interval $I_{\dot{q}_{max}}$. As shown in the figure, by combining these four curves into one continuous curve we do not directly obtain in this case the desired graph due to self-intersections. Such an intersection occurs, for instance, at a time close to $t_{min}(3)$ where the curves ${}^3\gamma$ and ${}^4\gamma$ intersect each other. Notice that for this particular time, there exist two different control strategies which solve the LVMP using a different number of switchings. For higher times, on the other hand, the optimal control strategies all require three switchings to solve the LVMP. This is especially true for $t = t_{min}(3)$ and we can thus conclude that control strategies solving the EMP do not necessarily solve the LVMP.

The four graphs depicted in Fig. 6.1.1 clearly validate our results regarding the time dependence of the maximal link velocity function. Furthermore, they also show how the parameters describing a control system can influence the attained maximal link velocity as well as the optimal control strategies required to reach this velocity. In the following section, we will take a closer look at this influence and show in particular how to systematically analyse it by making use of dimensionless parameters.

6.2 Parameter Dependence

In this section, we want to understand how the maximal link velocity of an EJ depends on its parameters. For this, we will analyse the properties of the *velocity gain function* (VGF) $\epsilon : (0, \infty) \times P_\Sigma \to (0, \infty)$ defined by

$$\epsilon(t; \boldsymbol{p}) = \frac{\dot{q}_{max}(t; \boldsymbol{p})}{\dot{\theta}_{max}}, \tag{6.2.1}$$

where $\dot{q}_{max}(.; \boldsymbol{p})$ denotes the maximal link velocity function for the system Σ corresponding to $\boldsymbol{p} = (M, \tau_J, \dot{\theta}_{max})$. Noting that abnormal extremals always lead to terminal link velocities which are an even multiple of the motor velocity, we will start our discussion by clarifying the relation between their terminal times and the parameter to which they correspond. In other words, we will first

investigate the influence of $\boldsymbol{p}$ on the function[4] $t_{min}(.;\boldsymbol{p})$. Our discussion will lead to a dimensionless time function which will explain some of the differences between the graphs in Fig. 6.1.1 (Left). In the second part of the section, we will then similarly introduce dimensionless parameters which can be used to simultaneously determine VGF's corresponding to different parameters.

6.2.1 Dimensionless Time Function

Let Σ be a control system corresponding to an arbitrary parameter $\boldsymbol{p} \in P_\Sigma$ and k a positive integer. From Prop. 11, it is then known that there exists a unique abnormal extremal such that the terminal link velocity $2k\dot{\theta}_{max}$ is reached at the final time $t_{min}(k;\boldsymbol{p})$. Consequently, the following inequality holds for the VGF according to (6.2.1):

$$\epsilon\left(t_{min}(k;\boldsymbol{p});\boldsymbol{p}\right) \geq 2k. \tag{6.2.2}$$

Clearly, the inequality above will hold with equality in case the abnormal extremal terminating at $t_{min}(k;\boldsymbol{p})$ is optimal. We have already seen in Fig. 6.1.1 (Left) that abnormal extremals can be optimal. In order to gain an insight on the properties of ϵ, we will therefore investigate in the following the relation between t_{min} and $\boldsymbol{p}$.

Notice first that for any given $\boldsymbol{p} \in P_\Sigma$, the function $t_{min}(.;\boldsymbol{p}) : \{1, 2, \ldots\} \to (0, \infty)$ is a strictly increasing function. This simply follows from the definition of t_{min} in (4.2.11)-(4.2.12) and the fact that periods of mass springs systems are always positive. In addition, according to the definition the image of $t_{min}(.;\boldsymbol{p})$ depends on all elements of $\boldsymbol{p}$. Indeed, the TDP determines the potential energy function while the link mass together with the motor velocity determine the relative energies stored along abnormal extremals. In addition, the mass and the TDP determine the period of the corresponding mass spring system. Analysing the influence of $\boldsymbol{p}$ on t_{min} requires us to consider all these dependences. The following proposition shows how this can be achieved by analysing dimensionless control systems for which both the mass and the maximum motor velocity are equal to one[5].

Proposition 21. *Let $\boldsymbol{p}$ be an arbitrary element of the parameter set P_Σ and*

---

[4]Similar to $\dot{q}_{max}(.;\boldsymbol{p})$, the additional argument in t_{min} is used to explicitly state its dependence on the parameter $\boldsymbol{p}$. In this section, we will adopt this same notation also for other previously defined functions (See also Sec. 2.2).

[5]In Prop. 21-26 as well as in our discussions to follow, we will be using the symbols "^" and "~" to distinguish the parameters $\hat{\boldsymbol{p}} = (\hat{M}, \hat{\tau}_J, \hat{\dot{\theta}}_{max})$ and $\tilde{\boldsymbol{p}} = (\tilde{M}, \tilde{\tau}_J, \tilde{\dot{\theta}}_{max})$ from $\boldsymbol{p}$. Consistent with this notation, we use $\hat{K}_J$ and $\tilde{K}_J$ to denote the SDP corresponding to $\hat{\tau}_J$ and $\tilde{\tau}_J$, respectively. Similarly, we use $\hat{\omega}_0 = \sqrt{\frac{\hat{K}_J(0)}{\hat{M}}}$ and $\tilde{\omega}_0 = \sqrt{\frac{\tilde{K}_J(0)}{\tilde{M}}}$ to denote the corresponding eigenfrequencies. Moreover, K_J will denote as before the SDP corresponding to τ_J and we will have $\omega_0 = \sqrt{\frac{K_J(0)}{M}}$. Finally, in Prop. 22-24 and Prop. 26 as well as in Lemma 57 the function $\tau_J(\phi)$ will be given by $K_e g(k_e \phi)$ and $\tilde{\tau}_J(\phi)$ by $\tilde{K}_e g(\tilde{k}_e \phi)$.

$\hat{\tau}_J : \mathbb{R} \to \mathbb{R}$ *the TDP defined by*

$$(\forall \phi \in \mathbb{R}) \left[\hat{\tau}_J(\phi) = \frac{\tau_J(\frac{\dot{\theta}_{max}}{\omega_0}\phi)}{M\omega_0\dot{\theta}_{max}} \right]. \tag{6.2.3}$$

Then, the parameter $\hat{p} = (1, \hat{\tau}_J, 1)$ *is an element of* P_Σ *and we have*

$$(\forall k \in \{1, 2, \ldots\}) \left[\omega_0 t_{min}(k; p) = t_{min}(k; \hat{p}) \right]. \tag{6.2.4}$$

Proof. See Appendix B.4.2. $\qquad\qquad\qquad\qquad\qquad\qquad\square$

Given a parameter $p \in P_\Sigma$, Prop. 21 shows how to construct a dimensionless parameter $\hat{p} = (1, \hat{\tau}_J, 1)$ such that the *dimensionless time function* (DTF) $\omega_0 t_{min}(.; p)$ is given directly by $t_{min}(.; \hat{p})$. It is important to realize here that there exist infinitely many elements of the set P_Σ for which application of Prop. 21 results in the same dimensionless parameter and thus in the same DTF. This is, in particular, true for elements of P_Σ with linear TDP's. Indeed, for these elements the DTF is always given by $k\pi$ with $k \in \{1, 2, \ldots\}$, see (4.2.11)-(4.2.12) and (6.2.3)-(6.2.4). The main value of Prop. 21 is therefore that it allows us to determine one particular function which can be used to analyse t_{min} for an infinite set of control system parameters. In the following proposition, we further exploit this property to introduce a subset of P_Σ for which the DTF can depend at most on one dimensionless variable.

Proposition 22. *Let* $g : \mathbb{R} \to \mathbb{R}$ *be an element of* $C^1_{\tau_J}$ *such that we have* $\frac{dg}{d\phi}(0) = 1$ *and let* P_{Σ_g} *be the set defined as follows:*

$$P_{\Sigma_g} = \left\{ (M, \tau_J, \dot{\theta}_{max}) \in P_\Sigma \middle| (\exists K_e > 0)(\exists k_e > 0) \right.$$
$$\left. (\forall \phi \in \mathbb{R}) \left[\tau_J(\phi) = K_e g(k_e \phi) \right] \right\}. \tag{6.2.5}$$

In addition, assume that $p = (M, \tau_J, \dot{\theta}_{max})$ *and* $\tilde{p} = (\tilde{M}, \tilde{\tau}_J, \tilde{\dot{\theta}}_{max})$ *are both elements of* P_{Σ_g} *such that the following equality holds:*

$$\frac{k_e \dot{\theta}_{max}}{\omega_0} = \frac{\tilde{k}_e \tilde{\dot{\theta}}_{max}}{\tilde{\omega}_0}.$$

Then, we have

$$(\forall k \in \{1, 2, \ldots\}) \left[\omega_0 t_{min}(k; p) = \tilde{\omega}_0 t_{min}(k; \tilde{p}) \right].$$

Proof. Let g, p and $\tilde{p}$ satisfy the hypotheses of the proposition. Then, for each $\phi \in \mathbb{R}$ we have

$$\frac{\tau_J(\frac{\dot{\theta}_{max}}{\omega_0}\phi)}{M\omega_0\dot{\theta}_{max}} = \frac{K_e g(\frac{k_e \dot{\theta}_{max}}{\omega_0}\phi)}{M\omega_0\dot{\theta}_{max}} = \frac{g(\frac{k_e \dot{\theta}_{max}}{\omega_0}\phi)}{\frac{k_e \dot{\theta}_{max}}{\omega_0}}$$

$$= \frac{g(\frac{\tilde{k}_e \tilde{\dot{\theta}}_{max}}{\tilde{\omega}_0}\phi)}{\frac{\tilde{k}_e \tilde{\dot{\theta}}_{max}}{\tilde{\omega}_0}} = \frac{\tilde{\tau}_J(\frac{\tilde{\dot{\theta}}_{max}}{\tilde{\omega}_0}\phi)}{\tilde{M}\tilde{\omega}_0\tilde{\dot{\theta}}_{max}}, \tag{6.2.6}$$

Σ	$\omega_0 t_{min}(k; \boldsymbol{p})$
Σ_g	$\sum_{l=0}^{k-1} \int_0^{2l+1} \dfrac{2\dot{\Theta}_{max}\mathrm{d}s}{g\left(E_{pot,g}^{-1}\left[\frac{\dot{\Theta}_{max}^2((2l+1)^2-s^2)}{2}\right]\right)}$
Σ_{sin}	$2\sum_{l=0}^{k-1} K\left(\frac{2l+1}{2}\dot{\Theta}_{max}\right), \dot{\Theta}_{max} \in \left(0, \frac{\sqrt{2}}{2k-1}\right)$
Σ_{id}	$k\pi$
Σ_{sinh}	$2\sum_{l=0}^{k-1} \dfrac{K\left(\left(1+\left(\frac{2}{2l+1}\frac{1}{\dot{\Theta}_{max}}\right)^2\right)^{-\frac{1}{2}}\right)}{\sqrt{1+\left(\frac{2l+1}{2}\dot{\Theta}_{max}\right)^2}}$
$g \in C_{\tau_J}^1, \frac{\mathrm{d}g}{\mathrm{d}\phi}(0) = 1, E_{pot,g}(\phi) = \int_0^\phi g(s)\mathrm{d}s,$	
$k \in \{1, 2, \ldots\}, \dot{\Theta}_{max} = \frac{k_e \dot{\theta}_{max}}{\omega_0} > 0.$	

Table 6.1: The Dimensionless Time Function $\omega_0 t_{min}$ for $\Sigma_{sin}, \Sigma_{id}, \Sigma_{sinh}$ and Σ_g

where we have used of the fact that ω_0 is given by $\sqrt{\frac{K_e k_e}{M}}$ and $\tilde{\omega}_0$ by $\sqrt{\frac{\tilde{K}_e \tilde{k}_e}{M}}$. If we now apply Prop. 21 once for the parameter $\boldsymbol{p}$ and once for the parameter $\tilde{\boldsymbol{p}}$, (6.2.6) implies that the resulting parameter will in both cases be equal to $\hat{\boldsymbol{p}} = (1, \hat{\tau}_J, 1)$ with $\hat{\tau}_J$ given by (6.2.3). Consequently, for each $k \in \{1, 2, \ldots\}$ we will have $\omega_0 t_{min}(k; \boldsymbol{p}) = \tilde{\omega}_0 t_{min}(k; \tilde{\boldsymbol{p}}) = t_{min}(k; \hat{\boldsymbol{p}})$ as desired. Since our choice for $g, \boldsymbol{p}$ and $\tilde{\boldsymbol{p}}$ was arbitrary, this concludes our proof. $\square$

Given an arbitrary function $g \in C_{\tau_J}^1$ with $\frac{\mathrm{d}g}{\mathrm{d}\phi}(0) = 1$, we can now see with Prop. 22 that for any element $\boldsymbol{p}$ in the set P_{Σ_g}, as defined by (2.2.2), the DTF is uniquely determined by the dimensionless ratio $\dot{\Theta}_{max} := \frac{k_e \dot{\theta}_{max}}{\omega_0}$. Consequently, for any $k \in \{1, 2, \ldots\}$ the product $\omega_0 t_{min}(k; \boldsymbol{p})$ can be expressed as a function of the dimensionless ratio $\dot{\Theta}_{max}$ when $\boldsymbol{p}$ is known to belong to P_{Σ_g}. This is indeed true as shown in[6] Table 6.1 where we provide a mathematical expression for the DTF depending only on g and $\dot{\Theta}_{max}$, see second row. For ease of readability, we give the derivation of this expression in Appendix B.4.2, see Lemma 57.

Focusing now on the three control systems $\Sigma_{sin}, \Sigma_{id}$ and Σ_{sinh} described in Table 4.1, the identity and the hyperbolic sine functions are clearly both valid candidates for the mapping g in Prop. 22. Furthermore, any element of $C_{\tau_J}^1$ which coincides with the sine function in a closed interval in $\left(-\frac{\pi}{2}, \frac{\pi}{2}\right)$ is a valid candidate. Consequently, we can substitute these three basic functions into the expression in the second row of Table 6.1 and find expressions for the DTF's of $\Sigma_{sin}, \Sigma_{id}$ and Σ_{sinh} as a function of k and $\dot{\Theta}_{max}$. These are provided again in[7]

---

[6] Given a $g \in C_{\tau_J}^1$ with $\frac{\mathrm{d}g}{\mathrm{d}\phi}(0) = 1$, we use Σ_g to denote any control system which corresponds to a parameter $\boldsymbol{p} \in P_{\Sigma_g}$. Moreover, we use $E_{pot,g}^{-1} : [0, \infty) \to [0, \infty)$ to denote the inverse of the function $E_{pot,g}|_{[0,\infty)}$ with $E_{pot,g} : \mathbb{R} \to [0, \infty)$ given by $E_{pot,g}(\phi) = \int_0^\phi g(s)\mathrm{d}s$, see Section 3.1.

[7] Notice that for the control system Σ_{sin}, the ratio $\dot{\Theta}_{max}$ is allowed to take values only in the bounded interval $(0, \frac{\sqrt{2}}{2k-1})$ which depends on the argument of $\omega_0 t_{min}(.; \boldsymbol{p})$. This is done in order to ensure that the assumptions $(A1) - (A3)$ from Sec. 2.1 hold. More specifically, for
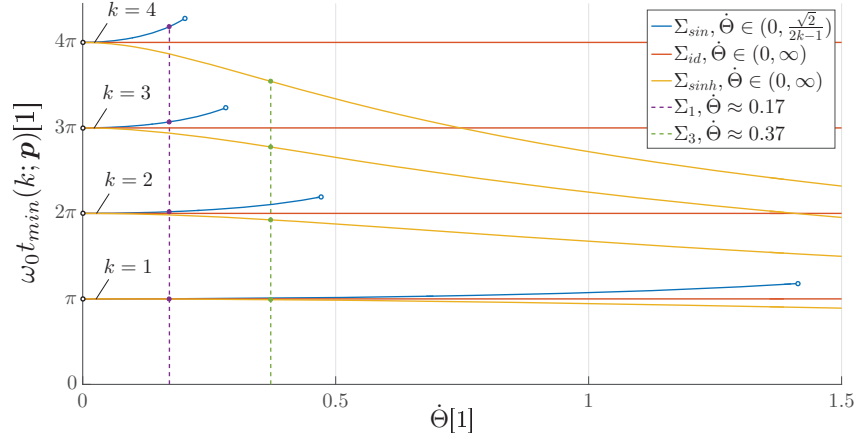
Figure 6.2.1: The Dimensionless Time Function $\omega_0 t_{min}$ for $\Sigma_{sin}, \Sigma_{id}$ and Σ_{sinh} ($\dot{\Theta}_{max} = \frac{k_e \dot{\theta}_{max}}{\omega_0}, k \in \{1, 2, 3, 4\}$)

Table 6.1 and are also graptically illusrated in Fig. 6.2.1. To better understand how the parameter $\boldsymbol{p}$ can influence t_{min}, we will next discuss this last figure and state two more propositions which will clarify for $\Sigma_{sin}, \Sigma_{id}$ and Σ_{sinh} the dependence of t_{min} on ω_0 and $\dot{\Theta}_{max}$. Moreover, we will show how the graphs in Fig. 6.1.1 (Left) are related to the graphs in Fig. 6.2.1.

We had already observed that for control systems with linear TDP's the dimensionless time function does not depend on the parameter $\boldsymbol{p}$. Consequently, the eigenfrequency ω_0 of these systems uniquely determine t_{min}. This is shown in Fig. 6.2.1 by the straight red lines which represent for each $k \in \{1, 2, 3, 4\}$ the product $\omega_0 t_{min}(k; \boldsymbol{p})$ as constant function of the ratio $\dot{\Theta}_{max}$. On the other hand, if we look at the blue lines, i.e. at the DTF's for the control systems with the TDP $\tau_{J,s}$, we can see that regardless of the value of k the product $\omega_0 t_{min}(k; \boldsymbol{p})$ strictly increases as the ratio $\dot{\Theta}_{max}$ increases. This means that even if we fix ω_0 we can still decrease in this case the time $t_{min}(k; \boldsymbol{p})$ by decreasing, for instance, the motor velocity. Conversely, for control systems with the TDP $\tau_{J,sh}$ the product $\omega_0 t_{min}(k; \boldsymbol{p})$ is always strictly decreasing when $\dot{\Theta}_{max}$ increases. This implies that for a given ω_0 and k the time $t_{min}(k; \boldsymbol{p})$ will decrease if we increase the motor velocity or the parameter k_e in the TDP.

These different possibilities regarding the dependence of t_{min} on $\boldsymbol{p}$ follow actually from the energy dependence of periods of MSS's and Prop. 22. This is exploited in the following proposition to introduce a particular set of control systems for which the relation between $\omega_0 t_{min}$ and $\boldsymbol{p}$ mainly depends on the spring characteristics.

---

each $k \in \{1, 2, \ldots\}$ the provided upper bound for $\dot{\Theta}_{max}$ ensures that the maximal magnitude of the deflection value, which is obtained along the abnormal extremal terminating at $t_{min}(k)$, is less than $\frac{\pi}{2k_e}$.

Proposition 23. *Let $g : \mathbb{R} \to \mathbb{R}$ be a two times continuously differentiable element of $C^1_{\tau_J}$ with $\frac{\mathrm{d}g}{\mathrm{d}\phi}(0) = 1$ and $\boldsymbol{p} = (M, \tau_J, \dot{\theta}_{max}), \tilde{\boldsymbol{p}} = (\tilde{M}, \tilde{\tau}_J, \dot{\tilde{\theta}}_{max})$ two elements of the set P_{Σ_g} defined by (6.2.5). Moreover, assume that there exists a positive integer k and a positive scalar $\Phi_{max} > 0$ such that the inequality*

$$E_{pot,g}(2\Phi_{max}) > \dot{\Theta}^2 \frac{(2k-1)^2}{2} \qquad (6.2.7)$$

holds for each $\dot{\Theta} \in \{ \frac{k_e \dot{\theta}_{max}}{\omega_0}, \frac{\tilde{k}_e \dot{\tilde{\theta}}_{max}}{\tilde{\omega}_0} \}$ and that we additionally have

$$(\forall \phi \in (0, 2\Phi_{max})) \left[\mathrm{sgn}\left(\frac{\mathrm{d}^2 g}{\mathrm{d}\phi^2}(\phi) \right) = const. \right]. \qquad (6.2.8)$$

Then, for each positive integer $l \in \{1, \ldots, k\}$ we have

$$\mathrm{sgn}\left[\omega_0 t_{min}(l; \boldsymbol{p}) - \tilde{\omega}_0 t_{min}(l; \tilde{\boldsymbol{p}}) \right] =$$

$$(-1) \,\mathrm{sgn}\left(\frac{\mathrm{d}^2 g}{\mathrm{d}\phi^2}(\Phi_{max}) \right) \mathrm{sgn}\left(\frac{k_e \dot{\theta}_{max}}{\omega_0} - \frac{\tilde{k}_e \dot{\tilde{\theta}}_{max}}{\tilde{\omega}_0} \right). \quad (6.2.9)$$

Proof. See Appendix B.4. $\qquad\qquad\qquad\qquad\qquad\qquad\qquad\qquad\square$

Prop. 23 clearly justifies our observations from Fig. 6.2.1 for the control systems $\Sigma_{sin}, \Sigma_{id}$ and Σ_{sinh}. More importantly, it shows that the relation between t_{min} and $\boldsymbol{p}$, as we have discussed above for these control systems, remains also valid for other control systems with softening and hardening springs. Indeed, it follows from the proposition and in particular (6.2.9) that for a TDP g, which can be obtained using a softening or a hardening spring and which satisfies $\frac{\mathrm{d}g}{\mathrm{d}\phi}(0) = 1$, the influence of $\dot{\Theta}_{max}$ on t_{min} is always described in terms of the sign of the derivative $\frac{\mathrm{d}^2 g}{\mathrm{d}\phi^2}$ if the eigenfrequency ω_0 is kept constant and $\boldsymbol{p}$ belongs to P_{Σ_g}.

It is important to note here that when the function g corresponds to a softening or a linear spring, (6.2.9) also implies that t_{min} will decrease if we increase the eigenfrequency ω_0 while keeping the product $k_e \dot{\theta}_{max}$ constant. When g corresponds to a hardening spring, however, the influence of ω_0 on t_{min} can not be uniquely determined by (6.2.9) in this case. The reason is that $\omega_0 t_{min}(k; \boldsymbol{p})$ is a strictly decreasing function of $\dot{\Theta}_{max}$ for each integer $k > 0$ and if the rate of this decrease is sufficiently high an increase in ω_0 might also increase[8] t_{min}. Nevertheless, this can never occur if g is given by the hyperbolic sine function. This is shown in the following proposition which provides sufficient conditions under which t_{min} always decreases with an increase in ω_0.

Proposition 24. *Let $g : \mathbb{R} \to \mathbb{R}$ be an element of $C^1_{\tau_J}$ with $\frac{\mathrm{d}g}{\mathrm{d}\phi}(0) = 1$. In addition, let $\boldsymbol{p} = (M, \tau_J, \dot{\theta}_{max})$ and $\tilde{\boldsymbol{p}} = (\tilde{M}, \tilde{\tau}_J, \dot{\tilde{\theta}}_{max})$ be two elements of the*

---

[8]As discussed in Appendix B.4.2, a function g for which such a dependence exists between ω_0 and t_{min} can be constructed.

set $P_{\Sigma,g}$ defined by (6.2.5) such that we have

$$k_e \dot{\theta}_{max} = \tilde{k}_e \dot{\tilde{\theta}}_{max}, \tag{6.2.10}$$

and

$$\omega_0 > \tilde{\omega}_0. \tag{6.2.11}$$

Morever, assume that there exists a positive integer k and a scalar $\Phi_{max} > 0$ with

$$E_{pot,g}(2\Phi_{max}) > \frac{1}{2}\left(\frac{\tilde{k}_e \dot{\tilde{\theta}}_{max}}{\tilde{\omega}_0}\right)^2 (2k-1)^2 \tag{6.2.12}$$

such that we have

$$(\forall \phi \in (0, 2\Phi_{max})) \left[\frac{E_{pot,g}(\phi)\frac{\mathrm{d}g}{\mathrm{d}\phi}(\phi)}{g^2(\phi)} < 1\right]. \tag{6.2.13}$$

Then, the following inequality holds for each positive integer $l \in \{1, \ldots, k\}$:

$$t_{min}(l; \boldsymbol{p}) < t_{min}(l; \tilde{\boldsymbol{p}}). \tag{6.2.14}$$

Proof. See Appendix B.4.2. □

According to Prop. 24, we can now see that for the three control systems $\Sigma_{sin}, \Sigma_{id}$ and Σ_{sinh} an abnormal extremal solving the EMP always requires less time if the eigenfrequency ω_0 is increased while keeping the product $k_e\dot{\theta}_{max}$ constant. Moreover, if we compare these times among each other it follows from Fig. 6.2.1 that for any given switching number they will approach each other by such an increase in ω_0.

Looking now back at Fig. 6.1.1 (Left), we can see that for the control system Σ_1 the velocity gains of $2, 4, 6$ and 8 are all attained in a smaller amount of time when compared with the systems Σ_2 and Σ_3. As the inequality in (6.2.2) holds with equality for these gains, this means that for each $k \in \{1, 2, 3, 4\}$ the time $t_{min}(k; \boldsymbol{p})$ is smallest for the system Σ_1. The values attained by the dimensionless product $\omega_0 t_{min}(k; \boldsymbol{p})$, on the other hand, is greatest for the system Σ_1 as we can see from Fig. 6.2.1. Consequently, the reason for the smaller time values for Σ_1 follows mainly from the fact that the eigenfrequency ω_0 is the highest for Σ_1, see Sec. 3.1.

A closer look at Fig. 6.2.1 also shows that for Σ_1 the difference $t_{min}(k) - t_{min}(k-1)$ is strictly increasing with increasing k. This follows directly from the fact that Σ_1 has a softening spring, see Prop. 1 and Prop. 4. Similarly, for the system Σ_3 the same difference is strictly decreasing with increasing k as this system has a hardening spring. As a consequence, we can see that in Fig. 6.1.1 (Left) the horizontal distance between the filled points is increasing for Σ_1 and decreasing for Σ_3. Nevertheless, these increases and decreases are not sufficiently high so that Σ_3 always requires the maximum amount of time to reach the velocity gains mentioned above. This is especially true for the gain $\epsilon = 8$, even though Σ_3 requires in this case the least amount of spring deflection to store the final relative energy ${}^3E_{rel} = 6.125$ while Σ_1 requires the maximal amount, see Sec. 3.1.

6.2.2 Velocity Gain Function

Given a parameter $\boldsymbol{p} \in P_\Sigma$, it follows from our discussions in Sec. 6.1.2 that the velocity gain function $\epsilon(.; \boldsymbol{p})$ must satisfy the following inequality for each $\beta \in (0, \infty)$:

$$\epsilon \left(t_S^{ext}(\beta; \boldsymbol{p}); \boldsymbol{p} \right) \geq \frac{x_{2S}^{ext}(\beta; \boldsymbol{p})}{\dot{\theta}_{max}}. \tag{6.2.15}$$

Furthermore, as already discussed there it follows from PMP that for each given final time $t_f > 0$ there exists at least one scalar $\beta > 0$ for which the final time is equal to $t_S^{ext}(\beta; \boldsymbol{p})$ and the inequality in (6.2.15) holds with equality. This particular property has been used in Sec. 6.1.2 together with the continuity properties of t_S^{ext} and x_{2S}^{ext} to introduce a construction procedure for the graph of $\dot{q}_{max}(.; \boldsymbol{p})$, see Fig. 6.1.1. Focusing particularly on the systems $\Sigma_{sin}, \Sigma_{id}$ and Σ_{sinh}, we want to show in the following how to use this same procedure to analyse the dependence of ϵ on t_f and $\boldsymbol{p}$.

Similar to Sec. 6.2.1, for analysing the influence of the final time and the system parameter on the velocity gain we will make use of dimensionless control systems in which both the mass and the maximal motor velocity are equal to one. The following proposition provides a basis for the construction of such systems.

Proposition 25. *Let $\boldsymbol{p}$ be an arbitrary element of the parameter set P_Σ and $t_f > 0$ an arbitrary scalar. Moreover, let $\hat{t}_f$ be an arbitrary positive scalar and $\hat{\tau}_J : \mathbb{R} \to \mathbb{R}$ the TDP defined by*

$$(\forall \phi \in \mathbb{R}) \left[\hat{\tau}_J(\phi) = \frac{\tau_J \left(\frac{\dot{\theta}_{max} t_f}{\hat{t}_f} \phi \right)}{\frac{M \dot{\theta}_{max} \hat{t}_f}{t_f}} \right]. \tag{6.2.16}$$

Then, the parameter $\hat{\boldsymbol{p}} = (1, \hat{\tau}_J, 1)$ is an element of P_Σ and we have

$$\epsilon(t_f; \boldsymbol{p}) = \epsilon(\hat{t}_f; \hat{\boldsymbol{p}}). \tag{6.2.17}$$

Proof. See Appendix B.4.2. $\qquad\qquad\square$

Given a parameter $\boldsymbol{p} \in P_\Sigma$ and final time $t_f > 0$, Prop. 25 provides a means to construct a dimensionless parameter $\hat{\boldsymbol{p}} = (1, \hat{\tau}_J, 1)$ and a dimensionless time $\hat{t}_f$ such that the two velocity gains $\epsilon(t_f; \boldsymbol{p})$ and $\epsilon(\hat{t}_f; \hat{\boldsymbol{p}})$ are equal to each other. It is important to note here that in this construction, the choice of $\hat{t}_f$ is arbitrary as long as it remains positive. More specifically, (6.2.16) will in general describe a different TDP for each choice of $\hat{t}_f$ and thus also a different parameter. Nevertheless, the equality (6.2.17) will hold in each case.

Given a dimensionless time and a dimensionless parameter, Prop. 25 can also be used to find different choices for the system parameter and final time such that the same velocity gain is attained. Indeed, it follows from (6.2.16) that for any two parameters $\boldsymbol{p}$ and $\tilde{\boldsymbol{p}}$ in the set P_Σ and any positive scalar t_f we will have

$$\epsilon(t_f; \boldsymbol{p}) = \epsilon(\frac{\dot{\theta}_{max}}{\tilde{\dot{\theta}}_{max}} t_f; \tilde{\boldsymbol{p}}), \tag{6.2.18}$$

provided $\tilde{\tau}_J$ is equal to $\frac{\tilde{M}\tilde{\dot{\theta}}_{max}^2}{M\dot{\theta}_{max}^2}\tau_J$. Note that this particular relation implies that given a control system and a desired velocity gain, the minimum time required to reach this gain will be reduced by half if the motor velocity is doubled and the mass is scaled down by four.

The equality (6.2.18) clearly illustrates how VGF's corresponding to different parameters can be closely related to each other. By focusing, as in Prop. 22, on a particular set of parameters, this relation can be further exploited to describe the velocity gain ϵ as a function of only two dimensionless parameters. This is shown in the following proposition.

Proposition 26. *Let* $g : \mathbb{R} \to \mathbb{R}$ *be an element of* $C_{\tau_J}^1$ *with* $\frac{\mathrm{d}g}{\mathrm{d}\phi}(0) = 1$ *and* $\boldsymbol{p} = (M, \tau_J, \dot{\theta}_{max}), \tilde{\boldsymbol{p}} = (\tilde{M}, \tilde{\tau}_J, \tilde{\dot{\theta}}_{max})$ *two elements of the set* P_{Σ_g} *defined by (6.2.5). Moreover, let* t_f *and* $\tilde{t}_f$ *be two arbitrary positive scalars such that the following two equalities hold:*

$$\frac{k_e \dot{\theta}_{max}}{\omega_0} = \frac{\tilde{k}_e \tilde{\dot{\theta}}_{max}}{\tilde{\omega}_0}, \tag{6.2.19}$$

and

$$\omega_0 t_f = \tilde{\omega}_0 \tilde{t}_f. \tag{6.2.20}$$

Then, we have

$$\epsilon(t_f, \boldsymbol{p}) = \epsilon(\tilde{t}_f, \tilde{\boldsymbol{p}}). \tag{6.2.21}$$

Proof. Let $g, \boldsymbol{p}, \tilde{\boldsymbol{p}}, t_f$ and $\tilde{t}_f$ satisfy the hypotheses of the proposition. By applying Prop. 25 once using the parameter $\boldsymbol{p}$ with t_f and once using the parameter $\tilde{\boldsymbol{p}}$ with $\tilde{t}_f$, it can then be shown that in both cases the same parameter $\hat{\boldsymbol{p}}$ will be obtained if $\hat{t}_f$ is set to $\omega_0 t_f = \tilde{\omega}_0 \tilde{t}_f$. Consequently, we will have $\epsilon(t_f; \boldsymbol{p}) = \epsilon(\tilde{t}_f; \tilde{\boldsymbol{p}}) = \epsilon(\hat{t}_f; \hat{\boldsymbol{p}})$ showing that (6.2.21) holds. $\square$

Given a function $g \in C_{\tau_J}^1$, with $\frac{\mathrm{d}g}{\mathrm{d}\phi}(0) = 1$, Prop. 26 shows that for any $\boldsymbol{p} \in P_{\Sigma_g}$ and $t_f > 0$ the velocity gain $\epsilon(t_f; \boldsymbol{p})$ can depend at most on two terms, namely the dimensionless ratio $\dot{\Theta}_{max}$ and the dimensionless final time $\omega_0 t_f$. Moreover, we can use the same proposition also to systematically analyse the influence of these two terms on ϵ. To see this, let us first set in the proposition both $\tilde{M}$ and $\tilde{\dot{\theta}}_{max}$ to one and let the TDP $\tilde{\tau}_J$ satisfy

$$(\forall \phi \in \mathbb{R}) \left[\tilde{\tau}_J(\phi) = \frac{g(\dot{\Theta}_{max}\phi)}{\dot{\Theta}_{max}} \right]. \tag{6.2.22}$$

The parameter $\tilde{\boldsymbol{p}}$ will then only depend on $\dot{\Theta}_{max}$. In addition, the equality (6.2.19) will hold since $\tilde{\omega}_0$ and $\tilde{k}_e$ are equal to one and $\dot{\Theta}_{max}$, respectively. Finally, it follows from (6.2.20)-(6.2.21) that for this particular parameter we will have

$$\epsilon(t_f; \boldsymbol{p}) = \epsilon(\omega_0 t_f; \tilde{\boldsymbol{p}}). \tag{6.2.23}$$
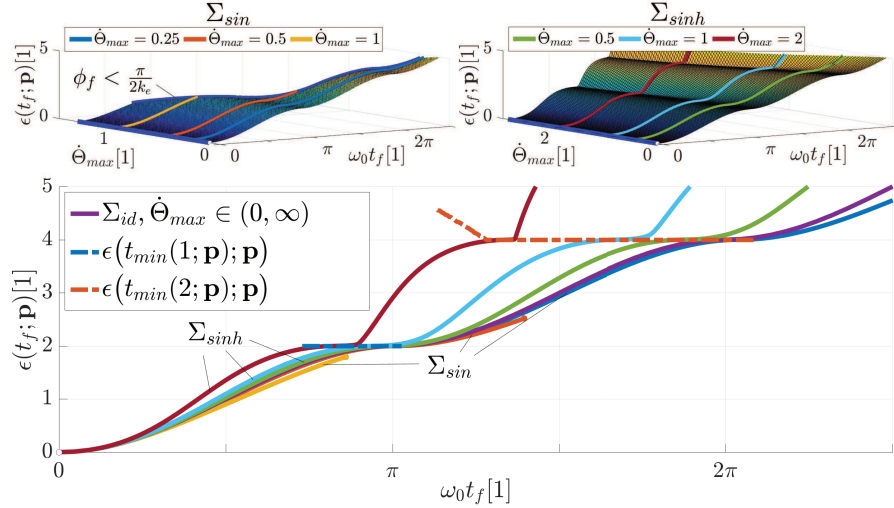
Figure 6.2.2: The Velocity Gain Function ϵ for $\Sigma_{sin}, \Sigma_{id}$ and Σ_{sinh}

The equality above shows now clearly that the velocity gain $\epsilon|_{(0,\infty) \times P_{\Sigma_g}}$ can be described as a function of $\dot{\Theta}_{max}$ and $\omega_0 t_f$. More importantly, it indicates that the graph of this function can be constructed using our results from Sec. 6.1.2 provided $\omega_0 t_f$ is constrained to take values in a closed interval $\tilde{I}_{\dot{q}_{max}} = (0, \omega_0 t_{f,max}] \subset (0, \infty)$. Indeed, using (6.2.22) we can first determine for each $\dot{\Theta}_{max} > 0$ a parameter $\tilde{\boldsymbol{p}} = (1, \tilde{\tau}_J, 1)$. For each of these parameters, the graph of $\dot{q}_{max}(.; \tilde{\boldsymbol{p}}) = \epsilon(.; \tilde{\boldsymbol{p}})$ can then be constructed in $\tilde{I}_{\dot{q}_{max}}$ by determining the set of the corresponding extremals terminating at a final time less than or equal to $\omega_0 t_{f,max}$. Finally, the union of these graphs will lead to the desired graph.

The procedure described above is graphically illustrated in Fig. 6.2.2 (Top) for the parameter sets $P_{\Sigma_{sin}}$ and $P_{\Sigma_{sinh}}$ and in Fig. 6.2.2 (Bottom) for the set $P_{\Sigma_{id}}$. As shown there, for the first two sets we have additionally constrained the ratio $\dot{\Theta}_{max}$ to take values in a closed interval. More specifically, for the set $P_{\Sigma_{sin}}$ the ratio $\dot{\Theta}_{max}$ was constrained to take values in the interval $[0.1, 1.414]$ and for the set $P_{\Sigma_{sinh}}$ in the interval $[0.1, 3]$. In addition, for the sets $P_{\Sigma_{sinh}}$ and $P_{\Sigma_{id}}$ the final time $\omega_0 t_{f,max}$ was set to $\frac{5}{2}\pi$. For the set $P_{\Sigma_{sin}}$, on the other hand, the same final time was only used for sufficiently small ratios. For larger ratios, the final time was further decreased until it could be numerically ensured that the final deflection value ϕ_f, which can be attained by an extremal corresponding to $\boldsymbol{p}$, is always less than $\frac{\pi}{2k_e}$. We want to next conclude our discussion on VGF's by elaborating on the properties of the depicted functions.

Taking a closer look at Fig. 6.2.2 (Bottom), it can be first seen that for each $\boldsymbol{p} \in P_{\Sigma_{id}}$ the VGF $\epsilon(.; \boldsymbol{p})$ can be described by the exact same function with only the dimensionless time $\omega_0 t_f$ as its argument. This property follows actually directly from (6.2.22) and (6.2.23), as the TDP defined by the former relation is not depending on $\dot{\Theta}_{max}$ when g is the identity function. Furthermore, using

Σ	$\epsilon(t_f; \boldsymbol{p})$
Σ_{id}	$2k - 1 + (-1)^k \cos(\omega_0 t_f)$
$k = \left\lfloor \frac{\omega_0 t_f}{\pi} \right\rfloor$	$, \omega_0 t_f \in (0, \infty)$

Table 6.2: The Velocity Gain Function ϵ for Σ_{id}

the expressions for t_S^{ext} and $\boldsymbol{x}_S^{ext}$ in Table 5.5b and the fact that (6.2.15) always holds with equality for linear SEA's, an analytical expression for this function describing the VGF can also be obtained. The corresponding expression is provided in Table 6.2.

In Fig. 6.2.2 (Bottom), VGF's corresponding to different parameters in the sets $P_{\Sigma_{sin}}$ and $P_{\Sigma_{sinh}}$ have been illustrated as a function of $\omega_0 t_f$ as well. As shown there and in the two graphs in Fig. 6.2.2 (Top), the depicted functions all correspond to a certain ratio $\dot{\Theta}_{max}$ and do not intersect each other. Furthermore, the way how $\dot{\Theta}_{max}$ influences these functions depends on the stiffness characteristics of the TDP's similar to the way how $\dot{\Theta}_{max}$ influences DTF's. Indeed, it follows from Fig. 6.2.2 (Top) that for the constructed VGF's, which correspond to parameters in $P_{\Sigma_{sin}}$, the dimensionless time required to reach a certain velocity gain always increases with increasing $\dot{\Theta}_{max}$. For the VGF's corresponding to parameters in $P_{\Sigma_{sinh}}$, on the other hand, the same time decreases with increasing $\dot{\Theta}_{max}$. Consequently, we observe that the function which is depicted in Fig. 6.2.2 (Bottom) to illustrate the VGF for linear SEA's divides the plot into two seperate parts.

We had already observed in Fig. 6.1.1 that abnormal extremals can be optimal or non-optimal depending on their final time as well as the parameters describing the control system. In Fig. 6.2.2 (Bottom), this dependence is also clarified by depicting $\epsilon(t_{min}(k; \boldsymbol{p}); \boldsymbol{p})$, with $k \in \{1, 2\}$, as a function of $\omega_0 t_f = \omega_0 t_{min}(k; \boldsymbol{p})$, see the dot-dashed lines. More specifically, for each of the ratios $\dot{\Theta}_{max}$ and TDP's used to construct the VGF's in Fig. 6.2.2, the two lines show the values attained by ϵ at the final times $t_{min}(1; \boldsymbol{p})$ and $t_{min}(2; \boldsymbol{p})$, respectively. Notice that according to the blue line, we can see that a velocity gain of 2 is always attained at $t_f = t_{min}(1; \boldsymbol{p})$ regardless of the ratio $\dot{\Theta}_{max}$ or the TDP. That is, abnormal extremals terminating at $t_{min}(1)$ are always optimal for these parameters and TDP's. Similarly, the orange line shows that a velocity gain of 4 is always attained at $t_f = t_{min}(2; \boldsymbol{p})$ when the parameter $\boldsymbol{p}$ belongs to $P_{\Sigma_{id}}$ or $P_{\Sigma_{sin}}$. If, however, $\boldsymbol{p}$ belongs to $P_{\Sigma_{sinh}}$ we can see that the same gain is attained at a time smaller than $t_{min}(2; \boldsymbol{p})$ when $\dot{\Theta}_{max}$ is sufficiently high. These results are consistent with the depicted graphs in Fig. 6.1.1.

It is important to note here that our results from Sec. 6.2.1 already implied a similarity between the parameter dependence of the DTF and the VGF when the velocity gain is a positive even integer and when abnormal extremals leading to this gain provide an optimal solution. Nevertheless, Fig. 6.2.2 suggests that for the three control systems $\Sigma_{sin}, \Sigma_{id}$ and Σ_{sinh} this similarity remains valid for any gain regardless of whether abnormal extremals are optimal or not. In
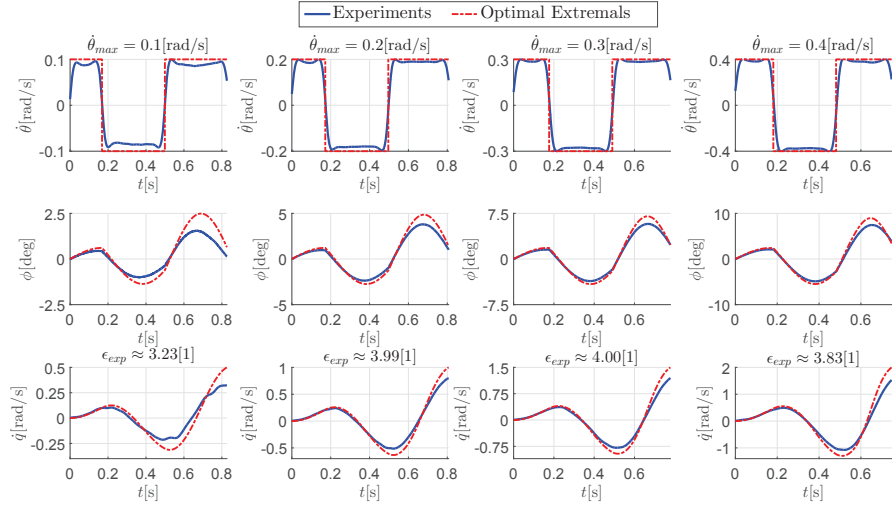
Figure 6.3.1: Experimental Results with the DLR FSJ
$(\Sigma_{FSJ,i}, i \in \{0.1, 0.2, 0.3, 0.4\})$

particular, it suggests that for a control system Σ_{sin} an increase in the maximal motor velocity always leads to an increase in the final time required to reach a given velocity gain. Conversely, for a control system Σ_{sinh} the required final time is expected to decrease in the same scenario. In the following section, we will use the DLR FSJ to show how by increasing the motor velocity the same velocity gain can indeed be obtained in a smaller amount of time both in theory and in practice.

6.3 Experimental Results

The experiments were conducted with the DLR Hand Arm System [18]. More specifically, using simple PD controllers with gravity compensation the torque controlled arm of the system has been first constrained to move on a horizontal plane. This ensured that the motion of the system was mainly caused by the forces in the elastic spring of the second shoulder joint which is a DLR FSJ. Then, the stiffness adjuster motor in this joint was set to 5 degrees in order to have a fixed TDP which is described by a hyperbolic sine function, see [59]. The motion of the arm could then be described by the control system $\Sigma_{FSJ,i}$ in Table 4.1. Note that i denotes here the maximal motor velocity $\dot{\theta}_{max}$ applied by the main motor in the second joint. Choosing four different values for $\dot{\theta}_{max} \in \{0.1\frac{rad}{s}, 0.2\frac{rad}{s}, 0.3\frac{rad}{s}, 0.4\frac{rad}{s}\}$, the optimal control strategy for the motor velocity has been computed afterwards such that in each case a velocity gain of $\epsilon = 5$ could be theoretically obtained. Finally, the computed strategies were implemented on the shoulder joint using again a fairly simple motor torque controller. The controller consisted of only a feed-forward term canceling the joint

torque and a proportional gain controller accounting for the difference between the optimal and measured motor velocity.

Figure 6.3.1 illustrates the control and state trajectories obtained during the experiments[9]. More specifically, the blue lines in the first row show the trajectories of the motor velocity for all the four experiments. The dashed red lines, on the other hand, depict the desired optimal motor control strategies. Similarly, the blue lines in the second and third rows depict the trajectories of the deflection and link velocity, respectively; while the dashed red lines stand for the optimal trajectories. Notice that based on the depicted blue and red lines, we can easily see that the experimental results correspond very well with the theoretical results. Clearly, unmodeled damping forces prevent the system to attain the theoretically achievable velocity gain. This is most obvious when the maximal motor velocity $\dot{\theta}_{max}$ is at its lowest value. Moreover, the unmodeled motor dynamics also has a negative influence as the desired motor velocities can never be exactly tracked. Nevertheless, regardless of these model deficiencies the experimentally obtained velocity gain ϵ_{exp}, i.e. the ratio of the terminal link velocity as obtained by the experiments to $\dot{\theta}_{max}$, is always higher than 3 and can even reach values as high as 4. Moreover, note that the time required to reach these gains strictly decrease when $\dot{\theta}_{max}$ is increased. This clearly agrees with our results from Sec. 6.2.2.

---

[9]For the trajectories of the motor and link velocity, a low pass filter with a cutoff frequency of 15Hz has been used.

Chapter 7

Influence of Damping and Stiffness Actuation

The purpose of this chapter is to discuss the structure of OC strategies for EJ's with variable impedance. In particular, we want to show how they are related to the strategies we have so far derived for EJ's with linear and nonlinear impedance. Moreover, we want to show how the concept of resonance energies, as we introduced for EJ's with SEA's, can also be extended to these more complex joints. The tasks we will investigate will again be related to explosive motion tasks, but our choice for the cost functionals will be more general. We start our discussion with the analysis of OC strategies for EJ's with variable damping actuators[1].

7.1 Influence of Variable Damping

In this section, we will focus on an EJ model that consists of a VDA, see Fig. 7.1.1. The TDP will be assumed to be described by the linear function $\tau_{J,l}$ in Table 3.1a. Similarly, we will assume that the adjustable damping torque $\tau_{J,D}$ is linear in each of its arguments and that the damping variable σ_d can be directly controlled. Finally, we will assume that the velocity of the motor can also be directly controlled and that the system is initially at rest. Under these assumptions, we want to discuss the structure of OC strategies minimizing a non-trivial linear combination of the terminal link velocity and spring deflection. We first give a mathematical formulation of this problem.

7.1.1 Problem Formulation

As in Chapter 2, we will first introduce the control system Σ for the above described EJ model and then formulate our desired OC problem. Notice that

---

[1]For our discussions on EJ's with VDA's and VSA's, we will make use of the references [41] and [42, 43], respectively.
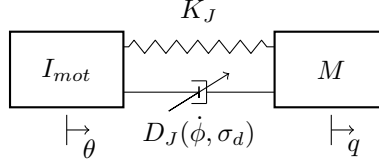
Figure 7.1.1: EJ Model with a VDA

for an EJ with a VDA, the torques acting between the motor and the link are not only due to the spring but also due to the VDA, i.e. $\tau_J = \tau_{J,S} + \tau_{J,D}$. Taking the state as $\boldsymbol{x} = \begin{pmatrix} \phi & \dot{q} \end{pmatrix}^T \in \mathbb{X} = \mathbb{R}^2$ and considering the assumptions introduced in the beginning of this section, the dynamics of Σ can be described, according to (2.1.1)-(2.1.2), by the function $\boldsymbol{f} : \mathbb{R}^2 \times \mathbb{R}^2 \to \mathbb{R}^2$ with

$$
\begin{aligned}
\boldsymbol{f}(\boldsymbol{x}, \boldsymbol{u}) &= \begin{pmatrix} u_1 - x_2 \\ \frac{K_e k_e}{M} x_1 + \frac{\sigma_d(u_2)}{M} \dot{x}_1 \end{pmatrix} \\
&= \begin{pmatrix} u_1 - x_2 \\ \omega_0^2 x_1 + 2 u_2 \omega_0 (u_1 - x_2) \end{pmatrix},
\end{aligned} \tag{7.1.1}
$$

where $\boldsymbol{u} = \begin{pmatrix} u_1 & u_2 \end{pmatrix}^T$ and $\sigma_d(u_2) = 2 u_2 \omega_0 M$. Notice that the first control u_1 denotes the motor velocity of the EJ whose magnitude will be bounded by $\dot{\theta}_{max} > 0$. The second control u_2, on the other hand, represents an adjustable damping ratio [35]. In particular, in case the control u_1 is constant and u_2 is continuous it follows from (7.1.1) that the deflection x_1 is two-times continuously differentiable and described by the following second-order differential equation:

$$
\ddot{x}_1 + 2 u_2 \omega_0 \dot{x}_1 + \omega_0^2 x_1 = 0. \tag{7.1.2}
$$

Equation (7.1.2) describes a damped MSS and we will constrain the second control to the set $[D_{J,min}, D_{J,max}] \subset [0, 1)$, with $D_{J,max} > D_{J,min}$, so that for constant u_2 this system is either undamped or underdamped. This leads us to the following convex control set:

$$
\mathbb{U} = [-\dot{\theta}_{max}, \dot{\theta}_{max}] \times [D_{J,min}, D_{J,max}]. \tag{7.1.3}
$$

Finally, we will take $\mathcal{PC}_{\mathbb{U}}$ as the class of admissible controls $\mathcal{U}$.

Our discussion so far fully describes the control system $\Sigma = (\mathbb{X}, \boldsymbol{f}, \mathbb{U}, \mathcal{U})$. Based on this system, we can now introduce the cost functional $J : \mathcal{U} \times (\mathbb{R}^2)^* \backslash \{\boldsymbol{0}\} \to \mathbb{R}$ with

$$
J(\boldsymbol{u}, \boldsymbol{\kappa}_f) = \boldsymbol{\kappa}_f \boldsymbol{x}_f, \tag{7.1.4}
$$

where $\boldsymbol{x}_f$ denotes the terminal state of the trajectory $\boldsymbol{x}$ which starts from $\boldsymbol{x}_0 = \boldsymbol{0}$ and corresponds to the control $\boldsymbol{u}$. Making use of this cost functional, our desired OC problem can be formulated as follows.

Linear Terminal Cost Problem (LTCP): Given a final time $t_f > 0$ and a non-trivial vector $\boldsymbol{\kappa}_f \in (\mathbb{R}^2)^*$ find the control $\boldsymbol{u}^{opt}$ which minimizes $J(\boldsymbol{u}, \boldsymbol{\kappa}_f)$ over all admissible controls $\boldsymbol{u} \in \mathcal{U}$ defined on $D = [0, t_f]$.

7.1.2 Optimal Control Strategies

In this subsection, we will first apply PMP to derive necessary conditions which need to be satisfied by the OC to solve the LTCP. In particular, we show that this control must be a switching control and provide analytical expressions for the corresponding trajectories and costates. Focusing mainly on control strategies where the motor velocity and damping ratio do not switch simultaneously, we then use these analytical descriptions to show the existence of certain switching patterns for OC strategies. Finally, for one of these patterns we provide an interpretation in terms of the energies attained by the EJ. This interpretation will show that the concept of resonance energies can also be extended to joints with adjustable viscous damping. In addition, it will reveal a non-trivial relation between the derived switching patterns and the optimal switching patterns for EJ's with adjustable linear stiffness [39, 21].

7.1.2.1 Basic Properties

We will call the pair $(\boldsymbol{x}, \boldsymbol{u})$ an optimally controlled trajectory if there exists a non-trivial $\boldsymbol{\kappa}_f \in (\mathbb{R}^2)^*$ and a terminal time $t_f > 0$ such that $\boldsymbol{u} : [0, t_f] \to \mathbb{R}^2$ solves the corresponding LTCP, $\boldsymbol{x}$ is a trajectory corresponding to $\boldsymbol{u}$ and $\boldsymbol{x}_0 = \boldsymbol{0}$. According to PMP, we have the following necessary condition for such trajectories.

Proposition 27. *Let $(\boldsymbol{x}, \boldsymbol{u})$ be an optimally controlled trajectory defined on the interval $D = [0, t_f]$ such that $\boldsymbol{u}$ minimizes the cost functional (7.1.4) with $\boldsymbol{\kappa}_f \in (\mathbb{R}^2)^* \backslash \{\boldsymbol{0}\}$. Then, there exists a piecewise continuously differentiable costate $\boldsymbol{\lambda} : D \to (\mathbb{R}^2)^*$ such that the first of the following conditions holds at every $t \in D$ at which u_2 is continuous, the second and third at every $t \in D$, and finally the fourth condition at the final time t_f:*

1. *Costate Dynamics*

$$\dot{\boldsymbol{\lambda}}(t) = \begin{pmatrix} -\omega_0^2 \lambda_2(t) & \lambda_1(t) + 2u_2(t)\omega_0\lambda_2(t) \end{pmatrix}. \qquad (7.1.5)$$

2. *Minimum Condition*

$$\mathbb{H}\left(\boldsymbol{x}(t), \boldsymbol{u}(t), \boldsymbol{\lambda}(t)\right) = \min_{\boldsymbol{v} \in \mathbb{U}} \mathbb{H}\left(\boldsymbol{x}(t), \boldsymbol{v}, \boldsymbol{\lambda}(t)\right), \qquad (7.1.6)$$

where $\mathbb{H} : \mathbb{R}^2 \times \mathbb{U} \times (\mathbb{R}^2)^* \to \mathbb{R}$ denotes the Hamiltonian function given by

$$\begin{aligned} \mathbb{H}(\boldsymbol{x}, \boldsymbol{u}, \boldsymbol{\lambda}) &= \boldsymbol{\lambda} \boldsymbol{f}(\boldsymbol{x}, \boldsymbol{u}) \\ &= \lambda_1(u_1 - x_2) + \lambda_2 \left(\omega_0^2 x_1 + 2u_2\omega_0(u_1 - x_2)\right). (7.1.7) \end{aligned}$$

3. *Hamiltonian Condition*

$$\mathbb{H}\left(\boldsymbol{x}(t), \boldsymbol{u}(t), \boldsymbol{\lambda}(t)\right) = -\lambda_a, \qquad (7.1.8)$$

where $\lambda_a \in \{0, 1\}$ is a constant scalar.

4. Transversality Condition

$$\boldsymbol{\lambda}(t_f) = v\boldsymbol{\kappa}_f, \qquad (7.1.9)$$

where v is a positive constant scalar.

Proof. The proof follows directly from applying PMP to the LTCP and is omitted for brevity. □

Following the definitions we introduced in Section 5.2.1, we will call the 4−tuple $\Lambda = (\boldsymbol{x}, \boldsymbol{u}, \boldsymbol{\lambda}, \lambda_a)$ consisting of an admissible controlled trajectory $(\boldsymbol{x}, \boldsymbol{u})$, a costate $\boldsymbol{\lambda}$ and a scalar $\lambda_a \in \{0, 1\}$ for which the conditions in Prop. 27 are satisfied an extremal lift for the LTCP. Looking at the Minimum Condition of this proposition and taking the partial derivative of the Hamiltonian $\mathbb{H}$ with respect to the first control, we can see that for such an extremal lift Λ we always have the following condition for u_1:

$$u_1(t) = \begin{cases} -\dot{\theta}_{max} & \dot{\lambda}_2(t) > 0 \\ \dot{\theta}_{max} & \dot{\lambda}_2(t) < 0 \end{cases}, \qquad (7.1.10)$$

with $\dot{\lambda}_2(t) = \lambda_1(t) + 2u_2(t)\omega_0\lambda_2(t)$, see (7.1.5). Similarly, taking the partial derivative of the Hamiltonian $\mathbb{H}$ with respect to u_2 we get

$$u_2(t) = \begin{cases} D_{J,min} & \lambda_2(t)\dot{x}_1(t) > 0 \\ D_{J,max} & \lambda_2(t)\dot{x}_1(t) < 0 \end{cases}, \qquad (7.1.11)$$

with $\dot{x}_1(t) = u_1(t) - x_2(t)$.

It is important to remark here that the condition (7.1.10) for the motor velocity depends, in contrary to EJ's with SEA's, not only on $\boldsymbol{\lambda}$ but also on the second control. This can be best explained if we refer to the description of costates in terms of impulse response functions of linear systems[2] as described in [40]. Indeed, if we choose an admissible control strategy for the second control u_2 and substitute it into (7.1.1), the resulting system will correspond to a linear time-varying system. The impulse response functions of this new system will then only depend on the eigenfrequency ω_0 and u_2, and $\boldsymbol{\lambda}$ is a linear combination of these functions. More specifically, the costates λ_1 and λ_2 give the response of the linear combination $v\boldsymbol{\kappa}_f\boldsymbol{x}_f$ to unit impulse functions applied to the first and second state, respectively. The reason behind the dependence of u_1 on u_2, as given by (7.1.10), follows finally from the fact that a jump in the control u_1 not only results in a jump in the time-derivative of the deflection but also in a jump in the damper torque which in turn depends on u_2, see (7.1.1). The following proposition clarifies the relation between u_1, u_2 and the cost functional $J(\boldsymbol{u}, \boldsymbol{\kappa}_f)$.

Proposition 28. *Let $(\boldsymbol{x}, \boldsymbol{u})$ be an admissible controlled trajectory defined on $D = [0, t_f]$ and $\boldsymbol{\lambda} : D \to (\mathbb{R}^2)^*$ a solution to (7.1.5). Then, for each $t \in D$ we have*

$$\boldsymbol{\lambda}(t)\boldsymbol{x}(t) - \boldsymbol{\lambda}_0\boldsymbol{x}_0 = \int_0^t \dot{\lambda}_2(s)u_1(s)\mathrm{d}s. \qquad (7.1.12)$$

---

[2]See for instance [12] for the definition of impulse response functions.

Proof. The proof directly follows from integrating the derivative $\frac{\mathrm{d}(\boldsymbol{\lambda}\boldsymbol{x})}{\mathrm{d}t}$ from 0 to t, see also Lemma 53 in Appendix B.3.4. $\qquad\square$

Applying Prop. 28 and using in particular (7.1.12), with $\boldsymbol{x}_0 = \boldsymbol{0}$, $t = t_f$ and $\boldsymbol{\lambda}_f = v\boldsymbol{\kappa}_f$, it is clear that (7.1.10) must hold if Λ is optimal. Moreover, the same proposition can also be used to analyse the dependence of the minimal value of $\boldsymbol{\kappa}_f\boldsymbol{x}_f$ on the given terminal time. To see this, let us first note that the dynamics of the second costate is described, similar to the first state, by the following second-order differential equation if the control $u_2 \equiv D_J$ is constant:

$$\ddot{\lambda}_2 - 2D_J\omega_0\dot{\lambda}_2 + \omega_0^2\lambda_2 = 0, \tag{7.1.13}$$

where we have simply used (7.1.5). According to (7.1.13), λ_2 physically describes the position of a MSS with an energy source modeled as a negative damper. Moreover, both the system's position λ_2 and velocity $\dot{\lambda}_2$ will oscillate with the damped eigenfrequency $\omega_d = \sqrt{1 - D_J^2}\omega_0$ provided the system is not at its equilibrium position. This means that the zeros of $\dot{\lambda}_2$ will in this case all be isolated. Taking into account the transversality condition and (7.1.12), this leads us then to the following proposition.

Proposition 29. *Let $\boldsymbol{\kappa}_f \in (\mathbb{R}^2)^*\backslash\{\boldsymbol{0}\}$ be given and assume that the controls $\bar{\boldsymbol{u}} : [0, \bar{t}_f] \to \mathbb{U}$ and $\boldsymbol{u} : [0, t_f] \to \mathbb{U}$ solve the corresponding LTCP with $t_f > \bar{t}_f$. Moreover, let $(\bar{\boldsymbol{x}}, \bar{\boldsymbol{u}})$ and $(\boldsymbol{x}, \boldsymbol{u})$ be both optimally controlled trajectories. Then, we have*

$$\boldsymbol{\kappa}_f\boldsymbol{x}_f < \boldsymbol{\kappa}_f\bar{\boldsymbol{x}}_f < 0.$$

Proof. See [41]. $\qquad\square$

With Prop. 29, we can now see that the minimum value of the product $\boldsymbol{\kappa}_f\boldsymbol{x}_f$ is a strictly decreasing function of the terminal time. Moreover, since the origin is an equilibrium position of (7.1.1) when $\boldsymbol{u} \equiv \boldsymbol{0}$, we can follow the same arguments as used in Sec. 5.4 to conclude that trajectories in optimal extremal lifts are also time-optimal. This suggests us that the costates can be again regarded, under some smoothness assumptions, as the gradient of the time function which for a given initial state in the set $\text{Reach}_{\Sigma_{t_f}}(\boldsymbol{0})$ gives the minimum time required to reach the boundary of this set. The condition (7.1.11) for the second control can then be physically explained using this interpretation and the Minimum Condition. A detailed analysis of conditions ensuring the required degree of smoothness for this time function, as done in Sec. 5.4, is beyond the scope of this thesis and left out for future work.

Based on the two conditions (7.1.10)-(7.1.11), it is tempting to assume that in an extremal lift Λ the value of the control $\boldsymbol{u}(t)$ is equal to one of the four extreme points of the control set $\mathbb{U}$ at each time $t \in D$. However, for the case when $\dot{\lambda}_2$ or $\lambda_2\dot{x}_1$ remains zero on a finite time-interval these conditions are not sufficient to uniquely determine the OC strategy. In such a case, the extremal lift is called singular [53]. In general, when searching for OC strategies singular lifts need to be also investigated. Nevertheless, as the following proposition

$\begin{pmatrix} x_1(s+t_{S,k}) \\ \dot{x}_1(s+t_{S,k}) \end{pmatrix}$	$e^{-u_2\omega_0 s} \begin{pmatrix} {}^k x_1 & \dfrac{{}^k \dot{x}_1 + u_2\omega_0\,{}^k x_1}{\omega_d} \\ {}^k \dot{x}_1 & -\dfrac{\omega_0^2\,{}^k x_1 + u_2\omega_0\,{}^k \dot{x}_1}{\omega_d} \end{pmatrix} \begin{pmatrix} \cos(\omega_d s) \\ \sin(\omega_d s) \end{pmatrix}$
$x_2(t)$	$\dot{x}_1(t) - u_1(t)$
$\begin{pmatrix} \lambda_2(s+t_{S,k}) \\ \dot{\lambda}_2(s+t_{S,k}) \end{pmatrix}$	$e^{u_2\omega_0 s} \begin{pmatrix} {}^k \lambda_2 & \dfrac{{}^k \lambda_2 - u_2\omega_0\,{}^k \lambda_2}{\omega_d} \\ {}^k \dot{\lambda}_2 & -\dfrac{\omega^2\,{}^k \lambda_2 - u_2\omega_0\,{}^k \dot{\lambda}_2}{\omega_d} \end{pmatrix} \begin{pmatrix} \cos(\omega_d s) \\ \sin(\omega_d s) \end{pmatrix}$
$\lambda_1(t)$	$\dot{\lambda}_2(t) - 2u_2\omega_0\lambda_2(t)$
$t \in D_k, s = t - t_{S,k}, \omega_d = \sqrt{1-u_2^2}\,\omega_0, \omega_0 = \sqrt{\dfrac{K_e k_e}{M}}$	

Table 7.1: States and Costates in D_k $(i \geq 0, k \in S_i)$

shows optimal extremal lifts for the LTCP are never singular. Consequently, we can always focus on control strategies taking values from the set of extreme points of $\mathbb{U}$ when searching for OC strategies.

Proposition 30. *Let $\Lambda = (\boldsymbol{x}, \boldsymbol{u}, \boldsymbol{\lambda}, \lambda_a)$ be an optimal extremal lift for the LTCP which is defined on $D = [0, t_f]$. Then, this extremal lift is non-singular and for each $t \in D$ we have*

$$\boldsymbol{u}(t) \in \mathbb{U}_{ext} = \left\{ \begin{pmatrix} -\dot{\theta}_{max} \\ D_{J,min} \end{pmatrix}, \begin{pmatrix} -\dot{\theta}_{max} \\ D_{J,max} \end{pmatrix}, \begin{pmatrix} \dot{\theta}_{max} \\ D_{J,min} \end{pmatrix}, \begin{pmatrix} \dot{\theta}_{max} \\ D_{J,max} \end{pmatrix} \right\}. \quad (7.1.14)$$

Proof. See [41]. $\qquad\square$

According to Prop. 30, an OC strategy solving the LTCP can take only a finite number of values. Consequently, determining such a strategy is equivalent to determining the initial value and the switching times of both the motor velocity and damping ratio. Notice that for a given constant control, the two differential equations (7.1.2) and (7.1.13) can be analytically solved. Consequently, using the corresponding solutions together with (7.1.1) and (7.1.5) we can analytically construct $\boldsymbol{x}$ and $\boldsymbol{\lambda}$ if we know their values at the initial time as well as the switching times. Table 7.1 provides the expressions required for this construction. We next show how to use these descriptions to find switching patterns for OC strategies.

7.1.2.2 Switching Patterns

Let Λ be an extremal lift for the LTCP which is defined on $D = [0, t_f]$. As already discussed, both the dynamics of the costate and the condition (7.1.10) for the first control u_1 depend on the second control u_2 which is not necessarily continuous. Consequently, even if we know the value of the costate at a given time the condition (7.1.10) might, in a sufficiently small neighborhood of this time, be simultaneously satisfied by different values of the set $\mathbb{U}_{ext}$ in (7.1.14). In other words, (7.1.5) and (7.1.10) do not always uniquely determine the control $u_1(t)$, with $t \in D$, even if the value of the costate $\boldsymbol{\lambda}(t)$ is known. Such a case did not occur for the LVMP we analysed in Chapter 5, as for that problem the

control only depended on the first costate having isolated zeros. Similarly, the condition (7.1.11) depends on the possibly discontinuous time-derivative of the deflection and this complicates the analysis of the set of all control strategies in extremal lifts.

In the following, we will mainly focus on those control strategies along which the motor velocity and the damping ratio do not change simultaneously. Their analysis is more straight-forward, as for an extremal lift containing such a control the right-hand side of (7.1.10) or (7.1.11) must be zero at a switching time. Since between two consecutive switching times both right-hand sides are continuous, this suggests us to construct extremal lifts for the LTCP as follows. First, choose an initial costate $\boldsymbol{\lambda}_0$ and an initial control $\boldsymbol{u}_0$, for which (7.1.10)-(7.1.11) are satisfied. Then, construct the lift in D_0 by investigating the sign changes of $\dot{\lambda}_2$ and $\lambda_2 \dot{x}_1$. Finally, if the control $\boldsymbol{u}$ has $i \geq 1$ switchings, construct successively for each $k \in \{1, \ldots, i\}$ the lift in D_k by determining the control $^k\boldsymbol{u}$ using (7.1.10)-(7.1.11) and by analysing again the sign changes of $\dot{\lambda}_2$ and $\lambda_2 \dot{x}_1$. Table 7.2 provides a more detailed description of this construction procedure, where we have additionally made use of (7.1.5)-(7.1.9) to systematically determine a pair $(\boldsymbol{\lambda}_0, \boldsymbol{u}_0)$ for which (7.1.10)-(7.1.11) hold. In particular, notice that by evaluating (7.1.8) at the initial time, where $\boldsymbol{x}_0 = \boldsymbol{0}$, and using (7.1.5) we can obtain the following relation:

$$\dot{\lambda}_{20} u_{10} = -\lambda_a \in \{0, 1\}, \tag{7.1.15}$$

with $\dot{\lambda}_{20} = \dot{\lambda}_2(0)$. Since according to the transversality condition the costate $\boldsymbol{\lambda}$ can never be equal to zero, this in turn implies by (7.1.5)- (7.1.6) the following conditions for λ_{20} and $\dot{\lambda}_{20}$:

$$\dot{\lambda}_{20} \in \{-\frac{1}{\dot{\theta}_{max}}, 0, \frac{1}{\dot{\theta}_{max}}\} \wedge \begin{pmatrix} \lambda_{20} & \dot{\lambda}_{20} \end{pmatrix} \neq \boldsymbol{0}, \tag{7.1.16}$$

in accordance with the procedure in Table 7.2.

In order to obtain switching patterns explaining the structure of the OC strategies, we want to next make use of the proposed construction procedure and investigate the switching times of u_1 and u_2 which result from different choices for the pair $\begin{pmatrix} \lambda_{20} & \dot{\lambda}_{20} \end{pmatrix} \in (\mathbb{R}^2)^*\backslash\{\boldsymbol{0}\}$. In particular, we will introduce as in Section 5.3.3 a one-dimensional and dimensionless variable $\alpha_0 \in \mathbb{R}$ defined by

$$\alpha_0 = -\frac{\dot{\lambda}_{20}}{\omega_0 \lambda_{20}}, \tag{7.1.17}$$

and use the expressions from Table 7.1 to construct extremal lifts corresponding to different values for α_0. Depending on the sign of α_0, we will then find five different switching patterns. We start our discussion by investigating the extremal lifts corresponding to $\alpha_0 = 0$, i.e. abnormal extremal lifts, see (7.1.15) and (7.1.17).

$\bullet \ \alpha_0 = 0:$ In order for α_0 to be zero, $\dot{\lambda}_{20} = 0$ must hold with $\lambda_{20} \neq 0$. Assume without loss of generality that $\lambda_{20} < 0$ holds. Then, by the continuity of $\dot{\lambda}_2$

Data : $M, K_e, k_e, \dot{\theta}_{max}, D_{J,min}, D_{J,max}, t_f$

Result : An Extremal Lift Λ for the LTCP defined on $D = [0, t_f]$

Initialization;

- Choose $\lambda_{20} \in \mathbb{R}$ and $\dot{\lambda}_{20} \in \{-\frac{1}{\dot{\theta}_{max}}, 0, \frac{1}{\dot{\theta}_{max}}\}$ such that $(\lambda_{20}, \dot{\lambda}_{20}) \neq \mathbf{0}$.

- Find $u_{10} = \dot{x}_{10} \in \{-\dot{\theta}_{max}, \dot{\theta}_{max}\}$ using (7.1.10).

- Determine $u_{20} \in \{D_{J,min}, D_{J,max}\}$ using (7.1.11).

- Set k to 0.

while $t_{S,k} < t_f$ **do**

    - Assuming $k = i$, construct $\lambda_2, \dot{\lambda}_2, x_1$ and $\dot{x}_1$ in $[t_{S,k}, t_f]$.

    - Find the maximal time interval $[t_{S,k}, t_{S,k+1}] \subset [t_{S,k}, t_f]$ for which (7.1.10)-(7.1.11) remain true.

    if $t_{S,k+1} = t_f$ **then**

    | - break.

    else

        - Find the control $^{k+1}\mathbf{u}$ which ensures that (7.1.10)-(7.1.11) are not violated in a sufficiently small neighborhood of $t_{S,k+1}$.

        - Set k to $k+1$.

    end

end

Table 7.2: Construction Procedure for an Extremal Lift for the LTCP ($i \in \{0, 1, \ldots\}$ denotes the switching number of $\mathbf{u}$ and depends on t_f)

in D_0 it follows from (7.1.13) that there exists a sufficiently small ε such that $\dot{\lambda}_2(t)$ is positive for each $t \in (0, \varepsilon] \subset D_0$. According to (7.1.10) this means that $u_{10} = -\dot{\theta}_{max}$, and since the joint starts from rest we also have $\dot{x}_{10} = -\dot{\theta}_{max}$. Based on our initial assumption on the sign of λ_{20} together with the continuity of λ_2 and $\dot{x}_1$ in D_0, (7.1.11) determines then uniquely the initial control:

$$^0\mathbf{u} = \begin{pmatrix} -\dot{\theta}_{max} \\ D_{J,min} \end{pmatrix}. \tag{7.1.18}$$

Using now (7.1.18) together with Table 7.1 and $\dot{\lambda}_{20} = 0$, we can find the following expressions for λ_2 and $\dot{\lambda}_2$:

$$\lambda_2(t) = e^{D_{J,min}\omega_0 t} \lambda_{20} \left(\cos(\omega_{d,max}t) - \frac{D_{J,min}\omega_0 \sin(\omega_{d,max}t)}{\omega_{d,max}} \right), \tag{7.1.19}$$

$$\dot{\lambda}_2(t) = -e^{D_{J,min}\omega_0 t} \frac{\omega_0^2 \lambda_{20}}{\omega_{d,max}} \sin(\omega_{d,max}t), \tag{7.1.20}$$

where $t \in D_0$ and $\omega_{d,max} = \omega_0 \sqrt{1 - D_{J,min}^2}$. Similarly, using the fact that $\mathbf{x}_0 = \mathbf{0}$ we have the following two expressions for x_1 and $\dot{x}_1$ which are valid on

D_0:

$$x_1(t) = e^{-D_{J,min}\omega_0 t}\dot{x}_{10}\frac{\sin(\omega_{d,max}t)}{\omega_{d,max}}, \tag{7.1.21}$$

$$\dot{x}_1(t) = e^{-D_{J,min}\omega_0 t}\dot{x}_{10}\left(\cos(\omega_{d,max}t) - \frac{D_{J,min}\omega_0\sin(\omega_{d,max}t)}{\omega_{d,max}}\right). \tag{7.1.22}$$

To fully determine the extremal lift Λ in D_0, we need to still find the value of $t_{S,1} \leq t_f$. By investigating the times at which $\dot{\lambda}_2$ and the product $\lambda_2\dot{x}_1$ can change their signs, we show next how to determine this time under the assumption that t_f is sufficiently large.

Let us first take a closer look at (7.1.19)-(7.1.20) and (7.1.22). Then, assuming that the control remains constant both $\dot{x}_1$ and λ_2 change their signs simultaneously at the times

$$t = \frac{\arctan(\frac{\omega_{d,max}}{\omega_0 D_{J,min}})}{\omega_{d,max}} + k\frac{T_{D_{J,min}}}{2}, \tag{7.1.23}$$

where $T_{D_{J,min}} = \frac{2\pi}{\omega_{d,max}}$ and k is a non-negative integer such that $t \leq t_f$. Moreover, since both quantities change their signs simultaneously the sign of their product remains non-negative.

Focusing now on $\dot{\lambda}_2$, it follows from (7.1.20) that $\dot{\lambda}_2$ will change its sign at the times

$$t = k\frac{T_{D_{J,min}}}{2}, \tag{7.1.24}$$

with $k \geq 1$ denoting this time a positive integer for which $t \leq t_f$. Notice that at each of these times, the deflection x_1 is also zero, see (7.1.21). According to (7.1.24), the first time $\dot{\lambda}_2$ changes its sign is equal to $\frac{T_{D_{J,min}}}{2}$ and based on the construction procedure from Table 7.2 we have

$$t_{S,1} = \frac{T_{D_{J,min}}}{2} \wedge {}^1\boldsymbol{u} = \begin{pmatrix} \dot{\theta}_{max} \\ D_{J,min} \end{pmatrix}. \tag{7.1.25}$$

Notice that the change in the control as given by (7.1.25) increases $\dot{x}_1$ instantaneously by $2\dot{\theta}_{max}$ but does not influence $\dot{\lambda}_2$. Consequently, evaluating (7.1.19)-(7.1.22) at $t_{S,1}$ we can see that ${}^1\lambda_2$ and ${}^1\dot{x}_1$ are both positive while ${}^1x_1$ and ${}^1\dot{\lambda}_2$ are both equal to zero[3]. Assuming, as before, that the control remains constant after $t_{S,1}$ we can then again make use of Table 7.1 to see that the product $\lambda_2\dot{x}_1$ is positive almost everywhere in D_1. Furthermore, $\dot{\lambda}_2$ will change its sign, for the first time after $t_{S,1}$, at $t_{S,2} = 2t_{S,1}$ and at this time u_1 will switch from $\dot{\theta}_{max}$ to $-\dot{\theta}_{max}$. The second control u_2, on the other hand, remains the same. Consequently, ${}^2\lambda_2$ and ${}^2\dot{x}_1$ are both negative, and ${}^2x_1$ and ${}^2\dot{\lambda}_2$ are both equal to zero. Repeating the analysis above, we can finally conclude that

---

[3]Note that for $\lambda_{20} > 0$ the sign of these values at $t_{S,1}$ correspond exactly to the signs of $x_{10}, \dot{x}_{10}, \lambda_{20}$ and $\dot{\lambda}_{20}$.

	$k=0$	$k \geq 1$
$t_{S,k}$	0	$k\dfrac{T_{D_{J,min}}}{2}$
$^k\boldsymbol{u}$	$\begin{pmatrix}\dfrac{\dot\theta_{max}}{\mathrm{sgn}(\lambda_{20})}\\[2mm] D_{J,min}\end{pmatrix}$	$\begin{pmatrix}\dfrac{(-1)^k\,\dot\theta_{max}}{\mathrm{sgn}(\lambda_{20})}\\[2mm] D_{J,min}\end{pmatrix}$
$\begin{pmatrix}^kx_1\\ ^k\dot x_1\end{pmatrix}$	$\begin{pmatrix}0\\[2mm]\dfrac{\dot\theta_{max}}{\mathrm{sgn}(\lambda_{20})}\end{pmatrix}$	$\begin{pmatrix}0\\[2mm]2\,^ku_1-\dfrac{^{k-1}\dot x_1}{F(\frac{T_{D_{J,min}}}{2},0)}\end{pmatrix}$
$^kx_2$	0	$^ku_1-\,^k\dot x_1$
$\begin{pmatrix}^k\lambda_2\\ ^k\dot\lambda_2\end{pmatrix}$	$\begin{pmatrix}\lambda_{20}\\0\end{pmatrix}$	$(-1)^k\,F_{exp}(t_{S,k},0)\begin{pmatrix}\lambda_{20}\\0\end{pmatrix}$
$^k\lambda_1$	$-2D_{J,min}\omega_0\lambda_{20}$	$-2D_{J,min}\omega_0\,^k\lambda_2$
$F_{exp}(t_1,t_2)=e^{\omega_0(D_{J,min}t_1+D_{J,max}t_2)}$		

Table 7.3: Extremal Lifts at the Switching Times ($\alpha_0 = 0$, $k \in \{0,\dots,i\}$)

the same switching pattern repeats itself. The damping u_2 is therefore always equal to its minimum value $D_{J,min}$ and (7.1.19)-(7.1.20) actually hold for each $t \in D$. The first control u_1, on the other hand, switches at $t_{S,k} = k\frac{T_{D_{J,min}}}{2}$, with $k \in \{1,\dots,i\}$, and the change in $\dot x_1$ at these switchings must be accounted for when constructing $\boldsymbol{x}$.

Table 7.3 summarizes[4] the values of the switching times as well as the values of $\boldsymbol{u}, \boldsymbol{x}$ and $\boldsymbol{\lambda}$ attained at these times. They can be used together with Table 7.1 to construct the extremal lift when $\alpha_0 = 0$. Note that if λ_{20} is positive and not negative as assumed in the beginning, the only difference in the resulting control trajectory is the positive sign of the initial value $u_{10} = \dot\theta_{max}$, while the switching structure remains the same. Figure 7.1.2 (Left) illustrates the described switching pattern for $\alpha_0 = 0$ and $\lambda_{20} < 0$ using phase plots.

We next discuss the switching patterns for $\alpha_0 > 0$. This structure is more complicated, since λ_2 and $\dot x_1$ will not change their signs simultaneously anymore and neither will $\dot\lambda_2$ and x_1.

• $\alpha_0 > 0$: When α_0 is positive, the initial value λ_{20} of the second costate has the opposite sign as its derivative $\dot\lambda_{20}$. According to (7.1.10), this means that both u_{10} and λ_{20} have the same sign. Furthermore, since the joint is initially at rest $\dot x_{10} = u_{10}$ the product $\lambda_2\dot x_1$ is positive at the beginning of the trajectory. Assuming without loss of generality that $\dot\lambda_{20}$ is positive, it follows then from (7.1.10)-(7.1.11) that we have

$$^0\boldsymbol{u} = \begin{pmatrix}-\dot\theta_{max}\\ D_{J,min}\end{pmatrix}. \qquad (7.1.26)$$

In the interval D_0, the trajectory $\boldsymbol{x}$ can thus still be described by (7.1.21)-(7.1.22), while the costate can be obtained from Table 7.1 by considering the

---

[4]Notice that the term $F_{exp}(t_1,t_2)$ there accounts for the exponential decrease of $\boldsymbol{x}$ and increase of $\boldsymbol{\lambda}$.
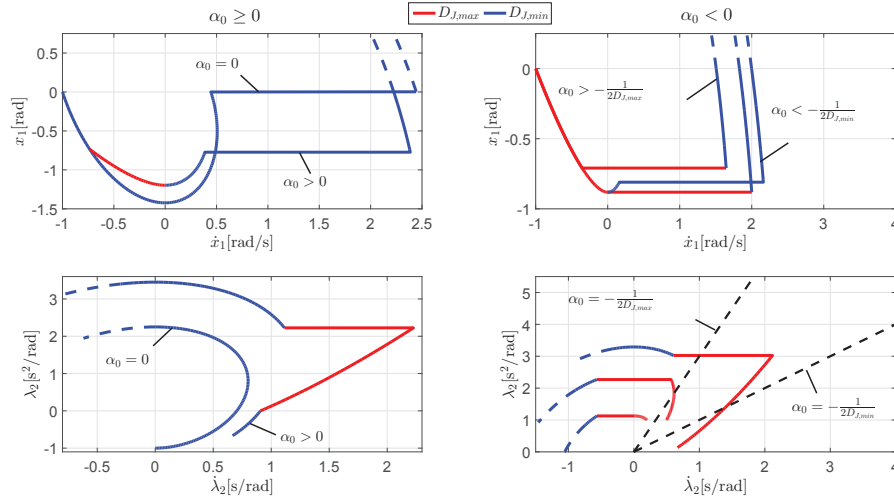
Figure 7.1.2: Switching Patterns for EJ's with Variable Damping
(Adapted from [41], ©2014 IEEE)

non-zero quantity $\dot{\lambda}_{20} = -\alpha_0 \lambda_{20}$. If we now follow the steps from the construction procedure described in Table 7.2, it is possible to see that for $\alpha_0 > 0$ the switching order always stays the same. More specifically, let l denote the number of times at which the deflection equals to zero in the interior of D and for each $k \in S_l$ let $\bar{t}_k$ denote the corresponding time, i.e. $x_1(\bar{t}_k) = 0$. Using this notation and assuming again that t_f is sufficiently large, we can describe for each $j \in S_l$ the resulting switching pattern as follows[5]:

- First, λ_2 changes its sign so that u_2 switches from $D_{J,min}$ to $D_{J,max}$ $(t = \bar{t}_j + t_j^*, x_1(\bar{t}_j) = 0)$.

- Then, $\dot{x}_1$ changes its sign so that u_2 switches from $D_{J,max}$ back to $D_{J,min}$ $(t = \bar{t}_j + t_j^* + \hat{t}_j)$. Since at this point the second costate is non-zero, $\dot{\lambda}_2$ has a jump discontinuity. However, its sign remains the same.

- After the switch of u_2, $\dot{\lambda}_2$ changes next its sign so that u_1 switches $(t = t_{M_{j+1}})$. This results in an increase in the magnitude of $\dot{x}_1$ by $2\dot{\theta}_{max}$.

- Finally, the angular deflection x_1 goes to zero and the switching structure repeats itself $(t = \bar{t}_j + T_{j+1} = \bar{t}_{j+1}, x_1(\bar{t}_{j+1}) = 0)$.

This switching pattern is illustrated in Figure 7.1.2 (Left).

Taking a closer look at the described structure, it can be observed that for each $k \in S_{l-1}$ the first control switches exactly once in the interval $(\bar{t}_k, \bar{t}_{k+1})$.

---

[5] A thorough discussion on finding the switching order of $\lambda_2 - \dot{x}_1 - \dot{\lambda}_2 - x_1 - \ldots$ as described below is omitted for brevity. The existence of this order can be shown by subsequently using the equations in Table 7.1 and taking into account the discontinuities of $\dot{x}_1$ and $\dot{\lambda}_2$ at the switching times, see also Table 7.4.

The second control, on the other hand, switches twice in the same interval and the switchings of both controls never occur simultaneously. Finally, the sign of $\dot{\lambda}_{20}$ only influences the sign of the motor velocity but not the switching pattern or the switching times. This can be observed from Table 7.4a which provides analytical expressions for the switching times as well as the values of $\boldsymbol{u}, \boldsymbol{x}$ and $\boldsymbol{\lambda}$ at these times. The used notation is clarified in Table 7.4b. In both tables, the integer $j \geq 0$ denotes the number how many times the motor velocity u_1 switched so far.

It is important to note here that whenever x_1 is zero along the trajectory for the j'th time, with $j \geq 1$, the ratio $\alpha_j = -\frac{\dot{\lambda}_2(\bar{t}_j)}{\omega_0 \lambda_2(\bar{t}_j)}$, obtained after the j'th switch of u_1, remains positive. More specifically, using Table 7.4, it is possible to show that this ratio not only remains positive but also decreases with every switch of u_1. Indeed, according to Table 7.4 we have the following relations:

$$
\begin{aligned}
\alpha_{j+1} &= -\frac{\dot{\lambda}_2(\bar{t}_{j+1})}{\omega_0 \lambda_2(\bar{t}_{j+1})} = \frac{1}{\beta_j - 2D_{J,min}}, \\
\beta_j &= -\frac{\dot{x}_1(\bar{t}_j + t_{M_{j+1}})}{\omega_0 x_1(\bar{t}_j + t_{M_{j+1}})} = 2D_{J,min} + \frac{1}{\alpha_j} \\
&+ \frac{2\dot{\theta}_{max} F_{exp}(t_{M_{j+1}} - \hat{t}_j, \hat{t}_j) K_1^2(\alpha_j)}{K_2(\alpha_j)\alpha_j |\dot{x}_1(\bar{t}_j)|} \\
\Rightarrow \alpha_{j+1} &= \frac{\alpha_j}{1 + \frac{2\dot{\theta}_{max} F_{exp}(t_{M_{j+1}} - \hat{t}_j, \hat{t}_j) K_1^2(\alpha_j)}{K_2(\alpha_j)|\dot{x}_1(\bar{t}_j)|}} < \alpha_j. \qquad (7.1.27)
\end{aligned}
$$

According to (7.1.27), the positive ratio α_j is approaching zero with increased j. This indicates that with every switch of the motor velocity the switching pattern followed by the control strategy resembles more and more to the pattern we have found for $\alpha_0 = 0$.

• $\alpha_0 < 0$: If the ratio α_0 is negative, the product $\dot{x}_1 \lambda_2$ is initially negative as well[6] and due to (7.1.11) the damping ratio u_2 starts with its maximum value. Assuming without loss of generality that $\dot{\lambda}_{20}$ is positive, we then have

$$
^0\boldsymbol{u} = \begin{pmatrix} -\dot{\theta}_{max} \\ D_{J,max} \end{pmatrix}. \qquad (7.1.28)
$$

With this initial value, we can now again make use of Table 7.1, as done for positive α_0, and follow the procedure described in Table 7.2 to search for a switching pattern. When deriving the switching structure for $\alpha_0 > 0$, we found that the order, with which $x_1, \dot{x}_1, \lambda_2, \dot{\lambda}_2$ change their signs, remained the same regardless of the value of α_0. For $\alpha_0 < 0$, on the other hand, this order depends on the magnitude of α_0 as well. More specifically, assuming that t_f is sufficiently large the following three switching patterns can exist in the interval $[0, \bar{t}_1]$, where

---

[6]Note that for $\alpha_0 < 0$, both λ_{20} and $\dot{\lambda}_{20}$ have the same sign and according to (7.1.10) we have $\text{sgn}(\dot{x}_{10}) = \text{sgn}(u_{10}) = -\text{sgn}(\dot{\lambda}_{20})$.

$t-\bar{t}_j$	0	$\dfrac{\arctan\left(\frac{\omega_{d,max}}{\omega_0(D_{J,min}+\alpha_j)}\right)}{\omega_{d,max}}=t_j^*$	$t_j^*+\dfrac{\arctan\left(\frac{\omega_{d,min}}{\omega_0(D_{J,max}+\alpha_j)}+\hat{t}_j\right)}{\omega_{d,min}}=\hat{t}_j$	$t_{M_{j+1}}=t_j^*+\hat{t}_j+\dfrac{\arctan\left(\frac{\omega_{d,max}}{\frac{\omega_0(\frac{1}{\alpha_j}+2D_{J,min})}{\omega_{d,max}}-D_{J,min}}\right)}{\omega_{d,max}}=t_{m_{j+1}}$	$T_{j+1}=\bar{t}_{j+1}-\bar{t}_j$
$u(t)$	$\left(\frac{(-1)^j\theta_{max}}{\text{sgn}(\lambda_{20})}\right)D_{J,min}$	$\left(\frac{(-1)^j\theta_{max}}{\text{sgn}(\lambda_{20})}\right)D_{J,max}$	$\left(\frac{(-1)^{j+1}\theta_{max}}{\text{sgn}(\lambda_{20})}\right)D_{J,min}$	$\left(\frac{(-1)^{j+1}\theta_{max}}{\text{sgn}(\lambda_{20})}\right)D_{J,min}$	$\left(\frac{(-1)^{j+1}\theta_{max}}{\text{sgn}(\lambda_{20})}\right)D_{J,max}$
$x_1(t)$	0	$\dot{x}_1(\bar{t}_j)\frac{F_{exp}(-t_j^*,0)}{\omega_0 K_1(\alpha_j)}$	0	$\dot{x}_1(\bar{t}_j)\frac{K_2(\alpha_j)\alpha_j}{\omega_0 K_1^2(\alpha_j)F_{exp}(t_{M_{j+1}}-t_j,t_j)}$	0
$\dot{x}_1(t)$	$\dot{x}_1(\bar{t}_j)$	$\dot{x}_1(\bar{t}_j)\frac{\alpha_j F_{exp}(-t_j^*,0)}{K_1(\alpha_j)}$	0	$-\dot{x}_1(\bar{t}_j)\frac{K_2(\alpha_j)\alpha_j(1+2\alpha_j D_{J,min})}{K_1^2(\alpha_j)F_{exp}(t_{M_{j+1}}-t_j,t_j)}-2\frac{\theta_{max}}{\text{sgn}(\dot{x}_1(t_j))}$	$-\dot{x}_1(\bar{t}_j)\frac{K_1(-\beta_j)K_2(\alpha_j)\alpha_j}{K_1^2(\alpha_j)F_{exp}(T_{j+1}-t_j,t_j)}$
$x_2(t)$		$(-1)^j\text{sgn}(\lambda_{20})\theta_{max}-\dot{x}_1(t)$		$(-1)^{j+1}\text{sgn}(\lambda_{20})\theta_{max}-\dot{x}_1(t)$	
$\lambda_2(t)$	$\lambda_2(\bar{t}_j)$	0	$-\lambda_2(\bar{t}_j)\frac{\alpha_j K_1(\alpha_j)}{K_2(\alpha_j)F_{exp}(-t_j^*,-t_j)}$	$-\lambda_2(\bar{t}_j)\frac{K_1^2(\alpha_j)F_{exp}(t_{M_{j+1}}-t_j,t_j)}{K_2(\alpha_j)}$	$-\lambda_2(\bar{t}_j)\frac{K_1^2(\alpha_j)F_{exp}(T_{j+1}-t_j,t_j)(\beta_j-2D_{J,min})}{K_2(\alpha_j)K_1(-\beta_j)}$
$\dot{\lambda}_2(t)$	$-\alpha_j\omega_0\lambda_2(\bar{t}_j)$	$-\lambda_2(\bar{t}_j)\frac{\omega_0 F_{exp}(t_j^*,0)}{K_1^{-1}(\alpha_j)}$	$-\lambda_2(\bar{t}_j)\frac{\omega_0 K_1(\alpha_j)(1+2\alpha_j D_{J,min})}{K_2(\alpha_j)F_{exp}(-t_j^*,-t_j)}$	0	$\lambda_2(\bar{t}_j)\frac{F_{exp}(T_{j+1}-t_j,t_j)\omega_0 K_1^2(\alpha_j)}{K_2(\alpha_j)K_1(-\beta_j)}$
$\lambda_1(t)$	$\dot{\lambda}_2(t)-\frac{2\omega_0\lambda_2(t)}{D_{J,min}^{-1}}$	$\dot{\lambda}_2(t)-\frac{2\omega_0\lambda_2(t)}{D_{J,max}^{-1}}$	$\dot{\lambda}_2(t)-\frac{2\omega_0\lambda_2(t)}{D_{J,min}^{-1}}$		

(a) Controls, States and Costates at Zero Deflection and at the Switching Times

$\bar{t}_j$	$T_{j+1}-t_{M_{j+1}}$	α_j	β_j	$\bar{t}_0$	$K_1(\alpha_j)$	$K_2(\alpha_j)$	$F_{exp}(t_1,t_2)$
$\sum_{k=0}^{j}T_k$	$\dfrac{\arctan\left(\frac{\omega_{d,max}}{\omega_0(D_{J,min}-\frac{1}{\beta_j})}\right)}{\omega_{d,max}}$	$-\dfrac{\dot{\lambda}_2(\bar{t}_j)}{\omega_0\lambda_2(\bar{t}_j)}$	$\dfrac{\dot{x}_1(\bar{t}_j+t_{M_{j+1}})}{-\omega_0 x_1(\bar{t}_j+t_{M_{j+1}})}$	$T_0=0$	$\sqrt{\alpha_j^2+2\alpha_j D_{J,min}+1}$	$\sqrt{\alpha_j^2+2\alpha_j D_{J,max}+1}$	$e^{\omega_0(D_{min}t_1+D_{max}t_2)}$

(b) Notation

Table 7.4: Switching Pattern for $\alpha_j>0$ ($j\in\{0,1,2,\ldots\}$, $t\in[\bar{t}_j,\bar{t}_{j+1}]$)
(Adapted from [41], ©2014 IEEE)

$\bar{t}_1$ denotes as before the first time the deflection becomes zero in the interior of D.

1. $\alpha_0 \in (-\infty, \frac{1}{2D_{J,min}})$: In this case, $\dot{x}_1$ switches first so that u_2 changes from $D_{J,max}$ to $D_{J,min}$ $(t = \hat{t}_0)$. According to (7.1.5), the change in u_2 also results in an instantaneous change of $\dot{\lambda}_2$ and this quantity approaches zero without changing its sign. Then, λ_2 changes its sign and u_1 switches $(t = t_{M_1} > \hat{t}_0)$. The magnitude of $\dot{x}_1$ is then increased and the angular deflection x_1 changes its sign before λ_2 does $(t = T_1 = \bar{t}_1)$.

2. $\alpha_0 \in [-\frac{1}{2D_{min}}, -\frac{1}{2D_{max}}]$: If α_0 belongs to this interval, $\dot{x}_1$ switches again before $\dot{\lambda}_2$ and u_2 switches to $D_{J,min}(t = \hat{t}_0)$. This also results in an instantaneous change in $\dot{\lambda}_2$. Unlike the previous case, however, this change results in a sign change of $\dot{\lambda}_2$ as well. Consequently, u_1 switches its sign simultaneously with u_2 $(t = \hat{t}_0 = t_{M_1})$. The magnitude of $\dot{x}_1$ is again increased by $2\dot{\theta}_{max}$ and afterwards x_1 changes its sign $(t = T_1 = \bar{t}_1)$.

3. $\alpha_0 \in (-\frac{1}{2D_{J,max}}, 0)$: In this case, $\dot{\lambda}_2$ changes its sign at first and u_1 switches $(t = t_{M_1})$. Consequently, $\dot{x}_1$ has a discontinuity at this time instant. Since $\lim_{t \to t_{M_1}^-} |\dot{x}_1(t)| < u_{1max}$ holds, $\dot{x}_1$ will have the opposite sign of this limit. This means according to (7.1.10) that u_2 switches its sign at this time instant as well $(\hat{t}_0 = t_{M_1})$. The quantity, that first changes its sign afterwards, is again $x_1(t = T_1 = \bar{t}_1)$.

These three possible switching patterns described above are illustrated in Figure 7.1.2 (Right) using again phase plots. The two straight dashed lines depicted there, i.e. the lines defined by the equalities $\alpha_0 = -\frac{1}{D_{J,max}}$ and $\alpha_0 = -\frac{1}{D_{J,min}}$, can be used to identify the patterns. Table 7.5 provides analytical expressions for the time instants $\hat{t}_0, t_{M_1}$ and $\bar{t}_1 = T_1$. Notice that the sign of $\dot{\lambda}_{20}$ does again not have any influence on these times.

Based on the last two switching patterns described above, we can now see that the construction procedure described in Table 7.2 can, for certain negative values of α_0, lead to control strategies with simultaneous switchings at the first switching time instant. Nevertheless, looking at the corresponding expressions for λ_2 and $\dot{\lambda}_2$ it can be seen that regardless of the value of $\alpha_0 < 0$ the signs of λ_2 and $\dot{\lambda}_2$ are different at $t = \bar{t}_1$. More specifically, by the time the angular deflection x_1 is zero again, the second costate λ_2 has not changed its sign, while $\dot{\lambda}_2$ has. This means that the ratio $\alpha_1 = -\frac{\dot{\lambda}_2^*(\bar{t}_1)}{\omega_0 \lambda_2^*(\bar{t}_1)}$ is positive for each of the three possibilities. Consequently, the switching pattern after $\bar{t}_1$ will be the pattern we have found for $\alpha_0 > 0$ and the controls u_1 and u_2 will never switch simultaneously after this time. This also means that the extremal lift can be fully constructed using first Table 7.5, to construct the lift in $[0, \bar{t}_1]$, and then Table 7.4 with $j \in \{1, \ldots, l\}$.

Before concluding our discussion on the switching patterns, it is important to remark here that our results so far actually consider every possible pair

$\tan\!\left(\frac{\omega_{d,min}}{\hat{t}_0}-1\right)$	$\tan\!\left(\frac{\omega_{d,max}-\hat{t}_0}{\hat{t}_0}-1\right)$	$\tan\!\left(\frac{\omega_{d,max}}{(T_1-t_{M_1})}-1\right)$	β_0	α_1	$\dot{x}_1(\bar{t}_1)$
$\dfrac{\omega_{d,min}}{\omega_0 D_{J,max}}$	$\dfrac{\frac{\omega_{d,max}}{\omega_0}}{\left(\frac{1}{2D_{J,min}}+\frac{1}{\alpha_0}-D_{J,min}\right)}$	$\dfrac{\frac{\omega_{d,max}}{\omega_0}}{\left(D_{J,min}+\frac{K_3(\alpha_0)}{\alpha_0}\right)}$	$2D_{J,min}+\dfrac{K_3(\alpha_0)}{\alpha_0}$	$\dfrac{\alpha_0}{K_3(\alpha_0)}$	$-\alpha_0\dfrac{F_{exp}(-T_1+\hat{t}_0,-\hat{t}_0)K_1(-\beta_0)\theta_{max}}{K_1(\alpha_0)\,\mathrm{sgn}(\lambda_{20})}$
$\dfrac{\omega_{d,min}}{\omega_0 D_{J,max}}$	0	$\dfrac{\frac{\omega_{d,max}}{\omega_0}}{\left(-D_{J,min}+2F_{exp}(0,\hat{t}_0)\right)}$	$2F_{exp}(0,\hat{t}_0)$	$\dfrac{F_{exp}(0,-\hat{t}_0)-4D_{J,min}-\frac{2}{\alpha_0}}{2+\frac{1}{\alpha_0}F_{exp}(0,-\hat{t}_0)}$	$\dfrac{K_1(-\beta_0)\theta_{max}}{F_{exp}(T_1-\hat{t}_0,\hat{t}_0)\,\mathrm{sgn}(\lambda_{20})}$
$\dfrac{\omega_{d,min}}{\omega_0\left(-\frac{1}{\alpha_0}-D_{J,max}\right)}$	0	$\dfrac{\frac{\omega_{d,max}}{\omega_0}}{\left(-D_{J,min}+2D_{J,max}+\frac{K_4(\alpha_0)}{\alpha_0}\right)}$	$2D_{J,max}+\dfrac{K_4(\alpha_0)}{\alpha_0}$	$\dfrac{2(D_{J,max}-D_{J,min})\beta_0+1}{\beta_0-2D_{J,max}}$	$-\alpha_0\dfrac{F_{exp}(-T_1+\hat{t}_0,-\hat{t}_0)K_1(-\beta_0)\theta_{max}}{K_2(\alpha_0)\,\mathrm{sgn}(\lambda_{20})}$

$$K_3(\alpha_0)=1-2K_1(\alpha_0)F_{exp}(t_{M_1}-\hat{t}_0,\hat{t}_0)<0,\; K_4(\alpha_0)=1-2K_2(\alpha_0)F_{exp}(0,\hat{t}_0)<0$$

Table 7.5: Switching Pattern for $\alpha_0<0$ ($t\in[0,\bar{t}_1]$)
First Row: $\alpha_0\in\left(-\infty,\frac{1}{2D_{min}}\right]$, Second Row: $\alpha_0\in\left[-\frac{1}{2D_{min}},-\frac{1}{2D_{max}}\right]$, Third Row: $\alpha_0\in\left(-\frac{1}{2D_{max}},0\right)$.
(Adapted from [41], ©2014 IEEE)

$\left(\lambda_{20} \quad \dot{\lambda}_{20}\right)$ satisfying (7.1.16) except the two pairs $\left(0 \quad \frac{1}{\dot{\theta}_{max}}\right)$ and $\left(0 \quad -\frac{1}{\dot{\theta}_{max}}\right)$ for which α_0 is not defined. Nevertheless, in accordance with the illustrated phase plot in Fig. 7.1.2, it can be shown[7] that for both of these pairs the resulting control structure will correspond exactly to the structure for $\alpha_0 \in (-\infty, \frac{1}{2D_{J,min}})$. More specifically, by taking the limit of the expressions provided in the first row of Table 7.5 as α_0 goes to minus infinity, we can use the resulting limits and Table 7.4 to fully construct the corresponding extremal lifts and thus also the control strategies.

7.1.2.3 Energy Interpretation

We have so far shown the existence of five different switching patterns which are followed by control strategies in extremal lifts, provided that the right-hand side of (7.1.10) or (7.1.11) is equal to zero at each switching time. We have further seen that under this assumption, control strategies along normal extremal lifts follow the exact switching pattern once the torque in the spring equals to zero for the first time after the start of the motion. More specifically, they all follow the pattern we have found for $\alpha_0 > 0$, see Fig. 7.1.2 (Left). In the remainder of this section, we want to find a physical law describing this pattern in terms of the relative energy of Σ along its extremals. Moreover, we also want to show how this law relates to the optimal switching patterns for EJ's with adjustable linear stiffness.

Let $\Lambda = (\boldsymbol{x}, \boldsymbol{u}, \boldsymbol{\lambda}, \lambda_a)$ be a normal extremal lift for the LTCP which is defined on a sufficiently large interval. Moreover, assume that x_1 changes its sign $l \geq 2$ times and let $k \in S_{l-1} \backslash \{0\}$. Then, at the switching time $\bar{t}_k + t_k^*$ at which the damping ratio u_2 switches from $D_{J,min}$ to $D_{J,max}$, the ratio of the relative kinetic energy $E_{kin}(\dot{x}_1)$ of the system Σ to its potential energy, which we will refer to as the *energy ratio*, is given by

$$r_k^* = \frac{E_{kin}\left(\dot{x}_1(\bar{t}_k + t_k^*)\right)}{E_{pot}\left(x_1(\bar{t}_k + t_k^*)\right)}$$
$$= \alpha_k^2, \tag{7.1.29}$$

where we have used Table 7.4. According to (7.1.29), we thus see that the ratio $\alpha_k > 0$ of the costates at the time $\bar{t}_k$ uniquely determine the energy ratio at the first switching time after $\bar{t}_k$. Notice that after this switching time, i.e. after $t = \bar{t}_k + t_k^*$, the link is being pulled with the maximum damping ratio until $\dot{x}_1$ and thus the damping torque changes its sign. At this time the energy ratio $\hat{r}_k$ is equal to zero and u_2 switches again back to $D_{J,min}$. Afterwards, when the energy ratio is equal to $r_{M_{k+1}}^- = \frac{(1+\alpha_k D_{J,min})^2}{\alpha_k^2}$ the motor velocity u_1 switches and the new energy ratio $r_{M_{k+1}} = \beta_k^2(\alpha_k)$ is obtained. Finally, the deflection becomes zero and the same switching pattern repeats itself now with the ratio $r_{k+1}^* = \frac{1}{(\beta_k - 2D_{J,min})^2} \overset{!}{=} \alpha_{k+1}^2$. Figure 7.1.3 (Right) illustrates qualitatively on

---

[7] By following again the procedure in Table 7.2 and using (7.1.10)-(7.1.11) together with Table 7.1.
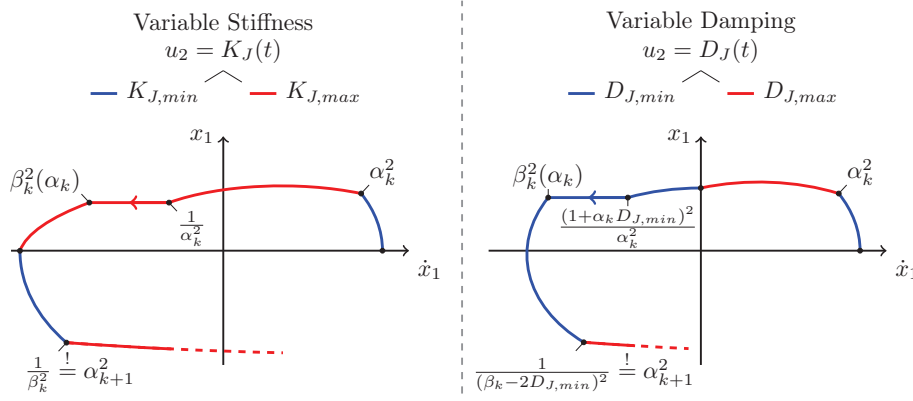
Figure 7.1.3: Comparison of Switching Patterns for EJ's with Variable Impedance (Adapted from [41], ©2014 IEEE)

a phase plot the changes of the energy ratio. It is important to remark here that knowing the value of r_1^*, all the switching times after $t = \bar{t}_1 + t_1^*$ can be uniquely determined by this physical law that is described in terms of the system's potential and relative energy. Therefore, the law provides our desired extension of the concept of resonance energies to EJ's with adjustable viscous damping.

Finally, optimal control strategies for EJ's with adjustable linear stiffness can also be uniquely described in terms of the energy ratio[8] in (7.1.29), see [39, 21]. The change of this ratio, for the case when the stiffness takes its minimum value at zero deflection, is depicted in Fig. 7.1.3 (Left) . A closer look at both systems show now that for $D_{J,min} = 0$, the two switching patterns follow the exact same physical law, eventhough they significantly differ in the way how their system properties are controlled. This clearly indicates the generality of our concept of resonance energies.

7.2 Influence of Variable Stiffness

In this section, we will analyse OC strategies for an EJ model with a VSA as depicted in Fig. 7.2.1. In particular, we will assume that the adjustable TDP of the system can be directly controlled. Furthermore, the motor velocity will be again modeled as a velocity source and the system will be assumed to start from a given position. Nevertheless, the initial state will this time not be necessarily the system's equilibrium position. In addition, the cost functional will be described by a *terminal cost function* which we will only require to have a non-zero gradient. This additional generality is motivated by the fact

---

[8]For variable stiffness joints the potential energy is computed using the maximum value $K_{J,max} > K_{J,min}$ for the stiffness, i.e. $E_{pot}(\phi) = \frac{1}{2}K_{J,max}\phi^2$.
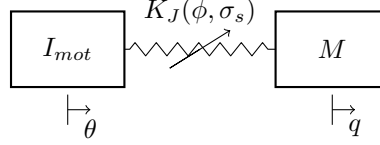
Figure 7.2.1: EJ Model with a VSA

that the concept of resonance frequency, as it exists for EJ's with LSEA's, is independent of the system's initial state and remains also valid for a large class of cost functionals, see [40]. We next provide a mathematical formulation to the general OC problem we just described and also clarify the assumptions on the TDP of the investigated model as well as the cost functional.

7.2.1 Problem Formulation

Similar to an EJ with a NSEA, for an EJ with a VSA the torque between the motor and the link is only due to the elastic elements in the VSA, i.e. $\tau_J = \tau_{J,S}$. Nevertheless, in contrary to a NSEA this torque does not only depend on the deflection ϕ but also on the stiffness variable σ_s. In other words, τ_J is a function of ϕ and σ_s. In our model, we will assume that this function is constrained between two elements of $C^1_{\tau_J}$, $\tau_{J,1}$ and $\tau_{J,2}$, which satisfy

$$(\forall \phi \in (0, \infty)) \left[\tau_{J,1}(\phi) < \tau_{J,2}(\phi) \right]. \tag{7.2.1}$$

Constraining σ_s to take values in the interval $[-1, 1]$, this assumption leads us then to the adjustable TDP $\tau_J : \mathbb{R} \times [-1, 1] \rightarrow \mathbb{R}$ with

$$\tau_J(\phi, \sigma_s) = \frac{\tau_{J,2}(\phi) + \tau_{J,1}(\phi)}{2} + \sigma_s \frac{\tau_{J,2}(\phi) - \tau_{J,1}(\phi)}{2}. \tag{7.2.2}$$

Figure 7.2.2 qualitatively illustrates one possible choice for $\tau_{J,1}, \tau_{J,2}$ and the resulting $\tau_J(., \sigma_s)$ for a piecewise continuous σ_s and $\phi \geq 0$. Notice that the SDP corresponding to τ_J, i.e. K_J, is given by the partial derivative $\frac{\partial \tau_J}{\partial \phi}$ and is thus also a function of ϕ and σ_s.

For the control system Σ describing our EJ model, we will take again $\boldsymbol{x} = \left(\phi \quad \dot{q} \right)^T \in \mathbb{X} = \mathbb{R}^2$ as the state variable and assume that both the motor velocity and the stiffness variable can be directly controlled. The dynamics of Σ can then be described, in accordance with (2.1.4) and (7.2.2), using the function $\boldsymbol{f} : \mathbb{R}^2 \times \mathbb{R}^2 \rightarrow \mathbb{R}^2$ with

$$\boldsymbol{f}(\boldsymbol{x}, \boldsymbol{u}) = \begin{pmatrix} u_1 - x_2 \\ \frac{\tau_J(x_1, u_2)}{M} \end{pmatrix}, \tag{7.2.3}$$

where u_1 and u_2 denote the motor velocity and stiffness variable, respectively. This also leads to the control set

$$\mathbb{U} = [-\dot{\theta}_{max}, \dot{\theta}_{max}] \times [-1, 1],$$
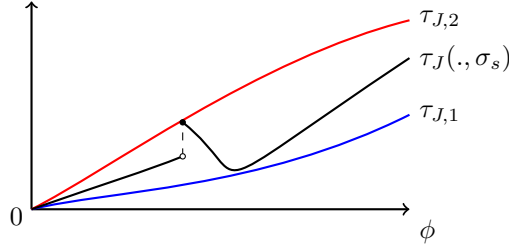
Figure 7.2.2: Adjustable TDP τ_J in the VSA
(Adapted from [42], ©2014 IFAC)

where $\dot{\theta}_{max} > 0$ denotes the maximal motor velocity. Choosing $\mathcal{PC}_{\mathbb{U}}$ as the class of admissible controls $\mathcal{U}$, we have thus fully determined the control system $\Sigma = (\mathbb{X}, \boldsymbol{f}, \mathbb{U}, \mathcal{U})$.

As already mentioned, for the OC problems we want to investigate in this section we will allow the initial state of the system to be chosen arbitrarily. Similarly, we will let the terminal cost function $\mathcal{V} : \mathbb{R}^2 \to \mathbb{R}$ to be an arbitrary continuously differentiable function and further assume that its gradient is always non-zero. Using $\mathcal{C}_\mathcal{V}$ to denote the set of all such functions[9], this leads us then to the cost functional $J : \mathcal{PC}_{\mathbb{U}} \times \mathbb{R}^2 \times \mathcal{C}_\mathcal{V} \to \mathbb{R}$ with

$$J(\boldsymbol{u}, \boldsymbol{x}_0, \mathcal{V}) = \mathcal{V}(\boldsymbol{x}_f), \qquad (7.2.4)$$

where $\boldsymbol{x}_f$ denotes the terminal state of the trajectory $\boldsymbol{x}$ which starts from $\boldsymbol{x}_0$ and correspons to the control $\boldsymbol{u}$. Our general OC problem can finally be formulated as follows.

General Terminal Cost Problem (GTCP): Given a final time $t_f > 0$, an initial state $\boldsymbol{x}_0 \in \mathbb{R}^2$ and a continuously differentiable function $\mathcal{V} \in \mathcal{C}_\mathcal{V}$ find the control $\boldsymbol{u}^{opt}$ which minimizes $J(\boldsymbol{u}, \boldsymbol{x}_0, \mathcal{V})$ over all admissible controls $\boldsymbol{u} \in \mathcal{U}$ defined on $D = [0, t_f]$.

7.2.2 Optimal Control Strategies

In this subsection, we will first make use of PMP to derive necessary conditions which need to be satisfied by the OC strategies solving the GTCP. More specifically, we will show that these strategies are all switching controls if the corresponding trajectories are time-optimal. Moreover, we will show that the relation between the switching times of the optimal motor velocity and the sign of the deflection, as we have found for the LVMP, remains also valid for the GTCP. In addition, regarding the adjustable TDP we show the existence of a similar but less informative relation for the switching times of the second control which depends on the system's state as well as the sign of the controlled motor velocity. Then, we make use of our results on the construction of costate

---

[9]That is $\mathcal{C}_\mathcal{V}$ is the set of all continuously differentiable functions $\mathcal{V} : \mathbb{R}^2 \to \mathbb{R}$ such that $\frac{\partial \mathcal{V}}{\partial \boldsymbol{x}}(\boldsymbol{x}) \neq \boldsymbol{0}$ holds for each $\boldsymbol{x} \in \mathbb{R}^2$.

trajectories from Sec. 5.2.2 to reformulate the derived conditions from PMP as state dependent switching conditions for OC strategies. This will show how to determine the possible switching patterns for the OC strategies and lead to an extension of the concept of resonance energies for EJ's with SEA's to EJ's with VSA's.

7.2.2.1 Basic Properties

In accordance with our previous definitions, we will call an admissible controlled trajectory $(\boldsymbol{x}, \boldsymbol{u})$ an optimally controlled trajectory if there exists a terminal time $t_f > 0$ and a function $\mathcal{V} \in \mathcal{C}_\mathcal{V}$ such that $\boldsymbol{u} : [0, t_f] \to \mathbb{R}^2$ solves the corresponding GTCP with the initial state $\boldsymbol{x}_0$. For such trajectories, PMP provides the following necessary condition.

Proposition 31. *Let $(\boldsymbol{x}, \boldsymbol{u})$ be an optimally controlled trajectory defined on the interval $D = [0, t_f]$ such that $\boldsymbol{u}$ minimizes the cost functional (7.2.4) with a continuously differentiable function $\mathcal{V} \in \mathcal{C}_\mathcal{V}$. Then, there exists a piecewise continuously differentiable costate $\boldsymbol{\lambda} : D \to (\mathbb{R}^2)^*$ such that the first of the following conditions holds at every $t \in D$ at which u_2 is continuous, the second and third at every $t \in D$, and finally the fourth condition at the final time t_f:*

1. *Costate Dynamics*

$$\dot{\boldsymbol{\lambda}}(t) = \left(-\frac{K_J(x_1(t), u_2(t))}{M} \lambda_2(t) \quad \lambda_1(t) \right). \tag{7.2.5}$$

2. *Minimum Condition*

$$\mathbb{H}\left(\boldsymbol{x}(t), \boldsymbol{u}(t), \boldsymbol{\lambda}(t)\right) = \min_{\boldsymbol{v} \in \mathbb{U}} \mathbb{H}\left(\boldsymbol{x}(t), \boldsymbol{v}, \boldsymbol{\lambda}(t)\right), \tag{7.2.6}$$

where $\mathbb{H} : \mathbb{R}^2 \times \mathbb{U} \times (\mathbb{R}^2)^* \to \mathbb{R}$ denotes the Hamiltonian function given by

$$\begin{aligned} \mathbb{H}(\boldsymbol{x}, \boldsymbol{u}, \boldsymbol{\lambda}) &= \boldsymbol{\lambda} \boldsymbol{f}(\boldsymbol{x}, \boldsymbol{u}) \\ &= \lambda_1(u_1 - x_2) + \lambda_2 \frac{\tau_J(x_1, u_2)}{M}. \end{aligned} \tag{7.2.7}$$

3. *Hamiltonian Condition*

$$\mathbb{H}\left(\boldsymbol{x}(t), \boldsymbol{u}(t), \boldsymbol{\lambda}(t)\right) = -\lambda_a, \tag{7.2.8}$$

where $\lambda_a \in \{-1, 0, 1\}$ is a constant scalar.

4. *Transversality Condition*

$$\boldsymbol{\lambda}(t_f) = v \frac{\partial \mathcal{V}}{\partial \boldsymbol{x}}(\boldsymbol{x}_f), \tag{7.2.9}$$

where v is a positive constant scalar.

Proof. The proof follows directly from applying PMP to the GTCP and is omitted for brevity. □

It is important to remark here that the conditions provided by Prop. 31 for the GCTP are very similar to those provided by Prop. 7 for the LVMP. This directly follows from the similarities between the dynamics of the corresponding control systems as well as the fact that in our formulation for the LVMP we only required to maximize the terminal link velocity, i.e. we had a terminal cost function. We want to next show how these similar conditions also lead to similar properties for the corresponding OC strategies.

Let $\Lambda = (\boldsymbol{x}, \boldsymbol{u}, \boldsymbol{\lambda}, \lambda_a)$ be an extremal lift for the GCTP, i.e. a 4$-$tuple consisting of an admissible controlled trajectory $(\boldsymbol{x}, \boldsymbol{u})$, a costate $\boldsymbol{\lambda}$ and a scalar $\lambda_a \in \{0, 1\}$ such that the conditions in Prop. 31 are satisfied with a terminal cost $\mathcal{V} \in \mathcal{C}_\mathcal{V}$. Focusing first on the control u_1, i.e. the velocity of the motor, we can see that the Minimum Condition (5.2.2) implies, as for the LVMP, the following equality:

$$u_1(t) = \begin{cases} -\dot{\theta}_{max} & \lambda_1(t) > 0 \\ \dot{\theta}_{max} & \lambda_1(t) < 0 \end{cases}, \tag{7.2.10}$$

where $t \in D = [0, t_f]$. According to (7.2.10), the value of u_1 is thus uniquely determined by the sign of the first costate whenever it is non-zero. Moreover, since the gradient of elements of $\mathcal{C}_\mathcal{V}$ and thus of $\mathcal{V}$ is everywhere non-zero the transversality condition (7.2.9), the costate dynamics (7.2.5) and our assumptions on the TDP τ_J ensure that the sign of $\dot{\lambda}_1 = -\frac{K_J(x_1, u_2)}{M} \lambda_2$ is always non-zero whenever λ_1 is equal to zero. Consequently, we can conclude that u_1 is a switching control whose switching times are uniquely determined by the zeros of λ_1. More generally, we have the following proposition which basically shows how to generalize Prop. 8 to extremal lifts for the GTCP.

Proposition 32. *Let $\Lambda = (\boldsymbol{x}, \boldsymbol{u}, \boldsymbol{\lambda}, \lambda_a)$ be an extremal lift for the GTCP which is defined on the interval $D = [0, t_f]$ and let $v_{u_{1_0}}$ and $v_{u_{1_f}}$ denote the integers*

$$v_{u_{1_0}} = \begin{cases} \mathrm{sgn}\left(\dot{\lambda}_1(0)\right) & \lambda_1(0) = 0 \\ \mathrm{sgn}\left(\lambda_1(0)\right) & \lambda_1(0) \neq 0 \end{cases}, \tag{7.2.11}$$

and

$$v_{u_{1_f}} = \begin{cases} \mathrm{sgn}\left(\frac{\partial \mathcal{V}}{\partial x_2}(\boldsymbol{x}_f)\right) & \frac{\partial \mathcal{V}}{\partial x_1}(\boldsymbol{x}_f) = 0 \\ \mathrm{sgn}\left(\frac{\partial \mathcal{V}}{\partial x_1}(\boldsymbol{x}_f)\right) & \frac{\partial \mathcal{V}}{\partial x_1}(\boldsymbol{x}_f) \neq 0 \end{cases}, \tag{7.2.12}$$

both of which are necessarily non-zero. Then, u_1 is a switching control with its initial value given by

$$^0u_1 = -v_{u_{1_0}}\dot{\theta}_{max}. \tag{7.2.13}$$

In addition, $t_S \in (0, t_f)$ is a switching time of u_1 if and only if $\lambda_1(t_S)$ is equal to zero in which case we have

$$\frac{\tau_J\left(x_1(t_S), u_2(t_S)\right) \lambda_2(t_S)}{M} = -\lambda_a, \tag{7.2.14}$$

with $\lambda_2(t_S) \neq 0$. Finally, if the control u_1 has $i_{u_1} \geq 1$ switchings we have

$$\left(\forall k \in S_{i_{u_1}} \backslash \{0\}\right) \left[\operatorname{sgn}\left(x_1(t_{S,k_{u_1}})\right) = (-1)^{k+i_{u_1}} v_{u_{1f}} \lambda_a\right], \tag{7.2.15}$$

where $t_{S,k_{u_1}}$ denotes the k'th switching time of u_1.

Proof. The proposition can be derived using the proof of Prop. 8 if we additionally consider the new transversality condition (7.2.9) according to which $\lambda_1(t_f)$ is now not necessarily zero, cf. (5.2.5). □

According to Prop. 32 and in particular (7.2.15), we can see that in case Λ is an abnormal extremal lift the control u_1 only switches when the deflection is equal to zero. On the other hand, if Λ is normal the deflection is non-zero at the switching times of u_1. Moreover, the sign of the deflection always changes between two switchings of u_1. These properties suggest a switching structure for the control u_1 similar to the one we have found for the solutions to the LVMP.

Regarding the second control u_2, we can again make use of the Minimum Condition (7.2.6) which together with our assumptions on the adjustable TDP yields the following relation:

$$u_2(t) = \begin{cases} -1 & \lambda_2(t)x_1(t) > 0 \\ 1 & \lambda_2(t)x_1(t) < 0 \end{cases}, \tag{7.2.16}$$

where $t \in D$. The value of u_2 is thus uniquely determined by the sign of the continuous product $\lambda_2 x_1$ whenever this sign is non-zero. As for the first costate λ_1, the costate dynamics (7.2.5) and the transversality condition (7.2.9) ensure that the zeros of λ_2 are all isolated. The same is, however, not true for the first state x_1. Indeed, according to (7.2.3) it is possible that the deflection remains zero on a finite time interval if both the motor and the link rotate with the same velocity, i.e. $u_1 = x_2$. In such a case, (7.2.16) does not provide any information on the control u_2 and Λ becomes a singular extremal lift. This is in accordance with the observation that at zero deflection the control u_2 does not have any influence on the system's dynamics as we have $\tau_J(0,.) \equiv 0$, see (7.2.2). Moreover, notice that in this case the system's relative energy becomes zero. As the following proposition shows this is a necessary and sufficient condition for an extremal lift for the GCTP to be singular.

Proposition 33. *Let $\Lambda = (\boldsymbol{x}, \boldsymbol{u}, \boldsymbol{\lambda}, \lambda_a)$ be an extremal lift for the GTCP which is defined on $D = [0, t_f]$. Then, Λ is singular if and only if there exists a time $\bar{t} \in D$ such that*

$$E_{pot}\left(x_1(\bar{t})\right) + E_{kin}\left(\dot{x}_1(\bar{t})\right) = 0.$$

Moreover, in this case Λ is abnormal, $\boldsymbol{x}$ is not time-optimal, and there exists a closed and non-degenerate time interval $\bar{D} \subset D$, containing $\bar{t}$, such that

$$\left(\forall t \in \bar{D}\right) \left[\boldsymbol{x}(t) = \begin{pmatrix} 0 \\ u_1(t) \end{pmatrix} \in \left\{\begin{pmatrix} 0 \\ \dot{\theta}_{max} \end{pmatrix}, \begin{pmatrix} 0 \\ -\dot{\theta}_{max} \end{pmatrix}\right\}\right].$$

Proof. See [43]. □

When analysing the extremal lifts for the LVMP, we have shown that the relative energy is always positive along their trajectories. Moreover, for optimal extremal lifts we have observed that these trajectories are all time-optimal. Based on these observations, we will from now on focus on non-singular extremal lifts for the GCTP.

Assuming that Λ is non-singular, neither λ_2 nor x_1 can remain at zero in a finite time-interval. Consequently, all the zeros of $\lambda_2 x_1$ are isolated and this means that u_2 will in this case also be a switching control, see (7.2.16). Moreover, at the switching times of u_2 the product $\lambda_2 x_1$ must be necessarily equal to zero. However, in contrary to u_1 this is not a sufficient condition. In particular, if there exists a time in the interior of D, at which both λ_2 and x_1 become simultaneously zero, the product $\lambda_2 x_1$ will attain the same sign in a deleted neighborhood[10] of this time. Nevertheless, there is still a certain relation between the switching times of u_2 and the sign of the deflection as well as its time-derivative. The following proposition clarifies this relation and can be regarded as an analogue of Prop. 32 for the second control.

Proposition 34. *Let $\Lambda = (\boldsymbol{x}, \boldsymbol{u}, \boldsymbol{\lambda}, \lambda_a)$ be a non-singular extremal lift for the GTCP which is defined on the interval $D = [0, t_f]$ and $\boldsymbol{\sigma} : D \to (\mathbb{R}^2)^*, t \to \begin{pmatrix} \sigma_1 & \sigma_2 \end{pmatrix}$ the function defined by*

$$\boldsymbol{\sigma}(t) = \boldsymbol{\lambda}(t) \begin{pmatrix} 0 & x_1(t) \\ x_1(t) & \dot{x}_1(t) \end{pmatrix}. \tag{7.2.17}$$

Moreover, let $v_{u_{20}}$ denote the integer

$$v_{u_{20}} = \begin{cases} \operatorname{sgn}\left(\sigma_2(0)\right) & \sigma_1(0) = 0 \\ \operatorname{sgn}\left(\sigma_1(0)\right) & \sigma_1(0) \neq 0 \end{cases}. \tag{7.2.18}$$

Then, u_2 is a switching control with its initial value given by

$$^0 u_2 = \begin{cases} -v_{u_{20}} & \boldsymbol{\sigma}(0) \neq \boldsymbol{0} \\ \lambda_a & \boldsymbol{\sigma}(0) = \boldsymbol{0} \end{cases}. \tag{7.2.19}$$

In addition, $t_S \in (0, t_f)$ is a switching time of u_2 if and only if we have

$$\sigma_1(t_S) = 0 \wedge \sigma_2(t_S) \neq 0. \tag{7.2.20}$$

Finally, in this case we have

$$\begin{pmatrix} x_1(t_S) & \lambda_2(t_S) \end{pmatrix} \neq \boldsymbol{0}, \tag{7.2.21}$$

and

$$\lambda_2(t_S) = 0 \Rightarrow \dot{x}_1(t_S) = -\frac{\lambda_a}{\lambda_1(t_S)} \wedge \operatorname{sgn}\left(\dot{x}_1(t_S)\right) = \operatorname{sgn}\left(\lambda_a u_1(t_S)\right), \tag{7.2.22}$$

with $\boldsymbol{\lambda}(t_S) \neq \boldsymbol{0}$.

---

[10]See for instance [62] for the definition of a deleted neighborhood.

Proof. The proof follows from (7.2.5)-(7.2.9) and our discussion above if we additionally note that σ_2 in (7.2.17) gives the time-derivative of the product $\sigma_1 = \lambda_2 x_1$ whenever this derivative exists, and similarly $2\lambda_1 \dot{x}_1$ its second time-derivative whenever this derivative exists and $\lambda_2 = x_1 = 0$. $\qquad\square$

Comparing Prop. 32 and Prop. 34, it can be observed that the latter proposition does not give a specific order on how the sign of the deflection or its time-derivative change between the switchings of u_2. It can only relate the sign of $\dot{x}_1$ at the switchings to the sign of the motor velocity assuming that the deflection is non-zero, see (7.2.22). Furthermore, in contrary to Prop. 32 it does not directly show how the transversality condition influence the switching structure of u_2, cf. (7.2.15). This influence is only implied indirectly by the sign of u_1. In order to better understand the switching structure of u_2, and more generally of $\boldsymbol{u}$, we will next provide a graphical illustration which can be used to determine control strategies satisfying (7.2.10) and (7.2.16) depending on the system's state.

7.2.2.2 Switching Conditions

Let $\Lambda = (\boldsymbol{x}, \boldsymbol{u}, \boldsymbol{\lambda}, \lambda_a)$ be a non-singular extremal lift for the GCTP which is defined on $D = [0, t_f]$. By Prop. 32 and Prop. 34, we know that in this case $\boldsymbol{u}$ will be a switching control with $i \geq 0$ switchings. Consequently, given an integer $k \in S_i$ the restriction of $\boldsymbol{x}$ to the interval D_k can be regarded as a trajectory of an EJ with a SEA. More specifically, $\boldsymbol{x}|_{D_k}$ will be a trajectory of the control system from Sec. 2.1 with the TDP $\tau_J(., {}^k u_2)$. Moreover, substituting the control ${}^k u_2$ into the costate dynamics (7.2.5) it can be seen that the restriction $\boldsymbol{\lambda}|_{D_k}$ will be a solution to (5.2.1) with the SDP $K_J(., {}^k u_2)$. Noting that along non-singular extremal lifts the relative energy is always positive, this means that we can make use of Prop. 9 to express $\boldsymbol{\lambda}|_{D_k}$ as a function of x_1, ${}^k \phi_{max}$ and the sign of $\dot{x}_1$ as done in Sec. 5.2.2. More specifically, making use of the notation introduced there[11] together with the equality (5.2.15) and Table 5.1 we have for each $j \in S_{m_k}$ and $t \in D_{k_j}$

$$\lambda_1(t) = - \lim_{D_{k_j} \ni s \to t} \frac{\tau_J \left(x_1(s), {}^k u_2 \right) {}^k v_{\phi,j}}{M \, {}^k \dot{\phi}_{max}} \left[{}^k \eta_{0,j} - \lambda_a C_{u_2}(x_1(s), {}^k \phi_{max}) \right],$$

(7.2.23)

and

$$\lambda_2(t) = \frac{|\dot{\phi}_{u_2}|(x_1(t), {}^k \phi_{max})}{{}^k \dot{\phi}_{max}} \left[{}^k \eta_{0,j} - \lambda_a J_{u_2}(x_1(t), {}^k \phi_{max}) \right],$$

(7.2.24)

where $J_{u_2} : D_{T_\phi} \to \mathbb{R}$ is the function given by

$$J_{u_2}(x, \phi_{max}) = - \frac{M \dot{\phi}_{max}}{\tau_J(\phi_{max}, {}^k u_2)} \frac{\partial T_{\phi_{u_2}}}{\partial \phi_{max}}(x, \phi_{max}),$$

(7.2.25)

---

[11]Recall that $m_k \geq 0$ gives the number of times the time-derivative $\dot{x}_1$ is equal to zero in the interior of D_k.

and the additional subscript u_2 is used to indicate the dependence of the functions $|\dot{\phi}|$, T_ϕ and C on the TDP $\tau_J(., u_2)$, see (3.1.6), (3.2.7) and (5.2.23).

Focusing now on the time interval D_{k_j}, with $j \in S_{m_k}$, the two expressions (7.2.23)-(7.2.24) can be used to rewrite the conditions (7.2.10) and (7.2.16) on the control as a function of the time-varying deflection x_1 and the constant parameters ${}^k v_{\phi,j}, {}^k \phi_{max}, {}^k \eta_{0,j}$ and λ_a. In the following, we will show how to use the resulting functions to reveal the switching structure of the control $\boldsymbol{u}$. More specifically, we will show how to graphically analyse the sign of these functions which can be used to find all the possible switching patterns for $\boldsymbol{u}$. It is important to remark here that we have actually already made use of the expression (7.2.23) for the first costate when deriving conditions for the controls solving the LVMP, see Sec. 5.2.3. There we have observed that the value of the control and its switching patterns can be graphically determined if we additionally distinguish between abnormal and normal extremal lifts, see Fig. 5.2.2. We will next show that this is also true for the control $\boldsymbol{u}$. We start our discussion by analysing controls in abnormal extremal lifts.

Abnormal Extremal Lifts Let us assume that Λ is an abnormal extremal lift, i.e. $\lambda_a = 0$. Following the exact same arguments as used in Sec. 5.2.3, with the transversality condition (7.2.9) instead of (5.2.5), we can then see that ${}^k \eta_{0,j} \neq 0$. Moreover, for each $t \in D_{k_j}$ the sign of $x_1(t)$ is non-zero and by definition we have $|x_1(t)| < {}^k \phi_{max}$. If we therefore plot the possible values for the parameter ${}^k \eta_{0,j}$ against the deflection x_1, as done in Fig. 5.2.2 (Left), we know that the horizontal curve $\left(x_1(t), {}^k \eta_{0,j} \right)$ will remain in the same quadrant for $t \in D_{k_j}$. Moreover, the value of the control u_1 along this curve will be given by

$$u_1(t) = \dot{\theta}_{max} \operatorname{sgn} \left(\frac{{}^k \eta_{0,j}}{{}^k v_{0,j}} x_1(t) \right), \qquad (7.2.26)$$

where $t \in D_{k_j}$, see (7.2.10) and (7.2.23). Similarly, according to (7.2.16) and (7.2.24) the second control u_2 will be given by

$$u_2(t) = - \operatorname{sgn} \left({}^k \eta_{0,j} x_1(t) \right), \qquad (7.2.27)$$

where $t \in D_{k_j}$. The two equalities (7.2.26) and (7.2.27) lead to the graphical illustration in Fig. 7.2.3 which provides the value of the control $\boldsymbol{u}$ in D_{k_j} depending on the constant parameters ${}^k \eta_{0,j} \in \mathbb{R} \backslash \{0\}, {}^k v_{0,j} \in \{-1, 1\}$ and the strictly decreasing or increasing deflection $x_1 \in (-{}^k \phi_{max}, {}^k \phi_{max}) \backslash \{0\}$.

Fig. 7.2.3 can also be used to determine the deflection values attained at the switching times of $\boldsymbol{u}$. To see this, notice first that at zero deflection the first costate is always equal to zero, see (7.2.23). Consequently, if the curve $\left(x_1(t), {}^k \eta_{0,j} \right)$ intersects the vertical axis at $t = t_{S_{k_{j+1}}} < t_f$ the control u_1 will have a switching according to Prop. 32. Moreover, since at zero deflection the second costate is equal to ${}^k \eta_{0,j} \neq 0$ the second control u_2 will also switch in this case, see Prop. 34. In other words, the controls u_1 and u_2 switch simultaneously.

A switching of u_2 and thus of $\boldsymbol{u}$ can also occur if the second costate is equal to zero while the deflection is non-zero. Taking a closer look at (7.2.24), we
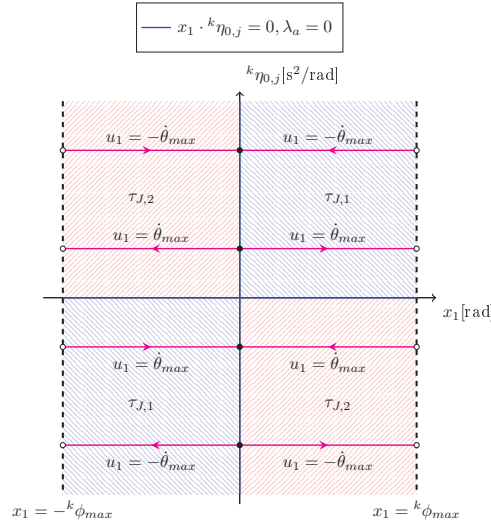
Figure 7.2.3: Controls along Abnormal Extremal Lifts
$(t \in D_{k_j}, i \in \{0, 1, \ldots\}, k \in S_i, j = m_k = 0, {}^k\phi_{max} > 0)$

can see that this is always the case when $|x_1(t_{S_{k_{j+1}}})| = {}^k\phi_{max}$. In other words, there always exists a switching of u_2 when the curve $\left(x_1(t), {}^k\eta_{0,j}\right)$ intersects one of the two vertical curves $x_1 = -{}^k\phi_{max}$ or $x_1 = {}^k\phi_{max}$ at $t = t_{S_{k_{j+1}}} < t_f$. Notice that this also shows that for abnormal extremal lifts we necessarily have $m_k = 0$.

Our discussion so far considers all the possible switchings of the control $\boldsymbol{u}$ which can occur in $D_{k_j} = D_{k_0}$. Since our choice for k was arbitrary, we can thus conclude that u_1 switches in the interior of D if and only if the deflection is equal to zero. Similarly, u_2 switches in the interior of D if and only if the deflection or its time-derivative is equal to zero. Defining the constant ${}^k\kappa = \text{sgn}\left(\frac{{}^k\eta_{0,j}}{{}^kv_{0,j}}\right)$, this switching law can then be formulated in terms of the deflection and its time-derivative as follows:

$$\boldsymbol{u}(t) = {}^k\kappa \begin{pmatrix} \dot{\theta}_{max} \, \text{sgn}\left(x_1(t)\right) \\ -\text{sgn}\left(x_1(t)\dot{x}_1(t)\right) \end{pmatrix}, \tag{7.2.28}$$

where $t \in D_{k_0}$ and $k \in S_i$. Notice that for the case when ${}^k\kappa = 1$ holds for each $k \in S_i$, the switching law for the first control above has been shown to solve the EMP for an EJ with a SEA, see Sec. 4.2. With (7.2.28), we see now the existence of a similar law which is valid for a more general class of EJ models.

Normal Extremal Lifts   Let us assume that Λ is a normal extremal lift so that $\lambda_a \in \{-1, 1\}$. Substituting the expressions (7.2.23)-(7.2.24) into (7.2.10)
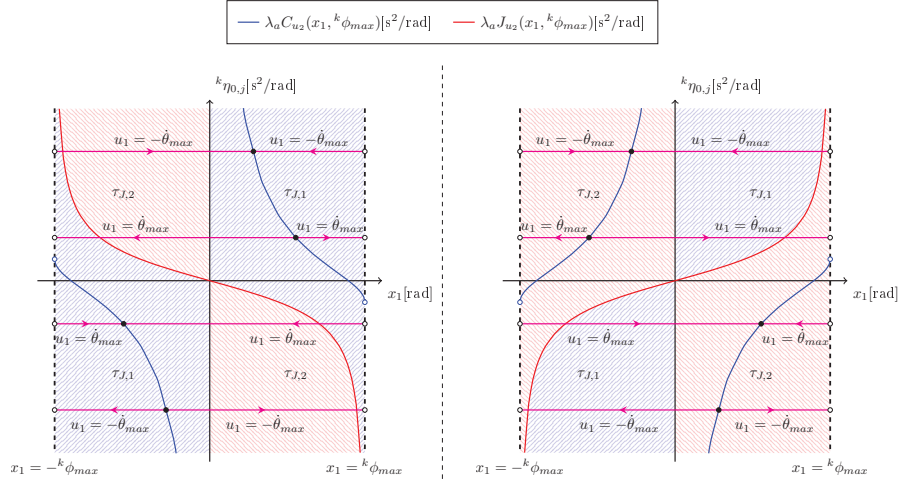
Figure 7.2.4: Controls along Normal Extremal Lifts
$(\lambda_a \in \{-1, 1\}, t \in D_{k_j}, i \in \{0, 1, \dots\}, k \in S_i, j \in S_{m_k}, {}^k\phi_{max} > 0,$
Left: $\lambda_a = -1$, Right: $\lambda_a = 1$)

and (7.2.16), we have then the following equalities for $\boldsymbol{u}$:

$$u_1(t) = \dot{\theta}_{max} \lim_{D_{k_j} \ni s \to t} \frac{\operatorname{sgn}\left(\left[{}^k\eta_{0,j} - \lambda_a C_{u_2}(x_1(s), {}^k\phi_{max})\right] x_1(s)\right)}{{}^k v_{\phi,j}}, \qquad (7.2.29)$$

and

$$u_2(t) = - \lim_{D_{k_j} \ni s \to t} \operatorname{sgn}\left(\left[{}^k\eta_{0,j} - \lambda_a J_{u_2}(x_1(s), {}^k\phi_{max})\right] x_1(s)\right), \qquad (7.2.30)$$

where $t \in D_{k_j}$. As already mentioned, the dependence of the motor velocity on the first costate is exactly the same as for the LVMP, see Prop. 32. Consequently, the value of u_1 can be graphically illustrated as done in Sec. 5.2.3. This is shown in Fig. 7.2.4 with the only difference being the additional possibility for λ_a to be negative. In this case the graph of $-C_{u_2}(., {}^k\phi_{max})$ needs to be used, see (7.2.29).

As illustrated in Fig. 7.2.4, it is possible to graphically determine the value of u_2, as well. In particular, since the function $J_{u_2}(., {}^k\phi_{max})$ is strictly increasing[12] the graph of $\lambda_a J_{u_2}(., {}^k\phi_{max})$ together with the vertical axis lead to four open regions in the set $\left\{(x, \phi_{max}) \in \mathbb{R}^2 \,\big|\, |x| <^k \phi_{max}\right\}$. In each of these regions, (7.2.30) yields the same value for the control u_2. In addition, for a given ${}^k v_{\phi,j}$ the value of the control u_1 is also constant in these regions. This follows from the fact that the two functions J_{u_2} and C_{u_2} are related to each other by

$$C_{u_2}(\phi, {}^k\phi_{max}) - J_{u_2}(\phi, {}^k\phi_{max}) = -\frac{M \, {}^k\dot{\phi}_{max}}{\tau_J(\phi, {}^k u_2)|\dot{\phi}_{u_2}|(\phi, {}^k\phi_{max})}, \qquad (7.2.31)$$

_____

[12]See (3.2.7) and (7.2.25).

for each $\phi \in (-^k\phi_{max}, {}^k\phi_{max})\backslash\{0\}$. Based on this, we can now see that there will always exist six open regions determined by C_{u_2}, J_{u_2} and λ_a to which the horizontal curve $(x_1(t), {}^k\eta_{0,j})$ must belong in D_{k_j} unless there exists a time $\bar{t} \in D_{k_j}$ with $x_1(\bar{t}) = {}^k\eta_{0,j} = 0$, see Fig. 7.2.4, Prop. 32 and Prop. 34. In the case when both x_1 and λ_2 are simultaneously equal to zero, the value of the control u_2 is given by λ_a in accordance with (7.2.30).

As with abnormal extremal lifts, Fig. 7.2.4 can be used to determine the values of the deflection at the switching times as well. In particular, assuming $k \leq i - 1$ this can be done by investigating the intersection points of the horizontal curve $(x_1(t), {}^k\eta_{0,j})$ with the graphs of C_{u_2} and J_{u_2} and the vertical axis. Indeed, at an intersection with the graph of C_{u_2}, or its continuous extension at $|x_1(t)| = {}^k\phi_{max}$, the first costate will be zero and the first control switches. Similarly, at an intersection with J_{u_2} the second costate will be zero and unless the deflection is also zero, which is the case when ${}^k\eta_{0,j} = 0$, the second control switches. Finally, at the vertical axis there will exist a switching of u_2 if again ${}^k\eta_{0,j} \neq 0$.

Our discussion above accounts for all the possible switchings of the control and shows that there never exists a simultanuous switching of the motor velocity and adjustable TDP in contrary to abnormal extremals. Nevertheless, with Fig. 7.2.3-7.2.4 we see that controls in non-singular extremal lifts can always be described in terms of the system's relative and potential energy at the switchings times. That is, we can explain the OC strategies solving the GCTP again using the concept of resonance energies according to which the system must attain a certain sequence of relative energies by changing the control at also a certain sequence of potential energies.

Chapter 8

Conclusion and Outlook

In this thesis, we have thoroughly analysed the problem of maximizing the link velocity of EJ's with velocity-sourced NSEA's. In particular, we have found a construction method for the control strategies solving this problem such that they are described in terms of analytical expressions. Furthermore, we used the proposed method to analyse the dependence of the maximal link velocity of these joints on the final time as well as the system parameters such as the maximal motor velocity, stiffness characteristics, etc. Finally, we have extended our results on the structure of OC strategies to EJ's with variable impedance. Our discussions have led to various results regarding the control and design of SEA's, both of theoretical and practical importance. Taking also our discussions in the two appendices into account, the main contributions of the thesis can be summarized under the following points:

- **Energy Maximization under a limited number of control switchings (Prop. 2-4 and 11)**

  Before solving the LVMP, we have analysed the intuitive control strategy of rotating the motor with its maximal velocity against the spring torque. Assuming that the terminal spring deflection is equal to zero, our results show that this strategy always maximizes the total energy stored in EJ's when there is a constraint on the switching number of the motor velocity. Moreover, the same strategy also maximizes the link velocity under the same constraints provided the sign of the initial control is chosen appropriately. Finally, in the latter case this strategy is also a solution candidate for the LVMP.

- **Existence of Piecewise Continuous Optimal Control Strategies (Prop. 5-6)**

  For control affine systems with convex and compact control sets, the reachable sets are also compact if the trajectories of these systems can be constrained to a compact set [2]. We provide such a compact set for trajectories of EJ's depending only on the motor velocity and the final time. This

enables us to use Filippov's Theorem [11] to conclude that there always exists a measurable control strategy maximizing the terminal link velocity. Applying Pontryagin's Minimum Principle [44] and Sturm-Liouville Theory [3], we then show how for each such control strategy we can also construct a piecewise continuous control leading to the same terminal link velocity and thus solving the LVMP.

- **Link Velocity Maximization of SEA's under limited final time (Prop. 1 and 7-15)**

  For determining the controls solving the LVMP, we show how to analytically describe extremal lifts in terms of only their initial costate and the switching number of their control. Moreover, we clarify how the stiffness characteristics of SEA's influence these extremal lifts by leading to different conditions for the trajectories of their costates and thus to different switching structures for their controls. Finally, by exploiting the dependence of extremal lifts on their initial costate we show how to parameterize the set of all extremals. This leads to a reformulation of the LVMP as a one-dimensional NPP, which can be solved numerically as well as graphically.

- **Resonance Energies (Prop. 1, 10 and 16-18)**

  Fixing a coordinate frame to its motor, the dynamics of an EJ with a velocity-sourced SEA can be described by a mass-spring system if the motor velocity remains constant. Consequently, whenever such a joint is controlled by a switching control the joint's trajectory can be constructed by combining trajectories of mass-spring systems with different relative energies, see Chapter 4. Our results show that the switching times of a strategy solving the LVMP, or more generally of a time-optimal control strategy, are uniquely determined as soon as the system's potential and relative energy are known at its initial switching time. This relation is described by the time properties of the EJ and thus depends on the spring characteristics of the SEA, see Fig. 5.2.2 and Fig. 5.3.2. According to the switching structures depicted there, for SEA's with linear springs each structure leads to a harmonic excitation with the joint's eigenfrequency. For SEA's with nonlinear springs, the corresponding structures are more complex but ensure that a switching always occurs either at zero deflection or after a sign change in the spring torque. In this context, we extend the concept of resonance frequency to the concept of resonance energies.

- **Influence of Final Time and System Parameters on the Maximal Link Velocity (Prop. 19-26)**

  The maximal link velocity of an EJ with a velocity-sourced SEA can be regarded as a function of both the final time and the system parameters. For given parameters, we first show in our analysis that this function is continuous in the final time and strictly increasing. Moreover, we also provide a graphical construction method for the graph of this function

based on the introduced parameterization for the set of extremals. Turning then our attention to the role of the system parameters, we show that graphs illustrating the dependence of the maximal link velocity on the final time can also be used to investigate its dependence on these parameters. More specifically, we show that using only two dimensionless parameters we can simultaneously analyse the influence of both the final time and the system parameters on the velocity gain, i.e. the ratio between the maximal link and motor velocity. Regarding their influence, we have especially observed that for a SEA with hardening springs this gain can be increased if the maximal motor velocity is increased. For SEA's with softening springs, on the other hand, the same gain can be increased with decreasing motor velocity. Finally, for SEA's with linear springs the maximal motor velocity does not have any influence, see Fig 6.2.1-6.2.2.

- **Experimental Verification**

  Our theoretical results on optimal control strategies and on the influence of system parameters on the maximal link velocity have been both experimentally verified using the DLR FSJ [59], see Fig. 6.3.1.

- **Influence of Variable Impedance on Optimal Control Strategies (Prop. 27-34)**

  We have applied PMP to analyse OC strategies for two different EJ models with variable impedance. Focusing first on EJ's with adjustable linear damping, we have shown the existence of switching patterns, for both the motor velocity and damping ratio, which maximize a non-trivial linear combination of the terminal deflection and link velocity. For one of these patterns, we have furthermore found a physical law which under certain assumptions on the minimal damping ratio fully agrees with the law for EJ's with adjustable linear stiffness. Then, we have analysed EJ's with adjustable nonlinear stiffness and shown how to graphically determine the switching structure for a general class of cost functionals. For both models, our results indicate that the introduced concept of resonance energies also apply to EJ's with variable impedance.

- **Second Order Minimum Principle (Theorem 39)**

  When searching for a global minimum of a differentiable real-valued cost function over a given subset of the n-dimensional real space, it is well-known that the cost function must satisfy certain conditions at such a minimum [62, 5]. In particular, the gradient of the cost function must be equal to the zero vector in case the minimum is an interior point of the given set. This condition is, however, in general not sufficient as it can be also satisfied by local minimas and maximas. Nevertheless, if the cost function is two-times continuously differentiable it is possible to obtain additional conditions using the corresponding Hessian, and these conditions can be used to distinguish between local minimas and maximas. In full analogy, the conditions provided by PMP are only necessary for a control

strategy to minimize a given cost functional over a given set of admissible controlled trajectories. Nevertheless, additional conditions can be derived if we assume that each element of the system dynamics is two-times continuously differentiable with respect to the state and if we additionally have a terminal cost function that is two-times continuously differentiable. This is shown in Appendix A, where we make use of properties of transition maps to derive the Second Order Minimum Principle.

There are several ways to extend our results on control strategies solving the LVMP. First of all, since boundary trajectories starting from the origin are necessarily contained in extremals, our proposed construction method for extremals can actually be used directly to construct reachable sets of initially resting elastic joints, as well. This is partially illustrated in Fig. 5.4.1 (Left), where we focus on a particular subset of optimal extremals and further restrict them to the same time interval. To fully understand the structure of these reachable sets, however, we need to further study the properties of the functions from Prop. 13 to determine whether and when extremals intersect each other [53]. This is still an open question, but can now be dealt with by making use of the analytical expressions we derived for these functions. Clearly, knowing this structure one can also construct the time-optimal synthesis to brake elastic joints in a time optimal way [6]. This time-optimal synthesis can in turn be used to derive new closed-loop control laws to control EJ robots. Noting that our results on EJ's with variable impedance also provide a means to construct families of extremals terminating at a given state, these results can be used to derive control laws for EJ robots as well.

Regarding the maximal link velocity of elastic joints, our analysis have led to several non-intuitive results which only apply to EJ's with nonlinear SEA's. Besides the dependence of the velocity gain function on the stiffness characteristics as discussed above, we have for instance seen that a given maximal velocity could be attained faster by an EJ with softening springs even though a larger deflection was required. Focusing only on linear springs, requiring a larger deflection to store a given energy is equivalent to decreasing the eigenfrequency of the joint and thus would not result in a faster motion in this case. The main reason why a faster motion, nevertheless, occurs when EJ's are equipped with nonlinear springs lies in the non-trivial relation between the attained relative energies and the corresponding periods. Our study on the maximal link velocity of EJ's with different spring characteristics clarifies how to exploit this relation to increase the velocity gain of such joints and thus lead to new design criteria for more performant SEA's in robotic systems.

Finally, when using PMP to construct candidates for optimal control strategies the resulting extremals might lead to non-optimal strategies with fairly low performance, see for instance Fig. 6.1.1 (Right). The Second Order Minimum Principle, which we introduce in Appendix A, provides a means to further decrease the set of such candidates under a practically relevant assumption on the system dynamics and cost functional. For the EJ models and OC problems which we have investigated in the thesis, this assumption is satisfied whenever

the TDP is two-times continuously differentiable. This means that this new principle can be used to further analyse, for instance, EJ models with softening and hardening springs, and this might in turn lead to additional information on the optimality/non-optimality of the derived switching structures along the corresponding extremals. More generally, the proposed principle can be used to analyse optimal control strategies for any deterministic system, both analytically and numerically, as long as the dynamics of the system can be described in terms of sufficiently smooth first-order differential equations.

Appendix A

Minimum Principles

In the thesis, we make substantial use of Pontryagin's Minimum Principle [44] and in this appendix we will provide a novel proof to this principle. More specifically, making use of the concept of parameterized families of controlled trajectories [53] we will show how to prove this principle for a general OC problem (GOCP) that accounts for all the three OC problems considered in the thesis, i.e. LVMP, LTCP and GTCP. Moreover, we will also show how using our approach we can further extend this principle assuming an additional degree in the smoothness of the system dynamics and cost functional. This will lead us to what we will call the *Second Order Minimum Principle* (SMP). Our approach is similar to the one pursued in [28], but differs in the requirement on the smoothness of control strategies. In particular, when deriving the SMP we will require the optimal control strategy to be only piecewise continuous. In addition, when deriving both PMP and SMP we will not make use of any separation theorems on convex sets. All our results will basically follow from investigating two types of control variations and the resulting transition maps. We start our discussion by providing a formulation for the GOCP in terms of transition maps and also clarifying some of the properties of these maps which we will require for our proofs of PMP and SMP.

A.1 Problem Formulation

Let $\Sigma = (\mathbb{X}, \boldsymbol{f}, \mathbb{U}, \mathcal{U})$ be a general control system which satisfies the following assumptions:

(B1) The state-space $\mathbb{X}$ is a non-empty open subset of $\mathbb{R}^n$ with $n \geq 1$ being a positive integer.

(B2) The control set $\mathbb{U}$ is a non-empty subset of $\mathbb{R}^m$ with $m \geq 1$ being a positive integer.

(B3) The system dynamics $\boldsymbol{f} : \mathbb{X} \times \mathbb{U} \to \mathbb{R}^n$ is a continuous function. Moreover,

for each $(\boldsymbol{x}, \boldsymbol{v}) \in \mathbb{X} \times \mathbb{U}$ the Jacobian

$$
\frac{\partial \boldsymbol{f}}{\partial \boldsymbol{x}}(\boldsymbol{x}, \boldsymbol{v}) = \begin{pmatrix} \frac{\partial f_1}{\partial x_1}(\boldsymbol{x}, \boldsymbol{v}) & \cdots & \frac{\partial f_1}{\partial x_n}(\boldsymbol{x}, \boldsymbol{v}) \\ \vdots & \ddots & \vdots \\ \frac{\partial f_n}{\partial x_1}(\boldsymbol{x}, \boldsymbol{v}) & \cdots & \frac{\partial f_n}{\partial x_n}(\boldsymbol{x}, \boldsymbol{v}) \end{pmatrix}
$$

exists and the corresponding function $\frac{\partial \boldsymbol{f}}{\partial \boldsymbol{x}} : \mathbb{X} \times \mathbb{U} \to \mathbb{R}^{n \times n}$ is continuous[1].

(B4) $\mathcal{U} = \mathcal{PC}_{\mathbb{U}}$, i.e. the class of admissible controls is the set of all piecewise continuous functions $\boldsymbol{u} : [0, t_f] \to \mathbb{U}$ with $t_f > 0$.

It is important to remark here that our assumptions on the system dynamics ensure that for each piecewise continuous function $\boldsymbol{w} : \mathbb{R} \to \mathbb{U}$ and each pair $(t_0, \boldsymbol{y}_0) \subset \mathbb{R} \times \mathbb{X}$ of initial time and state, the initial value problem

$$
\dot{\boldsymbol{y}}(t) = \boldsymbol{f}(\boldsymbol{y}(t), \boldsymbol{w}(t)), \ \boldsymbol{y}(t_0) = \boldsymbol{y}_0 \in \mathbb{X}, \ t_0 \in \mathbb{R}, \tag{A.1.1}
$$

has a unique maximal solution $\boldsymbol{y} : D_{\boldsymbol{w}}(t_0, \boldsymbol{y}_0) \to \mathbb{X}$, where $D_{\boldsymbol{w}}(t_0, \boldsymbol{y}_0)$ denotes the maximal interval of existence of the solution which is necesarily a non-empty open interval containing t_0, see [34]. More specifically, since the function $\boldsymbol{f}_{\boldsymbol{w}} : \mathbb{X} \times \mathbb{R} \to \mathbb{R}^n$ with

$$
\boldsymbol{f}_{\boldsymbol{w}}(\boldsymbol{x}, t) = \boldsymbol{f}(\boldsymbol{x}, \boldsymbol{w}(t)), \tag{A.1.2}
$$

is locally Lipschitz with respect to its first argument, the function $\boldsymbol{w}$ gives rise to a locally Lipschitz transition map $\boldsymbol{\psi}_{\boldsymbol{w}} : \operatorname{dom}(\boldsymbol{\psi}_{\boldsymbol{w}}) \to \mathbb{X}$ such that for each $(t_0, \boldsymbol{y}_0) \subset \mathbb{R} \times \mathbb{X}$ the function $\boldsymbol{\psi}_{\boldsymbol{w}}(., t_0, \boldsymbol{y}_0)$ gives the maximal solution to (A.1.1). Moreover, the domain of this map, given by $\operatorname{dom}(\boldsymbol{\psi}_{\boldsymbol{w}}) = \left\{ (t, t_0, \boldsymbol{y}_0) \in \mathbb{R}^2 \times \mathbb{X} \, | \, t \in D_{\boldsymbol{w}}(t_0, \boldsymbol{y}_0) \right\}$, is an open set in $\mathbb{R}^{n+2}$, see Theorem 4.29 in [34]. We will call $\boldsymbol{\psi}_{\boldsymbol{w}}$ *the transition map of* Σ *corresponding* to $\boldsymbol{w}$.

When proving PMP and SMP, we will need several properties of partial derivatives of transition maps. Focusing on the transition map $\boldsymbol{\psi}_{\boldsymbol{w}}$ introduced above, let $E_{\boldsymbol{w}} \subset \mathbb{R}$ denote the set of times at which $\boldsymbol{w}$ is not continuous. Regarding the partial derivative $\frac{\partial \boldsymbol{\psi}_{\boldsymbol{w}}}{\partial t}$, it is by definition clear that this derivative exists at each $(t, t_0, \boldsymbol{y}_0) \in (D_{\boldsymbol{w}}(t_0, \boldsymbol{y}_0) \backslash E_{\boldsymbol{w}}) \times \mathbb{R} \times \mathbb{X}$ with

$$
\frac{\partial \boldsymbol{\psi}_{\boldsymbol{w}}}{\partial t}(t, t_0, \boldsymbol{y}_0) = \boldsymbol{f}(\boldsymbol{\psi}_{\boldsymbol{w}}(t, t_0, \boldsymbol{y}_0), \boldsymbol{w}(t)). \tag{A.1.3}
$$

Moreover, according to the properties of $\boldsymbol{f}, \boldsymbol{\psi}_{\boldsymbol{w}}$ and $\boldsymbol{w}$ the corresponding function $\frac{\partial \boldsymbol{\psi}_{\boldsymbol{w}}}{\partial t} : (D_{\boldsymbol{w}}(t_0, \boldsymbol{y}_0) \backslash E_{\boldsymbol{w}}) \times \mathbb{R} \times \mathbb{X} \to \mathbb{R}^n$ is continuous. In addition, introducing for each $t \in \{\tau \in D_{\boldsymbol{w}}(t_0, \boldsymbol{y}_0) \, | \, (t_0 \in \mathbb{R} \wedge \boldsymbol{y}_0 \in \mathbb{X})\}$ the sets

$$
H^-(t) = \{(\tau, \tau_0, \boldsymbol{\xi}_0) \in \operatorname{dom}(\boldsymbol{\psi}_{\boldsymbol{w}}) \, | \, \tau < t\},
$$

and

$$
H^+(t) = \{(\tau, \tau_0, \boldsymbol{\xi}_0) \in \operatorname{dom}(\boldsymbol{\psi}_{\boldsymbol{w}}) \, | \, \tau > t\},
$$

---

[1] That is for each $(i, j) \in \{1, \ldots, n\}^2$ the function $\frac{\partial f_i}{\partial x_j} : \mathbb{X} \times \mathbb{U} \to \mathbb{R}$ is continuous.

the following equality holds for the *left time-derivative* $\frac{\partial \boldsymbol{\psi}_w^-}{\partial t} : dom(\boldsymbol{\psi}_w) \to \mathbb{R}^n$:

$$\begin{aligned}
\frac{\partial \boldsymbol{\psi}_w^-}{\partial t}(t, t_0, \boldsymbol{y}_0) &:= \lim_{H^-(t) \ni (\tau, \tau_0, \boldsymbol{\xi}_0) \to (t, t_0, \boldsymbol{y}_0)} \frac{\partial \boldsymbol{\psi}_w}{\partial t}(\tau, \tau_0, \boldsymbol{\xi}_0) \\
&= \boldsymbol{f}\left(\boldsymbol{\psi}_w(t, t_0, \boldsymbol{y}_0), \lim_{\tau \to t^-} \boldsymbol{w}(\tau)\right),
\end{aligned}$$

while for the *right time-derivative* $\frac{\partial \boldsymbol{\psi}_w^+}{\partial t} : dom(\boldsymbol{\psi}_w) \to \mathbb{R}^n$ we have

$$\begin{aligned}
\frac{\partial \boldsymbol{\psi}_w^+}{\partial t}(t, t_0, \boldsymbol{y}_0) &:= \lim_{H^+(t) \ni (\tau, \tau_0, \boldsymbol{\xi}_0) \to (t, t_0, \boldsymbol{y}_0)} \frac{\partial \boldsymbol{\psi}_w}{\partial t}(\tau, \tau_0, \boldsymbol{\xi}_0) \\
&= \boldsymbol{f}\left(\boldsymbol{\psi}_w(t, t_0, \boldsymbol{y}_0), \boldsymbol{w}(t)\right).
\end{aligned}$$

Similar properties also hold for the partial derivatives $\frac{\partial \boldsymbol{\psi}_w}{\partial t_0}$ and $\frac{\partial \boldsymbol{\psi}_w}{\partial \boldsymbol{y}_0}$. This is shown in the following lemma, where for each $t_0 \in \mathbb{R}$ we use $H_0^-(t_0)$ and $H_0^+(t_0)$ to denote the sets

$$H_0^-(t_0) = \{(\tau, \tau_0, \boldsymbol{\xi}_0) \in dom(\boldsymbol{\psi}_w) \,|\, \tau_0 < t_0\},$$

and

$$H_0^+(t_0) = \{(\tau, \tau_0, \boldsymbol{\xi}_0) \in dom(\boldsymbol{\psi}_w) \,|\, \tau_0 > t_0\}.$$

Lemma 35. *Let Σ satisfy assumptions (B1)-(B4), $\boldsymbol{w} : \mathbb{R} \to \mathbb{U}$ be a piecewise continuous function and $\boldsymbol{\psi}_w : dom(\boldsymbol{\psi}_w) \to \mathbb{X}$ the locally Lipschitz transition map of Σ corresponding to $\boldsymbol{w}$. Moreover, let E_w denote the set of times at which $\boldsymbol{w}$ is not continuous. Then, the partial derivative $\frac{\partial \boldsymbol{\psi}_w}{\partial \boldsymbol{y}_0}$ exists at each $(t, t_0, \boldsymbol{y}_0) \in dom(\boldsymbol{\psi}_w)$ and the corresponding function $\frac{\partial \boldsymbol{\psi}_w}{\partial \boldsymbol{y}_0} : dom(\boldsymbol{\psi}_w) \to \mathbb{R}^{n \times n}$ is continuous. Similarly, the partial derivative $\frac{\partial \boldsymbol{\psi}_w}{\partial t_0}$ exists at each $(t, t_0, \boldsymbol{y}_0) \in dom(\boldsymbol{\psi}_w)$ for which $t_0 \notin E_w$ and the corresponding function $\frac{\partial \boldsymbol{\psi}_w}{\partial t_0} : D_w(t_0, \boldsymbol{y}_0) \times (\mathbb{R} \backslash E_w) \times \mathbb{X} \to \mathbb{R}^n$ is continuous. Moreover, both the left initial time-derivative $\frac{\partial \boldsymbol{\psi}_w^-}{\partial t_0}$ with*

$$\frac{\partial \boldsymbol{\psi}_w^-}{\partial t_0}(t, t_0, \boldsymbol{y}_0) := \lim_{H_0^-(t_0) \ni (\tau, \tau_0, \boldsymbol{\xi}_0) \to (t, t_0, \boldsymbol{y}_0)} \frac{\partial \boldsymbol{\psi}_w}{\partial t_0}(\tau, \tau_0, \boldsymbol{\xi}_0),$$

and the right initial time-derivative $\frac{\partial \boldsymbol{\psi}_w^+}{\partial t_0}$ with

$$\frac{\partial \boldsymbol{\psi}_w^+}{\partial t_0}(t, t_0, \boldsymbol{y}_0) := \lim_{H_0^+(t_0) \ni (\tau, \tau_0, \boldsymbol{\xi}_0) \to (t, t_0, \boldsymbol{y}_0)} \frac{\partial \boldsymbol{\psi}_w}{\partial t_0}(\tau, \tau_0, \boldsymbol{\xi}_0),$$

exist at each $(t, t_0, \boldsymbol{y}_0) \in dom(\boldsymbol{\psi}_w)$, and are given by

$$\frac{\partial \boldsymbol{\psi}_w^-}{\partial t_0}(t, t_0, \boldsymbol{y}_0) = -\frac{\partial \boldsymbol{\psi}_w}{\partial \boldsymbol{y}_0}(t, t_0, \boldsymbol{y}_0)\boldsymbol{f}\left(\boldsymbol{y}_0, \lim_{\tau \to t_0^-} \boldsymbol{w}(\tau)\right), \qquad (A.1.4)$$

and

$$\frac{\partial \boldsymbol{\psi}_{\boldsymbol{w}}^{+}}{\partial t_0}(t, t_0, \boldsymbol{y}_0) = -\frac{\partial \boldsymbol{\psi}_{\boldsymbol{w}}}{\partial \boldsymbol{y}_0}(t, t_0, \boldsymbol{y}_0)\boldsymbol{f}(\boldsymbol{y}_0, \boldsymbol{w}(t_0)),\qquad \text{(A.1.5)}$$

respectively.

Proof. Let $\Sigma, \boldsymbol{w}, \boldsymbol{\psi}_{\boldsymbol{w}}$ and $E_{\boldsymbol{w}}$ satisfy the hypothesis of the lemma. Assume first that $E_{\boldsymbol{w}}$ is empty. Then, both $\boldsymbol{w}$ and the function $\boldsymbol{f}_{\boldsymbol{w}}$ in (A.1.2) are continuous. Moreover, the partial derivative of $\boldsymbol{f}_{\boldsymbol{w}}$ with respect to its first argument exists and is continuous for each $(\boldsymbol{x}, t) \in \mathbb{X} \times \mathbb{R}$. It follows then from Theorem 7.1 and 7.2 in Chapter 1 of [13] that both $\frac{\partial \boldsymbol{\psi}_{\boldsymbol{w}}}{\partial t_0} : \mathrm{dom}(\boldsymbol{\psi}_{\boldsymbol{w}}) \to \mathbb{R}^n$ and $\frac{\partial \boldsymbol{\psi}_{\boldsymbol{w}}}{\partial \boldsymbol{y}_0} : \mathrm{dom}(\boldsymbol{\psi}_{\boldsymbol{w}}) \to \mathbb{R}^{n \times n}$ exist and are continuous. Consequently, the initial time-derivatives $\frac{\partial \boldsymbol{\psi}_{\boldsymbol{w}}^{-}}{\partial t_0}$ and $\frac{\partial \boldsymbol{\psi}_{\boldsymbol{w}}^{+}}{\partial t_0}$ also exist. Finally, the fact that the partial derivatives $\frac{\partial \boldsymbol{\psi}_{\boldsymbol{w}}}{\partial t_0}$ and $\frac{\partial \boldsymbol{\psi}_{\boldsymbol{w}}}{\partial \boldsymbol{y}_0}$ satisfy the same linear differential equation with the boundary conditions[2]

$$\frac{\partial \boldsymbol{\psi}_{\boldsymbol{w}}}{\partial \boldsymbol{y}_0}(t_0, t_0, \boldsymbol{y}_0) = \boldsymbol{I}_d,$$

and

$$\frac{\partial \boldsymbol{\psi}_{\boldsymbol{w}}}{\partial t_0}(t_0, t_0, \boldsymbol{y}_0) = -\boldsymbol{f}(\boldsymbol{y}_0, \boldsymbol{w}(t_0)),\qquad \text{(A.1.6)}$$

see for instance Theorem B.2.2 in [53], imply that (A.1.4) and (A.1.5) both hold. This shows the truth of the lemma for $E_{\boldsymbol{w}} = \emptyset$.

In the remainder of the proof, we want to now show that the lemma is also true when $\boldsymbol{w}$ is piecewise continuous with $E_{\boldsymbol{w}} \neq \emptyset$. For this, let $(\bar{t}_f, \bar{t}_0, \bar{\boldsymbol{y}}_0)$ be an arbitrary element of $\mathrm{dom}(\boldsymbol{\psi}_{\boldsymbol{w}})$. Assuming first that $\bar{t}_f \geq \bar{t}_0$, let $\bar{D} = [\bar{t}_0, \bar{t}_f]$ and introduce the continuous function $\bar{\boldsymbol{y}} : D(\bar{t}_0, \bar{\boldsymbol{y}}_0) \to \mathbb{X}$ with

$$\bar{\boldsymbol{y}}(t) = \boldsymbol{\psi}_{\boldsymbol{w}}(t, \bar{t}_0, \bar{\boldsymbol{y}}_0).$$

Since the image of $\bar{\boldsymbol{y}}|_{\bar{D}}$ is compact and $\mathrm{dom}(\boldsymbol{\psi}_{\boldsymbol{w}})$ is open, we can then find a scalar $\tilde{\varepsilon} > 0$ such that the set

$$\tilde{S} = \left\{ (t, t_0, \boldsymbol{y}_0) \in \mathbb{R}^{n+2} \,\middle|\, t \in (\bar{t}_0 - \tilde{\varepsilon}, \bar{t}_f + \tilde{\varepsilon}) \wedge (t_0, \boldsymbol{y}_0) \in B\left((t, \bar{\boldsymbol{y}}(t))\,; \tilde{\varepsilon}\right) \right\}$$

is a subset of $\mathrm{dom}(\boldsymbol{\psi}_{\boldsymbol{w}})$. Moreover, by choosing $\tilde{\varepsilon} > 0$ sufficiently small we can additionally ensure that the control $\boldsymbol{w}$ is continuous at each $t \in (\bar{t}_0 - \tilde{\varepsilon}, \bar{t}_0) \cup (\bar{t}_f, \bar{t}_f + \tilde{\varepsilon})$. Under this assumption, let $\tilde{t}_0 = \bar{t}_0 - \frac{\tilde{\varepsilon}}{2}$ and $\tilde{t}_f = \bar{t}_f + \frac{\tilde{\varepsilon}}{2}$. Moreover, let $\tilde{D} = [\tilde{t}_0, \tilde{t}_f]$ and introduce the necessarily finite set $\tilde{E}_{\boldsymbol{w}} = (\tilde{t}_0, \tilde{t}_f) \cap E_{\boldsymbol{w}}$ with $\tilde{n} \geq 0$ elements. Set $\tilde{t}_0 = \tilde{t}_{S,0}$ and $\tilde{t}_f = \tilde{t}_{S,\tilde{n}+1}$, and in case the set $\tilde{E}_{\boldsymbol{w}}$ is non-empty let $\tilde{t}_{S,1} < \cdots < \tilde{t}_{S,\tilde{n}}$ denote its elements. Finally, construct for each $k \in \{0, \ldots, \tilde{n}\}$ the continuous control function $\boldsymbol{w}_k : \mathbb{R} \to \mathbb{U}$ with

$$\boldsymbol{w}_k(t) = \begin{cases} \boldsymbol{w}(\tilde{t}_{S,k}) & t \leq \tilde{t}_{S,k} \\ \boldsymbol{w}(t) & t \in (\tilde{t}_{S,k}, \tilde{t}_{S,k+1}), \\ \lim_{t \to \tilde{t}_{S,k+1}^{-}} \boldsymbol{w}(t) & t \geq \tilde{t}_{S,k+1} \end{cases} \qquad \text{(A.1.7)}$$

---

[2]$\boldsymbol{I}_d \in \mathbb{R}^{n \times n}$ denotes the identity matrix.

together with the corresponding transition map $\boldsymbol{\psi}_{\boldsymbol{w}_k}$. In addition, starting from $k = 0$ iteratively define for each $k \in \{0, \dots, \tilde{n}\}$ the state function ${}^k\boldsymbol{\xi}$: $B\left(\left(\tilde{t}_0, \bar{\boldsymbol{y}}(\tilde{t}_0)\right); \tilde{\varepsilon}\right) \to \mathbb{X}$ with

$$
{}^k\boldsymbol{\xi}(t_0, \boldsymbol{y}_0) = \begin{cases} \boldsymbol{y}_0 & k = 0 \\ \boldsymbol{\psi}_{\boldsymbol{w}_{k-1}}\left(\tilde{t}_{S,k}, \tilde{t}_{S,k-1}, {}^{k-1}\boldsymbol{\xi}(t_0, \boldsymbol{y}_0)\right) & k \geq 1 \end{cases}. \qquad (A.1.8)
$$

Based on our discussions in the beginning of the proof, we know that the constructed transition maps $\boldsymbol{\psi}_{\boldsymbol{w}_k}$ are all continuously differentiable. According to (A.1.8), this implies that the state functions ${}^k\boldsymbol{\xi}$ are also all continuously differentiable. To simplify our discussion, we will next distinguish between three different cases depending on whether the times $\bar{t}_0$ and $\bar{t}_f$ belong to $E_{\boldsymbol{w}}$ or not.

First Case $(\bar{t}_0 \notin E_{\boldsymbol{w}} \wedge \bar{t}_f \notin E_{\boldsymbol{w}})$ In this case, we can find a scalar $\bar{\varepsilon} < \tilde{\varepsilon}$ such that the union $(\bar{t}_0 - \bar{\varepsilon}, \bar{t}_0 + \bar{\varepsilon}) \cup (\bar{t}_f - \bar{\varepsilon}, \bar{t}_f + \bar{\varepsilon})$ and the set $E_{\boldsymbol{w}}$ are disjoint. Consequently, we can also find a sufficiently small neighborhood $\bar{V} \subset \mathbb{R}^{n+2}$ of $(\bar{t}_f, \bar{t}_0, \bar{\boldsymbol{y}}_0)$ such that for each $(t, t_0, \boldsymbol{y}_0) \in \bar{V}$ we have

$$
\boldsymbol{\psi}_{\boldsymbol{w}}(t, t_0, \boldsymbol{y}_0) = \boldsymbol{\psi}_{\boldsymbol{w}_{\tilde{n}}}\left(t, \tilde{t}_{S,\tilde{n}}, {}^{\tilde{n}}\boldsymbol{\xi}(t_0, \boldsymbol{y}_0)\right).
$$

Since the functions $\boldsymbol{\psi}_{\boldsymbol{w}_{\tilde{n}}}$ and ${}^{\tilde{n}}\boldsymbol{\xi}$ are both continuously differentiable, we can conclude that at each point of $\bar{V}$, including $(\bar{t}_f, \bar{t}_0, \bar{\boldsymbol{y}}_0)$, the partial derivatives $\frac{\partial \boldsymbol{\psi}_{\boldsymbol{w}}}{\partial t_0}$ and $\frac{\partial \boldsymbol{\psi}_{\boldsymbol{w}}}{\partial \boldsymbol{y}_0}$ exist and are continuous.

Second Case $(\bar{t}_0 \notin E_{\boldsymbol{w}} \wedge \bar{t}_f \in E_{\boldsymbol{w}})$ In this case, $\bar{t}_f = \tilde{t}_{S,\tilde{n}} > \bar{t}_0$ and we can find a scalar $\bar{\varepsilon} < \tilde{\varepsilon}$ such that the union $(\bar{t}_0 - \bar{\varepsilon}, \bar{t}_0 + \bar{\varepsilon}) \cup (\bar{t}_f - \bar{\varepsilon}, \bar{t}_f) \cup (\bar{t}_f, \bar{t}_f + \bar{\varepsilon})$ and the set $E_{\boldsymbol{w}}$ are disjoint. Consequently, we can also find a sufficiently small neighborhood $\bar{V}$ of $(\bar{t}_f, \bar{t}_0, \bar{\boldsymbol{y}}_0)$ such that for each $(t, t_0, \boldsymbol{y}_0) \in \bar{V}$ we have

$$
\boldsymbol{\psi}_{\boldsymbol{w}}(t, t_0, \boldsymbol{y}_0) = \begin{cases} \boldsymbol{\psi}_{\boldsymbol{w}_{\tilde{n}-1}}\left(t, \bar{t}_f, {}^{\tilde{n}}\boldsymbol{\xi}(t_0, \boldsymbol{y}_0)\right) & t < \bar{t}_f \\ \boldsymbol{\psi}_{\boldsymbol{w}_{\tilde{n}}}\left(t, \bar{t}_f, {}^{\tilde{n}}\boldsymbol{\xi}(t_0, \boldsymbol{y}_0)\right) & t \geq \bar{t}_f \end{cases}. \qquad (A.1.9)
$$

Notice that since the functions ${}^{\tilde{n}}\boldsymbol{\xi}, \boldsymbol{\psi}_{\boldsymbol{w}_{\tilde{n}-1}}$ and $\boldsymbol{\psi}_{\boldsymbol{w}_{\tilde{n}}}$ are all continuously differentiable, the partial derivatives $\frac{\partial \boldsymbol{\psi}_{\boldsymbol{w}}}{\partial t_0}$ and $\frac{\partial \boldsymbol{\psi}_{\boldsymbol{w}}}{\partial \boldsymbol{y}_0}$ exist again at each point of $\bar{V}$, including $(\bar{t}_f, \bar{t}_0, \bar{\boldsymbol{y}}_0)$, with

$$
\frac{\partial \boldsymbol{\psi}_{\boldsymbol{w}}}{\partial t_0}(t, t_0, \boldsymbol{y}_0) = \begin{cases} \frac{\partial \boldsymbol{\psi}_{\boldsymbol{w}_{\tilde{n}-1}}}{\partial \boldsymbol{y}_0}\left(t, \bar{t}_f, {}^{\tilde{n}}\boldsymbol{\xi}(t_0, \boldsymbol{y}_0)\right) \frac{\partial {}^{\tilde{n}}\boldsymbol{\xi}}{\partial t_0}(t_0, \boldsymbol{y}_0) & t < \bar{t}_f \\ \frac{\partial \boldsymbol{\psi}_{\boldsymbol{w}_{\tilde{n}}}}{\partial \boldsymbol{y}_0}\left(t, \bar{t}_f, {}^{\tilde{n}}\boldsymbol{\xi}(t_0, \boldsymbol{y}_0)\right) \frac{\partial {}^{\tilde{n}}\boldsymbol{\xi}}{\partial t_0}(t_0, \boldsymbol{y}_0) & t \geq \bar{t}_f \end{cases}, \qquad (A.1.10)
$$

and

$$
\frac{\partial \boldsymbol{\psi}_{\boldsymbol{w}}}{\partial \boldsymbol{y}_0}(t, t_0, \boldsymbol{y}_0) = \begin{cases} \frac{\partial \boldsymbol{\psi}_{\boldsymbol{w}_{\tilde{n}-1}}}{\partial \boldsymbol{y}_0}\left(t, \bar{t}_f, {}^{\tilde{n}}\boldsymbol{\xi}(t_0, \boldsymbol{y}_0)\right) \frac{\partial {}^{\tilde{n}}\boldsymbol{\xi}}{\partial \boldsymbol{y}_0}(t_0, \boldsymbol{y}_0) & t < \bar{t}_f \\ \frac{\partial \boldsymbol{\psi}_{\boldsymbol{w}_{\tilde{n}}}}{\partial \boldsymbol{y}_0}\left(t, \bar{t}_f, {}^{\tilde{n}}\boldsymbol{\xi}(t_0, \boldsymbol{y}_0)\right) \frac{\partial {}^{\tilde{n}}\boldsymbol{\xi}}{\partial \boldsymbol{y}_0}(t_0, \boldsymbol{y}_0) & t \geq \bar{t}_f \end{cases}. \qquad (A.1.11)
$$

The fact that these partial derivatives are also continuous at each point of $\bar{V}$, and in particular at $(\bar{t}, \bar{t}_0, \bar{\boldsymbol{y}}_0)$, follows from the fact that the two expressions on the right-hand side of (A.1.10), respectively of (A.1.11), take the same value at $t = \bar{t}_f$ since we have

$$\frac{\partial \boldsymbol{\psi}_{\boldsymbol{w}_{\tilde{n}-1}}}{\partial \boldsymbol{y}_0} (\bar{t}_f, \bar{t}_f, .) \equiv \frac{\partial \boldsymbol{\psi}_{\boldsymbol{w}_{\tilde{n}}}}{\partial \boldsymbol{y}_0} (\bar{t}_f, \bar{t}_f, .) \equiv \boldsymbol{I}_d.$$

Third Case $(\bar{t}_0 \in E_{\boldsymbol{w}})$ In this case, we have $\bar{t}_0 = \tilde{t}_{S,1}$ and we can therefore find a sufficiently small neighborhood $\bar{V}$ of $(\bar{t}_f, \bar{t}_0, \bar{\boldsymbol{y}}_0)$ such that for each point of $\bar{V}$ we have

$$\boldsymbol{\psi}_{\boldsymbol{w}}(t, t_0, \boldsymbol{y}_0) = \boldsymbol{\psi}_{\boldsymbol{w}} \left(t, \tilde{t}_0, \boldsymbol{\psi}_{\boldsymbol{w}}(\tilde{t}_0, t_0, \boldsymbol{y}_0) \right), \qquad (A.1.12)$$

with

$$\boldsymbol{\psi}_{\boldsymbol{w}}(\tilde{t}_0, t_0, \boldsymbol{y}_0) = \begin{cases} \boldsymbol{\psi}_{\boldsymbol{w}_0} \left(\tilde{t}_0, t_0, \boldsymbol{y}_0 \right) & t_0 < \bar{t}_0 \\ \boldsymbol{\psi}_{\boldsymbol{w}_0} \left(\tilde{t}_0, \bar{t}_0, \boldsymbol{\psi}_{\boldsymbol{w}_1} \left(\bar{t}_0, t_0, \boldsymbol{y}_0 \right) \right) & t_0 \geq \bar{t}_0 \end{cases}. \qquad (A.1.13)$$

By our discussion on the first two cases, the function on the right-hand side of (A.1.12) can be continuously differentiated with respect to its third argument. Similarly, the function in (A.1.13) can be differentiated with respect to its third argument with

$$\frac{\partial \boldsymbol{\psi}_{\boldsymbol{w}}}{\partial \boldsymbol{y}_0}(\tilde{t}_0, t_0, \boldsymbol{y}_0) = \begin{cases} \frac{\partial \boldsymbol{\psi}_{\boldsymbol{w}_0}}{\partial \boldsymbol{y}_0} \left(\tilde{t}_0, t_0, \boldsymbol{y}_0 \right) & t_0 < \bar{t}_0 \\ \frac{\partial \boldsymbol{\psi}_{\boldsymbol{w}_0}}{\partial \boldsymbol{y}_0} \left(\tilde{t}_0, \bar{t}_0, \boldsymbol{\psi}_{\boldsymbol{w}_1} \left(\bar{t}_0, t_0, \boldsymbol{y}_0 \right) \right) \frac{\partial \boldsymbol{\psi}_{\boldsymbol{w}_1}}{\partial \boldsymbol{y}_0} \left(\bar{t}_0, t_0, \boldsymbol{y}_0 \right) & t_0 \geq \bar{t}_0 \end{cases}. $$
$$(A.1.14)$$

Now, both of the expressions in the right-hand side of (A.1.14) can be regarded as continuous functions of the pair $(t_0, \boldsymbol{y}_0)$ and they both take the same value at $t_0 = \bar{t}_0$ since we have $\boldsymbol{\psi}_{\boldsymbol{w}_1} \left(\bar{t}_0, \bar{t}_0, \boldsymbol{y}_0 \right) = \boldsymbol{y}_0$ and $\frac{\partial \boldsymbol{\psi}_{\boldsymbol{w}_1}}{\partial \boldsymbol{y}_0} \left(\bar{t}_0, \bar{t}_0, \boldsymbol{y}_0 \right) = \boldsymbol{I}_d$. By the equality (A.1.12) and chain rule [62], we can then conclude that $\frac{\partial \boldsymbol{\psi}_{\boldsymbol{w}}}{\partial \boldsymbol{y}_0}$ exists again and is continuous at each point of $\bar{V}$. On the other hand, when focusing on points of $\bar{V}$ with $t_0 \neq \bar{t}_0$ we have

$$\frac{\partial \boldsymbol{\psi}_{\boldsymbol{w}}}{\partial t_0}(\tilde{t}_0, t_0, \boldsymbol{y}_0) = \begin{cases} \frac{\partial \boldsymbol{\psi}_{\boldsymbol{w}_0}}{\partial t_0} \left(\tilde{t}_0, t_0, \boldsymbol{y}_0 \right) & t_0 < \bar{t}_0 \\ \frac{\partial \boldsymbol{\psi}_{\boldsymbol{w}_0}}{\partial \boldsymbol{y}_0} \left(\tilde{t}_0, \bar{t}_0, \boldsymbol{\psi}_{\boldsymbol{w}_1} \left(\bar{t}_0, t_0, \boldsymbol{y}_0 \right) \right) \frac{\partial \boldsymbol{\psi}_{\boldsymbol{w}_1}}{\partial t_0} \left(\bar{t}_0, t_0, \boldsymbol{y}_0 \right) & t_0 > \bar{t}_0 \end{cases},$$

which by an application of the chain rule implies

$$\frac{\partial \boldsymbol{\psi}_{\boldsymbol{w}}^-}{\partial t_0}(\bar{t}_f, \bar{t}_0, \bar{\boldsymbol{y}}_0) = (-1) \frac{\partial \boldsymbol{\psi}_{\boldsymbol{w}}}{\partial \boldsymbol{y}_0} (\bar{t}_f, \bar{t}_0, \bar{\boldsymbol{y}}_0) \boldsymbol{f} \left(\bar{\boldsymbol{y}}_0, \lim_{t \to \bar{t}_0^-} \boldsymbol{w}(t) \right), \qquad (A.1.15)$$

and

$$\frac{\partial \boldsymbol{\psi}_{\boldsymbol{w}}^+}{\partial t_0}(\bar{t}_f, \bar{t}_0, \bar{\boldsymbol{y}}_0) = \frac{\partial \boldsymbol{\psi}_{\boldsymbol{w}}}{\partial \boldsymbol{y}_0} (\bar{t}_f, \bar{t}_0, \bar{\boldsymbol{y}}_0) \boldsymbol{f} \left(\bar{\boldsymbol{y}}_0, \boldsymbol{w}(\bar{t}_0) \right), \qquad (A.1.16)$$

where we have made use of the fact that (A.1.6) also holds for $\boldsymbol{w} = \boldsymbol{w}_1$ and $\boldsymbol{w} = \boldsymbol{w}_2$ since they are both continuous. Notice that the two expressions in (A.1.15) and (A.1.16) will in general be different and this shows why, in contrary to $\frac{\partial \boldsymbol{\psi}_{\boldsymbol{w}}}{\partial \boldsymbol{y}_0}$, the partial derivative $\frac{\partial \boldsymbol{\psi}_{\boldsymbol{w}}}{\partial t_0}$ might not exist in this third case.

Assuming the inequality $\bar{t}_f \geq \bar{t}_0$, our discussion of the three different cases proves all the desired properties of the partial derivatives $\frac{\partial \boldsymbol{\psi}_{\boldsymbol{w}}}{\partial t_0}$ and $\frac{\partial \boldsymbol{\psi}_{\boldsymbol{w}}}{\partial \boldsymbol{y}_0}$. Moreover, noting that (A.1.12) actually holds in all the three cases in a sufficiently small neighborhood of $(\bar{t}_f, \bar{t}_0, \bar{\boldsymbol{y}}_0)$ we can see that the equalities (A.1.15) and (A.1.16) also hold when $\bar{t}_f \geq \bar{t}_0$. To conclude the proof, we thus require to show that our results so far are also valid when $\bar{t}_f < \bar{t}_0$. This can be done analogously by letting $\bar{D} = [\bar{t}_f, \bar{t}_0]$, finding a positive scalar $\tilde{\varepsilon} > 0$ such that the set $\tilde{S}$ with

$$\tilde{S} = \left\{ (t, t_0, \boldsymbol{y}_0) \in \mathbb{R}^{n+2} \, | \, t \in (\bar{t}_f - \tilde{\varepsilon}, \bar{t}_0 + \tilde{\varepsilon}) \wedge (t_0, \boldsymbol{y}_0) \in B\left((t, \bar{\boldsymbol{y}}(t)) ; \tilde{\varepsilon} \right) \right\},$$

is a subset of $\operatorname{dom}(\boldsymbol{\psi}_{\boldsymbol{w}})$ and finally setting $\tilde{t}_0 = \bar{t}_f - \frac{\tilde{\varepsilon}}{2}$ and $\tilde{t}_f = \bar{t}_0 + \frac{\tilde{\varepsilon}}{2}$. $\square$

Given an admissible control strategy $\boldsymbol{u} \in \mathcal{PC}_{\mathbb{U}}$ defined on $D = [0, t_f]$, let us now introduce *the extended function* $\boldsymbol{u}_{ex} : \mathbb{R} \to \mathbb{U}$ *corresponding to* $\boldsymbol{u}$ with

$$\boldsymbol{u}_{ex}(t) = \begin{cases} \boldsymbol{u}(0) & t \leq 0 \\ \boldsymbol{u}(t) & t \in (0, t_f) \\ \boldsymbol{u}(t_f) & t \geq t_f \end{cases} . \tag{A.1.17}$$

Clearly $\boldsymbol{u}_{ex}$ is then also a piecewise continuous function and will lead to the transition map $\boldsymbol{\psi}_{\boldsymbol{u}_{ex}}$. Using this map, we can now define the following OC problem.

General Optimal Control Problem (GOCP): Given a final time $t_f > 0$, an initial state $\boldsymbol{x}_0 \in \mathbb{X}$ and a continuously differentiable function $\mathcal{V} : \mathbb{X} \to \mathbb{R}$ find the control $\boldsymbol{u}^{opt}$ which minimizes $\mathcal{V}\left(\boldsymbol{\psi}_{\boldsymbol{u}_{ex}}(t_f, 0, \boldsymbol{x}_0) \right)$ over all admissible controls $\boldsymbol{u} \in \mathcal{PC}_{\mathbb{U}}$.

We want to next show how we can derive PMP for this problem by exploiting the properties of transition maps.

A.2   Pontryagin's Minimum Principle

To motivate our proof for the PMP, we will start with the following lemma which illustrates how trajectories corresponding to the same control strategy can be related to each other.

Lemma 36. *Let Σ be a control system satisfying assumptions (B1)-(B4). Moreover, let $\boldsymbol{w} : \mathbb{R} \to \mathbb{U}$ be a piecewise continuous function and let $E_{\boldsymbol{w}} \subset \mathbb{R}$ denote the set of times at which $\boldsymbol{w}$ is discontinuous. Furthermore, let $\boldsymbol{\xi} : I_\gamma \times I_t \to \mathbb{X}, (\gamma, t) \to \boldsymbol{\xi}(\gamma, t)$ be a continuous function satisfying the following conditions:*

1. $I_\gamma \subset \mathbb{R}$ and $I_t \subset \mathbb{R}$ are two non-empty open intervals.

2. *The partial derivative $\frac{\partial \boldsymbol{\xi}}{\partial t}$ exists at each $(\gamma, t) \in I_\gamma \times (I_t \backslash E_{\boldsymbol{w}})$ with*

$$\frac{\partial \boldsymbol{\xi}}{\partial t}(\gamma, t) = \boldsymbol{f}\left(\boldsymbol{\xi}(\gamma, t), \boldsymbol{w}(t)\right).$$

3. *The partial derivative $\frac{\partial \boldsymbol{\xi}}{\partial \gamma}$ exists at each $(\gamma, t) \in I_\gamma \times I_t$ and is continuous.*

Then, $\frac{\partial \boldsymbol{\xi}}{\partial \gamma}$ satisfies at each $(\gamma, t) \in I_\gamma \times (I_t \backslash E_{\boldsymbol{w}})$ the following differential equation:

$$\frac{\partial}{\partial t}\left(\frac{\partial \boldsymbol{\xi}}{\partial \gamma}\right)(\gamma, t) = \frac{\partial \boldsymbol{f}}{\partial \boldsymbol{x}}\left(\boldsymbol{\xi}(\gamma, t), \boldsymbol{w}(t)\right)\frac{\partial \boldsymbol{\xi}}{\partial \gamma}(\gamma, t). \tag{A.2.1}$$

Proof. Let $\Sigma, \boldsymbol{w}, E_{\boldsymbol{w}}, \boldsymbol{\xi}, I_\gamma$ and I_t satisfy the hypothesis of the proposition. By definition, we have then for each $(\gamma, t, t_0) \in I_\gamma \times I_t^2$

$$
\begin{aligned}
\boldsymbol{\xi}(\gamma, t) &= \boldsymbol{\psi_w}\left(t, t_0, \boldsymbol{\xi}(\gamma, t_0)\right) \\
&= \boldsymbol{\xi}(\gamma, t_0) + \int_{t_0}^{t} \boldsymbol{f}\left(\boldsymbol{\psi_w}\left(s, t_0, \boldsymbol{\xi}(\gamma, t_0)\right), \boldsymbol{w}(s)\right) \mathrm{d}s \\
&= \boldsymbol{\xi}(\gamma, t_0) + \int_{t_0}^{t} \boldsymbol{f}\left(\boldsymbol{\xi}(\gamma, s), \boldsymbol{w}(s)\right) \mathrm{d}s.
\end{aligned}
$$

Since $\boldsymbol{f}$ and $\frac{\partial \boldsymbol{\xi}}{\partial \gamma}$ are both continuous and since $E_{\boldsymbol{w}} \cap I_t$ is a finite set, we can apply Leibniz rule [61] to differentiate both sides of the equality above with respect to γ and this leads to

$$\frac{\partial \boldsymbol{\xi}}{\partial \gamma}(\gamma, t) = \frac{\partial \boldsymbol{\xi}}{\partial \gamma}(\gamma, t_0) + \int_{t_0}^{t} \frac{\partial \boldsymbol{f}}{\partial \boldsymbol{x}}\left(\boldsymbol{\xi}(\gamma, s), \boldsymbol{w}(s)\right)\frac{\partial \boldsymbol{\xi}}{\partial \gamma}(\gamma, s)\mathrm{d}s,$$

which again holds for each $(\gamma, t, t_0) \in I_\gamma \times I_t^2$. Finally, noting that this last relation can be differentiated with respect to time t when $t \notin E_{\boldsymbol{w}}$ we see that (A.3.5) must hold for each $(\gamma, t) \in I_\gamma \times (I_t \backslash E_{\boldsymbol{w}})$, as desired. $\qquad \square$

Given a control system Σ and an admissible control strategy $\boldsymbol{u}$, we can clearly build the extended function $\boldsymbol{u}_{ex}$ and use the corresponding transition map $\boldsymbol{\psi}_{\boldsymbol{u}_{ex}}$ to construct different trajectories of Σ. Lemma 36 provides a means to compare such trajectories at any time along their domain of definition provided they can be combined in a sufficiently smooth manner. More specifically, if these trajectories can be described using a parameterized family of controlled trajectories satisfying the three conditions of the lemma, their relation to each other can be analysed using a linear homogeneous differential equation, see (A.2.1). In our proof of the PMP we will introduce two types of such families. A comparison of the trajectories in these families will then for each type lead to a different condition for a control strategy to solve the GOCP. By the differentiability properties of the constructed families, these conditions will in turn imply the well-known optimality conditions provided by PMP.

Theorem 37. *(Pontryagin's Minimum Principle) Let Σ be a control system satisfying assumptions (B1)-(B4), and $(\boldsymbol{x}, \boldsymbol{u})$ an admissible controlled trajectory which is defined on $D = [0, t_f]$. Moreover, let $E \subset D$ denote the finite set of times at which $\boldsymbol{u}$ is not continuous. Finally, assume that the control $\boldsymbol{u}$ solves the GOCP with the final time $t_f > 0$, the initial state $\boldsymbol{x}_0 \in \mathbb{X}$ and the continuously differentiable function $\mathcal{V} : \mathbb{X} \to \mathbb{R}$. Then, there exists a piecewise continuously differentiable costate $\boldsymbol{\lambda} : D \to (\mathbb{R}^n)^*$ such that the first of the following conditions holds at each $t \in D \backslash E$, the second and third at each $t \in D$, and finally the fourth condition at the final time t_f:*

1. *Costate Dynamics*

$$\dot{\boldsymbol{\lambda}}(t) = -\boldsymbol{\lambda}(t) \frac{\partial \boldsymbol{f}}{\partial \boldsymbol{x}} \left(\boldsymbol{x}(t), \boldsymbol{u}(t) \right). \tag{A.2.2}$$

2. *Minimum Condition*

$$\mathbb{H} \left(\boldsymbol{x}(t), \boldsymbol{u}(t), \boldsymbol{\lambda}(t) \right) = \min_{\boldsymbol{v} \in \mathbb{U}} \mathbb{H} \left(\boldsymbol{x}(t), \boldsymbol{v}, \boldsymbol{\lambda}(t) \right), \tag{A.2.3}$$

where $\mathbb{H} : \mathbb{X} \times \mathbb{U} \times (\mathbb{R}^n)^* \to \mathbb{R}$ denotes the Hamiltonian function given by

$$\mathbb{H}(\boldsymbol{x}, \boldsymbol{u}, \boldsymbol{\lambda}) = \boldsymbol{\lambda} \boldsymbol{f}(\boldsymbol{x}, \boldsymbol{u}). \tag{A.2.4}$$

3. *Hamiltonian Condition*

$$\mathbb{H} \left(\boldsymbol{x}(t), \boldsymbol{u}(t), \boldsymbol{\lambda}(t) \right) = -\lambda_a, \tag{A.2.5}$$

where $\lambda_a \in \{-1, 0, 1\}$ is a constant scalar.

4. *Transversality Condition*

$$\boldsymbol{\lambda}(t_f) = v \frac{\partial \mathcal{V}}{\partial \boldsymbol{x}} \left(\boldsymbol{x}(t_f) \right), \tag{A.2.6}$$

where v is a positive constant scalar.

Proof. Let $\Sigma, (\boldsymbol{x}, \boldsymbol{u}), D = [0, t_f], E \subset D, \boldsymbol{x}_0 \in \mathbb{X}$ and $\mathcal{V}$ satisfy the hypothesis of the theorem. Moreover, let $\boldsymbol{u}_{ex}$ denote the extended function corresponding to $\boldsymbol{u}$ and $\boldsymbol{\psi}_{\boldsymbol{u}_{ex}}$ the transition map of Σ corresponding to $\boldsymbol{u}_{ex}$. Notice that since $(\boldsymbol{x}, \boldsymbol{u})$ is an admissible controlled trajectory, we have for each $\tau_0 \in D$

$$S_{ex}(\tau_0) = \{ (t, \tau_0, \boldsymbol{x}(\tau_0)) \, | \, t \in D \} \subset \text{dom}(\boldsymbol{\psi}_{\boldsymbol{u}_{ex}}). \tag{A.2.7}$$

Consequently, since $S_{ex}(\tau_0)$ is a compact subset of $\mathbb{R}^{n+2}$ we can always find a scalar $\varepsilon_{\tau_0} > 0$ such that the set $\tilde{S}_{ex}(\tau_0, \varepsilon_{\tau_0})$ given by

$$\tilde{S}_{ex}(\tau_0, \varepsilon_{\tau_0}) = \{ (t, \tilde{\tau}_0, \tilde{\boldsymbol{y}}_0) \, | \, t \in (-\varepsilon_{\tau_0}, t_f + \varepsilon_{\tau_0}) \wedge (\tilde{\tau}_0, \tilde{\boldsymbol{y}}_0) \in B \left((\tau_0, \boldsymbol{x}(\tau_0)) \, ; \varepsilon_{\tau_0} \right) \} \tag{A.2.8}$$

is a subset of $\text{dom}(\boldsymbol{\psi}_{\boldsymbol{u}_{ex}})$, i.e.

$$\tilde{S}_{ex}(\tau_0, \varepsilon_{\tau_0}) \subset \text{dom}(\boldsymbol{\psi}_{\boldsymbol{u}_{ex}}). \tag{A.2.9}$$

We will now prove the theorem in seven steps.

1. Construction of $\boldsymbol{\xi}_s$: A family of controlled trajectories described by a shift in the time along the applied control strategy

Let $t_\beta \in (0, t_f) \backslash E$ and $\varepsilon_{t_\beta} > 0$ be a scalar for which the set $\tilde{S}_{ex}(t_\beta, \varepsilon_{t_\beta})$ defined by (A.2.8) is a subset of $\mathrm{dom}(\boldsymbol{\psi}_{\boldsymbol{u}_{ex}})$. There exists then a $\delta_s \in (0, \varepsilon_{t_\beta}]$ such that $I_\beta = (t_\beta - \delta_s, t_\beta + \delta_s)$ is a subset of $D \backslash E$ and we have

$$S_{t_\beta} = \{ (t, \beta, x(t_\beta)) \, | \, t \in (-\delta_s, t_f + \delta_s) \wedge \beta \in I_\beta \} \subset \tilde{S}_{ex}(t_\beta, \varepsilon_{t_\beta}). \qquad \text{(A.2.10)}$$

Choosing now a $\beta \in I_\beta$ and constructing the admissible control strategy $\bar{\boldsymbol{u}}_s : D \to \mathbb{U}$ with

$$\bar{\boldsymbol{u}}_s(t) = \begin{cases} \boldsymbol{u}(t) & t \in [0, t_\beta) \\ \boldsymbol{u}_{ex}(t + \beta - t_\beta) & t \in [t_\beta, t_f] \end{cases}, \qquad \text{(A.2.11)}$$

it follows then from (A.2.9) and (A.2.10) that there exists a unique trajectory $\bar{\boldsymbol{x}}_s : D \to \mathbb{X}$ which starts from $\boldsymbol{x}_0$ and corresponds to $\bar{\boldsymbol{u}}_s$. Moreover, this trajectory can be described in terms of the transition map $\boldsymbol{\psi}_{\boldsymbol{u}_{ex}}$ as follows:

$$\bar{\boldsymbol{x}}_s(t) = \begin{cases} \boldsymbol{\psi}_{\boldsymbol{u}_{ex}}(t, 0, \boldsymbol{x}_0) & t \in [0, t_\beta) \\ \boldsymbol{\psi}_{\boldsymbol{u}_{ex}}(t + \beta - t_\beta, \beta, \boldsymbol{x}(t_\beta)) & t \in [t_\beta, t_f] \end{cases}. \qquad \text{(A.2.12)}$$

Since $(\bar{\boldsymbol{x}}_s, \bar{\boldsymbol{u}}_s)$ is an admissible controlled trajectory, the optimality of $(\boldsymbol{x}, \boldsymbol{u})$ results then to the following condition:

$$\mathcal{V}(\boldsymbol{x}(t_f)) \leq \mathcal{V}(\bar{\boldsymbol{x}}_s(t_f)). \qquad \text{(A.2.13)}$$

Notice that our choice for $\beta \in I_\beta$ was arbitrary and the condition above should therefore hold for any such choice. Based on this observation, let us introduce the map $\boldsymbol{\xi}_s : I_\beta \times (-\delta_s, t_f + \delta_s) \to \mathbb{X}$ with

$$\begin{aligned} \boldsymbol{\xi}_s(\beta, t) &= \boldsymbol{\psi}_{\boldsymbol{u}_{ex}}(t, \beta, \boldsymbol{x}(t_\beta)) & \text{(A.2.14)} \\ &= \boldsymbol{x}(t_\beta) + \int_\beta^t \boldsymbol{f}\left(\boldsymbol{\psi}_{\boldsymbol{u}_{ex}}(s, \beta, \boldsymbol{x}(t_\beta)), \boldsymbol{u}_{ex}(s)\right) \mathrm{d}s, & \text{(A.2.15)} \end{aligned}$$

which for $\beta = t_\beta$ and $t = t_f$ takes the value $\boldsymbol{x}(t_f)$. With the mapping $\boldsymbol{\xi}_s$, (A.2.12) and (A.2.13), we can finally arrive at the condition

$$(\forall \beta \in (t_\beta - \delta_s, t_\beta + \delta_s)) \left[\mathcal{V}(\boldsymbol{\xi}_s(t_\beta, t_f)) \leq \mathcal{V}(\boldsymbol{\xi}_s(\beta, t_f + \beta - t_\beta)) \right], \qquad \text{(A.2.16)}$$

which needs to be satisfied in order for $(\boldsymbol{x}, \boldsymbol{u})$ to be an optimally controlled trajectory. In the sixth step of the proof, we will show how to exploit this last condition and the differentiability properties of $\boldsymbol{\xi}_s$ to derive the Hamiltonian Condition.

2. Construction of $\boldsymbol{\xi}_c$: A family of controlled trajectories described by a change in the value of the applied control strategy

Let $\boldsymbol{v} \in \mathbb{U}$ be an arbitrary element of the control set, $\boldsymbol{w} : \mathbb{R} \to \mathbb{U}$ the constant function with $\boldsymbol{w} \equiv \boldsymbol{v}$ and $\boldsymbol{\psi}_{\boldsymbol{w}} : \mathrm{dom}(\boldsymbol{\psi}_{\boldsymbol{w}}) \to \mathbb{X}$ the transition map of Σ corresponding to $\boldsymbol{w}$. Moreover, let $t_\alpha \in [0, t_f) \backslash E$. Focusing on the initial value problem (A.1.1), with $t_0 = t_\alpha$ and $\boldsymbol{y}_0 = \boldsymbol{x}(t_\alpha)$, the corresponding maximal solution $\boldsymbol{y} : D_{\boldsymbol{w}}(t_\alpha, \boldsymbol{x}(t_\alpha)) \to \mathbb{R}^n$ will then be defined in an open interval containing t_α. Moreover, if $\varepsilon_{t_\alpha} > 0$ denotes a positive scalar for which (A.2.8)-(A.2.9) hold with $\tau_0 = t_\alpha$ and $\varepsilon_{t_\alpha} = \varepsilon_{\tau_0}$, it follows from the continuity of the solution $\boldsymbol{y}$ that we can find a sufficiently small $\delta_{\boldsymbol{w}} \in (0, \varepsilon_{t_\alpha}]$ such that

$$I_{\boldsymbol{w}} = (t_\alpha - \delta_{\boldsymbol{w}}, t_\alpha + \delta_{\boldsymbol{w}}) \subset (-\infty, t_f) \cap D_{\boldsymbol{w}}(t_\alpha, \boldsymbol{x}(t_\alpha)) \backslash E, \qquad \text{(A.2.17)}$$

and

$$(\forall t \in I_{\boldsymbol{w}}) \left[(t, \boldsymbol{y}(t)) \in B\left((t_\alpha, \boldsymbol{x}(t_\alpha)) ; \varepsilon_{t_\alpha} \right) \right]. \qquad \text{(A.2.18)}$$

Let us now first choose an element α of the interval $I_{\boldsymbol{w}}$ with $\alpha > t_\alpha$. According to (A.2.8)-(A.2.9) and (A.2.17)-(A.2.18), the set

$$S_{\boldsymbol{w}}(\alpha) := \{ (t, \alpha, \boldsymbol{y}(\alpha)) \, | \, t \in D \} \qquad \text{(A.2.19)}$$

will be a subset of $\mathrm{dom}(\boldsymbol{\psi}_{\boldsymbol{u}_{ex}})$. Consequently, once the state $\boldsymbol{x}(t_\alpha)$ is reached it is possible to apply the constant control strategy $\boldsymbol{w}$ in the time-interval $[t_\alpha, \alpha) \subset I_{\boldsymbol{w}}$ and then again the control strategy $\boldsymbol{u}$ in $[\alpha, t_f] \subset D$. This can be regarded as a spatial control perturbation as discussed in [32] and leads to the control strategy $\bar{\boldsymbol{u}}_c : D \to \mathbb{U}$ with

$$\bar{\boldsymbol{u}}_c(t) = \begin{cases} \boldsymbol{u}(t) & t \in [0, t_\alpha) \\ \boldsymbol{v} & t \in [t_\alpha, \alpha). \\ \boldsymbol{u}(t) & t \in [\alpha, t_f] \end{cases} \qquad \text{(A.2.20)}$$

It is important to realize here that the control $\bar{\boldsymbol{u}}_c$ as defined above is an admissible control strategy. Moreover, the trajectory $\bar{\boldsymbol{x}}_c : D \to \mathbb{X}$ described by the transition maps $\boldsymbol{\psi}_{\boldsymbol{u}_{ex}}$ and $\boldsymbol{\psi}_{\boldsymbol{w}}$ with

$$\bar{\boldsymbol{x}}_c(t) = \begin{cases} \boldsymbol{\psi}_{\boldsymbol{u}_{ex}}(t, 0, \boldsymbol{x}_0) & t \in [0, t_\alpha) \\ \boldsymbol{\psi}_{\boldsymbol{w}}(t, t_\alpha, \boldsymbol{x}(t_\alpha)) & t \in [t_\alpha, \alpha] \, , \\ \boldsymbol{\psi}_{\boldsymbol{u}_{ex}}(t, \alpha, \boldsymbol{\psi}_{\boldsymbol{w}}(\alpha, t_\alpha, \boldsymbol{x}(t_\alpha))) & t \in (\alpha, t_f] \end{cases} \qquad \text{(A.2.21)}$$

is the unique trajectory which starts from $\boldsymbol{x}_0$ and corresponds to $\bar{\boldsymbol{u}}_c$. Consequently, $(\bar{\boldsymbol{x}}_c, \bar{\boldsymbol{u}}_c)$ is an admissible controlled trajectory and in order for $(\boldsymbol{x}, \boldsymbol{u})$ to be optimal we must have

$$\mathcal{V}(\boldsymbol{x}(t_f)) \le \mathcal{V}(\bar{\boldsymbol{x}}_c(t_f)). \qquad \text{(A.2.22)}$$

Notice now that our choice for $\alpha \in (t_\alpha, t_\alpha + \delta_{\boldsymbol{w}})$ was arbitrary and the inequality in (A.2.22) must actually hold for each trajectory $\bar{\boldsymbol{x}}_c$ arising from such a choice.

This suggests us to define the continuous map $\boldsymbol{\xi}_c : I_{\boldsymbol{w}} \times (-\delta_{\boldsymbol{w}}, t_f + \delta_{\boldsymbol{w}}) \to \mathbb{X}$ with

$$
\begin{aligned}
\boldsymbol{\xi}_c(\alpha, t) &= \boldsymbol{\psi}_{\boldsymbol{u}_{ex}} \left(t, \alpha, \boldsymbol{\psi}_{\boldsymbol{w}} \left(\alpha, t_\alpha, \boldsymbol{x}(t_\alpha) \right) \right) & \text{(A.2.23)} \\
&= \boldsymbol{x}(t_\alpha) + \int_{t_\alpha}^{\alpha} \boldsymbol{f} \left(\boldsymbol{\psi}_{\boldsymbol{w}} \left(s, t_\alpha, \boldsymbol{x}(t_\alpha) \right), \boldsymbol{v} \right) \mathrm{d}s & \text{(A.2.24)} \\
&\quad + \int_{\alpha}^{t} \boldsymbol{f} \left(\boldsymbol{\psi}_{\boldsymbol{u}_{ex}} \left(s, \alpha, \boldsymbol{\psi}_{\boldsymbol{w}} \left(\alpha, t_\alpha, \boldsymbol{x}(t_\alpha) \right) \right), \boldsymbol{u}_{ex}(s) \right) \mathrm{d}s, & \text{(A.2.25)}
\end{aligned}
$$

which for $\alpha = t_\alpha$ and $t = t_f$ takes the value $\boldsymbol{x}(t_f)$. With the map $\boldsymbol{\xi}_c$ and (A.2.21)-(A.2.22), we can arrive, similar to (A.2.16), at the condition

$$
(\forall \alpha \in [t_\alpha, t_\alpha + \delta_{\boldsymbol{w}})) \left[\mathcal{V} \left(\boldsymbol{\xi}_c(t_\alpha, t_f) \right) \leq \mathcal{V} \left(\boldsymbol{\xi}_c(\alpha, t_f) \right) \right], \tag{A.2.26}
$$

which needs to be satisfied in order for $(\boldsymbol{x}, \boldsymbol{u})$ to be an optimally controlled trajectory. In the final step of the proof, we will show how to exploit this relation and the differentiability properties of $\boldsymbol{\xi}_c$ to derive the Minimum Condition.

3. Computation of $\frac{\partial \boldsymbol{\xi}_s}{\partial \beta} : I_\beta \times (-\delta_s, t_f + \delta_s) \to \mathbb{X}$

By Lemma 35, we know that the partial derivative $\frac{\partial \boldsymbol{\psi}_{\boldsymbol{u}_{ex}}}{\partial t_0}(t, t_0, \boldsymbol{y}_0)$ exists and is continuous at each $(t, t_0, \boldsymbol{y}_0) \in \{(\tau, \beta, \boldsymbol{x}(t_\beta)) \,|\, \tau \in (-\delta_s, t_f + \delta_s) \wedge \beta \in I_\beta \}$ since $I_\beta \cap E = \emptyset$ holds by construction. Similarly, since $\boldsymbol{u}_{ex}$ is continuous at each $\beta \in I_\beta$ and since the set $(-\delta_s, t_f + \delta_s) \cap E$ is finite, we can use Leibniz rule to differentiate the right-and side of (A.2.15) with respect to β and this leads to the continuous map $\frac{\partial \boldsymbol{\xi}_s}{\partial \beta} : I_\beta \times (-\delta_s, t_f + \delta_s) \to \mathbb{X}$ with

$$
\begin{aligned}
\frac{\partial \boldsymbol{\xi}_s}{\partial \beta}(\beta, t) &= -\boldsymbol{f} \left(\boldsymbol{\psi}_{\boldsymbol{u}_{ex}} \left(\beta, \beta, \boldsymbol{x}(t_\beta) \right), \boldsymbol{u}_{ex}(\beta) \right) \\
&\quad + \int_{\beta}^{t} \frac{\partial \boldsymbol{f}}{\partial \boldsymbol{x}} \left(\boldsymbol{\psi}_{\boldsymbol{u}_{ex}} \left(s, \beta, \boldsymbol{x}(t_\beta) \right), \boldsymbol{u}_{ex}(s) \right) \frac{\partial \boldsymbol{\psi}_{\boldsymbol{u}_{ex}}}{\partial t_0} \left(s, \beta, \boldsymbol{x}(t_\beta) \right) \mathrm{d}s \\
&= -\boldsymbol{f} \left(\boldsymbol{x}(t_\beta), \boldsymbol{u}_{ex}(\beta) \right) \\
&\quad + \int_{\beta}^{t} \frac{\partial \boldsymbol{f}}{\partial \boldsymbol{x}} \left(\boldsymbol{\xi}_s(\beta, s), \boldsymbol{u}_{ex}(s) \right) \frac{\partial \boldsymbol{\xi}_s}{\partial \beta}(\beta, s) \mathrm{d}s. \tag{A.2.27}
\end{aligned}
$$

According to (A.2.27), we can now see that $\frac{\partial \boldsymbol{\xi}_s}{\partial \beta}(\beta, .)$ is differentiable with respect to time at each $t \in (-\delta_s, t_f + \delta_s) \backslash E$. More specifically, it solves the initial value problem

$$
\frac{\partial}{\partial t} \left(\frac{\partial \boldsymbol{\xi}_s}{\partial \beta} \right)(\beta, t) = \frac{\partial \boldsymbol{f}}{\partial \boldsymbol{x}} \left(\boldsymbol{\xi}_s(\beta, t), \boldsymbol{u}_{ex}(t) \right) \frac{\partial \boldsymbol{\xi}_s}{\partial \beta}(\beta, t), \tag{A.2.28}
$$

with the boundary condition

$$
\frac{\partial \boldsymbol{\xi}_s}{\partial \beta}(\beta, \beta) = -\boldsymbol{f} \left(\boldsymbol{x}(t_\beta), \boldsymbol{u}_{ex}(\beta) \right). \tag{A.2.29}
$$

Notice that the initial value problem (A.2.28)-(A.2.29) is described by a homogeneous linear differential equation. Therefore, its solution can be explicitly formulated using the transition matrix function generated by $\frac{\partial \boldsymbol{f}}{\partial \boldsymbol{x}}\left(\boldsymbol{\xi}_s(\beta, .), \boldsymbol{u}_{ex}(.)\right)$, see [34]. Let $\Phi_s : I_\beta \times (-\delta_s, t_f + \delta_s)^2 \to \mathbb{R}^{n \times n}$ be the matrix-valued function such that $\Phi_s(\beta, ., .)$ is equal to this transition matrix function for each $\beta \in I_\beta$. We have then for each $(\beta, t, t_0) \in I_\beta \times (-\delta_s, t_f + \delta_s)^2$

$$
\begin{aligned}
\frac{\partial \boldsymbol{\xi}_s}{\partial \beta}(\beta, t) &= \Phi_s(\beta, t, t_0)\frac{\partial \boldsymbol{\xi}}{\partial \alpha}(\beta, t_0) \\
&= -\Phi_s(\beta, t, \beta)\boldsymbol{f}\left(\boldsymbol{x}(t_\beta), \boldsymbol{u}_{ex}(\beta)\right),
\end{aligned} \tag{A.2.30}
$$

where for the last inequality we have set $t_0 = \beta$, see (A.2.29).

4. Computation of $\frac{\partial \boldsymbol{\xi}_c}{\partial \alpha} : I_{\boldsymbol{w}} \times (-\delta_{\boldsymbol{w}}, t_f + \delta_{\boldsymbol{w}}) \to \mathbb{X}$

Following the same arguments as used in the third step and noting by Lemma 35 that $\boldsymbol{\psi}_{\boldsymbol{w}}$ is continuously differentiable since $\boldsymbol{w}$ is continuous, we can differentiate the right-and side of (A.2.24)-(A.2.25) with respect to α and this leads to the continuous map $\frac{\partial \boldsymbol{\xi}_c}{\partial \alpha} : I_{\boldsymbol{w}} \times (-\delta_{\boldsymbol{w}}, t_f + \delta_{\boldsymbol{w}}) \to \mathbb{X}$ with

$$
\begin{aligned}
\frac{\partial \boldsymbol{\xi}_c}{\partial \alpha}(\alpha, t) &= \boldsymbol{f}\left(\boldsymbol{\psi}_{\boldsymbol{w}}\left(\alpha, t_\alpha, \boldsymbol{x}(t_\alpha)\right), \boldsymbol{v}\right) - \boldsymbol{f}\left(\boldsymbol{\psi}_{\boldsymbol{w}}\left(\alpha, t_\alpha, \boldsymbol{x}(t_\alpha)\right), \boldsymbol{u}_{ex}(\alpha)\right) \\
&\quad + \int_\alpha^t \frac{\partial \boldsymbol{f}}{\partial \boldsymbol{x}}\left(\boldsymbol{\psi}_{\boldsymbol{u}_{ex}}\left(s, \alpha, \boldsymbol{\xi}_c(\alpha, \alpha)\right), \boldsymbol{u}_{ex}(s)\right)\left\{\frac{\partial \boldsymbol{\psi}_{\boldsymbol{u}_{ex}}}{\partial t_0}\left(s, \alpha, \boldsymbol{\xi}_c(\alpha, \alpha)\right) + \right. \\
&\quad \left. \frac{\partial \boldsymbol{\psi}_{\boldsymbol{u}_{ex}}}{\partial \boldsymbol{y}_0}\left(s, \alpha, \boldsymbol{\xi}_c(\alpha, \alpha)\right)\frac{\partial \boldsymbol{\psi}_{\boldsymbol{w}}}{\partial t}\left(\alpha, t_\alpha, \boldsymbol{x}(t_\alpha)\right)\right\}\mathrm{d}s \\
&= \boldsymbol{f}\left(\boldsymbol{\xi}_c(\alpha, \alpha), \boldsymbol{v}\right) - \boldsymbol{f}\left(\boldsymbol{\xi}_c(\alpha, \alpha), \boldsymbol{u}_{ex}(\alpha)\right) \\
&\quad + \int_\alpha^t \frac{\partial \boldsymbol{f}}{\partial \boldsymbol{x}}\left(\boldsymbol{\xi}_c(\alpha, s), \boldsymbol{u}_{ex}(s)\right)\frac{\partial \boldsymbol{\xi}_c}{\partial \alpha}(\alpha, s)\mathrm{d}s.
\end{aligned} \tag{A.2.31}
$$

According to (A.2.31), we now see that $\frac{\partial \boldsymbol{\xi}_c}{\partial \alpha}(\alpha, .)$ is also differentiable with respect to time at each $t \in (-\delta_{\boldsymbol{w}}, t_f + \delta_{\boldsymbol{w}})\backslash E$ and solves the initial value problem

$$
\frac{\partial}{\partial t}\left(\frac{\partial \boldsymbol{\xi}_c}{\partial \alpha}\right)(\alpha, t) = \frac{\partial \boldsymbol{f}}{\partial \boldsymbol{x}}\left(\boldsymbol{\xi}_c(\alpha, t), \boldsymbol{u}_{ex}(t)\right)\frac{\partial \boldsymbol{\xi}_c}{\partial \alpha}(\alpha, t), \tag{A.2.32}
$$

with the boundary condition

$$
\frac{\partial \boldsymbol{\xi}_c}{\partial \alpha}(\alpha, \alpha) = \boldsymbol{f}\left(\boldsymbol{\xi}_c(\alpha, \alpha), \boldsymbol{v}\right) - \boldsymbol{f}\left(\boldsymbol{\xi}_c(\alpha, \alpha), \boldsymbol{u}_{ex}(\alpha)\right). \tag{A.2.33}
$$

As done in the third step for $\frac{\partial \boldsymbol{\xi}_s}{\partial \beta}$, let us introduce the matrix-valued function $\Phi_c : I_{\boldsymbol{w}} \times (-\delta_{\boldsymbol{w}}, t_f + \delta_{\boldsymbol{w}})^2 \to \mathbb{R}^{n \times n}$ such that $\Phi_c(\alpha, ., .)$ gives for each $\alpha \in I_{\boldsymbol{w}}$ the transition matrix function generated by $\frac{\partial \boldsymbol{f}}{\partial \boldsymbol{x}}\left(\boldsymbol{\xi}_c(\alpha, .), \boldsymbol{u}_{ex}(.)\right)$. We have then for each $(\alpha, t) \in I_{\boldsymbol{w}} \times (-\delta_{\boldsymbol{w}}, t_f + \delta_{\boldsymbol{w}})$

$$
\frac{\partial \boldsymbol{\xi}_c}{\partial \alpha}(\alpha, t) = \Phi_c(\alpha, t, \alpha)\left[\boldsymbol{f}\left(\boldsymbol{\xi}_c(\alpha, \alpha), \boldsymbol{v}\right) - \boldsymbol{f}\left(\boldsymbol{\xi}_c(\alpha, \alpha), \boldsymbol{u}_{ex}(\alpha)\right)\right]. \tag{A.2.34}
$$

5. *Construction of $\boldsymbol{\eta}_s$ and $\boldsymbol{\eta}_c$: A family of solutions to adjoint equations*

In this fifth step, we will simply introduce two functions $\boldsymbol{\eta}_s$ and $\boldsymbol{\eta}_c$ which can be used to refer to solutions of the differential equations that are adjoint to (A.2.28) and (A.2.32). More specifically, we define $\boldsymbol{\eta}_s : I_\beta \times (-\delta_s, t_f + \delta_s) \times (\mathbb{R}^n)^* \to (\mathbb{R}^n)^*, (\beta, t, \boldsymbol{\eta}_f) \to \boldsymbol{\eta}_s(\beta, t, \boldsymbol{\eta}_f)$ such that for each $(\beta, \boldsymbol{\eta}_f) \in I_\beta \times (\mathbb{R}^n)^*$ the function $\boldsymbol{\eta}_s(\beta, ., \boldsymbol{\eta}_f)$ satisfies at each $t \in (-\delta_s, t_f + \delta_s) \backslash E$ the differential equation

$$\frac{\partial \boldsymbol{\eta}_s}{\partial t}(\beta, t, \boldsymbol{\eta}_f) = -\boldsymbol{\eta}_s(\beta, t, \boldsymbol{\eta}_f)\frac{\partial \boldsymbol{f}}{\partial \boldsymbol{x}}\left(\boldsymbol{\xi}_s(\beta, t), \boldsymbol{u}_{ex}(t)\right), \tag{A.2.35}$$

with the boundary condition

$$\boldsymbol{\eta}_s(\beta, t_f, \boldsymbol{\eta}_f) = \boldsymbol{\eta}_f. \tag{A.2.36}$$

Similarly, we define $\boldsymbol{\eta}_c : I_{\boldsymbol{w}} \times (-\delta_{\boldsymbol{w}}, t_f + \delta_{\boldsymbol{w}}) \times (\mathbb{R}^n)^* \to (\mathbb{R}^n)^*, (\alpha, t, \boldsymbol{\eta}_f) \to \boldsymbol{\eta}_c(\alpha, t, \boldsymbol{\eta}_f)$ such that for each $(\alpha, \boldsymbol{\eta}_f) \in I_{\boldsymbol{w}} \times (\mathbb{R}^n)^*$ the function $\boldsymbol{\eta}_c(\alpha, ., \boldsymbol{\eta}_f)$ satisfies at each $t \in (-\delta_{\boldsymbol{w}}, t_f + \delta_{\boldsymbol{w}}) \backslash E$ the differential equation

$$\frac{\partial \boldsymbol{\eta}_c}{\partial t}(\alpha, t, \boldsymbol{\eta}_f) = -\boldsymbol{\eta}_c(\alpha, t, \boldsymbol{\eta}_f)\frac{\partial \boldsymbol{f}}{\partial \boldsymbol{x}}\left(\boldsymbol{\xi}_c(\alpha, t), \boldsymbol{u}_{ex}(t)\right), \tag{A.2.37}$$

with the boundary condition

$$\boldsymbol{\eta}_c(\alpha, t_f, \boldsymbol{\eta}_f) = \boldsymbol{\eta}_f. \tag{A.2.38}$$

Notice that since $\frac{\partial \boldsymbol{f}}{\partial \boldsymbol{x}}, \boldsymbol{\xi}_s$ and $\boldsymbol{\xi}_c$ are all continuous functions and $\boldsymbol{u}_{ex}$ is piecewise continuous, solutions to the initial value problems (A.2.35)-(A.2.36) and (A.2.37)-(A.2.38) uniquely exist. In particular, since (A.2.35) is adjoint to (A.2.28) $\boldsymbol{\eta}_s$ is given by

$$\boldsymbol{\eta}_s(\beta, t, \boldsymbol{\eta}_f) = \boldsymbol{\eta}_f \Phi_s(\beta, t_f, t), \tag{A.2.39}$$

while $\boldsymbol{\eta}_c$ is given by

$$\boldsymbol{\eta}_c(\alpha, t, \boldsymbol{\eta}_f) = \boldsymbol{\eta}_f \Phi_c(\alpha, t_f, t), \tag{A.2.40}$$

since (A.2.37) is adjoint to (A.2.32), see [34]. Finally, by setting $\beta = t_\beta$ and $\alpha = t_\alpha$ it is possible to relate these solutions to the function $\boldsymbol{\lambda} : D \to (\mathbb{R}^n)^*$ solving (A.2.2) with (A.2.6). Indeed, according to (A.2.14) and (A.2.23) we have for each $t \in D$

$$
\begin{aligned}
\boldsymbol{\lambda}(t) &= \boldsymbol{\eta}_s\left(t_\beta, t, v\frac{\partial \mathcal{V}}{\partial \boldsymbol{x}}\left(\boldsymbol{x}(t_f)\right)\right) \\
&= \boldsymbol{\eta}_c\left(t_\alpha, t, v\frac{\partial \mathcal{V}}{\partial \boldsymbol{x}}\left(\boldsymbol{x}(t_f)\right)\right).
\end{aligned}
\tag{A.2.41}
$$

This shows the existence of $\boldsymbol{\lambda}$ for each possible value of $v > 0$ in (A.2.6). We will next prove the Hamiltonian Condition and also specify the scalar $v > 0$.

6. Proving the Hamiltonian Condition

We have already shown that $\boldsymbol{\xi}_s : I_\beta \times (-\delta_s, t_f + \delta_s) \to \mathbb{X}$ is continuously differentiable with respect to its first argument. Similarly, at each $(\beta, t) \in I_\beta \times (-\delta_s, t_f + \delta_s) \backslash E$ it is also continuously differentiable with respect to its second argument with

$$\frac{\partial \boldsymbol{\xi}_s}{\partial t}(\beta, t) = \boldsymbol{f}\left(\boldsymbol{\xi}_s(\beta, t), \boldsymbol{u}_{ex}(t)\right), \tag{A.2.42}$$

see (A.2.14)-(A.2.15). Notice now that by definition, $\boldsymbol{u}_{ex} \in \mathcal{PC}_\mathbb{U}$ must be continuous at t_f. Consequently, we can find a sufficiently small interval $I_{\bar{\beta}} = (t_\beta - \bar{\delta}_s, t_\beta + \bar{\delta}_s) \subset I_\beta$, with $\bar{\delta}_s \in (0, \delta_s]$, such that the function $\boldsymbol{\xi}_{s,f} : I_{\bar{\beta}} \to \mathbb{X}$ with

$$\boldsymbol{\xi}_{s,f}(\beta) = \boldsymbol{\xi}_s(\beta, t_f + \beta - t_\beta), \tag{A.2.43}$$

is continuously differentiable with the derivative $\frac{\mathrm{d}\boldsymbol{\xi}_{s,f}}{\mathrm{d}\beta} : I_{\bar{\beta}} \to \mathbb{X}$ given by

$$\begin{aligned}
\frac{\mathrm{d}\boldsymbol{\xi}_{s,f}}{\mathrm{d}\beta}(\beta) &= \frac{\partial \boldsymbol{\xi}_s}{\partial \beta}(\beta, t_f + \beta - t_\beta) + \frac{\partial \boldsymbol{\xi}_s}{\partial t}(\beta, t_f + \beta - t_\beta) \\
&= -\Phi_s(\beta, t_f + \beta - t_\beta, \beta)\boldsymbol{f}\left(\boldsymbol{x}(t_\beta), \boldsymbol{u}_{ex}(\beta)\right) \\
&+ \boldsymbol{f}\left(\boldsymbol{\xi}_s(\beta, t_f + \beta - t_\beta), \boldsymbol{u}_{ex}(t_f + \beta - t_\beta)\right), \tag{A.2.44}
\end{aligned}$$

see (A.2.30) and (A.2.42). Since $\mathcal{V}$ is also continuously differentiable, the condition (A.2.16) implies by the fundemental theorem of calculus the following relation:

$$\left(\forall \beta \in I_{\bar{\beta}}\right) \left[\int_{t_\beta}^{\beta} \frac{\partial \mathcal{V}}{\partial \boldsymbol{x}}\left(\boldsymbol{\xi}_{s,f}(s)\right) \frac{\mathrm{d}\boldsymbol{\xi}_{s,f}}{\mathrm{d}\beta}(s)\mathrm{d}s \geq 0 \right]. \tag{A.2.45}$$

As t_β belongs to the interior of $I_{\bar{\beta}}$ a necessary condition for (A.2.45) to be true is now that the integrand is equal to zero at $s = t_\beta$. According to (A.2.43)-(A.2.44), this leads to

$$\begin{aligned}
\frac{\partial \mathcal{V}}{\partial \boldsymbol{x}}\left(\boldsymbol{\xi}_{s,f}(t_\beta)\right) \frac{\mathrm{d}\boldsymbol{\xi}_{s,f}}{\mathrm{d}\beta}(t_\beta) &= \frac{\partial \mathcal{V}}{\partial \boldsymbol{x}}\left(\boldsymbol{x}(t_f)\right) \frac{\mathrm{d}\boldsymbol{\xi}_{s,f}}{\mathrm{d}\beta}(t_\beta) \\
&= \frac{\partial \mathcal{V}}{\partial \boldsymbol{x}}\left(\boldsymbol{x}(t_f)\right) \boldsymbol{f}\left(\boldsymbol{x}(t_f), \boldsymbol{u}(t_f)\right) \\
&- \frac{\partial \mathcal{V}}{\partial \boldsymbol{x}}\left(\boldsymbol{x}(t_f)\right) \Phi_s(t_\beta, t_f, t_\beta)\boldsymbol{f}\left(\boldsymbol{x}(t_\beta), \boldsymbol{u}(t_\beta)\right) \\
&\overset{!}{=} 0 \\
\Rightarrow \frac{\partial \mathcal{V}}{\partial \boldsymbol{x}}\left(\boldsymbol{x}(t_f)\right) \boldsymbol{f}\left(\boldsymbol{x}(t_f), \boldsymbol{u}(t_f)\right) &= \frac{\partial \mathcal{V}}{\partial \boldsymbol{x}}\left(\boldsymbol{x}(t_f)\right) \Phi_s(t_\beta, t_f, t_\beta)\boldsymbol{f}\left(\boldsymbol{x}(t_\beta), \boldsymbol{u}(t_\beta)\right).
\end{aligned}$$
$$\tag{A.2.46}$$

Let us now define the scalar v as follows:

$$v = \begin{cases} 1 & \frac{\partial \mathcal{V}}{\partial \boldsymbol{x}}\left(\boldsymbol{x}(t_f)\right) \boldsymbol{f}\left(\boldsymbol{x}(t_f), \boldsymbol{u}(t_f)\right) = 0 \\ \frac{1}{\left|\frac{\partial \mathcal{V}}{\partial \boldsymbol{x}}(\boldsymbol{x}(t_f))\boldsymbol{f}(\boldsymbol{x}(t_f), \boldsymbol{u}(t_f))\right|} & \frac{\partial \mathcal{V}}{\partial \boldsymbol{x}}\left(\boldsymbol{x}(t_f)\right) \boldsymbol{f}\left(\boldsymbol{x}(t_f), \boldsymbol{u}(t_f)\right) \neq 0 \end{cases}.$$

Multiplying both sides of the equality (A.2.46) with this positive scalar v, we get then using (A.2.39) and (A.2.41)

$$\boldsymbol{\lambda}(t_f)\boldsymbol{f}\left(\boldsymbol{x}(t_f),\boldsymbol{u}(t_f)\right) = \boldsymbol{\lambda}(t_\beta)\boldsymbol{f}\left(\boldsymbol{x}(t_\beta),\boldsymbol{u}(t_\beta)\right) = -\lambda_a, \qquad (A.2.47)$$

with $\lambda_a \in \{-1,0,1\}$. Since our choice for $t_\beta \in (0,t_f)\backslash E$ was arbitrary, we can finally conclude that the Hamiltonian $\mathbb{H}\left(\boldsymbol{x}(t),\boldsymbol{u}(t),\boldsymbol{\lambda}(t)\right)$ takes the same value for each such t_β. The fact that the Hamiltonian $\mathbb{H}$ also takes the same value at $\{0,t_f\}\cup E$ follows from the continuity of $\boldsymbol{x},\boldsymbol{\lambda}$ and $\boldsymbol{f}$, and the piecewise continuity of $\boldsymbol{u}$.

7. Proving the Minimum Condition

In the fourth step of the proof, we have shown that the function $\boldsymbol{\xi}_c$, which arises by a spatial control perturbation at $t_\alpha \notin E$, is differentiable with respect to α at each $t \in (-\delta_{\boldsymbol{w}},t_f + \delta_{\boldsymbol{w}})$ and thus also at the terminal time. Since $\mathcal{V}$ is also continuously differentiable, it follows then from the Chain rule and the fundamental theorem of calculus that the condition (A.2.26) can be equivalently written as

$$(\forall \alpha \in [t_\alpha, t_\alpha + \delta_{\boldsymbol{w}})) \left[\int_{t_\alpha}^{\alpha} \frac{\partial \mathcal{V}}{\partial \boldsymbol{x}}\left(\boldsymbol{\xi}_c(s,t_f)\right) \frac{\partial \boldsymbol{\xi}_c}{\partial \alpha}(s,t_f)\mathrm{d}s \geq 0 \right], \qquad (A.2.48)$$

or using the expressions for $\frac{\partial \boldsymbol{\xi}_c}{\partial \alpha}(\alpha,t)$ and $\boldsymbol{\eta}_c(\alpha,t,\boldsymbol{\eta}_f)$ in (A.2.34) and (A.2.40) as

$$\int_{t_\alpha}^{\alpha} \boldsymbol{\eta}_c\left(s,s,\frac{\partial \mathcal{V}}{\partial \boldsymbol{x}}\left(\boldsymbol{\xi}_c(s,t_f)\right)\right)\left[\boldsymbol{f}\left(\boldsymbol{\xi}_c(s,s),\boldsymbol{v}\right) - \boldsymbol{f}\left(\boldsymbol{\xi}_c(s,s),\boldsymbol{u}(s)\right)\right]\mathrm{d}s \geq 0,$$
$$(A.2.49)$$

which must hold for each $\alpha \in [t_\alpha, t_\alpha + \delta_{\boldsymbol{w}})$. A necessary condition for (A.2.49) to hold is that the continuous integrand on the left-hand side of the inequality is non-negative at $s = t_\alpha$. Multiplying the resulting term with $v > 0$, this leads then according to (A.2.37)-(A.2.38) and (A.2.41) to the inequality

$$\boldsymbol{\lambda}(t_\alpha)\left[\boldsymbol{f}\left(\boldsymbol{x}(t_\alpha),\boldsymbol{u}(t_\alpha)\right) - \boldsymbol{f}\left(\boldsymbol{x}(t_\alpha),\boldsymbol{v}\right)\right] \quad \leq \quad 0,$$

and thus by (A.2.4) to

$$\mathbb{H}\left(\boldsymbol{x}(t_\alpha),\boldsymbol{u}(t_\alpha),\boldsymbol{\lambda}(t_\alpha)\right) \leq \mathbb{H}\left(\boldsymbol{x}(t_\alpha),\boldsymbol{v},\boldsymbol{\lambda}(t_\alpha)\right). \qquad (A.2.50)$$

Since our choice for $t_\alpha \in [0,t_f)\backslash E$ and $\boldsymbol{v}$ was arbitrary we have actually shown the truth of the following relation:

$$(\forall t \in [0,t_f)\backslash E)\left[\mathbb{H}\left(\boldsymbol{x}(t),\boldsymbol{u}(t),\boldsymbol{\lambda}(t)\right) = \min_{\boldsymbol{v}\in\mathbb{U}}\mathbb{H}\left(\boldsymbol{x}(t),\boldsymbol{v},\boldsymbol{\lambda}(t)\right)\right]. \qquad (A.2.51)$$

To prove that the relation above also holds for $t \in \{t_f\}\cup E$, assume by contradiction that there exists a time[3] $t_S \in E$ such that $\mathbb{H}\left(\boldsymbol{x}(t_S),\boldsymbol{u}(t_S),\boldsymbol{\lambda}(t_S)\right) >$

---

[3]The case with $t_S = t_f$ can be proved very similarly by noting that $\lim_{D\ni t\to t_f}\mathbb{H}\left(\boldsymbol{x}(.),\boldsymbol{u}(.),\boldsymbol{\lambda}(.)\right) = \mathbb{H}\left(\boldsymbol{x}(t_f),\boldsymbol{u}(t_f),\boldsymbol{\lambda}(t_f)\right)$ since $\boldsymbol{u}$ is continuous at t_f.

$\min_{\boldsymbol{v}\in\mathbb{U}}\mathbb{H}\left(\boldsymbol{x}(t),\boldsymbol{v},\boldsymbol{\lambda}(t)\right)$. Since $\boldsymbol{x}, \boldsymbol{\lambda}$ and $\boldsymbol{f}$ are continuous and since the control $\boldsymbol{u}$ is left-continuous, there exists then a control $\bar{\boldsymbol{v}} \in \mathbb{U}$ and a sufficiently small time-interval $[t_S, t_S + \varepsilon_S) \subset D$ in which the difference $\mathbb{H}\left(\boldsymbol{x}(t), \boldsymbol{u}(t), \boldsymbol{\lambda}(t)\right) - \mathbb{H}\left(\boldsymbol{x}(t), \bar{\boldsymbol{v}}, \boldsymbol{\lambda}(t)\right)$ remains positive. As the union $\{t_f\} \cup E$ is finite, we can then find a time $t_\alpha \in (t_S, t_S + \varepsilon_S)$ in this interval which also belongs to $[0, t_f) \backslash E$ and this in turn contradicts (A.2.51). $\qquad\square$

The main advantage of our proposed proof of Theorem 37 is that it clearly illustrates why PMP in general only provides sufficient conditions for optimal control strategies. Indeed, the Hamiltonian Condition (A.2.5) in the theorem is derived by first constructing, for each time $t_\beta \in (0, t_f)$ at which $\boldsymbol{u}$ is continuous, a parameterized family of controlled trajectories using the map $\boldsymbol{\xi}_s$. This leads then to a continuously differentiable curve which is defined on an open set and which must have a global minimum at t_β for $(\boldsymbol{x}, \boldsymbol{u})$ to be an optimally controlled trajectory, see (A.2.45). Nevertheless, for the derivation of (A.2.5) we only require the fact that the derivative of this curve must be zero at t_β, a necessary condition which can also be satisfied by local maximas. Similarly, to prove the Minimizing Condition (A.2.3) a continuously differentiable curve is constructed which must attain its global minimum at the boundary of a half-open interval, see (A.2.48). However, the inequality (A.2.50) can only ensure that this boundary is a local minimum if the inequality is strict.

Our discussion above suggests that we can attain additional necessary conditions for optimal control strategies in case the two curves described above have additional smoothness properties. In the following, we show how to ensure such properties by providing additional assumptions on the system dynamics $\boldsymbol{f}$ and the terminal cost function $\mathcal{V}$. This will lead to the SMP which under these assumptions extends PMP for the GOCP.

A.3 Second Order Minimum Principle

Let $\Sigma = (\mathbb{X}, \boldsymbol{f}, \mathbb{U}, \mathcal{U})$ be a general control system which satisfies, in addition to assumptions (B1)-(B4), the following assumption:

(B5) For each $k \in \{1, \ldots, n\}$, the Hessian

$$\frac{\partial^2 f_k}{\partial \boldsymbol{x}^2}(\boldsymbol{x}, \boldsymbol{v}) = \begin{pmatrix} \frac{\partial^2 f_k}{\partial x_1^2}(\boldsymbol{x}, \boldsymbol{v}) & \cdots & \frac{\partial^2 f_k}{\partial x_1 \partial x_n}(\boldsymbol{x}, \boldsymbol{v}) \\ \vdots & \ddots & \vdots \\ \frac{\partial^2 f_k}{\partial x_n \partial x_1}(\boldsymbol{x}, \boldsymbol{v}) & \cdots & \frac{\partial^2 f_k}{\partial x_n^2}(\boldsymbol{x}, \boldsymbol{v}) \end{pmatrix}$$

exists at each $(\boldsymbol{x}, \boldsymbol{v}) \in \mathbb{X} \times \mathbb{U}$ and the corresponding function $\frac{\partial^2 f_k}{\partial \boldsymbol{x}^2} : \mathbb{X} \times \mathbb{U} \to \mathbb{R}^{n \times n}$ is continuous.

Clearly, the properties of transition maps as we discussed in the beginning of this appendix still holds for the control system Σ. In particular, given a piecewise continuous function $\boldsymbol{w} : \mathbb{R} \to \mathbb{U}$ there exists a transition map $\boldsymbol{\psi}_{\boldsymbol{w}}$ which can be

used to construct trajectories of Σ which correspond to controls $\boldsymbol{u} = \boldsymbol{w}|_D$, where $D = [0, t_f]$ denotes a closed interval with $t_f > 0$. Let $\boldsymbol{y} : D \to \mathbb{X}$ be such a trajectory and assume that $\bar{t} \in D$ is a time at which $\boldsymbol{w}$ is continuous. Moreover, let $E_{\boldsymbol{w}}$ denote the set of times at which $\boldsymbol{w}$ is discontinuous and $\bar{\delta} > 0$ a scalar such that the interval $\bar{I}_\gamma = (-\bar{\delta} + \bar{t}, \bar{t} + \bar{\delta})$ and $E_{\boldsymbol{w}}$ are disjoint. We can then construct, as done in our proof of PMP, a parameterized family of trajectories $\bar{\boldsymbol{\xi}} : \bar{I}_\gamma \times \bar{I}_t \to \mathbb{X}$, with $\bar{I}_t = (-\bar{\delta}, t_f + \bar{\delta})$, such that for each $\gamma \in \bar{I}_\gamma$ the function $\bar{\boldsymbol{\xi}}(\gamma, .)$ solves the initial value problem

$$\frac{\partial \bar{\boldsymbol{\xi}}}{\partial t}(\gamma, t) = \boldsymbol{f}\left(\bar{\boldsymbol{\xi}}(\gamma, t), \boldsymbol{w}(t)\right), \ \bar{\boldsymbol{\xi}}(\gamma, \gamma) = \bar{\boldsymbol{z}}_0(\gamma) \in \mathbb{X}, \qquad (A.3.1)$$

where $\bar{\boldsymbol{z}}_0 : \bar{I}_\gamma \to \mathbb{X}$ is a continuously differentiable function which can be chosen arbitrarily. Using the properties of transition maps and Leibniz rule, we can then see that the partial derivative $\frac{\partial \bar{\boldsymbol{\xi}}}{\partial \gamma}$ is continuous and solves the initial value problem[4]

$$\frac{\partial}{\partial t}\left(\frac{\partial \bar{\boldsymbol{\xi}}}{\partial \gamma}\right)(\gamma, t) = \frac{\partial \boldsymbol{f}}{\partial \boldsymbol{x}}\left(\bar{\boldsymbol{\xi}}(\gamma, t), \boldsymbol{w}(t)\right)\frac{\partial \bar{\boldsymbol{\xi}}}{\partial \gamma}(\gamma, t), \qquad (A.3.2)$$

with

$$\begin{aligned}
\frac{\partial \bar{\boldsymbol{\xi}}}{\partial \gamma}(\gamma, \gamma) &= \frac{\mathrm{d}\bar{\boldsymbol{z}}_0}{\mathrm{d}\gamma}(\gamma) - \frac{\partial \bar{\boldsymbol{\xi}}}{\partial t}(\gamma, \gamma) \\
&= \frac{\mathrm{d}\bar{\boldsymbol{z}}_0}{\mathrm{d}\gamma}(\gamma) - \boldsymbol{f}\left(\bar{\boldsymbol{\xi}}(\gamma, \gamma), \boldsymbol{w}(\gamma)\right).
\end{aligned}$$

Finally, since (A.3.2) is a linear homogeneous differential equation, the derivative $\frac{\partial \bar{\boldsymbol{\xi}}}{\partial \gamma}$ can be explicitly described using the matrix-valued function $\bar{\Phi} : \bar{I}_\gamma \times \bar{I}_t^2 \to \mathbb{R}^{n \times n}$ with

$$\begin{aligned}
\frac{\partial \bar{\boldsymbol{\xi}}}{\partial \gamma}(\gamma, t) &= \bar{\Phi}(\gamma, t, \gamma)\frac{\partial \bar{\boldsymbol{\xi}}}{\partial \gamma}(\gamma, \gamma) \\
&= \bar{\Phi}(\gamma, t, \gamma)\left(\frac{\mathrm{d}\bar{\boldsymbol{z}}_0}{\mathrm{d}\gamma}(\gamma) - \boldsymbol{f}\left(\bar{\boldsymbol{\xi}}(\gamma, \gamma), \boldsymbol{w}(\gamma)\right)\right), \qquad (A.3.3)
\end{aligned}$$

where $\bar{\Phi}(\gamma, ., .)$ denotes for each $\gamma \in \bar{I}_\gamma$ the transition matrix function generated by $\frac{\partial \boldsymbol{f}}{\partial \boldsymbol{x}}\left(\bar{\boldsymbol{\xi}}(\gamma, .), \boldsymbol{w}(.)\right)$.

Taking now a closer look at this last expression for $\frac{\partial \bar{\boldsymbol{\xi}}}{\partial \gamma}$, it is clear that we can not ensure that this term is differentiable with respect to γ unless we introduce additional assumptions on the control strategy $\boldsymbol{w}$, the dependence of $\boldsymbol{f}$ on its second argument and the function $\bar{\boldsymbol{z}}_0$. Nevertheless, being generated by a set of piecewise continuous functions we know for certain that the partial derivative $\frac{\partial \bar{\Phi}}{\partial t}$ exists at each point $(\gamma, t, t_0) \in \bar{I}_\gamma \times \left(\bar{I}_t \backslash E_{\boldsymbol{w}}\right) \times \bar{I}_t$ with

$$\frac{\partial \bar{\Phi}}{\partial t}(\gamma, t, t_0) = \frac{\partial \boldsymbol{f}}{\partial \boldsymbol{x}}\left(\bar{\boldsymbol{\xi}}(\gamma, t), \boldsymbol{w}(t)\right)\bar{\Phi}(\gamma, t, t_0). \qquad (A.3.4)$$

---

[4]See the third and fourth step in the proof of Theorem 37.

Similarly, noting that for each pair $(\gamma, t_0) \in \bar{I}_\gamma \times \bar{I}_t$ the matrix-valued function $\bar{\Phi}(\gamma, ., t_0)$ solves the initial value problem (A.3.4) with

$$\bar{\Phi}(\gamma, t_0, t_0) = \boldsymbol{I}_d,$$

we can apply Lemma 35, with an appropriate choice for the control system, to see that $\frac{\partial \bar{\Phi}}{\partial t_0}$ exists at each $(\gamma, t, t_0) \in \bar{I}_\gamma \times \bar{I}_t \times \left(\bar{I}_t \backslash E_{\boldsymbol{w}} \right)$. Finally, using the relation

$$\left(\forall (\gamma, t, t_0) \in \bar{I}_\gamma \times \bar{I}_t^2 \right) \left[\bar{\Phi}(\gamma, t_0, t) \bar{\Phi}(\gamma, t, t_0) = \boldsymbol{I}_d \right],$$

and the chain rule we can see that the corresponding function $\frac{\partial \bar{\Phi}}{\partial t_0} : \bar{I}_\gamma \times \bar{I}_t \times \left(\bar{I}_t \backslash E_{\boldsymbol{w}} \right) \to \mathbb{R}^{n \times n}$ is given by

$$\frac{\partial \bar{\Phi}}{\partial t_0}(\gamma, t, t_0) = -\bar{\Phi}(\gamma, t, t_0) \frac{\partial \boldsymbol{f}}{\partial \boldsymbol{x}} \left(\bar{\boldsymbol{\xi}}(\gamma, t_0), \boldsymbol{w}(t_0) \right).$$

It is important to remark here that to establish the differentiability properties of $\bar{\Phi}$ discussed so far we did not make use of our additional assumption (B5). The following lemma shows that this assumption ensures that $\bar{\Phi}$ is continuously differentiable with respect to its first argument at each point of $\bar{I}_\gamma \times \bar{I}_t^2$.

Lemma 38. *Let Σ be a control system satisfying assumptions (B1)-(B5). Moreover, let $\boldsymbol{w} : \mathbb{R} \to \mathbb{U}$ be a piecewise continuous function and let $E_{\boldsymbol{w}} \subset \mathbb{R}$ denote the set of times at which $\boldsymbol{w}$ is discontinuous. Furthermore, let $\boldsymbol{\xi} : I_\gamma \times I_t \to \mathbb{X}, (\gamma, t) \to \boldsymbol{\xi}(\gamma, t)$ be a continuous function satisfying the following conditions:*

1. *$I_\gamma \subset \mathbb{R}$ and $I_t \subset \mathbb{R}$ are two non-empty open intervals.*

2. *The partial derivative $\frac{\partial \boldsymbol{\xi}}{\partial t}$ exists at each $(\gamma, t) \in I_\gamma \times (I_t \backslash E_{\boldsymbol{w}})$ with*

$$\frac{\partial \boldsymbol{\xi}}{\partial t}(\gamma, t) = \boldsymbol{f} \left(\boldsymbol{\xi}(\gamma, t), \boldsymbol{w}(t) \right).$$

3. *The partial derivative $\frac{\partial \boldsymbol{\xi}}{\partial \gamma}$ exists at each $(\gamma, t) \in I_\gamma \times I_t$ and is continuous so that at each $(\gamma, t) \in I_\gamma \times (I_t \backslash E_{\boldsymbol{w}})$ it satisfies the differential equation*

$$\frac{\partial}{\partial t} \left(\frac{\partial \boldsymbol{\xi}}{\partial \gamma} \right) (\gamma, t) = \frac{\partial \boldsymbol{f}}{\partial \boldsymbol{x}} \left(\boldsymbol{\xi}(\gamma, t), \boldsymbol{w}(t) \right) \frac{\partial \boldsymbol{\xi}}{\partial \gamma}(\gamma, t). \qquad (A.3.5)$$

Finally, let $\Phi : I_\gamma \times I_t^2 \to \mathbb{R}^{n \times n}, (\gamma, t, t_0) \to \Phi(\gamma, t, t_0)$ denote the matrix-valued function with $\Phi(\gamma, ., .)$ being the transition matrix function generated by $\frac{\partial \boldsymbol{f}}{\partial \boldsymbol{x}} \left(\boldsymbol{\xi}(\gamma, .), \boldsymbol{w}(.) \right)$ so that we have

$$\frac{\partial \boldsymbol{\xi}}{\partial \gamma}(\gamma, t_2) = \Phi(\gamma, t_2, t_1) \frac{\partial \boldsymbol{\xi}}{\partial \gamma}(\gamma, t_1), \qquad (A.3.6)$$

for each $(\gamma, t_2, t_1) \in I_\gamma \times I_t^2$. *Then, the partial derivative* $\frac{\partial \Phi}{\partial \gamma} : I_\gamma \times I_t^2 \to \mathbb{R}^{n \times n}$ *exists at each* $(\gamma, t_0, t) \in I_\gamma \times I_t^2$ *and is given by the continuous function*

$$\frac{\partial \Phi}{\partial \gamma}(\gamma, t, t_0) = \int_{t_0}^{t} \Phi(\gamma, t, s) \begin{pmatrix} \left(\frac{\partial \boldsymbol{\xi}}{\partial \gamma}(\gamma, s)\right)^T \frac{\partial^2 f_1}{\partial \boldsymbol{x}^2}(\boldsymbol{\xi}(\gamma, s), \boldsymbol{w}(s)) \\ \vdots \\ \left(\frac{\partial \boldsymbol{\xi}}{\partial \gamma}(\gamma, s)\right)^T \frac{\partial^2 f_n}{\partial \boldsymbol{x}^2}(\boldsymbol{\xi}(\gamma, s), \boldsymbol{w}(s)) \end{pmatrix} \Phi(\gamma, s, t_0) \mathrm{d}s.$$

(A.3.7)

Proof. Let $\Sigma, \boldsymbol{w}, E_{\boldsymbol{w}}, \boldsymbol{\xi}, I_\gamma, I_t$ and Φ satisfy the hypothesis of the lemma. Notice that the fact that (A.3.5) holds has been already established in Lemma 36. To prove the current lemma, we will first show the existence of the partial derivative $\frac{\partial \Phi}{\partial \gamma}$ by making use of Lemma 35. Then, we will use Leibniz rule to show the truth of (A.3.7).

For each $k \in \{1, \ldots, n\}$, introduce the column vector $\boldsymbol{e}_k = \begin{pmatrix} e_{k,1} & \cdots & e_{k,n} \end{pmatrix}^T$ given by

$$(\forall j \in \{1, \ldots, n\}) \left[e_{k,j} = \begin{cases} 0 & j \neq k \\ 1 & j = k \end{cases} \right].$$

Moreover, let $\tilde{\mathbb{X}} = \mathbb{X} \times I_\gamma$ and introduce the function $\boldsymbol{g} : \tilde{\mathbb{X}} \times I_t \to \mathbb{R}^{n+1}$ with

$$\boldsymbol{g}(\tilde{\boldsymbol{x}}, t) = \begin{pmatrix} g_1(\tilde{\boldsymbol{x}}, t) \\ \vdots \\ g_n(\tilde{\boldsymbol{x}}, t) \\ g_{n+1}(\tilde{\boldsymbol{x}}, t) \end{pmatrix} = \begin{pmatrix} \frac{\partial \boldsymbol{f}}{\partial \boldsymbol{x}}(\boldsymbol{\xi}(\tilde{x}_{n+1}, t), \boldsymbol{w}(t)) \begin{pmatrix} \tilde{x}_1 \\ \vdots \\ \tilde{x}_n \end{pmatrix} \\ 0 \end{pmatrix}, \qquad (A.3.8)$$

where $\tilde{\boldsymbol{x}} = \begin{pmatrix} \tilde{x}_1 & \cdots & \tilde{x}_{n+1} \end{pmatrix}^T$. Finally, let $\boldsymbol{\chi_w} : \mathrm{dom}(\boldsymbol{\chi_w}) \to \tilde{\mathbb{X}}$ denote the transition map such that for each $(t_0, \tilde{\boldsymbol{y}}_0) \in I_t \times \tilde{\mathbb{X}}$, the function $\boldsymbol{\chi_w}(., t_0, \tilde{\boldsymbol{y}}_0)$ provides the maximal solution $\tilde{\boldsymbol{y}} : D_{\boldsymbol{w}}(t_0, \tilde{\boldsymbol{y}}_0) \to \tilde{\mathbb{X}}$ to the initial value problem

$$\dot{\tilde{\boldsymbol{y}}}(t) = \boldsymbol{g}(\tilde{\boldsymbol{y}}(t), t), \ \tilde{\boldsymbol{y}}(0) = \tilde{\boldsymbol{y}}_0 \in \tilde{\mathbb{X}}, \ t_0 \in I_t. \qquad (A.3.9)$$

A closer look at (A.3.8) shows then that $D_{\boldsymbol{w}}(t_0, \tilde{\boldsymbol{y}}_0)$ must always be equal to I_t since the $n+1$'th state remains constant and the remaining n states satisfy a linear differential equation. Consequently, we have $\mathrm{dom}(\boldsymbol{\chi_w}) = I_t^2 \times \tilde{\mathbb{X}}$.

Let us now choose an arbitrary integer $k \in \{1, \ldots, n\}$ and a parameter $\gamma \in I_\gamma$. Evaluating the transition map $\boldsymbol{\chi_w}$ at an arbitrary pair of times $(t, t_0) \in I_t^2$ and at the initial state $\tilde{\boldsymbol{y}}_0 = \begin{pmatrix} \boldsymbol{e}_k^T & \gamma \end{pmatrix}^T$, we have then according to (A.3.5)-(A.3.6) and (A.3.8)-(A.3.9)

$$\boldsymbol{\chi_w}\left(t, t_0, \begin{pmatrix} \boldsymbol{e}_k \\ \gamma \end{pmatrix}\right) = \begin{pmatrix} \Phi(\gamma, t, t_0) \boldsymbol{e}_k \\ \gamma \end{pmatrix}. \qquad (A.3.10)$$

Since our choice for k was arbitrary, this shows that each column of Φ can be related to the first n elements of the transition map $\boldsymbol{\chi_w}$ if t_0 and $\tilde{\boldsymbol{y}}_0$ are

appropriately chosen. It is important to notice here that by assumption (B5) the partial derivative of $\boldsymbol{g}$ with respect to its first argument is described by a continuous function $\frac{\partial \boldsymbol{g}}{\partial \tilde{\boldsymbol{x}}} : \mathbb{X} \times I_t \to \mathbb{R}^{(n+1) \times (n+1)}$. Since $\boldsymbol{w}$ has a finite number of discontinuities in I_t, this in turn means that $\boldsymbol{g}$ is locally Lipschitz with respect to its first argument and that the transition map $\boldsymbol{\chi}_{\boldsymbol{w}}$ is continuously differentiable with respect to the initial state $\tilde{\boldsymbol{y}}_0$, see Lemma 35. This finally implies by (A.3.10) that the partial derivative of Φ with respect to γ always exists and is described by a continuous function which we denote by $\frac{\partial \Phi}{\partial \gamma} : I_\gamma \times I_t^2 \to \mathbb{R}^{n \times n}$. We will next show how to derive an expression for this function in terms of $\boldsymbol{\xi}, \boldsymbol{f}$ and Φ.

As we can see from our discussion above, for each given $(\gamma, t_0) \in I_\gamma \times I_t$ the columns of the transition matrix $\Phi(\gamma, ., t_0)$ solve the linear differential equation given by (A.3.5), see (A.3.8)-(A.3.10). Consequently, by integrating this equation and making use of the different initial states described by the vectors $\boldsymbol{e}_k$, with $k \in \{1, \dots, n\}$, we can see that for each $(\gamma, t, t_0) \in I_\gamma \times I_t^2$ we have

$$\Phi(\gamma, t, t_0) = \boldsymbol{I}_d + \int_{t_0}^t \frac{\partial \boldsymbol{f}}{\partial \boldsymbol{x}} \left(\boldsymbol{\xi}(\gamma, s), \boldsymbol{w}(s) \right) \Phi(\gamma, s, t_0) \mathrm{d}s.$$

Since the product in the above integral is continuously differentiable with respect to γ at each $(\gamma, s, t_0) \in I_\gamma \times (I_t \backslash E_{\boldsymbol{w}}) \times I_t$ and since $I_t \cap E_{\boldsymbol{w}}$ is finite, we can then apply Leibniz rule to obtain the following relation:

$$\frac{\partial \Phi}{\partial \gamma}(\gamma, t, t_0) = \int_{t_0}^t \begin{pmatrix} \left(\frac{\partial \boldsymbol{\xi}}{\partial \gamma}(\gamma, s) \right)^T \frac{\partial^2 f_1}{\partial \boldsymbol{x}^2} \left(\boldsymbol{\xi}(\gamma, s), \boldsymbol{w}(s) \right) \\ \vdots \\ \left(\frac{\partial \boldsymbol{\xi}}{\partial \gamma}(\gamma, s) \right)^T \frac{\partial^2 f_n}{\partial \boldsymbol{x}^2} \left(\boldsymbol{\xi}(\gamma, s), \boldsymbol{w}(s) \right) \end{pmatrix} \Phi(\gamma, s, t_0) \mathrm{d}s$$
$$+ \int_{t_0}^t \frac{\partial \boldsymbol{f}}{\partial \boldsymbol{x}} \left(\boldsymbol{\xi}(\gamma, s), \boldsymbol{w}(s) \right) \frac{\partial \Phi}{\partial \gamma}(\gamma, s, t_0) \mathrm{d}s, \qquad (A.3.11)$$

where $(\gamma, t, t_0) \in I_\gamma \times I_t^2$. Differentiating the expression above with respect to time, we can now see that $\frac{\partial \Phi}{\partial \gamma}(\gamma, ., t_0)$ solves an inhomogeneous linear differential equation with the boundary condition $\frac{\partial \Phi}{\partial \gamma}(\gamma, t_0, t_0) = \boldsymbol{0}$. Furthermore, the solution to this differential equation can be explicitly described using the transition matrix function $\Phi(\gamma, ., .)$ generated by $\frac{\partial \boldsymbol{f}}{\partial \boldsymbol{x}}(\boldsymbol{\xi}(\gamma, .), \boldsymbol{w}(.))$ and this finally leads to the equality (A.3.7), as desired[5]. $\qquad \square$

Making use of Lemma 38 we can finally extend PMP as follows.

Theorem 39. *(Second Order Minimum Principle) Let Σ be a control system satisfying assumptions (B1)-(B5), and $(\boldsymbol{x}, \boldsymbol{u})$ an admissible controlled trajectory which is defined on $D = [0, t_f]$. Moreover, assume that the control $\boldsymbol{u}$ solves the GOCP with the final time $t_f > 0$, the initial state $\boldsymbol{x}_0 \in \mathbb{X}$ and the two-times*

---

[5]See for instance Theorem 2.15 in [34] for the description of solutions to inhomogeneous linear differential equations in terms of transition matrix functions.

continuously differentiable function $\mathcal{V} : \mathbb{X} \to \mathbb{R}$. *In addition, let* $\boldsymbol{\lambda} : D \to (\mathbb{R}^n)^*$ *be the piecewise continuously differentiable function which solves the initial value problem*

$$\dot{\boldsymbol{\lambda}}(t) = -\boldsymbol{\lambda}(t)\frac{\partial \boldsymbol{f}}{\partial \boldsymbol{x}}\left(\boldsymbol{x}(t), \boldsymbol{u}(t)\right), \tag{A.3.12}$$

with the boundary condition

$$\boldsymbol{\lambda}(t_f) = \frac{\partial \mathcal{V}}{\partial \boldsymbol{x}}\left(\boldsymbol{x}(t_f)\right). \tag{A.3.13}$$

Furthermore, let $\boldsymbol{\mu}_s : D \times D \to \mathbb{R}^n, (t_\beta, t) \to \boldsymbol{\mu}_s(t_\beta, t)$ *be the variational vector solving the initial value problem*

$$\frac{\partial \boldsymbol{\mu}_s}{\partial t}(t_\beta, t) = \frac{\partial \boldsymbol{f}}{\partial \boldsymbol{x}}\left(\boldsymbol{x}(t), \boldsymbol{u}(t)\right)\boldsymbol{\mu}_s(t_\beta, t),$$

with the boundary condition

$$\boldsymbol{\mu}_s(t_\beta, t_\beta) = -\boldsymbol{f}\left(\boldsymbol{x}(t_\beta), \boldsymbol{u}(t_\beta)\right),$$

and $\boldsymbol{\mu}_{s,f} : D \to \mathbb{R}^n$ *the function given by*

$$\boldsymbol{\mu}_{s,f}(t_\beta) = \boldsymbol{\mu}_s(t_\beta, t_f) + \boldsymbol{f}\left(\boldsymbol{x}(t_f), \boldsymbol{u}(t_f)\right).$$

Similarly, let $\boldsymbol{\mu}_c : D \times \mathbb{U} \times D \to \mathbb{R}^n, (t_\alpha, \boldsymbol{v}, t) \to \boldsymbol{\mu}_c(t_\alpha, \boldsymbol{v}, t)$ *be the variational vector solving the initial value problem*

$$\frac{\partial \boldsymbol{\mu}_c}{\partial t}(t_\alpha, \boldsymbol{v}, t) = \frac{\partial \boldsymbol{f}}{\partial \boldsymbol{x}}\left(\boldsymbol{x}(t), \boldsymbol{u}(t)\right)\boldsymbol{\mu}_c(t_\alpha, \boldsymbol{v}, t),$$

with the boundary condition

$$\boldsymbol{\mu}_c(t_\alpha, \boldsymbol{v}, t_\alpha) = \boldsymbol{f}\left(\boldsymbol{x}(t_\alpha), \boldsymbol{v}\right) - \boldsymbol{f}\left(\boldsymbol{x}(t_\alpha), \boldsymbol{u}(t_\alpha)\right).$$

Finally, let $\mathbb{H} : \mathbb{X} \times \mathbb{U} \times (\mathbb{R}^n)^* \to \mathbb{R}$ *denote the Hamiltonian function given by (A.2.4) and* $E_\mathbb{H} : \mathbb{U} \rightrightarrows D$ *the set-valued function given by*

$$E_\mathbb{H}(\boldsymbol{v}) = \{t \in [0, t_f] | \mathbb{H}\left(\boldsymbol{x}(t), \boldsymbol{u}(t), \boldsymbol{\lambda}(t)\right) = \mathbb{H}\left(\boldsymbol{x}(t), \boldsymbol{v}, \boldsymbol{\lambda}(t)\right)\}. \tag{A.3.14}$$

Then, the following four conditions hold.

1. *First Minimum Condition: For each* $t \in D$, *we have*

$$\mathbb{H}\left(\boldsymbol{x}(t), \boldsymbol{u}(t), \boldsymbol{\lambda}(t)\right) = \min_{\boldsymbol{v} \in \mathbb{U}} \mathbb{H}\left(\boldsymbol{x}(t), \boldsymbol{v}, \boldsymbol{\lambda}(t)\right). \tag{A.3.15}$$

2. *Second Minimum Condition: For each* $\boldsymbol{v} \in \mathbb{U}$ *and each* $t_\alpha \in E_\mathbb{H}(\boldsymbol{v})$ *we have*

$$\int_{t_\alpha}^{t_f} \boldsymbol{\mu}_c^T(t_\alpha, \boldsymbol{v}, s)\frac{\partial^2 \mathbb{H}}{\partial \boldsymbol{x}^2}\left(\boldsymbol{x}(s), \boldsymbol{u}(s), \boldsymbol{\lambda}(s)\right)\boldsymbol{\mu}_c(t_\alpha, \boldsymbol{v}, s)\mathrm{d}s +$$

$$\boldsymbol{\mu}_c^T(t_\alpha, \boldsymbol{v}, t_f)\frac{\partial^2 \mathcal{V}}{\partial \boldsymbol{x}^2}\left(\boldsymbol{x}(t_f)\right)\boldsymbol{\mu}_c(t_\alpha, \boldsymbol{v}, t_f) +$$

$$\boldsymbol{\lambda}(t_\alpha)\left[\frac{\partial \boldsymbol{f}}{\partial \boldsymbol{x}}\left(\boldsymbol{x}(t_\alpha), \boldsymbol{v}\right) - 2\frac{\partial \boldsymbol{f}}{\partial \boldsymbol{x}}\left(\boldsymbol{x}(t_\alpha), \boldsymbol{u}(t_\alpha)\right)\right]\boldsymbol{f}\left(\boldsymbol{x}(t_\alpha), \boldsymbol{v}\right) +$$

$$\boldsymbol{\lambda}(t_\alpha)\frac{\partial \boldsymbol{f}}{\partial \boldsymbol{x}}\left(\boldsymbol{x}(t_\alpha), \boldsymbol{u}(t_\alpha)\right)\boldsymbol{f}\left(\boldsymbol{x}(t_\alpha), \boldsymbol{u}(t_\alpha)\right) \geq 0. \tag{A.3.16}$$

3. *First Hamiltonian Condition: For each $t \in D$, we have*

$$\mathbb{H}\left(\boldsymbol{x}(t), \boldsymbol{u}(t), \boldsymbol{\lambda}(t)\right) = -\lambda_a, \qquad (A.3.17)$$

where $\lambda_a \in \mathbb{R}$ is a constant scalar.

4. *Second Hamiltonian Condition: For each $t_\beta \in D$, we have*

$$\int_{t_\beta}^{t_f} \boldsymbol{\mu}_s^T(t_\beta, s) \frac{\partial^2 \mathbb{H}}{\partial \boldsymbol{x}^2}\left(\boldsymbol{x}(s), \boldsymbol{u}(s), \boldsymbol{\lambda}(s)\right) \boldsymbol{\mu}_s(t_\beta, s)\mathrm{d}s +$$

$$\boldsymbol{\mu}_{s,f}^T(t_\beta) \frac{\partial^2 \mathcal{V}}{\partial \boldsymbol{x}^2}\left(\boldsymbol{x}(t_f)\right) \boldsymbol{\mu}_{s,f}(t_\beta) +$$

$$\boldsymbol{\lambda}(t_f)\left[\frac{\partial \boldsymbol{f}}{\partial \boldsymbol{x}}\left(\boldsymbol{x}(t_f), \boldsymbol{u}(t_f)\right) + \frac{\partial \boldsymbol{f}}{\partial \boldsymbol{x}}\left(\boldsymbol{x}(t_\beta), \boldsymbol{u}(t_\beta)\right)\right] \boldsymbol{\mu}_s(t_\beta, t_f) +$$

$$\boldsymbol{\lambda}(t_\beta)\frac{\partial \boldsymbol{f}}{\partial \boldsymbol{x}}\left(\boldsymbol{x}(t_\beta), \boldsymbol{u}(t_\beta)\right) \boldsymbol{f}\left(\boldsymbol{x}(t_\beta), \boldsymbol{u}(t_\beta)\right) +$$

$$\boldsymbol{\lambda}(t_f)\frac{\partial \boldsymbol{f}}{\partial \boldsymbol{x}}\left(\boldsymbol{x}(t_f), \boldsymbol{u}(t_f)\right) \boldsymbol{f}\left(\boldsymbol{x}(t_f), \boldsymbol{u}(t_f)\right) \geq 0. \quad (A.3.18)$$

Proof. Let $\Sigma, (\boldsymbol{x}, \boldsymbol{u}), D, \mathcal{V}, \boldsymbol{\lambda}, \boldsymbol{\mu}_s, \boldsymbol{\mu}_{s,f}, \boldsymbol{\mu}_c, \mathbb{H}$ and $E_\mathbb{H}$ satisfy the hypotheses of the theorem. Moreover, let $E \subset D$ denote the finite set of times at which $\boldsymbol{u}$ is not continuous. According to Theorem 37, there exists then a costate $\tilde{\boldsymbol{\lambda}} : D \to (\mathbb{R}^n)^*$ which solves the initial value problem (A.3.12) with the boundary condition

$$\tilde{\boldsymbol{\lambda}}(t_f) = v\frac{\partial \mathcal{V}}{\partial \boldsymbol{x}}\left(\boldsymbol{x}(t_f)\right),$$

where $v > 0$ is a positive scalar. Moreover, according to (A.2.3) and (A.2.5) we have for each $t \in D$

$$\mathbb{H}\left(\boldsymbol{x}(t), \boldsymbol{u}(t), \tilde{\boldsymbol{\lambda}}(t)\right) = \min_{\boldsymbol{v} \in \mathbb{U}} \mathbb{H}\left(\boldsymbol{x}(t), \boldsymbol{v}, \tilde{\boldsymbol{\lambda}}(t)\right) = -\tilde{\lambda}_a, \qquad (A.3.19)$$

where $\tilde{\lambda}_a \in \{-1, 0, 1\}$ is a constant scalar. Notice that due to the linearity of the differential equation in (A.3.12) and the boundary condition (A.3.13), we have the equality $\boldsymbol{\lambda} = \frac{1}{v}\tilde{\boldsymbol{\lambda}}$. Consequently, by (A.3.19), the linearity of the Hamiltonian function $\mathbb{H}$ in its third argument and the positivity of v, the two conditions (A.3.15) and (A.3.17) both hold for each $t \in D$ if we set $\lambda_a = \frac{\tilde{\lambda}_a}{v} \in \mathbb{R}$. To conclude the proof, we will next derive, in two steps, the remaining conditions (A.3.16) and (A.3.18).

1. *Proving the Second Minimum Condition*

We will first show that the inequality in (A.3.16) must hold for each $\boldsymbol{v} \in \mathbb{U}$ and each $t_\alpha \in E_\mathbb{H}(\boldsymbol{v})$. For this, let $\boldsymbol{v}$ be an arbitrary element of $\mathbb{U}$ and t_α an element of the set $E_\mathbb{H}(\boldsymbol{v})$. Moreover, assume first that the control $\boldsymbol{u}$ is continuous at t_α, i.e. $t_\alpha \notin E$. Following the second step of the proof of Theorem 37, we can then construct, using (A.2.23), the function $\boldsymbol{\xi}_c : I_{\boldsymbol{w}} \times (-\delta_{\boldsymbol{w}}, t_f + \delta_{\boldsymbol{w}}) \to \mathbb{X}$ for which

the inequality (A.2.48) must hold if $(\boldsymbol{x}, \boldsymbol{u})$ is an optimally controlled trajectory. Based on this last inequality, let us introduce the continuously differentiable function $g_c : I_{\boldsymbol{w}} \to \mathbb{R}$ with

$$g_c(\alpha) = \int_{t_\alpha}^{\alpha} \frac{\partial \mathcal{V}}{\partial \boldsymbol{x}} \left(\boldsymbol{\xi}_c(s, t_f)\right) \frac{\partial \boldsymbol{\xi}_c}{\partial \alpha}(s, t_f) \mathrm{d}s. \tag{A.3.20}$$

According to (A.2.32)-(A.2.34), the derivative $\frac{\mathrm{d}g_c}{\mathrm{d}\alpha} : I_{\boldsymbol{w}} \to \mathbb{R}$ of this function is then given by

$$\begin{aligned} \frac{\mathrm{d}g_c}{\mathrm{d}\alpha}(\alpha) &= \frac{\partial \mathcal{V}}{\partial \boldsymbol{x}} \left(\boldsymbol{\xi}_c(\alpha, t_f)\right) \frac{\partial \boldsymbol{\xi}_c}{\partial \alpha}(\alpha, t_f) \\ &= \frac{\partial \mathcal{V}}{\partial \boldsymbol{x}} \left(\boldsymbol{\xi}_c(\alpha, t_f)\right) \Phi_c(\alpha, t_f, \alpha) \frac{\partial \boldsymbol{\xi}_c}{\partial \alpha}(\alpha, \alpha), \end{aligned} \tag{A.3.21}$$

where

$$\frac{\partial \boldsymbol{\xi}_c}{\partial \alpha}(\alpha, \alpha) = \boldsymbol{f}\left(\boldsymbol{\xi}_c(\alpha, \alpha), \boldsymbol{v}\right) - \boldsymbol{f}\left(\boldsymbol{\xi}_c(\alpha, \alpha), \boldsymbol{u}_{ex}(\alpha)\right). \tag{A.3.22}$$

Moreover, by construction we have for each $t \in D$

$$\boldsymbol{x}(t) = \boldsymbol{\xi}_c(t_\alpha, t) \wedge \boldsymbol{\lambda}(t) = \frac{\partial \mathcal{V}}{\partial \boldsymbol{x}} \left(\boldsymbol{\xi}_c(t_\alpha, t_f)\right) \Phi_c(t_\alpha, t_f, t). \tag{A.3.23}$$

Now, since $t_\alpha \in E_{\mathbb{H}}(\boldsymbol{v})$ it follows from (A.3.14) and (A.3.21)-(A.3.23) that the derivative $\frac{\mathrm{d}g_c}{\mathrm{d}\alpha}$ is equal to zero at $\alpha = t_\alpha$, i.e. $\frac{\mathrm{d}g_c}{\mathrm{d}\alpha}(t_\alpha) = 0$. Consequently, provided that g_c is two times differentiable at $\alpha = t_\alpha$ the condition (A.2.48) implies the following second-order condition:

$$\frac{\mathrm{d}^2 g_c}{\mathrm{d}\alpha^2}(t_\alpha) \geq 0. \tag{A.3.24}$$

In the following, we will make use of the Hamiltonian Condition (A.3.17), Lemma 38 and properties of transition matrix functions to show that the derivative in (A.3.24) indeed exists. This will also directly lead to the condition in (A.3.16).

In order to show that the derivative $\frac{\mathrm{d}^2 g_c}{\mathrm{d}\alpha^2}$ exists at $\alpha = t_\alpha$, we need to show that the limit $\lim_{h \to 0} \frac{\frac{\mathrm{d}g_c}{\mathrm{d}\alpha}(t_\alpha + h) - \frac{\mathrm{d}g_c}{\mathrm{d}\alpha}(t_\alpha)}{h}$ exists. For this, notice first that for each $t \in (-\delta_{\boldsymbol{w}}, t_f + \delta_{\boldsymbol{w}})$ we have

$$\frac{\partial \mathcal{V}}{\partial \boldsymbol{x}} \left(\boldsymbol{\xi}_c(t_\alpha, t_f)\right) \Phi_c(t_\alpha, t_f, t) \boldsymbol{f}\left(\boldsymbol{\xi}_c(t_\alpha, t), \boldsymbol{u}_{ex}(t)\right) = -\lambda_a. \tag{A.3.25}$$

Indeed, for $t \in D$ this follows directly from the Hamiltonian Condition (A.3.17). For $t \in (-\delta_{\boldsymbol{w}}, 0)$ and $t \in (t_f, t_f + \delta_{\boldsymbol{w}})$, on the other hand, it follows from the fact that $\boldsymbol{u}_{ex}$ remains constant on these intervals with $\boldsymbol{u}_{ex}(t) = \boldsymbol{u}(0)$ and $\boldsymbol{u}_{ex}(t) = \boldsymbol{u}(t_f)$, respectively. More specifically, taking the time-derivative of the left-hand side of (A.3.25) it can be seen that this term must remain constant

in these intervals. The provided equality follows then from the fact that the left-hand side of (A.3.25) must be continuous at $t = 0$ and $t = t_f$.

Let now $I_{c,h}$ denote the set $(-\delta_{\boldsymbol{w}}, \delta_{\boldsymbol{w}})$ and introduce the six real-valued continuous functions $K_{c,1}, K_{c,2}, K_{c,3}, K_{c,4}, K_{c,5}$ and $K_{c,6}$ defined on $I_{c,h}$ with

$$K_{c,1}(h) = \frac{\partial \mathcal{V}}{\partial \boldsymbol{x}} \left(\boldsymbol{\xi}_c(t_\alpha + h, t_f) \right) \Phi_c(t_\alpha + h, t_f, t_\alpha + h),$$

$$K_{c,2}(h) = \frac{\partial \mathcal{V}}{\partial \boldsymbol{x}} \left(\boldsymbol{\xi}_c(t_\alpha, t_f) \right) \Phi_c(t_\alpha, t_f, t_\alpha + h),$$

$$K_{c,3}(h) = \frac{\partial \boldsymbol{\xi}_c}{\partial \alpha}(t_\alpha + h, t_\alpha + h),$$

$$K_{c,4}(h) = \boldsymbol{f} \left(\boldsymbol{\xi}_c(t_\alpha + h, t_\alpha + h), \boldsymbol{v} \right),$$

$$K_{c,5}(h) = \boldsymbol{f} \left(\boldsymbol{\xi}_c(t_\alpha + h, t_\alpha + h), \boldsymbol{u}_{ex}(t_\alpha + h) \right),$$

and

$$K_{c,6}(h) = \boldsymbol{f} \left(\boldsymbol{\xi}_c(t_\alpha, t_\alpha + h), \boldsymbol{u}_{ex}(t_\alpha + h) \right).$$

According to (A.3.25), we have then by definition

$$(\forall h \in I_{c,h}) \left[K_{c,2}(h) K_{c,6}(h) = K_{c,1}(0) K_{c,5}(0) \right]. \tag{A.3.26}$$

Noting that we also have the equality $K_{c,1}(0) = K_{c,2}(0)$ and $K_{c,3}(h) = K_{c,4}(h) - K_{c,5}(h)$, we obtain the following expression for the desired limit:

$$
\begin{aligned}
\lim_{h \to 0} \frac{\frac{\mathrm{d}g_c}{\mathrm{d}\alpha}(t_\alpha + h) - \frac{\mathrm{d}g_c}{\mathrm{d}\alpha}(t_\alpha)}{h} &= \lim_{h \to 0} \frac{K_{c,1}(h) K_{c,3}(h) - K_{c,1}(0) K_{c,3}(0)}{h} \\
&= \lim_{h \to 0} \left[\frac{K_{c,1}(h) - K_{c,1}(0)}{h} K_{c,3}(h) \right. \\
&\quad \left. + K_{c,1}(0) \frac{K_{c,3}(h) - K_{c,3}(0)}{h} \right] \\
&= \lim_{h \to 0} \left[\frac{K_{c,1}(h) - K_{c,1}(0)}{h} K_{c,3}(h) \right. \\
&\quad \left. + K_{c,1}(0) \frac{K_{c,4}(h) - K_{c,4}(0)}{h} + K_{c,1}(0) \frac{K_{c,5}(0) - K_{c,5}(h)}{h} \right] \\
&= \lim_{h \to 0} \left[\frac{K_{c,1}(h) - K_{c,1}(0)}{h} K_{c,3}(h) \right. \\
&\quad + K_{c,1}(0) \frac{K_{c,4}(h) - K_{c,4}(0)}{h} + K_{c,2}(h) \frac{K_{c,6}(h) - K_{c,5}(h)}{h} \\
&\quad \left. + \frac{K_{c,2}(h) - K_{c,2}(0)}{h} K_{c,5}(h) \right]. \tag{A.3.27}
\end{aligned}
$$

By the smoothness properties of $\boldsymbol{\xi}_c, \Phi_c, \boldsymbol{f}$ and $\mathcal{V}$, we can take the limit of each of the four terms in the last equality as $h \to 0$. More specifically, for the first

term we have

$$
\lim_{h\to 0} \frac{K_{c,1}(h) - K_{c,1}(0)}{h} K_{c,3}(h) = \frac{\partial \boldsymbol{\xi}_c}{\partial \alpha}^T (t_\alpha, t_f) \frac{\partial^2 \mathcal{V}}{\partial \boldsymbol{x}^2} \left(\boldsymbol{x}(t_f) \right) \Phi_c(t_\alpha, t_f, t_\alpha) K_{c,3}(0)
$$
$$
+ \frac{\partial \mathcal{V}}{\partial \boldsymbol{x}} \left(\boldsymbol{x}(t_f) \right) \frac{\partial \Phi_c}{\partial \alpha}(t_\alpha, t_f, t_\alpha) K_{c,3}(0)
$$
$$
+ \frac{\partial \mathcal{V}}{\partial \boldsymbol{x}} \left(\boldsymbol{x}(t_f) \right) \frac{\partial \Phi_c}{\partial t_0}(t_\alpha, t_f, t_\alpha) K_{c,3}(0)
$$
$$
= \frac{\partial \boldsymbol{\xi}_c}{\partial \alpha}^T (t_\alpha, t_f) \frac{\partial^2 \mathcal{V}}{\partial \boldsymbol{x}^2} \left(\boldsymbol{x}(t_f) \right) \frac{\partial \boldsymbol{\xi}_c}{\partial \alpha}(t_\alpha, t_f)
$$
$$
+ \int_{t_\alpha}^{t_f} \boldsymbol{\lambda}(s) \begin{pmatrix} \left(\frac{\partial \boldsymbol{\xi}_c}{\partial \alpha}(\alpha, s) \right)^T \frac{\partial^2 f_1}{\partial \boldsymbol{x}^2} \left(\boldsymbol{\xi}(\alpha, s), \boldsymbol{u}_{ex}(s) \right) \frac{\partial \boldsymbol{\xi}_c}{\partial \alpha}(t_\alpha, s) \\ \vdots \\ \left(\frac{\partial \boldsymbol{\xi}_c}{\partial \alpha}(\alpha, s) \right)^T \frac{\partial^2 f_n}{\partial \boldsymbol{x}^2} \left(\boldsymbol{\xi}(\alpha, s), \boldsymbol{u}_{ex}(s) \right) \frac{\partial \boldsymbol{\xi}_c}{\partial \alpha}(t_\alpha, s) \end{pmatrix} \mathrm{d}s
$$
$$
- \boldsymbol{\lambda}(t_\alpha) \frac{\partial \boldsymbol{f}}{\partial \boldsymbol{x}} \left(\boldsymbol{x}(t_\alpha), \boldsymbol{u}_{ex}(t_\alpha) \right) \frac{\partial \boldsymbol{\xi}_c}{\partial \alpha}(t_\alpha, t_\alpha), \tag{A.3.28}
$$

where we have used of Lemma 38 when computing the partial derivative of Φ_c with respect to its first argument. Similarly, for the other three terms we have

$$
\lim_{h\to 0} K_{c,1}(0) \frac{K_{c,4}(h) - K_{c,4}(0)}{h} = \frac{\partial \mathcal{V}}{\partial \boldsymbol{x}} \left(\boldsymbol{x}(t_f) \right) \Phi_c(t_\alpha, t_f, t_\alpha) \frac{\partial \boldsymbol{f}}{\partial \boldsymbol{x}} \left(\boldsymbol{x}(t_\alpha), \boldsymbol{v} \right) \frac{\partial \boldsymbol{\xi}_c}{\partial \alpha}(t_\alpha, t_\alpha)
$$
$$
+ \frac{\partial \mathcal{V}}{\partial \boldsymbol{x}} \left(\boldsymbol{x}(t_f) \right) \Phi_c(t_\alpha, t_f, t_\alpha) \frac{\partial \boldsymbol{f}}{\partial \boldsymbol{x}} \left(\boldsymbol{x}(t_\alpha), \boldsymbol{v} \right) \frac{\partial \boldsymbol{\xi}_c}{\partial t}(t_\alpha, t_\alpha)
$$
$$
= \boldsymbol{\lambda}(t_\alpha) \frac{\partial \boldsymbol{f}}{\partial \boldsymbol{x}} \left(\boldsymbol{x}(t_\alpha), \boldsymbol{v} \right) \frac{\partial \boldsymbol{\xi}_c}{\partial \alpha}(t_\alpha, t_\alpha)
$$
$$
+ \boldsymbol{\lambda}(t_\alpha) \frac{\partial \boldsymbol{f}}{\partial \boldsymbol{x}} \left(\boldsymbol{x}(t_\alpha), \boldsymbol{v} \right) \boldsymbol{f} \left(\boldsymbol{x}(t_\alpha), \boldsymbol{u}_{ex}(t_\alpha) \right), \tag{A.3.29}
$$

$$
\lim_{h\to 0} K_{c,2}(h) \frac{K_{c,6}(h) - K_{c,5}(h)}{h} = -\frac{\partial \mathcal{V}}{\partial \boldsymbol{x}} \left(\boldsymbol{x}(t_f) \right) \Phi_c(t_\alpha, t_f, t_\alpha) \cdot
$$
$$
\frac{\partial \boldsymbol{f}}{\partial \boldsymbol{x}} \left(\boldsymbol{x}(t_\alpha), \boldsymbol{u}_{ex}(t_\alpha) \right) \frac{\partial \boldsymbol{\xi}_c}{\partial \alpha}(t_\alpha, t_\alpha)
$$
$$
= -\boldsymbol{\lambda}(t_\alpha) \frac{\partial \boldsymbol{f}}{\partial \boldsymbol{x}} \left(\boldsymbol{x}(t_\alpha), \boldsymbol{u}_{ex}(t_\alpha) \right) \frac{\partial \boldsymbol{\xi}_c}{\partial \alpha}(t_\alpha, t_\alpha), \tag{A.3.30}
$$

and

$$
\lim_{h\to 0} \frac{K_{c,2}(h) - K_{c,2}(0)}{h} K_{c,5}(h) = \frac{\partial \mathcal{V}}{\partial \boldsymbol{x}} \left(\boldsymbol{x}(t_f) \right) \frac{\partial \Phi_c}{\partial t_0}(t_\alpha, t_f, t_\alpha) \boldsymbol{f} \left(\boldsymbol{x}(t_\alpha), \boldsymbol{u}_{ex}(t_\alpha) \right),
$$
$$
= -\boldsymbol{\lambda}(t_\alpha) \frac{\partial \boldsymbol{f}}{\partial \boldsymbol{x}} \left(\boldsymbol{x}(t_\alpha), \boldsymbol{u}_{ex}(t_\alpha) \right) \boldsymbol{f} \left(\boldsymbol{x}(t_\alpha), \boldsymbol{u}_{ex}(t_\alpha) \right). \tag{A.3.31}
$$

Summing now all the four limits (A.3.28)-(A.3.31) and taking into account the definition of $\boldsymbol{u}_{ex}$, $\mathbb{H}$ and $\boldsymbol{\mu}_c$, we can see that the condition (A.3.16) is equivalent to (A.3.24). Moreover, since our choice for $t_\alpha \in E_{\mathbb{H}}(\boldsymbol{v}) \backslash E$ was arbitrary, we can conclude that (A.3.16) must hold whenever $\boldsymbol{u}$ is continuous at t_α.

To show that (A.3.16) also holds when $t_\alpha \in E$, we can make use of the fact that $\boldsymbol{u}$ is left-continuous at t_α. More specifically, let us introduce the control strategy $\tilde{\boldsymbol{u}}_{ex,t_\alpha} : \mathbb{R} \to \mathbb{U}$ with

$$
\tilde{\boldsymbol{u}}_{ex,t_\alpha} = \begin{cases} \boldsymbol{u}_{ex}(t_\alpha) & t \in (-\infty, t_\alpha) \\ \boldsymbol{u}_{ex}(t) & t \geq t_\alpha \end{cases} ,
$$

which is clearly continuous at t_α. Noting that the corresponding transition map $\boldsymbol{\psi}_{\tilde{\boldsymbol{u}}_{ex,t_\alpha}}$ will also lead to trajectories of Σ, we can use this map, instead of $\boldsymbol{\psi}_{\boldsymbol{u}_{ex}}$, to construct the parameterized family of controlled trajectories $\boldsymbol{\xi}_c$. Following the steps above, we will then obtain the exactly same condition. Noting finally that our choice for $\boldsymbol{v} \in \mathbb{U}$ was arbitrary, this shows the truth of the Second Minimum Condition.

2. *Proving the Second Hamiltonian Condition*

To conclude the proof of the theorem, we will show that (A.3.18) holds for each $t_\beta \in D$. For this, let us first assume that $t_\beta \in (0, t_f) \backslash E$. Following the first and sixth steps of Theorem 37, we can then construct the functions $\boldsymbol{\xi}_s : I_\beta \times (-\delta_s, t_f + \delta_s) \to \mathbb{X}$ and $\boldsymbol{\xi}_{s,f} : I_{\bar{\beta}} \to \mathbb{X}$, with $I_{\bar{\beta}} = (t_\beta - \bar{\delta}_s, t_\beta + \bar{\delta}_s) \subset I_\beta$, which will in turn lead to the optimality condition (A.2.45). Based on this condition, let us introduce the continuously differentiable function $g_s : I_{\bar{\beta}} \to \mathbb{R}$ with

$$
g_s(\beta) = \int_{t_\beta}^\beta \frac{\partial \mathcal{V}}{\partial \boldsymbol{x}} \left(\boldsymbol{\xi}_{s,f}(s) \right) \frac{\mathrm{d}\boldsymbol{\xi}_{s,f}}{\mathrm{d}\beta}(s) \mathrm{d}s. \tag{A.3.32}
$$

According to (A.2.44), the derivative $\frac{\mathrm{d}g_s}{\mathrm{d}\beta} : I_{\bar{\beta}} \to \mathbb{R}$ of this function is given by

$$
\begin{aligned}
\frac{\mathrm{d}g_s}{\mathrm{d}\beta}(\beta) &= \frac{\partial \mathcal{V}}{\partial \boldsymbol{x}} \left(\boldsymbol{\xi}_{s,f}(s) \right) \frac{\mathrm{d}\boldsymbol{\xi}_{s,f}}{\mathrm{d}\beta}(s) \\
&= \frac{\partial \mathcal{V}}{\partial \boldsymbol{x}} \left(\boldsymbol{\xi}_{s,f}(s) \right) \boldsymbol{f} \left(\boldsymbol{\xi}_s \left(\beta, t_f + \beta - t_\beta \right), \boldsymbol{u}_{ex}(t_f + \beta - t_\beta) \right) \\
&\quad - \frac{\partial \mathcal{V}}{\partial \boldsymbol{x}} \left(\boldsymbol{\xi}_{s,f}(s) \right) \Phi_s(\beta, t_f + \beta - t_\beta, \beta) \boldsymbol{f} \left(\boldsymbol{x}(t_\beta), \boldsymbol{u}_{ex}(\beta) \right), \quad \text{(A.3.33)}
\end{aligned}
$$

and is equal to zero at t_β, see (A.2.46). Consequently, provided that g_s is two times differentiable at this time (A.2.45) implies the following second-order condition:

$$
\frac{\mathrm{d}^2 g_s}{\mathrm{d}\beta^2}(t_\beta) \geq 0. \tag{A.3.34}
$$

We will next show that the derivative in (A.3.34) indeed exists. This will in turn lead to our desired condition (A.3.18).

Notice that by construction we have, as with $\boldsymbol{\xi}_c$ and Φ_c, for each $t \in D$

$$
\boldsymbol{x}(t) = \boldsymbol{\xi}_s(t_\beta, t) \wedge \boldsymbol{\lambda}(t) = \frac{\partial \mathcal{V}}{\partial \boldsymbol{x}} \left(\boldsymbol{\xi}_s(t_\alpha, t_f) \right) \Phi_s(t_\alpha, t_f, t).
$$

Consequently, following the arguments used in the first step of the current proof we get, similar to (A.3.25), the equality

$$\frac{\partial \mathcal{V}}{\partial \boldsymbol{x}}\left(\boldsymbol{\xi}_s(t_\beta, t_f)\right) \Phi_c(t_\beta, t_f, t) \boldsymbol{f}\left(\boldsymbol{\xi}_c(t_\beta, t), \boldsymbol{u}_{ex}(t)\right) = -\lambda_a, \qquad (\text{A.3.35})$$

which holds for each $t \in (-\bar{\delta}_s, t_f + \bar{\delta}_s)$. Let now $I_{s,h}$ denote the set $(-\bar{\delta}_s, \bar{\delta}_s)$ and introduce the six real-valued continuous functions $K_{s,1}, K_{s,2}, K_{s,3}, K_{s,4}, K_{s,5}$ and $K_{s,6}$ defined on $I_{s,h}$ with

$$K_{s,1}(h) = \frac{\partial \mathcal{V}}{\partial \boldsymbol{x}}\left(\boldsymbol{\xi}_{s,f}(t_\beta + h)\right),$$

$$K_{s,2}(h) = \Phi_s(t_\beta + h, t_f + h, t_\beta + h)\boldsymbol{f}\left(\boldsymbol{x}(t_\beta), \boldsymbol{u}_{ex}(t_\beta + h)\right),$$

$$K_{s,3}(h) = \boldsymbol{f}\left(\boldsymbol{\xi}_s(t_\beta + h, t_f + h), \boldsymbol{u}_{ex}(t_f + h)\right),$$

$$K_{s,4}(h) = \Phi_s(t_\beta, t_f, t_\beta + h)\boldsymbol{f}\left(\boldsymbol{\xi}_s(t_\beta, t_\beta + h), \boldsymbol{u}_{ex}(t_\beta + h)\right),$$

$$K_{s,5}(h) = \Phi_s(t_\beta, t_f, t_f + h)\boldsymbol{f}\left(\boldsymbol{\xi}_s(t_\beta, t_f + h), \boldsymbol{u}_{ex}(t_f + h)\right),$$

and

$$K_{s,6}(h) = K_{s,3}(h) - K_{s,2}(h).$$

It follows then from (A.3.35) and our definitions above that we have

$$\begin{aligned} K_{s,1}(0)K_{s,4}(h) = K_{s,1}(0)K_{s,5}(h) = \\ K_{s,1}(0)K_{s,3}(0) = K_{s,1}(0)K_{s,2}(0), \end{aligned} \qquad (\text{A.3.36})$$

for each $h \in I_{s,h}$. Exploiting the relation above, we can then obtain the following expression for the desired limit:

$$\begin{aligned} \lim_{h \to 0} \frac{\frac{\mathrm{d}g_s}{\mathrm{d}\beta}(t_\beta + h) - \frac{\mathrm{d}g_s}{\mathrm{d}\beta}(t_\beta)}{h} &= \lim_{h \to 0} \frac{K_{s,1}(h)K_{s,6}(h) - K_{s,1}(0)K_{s,6}(0)}{h} \\ &= \lim_{h \to 0} \left[\frac{K_{s,1}(h) - K_{s,1}(0)}{h} K_{s,6}(h) \right. \\ &\quad \left. + K_{s,1}(0)\frac{K_{s,6}(h) - K_{s,6}(0)}{h} \right] \\ &= \lim_{h \to 0} \left[\frac{K_{s,1}(h) - K_{s,1}(0)}{h} K_{s,6}(h) \right. \\ &\quad \left. + K_{s,1}(0)\frac{K_{s,3}(h) - K_{s,3}(0)}{h} - K_{s,1}(0)\frac{K_{s,2}(h) - K_{s,2}(0)}{h} \right] \\ &= \lim_{h \to 0} \left[\frac{K_{s,1}(h) - K_{s,1}(0)}{h} K_{s,6}(h) \right. \\ &\quad \left. + K_{s,1}(0)\frac{K_{s,3}(h) - K_{s,5}(h)}{h} - K_{s,1}(0)\frac{K_{s,2}(h) - K_{s,4}(h)}{h} \right]. \end{aligned}$$

$$(\text{A.3.37})$$

By the smoothness properties of $\boldsymbol{\xi}_s, \boldsymbol{\xi}_{s,f}, \Phi_s, \boldsymbol{f}$ and $\mathcal{V}$, we can take the limit of each of the three terms in the last equality as $h \to 0$. Indeed, for the first term we have

$$\lim_{h \to 0} \frac{K_{s,1}(h) - K_{s,1}(0)}{h} K_{s,6}(h) = \frac{\mathrm{d}\boldsymbol{\xi}_{s,f}}{\mathrm{d}\beta}^T (t_\beta) \frac{\partial^2 \mathcal{V}}{\partial \boldsymbol{x}^2} (\boldsymbol{x}(t_f)) \cdot$$
$$[\boldsymbol{f}(\boldsymbol{x}(t_f), \boldsymbol{u}_{ex}(t_f)) - \Phi_s(t_\beta, t_f, t_\beta) \boldsymbol{f}(\boldsymbol{x}(t_\beta), \boldsymbol{u}_{ex}(t_\beta))]$$
$$= \frac{\mathrm{d}\boldsymbol{\xi}_{s,f}}{\mathrm{d}\beta}^T (t_\beta) \frac{\partial^2 \mathcal{V}}{\partial \boldsymbol{x}^2} (\boldsymbol{x}(t_f)) \frac{\mathrm{d}\boldsymbol{\xi}_{s,f}}{\mathrm{d}\beta}(t_\beta). \qquad \text{(A.3.38)}$$

Similarly, for the ratio in the second term we have

$$\lim_{h \to 0} \frac{K_{s,3}(h) - K_{s,5}(h)}{h} = \lim_{h \to 0} \left[\frac{\Phi_s(t_\beta, t_f + h, t_f + h) \boldsymbol{f}(\boldsymbol{\xi}_s(t_\beta + h, t_f + h), \boldsymbol{u}_{ex}(t_f + h))}{h} \right.$$
$$\left. - \frac{\Phi_s(t_\beta, t_f, t_f + h) \boldsymbol{f}(\boldsymbol{\xi}_s(t_\beta, t_f + h), \boldsymbol{u}_{ex}(t_f + h))}{h} \right]$$
$$= \frac{\partial \Phi_s}{\partial t}(t_\beta, t_f, t_f) \boldsymbol{f}(\boldsymbol{x}(t_f), \boldsymbol{u}_{ex}(t_f))$$
$$+ \Phi_s(t_\beta, t_f, t_f) \frac{\partial \boldsymbol{f}}{\partial \boldsymbol{x}} (\boldsymbol{x}(t_f), \boldsymbol{u}_{ex}(t_f)) \frac{\partial \boldsymbol{\xi}_s}{\partial \beta}(t_\beta, t_f)$$
$$= \frac{\partial \boldsymbol{f}}{\partial \boldsymbol{x}} (\boldsymbol{x}(t_f), \boldsymbol{u}_{ex}(t_f)) \frac{\mathrm{d}\boldsymbol{\xi}_{s,f}}{\mathrm{d}\beta}(t_\beta), \qquad \text{(A.3.39)}$$

and for the ratio in the third term we have

$$\lim_{h \to 0} \frac{K_{s,2}(h) - K_{s,4}(h)}{h} = \lim_{h \to 0} \left[\frac{\Phi_s(t_\beta + h, t_f + h, t_\beta + h) \boldsymbol{f}(\boldsymbol{\xi}_s(t_\beta, t_\beta), \boldsymbol{u}_{ex}(t_\beta + h))}{h} \right.$$
$$\left. - \frac{\Phi_s(t_\beta, t_f, t_\beta + h) \boldsymbol{f}(\boldsymbol{\xi}_s(t_\beta, t_\beta + h), \boldsymbol{u}_{ex}(t_\beta + h))}{h} \right]$$
$$= -\Phi_s(t_\beta, t_f, t_\beta) \frac{\partial \boldsymbol{f}}{\partial \boldsymbol{x}} (\boldsymbol{x}(t_\beta), \boldsymbol{u}_{ex}(t_\beta)) \boldsymbol{f}(\boldsymbol{x}(t_\beta), \boldsymbol{u}_{ex}(t_\beta))$$
$$+ \frac{\partial \Phi_s}{\partial \beta}(t_\beta, t_f, t_\beta) \boldsymbol{f}(\boldsymbol{x}(t_\beta), \boldsymbol{u}_{ex}(t_\beta))$$
$$+ \frac{\partial \Phi_s}{\partial t}(t_\beta, t_f, t_\beta) \boldsymbol{f}(\boldsymbol{x}(t_\beta), \boldsymbol{u}_{ex}(t_\beta))$$
$$= -\Phi_s(t_\beta, t_f, t_\beta) \frac{\partial \boldsymbol{f}}{\partial \boldsymbol{x}} (\boldsymbol{x}(t_\beta), \boldsymbol{u}_{ex}(t_\beta)) \boldsymbol{f}(\boldsymbol{x}(t_\beta), \boldsymbol{u}_{ex}(t_\beta))$$
$$- \int_{t_\beta}^{t_f} \Phi_s(t_\beta, t_f, s) \begin{pmatrix} \left(\frac{\partial \boldsymbol{\xi}_s}{\partial \beta}(t_\beta, s)\right)^T \frac{\partial^2 f_1}{\partial \boldsymbol{x}^2} (\boldsymbol{\xi}_s(t_\beta, s), \boldsymbol{u}_{ex}(s)) \frac{\partial \boldsymbol{\xi}_s}{\partial \beta}(t_\beta, s) \\ \vdots \\ \left(\frac{\partial \boldsymbol{\xi}_s}{\partial \beta}(t_\beta, s)\right)^T \frac{\partial^2 f_n}{\partial \boldsymbol{x}^2} (\boldsymbol{\xi}_s(t_\beta, s), \boldsymbol{u}_{ex}(s)) \frac{\partial \boldsymbol{\xi}_s}{\partial \beta}(t_\beta, s) \end{pmatrix} \mathrm{d}s$$
$$+ \frac{\partial \boldsymbol{f}}{\partial \boldsymbol{x}} (\boldsymbol{x}(t_\beta), \boldsymbol{u}_{ex}(t_\beta)) \Phi_s(t_\beta, t_f, t_\beta) \boldsymbol{f}(\boldsymbol{x}(t_\beta), \boldsymbol{u}_{ex}(t_\beta)), \qquad \text{(A.3.40)}$$

where we have again made use of Lemma 38 when computing the derivative $\frac{\partial \Phi_s}{\partial \beta}$. Noting that $K_{s,1}(0)$ is equal to $\frac{\partial \mathcal{V}}{\partial \boldsymbol{x}} (\boldsymbol{x}(t_f)) = \boldsymbol{\lambda}(t_f)$, we can finally substitute the three limits (A.3.38)-(A.3.40) into (A.3.37) and this will lead to the desired condition (A.3.18) for $t_\beta \in (0, t_f) \backslash E$ if we additionally take account of the definitions of $\boldsymbol{u}_{ex}, \mathbb{H}, \boldsymbol{\mu}_s$ and $\boldsymbol{\mu}_{s,f}$. The fact that the condition also holds for $t_\beta \in \{0, t_f\} \cup E$ follows from the fact that the left-hand side of (A.3.18) is, as a function of t_β, left continuous at each point of the finite set $\{0\} \cup E$ and right continuous at t_f. $\qquad \square$

Appendix B

Proofs

In this appendix, we will show how to derive the propositions which are stated in Chapters 3-6 without proof.

B.1 Mass-Spring Systems

In this part of the appendix, we will prove Prop. 1 by mainly using (3.2.14). Before starting with the proof, however, we want to reformulate this equation such that the influence of the TDP on the sign of $\frac{\mathrm{d}T_p}{\mathrm{d}\phi_{max}}$ becomes more evident. For this, we start by making a change of variables in the two integrals on the right-hand side of (3.2.14) such that integration is done with respect to the torque in the spring. Since $\frac{\mathrm{d}T_p}{\mathrm{d}\phi_{max}}$ is only a function of ϕ_{max}, the resulting expression becomes independent of the value of $\tau_{J_s} = \tau_J(\phi_s) \in (0, \tau_J(\phi_{max}))$. Taking the limit of this expression as $\tau_{J_s} \to 0^+$ leads then to the desired reformulation:

$$\frac{\frac{dT_p}{\mathrm{d}\phi_{max}}(\phi_{max})}{4\tau_J(\phi_{max})} = \lim_{\tau_{J_s} \to 0^+} \left[\frac{\tau_{J_s}^{-1}}{|\dot{\phi}|\left(\tau_J^{-1}(\tau_{J_s}), \phi_{max}\right)} - \right.$$
$$\left. \int_{\tau_{J_s}}^{\tau_J(\phi_{max})} \frac{s^{-2}\mathrm{d}s}{|\dot{\phi}|\left(\tau_J^{-1}(s), \phi_{max}\right)} \right], \qquad \text{(B.1.1)}$$

where τ_J^{-1} denotes the continously differentiable inverse of τ_J. We will next show how to prove Prop. 1 using (B.1.1).

Proof of Prop. 1. Let τ_J be a TDP which satisfies the hypotheses of the proposition and choose a MSS having this TDP with an arbitrary mass $M > 0$. In order to prove the proposition, we need to consider three different cases depending on the sign of $\frac{\mathrm{d}^2\tau_J}{\mathrm{d}\phi^2}$.

Let us first assume that $\frac{\mathrm{d}^2\tau_J}{\mathrm{d}\phi^2}(\phi)$ is equal to zero for each $\phi \in (0, \varphi_{max})$. By $(A1) - (A3)$, $\tau_J(\phi)$ will then for each ϕ in the interval $(-\varphi_{max}, \varphi_{max})$ be equal to $\tau_{J,l}(\phi) = k_e\phi$ with $k_e = K_J(0) > 0$. Substituting this expression for τ_J into

(B.1.1) and using (3.1.6), we can conclude that for each $\phi_{max} \in (0, \varphi_{max})$ we have

$$\frac{\frac{dT_p}{d\phi_{max}}(\phi_{max})}{4\tau_J(\phi_{max})\sqrt{k_e M}} = \lim_{\tau_{J_s} \to 0^+} \frac{\tau_{J_s} \left(\tau_J^2(\phi_{max}) - \tau_{J_s}^2\right)^{-\frac{1}{2}}}{\tau_J^2(\phi_{max})}$$
$$= 0,$$

and thus $\frac{dT_p}{d\phi_{max}}(\phi_{max}) = 0$ as expected from Table 3.1d.

Looking now at the case where $\frac{d^2\tau_J}{d\phi^2}(\phi)$ is negative for each $\phi \in (0, \varphi_{max})$, we can not directly evaluate the limit in (B.1.1) as in the previous case. Nevertheless, in order to prove the proposition we only need to determine the sign of this limit for $\phi_{max} \in (0, \varphi_{max})$. To achieve this, we will next construct for an arbitrary ϕ_{max} in that interval a linear TDP $\bar{\tau}_J$ satisfying $\bar{\tau}_J(\phi_{max}) = \tau_J(\phi_{max})$. In addition, we will build the product $\frac{\dot{\phi}_{max}}{4\tau_J(\phi_{max})} \frac{dT_p}{d\phi_{max}}(\phi_{max})$ once for the chosen MSS and once for a MSS having the same mass as the chosen system but the linear TDP $\bar{\tau}_J$. The sign of the limit in (B.1.1) will then directly follow from comparing the resulting two products and using the sign of $\frac{d^2\tau_J}{d\phi^2}(\phi)$ together with the fact that the product for the second MSS is equal to zero due to the linearity of $\bar{\tau}_J$.

Let us first fix a $\phi_{max} \in (0, \varphi_{max})$ and construct the linear TDP $\bar{\tau}_J$ as just described. Moreover, construct a second MSS with the TDP $\bar{\tau}_J$ and the mass M. Using a bar to denote the various variables corresponding to this second MSS, let us also introduce the function $H : (0, \tau_J(\phi_{max})) \to \mathbb{R}$ given by

$$H(s) = \frac{\dot{\phi}_{max}}{|\dot{\phi}| \left(\tau_J^{-1}(s), \phi_{max}\right)} - \frac{\dot{\bar{\phi}}_{max}}{|\dot{\bar{\phi}}| \left(\bar{\tau}_J^{-1}(s), \phi_{max}\right)}. \tag{B.1.2}$$

Note that the first term in the right-hand side of (B.1.2) gives for the chosen MSS the ratio between the maximum velocity and the magnitude of the attained velocity at the torque value s. Similarly, the second term there gives the same ratio for the second MSS with the linear TDP. In both terms, the maximum deflection value is equal to ϕ_{max} and at this deflection both systems have the same torque in their springs. Comparing now the aforementioned products corresponding to these systems shows that $H(s)$ and $\frac{dT_p}{d\phi_{max}}$ are related as follows:

$$\frac{\dot{\phi}_{max} \frac{dT_p}{d\phi_{max}}(\phi_{max}) - \dot{\bar{\phi}}_{max} \frac{d\bar{T}_p}{d\phi_{max}}(\phi_{max})}{4\tau_J(\phi_{max})} \overset{(B.1.1)}{=}$$

$$\lim_{\tau_{J_s} \to 0^+} \left[\frac{H(\tau_{J_s})}{\tau_{J_s}} - \int_{\tau_{J_s}}^{\tau_J(\phi_{max})} \frac{H(s)}{s^2} ds\right]$$

$$\Rightarrow \frac{dT_p}{d\phi_{max}}(\phi_{max}) = -\lim_{\tau_{J_s} \to 0^+} \int_{\tau_{J_s}}^{\tau_J(\phi_{max})} \frac{4\tau_J(\phi_{max})H(s)ds}{\dot{\phi}_{max}s^2}, \tag{B.1.3}$$

where we have applied L'Hospital's rule to conclude that $\lim_{\tau_{J_s} \to 0^+} \frac{H(\tau_{J_s})}{\tau_{J_s}} = 0$

holds[1]. Moreover, we have also used the fact that $\frac{\mathrm{d}\bar{T}_p}{\mathrm{d}\phi_{max}}(\phi_{max}) = 0$ holds since $\bar{\tau}_J$ is a linear TDP.

It is important to notice here that the equality in (B.1.3) holds for any τ_J which satisfy the assumptions $(A1) - (A3)$. Indeed, in deriving this relation we have only used (B.1.1) and not considered any of the properties of the derivative $\frac{\mathrm{d}^2\tau_J}{\mathrm{d}\phi^2}$. For the current case we are investigating, this derivative is known to be negative for each $\phi \in (0, \phi_{max})$. As we next show, this property can be used together with (B.1.3) to find the sign of $\frac{\mathrm{d}T_p}{\mathrm{d}\phi_{max}}$.

Let us fix a $s \in (0, \tau_J(\phi_{max}))$ and focus on the first term of $H(s)$. From the negativity of $\frac{\mathrm{d}^2\tau_J}{\mathrm{d}\phi^2}$ it follows that K_J is strictly decreasing on $[0, \phi_{max}]$. By making use of this monoticity of K_J together with (3.1.4) and (3.1.6), we can see that the first term of $H(s)$ satisfies

$$
\begin{aligned}
\frac{\dot{\phi}_{max}}{|\dot{\phi}|\left(\tau_J^{-1}(s), \phi_{max}\right)} &= \sqrt{1 + \frac{E_{pot}\left(\tau_J^{-1}(s)\right)}{E_{pot}(\phi_{max}) - E_{pot}\left(\tau_J^{-1}(s)\right)}} \\
&= \sqrt{1 + \frac{\int_0^s \frac{\xi \mathrm{d}\xi}{K_J\left(\tau_J^{-1}(\xi)\right)}}{\int_s^{\tau_J(\phi_{max})} \frac{\xi \mathrm{d}\xi}{K_J\left(\tau_J^{-1}(\xi)\right)}}} \\
&< \sqrt{1 + \frac{s^2}{\tau_J(\phi_{max})^2 - s^2}} \\
&= \frac{\dot{\bar{\phi}}_{max}}{|\dot{\bar{\phi}}|\left(\bar{\tau}_J^{-1}(s), \phi_{max}\right)},
\end{aligned}
$$

where the last equality follows from Table 3.1b with $\bar{\tau}_J(\phi_{max}) = \tau_J(\phi_{max})$. From the inequality above it follows that the function $H(s)$ and thus the integrand in (B.1.3) are always negative when $s \in (0, \tau_J(\phi_{max}))$. Consequently, we can conclude that $\frac{\mathrm{d}T_p}{\mathrm{d}\phi_{max}}(\phi_{max})$ is positive.

Looking finally at the case where $\frac{\mathrm{d}^2\tau_J}{\mathrm{d}\phi^2}(\phi)$ is positive for each $\phi \in (0, \varphi_{max})$, we can use again (B.1.3) together with the sign of $\frac{\mathrm{d}^2\tau_J}{\mathrm{d}\phi^2}$ to show that for each $\phi_{max} \in (0, \varphi_{max})$ the resulting function H takes positive values in its domain of definition. This will then imply that $\frac{\mathrm{d}T_p}{\mathrm{d}\phi_{max}}(\phi_{max})$ is negative for each $\phi_{max} \in (0, \varphi_{max})$, as desired. $\qquad\square$

B.2 Switching Control Strategies

The main aim of this appendix is to provide the proofs of Prop. 2 and 4. Note that in both propositions switching control strategies satisfying the two conditions (4.2.6) and (4.2.7) play an important role. For that reason, we want to first clarify the implications of these two conditions on control strategies as

---

[1] Notice that we have $\lim_{s \to 0+} H(s) = \lim_{s \to 0+} \frac{\mathrm{d}H}{\mathrm{d}s}(s) = 0$.

well as on the corresponding trajectories. This is done by the following two lemmas.

Lemma 40. *Let $i \geq 0$ be a non-negative integer and $u_{S,i} : D_{S,i} \to \mathbb{U}$ an admissible switching control with $|^0 u_{S,i}| = \dot{\theta}_{max}$ and $D_{S,i} = [0, t_{min}(i+1)]$. Moreover, assume that $u_{S,i}$ has i switchings and that in case $i \neq 0$ holds we have both*

$$t_{S,k} = t_{min}(k), \tag{B.2.1}$$

and

$$^k u_{S,i} = (-1)^k \, ^0 u_{S,i}, \tag{B.2.2}$$

for each $k \in \{1, \ldots, i\}$. Then, along the trajectory $\boldsymbol{x}_{S,i}$ which corresponds to $u_{S,i}$ and which starts from the origin, i.e. $\boldsymbol{x}_{S,i}(0) = \boldsymbol{0}$, we have for each $k \in S_{i+1}$

$$^k \boldsymbol{x}_{S,i} = (-1)^{k+1} 2k \begin{pmatrix} 0 \\ ^0 u_{S,i} \end{pmatrix}. \tag{B.2.3}$$

Proof. To prove this lemma, we will use the principle of mathematical induction.

Base Case $(i = 0)$ For $i = 0$, the control $u_{S,i}$ satisfying the hypotheses of the lemma will be a constant function defined on $[0, t_{min}(1)]$ such that it is either equal to $-\dot{\theta}_{max}$ or $\dot{\theta}_{max}$. In both cases, along the trajectory $\boldsymbol{x}$ which corresponds to this control with $\boldsymbol{x}_0 = \boldsymbol{0}$ we will have $x_1(0) = 0$ and $\dot{x}_1(0) = \text{sgn}(^0 u_{S,i})\dot{\theta}_{max} = \text{sgn}(^0 u_{S,i}) \, ^0 \dot{\phi}_{max}$ leading to the relative energy $^0 E_{rel} = \frac{1}{2} M \dot{\theta}_{max}^2$. Note that by definition the period T_p related to this energy is given exactly by $2t_{min}(1)$, see (4.2.11)-(4.2.12). Using our results on trajectories of EJ's in Sec. 4.1, we can then see that $\boldsymbol{x}_f$ will be equal to $\text{sgn}(^0 u_{S,i}) \begin{pmatrix} 0 & 2\dot{\theta}_{max} \end{pmatrix}^T$. Comparing the initial and terminal values of $\boldsymbol{x}$ with the values provided by (B.2.3), we can finally conclude that the lemma holds for $i = 0$.

Inductive Step $(i \in \{0, 1, \ldots\})$ Let i be any non-negative integer and assume that Lemma 40 holds for this integer. We want to show that the same lemma holds for $i + 1$, as well. For this assume now that $u_{S,i+1} : D_{S,i+1} \to \mathbb{U}$ is an admissible switching control satisfying the hypotheses of the lemma. Then, since $i + 1 > 0$ we know that for each $k \in \{1, \ldots, i+1\}$ the two conditions (B.2.1) and (B.2.2) will hold. Let us now introduce the function $\bar{u}_{S,i} : [0, t_{min}(i)] \to \mathbb{U}$ with

$$\bar{u}_{S,i}(t) = \begin{cases} u_{S,i+1}(t) & t \in [0, t_{min}(i)) \\ -^i u_{S,i+1} & t = t_{min}(i) \end{cases}. \tag{B.2.4}$$

It can then be seen that the control $\bar{u}_{S,i}$ defined above satisfies the hypotheses of the lemma. Moreover, due to this definition the restriction of both controls $u_{S,i+1}$ and $\bar{u}_{S,i}$ to the time interval $[0, t_{min}(i))$ are equal to each other. From our induction hypothesis and from the continuity of the states it then follows that along the trajectory $\boldsymbol{x}$ corresponding to $u_{S,i+1}$ with $\boldsymbol{x}_0 = \boldsymbol{0}$, (B.2.3) holds for each $k \in S_{i+1}$. In order to prove the lemma, we need to now show that (B.2.3) also holds for $k = i + 2$.

Noting that ${}^{i}u_{S,i+1}$ equals to $(-1)^{i}\ {}^{0}u_{S,i}$, we have ${}^{i}x_1 = 0$ and ${}^{i}\dot{x}_1 = (-1)^{i}(2i+1)\ {}^{0}u_{S,i}$ along the trajectory $\boldsymbol{x}$, see (B.2.3). Consequently, the relative energy ${}^{i}E_{rel}$, which is constant in the time interval $[t_{min}(i), t_{min}(i+1)]$, equals to $\frac{1}{2}M(2i+1)^2\dot{\theta}_{max}^2$. According to (4.2.11)-(4.2.12) the period T_p related to this energy is now given by $2\left(t_{min}(i+1) - t_{min}(i)\right)$. Using again our results on trajectories of EJ's in Sec. 4.1 we can finally conclude that (B.2.3) also holds for $k = i + 2$ as desired.

$\square$

Lemma 41. *Let $(\boldsymbol{x}, u)$ be an admissible controlled trajectory such that $\boldsymbol{x}_0$ equals to $\boldsymbol{0}$ and u satisfies the two conditions (4.2.6) and (4.2.7). Then $u \in \mathcal{S}_{\mathbb{U}}$ is a switching control with the switching number i given by*

$$i = \min\left\{k \in \{1, 2, \ldots\}\Big| t_f \le t_{min}(k)\right\} - 1. \qquad (B.2.5)$$

Moreover, for each $k \in S_i$ ${}^{k}u$ and ${}^{k}\boldsymbol{x}$ are given by the right-hand sides of (B.2.2) and (B.2.3) with ${}^{0}u_{S,i} = {}^{0}u$, respectively. Finally, if $i \ge 1$ holds then for each $k \in \{1, \ldots, i\}$ the switching time $t_{S,k}$ is given by (B.2.1).

Proof. Let us note here first that the set of admissible controlled trajectories satisying the hypothesis of the lemma are not empty. This follows directly from Lemma 40 as for each non-negative integer i the controlled trajectory $(\boldsymbol{x}_{S,i}, u_{S,i})$ with $\boldsymbol{x}_{S,i}(0) = \boldsymbol{0}$ satisfies both (4.2.6) and (4.2.7), see Sec. 4.1. It is clear that these trajectories also satisfy the conclusions of the lemma.

Choose now any admissible controlled trajectory $(\boldsymbol{x}, u)$ satisfying the hypothesis of the lemma. Since $u \in \mathcal{PC}_{\mathbb{U}}$, condition (4.2.6) together with the initial condition $\boldsymbol{x}_0 = \boldsymbol{0}$ implies that we can always find a sufficiently small time $t_{\varepsilon,0}$ such that $\text{sgn}\,(x_1(t)) = \text{sgn}\,(u(0)) \ne 0$ holds for each $t \in (0, t_{\varepsilon,0}] \subset (0, t_f]$. Moreover, due to (4.2.7) $u(t)$ will then be equal to $u(0)$ in $[0, t_{\varepsilon,0}]$ with $|u(0)| = \dot{\theta}_{max}$. Depending on the value of the final time t_f we look at two different cases.

Case 1 $\left(t_f \in (0, t_{min}(1)]\right)$ We want to show that for this case $u(t)$ must be equal to $u(0)$ for each $t \in [0, t_f]$. Since u is an element of $\mathcal{PC}_{\mathbb{U}}$, it suffices to show that $u(t) = u(0)$ holds for each $t \in [0, t_f)$. Assume now by contradiction that there exists at least one $\bar{t} \in [0, t_f)$ such that $u(\bar{t}) \ne u(0)$ and let $S_{\bar{t},1}$ denote the non-empty set of all such times, i.e.

$$S_{\bar{t},1} := \{t \ge 0 | u(t) \ne u(0) \wedge t < t_f\}. \qquad (B.2.6)$$

By our discussion above, this set is then bounded below by $t_{\varepsilon,0} > 0$ and its infimum exists. Let $\tilde{t}_1 \in [t_{\varepsilon,0}, t_f)$ denote this infimum. From (4.2.7) and from the continuity of x_1, it then follows that $x_1(\tilde{t}_1)$ must be equal to 0. Moreover, since $\tilde{t}_1$ is the infimum of the set $S_{\bar{t},1}$ the control u is constant and equals to $u(0)$ in $t \in [0, \tilde{t}_1)$. This means that the relative energy along $(\boldsymbol{x}, u)$ is equal to $\frac{1}{2}M\dot{\theta}_{max}^2$ in this time interval. However, since $x_1(0) = 0$ and $\dot{x}_1(0) = u(0) \ne 0$ hold $t_{min}(1)$ is then the first time x_1 equals to zero after $t = 0$ and therefore we must have $\tilde{t}_1 \ge t_{min}(1)$, see (4.2.11)-(4.2.12) and Chapter 3. This leads to a

contradiction since $\tilde{t}_1$ is less than t_f and we conclude that the set $S_{\bar{t},1}$ must be empty.

We have thus shown that for any $t_f \in (0, t_{min}(1)]$ u is a switching control with $i = 0$ switchings consistent with (B.2.5). Moreover, for $k \in S_i$ it follows directly from the initial conditions on the state and controls that the values for ${}^k\boldsymbol{x}$ and ${}^k u$ are given by the right-hand sides of (B.2.2) and (B.2.3) with ${}^0 u_{S,i} = {}^0 u$, respectively.

Case 2 $\left(t_f > t_{min}(1)\right)$ For this case we will first use induction to show that t_f being greater than $t_{min}(i-1)$ implies for any $i \in \{2, ...\}$ that the controlled trajectory $(\boldsymbol{x}_{S,i}, u_{S,i})$ defined in Lemma 40 and the trajectory $(\boldsymbol{x}, u)$ are equal to each other if they are restricted to the time interval $[0, t_{min}(i-1)]$ and if we have $u_{S,i}(0) = u(0)$.

Let us first set i to 2 and show that $t_f > t_{min}(1)$ implies that $(\boldsymbol{x}(t), u(t)) = (\boldsymbol{x}_{S,2}(t), u_{S,2}(t))$ holds for each $t \in [0, t_{min}(1)]$. Recall that there always exists a $t_{\varepsilon,0} > 0$, such that the control u is equal to $u(0)$ for all $t \in [0, t_{\varepsilon,0}] \subset D$. The value of $t_{\varepsilon,0}$ must, however, in this case be less than t_f, since otherwise we would have $x_1(t_{min}(1)) = 0$ and $\dot{x}_1(t_{min}(1)) = -u(0)$ and there would then exist a time $t_{\varepsilon,1} > t_{min}(1)$ such that $\mathrm{sgn}\,(x_1(t)) = -\mathrm{sgn}\,(u(0))$ holds for $t \in (t_{min}(1), t_{\varepsilon,1}] \subset (t_{min}(1), t_f]$. This contradicts the condition (4.2.7).

We have thus just shown that the set $S_{\bar{t},1}$ as defined in (B.2.6) is not empty. Following the same arguments used for the first case, we can also conclude that $\tilde{t}_1 \geq t_{min}(1)$ must hold for the infimum of this set. We want to next show that $\tilde{t}_1$ is equal to $t_{min}(1)$ and that it is an element of $S_{\bar{t},1}$. For this, note that the control $u(t)$ must be equal to $u(0)$ for each $t \in [0, t_{min}(1)) \subset [0, \tilde{t}_0)$. From the continuity of the states, it then follows that $\boldsymbol{x}\,(t_{min}(1))$ equals to $\begin{pmatrix} 0 & 2u(0) \end{pmatrix}^T$. Since u is an admissible control, we know that at $t = t_{min}(1)$ $u(t) \in [-\dot{\theta}_{max}, \dot{\theta}_{max}]$ must hold. This means that regardless of the value of the control the sign of $\dot{x}_1\,(t_{min}(1)) = u\,(t_{min}(1)) - x_2\,(t_{min}(1))$ will always be equal to $-\mathrm{sgn}\,(u(0))$, as we have $|u(0)| = \dot{\theta}_{max}$. Consequently, we can find a time $t_{\varepsilon,1} > t_{min}(1)$ such that $\mathrm{sgn}\,(x_1(t)) = -\mathrm{sgn}\,(u(0))$ holds for each $t \in (t_{min}(1), t_{\varepsilon,1}] \subset (t_{min}(1), t_f]$. From condition (4.2.7) and from the continuity properties of elements of $\mathcal{PC}_{\mathbb{U}}$ it finally follows that at $u\,(t_{min}(1))$ must be equal to $-u(0)$ so that $t_{min}(1)$ is the infimum of the set $S_{\bar{t},1}$. We have thus shown that the restriction of u to the time interval $[0, t_{min}(1)]$ is equal to the restriction of $u_{S,2}$ to the same time-interval if $u(0) = u_{S,2}(0)$. The restriction of the two trajectories $\boldsymbol{x}$ and $\boldsymbol{x}_{S,i}$ to $[0, t_{min}(1)]$ will then also be equal to each other and this proves the desired implication for the base case with $i = 2$.

Let us now choose any $i \in \{2, 3, \ldots\}$ and assume that $t_f > t_{min}(i-1)$ implies that $(\boldsymbol{x}(t), u(t)) = (\boldsymbol{x}_{S,i}(t), u_{S,i}(t))$ holds for each $t \in [0, t_{min}(i-1)]$ if $u(0) = u_{S,i}(0)$. We want to now show that if $t_f > t_{min}(i)$ holds then $(\boldsymbol{x}(t), u(t)) = (\boldsymbol{x}_{S,i+1}(t), u_{S,i+1}(t))$ will also hold at each $t \in [0, t_{min}(i)]$ provided $u(0)$ equals to $u_{S,i+1}(0)$. For this, first note that $t_{min}(i)$ is greater than $t_{min}(i-1)$. By the induction hypothesis we have then for each $t \in [0, t_{min}(i-1)]$ that $(\boldsymbol{x}(t), u(t))$ is equal to $(\boldsymbol{x}_{S,i}(t), u_{S,i}(t))$ and thus also to $(\boldsymbol{x}_{S,i+1}(t), u_{S,i+1}(t))$

if $u(0) = u_{S,i}(0) = u_{S,i+1}(0)$. By Lemma 40, we have then $x_1(t_{S,i-1}) = 0$ and $\dot{x}_1(t_{S,i-1}) = (-1)^{i-1}u(0)(2i-1) \neq 0$. Introduce now the set $S_{\bar{t},i-1} = \{t \geq t_{min}(i-1)|u(t) \neq u(t_{min}(i-1)) \wedge t < t_f\}$. Following analogous arguments as done for the base case, it can be shown that the set $S_{\bar{t},i-1}$ is not empty and that its infimum $\tilde{t}_{i-1}$ is equal to $t_{min}(i)$ and thus an element of $S_{\bar{t},i-1}$. Finally, noting that a sign change of u must occur at $t = t_{min}(i)$, we arrive at the desired implication. This concludes the inductive step.

Note that as i goes to infinity, the magnitude of $\boldsymbol{x}_{S,i}$ at $t_{min}(i+1)$ goes to infinity. Using the fact that the state $\boldsymbol{x}$ defined on D must be bounded and the relation we have just shown to exist between $(\boldsymbol{x}, u)$ and the controlled trajectories described by Lemma 40, we can conclude that there must exist a positive integer $l \geq 2$ such that $t_f \in (t_{min}(l-1), t_{min}(l)]$ holds. The proof of the lemma for $t_f > t_{min}(1)$ follows now from the equalities (B.2.1)-(B.2.3) in Lemma 40 and that the sign of $x_1(t)$ must remain constant in $t \in (t_{min}(l-1), t_f]$. $\quad\square$

With Lemmas 40-41, Prop. 2 and 4 can easily be proved as we next show.

Proof of Prop. 2. We will again make use of mathematical induction.

Base case $(i = 0)$ Let $u \in \mathcal{S}_{\mathbb{U}}$ be a control with 0 switchings. Moreover, let $\boldsymbol{x}$ be the trajectory corresponding to u with $\boldsymbol{x}_0 = \boldsymbol{0}$. By definition, u is a constant function with $u \equiv {}^0u$ and it follows from (2.1.5) and (4.1.2) together with the condition on the initial state that the following relation holds for ${}^0E_{rel}$:

$$^0E_{rel} = \frac{1}{2}M\ {}^0u^2 \leq \frac{1}{2}M\dot{\theta}_{max}^2. \tag{B.2.7}$$

Assume now that both (4.2.6) and (4.2.7) hold for the control u as stated in the proposition. Then, ${}^0u$ is either equal to $-\dot{\theta}_{max}$ or $\dot{\theta}_{max}$. Moreover, we have $t_f \leq \frac{1}{2}T_p({}^0\phi_{max})$ with $E_{pot}({}^0\phi_{max}) = \frac{1}{2}M\dot{\theta}_{max}^2$, since for larger final times x_1 and thus u will change its sign. Regardless of these values we easily see from (B.2.7) that the inequality (4.2.5) holds with equality in this case.

Inductive step $(i \in \{0, 1, \ldots\})$ Let i be any non-negative integer and assume that Prop. 2 holds for this integer. We want to show that the same proposition holds for $i + 1$, as well. Let Σ be, as before, a given control system and $u \in \mathcal{S}_{\mathbb{U}}$ now a control with $i + 1$ switchings. Moreover, let $\boldsymbol{x}$ denote the trajectory corresponding to u with $\boldsymbol{x}_0 = \boldsymbol{0}$. According to (3.1.3) and (4.1.2)-(4.1.4), the two relative energies ${}^iE_{rel}$ and ${}^{i+1}E_{rel}$ along this trajectory are then related to

each other as follows:

$$
\begin{aligned}
{}^{i+1}E_{rel} \;=\; & E_{pot}({}^{i+1}x_1) + \\
& E_{kin}\left({}^{i+1}u - {}^{i}u + \lim_{t \to t_{S,i+1}^-} \dot{x}_1(t)\right) \\
=\; & {}^{i}E_{rel} + \lim_{t \to t_{S,i+1}^-} \dot{x}_1(t)M({}^{i+1}u - {}^{i}u) + \\
& \frac{1}{2}M({}^{i+1}u - {}^{i}u)^2 \qquad\qquad\qquad\qquad\text{(B.2.8)} \\
\leq\; & {}^{i}E_{rel} + 2M\dot{\theta}_{max}\left({}^{i}\dot{\phi}_{max} + \dot{\theta}_{max}\right), \qquad\quad\text{(B.2.9)}
\end{aligned}
$$

where we used the fact that ${}^{i}E_{rel}$ remains constant for $t \in D_i$ together with the continuity of E_{kin}, E_{pot} and $\boldsymbol{x}$. Clearly, the control u restricted to the time-interval $[0, t_{S,i+1})$ is a switching control with i switchings and from our induction hypothesis it follows that ${}^{k}E_{rel} \leq \frac{(2k+1)^2}{2}M\dot{\theta}^2_{max}$ for each $k \in S_i$. Note that this also implies that ${}^{i}\dot{\phi}_{max} \leq (2i+1)\dot{\theta}_{max}$. Using these two inequalities in (B.2.9), we have now

$$
{}^{i+1}E_{rel} \leq \frac{(2i+3)^2}{2}M\dot{\theta}^2_{max},
$$

showing that (4.2.5) holds for each $k \in S_{i+1}$.

Assume now that both (4.2.6) and (4.2.7) hold for the control u as stated in the proposition. From Lemma 40 it follows then that t_f must be an element of the interval $(t_{min}(i+1), t_{min}(i+2)]$. More importantly, according to this lemma (B.2.2)-(B.2.3) hold for each $k \in S_{i+1}$. Consequently, for each $k \in S_{i+1}$ ${}^{k}E_{rel}$ equals to $E_{kin}({}^{k}\dot{x}_1) = \frac{(2k+1)^2}{2}M\dot{\theta}^2_{max}$ as desired. $\qquad\square$

Proof of Prop. 4. Let $(\boldsymbol{x}, u)$ be any admissible controlled trajectory satisfying the hypothesis of the lemma. Since $E_{EJ}(u, t_f)$ equals to $E_{max}(i)$ it follows from (4.2.4)-(4.2.5) directly that ${}^{i}E_{rel}$ must be equal to $E_{r,max}(i)$. We want to first show that this is only possible if for each $k \in S_i$ the deflection at $t_{S,k}$ is equal to zero and the relative energy at that time equals to $E_{r.max}(k)$. For this we will make use of the following inequality for the relative energy ${}^{i}E_{rel}$:

$$
\begin{aligned}
{}^{i}E_{rel} - {}^{0}E_{rel} \;=\; & \sum_{k=0}^{i-1} {}^{k+1}E_{rel} - {}^{k}E_{rel} \\
=\; & \sum_{k=0}^{i-1} E_{kin}({}^{k+1}\dot{x}_1) - E_{kin}\left(\lim_{t \to t_{S,k+1}^-} \dot{x}_1(t)\right) \\
\overset{(4.1.4)}{=}\; & \frac{1}{2}M\sum_{k=0}^{i-1}({}^{k+1}u - {}^{k}u)^2 + \\
& M\sum_{k=0}^{i-1}({}^{k+1}u - {}^{k}u)\lim_{t \to t_{S,k+1}^-} \dot{x}_1(t) \qquad\text{(B.2.10)}
\end{aligned}
$$

$$\Rightarrow {}^{i}E_{rel} \le \frac{1}{2}M\,{}^{0}\dot{\phi}_{max}^{2} + 2M\dot{\theta}_{max}\left[i + \sum_{k \in 0}^{i-1}{}^{k}\dot{\phi}_{max}\right], \qquad \text{(B.2.11)}$$

where the last inequality can hold with equality only if ${}^{k}x_1 = 0$ holds for each $k \in \{1, \ldots, i\}$, see the second summation in (B.2.10).

Assume now by contradiction that there either exists a $\bar{k} \in S_i$ with ${}^{\bar{k}}x_1 \neq 0$ and thus $|{}^{\bar{k}}\dot{x}_1| < {}^{\bar{k}}\dot{\phi}_{max}$ or with ${}^{\bar{k}}E_{rel} \neq E_{r,max}(\bar{k})$. In the first case, $\bar{k}$ must be greater than 0 since we have $\boldsymbol{x}_0 = \boldsymbol{0}$. Consequently, (B.2.11) will hold with inequality. Noting from Prop. 2 that for each $k \in S_i$ the maximum value for ${}^{k}\dot{\phi}_{max}$ is equal to $(2k+1)\dot{\theta}_{max}$, we conclude then that ${}^{i}E_{rel}$ must be less than $E_{r,max}(i)$. In the second case, i.e. ${}^{\bar{k}}E_{rel} \neq E_{r,max}(\bar{k})$, $\bar{k}$ must clearly be less than i. Assuming that $\bar{k} \in S_{i-1}$, we know from Prop. 2 that ${}^{\bar{k}}\dot{\phi}_{max}$ must be less than $(2\bar{k}+1)\dot{\theta}_{max}$ and the inequality (B.2.11) will then again imply that ${}^{i}E_{rel}$ is less than $E_{r,max}(i)$.

Based on our discussion so far, we now know that for each $k \in S_i$ we must have ${}^{k}x_1 = 0$ and ${}^{k}E_{rel} = E_{r,max}(k) > 0$. Moreover, as already discussed in Sec. 4.2 it follows from (4.2.3)-(4.2.4) that ${}^{i+1}x_1 = x_1(t_f)$ must be equal to zero in order for $E_{EJ}(u, t_f)$ to be equal to $E_{max}(i)$. Note now that a MSS with the energy ${}^{k}E_{rel} > 0$ and with zero initial deflection requires at least $\frac{T_p({}^{k}\dot{\phi}_{max})}{2}$ to reach a deflection of zero for the second time, see Chapter 3. This proves the inequality (4.2.11).

Finally, using the exact same arguments just used to prove (4.2.11) we can show that in case this inequality holds with equality for $k = i+1$ it must also hold with equality for each $k \in S_i \backslash \{0\}$. From Lemma 40 and the properties of the trajectories of EJ's as discussed in Sec. 4.1 it follows then that in this case both (4.2.6) and (4.2.7) will hold in $t \in [0, t_f]$ with $x_1(t_f) = 0$ and $t_f = t_{min}(i+1)$. The fact that the three conditions (4.2.6), (4.2.7) and (4.2.9) are sufficient for the inequality (4.2.11) to hold with equality for each $k \in \{1, \ldots, i+1\}$ follows from Lemma 41. $\qquad \square$

B.3 Optimal Control Strategies

B.3.1 Existence

In this part of the appendix, we will first prove Prop. 5 by making use of the inequality (5.1.2). Then, making use of this proposition we establish the existence and uniqueness of solutions of (2.1.4) when an initial state is given together with an admissible control. Finally, using Filippov's Theorem, PMP and Sturm Comparison Theorem we prove Prop. 6. In order to simplify our discussions, we first give the following straightforward lemma clarifying the relation between the deflection x_1 and ψ_{max} along trajectories of Σ.

Lemma 42. *Let $\boldsymbol{x}$ be a trajectory of Σ defined on D and assume that along this trajectory $|x_1(t)|$ and $\psi_{max}(t)$ are equal to each other in a non-empty open*

time interval $\bar{D} \subset D$. Then, for each $t \in \bar{D}$ we have

$$\boldsymbol{x}(t) = \boldsymbol{0}. \tag{B.3.1}$$

Proof. Let $\boldsymbol{x}$ be an admissible controlled trajectory defined on D and $\bar{D}$ a time interval satisfying the hypothesis of the lemma. Notice that, according to (4.2.1) and (5.1.1) we must then have $x_2(t) = 0$ and thus $\dot{x}_2(t) = \frac{\tau_J(x_1(t))}{M} = 0$ for each $t \in \bar{D}$. This shows that $\boldsymbol{x}(t) = \dot{\boldsymbol{x}}(t) = \boldsymbol{0}$ must hold for each $t \in \bar{D}$. □

With Lemma 42, we can now see that along a trajectory of Σ with positive E_{EJ} the inequality (5.1.2) can never hold with equality in a finite time-interval. Using this property and rewriting (5.1.2) in terms of ψ_{max}, we can then prove Prop. 5 as follows.

Proof of Prop. 5. Let $(\boldsymbol{x}, u)$ be an admissible controlled trajectory defined on $D = [0, t_f]$. Depending on the value of ψ_{max} along $(\boldsymbol{x}, u)$, we will first discuss two different cases to prove (5.1.3).

Case 1 $(\forall t \in D)\,[\psi_{max}(t) \neq 0]$ In this case the maximal deflection ψ_{max} is always positive. Moreover, using (4.2.2) and (5.1.1) we can see that this deflection is differentiable almost everywhere with its derivative given by

$$\frac{\mathrm{d}\psi_{max}}{\mathrm{d}t}(t) = \frac{\tau_J\left(x_1(t)\right)}{\tau_J\left(\psi_{max}(t)\right)}u(t), \tag{B.3.2}$$

at each $t \in D$ where this derivative exists. Note that both the magnitude of u and x_1 are bounded by $\dot{\theta}_{max}$ and ψ_{max}, respectively. The relation (5.1.3) follows then from integrating (B.3.2) and using Lemma 42 together with the continuity of x_2.

Case 2 $(\exists \bar{t} \in D)\,[\psi_{max}(\bar{t}) = 0]$ By contradiction, assume that there exists a $\hat{t} \in (0, t_f]$ such that $|\psi_{max}(\hat{t}) - \psi_{max}(0)| \geq \dot{\theta}_{max}\hat{t}$ and define the set $S_{\bar{t}} := \{t \in [0, \hat{t}] | \psi_{max}(t) = 0\}$. Notice that if this set is empty, we can directly apply our results from the first case above to show that $|\psi_{max}(\hat{t}) - \psi_{max}(0)|$ must be less than $\dot{\theta}_{max}\hat{t}$ leading to a contradiction. Assuming therefore additionally that the set $S_{\bar{t}}$ is non-empty, let $\bar{t}_{inf}$ and $\bar{t}_{sup}$ denote its infimum and supremum, respectively. Our initial assumption on ψ_{max} implies that we have either $\psi_{max}(\hat{t}) \geq \psi_{max}(0) + \dot{\theta}_{max}\hat{t}$ or $\psi_{max}(\hat{t}) \leq \psi_{max}(0) - \dot{\theta}_{max}\hat{t}$. We want to next show that none of these two possibilities can actually occur.

Focusing on the first possibility, it follows from the continuity of ψ_{max} that we must have $\psi_{max}(\bar{t}_{sup}) = 0$, i.e. $\bar{t}_{sup} \in S_{\bar{t}}$. Furthermore, since $\psi_{max}(\hat{t})$ is positive $\psi_{max}(t)$ will be positive at each $t \in (\bar{t}_{sup,1}, \hat{t}]$ and thus also differentiable almost everywhere in this interval. Consequently, using again our results from

the first case and in particular (B.3.2) we get

$$
\begin{aligned}
\psi_{max}(\bar{t}_{sup}) &= \psi_{max}(\hat{t}) + \int_{\hat{t}}^{\bar{t}_{sup}} \frac{\tau_J\left(x_1(s)\right)}{\tau_J\left(\psi_{max}(s)\right)} u(s)\mathrm{d}s \\
&> \psi_{max}(\hat{t}) - \dot{\theta}_{max}(\hat{t} - \bar{t}_{sup}) \\
\Rightarrow \psi_{max}(\bar{t}_{sup}) &> \psi_{max}(0) + \dot{\theta}_{max}\bar{t}_{sup} \geq 0,
\end{aligned}
$$

which is a contradiction.

For the second possibility, it follows from the non-negativity of ψ_{max} that $\hat{t}$ must be less than or equal to $\min\{\frac{\psi_{max}(0)}{\dot{\theta}_{max}}, t_f\}$. Moreover, $\psi_{max}(0)$ must be positive, as $\hat{t}$ is positive, which implies together with the continuity of ψ_{max} that the infimum $\bar{t}_{inf}$ will be an element of $(0, \hat{t}]$ with $\psi_{max}(\bar{t}_{inf}) = 0$. It follows then that $\psi_{max}(t)$ is positive in $[0, \bar{t}_{inf})$ and thus also differentiable almost everywhere in this interval. Consequently, we have $\psi_{max}(\bar{t}_{inf}) = \psi_{max}(0) + \int_0^{\bar{t}_{inf}} \frac{\tau_J(x_1(s))}{\tau_J(\psi_{max}(s))} u(s)\mathrm{d}s > \psi_{max}(\hat{t})$ which leads again to a contradiction.

Our discussion above proves the relation (5.1.3). To prove the remaining part of the proposition, notice first that (5.1.3) together with the definitions (5.1.4)-(5.1.5) imply that $\psi_{max}(t) \in [\psi_{lb}, \psi_{ub}]$ holds, with $\psi_{ub} > \psi_{lb} \geq 0$, at each $t \in D$. With (3.1.2)-(3.1.4) and (4.2.1), this then directly implies (5.1.7) with the set S_{E_b} given by (5.1.6). Note that the compactness of S_{E_b} follows from the fact that the function E_{MSS} is continuous and radially unbounded. $\square$

When discussing the construction of trajectories corresponding to switching controls, we have seen in Sec. 4.1 that for each initial state and admissible switching control, there exists a unique trajectory of Σ which starts from this initial state and corresponds to that control. With Prop. 5, we can now show that this existence and uniqueness result actually holds for any admissible control. This is illustrated in the following lemma.

Lemma 43. *For each initial state $\boldsymbol{x}_0 \in \mathbb{R}^2$ and control $u \in \mathcal{PC}_{\mathbb{U}}$, there exists a unique trajectory $\boldsymbol{x} \in \mathit{Traj}(\Sigma)$ starting from $\boldsymbol{x}_0$ and corresponding to u.*

Proof. Let the initial state $\boldsymbol{x}_0 \in \mathbb{R}^2$ and the admissible control $u : [0, t_f] \to \mathbb{U}$ be given. Moreover, define the function $\bar{f}(t, \boldsymbol{x}) : [0, t_f] \times \mathbb{R}^2 \to \mathbb{R}^2$ with $\bar{\boldsymbol{f}}(t, \boldsymbol{x}) = \boldsymbol{f}(\boldsymbol{x}, u(t))$. Then, each term in the gradient $\frac{\partial \bar{\boldsymbol{f}}}{\partial \boldsymbol{x}}(t, \boldsymbol{x}) = \begin{pmatrix} 0 & -1 \\ \frac{K_J(x_1)}{M} & 0 \end{pmatrix}$ is continuous in $\boldsymbol{x}$ implying that $\bar{\boldsymbol{f}}$ is locally Lipschitz with respect to its second argument. Moreover, since u is piecewise continuous the function $t \to \bar{\boldsymbol{f}}(t, \boldsymbol{y}(t))$ is also piecewise continuous for each continuous function $\boldsymbol{y} : D \to \mathbb{R}^2$. Consequently, we can first apply Theorem 4.22 from [34] to conclude that there exists a unique maximal solution $\boldsymbol{x} : I \to \mathbb{R}^2$ to the initial value problem

$$
\dot{\boldsymbol{x}}(t) = \bar{\boldsymbol{f}}(t, \boldsymbol{x}(t)), \boldsymbol{x}(0) = \boldsymbol{x}_0, \tag{B.3.3}
$$

where $I \subset [0, t_f]$ is the maximal interval of existence containing the origin. Moreover, making use of Prop. 5 it can be also shown that this interval must

be exactly equal to D. Indeed, by contradiction assume that the necessarily bounded interval I is not equal to D and set $\omega = \sup I$. Then, for each compact set S there must exist a scalar $\sigma \in I$ with $\sigma < \omega$ such that $\boldsymbol{x}(t) \notin S$ for each $t \in (\sigma, \omega)$, see Theorem 4.25 in [34]. Choose now as a compact set the set S_{E_b} in (5.1.6) with $\psi_{lb} = 0$ and $\psi_{ub} = \theta_{max} t_f$. In addition, fix the scalar $\sigma \in I$ and choose an arbitrary time $\bar{t} \in (\sigma, \omega)$. Then, the restriction of $\boldsymbol{x}$ to the interval $[0, \bar{t}]$ is a trajectory of Σ. This, however, leads to a contradiction since we have $\boldsymbol{x}(\bar{t}) \in S_{E_b}$ by (5.1.7). Consequently, $I = [0, t_f]$ and $\boldsymbol{x}$ is the unique trajectory of Σ which starts from $\boldsymbol{x}_0$ and corresponds to u. $\qquad\square$

Prop. 5 remains also valid, if we define admissible controls as Lebesgue measurable functions taking values in $\mathbb{U}$ almost everywhere (a.e.) and if we further define the corresponding trajectories as absolutely continuous functions satisfying a.e. the differential equation (2.1.4). Indeed, the proof of the proposition can also be used for this more general case if the integrals there are regarded as Lebesgue integrals. Consequently, based on our discussion in Sec. 5.1 we can apply Filippov's Theorem to conclude that for each $t_f > 0$ there exists an optimal measurable control minimizing the cost functional (2.3.1). In the following, we want to show how to use this fact together with PMP to prove Prop. 6. The proof will require the following lemma which is mainly an application of the Sturm Comparison Theorem and which can be used to find a lower and an upper bound for the number of times at which optimal controls must necessarily switch. The lemma will also be of importance in Appendix B.3.3 when we prove Prop. 15.

Lemma 44. *Let t_f be a positive scalar, $\Omega : [0, t_f] \to (0, \infty)$ a continuous function and $\boldsymbol{\lambda} : [0, t_f] \to (\mathbb{R}^2)^*$ the unique solution to the initial value problem*

$$\dot{\boldsymbol{\lambda}}(t) = \boldsymbol{\lambda}(t) \begin{pmatrix} 0 & 1 \\ -\Omega^2(t) & 0 \end{pmatrix}, \ \boldsymbol{\lambda}(0) = \boldsymbol{\lambda}_0, \tag{B.3.4}$$

with $\boldsymbol{\lambda}_0 \in (\mathbb{R}^2)^* \backslash \{0\}$. Moreover, let Ω_{min} and Ω_{max} denote the minimal and maximal values of Ω, respectively; i.e.

$$\Omega_{min} = \min_{t \in [0, t_f]} \Omega(t) \wedge \Omega_{max} = \max_{t \in [0, t_f]} \Omega(t). \tag{B.3.5}$$

Finally, let S_{t_S} denote the set

$$S_{t_S} = \{t \in (0, t_f) | \lambda_1(t) = 0\}.$$

Then, S_{t_S} is finite. Moreover, using $i \geq 0$ to denote the number of elements of S_{t_S} and introducing the scalars

$$i_{lb} = \max \left\{ 0, \left\lceil \frac{\Omega_{min} t_f}{\pi} \right\rceil - 2 \right\}, \tag{B.3.6}$$

and

$$i_{ub} = \left\lceil \frac{\Omega_{max} t_f}{\pi} \right\rceil + 1, \tag{B.3.7}$$

we have

$$i_{lb} \le i \le i_{ub}. \tag{B.3.8}$$

Proof. Let Ω and $\boldsymbol{\lambda}$ be two given functions satisfying the hypothesis of the proposition with $t_f > 0$ and $\boldsymbol{\lambda}_0 \ne \mathbf{0}$. Note that being a continuous function defined on a compact interval, the minimum and maximum values of Ω, i.e. Ω_{min} and Ω_{max}, both exist and they will also be positive since Ω only takes positive values. We will prove the proposition in five steps. Our arguments will resemble to those used in Chapter 2.2 of [3] where the zeros of functions solving a homogeneous second-order differential equation are analysed.

1. Zeros of λ_1 and λ_2 are isolated.

Let us first note that since the differential equation in (B.3.4) is linear and since $\boldsymbol{\lambda}_0$ is non-zero, we have the following relation for $\boldsymbol{\lambda}$:

$$(\forall t \in [0, t_f]) \left[\boldsymbol{\lambda}(t) \ne \mathbf{0} \right]. \tag{B.3.9}$$

Assume now that there exists a $\bar{t} \in [0, t_f]$ such that $\lambda_1(\bar{t}) = 0$. Then, by (B.3.4) $\dot{\lambda}_1(\bar{t})$ is equal to $-\Omega^2(\bar{t})\lambda_2(\bar{t})$ and this product is non-zero since $\Omega(\bar{t})$ is positive by definition and $\lambda_2(\bar{t}) \ne 0$ by (B.3.9). Noting that both Ω and λ_2 are continuous, this also means that there exists a sufficiently small $\varepsilon > 0$ such that $\operatorname{sgn}\left(\dot{\lambda}_1\right)$ is constant and non-zero on the interval $(\bar{t} - \varepsilon, \bar{t} + \varepsilon) \cap [0, t_f]$. Consequently, on this interval λ_1 will be strictly monotone and thus be equal to zero only at $t = \bar{t}$. This shows that the zeros of λ_1 are all isolated.

Similarly, assume that there exists a $\bar{t} \in [0, t_f]$ such that $\lambda_2(\bar{t}) = 0$. Then, by (B.3.4) and (B.3.9) we have $\dot{\lambda}_2(\bar{t}) = \lambda_1(\bar{t}) \ne 0$. Since λ_1 is continuous, this implies as above that $\bar{t}$ is an isolated zero of λ_2. Consequently, we conclude that the zeros of λ_2 are also all isolated.

2. The set of zeros of λ_2 is finite.

We want to show that the set S_{τ_S} given by

$$S_{\tau_S} = \{t \in [0, t_f] | \lambda_2(t) = 0\},$$

is finite. For this, let us first take the time-derivative of the second column of (B.3.4) which according to its first column leads to the following second-order differential equation for λ_2:

$$\ddot{\lambda}_2(t) + \Omega^2(t)\lambda_2(t) = 0. \tag{B.3.10}$$

We will next compare the location of the zeros of λ_2 with the location of the zeros of the function $y_{max} : [0, t_f] \to \mathbb{R}, t \to y_{max}(t) = \sin(\Omega_{max}t)$, which is a solution to the differential equation

$$\ddot{y}_{max}(t) + \Omega_{max}^2 y_{max}(t) = 0. \tag{B.3.11}$$

Using the zeros of y_{max}, let us introduce a partition of the set $[0, t_f) = \cup_{j=1}^{k_{max}} {}^j I_{max}$ with

$$k_{max} := \left\lceil \frac{\Omega_{max} t_f}{\pi} \right\rceil \geq 1, \tag{B.3.12}$$

and

$${}^j I_{max} := \begin{cases} \left[\frac{\Omega_{max}}{\pi}(j-1), \frac{\Omega_{max}}{\pi} j \right) & j < k_{max} \\ \left[\frac{\Omega_{max}}{\pi}(j-1), t_f \right) & j = k_{max} \end{cases}.$$

Fixing now a positive integer $j \in S_{k_{max}} \backslash \{0\}$, we can see that the restriction of λ_2 to the interval ${}^j I_{max}$ can not have more than one zero in that interval. Indeed, this clearly holds if this restriction is equal to a non-zero multiple of $y_{max}|_{{}^j I_{max}}$. More specifically, in this case $\lambda_2|_{{}^j I_{max}}$ has exactly one zero at $t = \frac{\Omega_{max}}{\pi}(j-1)$. Similarly, in case λ_2 is not a non-zero multiple of y_{max} in ${}^j I_{max}$, λ_2 can still not have more than one zero in ${}^j I_{max}$. To see this, assume first by contradiction that there exist two consecutive[2] zeros $\tilde{\tau}$ and $\bar{\tau}$ of λ_2 in ${}^j I_{max}$ with $\tilde{\tau} < \bar{\tau}$ and $\lambda_2(\tilde{\tau}) = \lambda_2(\bar{\tau}) = 0$. Then, since λ_2 is a non-trivial solution to (B.3.10) and since Ω_{max} is the maximum value of Ω, it follows from Sturm Comparison Theorem[3] that y_{max} must have at least one zero in $(\tilde{\tau}, \bar{\tau}) \subset (\frac{\Omega_{max}}{\pi}(j-1), \frac{\Omega_{max}}{\pi} j)$. This is, however, not possible by the definition of y_{max} and leads to a contradiction.

Our discussion above shows that for each $j \in S_{k_{max}} \backslash \{0\}$, there can exist at most one zero of λ_2 in the interval ${}^j I_{max}$. Noting that the union of all such intervals is equal to $[0, t_f)$, we can thus conclude that the number of elements of S_τ is bounded above by $k_{max} + 1$ and that this set is finite.

3. The set S_{t_S} is finite.

By contradiction, assume that the set S_{t_S} is not finite and let $\tilde{t}_1$ denote the infimum of this set, i.e. $\tilde{t}_1 = \inf S_{t_S}$. Since λ_1 is continuous and since the zeros of λ_1 are isolated, $\tilde{t}_1$ is then necessarily an element of S_{t_S}. Similarly, since S_{t_S} has infinitely many elements we can inductively build a strictly increasing sequence $(\tilde{t}_k)_{k \geq 1}$ in S_{t_S} using the following relation:

$$\tilde{t}_{k+1} = \inf\{t \in S_{t_S} | t > \tilde{t}_k\}. \tag{B.3.13}$$

Fixing now a $k \geq 1$, let us note that by the continuity of λ_1 and by the definition in (B.3.13), the sign of λ_1 must remain constant and non-zero on $(\tilde{t}_k, \tilde{t}_{k+1})$. Moreover, according to (B.3.4) and (B.3.9) both $\dot{\lambda}_1(\tilde{t}_k)$ and $\dot{\lambda}_1(\tilde{t}_{k+1})$ will be non-zero and must therefore differ in their signs. This also means that $\lambda_2 = -\frac{\dot{\lambda}_1}{\Omega^2}$ will have at least one zero in $(\tilde{t}_k, \tilde{t}_{k+1})$, since λ_2 is continuous. In fact, there exists exactly one zero of λ_2 in this interval. This follows directly from the fact that the sign of $\dot{\lambda}_2 = \lambda_1$ is always non-zero and constant on $(\tilde{t}_k, \tilde{t}_{k+1})$ so that λ_2 is strictly monotone on $[\tilde{t}_k, \tilde{t}_{k+1}]$.

Noting that there exists exactly one zero of λ_2 in $(\tilde{t}_k, \tilde{t}_{k+1})$, our assumption on the set S_{t_S} being infinite implies that the set of zeros of λ_2 is also infinite. We have thus reached a contradiction showing that the set S_{t_S} must be finite.

---

[2]Note that the zeros of λ_2 are all isolated as shown in the first step.
[3]See Theorem 2.10 in [3].

4. Between two consecutive zeros of λ_2 there exists exactly one zero of λ_1

Assume that $\bar{t}_1$ and $\bar{t}_2$ are two consecutive zeros of λ_2 with $\bar{t}_1 < \bar{t}_2$. Then, the sign of $\dot{\lambda}_1 = -\Omega^2 \lambda_2$ will remain constant on $(\bar{t}_1, \bar{t}_2)$ and λ_1 will be strictly monotone on $[\bar{t}_1, \bar{t}_2]$. Moreover, the sign of $\dot{\lambda}_2 = \lambda_1$ will be non-zero both at $\bar{t}_1$ and $\bar{t}_2$ according to (5.3.1). Consequently, the sign of $\dot{\lambda}_2$, and thus of λ_1, at these two times must be different in order for the sign of λ_2 to remain constant on $(\bar{t}_1, \bar{t}_2)$. This implies that λ_1 indeed has exactly one zero in $(\bar{t}_1, \bar{t}_2)$.

5. The number of elements of S_{t_S} is bounded by i_{lb} and i_{ub}.

Let $i \geq 0$ denote the number of elements of the set S_{t_S}, which we know is finite. Moreover, let i_{lb} and i_{ub} be defined as in (B.3.6) and (B.3.7). We want to first show that $i \leq i_{ub}$.

If $i \in \{0, 1\}$, the inequality $i \leq i_{ub}$ clearly holds since we have $i_{ub} \geq 2$ according to (B.3.7). Let us now assume that $i \geq 2$ and set $\tilde{t}_1$ to $\inf S_{t_S}$. Furthermore, use (B.3.13), with $k \in \{1, \ldots, i-1\}$, to determine all the other elements of the set S_{t_S}. Following the arguments used in the third step, we can then see that for each $k \in \{1, \ldots, i-1\}$ there exists exactly one zero of λ_2 in the interior of the interval $[\tilde{t}_k, \tilde{t}_{k+1}]$. Consequently, there exists exactly $i-1$ zeros of λ_2 in the interior of the interval $[\tilde{t}_1, \tilde{t}_i]$ which is a strict subset of $(0, t_f)$. Recall now that in our discussion in the second step we have shown that the number of zeros of λ_2 in the interval $[0, t_f)$ is bounded above by k_{max}. This leads then as desired to the inequality $i \leq k_{max} + 1 = i_{ub}$.

In order to show that $i \geq i_{lb}$, let us note that for $t_f \in (0, \frac{2\pi}{\Omega_{min}}]$ this inequality is always satisfied as in this case we have $i_{lb} = 0$, see (B.3.6). Assume now that $t_f > \frac{2\pi}{\Omega_{min}}$ and introduce the function $y_{min} : [0, t_f] \to \mathbb{R}, t \to y_{min}(t) = \sin(\Omega_{min} t)$ which solves the differential equation

$$\ddot{y}(t) + \Omega_{min}^2 y(t) = 0.$$

Furthermore, introduce the partition of the interval $[0, t_f) = \cup_{j=1}^{k_{min}} {}^j I_{min}$ with

$$k_{min} := \left\lceil \frac{\Omega_{min} t_f}{\pi} \right\rceil \geq 3, \tag{B.3.14}$$

and

$${}^j I_{min} := \begin{cases} \left[\frac{\Omega_{min}}{\pi}(j-1), \frac{\Omega_{min}}{\pi}j\right) & j < k_{min} \\ \left[\frac{\Omega_{min}}{\pi}(j-1), t_f\right) & j = k_{min} \end{cases}.$$

Fixing now, as in the second step, the integer $j \in S_{k_{min}} \setminus \{0, k_{min}\}$ we can see that the restriction of λ_2 to the interval ${}^j I_{min}$ must have at least one zero in that interval. Indeed, this clearly holds if this restriction is equal to a non-zero multiple of $y_{min}|_{{}^j I_{min}}$. More specifically, in this case $\lambda_2|_{{}^j I_{min}}$ has exactly one zero at $t = \frac{\Omega_{min}}{\pi}(j-1)$. Similarly, in case λ_2 is not a non-zero multiple of y_{min} in ${}^j I_{min}$, λ_2 must still have at least one zero in ${}^j I_{min}$. This follows from Sturm Comparison Theorem, since λ_2 is a non-trivial solution to (B.3.10) and since Ω_{min} is the minimum value of Ω. Based on our discussion, we can thus now see

that the zeros of λ_2 in $[0, t_f]$ must be greater than or equal to $k_{min} - 1$ which under our assumption on t_f is equal to $i_{lb} + 1$, see (B.3.6). Since there is a zero of λ_1 between every two consecutive zeros of λ_2, as we have shown in the fourth step, this then leads to the inequality $i \geq i_{lb}$ as desired. $\qquad\square$

Using Lemma 44, we can now prove Prop. 6 as follows.

Proof of Prop. 6. Let $t_f > 0$ be an arbitrary scalar, $D = [0, t_f]$ and $u : D \to \mathbb{U}$ be the measurable control which minimizes the cost functional in (2.3.1) and whose existence is ensured by Filippov's Theorem. Moreover, let $\boldsymbol{x}$ be the absolutely continuous function defined on D such that $\boldsymbol{x}_0$ is the origin and the pair $(\boldsymbol{x}, u)$ satisfies a.e. the differential equation (2.1.4). Since u is an optimal control, it follows then from PMP that Prop. 7 still remains valid for $(\boldsymbol{x}, u)$, if we relax the second and third conditions, i.e. (5.2.2) and (5.2.4), such that they hold a.e. in D. Let $\boldsymbol{\lambda}$ denote the corresponding continuously differentiable costate from Prop. 7 which satisfies the differential equation (5.2.1). By introducing the continuous function $\Omega : D \to (0, \infty), t \to \Omega(t) = \sqrt{\frac{K_J(x_1(t))}{M}}$ and noting further that $\boldsymbol{\lambda}(t_f) \neq \boldsymbol{0}$ holds due to (5.2.5), we can then see that $\boldsymbol{\lambda}$ will solve the initial value problem in (B.3.4) with $\boldsymbol{\lambda}_0 \neq \boldsymbol{0}$. Consequently, we can apply the results from Lemma 44.

According to Lemma 44, the set of zeros of λ_1 in D, which we will denote by E, is finite. This means that the relation in (5.2.6) will uniquely determine a control $u_{PC} : D \to \mathbb{U}$ in the space $\mathcal{PC}_{\mathbb{U}}$. Furthermore, from the properties of the set E and the condition (5.2.2) it follows that $u(t)$ and $u_{PC}(t)$ are equal to each other a.e. in D. Therefore, $(\boldsymbol{x}, u_{PC})$ is an admissible controlled trajectory of Σ and u_{PC} is a solution to the LVMP as defined in Sec. 2.3. $\qquad\square$

B.3.2 Basic Properties

Minimum Principle

Proof of Prop. 8. Let $\Lambda = (\boldsymbol{x}, u, \boldsymbol{\lambda}, \lambda_a)$ be an extremal lift satisfying the hypothesis of the lemma. We want to first show that the first costate λ_1 can never be equal to zero in a finite time interval. To show this, we will prove that the time-derivative of λ_1 is non-zero whenever λ_1 equals to zero.

Assume that t_S is an element of D such that $\lambda_1(t_S) = 0$. According to (5.2.1), $\dot{\lambda}_1(t_S)$ is then given by the product $-\frac{K_J(x_1(t_S))}{M}\lambda_2(t_S)$. Due to our assumption on the SDP K_J the first term of this product is always negative. Moreover, $\lambda_2(t_S)$ must be non-zero since otherwise we would have $\boldsymbol{\lambda} \equiv \boldsymbol{0}$ due to the linearity of the costate dynamics in (5.2.1) which in turn would contradict the transversality condition (5.2.5) and thus the fact that Λ is an extremal lift. Being a product of a negative and a non-zero term, we can finally conclude that $\dot{\lambda}_1(t_S) \neq 0$ holds.

Based on our discussion above, it follows now from (5.2.6) that u is a switching control and satisfies (5.2.8) with $\dot{\lambda}_1(0) \neq 0$ in case $\lambda_1(0) = 0$. Moreover, if $t_S \in (0, t_f)$ is a switching time of u it follows from that same relation that $\lambda_1(t_S)$

must be equal to zero. Conversely, if $\lambda_1(t_S)$ is equal to zero it follows from the inequality $\dot{\lambda}_1(t_S) \neq 0$ that u will have a switching at t_S. The equality (5.2.9) follows then from (5.2.3)-(5.2.4) if we additionally use the relation between $\dot{\lambda}_1$ and λ_2 in (5.2.1) together with the fact that K_J is always positive.

In order to prove the last statement of the proposition, i.e. (5.2.10), let us first assume that i is an arbitrary non-negative integer. Then, by evaluating the Hamiltonian function in (5.2.4) at the final time $t_f = t_{S,i+1}$ and using (5.2.5) we can arrive at the following relation for $^{i+1}x_1$:

$$\tau_J(^{i+1}x_1) = \frac{M}{v}\lambda_a \geq 0. \tag{B.3.15}$$

This shows that the sign of $^{i+1}x_1$ is equal to $\lambda_a \in \{0,1\}$ and also proves (5.2.10) for the case when $i = 0$. Let us now assume that $i > 0$. If $\lambda_a = 0$, it follows directly from (5.2.9) and (B.3.15) that (5.2.10) is true. We will conclude the proof of the proposition by using the principle of mathematical induction to show that (5.2.10) also holds when $\lambda_a = 1$.

Let $\bar{k} \in S_{i+1}\backslash\{0\}$ and assume that we have $\text{sgn}(^{\bar{k}}x_1) = (-1)^{\bar{k}+i+1}$. Moreover, by contradiction assume that $\text{sgn}(^{\bar{k}-1}x_1) \neq 0$ has the same sign as $\text{sgn}(^{\bar{k}}x_1)$. Evaluating (5.2.9) once at $t_{S,\bar{k}-1}$ and once at $t_{S\bar{k}}$, we will then have $\text{sgn}(^{\bar{k}-1}\dot{\lambda}_1) = \text{sgn}(^{\bar{k}}\dot{\lambda}_1) \neq 0$. This, however, leads to a contradiction since λ_1 never changes its sign in $(t_{S,\bar{k}-1}, t_{S,\bar{k}})$ and is always non-zero. Consequently, $\text{sgn}(^{\bar{k}-1}x_1) = (-1)^{\bar{k}+i}$ and since we also have (B.3.15) it follows from induction that (5.2.10) is true when $\lambda_a = 1$. $\qquad\square$

Costates with $u \in \mathcal{S}_\mathbb{U}$ In this part of the appendix, we will show how to derive Prop. 9 which establishes a link between the solutions to the ordinary differential equation (5.2.1) and the solutions to the partial differential equation (5.2.12). For this, we will first state two lemmas which clarify the properties of solutions of (5.2.12). The mathematical expressions provided there are also made use of in Sec. 5.2.2 when constructing the trajectories of the costates, see Table 5.1.

Lemma 45. *Let* $\eta(x, \phi_{max}) : D_{T_\phi} \to \mathbb{R}$ *be a solution to the partial differential equation (5.2.12). Then, we have*

$$\eta(x, \phi_{max}) = \frac{|\dot{\phi}|(x, \phi_{max})}{\dot{\phi}_{max}}\left[\eta(0, \phi_{max}) + \right.$$
$$\left. \eta_c \frac{M\dot{\phi}_{max}}{\tau_J(\phi_{max})}\frac{\partial T_\phi}{\partial \phi_{max}}(x, \phi_{max})\right], \tag{B.3.16}$$

for each $(x, \phi_{max}) \in D_{T_\phi}$.

Proof. Assume that η is a solution to (5.2.12). Fixing an arbitrary $\bar{\phi}_{max} \in (0, \infty)$, we can then define a function $\bar{\eta} : (-\bar{\phi}_{max}, \bar{\phi}_{max}) \to \mathbb{R}$ such that $\bar{\eta}(x) =$

$\eta(x, \bar{\phi}_{max})$ holds at each $x \in (-\bar{\phi}_{max}, \bar{\phi}_{max})$. According to (5.2.12), this function satisfies the following first-order linear differential equation:

$$\frac{\mathrm{d}\bar{\eta}}{\mathrm{d}x} + \bar{a}(x)\bar{\eta} - \bar{b}(x) = 0, \tag{B.3.17}$$

where $\bar{a} : (-\bar{\phi}_{max}, \bar{\phi}_{max}) \to \mathbb{R}$ and $\bar{b} : (-\bar{\phi}_{max}, \bar{\phi}_{max}) \to \mathbb{R}$ are given by

$$\bar{a}(x) = \frac{\tau_J(x)}{2 \int_x^{\bar{\phi}_{max}} \tau_J(s)\mathrm{d}s}, \tag{B.3.18}$$

and

$$\bar{b}(x) = -\frac{\eta_c}{\left(|\dot{\phi}|(x, \bar{\phi}_{max})\right)^2}, \tag{B.3.19}$$

respectively. It is important to note here that $\bar{a}$ and $\bar{b}$ are both continuous functions. Consequently, we can solve (B.3.17) to express $\bar{\eta}$ in terms of these two functions together with the value of $\bar{\eta}$ at $x = 0$, i.e. $\bar{\eta}(0)$. Indeed, making use of the integrating factor $\bar{\mu} : (-\bar{\phi}_{max}, \bar{\phi}_{max}) \to (0, \infty)$ with

$$\bar{\mu}(x) = e^{\int_0^x \bar{a}(s)\mathrm{d}s}, \tag{B.3.20}$$

we can show that $\bar{\eta}$ is given by [8]:

$$\bar{\eta}(x) = \frac{\bar{\eta}(0) + \int_0^x \bar{\mu}(s)\bar{b}(s)\mathrm{d}s}{\bar{\mu}(x)}, \tag{B.3.21}$$

where $x \in (-\bar{\phi}_{max}, \bar{\phi}_{max})$.

Based on our discussion so far, we now know that for each $x \in (-\bar{\phi}_{max}, \bar{\phi}_{max})$, $\bar{\eta}(x)$ and thus $\eta(x, \bar{\phi}_{max})$ are given by the expression on the right-hand side of (B.3.21). In order to prove the lemma, we next show that this expression is exactly equal to the expression on the right-hand side of (B.3.16) if ϕ_{max} is set to $\bar{\phi}_{max}$.

Let us introduce the function $\bar{y} : (-\bar{\phi}_{max}, \bar{\phi}_{max}) \to (0, \infty)$ with $\bar{y}(x) = \int_x^{\bar{\phi}_{max}} \tau_J(\phi)\mathrm{d}\phi$. Using this function, we can apply a change of variables when evaluating the integral in (B.3.20) which in turn leads to a simplified expression for the integrating factor $\bar{\mu}$ as follows:

$$\begin{aligned}
\bar{\mu}(x) &= e^{\int_0^x \frac{\tau_J(s)}{2\bar{y}(s)}\mathrm{d}s} = e^{-\int_{\bar{y}(0)}^{\bar{y}(x)} \frac{\mathrm{d}s}{2s}} \\
&= \sqrt{\frac{\bar{y}(0)}{\bar{y}(x)}} = \sqrt{\frac{M\dot{\phi}_{max}^2}{2 \int_x^{\bar{\phi}_{max}} \tau_J(\phi)\mathrm{d}\phi}} \\
&= \frac{\dot{\phi}_{max}}{|\dot{\phi}|(x, \bar{\phi}_{max})}, \tag{B.3.22}
\end{aligned}$$

where $x \in (-\bar{\phi}_{max}, \bar{\phi}_{max})$ and $\dot{\phi}_{max} := |\dot{\phi}|(0, \bar{\phi}_{max})$. If we now substitute this new expression for $\bar{\mu}$ into (B.3.21) and use (B.3.18)-(B.3.19), we can find a

new expression for $\bar{\eta}$ as well. It is easily seen that this expression is, as desired, exactly equal to the expression on the right-hand side of (B.3.16) if $\phi_{max} = \bar{\phi}_{max}$ holds in the latter expression. Noting that our choice for $\bar{\phi}_{max}$ was arbitrary, we can finally conclude from the definition of $\bar{\eta}$ that (B.3.16) holds for each $(x, \phi_{max}) \in D_{T_\phi}$. $\qquad\square$

Having shown how to describe the solution of (5.2.12) in terms of physical quantities, we discuss in the following lemma the behaviour of this solution at the boundaries of its domain.

Lemma 46. *Let $\eta : D_{T_\phi} \to \mathbb{R}$ be a solution of (5.2.12) and ϕ_{max} an arbitrary positive scalar. Moreover, let ϕ_b a boundary point of the interval $D_\phi = (-\phi_{max}, \phi_{max})$. Then, the following equalities hold[4]:*

$$\lim_{D_\phi \ni x \to \phi_b} \eta(x, \phi_{max}) = -\operatorname{sgn}(\phi_b) \frac{M\eta_c}{\tau_J(\phi_{max})}, \qquad (B.3.23)$$

and

$$\lim_{D_\phi \ni x \to \phi_b} \frac{\frac{\partial \eta}{\partial x}(x, \phi_{max})}{\frac{1}{|\dot{\phi}|(x, \phi_{max})}} = -\frac{\eta_c}{4} \frac{\mathrm{d}T_p}{\mathrm{d}\phi_{max}}(\phi_{max})$$

$$- \operatorname{sgn}(\phi_b) \frac{\eta(0, \phi_{max})}{\frac{M\dot{\phi}_{max}}{\tau_J(\phi_{max})}}. \qquad (B.3.24)$$

Proof. Let η, ϕ_{max}, D_ϕ and ϕ_b all satisfy the hypotheses of the lemma. Since η is a solution to (5.2.12), we know by Lemma 45 that $\eta(x, \phi_{max})$ satisfies the equality in (B.3.16) for each $x \in D_\phi$. Taking the limit of both sides of this equality as $D_\phi \ni x \to \phi_b$ we then get

$$\lim_{D_\phi \ni x \to \phi_b} \eta(x, \phi_{max}) = \frac{M\eta_c}{\tau_J(\phi_{max})} \lim_{D_\phi \ni x \to \phi_b} \left\{ |\dot{\phi}|(|x|, \phi_{max}) \cdot \right.$$

$$\left. \operatorname{sgn}(x) \frac{\partial T_\phi}{\partial \phi_{max}}(|x|, \phi_{max}) \right\}$$

$$\overset{(3.2.14)}{=} \frac{M\eta_c \operatorname{sgn}(\phi_b)}{\tau_J(\phi_{max})} \lim_{x \to \phi_{max}^-} -\frac{\tau_J(\phi_{max})}{\tau_J(x)}$$

$$= -\operatorname{sgn}(\phi_b) \frac{M\eta_c}{\tau_J(\phi_{max})},$$

where we have made use of the symmetry properties of $|\dot{\phi}|$ and $\frac{\partial T_\phi}{\partial \phi_{max}}$ together with the fact that in (3.2.14) both ϕ_s and $\dot{\phi}_s$ can take arbitrary values as long as they are positive and satisfy $E_{MSS}(\phi_s, \dot{\phi}_s) = E_{pot}(\phi_{max})$ and $\dot{\phi}_s = |\dot{\phi}|(\phi_s, \phi_{max})$. This proves the equality (B.3.23).

---

[4]Given a nonempty subset $E \subset \mathbb{R}$ and a function $g : E \to \mathbb{R}$, $\lim_{E \ni x \to y} g(x)$ denotes the limit of this function as x goes to y in the set E, see [62].

In order to prove the equality (B.3.24), let us first note that η is a solution to (5.2.12) so that the following relation holds for the ratio $\frac{\frac{\partial \eta}{\partial x}(x, \phi_{max})}{\frac{1}{|\dot{\phi}|(x,\phi_{max})}}$ at each $x \in D_\phi$:

$$\frac{\frac{\partial \eta}{\partial x}(x, \phi_{max})}{\frac{1}{|\dot{\phi}|(x,\phi_{max})}} = -\frac{\left[\eta(x, \phi_{max})\frac{\tau_J(x)}{M} + \eta_c\right]}{|\dot{\phi}|(x, \phi_{max})}. \tag{B.3.25}$$

If we now substitute the expression in (B.3.16) for η into (B.3.25) and make use of the symmetry properties of $|\dot{\phi}|, \frac{\partial T_\phi}{\partial \phi_{max}}$ and τ_J, we can rewrite (B.3.25) as follows:

$$\frac{\frac{\partial \eta}{\partial x}(x, \phi_{max})}{\frac{1}{|\dot{\phi}|(x,\phi_{max})}} = -\frac{\tau_J(|x|)\eta_c}{\tau_J(\phi_{max})} \cdot \left[\frac{\partial T_\phi}{\partial \phi_{max}}(|x|, \phi_{max})+\right.$$
$$\left. \frac{\tau_J(\phi_{max})}{\tau_J(|x|) \cdot |\dot{\phi}|(|x|, \phi_{max})}\right] - \text{sgn}(x)\frac{\eta(0, \phi_{max})}{\frac{M\dot{\phi}_{max}}{\tau_J(|x|)}}. \tag{B.3.26}$$

Finally, taking the limit of (B.3.26) as $D_\phi \ni x \to \phi_b$ and using (3.2.14), we can see that (B.3.24) holds as desired. $\qquad\square$

With Lemmas 45-46, we can now finally prove Prop. 9.

Proof of Prop. 9. Let $\boldsymbol{x}, u, i, \boldsymbol{\lambda}, \eta, \eta_c, k, v_\phi$ and $\bar{D}_k = (\bar{t}_{k,0}, \bar{t}_{k,f}) \subset D_k$ all satisfy the hypotheses of the proposition and assume further that there exists a $\bar{t} \in \bar{D}_k$ such that both $\lambda_2(\bar{t}) = \eta\left(x_1(\bar{t}), {}^k\phi_{max}\right)$ and $\mathbb{H}\left(\boldsymbol{x}(\bar{t}), u(\bar{t}), \boldsymbol{\lambda}(\bar{t})\right) = -\eta_c$ hold. From our results in Chapter 4, we know first of all that $\dot{x}_1$ will be continuous in $\bar{D}_k$. Moreover, according to (5.2.13) the sign of $\dot{x}_1$ will remain constant and non-zero in that time interval. Consequently, the restriction of the first state on $\bar{D}_k$, i.e. $x_1|_{\bar{D}_k}$, will be a $\mathcal{C}^1-$diffeomorphism with a well-defined inverse $x_1|_{\bar{D}_k}^{-1}$. Finally, since $\dot{x}_1$ is non-zero the system's relative energy in $\bar{D}_k$ and thus ${}^k\phi_{max}$ will be positive.

In order to prove the proposition, we want to first show that the Hamiltonian $\mathbb{H}\left(\boldsymbol{x}(t), u(t), \boldsymbol{\lambda}(t)\right)$ is constant in the time interval $\bar{D}_k$. For this, let us introduce the function $h_k(t) : D_k \to \mathbb{R}$ with

$$h_k(t) = \mathbb{H}\left(\boldsymbol{x}(t), {}^ku, \boldsymbol{\lambda}(t)\right) = \boldsymbol{\lambda}(t)\boldsymbol{f}(\boldsymbol{x}(t), {}^ku). \tag{B.3.27}$$

Taking the time-derivative of this function, it follows then from (2.1.4),(5.2.1) and (5.2.3) that we have for each $t \in D_k$

$$\begin{aligned}
\dot{h}_k(t) &= \frac{\partial \mathbb{H}}{\partial \boldsymbol{x}}\left(\boldsymbol{x}(t), {}^ku, \boldsymbol{\lambda}(t)\right)\boldsymbol{f}\left(\boldsymbol{x}(t), {}^ku\right) \\
&+ \frac{\partial \mathbb{H}}{\partial \boldsymbol{\lambda}}\left(\boldsymbol{x}(t), {}^ku, \boldsymbol{\lambda}(t)\right)\dot{\boldsymbol{\lambda}}^T\left(\boldsymbol{x}(t), \boldsymbol{\lambda}(t)\right) \\
&= \boldsymbol{\lambda}(t)\frac{\partial \boldsymbol{f}}{\partial \boldsymbol{x}}\left(\boldsymbol{x}(t), {}^ku\right)\boldsymbol{f}\left(\boldsymbol{x}(t), {}^ku\right) \\
&- \boldsymbol{f}^T\left(\boldsymbol{x}(t), {}^ku\right)\frac{\partial \boldsymbol{f}^T}{\partial \boldsymbol{x}}\left(\boldsymbol{x}(t), {}^ku\right)\boldsymbol{\lambda}^T(t) \\
&= 0. \tag{B.3.28}
\end{aligned}$$

According to (B.3.28), we can now see that the Hamiltonian is indeed constant on $\bar{D}_k$. Consequently, our assumption on the value of the Hamiltonian at $\bar{t}$ implies that the following equality holds at each $t \in \bar{D}_k$:

$$\lambda_1(t)\dot{x}_1(t) + \lambda_2(t)\frac{\tau_J(x_1(t))}{M} + \eta_c = 0. \tag{B.3.29}$$

In the following, we will make use of this last equality to show that $\boldsymbol{\lambda}$ and η are related to each other as given by (5.2.15).

Without loss of generality, let us assume that x_1 is strictly increasing[5] on $\bar{D}_k$, i.e. $\dot{x}_1(t) > 0$ for each $t \in \bar{D}_k$. We can then define a function $\bar{\eta} : \bar{E}_k \to \mathbb{R}$ with $\bar{E}_k := (x_1(\bar{t}_{k,0}), x_1(\bar{t}_{k,f}))$ and

$$\bar{\eta}(x) = \lambda_2\left(x_1|_{\bar{D}_k}^{-1}(x)\right). \tag{B.3.30}$$

From the inverse function theorem and the chain rule, it follows that this function is differentiable with its derivative $\frac{\mathrm{d}\bar{\eta}}{\mathrm{d}x} : \bar{E}_k \to \mathbb{R}$ given by

$$\frac{\mathrm{d}\bar{\eta}}{\mathrm{d}x}(x) = \frac{\lambda_1\left(x_1|_{\bar{D}_k}^{-1}(x)\right)}{\dot{x}_1\left(x_1|_{\bar{D}_k}^{-1}(x)\right)}. \tag{B.3.31}$$

Notice that using the equalities $t = x_1|_{\bar{D}_k}^{-1}(x)$ and $\dot{x}_1(t) = |\dot{\phi}|(x, {}^k\phi_{max})$ together with (B.3.30)-(B.3.31), (B.3.29) can now be rewritten such that it becomes an equality depending only on x. More specifically, the resulting expression will be a differential equation for the function $\bar{\eta}$ which is given by

$$\left(|\dot{\phi}|(x, {}^k\phi_{max})\right)^2 \frac{\mathrm{d}\bar{\eta}}{\mathrm{d}x} + \frac{\tau_J(x)}{M}\bar{\eta} + \eta_c = 0, \tag{B.3.32}$$

with $x \in \bar{E}_k$.

It is important to remark here that the condition (5.2.13) ensures that $\bar{E}_k$ is a subset of $(-{}^k\phi_{max}, {}^k\phi_{max})$. Consequently, the coefficient of $\frac{\mathrm{d}\bar{\eta}}{\mathrm{d}x}$ in (B.3.32) remains non-zero. Being a first-order linear differential equation with coefficients that are continuous in x, $\bar{\eta}(x)$ is therefore the unique solution of (B.3.32) which attains the value $\lambda_2(\bar{t})$ at $x_1(\bar{t}) \in \bar{E}_k$, see (B.3.30). Comparing now (5.2.12) and (B.3.32), we can see that $\eta(x, {}^k\phi_{max})$ is also uniquely determined by the value of $\lambda_2(\bar{t})$ and equals to $\bar{\eta}(x)$ for each $x \in \bar{E}_k$. The equality in (5.2.15) follows finally from this relation between η and $\bar{\eta}$, (B.3.30)-(B.3.32) and the equality $\dot{x}_1(t) = v_\phi \cdot |\dot{\phi}|(x_1(t), {}^k\phi_{max})$.

To prove the remaining part of the proposition, let $\bar{t}_b$ be a boundary point of $\bar{D}_k$. It follows then from the continuity of $\boldsymbol{\lambda}$ that $\boldsymbol{\lambda}(\bar{t}_b)$ is given by the limit of the right-hand side of (5.2.15) as t goes to $\bar{t}_b$ in the set $\bar{D}_k$. Moreover, if $\lim_{\bar{D}_k \ni t \to \bar{t}_b} \dot{x}_1(\bar{t}_b)$ is non-zero it follows from the continuity properties of $x_1, \dot{x}_1, \tau_J$ and η that this limit can be directly obtained by evaluating

---

[5]The proof for the other case, where x_1 is strictly decreasing, can be done using the exact same arguments, if we define $\bar{E}_k$ as the interval $\left(x_1(\bar{t}_{k,f}), x_1(\bar{t}_{k,0})\right)$ and note that $\dot{x}_1(t)$ is given this time by the negative of $|\dot{\phi}|\left(x_1(t), {}^k\phi_{max}\right)$ for each $t \in \bar{D}_k$.

(5.2.15) at $t = \bar{t}_b$. Let us now assume that $\lim_{\bar{D}_k \ni t \to \bar{t}_b} \dot{x}_1(\bar{t}_b) = 0$ and let $\bar{x}_{1b} \in \{-{}^k\phi_{max}, {}^k\phi_{max}\}$ denote the deflection value attained at $\bar{t}_b$. Making use of (B.3.30)-(B.3.31) together with $x = x_1|_{\bar{D}_k}(t)$ and $t = x_1|_{\bar{D}_k}^{-1}(x)$, the desired limit can then be rewritten in this case as follows:

$$
\begin{aligned}
\lim_{\bar{D}_k \ni t \to \bar{t}_b} \boldsymbol{\lambda}(t) &= \lim_{\bar{D}_k \ni t \to \bar{t}_b} \left(\begin{array}{c} \frac{\partial \eta}{\partial x}(x_1(t), {}^k\phi_{max})\dot{x}_1(t) \\ \eta(x_1(t), {}^k\phi_{max}) \end{array} \right)^T \\
&= \lim_{\bar{E}_k \ni x \to \bar{x}_{1b}} \left(\begin{array}{c} v_\phi \frac{\frac{\partial \eta}{\partial x}(x, {}^k\phi_{max})}{|\dot{\phi}|(x, {}^k\phi_{max})} \\ \eta(x, {}^k\phi_{max}) \end{array} \right)^T.
\end{aligned}
$$

Finally, it follows from Lemma 46 that the last limit above is equal to (5.2.16).
□

Switching and Terminal State Conditions

Lemma 47. *Let $\Lambda = (\boldsymbol{x}, u, \boldsymbol{\lambda}, \lambda_a)$ be an extremal lift for the LVMP and u a control with $i \geq 0$ switchings. Moreover, let $k \in S_i$ such that ${}^k E_{rel} > 0$ and $j \in S_{m_k}$. Then, for each $t \in [t_{S,k_j}, t_{S,k_{j+1}}]$ we have*

$$
\lambda_1(t) = \lim_{D_{k_\phi} \backslash \{0\} \ni x \to x_1(t)} \frac{\left[\lambda_a C(x, {}^k\phi_{max}) - {}^k\eta_{0,j} \right] \tau_J(x)}{{}^k v_{\phi,j} M \, {}^k\dot{\phi}_{max}}, \tag{B.3.33}
$$

where $D_{k_\phi} = (-{}^k\phi_{max}, {}^k\phi_{max})$.

Proof. Let $\Lambda, i, k, {}^k E_{rel}$ and j all satisfy the hypotheses of the lemma. Furthermore, let $t \in [t_{S,k_j}, t_{S,k_{j+1}}]$. Since ${}^k E_{rel}$ is positive, ${}^k\phi_{max}$ is also positive and we have $|x_1(t)| \leq {}^k\phi_{max}$. Moreover, the sign of $\dot{x}_1$ in D_{k_j} is non-zero and constant so that we can always find a non-empty open time interval $\bar{D}_{k_j} \subset D_{k_j}$ such that t is a boundary point of $\bar{D}_{k_j}$ and the following relation holds:

$$
\left(\forall \tilde{t} \in \bar{D}_{k_j} \right) \left[|x_1(\tilde{t})| < {}^k\phi_{max} \wedge x_1(\tilde{t}) \neq 0 \right].
$$

The set $\{x_1(\tilde{t}) | \tilde{t} \in \bar{D}_{k_j}\} \subset D_{k_\phi}$ will then also be a non-empty open interval with $x_1(t)$ being one of its boundary points. Using now (5.2.15) in Prop. 9 together with the expression for the function η in Table 5.1a we can see that the following equality will hold for each $\tilde{t} \in \bar{D}_{k_j}$:

$$
\lambda_1(\tilde{t}) = \frac{\left[\lambda_a C \left(x_1(\tilde{t}), {}^k\phi_{max} \right) - {}^k\eta_{0,j} \right] \tau_J \left(x_1(\tilde{t}) \right)}{{}^k v_{\phi,j} M \, {}^k\dot{\phi}_{max}}. \tag{B.3.34}
$$

Notice that if on the right-hand side of (B.3.34) we set $x_1(\tilde{t})$ to x, the resulting expression becomes a continuous function of x which is defined on the set $D_{k_\phi} \backslash \{0\}$. Furthermore, for each boundary point ϕ_b of this set, i.e. for $\phi_b \in \{-{}^k\phi_{max}, 0, {}^k\phi_{max}\}$, the limit of the function as x approaches ϕ_b exists and is finite[6]. Clearly, since λ_1 is a continuous function $\lambda_1(t)$ will be equal to

---

[6]This directly follows from the definition of the function C and its properties, see (5.2.23), (5.2.27) and (5.2.30).

the limit $\lim_{\bar{D}_{k_j} \ni \tilde{t} \to t} \lambda_1(\tilde{t})$. It follows then from the equality in (B.3.34), the properties of its right-hand side just discussed and the continuity of x_1, that this limit is equal to the limit on the right-hand side of (B.3.33) as desired. $\qquad\square$

Proof of Prop. 10. Let $\Lambda, i, k, {}^k E_{rel}, j, t, \phi$ and S_{ϕ_b} all satisfy the hypotheses of the proposition. We will only prove the part of the proposition which gives a sufficient and necessary condition for t_{S,k_j} to be a switching time and which further provides the deflection value attained at such a time. The remaining part of the proposition can be proved very similarly and is omitted for brevity[7].

Let us first assume that t_{S,k_j} is the k'th switching time. By definition, we have then $k > 0, x_1(t_{S,k_j}) = {}^k x_1$ and $\mathrm{sgn}(\phi - {}^k x_1) = {}^k v_{\phi,j}$. We will next show that ${}^k x_1$ is an element of S_ϕ. First of all, notice that $|{}^k x_1| \leq {}^k \phi_{max}$ always holds. Furthermore, by Prop. 8 the first costate λ_1 is zero at t_{S,k_j}. Consequently, applying Lemma 47 and using the fact that $\lim_{D_{k_\phi} \setminus \{0\} \ni x \to s} \frac{s}{\tau_J(s)}$ is positive for each $s \in [-{}^k \phi_{max}, {}^k \phi_{max}]$, we can arrive at the following relation:

$$\lim_{D_{k_\phi} \setminus \{0\} \ni x \to {}^k x_1} \left[{}^k \eta_{0,j} - \lambda_a C(x, {}^k \phi_{max}) \right] x = 0. \tag{B.3.35}$$

With (B.3.35) we can finally conclude that ${}^k x_1 \in S_\phi$.

Conversely, assume that $k > 0$ and that there exists a $\phi_b \in S_{\phi_b}$ such that $\mathrm{sgn}(\phi - \phi_b) = {}^k v_{\phi,j}$. By contradiction, assume further that t_{S,k_j} is not a switching time. Then, $\lambda_1(\tilde{t})$ must be non-zero for each $\tilde{t} \in [t_{S,k_j}, t]$ and $x_1(t_{S,k_j})$ must be equal to $-{}^k v_{\phi,j} {}^k \phi_{max}$. Moreover, since we have $|\phi_b| \leq {}^k \phi_{max}$ and since $x_1|_{[t_{S,k_j}, t]}$ is a strictly monotone and continuous function, there must exist a time $t_b \in [t_{S,k_j}, t)$ such that $x_1(t_b) = \phi_b$. This, however, implies according to (5.2.24) and Lemma 47 that $\lambda_1(t_b)$ must be equal to zero and thus leads to a contradiction.

To conclude the proof, we need to now show that (5.2.25) holds if t_{S,k_j} is a switching time. For this, let us first note that λ_1 is always non-zero in D_{k_j}. Consequently, following the arguments we used to derive (B.3.35) we obtain the following inequality which holds at each $\tilde{t} \in D_{k_j}$:

$$\lim_{D_{k_\phi} \setminus \{0\} \ni x \to x_1(\tilde{t})} \left[{}^k \eta_{0,j} - \lambda_a C(x, {}^k \phi_{max}) \right] x \neq 0. \tag{B.3.36}$$

Assuming from now on that t_{S,k_j} is a switching time, recall that in this case ${}^k x_1$ is an element of S_ϕ. If now ${}^k v_{\phi,j} = -1$, the non-empty open interval $(\phi, {}^k x_1)$ will be a subset of the image of $x_1|_{D_{k_j}}$. According to (5.2.24) and (B.3.36), ${}^k x_1 \in S_{\phi_b}$ will then be the minimum of the set $\{\phi_b \in S_{\phi_b} | \phi_b > \phi\}$. Similarly, if ${}^k v_{\phi,j} = 1$ the non-empty open interval $({}^k x_1, \phi)$ will be a subset of the image of $x_1|_{D_{k_j}}$, and ${}^k x_1$ will be the maximum of $\{\phi_b \in S_{\phi_b} | \phi_b < \phi\}$. This proves (5.2.25) as desired. $\qquad\square$

---

[7]Notice that the first costate is equal to zero both at the switching times and at the terminal time, see (5.2.5) and Prop. 8.

B.3.3 Extremals for the LVMP

In this part of the appendix, we will first state three straight-forward lemmas and one corollary which are all related to extremal lifts for the LVMP. The lemmas follow mainly from the linearity of the costate dynamics, the fact that the system's admissible trajectories can always be constrained to a compact set and are uniquely determined by their control and initial state, see Prop. 5 and Lemma 43, and finally from the properties of the zeros of the first costate, see Prop. 44. They have been already used in our discussions in Sec. 5.3 and will also be used when proving Prop. 13.

Lemma 48. *Let $\Lambda = (\boldsymbol{x}, u, \boldsymbol{\lambda}, \lambda_a)$ be a four-tuple such that $(\boldsymbol{x}, u)$ is an admissible controlled trajectory defined on $D = [0, t_f]$, $\boldsymbol{\lambda} : D \to (\mathbb{R}^2)^*$ is the unique solution to (5.2.1) with the initial condition $\boldsymbol{\lambda}_0 \in (\mathbb{R}^2)^* \backslash \{\boldsymbol{0}\}$ and $\lambda_a = -\boldsymbol{\lambda}_0 \boldsymbol{f}(\boldsymbol{x}_0, u(0))$. Moreover, assume that the Minimum Condition (5.2.2) is satisfied. Then, u is a switching control. Moreover, for each scalar κ_s the pair $(\tilde{\boldsymbol{x}}, \tilde{u}) = (\operatorname{sgn}(\kappa_s)\boldsymbol{x}, \operatorname{sgn}(\kappa_s)u)$ is an admissible controlled trajectory, $\tilde{\boldsymbol{\lambda}} = \kappa_s \boldsymbol{\lambda}$ solves the differential equation (5.2.1) with $\tilde{\boldsymbol{\lambda}}_0 = \kappa_s \boldsymbol{\lambda}_0$ and for each $t \in D$ we have*

$$\mathbb{H}(\tilde{\boldsymbol{x}}(t), \tilde{u}(t), \tilde{\boldsymbol{\lambda}}(t)) = \min_{v \in \mathbb{U}} \mathbb{H}(\tilde{\boldsymbol{x}}(t), v, \tilde{\boldsymbol{\lambda}}(t)) = -|\kappa_s|\lambda_a.$$

Lemma 49. *Let $\boldsymbol{x}_0 \in \mathbb{R}^2$, $\boldsymbol{\lambda}_0 \in (\mathbb{R}^2)^* \backslash \{\boldsymbol{0}\}$ be given and introduce the following three variables:*

$$v_0 = \begin{cases} \dot{\theta}_{max} \operatorname{sgn}(\lambda_{20}) & \lambda_{10} = 0 \\ -\dot{\theta}_{max} \operatorname{sgn}(\lambda_{10}) & \lambda_{10} \neq 0 \end{cases},$$

$$\varphi_{max} = E_{pot}^{-1}\left(E_{kin}(v_0 - x_{20}) + E_{pot}(x_{10})\right),$$

and

$$\Omega_{min} = \min_{[0, \varphi_{max}]} \sqrt{\frac{K_J(\phi)}{M}}.$$

Then, there exists a unique four-tuple $\Lambda = (\boldsymbol{x}, u, \boldsymbol{\lambda}, \lambda_a)$ such that the following three conditions hold:

(1) $(\boldsymbol{x}, u)$ is an admissible controlled trajectory which starts from $\boldsymbol{x}_0$ and is defined on $D = [0, t_f]$.

(2) $\boldsymbol{\lambda} : D \to (\mathbb{R}^2)^*$ solves (5.2.1), starts from $\boldsymbol{\lambda}_0$, satisfies $\lambda_1(t) \neq 0$ for each $t \in (0, t_f)$ and terminates at $\boldsymbol{\lambda}_f = \begin{pmatrix} 0 & \lambda_{2f} \end{pmatrix} \in (\mathbb{R}^2)^* \backslash \{\boldsymbol{0}\}$.

(3) For each $t \in D$, we have

$$\mathbb{H}(\boldsymbol{x}(t), u(t), \boldsymbol{\lambda}(t)) = \min_{v \in \mathbb{U}} \mathbb{H}(\boldsymbol{x}(t), v, \boldsymbol{\lambda}(t)) = \boldsymbol{\lambda}_0 \boldsymbol{f}(\boldsymbol{x}_0, v_0).$$

Moreover, we have the following upper bound on the terminal time t_f:

$$t_f \leq \frac{2\pi}{\Omega_{min}}.$$

Lemma 50. *For each $t_f > 0, \boldsymbol{x}_0 \in \mathbb{R}^2$ and $\boldsymbol{\lambda}_0 \in (\mathbb{R}^2)^* \backslash \{\boldsymbol{0}\}$, there exists a unique four-tuple $\Lambda = (\boldsymbol{x}, u, \boldsymbol{\lambda}, \lambda_a)$ for which the following three conditions hold:*

(1) $(\boldsymbol{x}, u)$ is an admissible controlled trajectory which starts from $\boldsymbol{x}_0$ and is defined on $D = [0, t_f]$.

(2) $\boldsymbol{\lambda} : D \to (\mathbb{R}^2)^*$ solves (5.2.1) and starts from $\boldsymbol{\lambda}_0$.

(3) For each $t \in D$, we have

$$\mathbb{H}(\boldsymbol{x}(t), u(t), \boldsymbol{\lambda}(t)) = \min_{v \in \mathbb{U}} \mathbb{H}(\boldsymbol{x}(t), v, \boldsymbol{\lambda}(t)) = -\lambda_a,$$

with

$$\lambda_a = -\boldsymbol{\lambda}_0 \boldsymbol{f}\left(\boldsymbol{x}_0, u_0\right).$$

Similarly, for each $i \geq 0$, $\boldsymbol{x}_0 \in \mathbb{R}^2$ and $\boldsymbol{\lambda}_0 \in (\mathbb{R}^2)^* \backslash \{\boldsymbol{0}\}$ there exists a unique four-tuple $\Lambda = (\boldsymbol{x}, u, \boldsymbol{\lambda}, \lambda_a)$ for which the three conditions from above hold with the additional conditions that u switches i times and $\lambda_1(t_f) = 0$.

Corollary 51. *For each $i \geq 0$ and $\boldsymbol{\lambda}_0 \in (\mathbb{R}^2)^* \backslash \{\boldsymbol{0}\}$, for which the conditions (5.3.1)-(5.3.2) and (5.3.4)-(5.3.5) are satisfied, there exists a unique extremal lift $\Lambda = (\boldsymbol{x}, u, \boldsymbol{\lambda}, \lambda_a)$ for the LVMP such that $\boldsymbol{\lambda}$ starts from $\boldsymbol{\lambda}_0$ and the control u switches i times.*

Having clarified the properties of extremal lifts regarding their dependence on the initial costate, the final time and the switching number of their controls, we will next provide the proofs of Prop. 11-15.

Abnormal Extremal Lifts

Proof of Prop. 11. Let $(\boldsymbol{x}, u)$ satisfy the hypothesis of the proposition and assume first that $(\boldsymbol{x}, u)$ is an abnormal extremal. Then, there exists an abnormal extremal lift $\Lambda = (\boldsymbol{x}, u, \boldsymbol{\lambda}, \lambda_a)$ containing this extremal with $\lambda_{10} = \lambda_a = 0$ and $\lambda_{20} \neq 0$, see (5.3.1)-(5.3.2). Moreover, by Prop. 8 the control u is a switching control with $i \geq 0$ switchings and according to (5.3.3) the initial control is given by ${}^0 u = (-1)^i \dot{\theta}_{max}$. Our discussion in Sec. 5.3.1 already shows that u will solve the EMP if $i = 0$. We want to next show that u will also solve the EMP if $i > 0$. For this, we will use complete induction to show that for each positive integer i and $k \in S_i$ the following relations always hold:

$$ {}^k E_{rel} > 0 \wedge {}^k x_1 = {}^{k+1} x_1 = 0, \tag{B.3.37}$$

$$ \frac{{}^k \eta_{0,0}}{\lambda_{20}} = \frac{{}^k v_{\phi,0}}{\operatorname{sgn}(\lambda_{20})} = (-1)^k, \tag{B.3.38}$$

$$ t_{S,k+1} = t_{min}(k+1), \tag{B.3.39}$$

and

$$ (\forall t \in (t_{S,k}, t_{S,k+1})) \left[\frac{u(t)}{\dot{\theta}_{max}} = \operatorname{sgn}(x_1(t)) \neq 0 \right]. \tag{B.3.40}$$

Let $i > 0$ be fixed. Since the truth of (B.3.37)-(B.3.40) for $k = 0$ has already been established in the beginning of Sec. 5.3.1, it is sufficient to show the inductive step. Let $\bar{k} \in S_{i-1}$ and assume that (B.3.37)-(B.3.40) hold for each $k \in S_{\bar{k}}$. According to Table 5.2a, (5.2.4), (5.2.17) and (5.2.20) we then have $m_{\bar{k}} = 1$, ${}^{\bar{k}}v_{\phi,1} = -{}^{\bar{k}}v_{\phi,0}$ and ${}^{\bar{k}}\eta_{0,1} = -{}^{\bar{k}}\eta_{0,0}$. Moreover, by applying Prop. 9 and using (B.3.37)-(B.3.38) we can find the following equality for the costate $\boldsymbol{\lambda}$ at $t_{S,\bar{k}+1}$:

$$
{}^{\bar{k}+1}\boldsymbol{\lambda} = (-1)^{\bar{k}+1} \begin{pmatrix} 0 & \lambda_{20} \end{pmatrix}. \tag{B.3.41}
$$

In addition, if we use $\tilde{\boldsymbol{x}}$ to denote $\boldsymbol{x}|_{[0,t_{min}(\bar{k}+1)]}$ and $\tilde{u}$ to denote the continuous extension of $u|_{[0,t_{min}(\bar{k}+1))}$ to the interval $[0, t_{min}(\bar{k}+1)]$, the pair $(\tilde{\boldsymbol{x}}, \tilde{u})$ will be an admissible controlled trajectory which according to (B.3.39) will satisfy the hypothesis of Lemma 40. Therefore, using (B.2.3) we can also arrive at the following condition for the state $\boldsymbol{x}$ at $t_{S,\bar{k}+1} = t_{min}(\bar{k}+1)$:

$$
{}^{\bar{k}+1}\boldsymbol{x} = (-1)^{\bar{k}+i} 2(\bar{k}+1) \begin{pmatrix} 0 \\ \dot{\theta}_{max} \end{pmatrix}. \tag{B.3.42}
$$

According to (5.3.3), this last equality implies that we have

$$
\lim_{t \to t_{S,\bar{k}+1}^-} \dot{x}_1(t) = (-1)^{i+\bar{k}+1}(2\bar{k}+1)\dot{\theta}_{max}, \tag{B.3.43}
$$

and

$$
{}^{\bar{k}+1}\dot{x}_1 = {}^{k+1}\dot{\phi}_{max} = (-1)^{i+\bar{k}+1}(2\bar{k}+3)\dot{\theta}_{max}. \tag{B.3.44}
$$

Since $\bar{k} \geq 0$, both terms above are non-zero and share the same sign. Consequently, we have

$$
{}^{\bar{k}+1}E_{rel} > 0, \tag{B.3.45}
$$

and

$$
\frac{{}^{\bar{k}+1}v_{\phi,0}}{\text{sgn}(\lambda_{20})} = \frac{{}^{\bar{k}+1}\eta_{0,0}}{\lambda_{20}} = (-1)^{\bar{k}+1}, \tag{B.3.46}
$$

where we have also used (B.3.38), Prop. 9 and (B.3.41)-(B.3.42). Since ${}^{\bar{k}+1}E_{rel}$ is positive, we can now use, as above, Table 5.2a, (5.2.4), (5.2.17) and (5.2.20) to conclude that we have $m_{\bar{k}+1} = 1$, ${}^{\bar{k}+1}v_{\phi,1} = -{}^{\bar{k}+1}v_{\phi,0}$, ${}^{\bar{k}+1}\eta_{0,1} = -{}^{\bar{k}+1}\eta_{0,0}$ and

$$
{}^{\bar{k}+2}x_1 = 0. \tag{B.3.47}
$$

Moreover, according to (B.3.39) and (B.3.44) we can additionally arrive at the following equality:

$$
t_{S,\bar{k}+2} = t_{min}(\bar{k}+2). \tag{B.3.48}
$$

Note that (B.3.42) and (B.3.45)-(B.3.48) show that the relations (B.3.37)-(B.3.39) all hold for $k = \bar{k}+1$. Furthermore, if we evaluate (5.2.22) in $D_{\bar{k}+1_0}$ and $D_{\bar{k}+1_1}$ using the derived values for ${}^{\bar{k}+1}\eta_{0,0}, {}^{\bar{k}+1}\eta_{0,1}, {}^{\bar{k}+1}v_{\phi,0}$ and ${}^{\bar{k}+1}v_{\phi,1}$ we can see that (B.3.40) also holds for $k = \bar{k}+1$ since both u and the sign of x_1 remains constant in $(t_{S,\bar{k}+1}, t_{S,\bar{k}+1})$. This finally proves the inductive step. Since our choice for i

was arbitrary, we can now see that $(\boldsymbol{x}, u)$ will always satisfy the three conditions (4.2.6), (4.2.7) and (4.2.9) regardless of the value of $i > 0$. According to Prop. 3-4 this means that the control u always solves the EMP.

Conversely, assume now that the control u in the given admissible controlled trajectory $(\boldsymbol{x}, u)$ is a switching control with $i \geq 0$ switchings, solves the EMP and satisfies ${}^0 u = (-1)^i \dot{\theta}_{max}$. By Prop. 3-4 and Lemma 40, we then know that both (B.2.1) and (B.2.3) hold[8] for each $k \in S_{i+1} \backslash \{0\}$. Consequently, for each $k \in S_i$ we have $m_k = 1$ and ${}^k v_{\phi,1} = -{}^k v_{\phi,0} = (-1)^{i+k+1}$. Let $\boldsymbol{\lambda} : D \to (\mathbb{R}^2)^*$ denote now a solution of (5.2.1) such that $\lambda_{10} = 0$, $\lambda_{20} \in \mathbb{R}$ and $\mathrm{sgn}(\lambda_{20}) = (-1)^i$. Since the relative energy along $\boldsymbol{x}$ is always positive, we can make use of Prop. 9 to construct this costate $\boldsymbol{\lambda}$ as discussed in Sec. 5.2.2. In particular, noting that ${}^k x_1$ is equal to zero for each $k \in S_i$ we can use Prop. 9, (5.2.17), (5.2.20) and the principle of mathematical induction to show that we have[9]

$$(\forall k \in S_i) \left[{}^k \eta_c = 0, {}^k \eta_{0,1} = -{}^k \eta_{0,0} = (-1)^{k+1} \lambda_{20} \right], \tag{B.3.49}$$

and

$$(\forall k \in S_{i+1}) \left[{}^k \boldsymbol{\lambda} = (-1)^k (0, \lambda_{20}) \right]. \tag{B.3.50}$$

With (B.3.49)-(B.3.50) we can now easily see that for the 4-tuple $\Lambda = (\boldsymbol{x}, u, \boldsymbol{\lambda}, \lambda_a)$ with $\lambda_a = 0$ all the three conditions (5.2.1), (5.2.4) and (5.2.5) are satisfied. Moreover, the condition (5.2.2) is satisfied as well. To see this, let k be an arbitrary element of S_i and let $j \in S_{m_k}$. Substituting the values for ${}^k v_{\phi,j}$ and ${}^k \eta_{0,j}$ into the ratio on the left hand side of (5.2.22) and noting that $\mathrm{sgn}(x_1(t)) = {}^k v_{\phi,0}$ holds for each $t \in D_{k_j}$, we can then see that this expression is equal to $(-1)^{i+k} = \frac{{}^k u}{\dot{\theta}_{max}}$. That is the equality in (5.2.22) holds at each $t \in D_{k_j}$. Since our choice for k and j was arbitrary, it follows then from the continuity properties of the control u and from Prop. 9 that u indeed minimizes the Hamiltonian function in (5.2.2) at each $t \in D$. Therefore, we can conclude that Λ is an abnormal extremal lift and that $(\boldsymbol{x}, u)$ is an abnormal extremal.

Finally, to conclude the proof of the proposition we need to show that for an abnormal extremal $(\boldsymbol{x}, u)$ both (5.3.8) and (5.3.9) hold for each $k \in S_{i+1} \backslash \{0\}$. This directly follows from (B.3.39), which we have shown to hold for each $k \in S_i$, and from Lemma 40. $\qquad \square$

Proof of Prop. 12. Let $\Lambda = (\boldsymbol{x}, u, \boldsymbol{\lambda}, \lambda_a)$ be an abnormal extremal such that u is a control with $i \geq 0$ switchings. It follows then from our discussion in Sec. 5.3.1 and from the proof of Prop. 11, that for each $k \in S_i$ we will have ${}^k E_{rel} > 0$, $m_k = 1$, ${}^k \eta_{0,1} = -{}^k \eta_{0,0} = (-1)^{k+1} \lambda_{20}$ and ${}^k v_{\phi,1} = -{}^k v_{\phi,0} = (-1)^{k+1} \mathrm{sgn}(\lambda_{20})$ regardless of the value of i. If we now choose an arbitrary $k \in S_i$ and $t \in D_k$, t will either be an element of $D_{k_0} \cup D_{k_1}$ or a boundary point of this union. Consequently, using Prop. 9 and noting that we have ${}^k \eta_{0,0} \cdot {}^k v_{\phi,0} = {}^k \eta_{0,1} \cdot {}^k v_{\phi,1} = |\lambda_{20}|$ we can conclude that $\boldsymbol{\lambda}(t)$ will be given by

$$\boldsymbol{\lambda}(t) = \frac{|\lambda_{20}|}{{}^k \dot{\phi}_{max}} \left(-\frac{\tau_J(x_1(t))}{M} \quad \dot{x}_1(t) \right). \tag{B.3.51}$$

---

[8] with ${}^0 u_{S,i} = (-1)^i \dot{\theta}_{max}$ and ${}^k \boldsymbol{x}_{S,i} = {}^k \boldsymbol{x}$.

[9] This step is omitted for brevity.

This proves the proposition, since our choice for $k \in S_i$ and $t \in D_k$ was arbitrary.

$\square$

Parameterization of Extremals When proving Prop. 13, we will make use of the following lemma which for a constant control strategy shows that state and costate trajectories always depend continuously on their initial conditions. In addition, the lemma implies that the zeros of the first costate depend also continuously on these conditions when the initial costate is non-trivial.

Lemma 52. *Let $D = [0, t_f]$ and $I_\alpha \subset \mathbb{R}$ be two given non-degenerate intervals and $v \in \mathbb{U}$ a constant scalar. Moreover, let $^0\boldsymbol{\xi} : I_\alpha \to \mathbb{R}^2$ and $^0\boldsymbol{\eta} : I_\alpha \to (\mathbb{R}^2)^*$ be two continuous functions and assume that $^0\boldsymbol{\xi}$ is bounded. Finally, consider the following four conditions for the functions $\boldsymbol{\xi} : I_\alpha \times D \to \mathbb{R}^2$ and $\boldsymbol{\eta} : I_\alpha \times D \to (\mathbb{R}^2)^*$:*

(1) For each $\alpha \in I_\alpha$, $\boldsymbol{\xi}(\alpha, .)$ is the unique solution to the initial value problem

$$\frac{\partial \boldsymbol{\xi}}{\partial t}(\alpha, t) = \boldsymbol{f}\left(\boldsymbol{\xi}(\alpha, t), v\right), \ \boldsymbol{\xi}(\alpha, 0) = {}^0\boldsymbol{\xi}(\alpha). \tag{B.3.52}$$

(2) For each $\alpha \in I_\alpha$, $\boldsymbol{\eta}(\alpha, .)$ is the unique solution to the initial value problem

$$\frac{\partial \boldsymbol{\eta}}{\partial t}(\alpha, t) = \boldsymbol{\eta}(\alpha, t) \begin{pmatrix} 0 & 1 \\ -\frac{K_J(\xi_1(\alpha, t))}{M} & 0 \end{pmatrix}, \ \boldsymbol{\eta}(\alpha, 0) = {}^0\boldsymbol{\eta}(\alpha). \tag{B.3.53}$$

(3) There exists a scalar $\kappa \in \{-1, 1\}$ and an open set $U_\alpha \subset I_\alpha$ such that for each $\alpha \in U_\alpha$ we have

$${}^0\boldsymbol{\eta}(\alpha) \neq \boldsymbol{0}, \tag{B.3.54}$$

and either

$$\frac{\mathrm{sgn}\left({}^0\eta_1(\alpha)\right)}{\kappa} = 1, \tag{B.3.55}$$

or

$$\mathrm{sgn}\left({}^0\eta_1(\alpha)\right) = 0 \wedge \frac{\mathrm{sgn}\left({}^0\eta_2(\alpha)\right)}{\kappa} = -1. \tag{B.3.56}$$

In addition, for each $\alpha \in U_\alpha$ the set

$$S_{t_S}(\alpha) = \{\eta_1(\alpha, t) | t \in (0, t_f)\}, \tag{B.3.57}$$

is non-empty.

(4) The functions $^0\boldsymbol{\xi}$ and $^0\boldsymbol{\eta}$ are both continuously differentiable and the TDP τ_J is two-times continuously differentiable.

Then, if the conditions (1)-(2) are satisfied $\boldsymbol{\xi}$ and $\boldsymbol{\eta}$ are both continuous functions. In addition, if the conditions (1)-(3) are satisfied the function $t_S : U_\alpha \to (0, t_f)$ with

$$t_S(\alpha) = \inf S_{t_S}(\alpha), \tag{B.3.58}$$

is continuous and we have

$$(\forall \alpha \in U_\alpha) \left[\frac{\text{sgn}\left(\eta_2\left(\alpha, t_S(\alpha)\right)\right)}{\kappa} = 1 \right].$$ (B.3.59)

Finally, if the conditions (1), (2) and (4) are satisfied, then $\boldsymbol{\xi}$ and $\boldsymbol{\eta}$ are continuously differentiable and if all the four conditions are satisfied t_S is a continuously differentiable function.

Proof. Let $D, I_\alpha, v, {}^0\boldsymbol{\xi}, {}^0\boldsymbol{\eta}$ satisfy the hypothesis of the proposition and define the function $\bar{\boldsymbol{f}} : \mathbb{R}^2 \to \mathbb{R}^2$ with $\bar{\boldsymbol{f}}(\boldsymbol{x}) = \boldsymbol{f}(\boldsymbol{x}, v) = \left(v - x_2 \quad \frac{\tau_J(x_1)}{M} \right)$. From our discussions in Sec. 3.1 and 4.1, we know that for each $\boldsymbol{x}_0 \in \mathbb{R}^2$ there exists a unique maximal solution $\boldsymbol{x} : \mathbb{R} \to \mathbb{R}^2$ to the initial value problem

$$\dot{\boldsymbol{x}}(t) = \bar{\boldsymbol{f}}\left(\boldsymbol{x}(t)\right), \; \boldsymbol{x}(0) = \boldsymbol{x}_0 \in \mathbb{R}^2.$$ (B.3.60)

Consequently, we can define a flow $\boldsymbol{\xi}_F : \mathbb{R} \times \mathbb{R}^2 \to \mathbb{R}^2$ with the condition that for each $\boldsymbol{\xi}_0 \in \mathbb{R}^2$ the function $\boldsymbol{\xi}_F(., \boldsymbol{\xi}_0)$ gives the solution of (B.3.60) with $\boldsymbol{x}_0 = \boldsymbol{\xi}_0$. Notice that due to our assumption on the TDP τ_J being continuously differentiable, the function $\bar{\boldsymbol{f}}$ is also continuously differentiable. Consequently, both $\bar{\boldsymbol{f}}$ and $\boldsymbol{\xi}_F$ are locally Lipschitz which implies that $\boldsymbol{\xi}_F$ is continuous [34].

Assume first that the conditions *(1)-(2)* both hold. Based on the definitions of $\boldsymbol{\xi}$ and $\boldsymbol{\xi}_F$, we have then $\boldsymbol{\xi}(\alpha, t) = \boldsymbol{\xi}_F(t, {}^0\boldsymbol{\xi}(\alpha))$ for each $\alpha \in I_\alpha$ and $t \in D$. Since both ${}^0\boldsymbol{\xi}$ and $\boldsymbol{\xi}_F$ are continuous, this shows that $\boldsymbol{\xi}$ is continuous. Moreover, notice that the boundedness of ${}^0\boldsymbol{\xi}$ and D imply by Prop. 5 that $\boldsymbol{\xi}$ is bounded. To show the continuity of $\boldsymbol{\eta}$, let us fix an arbitrary pair $(\bar{\alpha}, \bar{t}) \in I_\alpha \times D$ and assume that $((\alpha_k, t_k))_{k \geq 1}$ is a sequence in $I_\alpha \times D$ which converges to $(\bar{\alpha}, \bar{t})$. Moreover, for each $k \in \{1, 2, \ldots\}$ introduce the following initial value problem for the continuously differentiable function $\boldsymbol{\lambda}_k : D \to (\mathbb{R}^2)^*$:

$$\dot{\boldsymbol{\lambda}}_k(t) = \boldsymbol{\lambda}_k(t)\boldsymbol{A}_k(t), \; \boldsymbol{\lambda}_k(0) = {}^0\boldsymbol{\eta}(\alpha_k) \in (\mathbb{R}^2)^*,$$ (B.3.61)

where $\boldsymbol{A}_k : D \to \mathbb{R}^{2 \times 2}$ is the matrix-valued function given by

$$\boldsymbol{A}_k(t) = \begin{pmatrix} 0 & 1 \\ -\frac{K_J(\xi_1(\alpha_k, t))}{M} & 0 \end{pmatrix}.$$ (B.3.62)

Comparing the two problems (B.3.53) and (B.3.61), one can see that for each $k \geq 1$ and $t \in D$ we have $\boldsymbol{\lambda}_k(t) = \boldsymbol{\eta}(\alpha_k, t)$. In order to prove that $\boldsymbol{\eta}$ is continuous at $(\bar{\alpha}, \bar{t})$, we need to therefore show that the sequence $(\boldsymbol{\lambda}_k(t_k))_{k \geq 1}$ converges to $\boldsymbol{\eta}(\bar{\alpha}, \bar{t})$. This can be done by exploiting the continuous parameter dependence of linear systems of differential equations as discussed in [38]. More specifically, the first theorem there can be applied for the introduced sequence of initial value problems in (B.3.61) since $\boldsymbol{\xi}, K_J$ and ${}^0\boldsymbol{\eta}$ are all continuous and since $\boldsymbol{\xi}$ is bounded. This leads us then to the fact that the sequence $(\boldsymbol{\lambda}_k(\bar{t}))_{k \geq 1}$ converges to $\boldsymbol{\eta}(\alpha_k, \bar{t})$. Using also the fact that solutions to (B.3.61) are always continuous

in D we then get[10]

$$
\begin{aligned}
\lim_{k \to \infty} \|\boldsymbol{\lambda}_k(t_k) - \boldsymbol{\eta}(\bar{\alpha}, \bar{t})\| \ &\leq \ \lim_{k \to \infty} \|\boldsymbol{\lambda}_k(t_k) - \boldsymbol{\lambda}_k(\bar{t})\| \\
&+ \ \lim_{k \to \infty} \|\boldsymbol{\lambda}_k(\bar{t}) - \boldsymbol{\eta}(\bar{\alpha}, \bar{t})\| \\
\Rightarrow \lim_{k \to \infty} \|\boldsymbol{\lambda}_k(t_k) - \boldsymbol{\eta}(\bar{\alpha}, \bar{t})\| \ &= \ 0.
\end{aligned} \tag{B.3.63}
$$

Equation (B.3.63) shows now that $\boldsymbol{\eta}$ is continuous at the pair $(\bar{\alpha}, \bar{t}) \in I_\alpha \times D$. Since our choice for this pair was arbitrary, we conclude that $\boldsymbol{\eta}$ is continuous.

Let us now assume that the conditions *(1)-(3)* hold with the scalar $\kappa \in \{-1, 1\}$ and the sets U_α and S_{t_S}. Following the proof of Prop. 44 with $\Omega : D \to (0, \infty), t \to \sqrt{\frac{K_J(\xi_1(\alpha, t))}{M}}$, $\boldsymbol{\lambda}_0 = {}^0\boldsymbol{\eta}(\alpha)$ and $\boldsymbol{\lambda} = \boldsymbol{\eta}(\alpha, .)$, it can then be seen that for each $\alpha \in U_\alpha$ the zeros of $\eta_1(\alpha, .)$ will be isolated. Consequently, the conditions *(1)-(3)* ensure that the function $t_S : U_\alpha \to (0, t_f)$ is well-defined by the relation (B.3.58). We want to show that this function is also continuous and that (B.3.59) holds. For this, choose an arbitrary $\bar{\alpha} \in U_\alpha$ and notice first that the following relation holds by the definition of t_S:

$$
\eta_1\left(\bar{\alpha}, t_S(\bar{\alpha})\right) = 0. \tag{B.3.64}
$$

In the following, we will use the implicit function theorem[11] in [29] together with the continuity of $\boldsymbol{\eta}$ and (B.3.53) to construct an open neighborhood $V_1^0 \subset U_\alpha$ of $\bar{\alpha}$ and an open neighborhood $V_2^0 \subset D$ of $\bar{t}_S := t_S(\bar{\alpha})$ such that for all $\tilde{\alpha} \in V_1^0$ the equality

$$
\eta_1(\tilde{\alpha}, \tilde{t}) = 0,
$$

has a unique solution $\tilde{t}$ in V_2^0 given by the continuous function $\tau_S : V_1^0 \to V_2^0$ with

$$
\tau_S(\tilde{\alpha}) = \tilde{t},
$$

and

$$
\tau_S(\bar{\alpha}) = t_S(\bar{\alpha}).
$$

Without loss of generality, assume that $\kappa = 1$. Then, either ${}^0\eta_1(\bar{\alpha})$ is positive or ${}^0\eta_1(\bar{\alpha})$ is equal to zero and the time-derivative $\frac{\partial \eta_1}{\partial t}(\bar{\alpha}, t)$ is positive, see (B.3.53) and (B.3.55)-(B.3.56). Moreover, since $\bar{t}_S$ is the first time $\eta_1(\bar{\alpha}, .)$ is equal to zero in $(0, t_f)$, $\eta_1(\bar{\alpha}, .)$ is positive on $(0, \bar{t}_S)$. Finally, since $\boldsymbol{\eta}(\bar{\alpha}, 0) \neq \mathbf{0}$ it follows from (B.3.53) that (B.3.59) holds, as desired, and that the derivative $\frac{\partial \eta_1}{\partial t}(\bar{\alpha}, \bar{t}_S)$ is negative. Notice that this derivative is continuous. Therefore, we can find a sufficiently small $\varepsilon_S > 0$ such that $\frac{\partial \eta_1}{\partial t}(\alpha, t)$ takes negative values for each pair $(\alpha, t) \in (\bar{\alpha} - \varepsilon_S, \bar{\alpha} + \varepsilon_S) \times (\bar{t}_S - \varepsilon_S, \bar{t}_S + \varepsilon_S) \subset U_\alpha \times D$. For each $\alpha \in (\bar{\alpha} - \varepsilon_S, \bar{\alpha} + \varepsilon_S)$ the function $\eta_1(\alpha, .)$ will then be strictly decreasing on $(\bar{t}_S - \varepsilon_S, \bar{t}_S + \varepsilon_S)$. This means that we have found an open neighborhood $V_1 = (\bar{\alpha} - \varepsilon_S, \bar{\alpha} + \varepsilon_S)$ of $\bar{\alpha}$ and an open neighborhood $V_2 = (\bar{t}_S - \varepsilon_S, \bar{t}_S + \varepsilon_S)$ of $\bar{t}_S$ such that for each $\alpha \in V_1$ the function $\eta_1(\alpha, .)$ is locally one-to-one. This

---

[10]We use "$\|.\|$" to denote the norm in $\mathbb{R}^2$, see for instance [62].

[11]See also [27].

shows according to Theorem 2.1 in [29] the existence of the two sets V_1^0 and V_2^0 and the continuous function τ_S as described above.

Using the function τ_S it is now possible to show that t_S is continuous at $\bar{\alpha}$. To see this more clearly, we will construct an open neighborhood $V_{\bar{\alpha}} \subset V_1^0$ of $\bar{\alpha}$ such that $t_S|_{V_{\bar{\alpha}}} = \tau_S|_{V_{\bar{\alpha}}}$. Notice first that we can use, similar to our discussion above, the continuity of $\boldsymbol{\eta}$, (B.3.53) and (B.3.55)-(B.3.56) to find a sufficiently small ε_0 such that η_1 is positive on $I_0 = (\bar{\alpha} - \varepsilon_0, \bar{\alpha} + \varepsilon_0) \times (0, \varepsilon_0] \subset U_\alpha \times D$ with the inequality $\varepsilon_0 < \tau_S(\alpha)$ holding for each $\alpha \in (\bar{\alpha} - \varepsilon_0, \bar{\alpha} + \varepsilon_0)$. Similarly, since $\tau_S(\bar{\alpha}) = t_S(\bar{\alpha})$ is the first time $\eta_1(\bar{\alpha}, .)$ equals to zero in $(0, t_f)$ it follows from the continuity and non-triviality of $\boldsymbol{\eta}(\bar{\alpha}, .)$ that $\eta_2(\bar{\alpha}, \tau_S(\bar{\alpha}))$ must be positive, see (B.3.53). Using the continuity of $K_J, \boldsymbol{\xi}, \boldsymbol{\eta}$ and τ_S, we can then find a sufficiently small ε_f such that the continuous derivative $\frac{\partial \eta_1}{\partial t}$ is negative on $I_f = \left\{ (\alpha, t) \in V_1^0 \times D \,\middle|\, |\alpha - \bar{\alpha}| < \varepsilon_f, t \in [\tau_S(\alpha) - \varepsilon_f, \tau_S(\alpha)] \right\}$. Finally, assume without loss of generality that we have $\varepsilon_0 + \varepsilon_f < t_f$ and build an open cover of the compact set $\{(\bar{\alpha}, t) \in U_\alpha \times D | t \in [\varepsilon_0, t_f - \varepsilon_f]\}$ by first choosing for each pair $(\bar{\alpha}, \tilde{t})$ of this set an open neighborhood $\tilde{I} = (\bar{\alpha} - \tilde{\varepsilon}, \bar{\alpha} + \tilde{\varepsilon}) \times (\tilde{t} - \tilde{\varepsilon}, \tilde{t} + \tilde{\varepsilon}) \subset U_\alpha \times D$, with $\tilde{\varepsilon} > 0$, such that η_1 is non-zero in this neighborhood and then building the union of the resulting neighborhoods. By extracting a finite subcover and taking the two sets I_0 and I_f into account, we can then find a sufficiently small scalar $\varepsilon > 0$ such that for each $\alpha \in V_{\bar{\alpha}} = (\bar{\alpha} - \varepsilon, \bar{\alpha} + \varepsilon)$ the following relation holds:

$$(\forall t \in (0, \tau_S(\alpha))) \, [\eta_1(\alpha, t) > 0]. \tag{B.3.65}$$

According to (B.3.65), we now see that for each $\alpha \in V_{\bar{\alpha}}$ the function $\eta_1(\alpha, .)$ will be equal to zero at $\tau_S(\alpha)$ for the first time in $(0, t_f)$. In other words, we have shown that $t_S|_{V_{\bar{\alpha}}}$ is equal to $\tau_S|_{V_{\bar{\alpha}}}$. Since τ_S is continuous, this also means that t_S will be continuous at $\bar{\alpha}$. Finally, since our choice for $\bar{\alpha} \in U_\alpha$ was arbitrary we conclude that t_S is a continuous function.

Assume now that conditions *(1)-(2)* and *(4)* are satisfied and consider the following initial value problem for the continuously differentiable function $\boldsymbol{\gamma}$: $\mathbb{R} \to \mathbb{R}^4$:

$$\dot{\boldsymbol{\gamma}}(t) = \boldsymbol{l}(\boldsymbol{\gamma}(t)), \; \boldsymbol{\gamma}(0) = \boldsymbol{\gamma}_0 \in \mathbb{R}^4, \tag{B.3.66}$$

where $\boldsymbol{l} : \mathbb{R}^4 \to \mathbb{R}^4$ is the function which at each $\boldsymbol{x} \in \mathbb{R}^4$ satisfies

$$\boldsymbol{l}(\boldsymbol{x}) = \begin{pmatrix} v - x_2 \\ \frac{\tau_J(x_1)}{M} \\ \frac{\tau_J(x_1)}{M} - \frac{K_J(x_1)}{M} x_4 \\ x_3 \end{pmatrix}. \tag{B.3.67}$$

The existence and uniqueness of a solution $\boldsymbol{\gamma} : \mathbb{R} \to \mathbb{R}^4$ to this problem follows from the uniqueness of solutions to the IVP's in (B.3.60)-(B.3.61). Moreover, based on this property we can again define a flow $\boldsymbol{\gamma}_F : \mathbb{R} \times \mathbb{R}^4$ with $\boldsymbol{\gamma}_F(., \boldsymbol{\gamma}_0)$ giving the solution to (B.3.66). As in this case τ_J is two-times continuously differentiable, the function $\boldsymbol{l}$ in *(B.3.67)* is continuously differentiable and therefore also the flow $\boldsymbol{\gamma}_F$ is continuously differentiable [52]. Finally, according to the def-

initions of $\boldsymbol{\xi}, \boldsymbol{\eta}$ and $\boldsymbol{\gamma}_F$ we have for each $(\alpha, t) \in I_\alpha \times D$

$$\begin{pmatrix} \boldsymbol{\xi}(\alpha, t) \\ \boldsymbol{\eta}^T(\alpha, t) \end{pmatrix} = \boldsymbol{\gamma}_F \left(t, \begin{pmatrix} {}^0\boldsymbol{\xi}(\alpha) \\ {}^0\boldsymbol{\eta}^T(\alpha) \end{pmatrix} \right), \tag{B.3.68}$$

and since both ${}^0\boldsymbol{\xi}$ and ${}^0\boldsymbol{\eta}$ are continuously differentiable this shows, as desired, that $\boldsymbol{\xi}$ and $\boldsymbol{\eta}$ are also continuously differentiable.

Finally, assume that the conditions *(1)-(4)* all hold so that $\boldsymbol{\xi}$ and $\boldsymbol{\eta}$ are continuously differentiable. We want to show that t_S is also continuously differentiable. Recall that conditions *(1)-(3)* already ensure that t_S is a continuous function. Moreover, by its definition, the positiveness of K_J and the nontriviality of ${}^0\boldsymbol{\eta}$ we have the following two conditions:

$$\eta_1\left(\alpha, t_S(\alpha)\right) = 0 \wedge \frac{\partial \eta_1}{\partial t}\left(\alpha, t_S(\alpha)\right) \neq 0,$$

which hold for each $\alpha \in U_\alpha$, see (B.3.53) and (B.3.58). Since $\boldsymbol{\eta}$ is continuously differentiable, we can then apply the classical implicit function theorem [62] to conclude that t_S is indeed continuously differentiable with its derivative $\frac{\mathrm{d}t_S}{\mathrm{d}\alpha}$: $U_\alpha \to \mathbb{R}$ given by

$$\frac{\mathrm{d}t_S}{\mathrm{d}\alpha}(\alpha) = \frac{M}{K_J\left(\xi_1(\alpha, t_S(\alpha))\right)} \frac{\frac{\partial \eta_1}{\partial \alpha}\left(\alpha, t_S(\alpha)\right)}{\eta_2(\alpha, t_S(\alpha))}.$$

$\square$

Using Lemma 52, we can now prove Prop. 13 as follows.

Proof of Prop. 13. Let us first note that for any extremal lift $\Lambda = (\boldsymbol{x}, u, \boldsymbol{\lambda}, \lambda_a)$ for the LVMP, the pair $(-\boldsymbol{x}, -u)$ will be an admissible controlled trajectory and the four-tuple $\tilde{\Lambda} = (-\boldsymbol{x}, -u, -\boldsymbol{\lambda}, \lambda_a)$ will satisfy all the first three conditions in Prop. 7, see Lemma 48. Moreover, using $i \geq 0$ to denote the switching number of the control u there will exist a unique extremal lift $\bar{\Lambda} = (\bar{\boldsymbol{x}}, \bar{u}, \bar{\boldsymbol{\lambda}}, \lambda_a)$ for the LVMP such that $\bar{u}$ is a switching control with $i+1$ switchings and $\bar{\boldsymbol{\lambda}}_0 = -\boldsymbol{\lambda}_0$, see Corollary 51. Finally, if t_f denotes the terminal time of u it follows from Lemma 50 that $\bar{\boldsymbol{x}} = -\boldsymbol{x}|_{[0, t_f]}$ and $\bar{\boldsymbol{\lambda}} = -\boldsymbol{\lambda}|_{[0, t_f]}$ must hold. Consequently, the terminal time of Λ and the $i+1$'th switching time of $\bar{\Lambda}$ will be equal to each other. Furthermore, the states reached at these times, i.e. $\boldsymbol{x}(t_f)$ and $\bar{\boldsymbol{x}}(t_f)$, will only differ in their signs. Noting that our choice for Λ was arbitrary and that the function $\boldsymbol{\lambda}_0^{ext}$ is symmetric with respect to the origin, this implies by the definition of the functions ${}^k t_S^{ext} : D_\alpha \to \mathbb{R}$ and ${}^k \boldsymbol{x}_S^{ext} : D_\alpha \to \mathbb{R}^2$ in Sec. 5.3.3 that the equalities (5.3.17) and (5.3.18) hold for each $k \in \{1, 2, \ldots\}$ and $\alpha \in D_\alpha$.

We want to next make use of mathematical induction to show that for each $k \in \{1, 2, \ldots\}$ the functions ${}^k t_S^{ext}$ and ${}^k \boldsymbol{x}_S^{ext}$ are continuous and satisfy the equalities (5.3.19)-(5.3.22).

Base Case $(k = 1)$ In view of Lemma 52, introduce the variables $I_\alpha = (0, 2\pi], v = \dot{\theta}_{max}$ and the continuous and bounded functions ${}^0\boldsymbol{\eta} : I_\alpha \to (\mathbb{R}^2)^*$ and ${}^0\boldsymbol{\xi} : I_\alpha \to \mathbb{R}^2$ given by

$$
{}^0\boldsymbol{\eta}(\gamma) = \begin{cases} \begin{pmatrix} -\sin(\gamma) & -\cos(\gamma) \end{pmatrix} & \gamma \in (0, \pi] \\ \begin{pmatrix} 0 & 1 \end{pmatrix} & \gamma \in (\pi, 2\pi] \end{cases}, \tag{B.3.69}
$$

and

$$
{}^0\boldsymbol{\xi}(\gamma) = \mathbf{0},
$$

respectively. Moreover, let $D = [0, t_f]$ be a non-degenerate interval and $\boldsymbol{\xi} : I_\alpha \times D \to \mathbb{R}^2$ and $\boldsymbol{\eta} : I_\alpha \times D \to \mathbb{R}^2$ functions defined by the first two conditions of Lemma 52, see (B.3.52) and (B.3.53). Finally, assume that for each $\alpha \in I_\alpha$ the set $S_{t_S}(\alpha)$ in (B.3.57) is non-empty which according to Lemma 49 can always be ensured if t_f is chosen sufficiently large. With the introduced variables and functions we can now directly apply Lemma 52. More specifically, since the first three conditions of this lemma are satisfied with $\kappa = -1$ and $U_\alpha = (0, 2\pi)$, we can conclude that $\boldsymbol{\xi}, \boldsymbol{\eta}$ and t_S are continuous where $t_S : U_\alpha \to (0, t_f)$ is the function given by (B.3.58).

Let us now choose an arbitrary parameter $\bar{\alpha} \in (0, 1) \subset D_\alpha$ and introduce the scalar $\bar{\gamma} \in (0, \pi)$ with

$$
\bar{\gamma} = \text{atan2}\left(-\lambda_{20}^{ext}(\bar{\alpha}), -\lambda_{10}^{ext}(\bar{\alpha})\right). \tag{B.3.70}
$$

Moreover, define the functions $\bar{\boldsymbol{x}} : \bar{D} \to \mathbb{R}^2, \bar{u} : \bar{D} \to \mathbb{U}$ and $\bar{\boldsymbol{\lambda}} : \bar{D} \to (\mathbb{R}^2)^*$, with $\bar{D} = [0, t_S(\bar{\gamma})]$, such that for each $t \in \bar{D}$ we have

$$
\bar{\boldsymbol{x}}(t) = \boldsymbol{\xi}(\bar{\gamma}, t) \wedge \bar{u}(t) = v \wedge \bar{\boldsymbol{\lambda}}(t) = \boldsymbol{\eta}(\bar{\gamma}, t). \tag{B.3.71}
$$

Then, by setting $\bar{\lambda}_a = v \sin \bar{\gamma} > 0$ we can see that the four tuple $\bar{\Lambda} = (\bar{\boldsymbol{x}}, \bar{u}, \bar{\boldsymbol{\lambda}}, \bar{\lambda}_a)$ satisfies the hypothesis of Lemma 48. Consequently, choosing $\kappa_s = \frac{1}{v \sin \bar{\gamma}}$ as a scaling factor we can see that $\Lambda = (\bar{\boldsymbol{x}}, \bar{u}, \kappa_s \bar{\boldsymbol{\lambda}}, 1)$ will be an extremal lift for the LVMP with $\boldsymbol{\lambda}_0 = \kappa_s \bar{\boldsymbol{\lambda}}_0 = \boldsymbol{\lambda}_0^{ext}(\bar{\alpha})$, see (B.3.69)-(B.3.71). This implies the following equalities for ${}^1t_S^{ext}$ and ${}^1\boldsymbol{x}_S^{ext}$:

$$
{}^1t_S^{ext}(\bar{\alpha}) = t_S(\bar{\gamma}), \tag{B.3.72}
$$

and

$$
\begin{aligned}
{}^1\boldsymbol{x}_S^{ext}(\bar{\alpha}) &= \bar{\boldsymbol{x}}\left(t_S\left(\bar{\gamma}\right)\right) \\
&= \boldsymbol{\xi}\left(t_S\left(\bar{\gamma}\right), \bar{\gamma}\right). \tag{B.3.73}
\end{aligned}
$$

Noting that our choice for $\bar{\alpha} \in (0, 1)$ was arbitrary, that the relation in (B.3.70) defines a continuous mapping from $(0, 1)$ to $(0, \pi)$, and finally that both t_S and $\boldsymbol{\xi}$ are continuous, the two equalities (B.3.72) and (B.3.73) show that ${}^1t_S^{ext}$ and ${}^1\boldsymbol{x}_S^{ext}$ are continuous on $(0, 1)$. More generally, since ${}^1t_S^{ext}$ is an even function and ${}^1\boldsymbol{x}_S^{ext}$ an odd function, these two functions are both continuous on D_α.

Taking the limit of the mapping described by (B.3.70) as $\bar{\alpha}$ goes to 1^- one can see that $\bar{\gamma}$ converges to π and thus $\bar{\boldsymbol{\lambda}}_0$ to $\begin{pmatrix} 0 & 1 \end{pmatrix}$, see (B.3.69). Noting that this initial costate leads to an abnormal extremal it follows then from (B.3.72)-(B.3.73) and Prop. 11 that the two equalities in (5.3.20) and (5.3.22) indeed hold for $k = 1$. The fact that the two equalities in (5.3.19) and (5.3.21) also hold for $k = 1$, can be seen from Table 5.3 if we set there i to zero and take the limit of the provided expressions as λ_{20} goes to minus infinity, see also the function $\boldsymbol{\lambda}_0^{ext}$ in Table 5.5a and $^1\boldsymbol{x}_S^{ext}$ in (5.3.11).

Inductive Step ($\bar{k} \in \{1, 2, \ldots\}$)   Let us assume that $^{\bar{k}}t_S^{ext}$ and $^{\bar{k}}\boldsymbol{x}_S^{ext}$ are both continuous and that the equalities in (5.3.19)-(5.3.22) all hold for $k = \bar{k}$. Similar to our discussion in the base case, we will make use of Lemma 52. For this, introduce the variables $I_\alpha = (-1, 2), v = (-1)^k\dot{\theta}_{max}$ and the continuous and bounded[12] functions $^0\boldsymbol{\eta} : I_\alpha \to (\mathbb{R}^2)^*$ and $^0\boldsymbol{\xi} : I_\alpha \to \mathbb{R}^2$ given by

$$^0\boldsymbol{\eta}(\alpha) = \begin{pmatrix} 0 & (-1)^k \end{pmatrix}, \tag{B.3.74}$$

and

$$^0\boldsymbol{\xi}(\alpha) = \begin{cases} \lim_{\alpha \to 0^+} {}^k\boldsymbol{x}_S^{ext}(\alpha) & \alpha \in (-1, 0] \\ {}^k\boldsymbol{x}_S^{ext}(\alpha) & \alpha \in (0, 1) \\ \lim_{\alpha \to 1^-} {}^k\boldsymbol{x}_S^{ext}(\alpha) & \alpha \in [1, 2) \end{cases}, \tag{B.3.75}$$

respectively. Moreover, let $D = [0, t_f]$ be a non-degenerate interval and $\boldsymbol{\xi} : I_\alpha \times D \to \mathbb{R}^2$ and $\boldsymbol{\eta} : I_\alpha \times D \to \mathbb{R}^2$ functions defined by the first two conditions of Lemma 52. Finally, assume that t_f is sufficiently large so that for each $\alpha \in I_\alpha$ the set $S_{t_S}(\alpha)$ in (B.3.57) is non-empty. It follows then from Lemma 52, with $\kappa = (-1)^{k-1}$ and $U_\alpha = I_\alpha$, that $\boldsymbol{\xi}, \boldsymbol{\eta}$ and t_S are continuous with $t_S : U_\alpha \to (0, t_f)$ being the function defined by (B.3.58).

Let us now choose an arbitrary scalar $\bar{\alpha} \in (0, 1)$ and define the functions $\bar{\boldsymbol{x}} : \bar{D} \to \mathbb{R}^2, \bar{u} : \bar{D} \to \mathbb{U}$ and $\bar{\boldsymbol{\lambda}} : \bar{D} \to (\mathbb{R}^2)^*$, with $\bar{D} = [0, t_S(\bar{\alpha})]$, such that for each $t \in \bar{D}$ we have

$$\bar{\boldsymbol{x}}(t) = \boldsymbol{\xi}(\bar{\alpha}, t) \wedge \bar{u}(t) = v \wedge \bar{\boldsymbol{\lambda}}(t) = \boldsymbol{\eta}(\bar{\alpha}, t). \tag{B.3.76}$$

Then, by setting[13] $\bar{\lambda}_a = (-1)^{k+1}\frac{\tau_J\left({}^k x_S^{ext}(\alpha)\right)}{M} > 0$ we can see that the four tuple $\bar{\Lambda} = (\bar{\boldsymbol{x}}, \bar{u}, \bar{\boldsymbol{\lambda}}, \bar{\lambda}_a)$ satisfies the hypothesis of Lemma 48. Consequently, choosing $\kappa_s = \frac{M}{\tau_J\left(\left|{}^k x_S^{ext}(\alpha)\right|\right)}$ as a scaling factor and using additionally Lemma 50 by setting $i, \boldsymbol{x}_0$ and $\boldsymbol{\lambda}_0$ once to $\bar{k}, \boldsymbol{0}$ and $\boldsymbol{\lambda}_0^{ext}(\bar{\alpha})$ and once to $0, \bar{\boldsymbol{x}}(0), \kappa_s\bar{\boldsymbol{\lambda}}(0)$ we get the following relations for $^{\bar{k}+1}t_S^{ext}$ and $^{\bar{k}+1}\boldsymbol{x}_S^{ext}$:

$$^{\bar{k}+1}t_S^{ext}(\bar{\alpha}) = {}^{\bar{k}}t_S^{ext}(\bar{\alpha}) + t_S(\bar{\alpha}), \tag{B.3.77}$$

and

$$\begin{aligned} ^{\bar{k}+1}\boldsymbol{x}_S^{ext}(\bar{\alpha}) &= \bar{\boldsymbol{x}}\left(t_S\left(\bar{\alpha}\right)\right) \\ &= \boldsymbol{\xi}\left(\bar{\alpha}, t_S\left(\bar{\alpha}\right)\right). \end{aligned} \tag{B.3.78}$$

---

[12]Notice that the boundedness of $^0\boldsymbol{\xi}$ follows from Prop. 3.

[13]Notice that the positivity of $\bar{\lambda}_a$ follows from Prop. 8 and in particular (5.2.10).

Noting that our choice for $\bar{\alpha} \in (0,1)$ was arbitrary, the two equalities (B.3.77) and (B.3.78) show, similar to the base case, the continuity of the functions $^{\bar{k}+1}t_S^{ext}$ and $^{\bar{k}+1}\boldsymbol{x}_S^{ext}$.

Finally, since the functions t_S and $\boldsymbol{\xi}$ are continuous on I_α and on $I_\alpha \times D$, respectively, it follows from (B.3.77)-(B.3.78) that the limits of $^{\bar{k}+1}t_S^{ext}$ and $^{\bar{k}+1}\boldsymbol{x}_S^{ext}$ as $\alpha \to 0^+$ and as $\alpha \to 1^-$ exist. Moreover, these limits can be computed by analysing the pair $(\bar{\boldsymbol{x}}, \bar{\boldsymbol{\lambda}})$ defined by (B.3.76) if we set $\bar{\alpha}$ once to 0 and once to 1. Noting the relation between abnormal extremal lifts and the initial conditions determined by (B.3.74)-(B.3.75), it follows then from Prop. 11 that all the equalities in (5.3.19)-(5.3.22) indeed hold for $k = \bar{k} + 1$.

In order to conclude the proof of the proposition, we need to show that for each $k \in \{1, 2, \ldots\}$ the functions $^k t_S^{ext}$ and $^k \boldsymbol{x}_S^{ext}$ are not only continuous but also continuously differentiable in case the TDP τ_J is two-times continuously differentiable. This can be done, as above, using Lemma 52 and mathematical induction if we additionally note that $\boldsymbol{\lambda}_0^{ext}$ is continuously differentiable, see (5.3.11) and Table 5.5a. The proof is very similar and omitted for brevity. $\qquad\square$

We conclude this part of the appendix with the proof of Prop. 15.

Proof of Prop. 15. Let $t_f > 0, \beta^{ext} \in (0, \infty)$ and assume that $t_f = t_S^{ext}(\beta^{ext})$ holds. Moreover, let ω_{min} and ω_{max} be given by (5.3.30) and (5.3.31), respectively. Finally, let $\alpha^{ext} = (-1)^i (\beta^{ext} - i)$ with $i = \lceil \beta^{ext} \rceil - 1$. Then, by definition there exists an extremal lift $\Lambda = (\boldsymbol{x}, u, \boldsymbol{\lambda}, \lambda_a)$ for the LVMP, defined on $D = [0, t_f]$, such that u has i switchings and $\boldsymbol{\lambda}_0 = \boldsymbol{\lambda}_0^{ext}(\alpha^{ext})$. Now, according to Prop. 8 the first costate λ_1 in this lift has exactly i zeros in the interval $(0, t_f)$. Consequently, applying Lemma 44 with $\Omega : D \to (0, \infty), t \to \Omega(t) = \sqrt{\frac{K_J(x_1(t))}{M}}$, we can see that the variables Ω_{min} and Ω_{max} in (B.3.5) provide a lower and an upper bound for the integer i, see (B.3.6)-(B.3.8). The desired relation (5.3.34) for β^{ext} follows then directly from these bounds by noting that we have $\omega_{min} \leq \Omega_{min}$ and $\omega_{max} \geq \Omega_{max}$ due to Prop. 5.

Let us now assume that β^{ext} solves the NPP described by (5.3.24)-(5.3.26) so that $(\boldsymbol{x}, u)$ is an optimal extremal and $x_2(t_f) = x_2^{ext}(\beta^{ext})$. Then, as we have already discussed in Sec. 5.1 it follows from Prop. 5 that the maximal energy attained by the extremal $(\boldsymbol{x}, u)$ will be bounded above by $E_{pot}(\dot{\theta}_{max} t_f)$. Consequently, in accordance with (5.3.35) we have $x_2^{ext}(\beta^{ext}) < \sqrt{\frac{2 E_{pot}(\dot{\theta}_{max} t_f)}{M}}$. Finally, since u solves the LVMP $x_{2S}^{ext}(\beta^{ext})$ must be greater than or equal to the terminal link velocity of each admissible controlled trajectory $(\bar{\boldsymbol{x}}, \bar{u})$ which is defined on D if $\bar{\boldsymbol{x}}_0 = \boldsymbol{0}$. Noting that the control $\bar{u} : D \to \mathbb{U}$ with

$$\bar{u}(t) = \begin{cases} 0 & \frac{t}{t_{min}(1)} < \left\lceil \frac{t_f}{t_{min}(1)} \right\rceil - 1 \\[2ex] \dot{\theta}_{max} & \frac{t}{t_{min}(1)} \geq \left\lceil \frac{t_f}{t_{min}(1)} \right\rceil - 1 \end{cases},$$

always leads to a positive velocity $\bar{x}_2(t_f) > 0$, see (2.1.4) and (5.3.11), we can conclude that $x_{2S}^{ext}(\beta^{ext})$ is positive. $\qquad\square$

B.3.4   Resonance Energies

In this part of the appendix, we will first provide the proof of Prop. 16 and then the proofs of Prop. 17-18. For the first proof, we will require the following lemma which clarifies for control systems with linear TDP's the relation between applied control strategies and the resulting inner products of state and costate trajectories[14].

Lemma 53. *Let τ_J be a linear TDP and $(\boldsymbol{x}, u)$ an admissible controlled trajectory which is defined on $D = [0, t_f]$. Moreover, let $\boldsymbol{\lambda} : D \to (\mathbb{R}^2)^*$ be a continuously differentiable function solving the differential equation (5.2.1). Then, for each $t \in D$ we have*

$$\boldsymbol{\lambda}(t)\boldsymbol{x}(t) - \boldsymbol{\lambda}_0 \boldsymbol{x}_0 = \int_0^t \lambda_1(s)u(s)\mathrm{d}s. \tag{B.3.79}$$

Proof. Let τ_J, $(\boldsymbol{x}, u)$ and $\boldsymbol{\lambda}$ satisfy the hypothesis of the lemma and let E denote the set of times at which u is discontinuous. Then, taking the time-derivative of the product $\boldsymbol{\lambda}\boldsymbol{x}$ and noting that the terms $\frac{\partial \boldsymbol{f}}{\partial \boldsymbol{x}}$ and $\frac{\partial \boldsymbol{f}}{\partial u}$ are constant we obtain the following equality which holds at each $s \in D \backslash E$:

$$
\begin{aligned}
\frac{\mathrm{d}(\boldsymbol{\lambda}\boldsymbol{x})}{\mathrm{d}t}(s) &= \dot{\boldsymbol{\lambda}}(s)\boldsymbol{x}(s) + \boldsymbol{\lambda}(s)\dot{\boldsymbol{x}}(s) \\
&= -\boldsymbol{\lambda}(s)\frac{\partial \boldsymbol{f}}{\partial \boldsymbol{x}}\left(\boldsymbol{x}(s), u(s)\right)\boldsymbol{x}(s) \\
&\quad + \boldsymbol{\lambda}(s)\left(\frac{\partial \boldsymbol{f}}{\partial \boldsymbol{x}}\left(\boldsymbol{x}(s), u(s)\right)\boldsymbol{x}(s) + \frac{\partial \boldsymbol{f}}{\partial u}\left(\boldsymbol{x}(s), u(s)\right)u(s)\right) \\
&= \lambda_1(s)u(s). \tag{B.3.80}
\end{aligned}
$$

The relation (B.3.79) follows now directly from integrating (B.3.80) from 0 to t. $\qquad \square$

With Lemma 53, we can now prove Prop. 16 as follows.

Proof of Prop. 16. Let τ_J be a linear TDP and $\Lambda = (\boldsymbol{x}, u, \boldsymbol{\lambda}, \lambda_a)$ an extremal lift for the LVMP which is defined on $D = [0, t_f]$. Similarly, assume that $(\bar{\boldsymbol{x}}, \bar{u})$ is an admissible controlled trajectory, defined on $\bar{D} = [0, \bar{t}_f] \subset D$, such that $\bar{\boldsymbol{x}}_0 = \boldsymbol{0}$. Let us first note that due to the linearity of τ_J the differential equation (5.2.1) does not depend on the state trajectory. Consequently, we can apply Lemma 53 by choosing $(\bar{\boldsymbol{x}}, \bar{u})$ as the admissible controlled trajectory and $\boldsymbol{\lambda}|_{\bar{D}}$ as the solution to (5.2.1). According to (B.3.79) this leads us to the following relations for the product $\boldsymbol{\lambda}(\bar{t}_f)\bar{\boldsymbol{x}}(\bar{t}_f)$:

$$
\begin{aligned}
\boldsymbol{\lambda}(\bar{t}_f)\bar{\boldsymbol{x}}(\bar{t}_f) &= \int_0^{\bar{t}_f} \lambda_1(s)\bar{u}(s)\mathrm{d}s \\
&\geq -\int_0^{\bar{t}_f} |\lambda_1(s)|\dot{\theta}_{max}\mathrm{d}s. \tag{B.3.81}
\end{aligned}
$$

---

[14]See also the discussion on the reachable sets of linear systems in [30].

Since our choice for $(\bar{\boldsymbol{x}}, \bar{u})$ was arbitrary, (B.3.81) shows that the product $\boldsymbol{\lambda}(\bar{t}_f)\bar{\boldsymbol{x}}_f$ is bounded below for any trajectory $\bar{\boldsymbol{x}}$ of Σ which starts from the origin and terminates at $\bar{t}_f \in (0, t_f]$. Notice now that the pair $(\boldsymbol{x}|_{\bar{D}}, \bar{u})$ is an admissible controlled trajectory containing such a trajectory if the control $\bar{u}$ is given by the relation (5.4.1). Moreover, by definition the control $\bar{u}$ and λ_1 always take opposite signs whenever λ_1 is non-zero, see (5.2.6). As the magnitude of $\bar{u}$ is always equal to $\dot{\theta}_{max}$, it follows then from (B.3.81) that $\bar{u}$ indeed minimizes the cost functional $\bar{J}$ in (5.4.2). The fact that $\bar{u}$ is the unique control follows from the fact that λ_1 never remains at zero in a finite time-interval, see the proof of Prop. 8.

Noting that our choice for $\bar{t}_f \in (0, t_f]$ was arbitrary, let us set now $\bar{t}_f$ to t_f. Then, $u = \bar{u}$ is the unique control minimizing the cost functional $\bar{J} = -\tilde{x}_{2f}$, see (5.2.5). Consequently, Λ is optimal and moreover $\boldsymbol{x}_f$ belongs to the boundary of the time-t_f-reachable set $\text{Reach}_{\Sigma, t_f}(\boldsymbol{0})$. Since the origin is an equilibrium point of Σ, this also means that[15] $\boldsymbol{x}_f \in \partial \text{Reach}_{\Sigma, \leq t_f}(\boldsymbol{0})$. We conclude the proof of the proposition by showing that $\boldsymbol{x}$ is a time-optimal trajectory. In view of Lemma 7.1.1 in [53] this will also show that $(\boldsymbol{x}, u)$ is a boundary trajectory.

By contradiction, assume that $\boldsymbol{x}$ is not a time-optimal trajectory so that there exists an admissible controlled trajectory $(\bar{\boldsymbol{x}}, \bar{u})$, as defined above, such that $\bar{t}_f < t_f$ and $\bar{\boldsymbol{x}}_f = \boldsymbol{x}_f$. Moreover, let $\bar{\boldsymbol{\lambda}} : \bar{D} \to (\mathbb{R}^2)^*$ be a solution to the differential equation (5.2.1) such that $\bar{\boldsymbol{\lambda}}_f = \boldsymbol{\lambda}_f$. Applying then Lemma 53 and making use of the fact that the linear differential equation described by (5.2.1) is time-independent, we can obtain the following relations:

$$
\begin{aligned}
\bar{\boldsymbol{\lambda}}(\bar{t}_f)\bar{\boldsymbol{x}}(\bar{t}_f) &= \int_0^{\bar{t}_f} \bar{\lambda}_1(s)\bar{u}(s)\mathrm{d}s \\
&= \int_0^{\bar{t}_f} \lambda_1(s + t_f - \bar{t}_f)\bar{u}(s)\mathrm{d}s \\
&\geq -\dot{\theta}_{max} \int_0^{\bar{t}_f} |\lambda_1(s + t_f - \bar{t}_f)|\mathrm{d}s \\
&= -\dot{\theta}_{max} \int_{t_f - \bar{t}_f}^{t_f} |\lambda_1(s)|\mathrm{d}s \\
\Rightarrow x_{2f} &> \bar{x}_{2f},
\end{aligned}
\tag{B.3.82}
$$

where for the last inequality we have again made use of the properties of the control u as well as the fact that λ_1 never remains at zero in a finite time-interval. Clearly, (B.3.82) contradicts the condition $\bar{\boldsymbol{x}}_f = \boldsymbol{x}_f$ and we conclude that $\boldsymbol{x}$ is a time-optimal trajectory. $\qquad\square$

Proof of Prop. 17. Let $(\boldsymbol{x}, u)$ be an optimally controlled trajectory, defined on $D = [0, t_f]$, so that u minimizes the cost functional J in (2.3.1). As we have discussed in the proof of Prop. 16 above, the terminal state $\boldsymbol{x}_f$ is then an element of $\partial \text{Reach}_{\Sigma, \leq t_f}(\boldsymbol{0})$. Consequently, in order to prove the proposition it is sufficient to show that $\boldsymbol{x}$ is a time-optimal trajectory, see Lemma 7.1.1 in [53].

---

[15]Notice that we have $\text{Reach}_{\Sigma, \leq t_f}(\boldsymbol{0}) = \cup_{t \in [0, t_f]} \text{Reach}_{\Sigma, t}(\boldsymbol{0})$.

By contradiction assume that $\boldsymbol{x}$ is not time-optimal. There exists then a trajectory $\bar{\boldsymbol{x}} \in \text{Traj}(\Sigma)$ with $\bar{\boldsymbol{x}}_f = \boldsymbol{x}_f$ and $\bar{t}_f = T(\bar{\boldsymbol{x}}) < t_f$. Noting that the origin is an equilibrium point of Σ, this implies that for each $\boldsymbol{y} \in \text{Traj}(\Sigma)$ we have

$$T(\boldsymbol{y}) \in [\bar{t}_f, t_f] \Rightarrow y_{2f} \leq x_{2f}. \tag{B.3.83}$$

Without loss of generality, assume now that $\bar{\Lambda} = (\bar{\boldsymbol{x}}, \bar{u}, \bar{\boldsymbol{\lambda}}, \bar{\lambda}_a)$ is an optimal extremal for the LVMP. Then, according to (B.3.83) the terminal link velocity $\bar{x}_{2f}$ must be equal to x_{2f}. Depending on the value of $\bar{\lambda}_a$, we consider next two different cases.

Case 1 ($\bar{\lambda}_a = 1$) In this case, we know from Prop. 8 and in particular (5.2.10) that $\bar{x}_{1f} > 0$ must hold. According to (2.1.3), this means that the acceleration $\dot{\bar{x}}_{2f}$ at the final time will also be positive. Consequently, by keeping the control constant after $\bar{t}_f$ we can always construct an admissible controlled trajectory $(\tilde{\boldsymbol{x}}, \tilde{u})$ with a final time $\tilde{t}_f \in (\bar{t}_f, t_f]$ and with a link velocity $\tilde{x}_{2f} > \bar{x}_{2f} = x_{2f}$. This contradicts (B.3.83).

Case 2 ($\bar{\lambda}_a = 0$) In this case, we can find a positive integer $i \geq 1$ such that $\bar{t}_f = t_{min}(i)$, see Prop. 11. Let us choose a final time $\tilde{t}_f \in (\bar{t}_f, t_f]$, with $\tilde{t}_f < t_{min}(i+1)$, and let $(\tilde{\boldsymbol{x}}, \tilde{u})$ denote the optimal extremal for the LVMP defined on $\tilde{D} = [0, \tilde{t}_f]$. According to (B.3.83), we have then $\tilde{x}_{2f} = x_{2f}$. Moreover, by Prop. 11 the pair $(\tilde{\boldsymbol{x}}, \tilde{u})$ is a normal extremal due to our choice for $\tilde{t}_f$. Consequently, based on our discussion for the first case above $\dot{\tilde{x}}_{2f}$ is positive and this leads again to a contradiction with (B.3.83).

Having shown the existence of a contradiction for each possibility for $\bar{\lambda}_a$, we can conclude that $\boldsymbol{x}$ is a time-optimal trajectory and that $(\boldsymbol{x}, u)$ is a boundary trajectory. $\qquad \square$

To prove Prop. 18, i.e. the last proposition of Sec. 5.4, we will make use of the following two lemmas.

Lemma 54. *Let $n \geq 2$ be a positive integer and $\boldsymbol{A} : \mathbb{R} \to \mathbb{R}^{n \times n}$ a matrix-valued function with continuous entries. Moreover, for each $k \in S_n \backslash \{0\}$ let $^k\boldsymbol{\xi} : \mathbb{R} \to \mathbb{R}^n$ be a continuously differentiable function such that we have*

$$^k\dot{\boldsymbol{\xi}}(t) = \boldsymbol{A}(t) \, {}^k\boldsymbol{\xi}(t), \tag{B.3.84}$$

for each $t \in \mathbb{R}$. Similarly, let $\boldsymbol{\eta} : \mathbb{R} \to (\mathbb{R}^n)^*$ be a continuously differentiable function which satisfies

$$\dot{\boldsymbol{\eta}}(t) = -\boldsymbol{\eta}(t)\boldsymbol{A}(t), \tag{B.3.85}$$

for each $t \in \mathbb{R}$. Finally, let $\boldsymbol{F} : \mathbb{R} \to \mathbb{R}^{n \times n}$ be the matrix-valued function given by

$$\boldsymbol{F}(t) = \begin{pmatrix} ^1\boldsymbol{\xi}(t) & \dots & {}^n\boldsymbol{\xi}(t) \end{pmatrix}.$$

Then, for each $t \in \mathbb{R}$ we have

$$\det \left(\boldsymbol{F}(t) \right) = \det \left(\boldsymbol{F}(0) \right) + \int_0^t tr \left(\boldsymbol{A}(s) \right) \det \left(\boldsymbol{F}(s) \right) \mathrm{d}s, \qquad (\text{B.3.86})$$

and

$$\boldsymbol{\eta}(t)\boldsymbol{F}(t) = \boldsymbol{\eta}(0)\boldsymbol{F}(0). \qquad (\text{B.3.87})$$

Proof. Let $n, \boldsymbol{A}, {}^k\boldsymbol{\xi}$, with $k \in S_n \backslash \{0\}$, $\boldsymbol{\eta}$ and $\boldsymbol{F}$ satisfy the hypothesis of the proposition. Moreover, let us introduce the functions $a_1 : \mathbb{R} \to \mathbb{R}, t \to a_1(t) = \det \left(\boldsymbol{F}(t) \right)$ and $\boldsymbol{a}_2 : \mathbb{R} \to (\mathbb{R}^n)^*, t \to \boldsymbol{a}_2(t) = \boldsymbol{\eta}(t)\boldsymbol{F}(t)$. Focusing first on the function a_1, we can use Jacobi's formula to take its time-derivative which leads to

$$
\begin{aligned}
\frac{\mathrm{d}a_1}{\mathrm{d}t}(s) \quad &= \quad tr \left(\mathrm{adj}\left(\boldsymbol{F}(s) \right) \frac{\mathrm{d}\boldsymbol{F}}{\mathrm{d}t}(s) \right) \\
&\overset{(\text{B.3.84})}{=} \quad tr \left(\mathrm{adj}\left(\boldsymbol{F}(s) \right) \boldsymbol{A}(s)\boldsymbol{F}(s) \right) \\
&= \quad tr \left(\boldsymbol{F}(s)\mathrm{adj}\left(\boldsymbol{F}(s) \right) \boldsymbol{A}(s) \right) \\
&= \quad \det \left(\boldsymbol{F}(s) \right) tr \left(\boldsymbol{A}(s) \right) = a_1(s) tr \left(\boldsymbol{A}(s) \right),
\end{aligned}
$$

where $s \in \mathbb{R}$. This shows that (B.3.86) holds.

Similarly, the truth of (B.3.87) can be shown by taking the time-derivative of $\boldsymbol{a}_2$. Indeed, by making use of (B.3.84) and (B.3.85) we get the following equality which holds at each $t \in \mathbb{R}$ and shows that $\boldsymbol{a}_2$ is constant:

$$
\begin{aligned}
\frac{\mathrm{d}\boldsymbol{a}_2}{\mathrm{d}t}(t) \quad &= \quad \dot{\boldsymbol{\eta}}(t)\boldsymbol{F}(t) + \boldsymbol{\eta}(t)\dot{\boldsymbol{F}}(t) \\
&= \quad \boldsymbol{\eta}(t)\boldsymbol{A}(t)\boldsymbol{F}(t)\left(-1 + 1 \right) \\
&= \quad \boldsymbol{0}.
\end{aligned}
$$

$\square$

Lemma 55. *Let $i \geq 1$ be a positive integer and $I_\alpha \in D_\alpha$ be an open interval. Moreover, assume that for each $k \in S_i \backslash \{0\}$ the functions ${}^k t_S^{ext}$ and ${}^k \boldsymbol{x}_S^{ext}$ are continuously differentiable on I_α. Finally, let $\mathring{D}_{\boldsymbol{x}^{ext}}$ denote the set[16]*

$$\mathring{D}_{\boldsymbol{x}^{ext}} := \left\{ (\alpha, t) \, \middle| \, \alpha \in I_{\alpha^{ext}} \wedge t \in \cup_{k=0}^{i} \left({}^k t_S^{ext}(\alpha), {}^{k+1} t_S^{ext}(\alpha) \right) \right\}.$$

Then, $\boldsymbol{x}^{ext}$ is continuously differentiable on $\mathring{D}_{\boldsymbol{x}^{ext}}$. Moreover, for each $(\alpha, t) \in I_{\alpha^{ext}} \times \left(0, {}^1 t_S^{ext}(\alpha) \right)$ we have

$$\frac{\partial \boldsymbol{x}^{ext}}{\partial \alpha}(\alpha, t) = \boldsymbol{0}. \qquad (\text{B.3.88})$$

---

[16]Notice that $\mathring{D}_{\boldsymbol{x}^{ext}}$ contains in this lemma, in contrary to Prop. 18, also the elements of the open set $I_{\alpha^{ext}} \times \left(0, {}^1 t_S^{ext}(\alpha) \right)$.

In addition, if $i \geq 2$ we have for each $k \in S_i \setminus \{0\}$ and $\alpha \in I_\alpha$

$$
\begin{aligned}
\lim_{t \to {}^k t_S^{ext}(\alpha)^+} \frac{\partial \boldsymbol{x}}{\partial \alpha}(\alpha, t) \;=\; & \lim_{t \to {}^k t_S^{ext}(\alpha)^-} \frac{\partial \boldsymbol{x}}{\partial \alpha}(\alpha, t) \\
& + \frac{2\dot{\theta}_{max} \frac{\mathrm{d}\, {}^k t_S^{ext}}{\mathrm{d}\alpha}(\alpha)}{(-1)^{\mathrm{sgn}(\alpha)+k+1}} \begin{pmatrix} 1 \\ 0 \end{pmatrix}.
\end{aligned}
\tag{B.3.89}
$$

Finally, for each $(\alpha, t) \in \mathring{D}_{\boldsymbol{x}^{ext}}$ we have

$$
\boldsymbol{\lambda}^{ext}(\alpha, t) \frac{\partial \boldsymbol{x}^{ext}}{\partial \alpha}(\alpha, t) = 0.
\tag{B.3.90}
$$

Proof. Let $k \in S_i$ and introduce the set ${}^k \mathring{D}_{\boldsymbol{x}^{ext}} = I_\alpha \times \left({}^k t_S^{ext}(\alpha), {}^{k+1} t_S^{ext}(\alpha) \right)$. Notice that for any extremal lift corresponding to the pair (α, i), with $\alpha \in I_\alpha$, the control will be constant on the interval $\left({}^k t_S^{ext}(\alpha), {}^{k+1} t_S^{ext}(\alpha) \right)$ and equal to ${}^k u = (-1)^{\mathrm{sgn}(\alpha)+k} \dot{\theta}_{max}$, see Prop. 8 and Table 5.5a. Following then the arguments used in the proof of Lemma 52 and noting that τ_J, ${}^k t_S^{ext}$ and ${}^k \boldsymbol{x}_S^{ext}$ are all continuously differentiable, we can conclude that the restriction $\boldsymbol{x}^{ext}|_{{}^k \mathring{D}_{\boldsymbol{x}^{ext}}}$ is continuously differentiable. Consequently, we can differentiate (5.4.3) with respect to α which leads to

$$
\begin{aligned}
\frac{\partial \boldsymbol{x}^{ext}}{\partial \alpha}(\alpha, t) = & \frac{\mathrm{d}\, {}^k \boldsymbol{x}_S^{ext}}{\mathrm{d}\alpha}(\alpha) - \boldsymbol{f}\left({}^k \boldsymbol{x}_S^{ext}(\alpha), {}^k u \right) \frac{\mathrm{d}\, {}^k t_S^{ext}}{\mathrm{d}\alpha}(\alpha) \\
& + \int_{{}^k t_S^{ext}(\alpha)}^{t} \frac{\partial \boldsymbol{f}}{\partial \boldsymbol{x}} \left(\boldsymbol{x}^{ext}(\alpha, s) \right) \frac{\partial \boldsymbol{x}^{ext}}{\partial \alpha}(\alpha, s)\mathrm{d}s,
\end{aligned}
\tag{B.3.91}
$$

for each $(\alpha, t) \in {}^k \mathring{D}_{\boldsymbol{x}^{ext}}$. Moreover, at each such pair the expression above can also be differentiated with respect to time so that we have

$$
\frac{\partial}{\partial t} \left(\frac{\partial \boldsymbol{x}^{ext}}{\partial \alpha}(\alpha, t) \right) = \frac{\partial \boldsymbol{f}}{\partial \boldsymbol{x}} \left(\boldsymbol{x}^{ext}(\alpha, t) \right) \frac{\partial \boldsymbol{x}^{ext}}{\partial \alpha}(\alpha, t).
\tag{B.3.92}
$$

Notice that since our choice for $k \in S_i$ was arbitrary, the two equations (B.3.91) and (B.3.92) are valid for each $(k, (\alpha, t)) \in S_i \times {}^k \mathring{D}_{\boldsymbol{x}^{ext}}$. Moreover, noting that the sets ${}^k \mathring{D}_{\boldsymbol{x}^{ext}}$, with $k \in S_i$, are all open our discussion also shows that $\boldsymbol{x}^{ext}|_{\mathring{D}_{\boldsymbol{x}^{ext}}}$ is continuously differentiable.

Assume now that $k = 0$ and recall that in this case we have, by definition, ${}^k \boldsymbol{x}_S^{ext} \equiv \boldsymbol{0}$ and ${}^k t_S^{ext} \equiv 0$. Consequently, given an arbitrary $\bar{\alpha} \in I_\alpha$ we have according to (B.3.91)

$$
\lim_{t \to 0^+} \frac{\partial \boldsymbol{x}^{ext}}{\partial \alpha}(\bar{\alpha}, t) = \boldsymbol{0},
$$

and this in turn implies by the linear differential equation (B.3.92) the relation

$$
\left(\forall t \in \left(0, {}^1 t_S^{ext}(\bar{\alpha}) \right) \right) \left[\frac{\partial \boldsymbol{x}^{ext}}{\partial \alpha}(\bar{\alpha}, t) = \boldsymbol{0} \right].
\tag{B.3.93}
$$

Since our choice for $\bar{\alpha} \in I_\alpha$ was arbitrary, we can conclude by (B.3.93) that (B.3.88) indeed holds.

Let us now assume that $i \geq 2$ and choose an arbitrary $k \in S_i \backslash \{0\}$. Moreover, let $\bar{\alpha}$ be again an arbitrary element of I_α. According to (B.3.91) the limit of $\frac{\partial \boldsymbol{x}^{ext}}{\partial \alpha}(\bar{\alpha}, t)$ as t approaches $^k t_S^{ext}(\bar{\alpha})$ from the right will then be given by

$$\lim_{t \to {}^k t_S^{ext}(\bar{\alpha})^+} \frac{\partial \boldsymbol{x}^{ext}}{\partial \alpha}(\bar{\alpha}, t) = \frac{\mathrm{d}\, {}^k \boldsymbol{x}_S^{ext}}{\mathrm{d}\alpha}(\bar{\alpha})$$
$$- \boldsymbol{f}\left({}^k \boldsymbol{x}_S^{ext}(\bar{\alpha}), {}^k u\right) \frac{\mathrm{d}\, {}^k t_S^{ext}}{\mathrm{d}\alpha}(\bar{\alpha}). \qquad (B.3.94)$$

To take the limit of $\frac{\partial \boldsymbol{x}^{ext}}{\partial \alpha}(\bar{\alpha}, t)$ as t approaches $^k t_S^{ext}(\bar{\alpha})$ from the left, let us first note that according to (5.4.3) we have

$$\boldsymbol{x}^{ext}(\alpha, t) = {}^k \boldsymbol{x}_S^{ext}(\alpha) - \int_t^{{}^k t_S^{ext}(\alpha)} \boldsymbol{f}(\boldsymbol{x}^{ext}(\alpha, s), {}^{k-1}u)\mathrm{d}s,$$

for each $(\alpha, t) \in {}^k \mathring{D}_{\boldsymbol{x}^{ext}}$. Consequently, taking the derivative of this expression with respect to α we can, as above, use the resulting expression to compute the limit of $\frac{\partial \boldsymbol{x}^{ext}}{\partial \alpha}(\bar{\alpha}, t)$ as t approaches $^k t_S^{ext}(\bar{\alpha})$ from the left. This leads to

$$\lim_{t \to {}^k t_S^{ext}(\bar{\alpha})^-} \frac{\partial \boldsymbol{x}^{ext}}{\partial \alpha}(\bar{\alpha}, t) = \frac{\mathrm{d}\, {}^k \boldsymbol{x}_S^{ext}}{\mathrm{d}\alpha}(\bar{\alpha})$$
$$- \boldsymbol{f}\left({}^k \boldsymbol{x}_S^{ext}(\bar{\alpha}), {}^{k-1}u\right) \frac{\mathrm{d}\, {}^k t_S^{ext}}{\mathrm{d}\alpha}(\bar{\alpha}). \qquad (B.3.95)$$

The equality in (B.3.89) follows now from (B.3.94), (B.3.95) and the equality $^k u = -{}^{k-1}u$.

To conclude the proof we want to show that (B.3.90) holds for each $(\alpha, t) \in \mathring{D}_{\boldsymbol{x}^{ext}}$. For this, choose first an arbitrary $\bar{\alpha} \in I_\alpha$ and define the continuous matrix-valued function $\bar{\boldsymbol{A}}(t) : \left(0, {}^{i+1} t_S^{ext}(\bar{\alpha})\right) \to \mathbb{R}^{2 \times 2}, t \to \bar{\boldsymbol{A}}(t) = \frac{\partial \boldsymbol{f}}{\partial \boldsymbol{x}}\left(\boldsymbol{x}^{ext}(\bar{\alpha}, t)\right)$. Notice that according to (B.3.92) $\frac{\partial \boldsymbol{x}^{ext}}{\partial \alpha}(\bar{\alpha}, .)$ satisfies the differential equation (B.3.84), with $\boldsymbol{A} = \bar{\boldsymbol{A}}$, at each $t \in \cup_{k=0}^{i+1}\left({}^k t_S^{ext}(\bar{\alpha}), {}^{k+1} t_S^{ext}(\bar{\alpha})\right)$. Similarly, according to (5.4.4) $\boldsymbol{\lambda}^{ext}(\bar{\alpha}, .)$ satisfies the differential equation (B.3.85), again with $\boldsymbol{A} = \bar{\boldsymbol{A}}$, at each $t \in \left(0, {}^{i+1} t_S^{ext}(\bar{\alpha})\right)$. Consequently, by Lemma 54 we conclude that for each $k \in S_i$ the product $\boldsymbol{\lambda}^{ext}(\bar{\alpha}, t)\frac{\partial \boldsymbol{x}^{ext}}{\partial \alpha}(\bar{\alpha}, t)$ remains constant on $\left({}^k t_S^{ext}(\bar{\alpha}), {}^{k+1} t_S^{ext}(\bar{\alpha})\right)$. In other words, for each $k \in S_i$ there exists a scalar s_k such that

$$\left(\forall t \in \left({}^k t_S^{ext}(\bar{\alpha}), {}^{k+1} t_S^{ext}(\bar{\alpha})\right)\right) \left[\boldsymbol{\lambda}^{ext}(\bar{\alpha}, t)\frac{\partial \boldsymbol{x}^{ext}}{\partial \alpha}(\bar{\alpha}, t) = s_k\right]. \qquad (B.3.96)$$

We next use mathematical induction to show that s_k is equal to zero for each $k \in S_i$.

Base Case $(\bar{k} = 0)$ Choose an arbitrary time $\bar{t}$ in the interval $\left(0, {}^k t_S^{ext}(\bar{\alpha})\right)$. Then, by (B.3.93) and (B.3.96) we have $s_0 = \boldsymbol{\lambda}^{ext}(\bar{\alpha}, \bar{t})\frac{\partial \boldsymbol{x}^{ext}}{\partial \alpha}(\bar{\alpha}, \bar{t}) = 0$.

Inductive Step ($\bar{k} \in S_{i-1}$) Let $\bar{k} \in S_{i-1}$ and assume that $s_{\bar{k}} = 0$. Then, taking the limit of the product in (B.3.96), with $k = \bar{k}$, as t goes to $^{\bar{k}+1}t_S^{ext}(\bar{\alpha})$ from the left we get the following expression for $s_{\bar{k}}$:

$$
\begin{aligned}
s_{\bar{k}} &= \lim_{t \to ^{\bar{k}+1}t_S^{ext}(\bar{\alpha})^-} \boldsymbol{\lambda}^{ext}(\bar{\alpha}, t) \frac{\partial \boldsymbol{x}^{ext}}{\partial \alpha}(\bar{\alpha}, t) \\
&= \boldsymbol{\lambda}^{ext}\left(\bar{\alpha}, {}^{\bar{k}+1}t_S^{ext}(\bar{\alpha})\right) \lim_{t \to ^{\bar{k}+1}t_S^{ext}(\bar{\alpha})^-} \frac{\partial \boldsymbol{x}^{ext}}{\partial \alpha}(\bar{\alpha}, t) \\
&= \lambda_2^{ext}\left(\bar{\alpha}, {}^{\bar{k}+1}t_S^{ext}(\bar{\alpha})\right) \lim_{t \to ^{\bar{k}+1}t_S^{ext}(\bar{\alpha})^-} \frac{\partial x_2^{ext}}{\partial \alpha}(\bar{\alpha}, t),
\end{aligned}
\tag{B.3.97}
$$

where we have used the fact that $\boldsymbol{\lambda}^{ext}(\bar{\alpha}, .)$ is continuous and that the first costate $\lambda_1^{ext}(\bar{\alpha}, .)$ is equal to zero at the switching time $^{\bar{k}+1}t_S^{ext}(\bar{\alpha})$, see Prop. 7-8. Similarly, taking the limit of the product in (B.3.96), with $k = \bar{k} + 1$, as t goes to $^{\bar{k}+1}t_S^{ext}(\bar{\alpha})$ from the right we get

$$
\begin{aligned}
s_{\bar{k}+1} &= \lim_{t \to ^{\bar{k}+1}t_S^{ext}(\bar{\alpha})^+} \boldsymbol{\lambda}^{ext}(\bar{\alpha}, t) \frac{\partial \boldsymbol{x}^{ext}}{\partial \alpha}(\bar{\alpha}, t) \\
&= \boldsymbol{\lambda}^{ext}\left(\bar{\alpha}, {}^{\bar{k}+1}t_S^{ext}(\bar{\alpha})\right) \lim_{t \to ^{\bar{k}+1}t_S^{ext}(\bar{\alpha})^+} \frac{\partial \boldsymbol{x}^{ext}}{\partial \alpha}(\bar{\alpha}, t) \\
&= \lambda_2^{ext}\left(\bar{\alpha}, {}^{\bar{k}+1}t_S^{ext}(\bar{\alpha})\right) \lim_{t \to ^{\bar{k}+1}t_S^{ext}(\bar{\alpha})^+} \frac{\partial x_2^{ext}}{\partial \alpha}(\bar{\alpha}, t),
\end{aligned}
$$

and this shows together with (B.3.97) that $\bar{s}_k + 1$ is exactly equal to $\bar{s}_k$ since according to (B.3.89) we have

$$
\lim_{t \to ^{\bar{k}+1}t_S^{ext}(\bar{\alpha})^-} \frac{\partial x_2^{ext}}{\partial \alpha}(\bar{\alpha}, t) = \lim_{t \to ^{\bar{k}+1}t_S^{ext}(\bar{\alpha})^+} \frac{\partial x_2^{ext}}{\partial \alpha}(\bar{\alpha}, t).
$$

Noting that our choice for $\bar{\alpha} \in I_\alpha$ was arbitrary, we finally conclude, as desired, that the relation in (B.3.90) is true for each $(\alpha, t) \in \mathring{D}_{\boldsymbol{x}^{ext}}$. $\qquad \square$

We conclude this part of the appendix by showing how to make use of Lemma 54-55 to prove Prop. 18.

Proof of Prop. 18. Let $i \geq 1$, $I_{\alpha^{ext}} \subset D_\alpha$, the functions $^k t_S^{ext}$ and $^k \boldsymbol{x}_S^{ext}$, with $k \in S_i \backslash \{0\}$, and $\boldsymbol{x}^{ext}$ satisfy the hypotheses of the proposition. By Lemma 55, $\boldsymbol{x}^{ext}$ is then continuously differentiable on the open set $\mathring{D}_{\boldsymbol{x}^{ext}}$. Moreover, we can define the matrix-valued function $\boldsymbol{F} : \mathring{D}_{\boldsymbol{x}^{ext}} \to \mathbb{R}^{2 \times 2}$ with

$$
\boldsymbol{F}(\alpha, t) = \left(\frac{\partial \boldsymbol{x}^{ext}}{\partial \alpha}(\alpha, t) \quad \frac{\partial \boldsymbol{x}^{ext}}{\partial t}(\alpha, t) \right),
\tag{B.3.98}
$$

such that $\boldsymbol{F}$ maps each element of $\mathring{D}_{\boldsymbol{x}^{ext}}$ to the Jacobi matrix of $\boldsymbol{x}^{ext}$ at this element. We want to next show that the determinant of this matrix is always positive.

Let $(\bar{\alpha}, \bar{t})$ be an arbitrary element of $\mathring{D}_{\boldsymbol{x}^{ext}}$. Then, there must exist an integer $k \in S_i \backslash \{0\}$ such that $\bar{t} \in \left({}^k t_S^{ext}(\bar{\alpha}), {}^{k+1} t_S^{ext}(\bar{\alpha})\right)$. Moreover, noting that the control on this interval is constant we can, according to (2.1.4) and (B.3.91), differentiate each term in $\boldsymbol{F}(\bar{\alpha}, .)$ with respect to time which leads to

$$\frac{\partial \boldsymbol{F}}{\partial t}(\bar{\alpha}, t) = \frac{\partial \boldsymbol{f}}{\partial \boldsymbol{x}}\left(\boldsymbol{x}^{ext}(\bar{\alpha}, t)\right) \boldsymbol{F}(\bar{\alpha}, t), \tag{B.3.99}$$

for each $t \in \left({}^k t_S^{ext}(\bar{\alpha}), {}^{k+1} t_S^{ext}(\bar{\alpha})\right)$. Noting now that the trace of $\frac{\partial \boldsymbol{f}}{\partial \boldsymbol{x}}$ is equal to zero, we can use Lemma 54 to determine the determinant of $\boldsymbol{F}(\bar{\alpha}, \bar{t})$ as follows:

$$\det\left(\boldsymbol{F}(\bar{\alpha}, \bar{t})\right) = \lim_{t \to {}^k t_S^{ext+}(\bar{\alpha})} \det\left(\boldsymbol{F}(\bar{\alpha}, t)\right) \tag{B.3.100}$$

$$\overset{(B.3.91)}{=} \det\left(\frac{\mathrm{d}\, {}^k \boldsymbol{x}_S^{ext}}{\mathrm{d}\alpha}(\bar{\alpha}) \quad \boldsymbol{f}({}^k \boldsymbol{x}_S^{ext}(\bar{\alpha}), {}^k u)\right)$$

$$\overset{(3.1.4)}{=} \frac{\partial E_{MSS}}{\partial \boldsymbol{x}}\left({}^k x_{1S}^{ext}(\bar{\alpha}), {}^k x_{2S}^{ext}(\bar{\alpha}) - {}^k u\right) \frac{\mathrm{d}{}^k x_S^{ext}}{\mathrm{d}\alpha}(\bar{\alpha})$$

$$\overset{(5.4.13)}{\Rightarrow} \det\left(\boldsymbol{F}(\bar{\alpha}, \bar{t})\right) > 0. \tag{B.3.101}$$

Noting that our choice for $(\bar{\alpha}, \bar{t}) \in \mathring{D}_{\boldsymbol{x}^{ext}}$ was arbitrary we conclude that (5.4.14) indeed holds.

To conclude the proof of the proposition, let us first note that there exists an inverse of the restriction $\boldsymbol{x}^{ext}$ to $D_{\boldsymbol{x}^{ext}}$, with the set $D_{t_f^{ext}}$ as its range, since $\boldsymbol{x}^{ext}$ is a surjective function by assumption. Using $\boldsymbol{\mu}^{ext} : D_{t_f^{ext}} \to D_{\boldsymbol{x}^{ext}}, \boldsymbol{x} \to \boldsymbol{\mu}^{ext}(\boldsymbol{x}) = \begin{pmatrix} \mu_1^{ext} & \mu_2^{ext} \end{pmatrix}^T$ to denote this inverse, we clearly have

$$(\forall (\alpha, t) \in D_{\boldsymbol{x}^{ext}}) \left[\boldsymbol{\mu}^{ext}\left(\boldsymbol{x}^{ext}(\alpha, t)\right) = \begin{pmatrix} \alpha \\ t \end{pmatrix}\right], \tag{B.3.102}$$

and the desired function t_f^{ext} in the proposition is uniquely determined by μ_2^{ext}. Now, it follows from (5.4.14) and the inverse function theorem [62] that the restriction of t_f^{ext} to $\mathring{D}_{\boldsymbol{x}^{ext}}$ is continuously differentiable and satisfies, in accordance with (B.3.102), the equality

$$\frac{\partial t_f^{ext}}{\partial \boldsymbol{x}}\left(\boldsymbol{x}^{ext}(\alpha, t)\right) \boldsymbol{F}(\alpha, t) \;\; = \;\; \begin{pmatrix} 0 & 1 \end{pmatrix},$$

for each $(\alpha, t) \in \mathring{D}_{\boldsymbol{x}^{ext}}$. In addition, notice that by the Hamiltonian condition in (5.2.4) and the condition (B.3.90) in Lemma 55, we similarly have

$$\boldsymbol{\lambda}^{ext}(\alpha, t) \boldsymbol{F}(\alpha, t) = \begin{pmatrix} 0 & -1 \end{pmatrix}.$$

According to (5.4.14), this shows that (5.4.16)-(5.4.17) must hold for each $(\alpha, t) \in D_{\boldsymbol{x}^{ext}} \backslash \mathring{D}_{\boldsymbol{x}^{ext}}$. The fact that the relation (5.4.17) also holds at points $(\alpha, t) \in D_{\boldsymbol{x}^{ext}} \backslash \mathring{D}_{\boldsymbol{x}^{ext}}$ follows from the continuity of $\boldsymbol{\lambda}^{ext}$, as one can show using Lemma 52, and the fact that the determinant of $\boldsymbol{F}(\alpha, t)$ is positive for each $(\alpha, t) \in \mathring{D}_{\boldsymbol{x}^{ext}}$, see also Theorem 6.1.1 in [53]. This finally shows that t_f^{ext} is continuously differentiable, as desired. $\qquad \square$

B.4 Maximal Link Velocity

B.4.1 Final Time Dependence

In this first part of the appendix, we will provide the proofs of the two propositions from Sec. 6.1.

Proof of Prop. 19. Let $(\boldsymbol{x}, u)$ be an optimally controlled trajectory with the final time $t_f > 0$. Moreover, let $\dot{q}_{lb} : (0, \infty) \to \mathbb{R}$ and $\dot{q}_{ub} : (0, \infty) \to \mathbb{R}$ be the two functions defined by (6.1.5) and (6.1.6), respectively. It follows then from the continuity of $\boldsymbol{x}$ and E_{pot} that both $\dot{q}_{lb}$ and $\dot{q}_{ub}$ are continuous on the intervals $(0, t_f)$ and (t_f, ∞). Moreover, since the limits of $\dot{q}_{lb}$ and $\dot{q}_{ub}$, as t goes to t_f, are both equal to $x_2(t_f)$ these two functions are continuous at t_f, as well. Consequently, we conclude that $\dot{q}_{lb}$ and $\dot{q}_{ub}$ are continuous.

Evaluating now $\dot{q}_{lb}$ and $\dot{q}_{ub}$ at t_f and noting that $\boldsymbol{x}$ is an optimal trajectory, we can directly see that we have $\dot{q}_{lb}(t_f) = \dot{q}_{ub}(t_f) = \dot{q}_{max}(t_f)$. This shows that the inequalities in (6.1.7) hold with equality if t equals to t_f. Moreover, notice that our discussion in the beginning of Sec. 6.1 and in particular the relations (6.1.3)-(6.1.4) directly imply that $\dot{q}_{lb}(t) \leq \dot{q}_{max}(t)$ holds for each $t \in (0, \infty)$. In order to prove the proposition, it is thus sufficient to show the truth of the following statement:

$$(\forall t \in (0, t_f) \cup (t_f, \infty)) \left[\dot{q}_{max}(t) \leq \dot{q}_{ub}(t) \right]. \tag{B.4.1}$$

In the remaining of the proof, we will show that the statement above is indeed true.

Let $\bar{t}_f$ be an arbitrary element of $(0, t_f) \cup (t_f, \infty)$. Then, by Prop. 6 there exists an optimally controlled trajectory $(\bar{\boldsymbol{x}}, \bar{u})$ with the final time $\bar{t}_f$ such that $\bar{x}_2(\bar{t}_f)$ equals to $\dot{q}_{max}(\bar{t}_f)$. In order to prove (B.4.1), we need to show that $\dot{q}_{max}(\bar{t}_f)$ is less than or equal to $\dot{q}_{ub}(\bar{t}_f)$. For this, we will investigate two different cases depending on the value of $\bar{t}_f$.

Case 1 $\left(\bar{t}_f \in (0, t_f)\right)$ Notice that the relation (6.1.3) holds for any optimally controlled trajectory and thus also for $(\bar{\boldsymbol{x}}, \bar{u})$. Consequently, we have the following condition for $\dot{q}_{max}$:

$$(\forall t \in (\bar{t}_f, \infty)) \left[\bar{x}_2(\bar{t}_f) = \dot{q}_{max}(\bar{t}_f) \leq \dot{q}_{max}(t) \right].$$

Since in this first case t_f is greater than $\bar{t}_f$, the condition above implies then, as desired, that $\dot{q}_{max}(\bar{t}_f)$ is less than or equal to $\dot{q}_{ub}(\bar{t}_f) = \dot{q}_{max}(t_f)$.

Case 2 $\left(\bar{t}_f \in (t_f, \infty)\right)$ Due to the optimality of $(\bar{\boldsymbol{x}}, \bar{u})$ and the system dynamics in (2.1.4), the following equality holds for the value of $\dot{q}_{max}$ at $\bar{t}_f$:

$$\begin{aligned} \dot{q}_{max}(\bar{t}_f) &= \bar{x}_2(\bar{t}_f) \\ &= \bar{x}_2(t_f) + \int_{t_f}^{\bar{t}_f} \frac{\tau_J\left(\bar{x}_1(s)\right)}{M} \mathrm{d}s. \end{aligned} \tag{B.4.2}$$

Now, based on the definition of $\dot{q}_{max}$ it is clear that $\bar{x}_2(t_f) \leq \dot{q}_{max}(t_f) = x_2(t_f)$ must hold. Moreover, since $\bar{\boldsymbol{x}}$ starts from the origin it follows from Prop. 5 that we will have $\bar{x}_1(t) < \dot{\theta}_{max}t$ for each $t \in (0, \bar{t}_f]$. Using these two inequalities together with (B.4.2) and the fact that $\bar{t}_f$ is greater than t_f, we arrive then at the following relation for $\dot{q}_{max}$:

$$
\begin{aligned}
\dot{q}_{max}(\bar{t}_f) \quad &< \quad x_2(t_f) + \int_{t_f}^{\bar{t}_f} \frac{\tau_J(\dot{\theta}_{max}s)}{M}\mathrm{d}s \\
&= \quad x_2(t_f) + \int_{\dot{\theta}_{max}t_f}^{\dot{\theta}_{max}\bar{t}_f} \frac{\tau_J(s)}{M\dot{\theta}_{max}}\mathrm{d}s \\
\stackrel{(6.1.6)}{\Rightarrow} \dot{q}_{max}(\bar{t}_f) \quad &< \quad \dot{q}_{ub}(\bar{t}_f).
\end{aligned}
$$

With the relation above, we finally conclude that in this second case the inequality in (B.4.1) holds for $t = \bar{t}_f$, as well. $\qquad\square$

Proof of Prop. 20. We will first show that $\dot{q}_{max}$ is a continuous function. For this, let t_f be an arbitrary positive scalar. By Prop. 6, there exists then an optimally controlled trajectory $(\boldsymbol{x}, u)$ defined on $D = [0, t_f]$ with $x_2(t_f) = \dot{q}_{max}(t_f)$. Moreover, using Prop. 19 and in particular (6.1.5)-(6.1.6) we can construct two continuous functions, $\dot{q}_{lb}$ and $\dot{q}_{ub}$, for which (6.1.7) will hold. From the continuity of these functions and the fact that they are both equal to $\dot{q}_{max}(t_f)$ at t_f, it follows that for each scalar $\varepsilon > 0$ there exists a $\delta \in (0, t_f)$ such that for each $t \in B_{t_f}(\delta) := (t_f - \delta, t_f + \delta)$ we have

$$
|\dot{q}_{lb}(t) - \dot{q}_{max}(t_f)| < \frac{\varepsilon}{2} \wedge |\dot{q}_{ub}(t) - \dot{q}_{lb}(t)| < \frac{\varepsilon}{2}.
$$

Looking now at the difference $|\dot{q}_{max}(t) - \dot{q}_{max}(t_f)|$, we have for each t in $B_{t_f}(\delta)$

$$
\begin{aligned}
|\dot{q}_{max}(t) - \dot{q}_{max}(t_f)| \quad &\leq \quad |\dot{q}_{max}(t) - \dot{q}_{lb}(t)| + \\
& \qquad |\dot{q}_{lb}(t) - \dot{q}_{max}(t_f)| \\
&\stackrel{(6.1.7)}{\leq} \quad |\dot{q}_{ub}(t) - \dot{q}_{lb}(t)| + \\
& \qquad |\dot{q}_{lb}(t) - \dot{q}_{max}(t_f)| \\
&< \quad \varepsilon.
\end{aligned}
$$

Since the choice of ε was arbitrary, the inequality above proves the continuity of $\dot{q}_{max}$ at t_f. Similarly, since the choice of t_f was also arbitrary we conclude that $\dot{q}_{max}$ is a continuous function. We next prove that $\dot{q}_{max}$ is a strictly increasing function.

Let t_f and $\bar{t}_f$ be two arbitrary scalars with $\bar{t}_f > t_f > 0$. Moreover, let $(\boldsymbol{x}, u)$ as above an optimally controlled trajectory defined on $D = [0, t_f]$ and $\dot{q}_{lb}$ the continuous lower bound defined by (6.1.5). Evaluating the inequality (6.1.7) at $t = \bar{t}_f$, we can then arrive directly at the following condition for $\dot{q}_{max}$:

$$
\dot{q}_{ub}(\bar{t}_f) = \dot{q}_{max}(t_f) \leq \dot{q}_{max}(\bar{t}_f).
$$

Since our choice for t_f and $\bar{t}_f$ was arbitrary, the inequality above shows that $\dot{q}_{max}$ is an increasing function. To prove now that $\dot{q}_{max}$ is a strictly increasing function, assume by contradiction that there exist two scalars $t_f, \bar{t}_f$ with $\bar{t}_f > t_f > 0$ and $\dot{q}_{max}(\bar{t}_f) = \dot{q}_{max}(t_f)$. Since $\dot{q}_{max}$ is an increasing function, $\dot{q}_{max}$ must then be constant in the interval $[t_f, \bar{t}_f]$, i.e. we must have

$$(\forall t \in [t_f, \bar{t}_f]) \left[\dot{q}_{max}(t) = \dot{q}_{max}(t_f) \right]. \tag{B.4.3}$$

Notice that by Prop. 6 and Prop. 7 there exists an extremal lift $\Lambda = (\boldsymbol{x}, u, \boldsymbol{\lambda}, \lambda_a)$ for the LVMP such that $(\boldsymbol{x}, u)$ is an optimally controlled trajectory defined on $D = [0, t_f]$. In addition, according to (5.2.3)-(5.2.5) the following equality will hold for the terminal spring deflection x_{1f}:

$$\frac{\tau_J(x_{1f})}{M} = \frac{\lambda_a}{v}, \tag{B.4.4}$$

where v is a positive scalar and $\lambda_a \in \{0, 1\}$. In the following, we investigate two cases depending on the value of λ_a and show that in each case (B.4.3) leads to a contradiction.

Case 1 $\left(\lambda_a = 1\right)$ In this case, the terminal deflection x_{1f} will be positive due to (B.4.4). Defining now a control $\bar{u} : [0, \bar{t}_f] \to \mathbb{U}$ with

$$\bar{u}(t) = \begin{cases} u(t) & t < t_f \\ u(t_f) & t \geq t_f \end{cases},$$

we can see that the trajectory $\bar{\boldsymbol{x}}$ which starts from the origin and corresponds to $\bar{u}$ will coincide with the optimal trajectory $\boldsymbol{x}$ in the interval D. Moreover, the time-derivative of $\bar{x}_2$ at $t = t_f$ will be positive since it equals to $\frac{\tau_J(x_{1f})}{M}$, see (2.1.4). Consequently, we can find a time $\tilde{t}_f \in (t_f, \bar{t}_f]$ at which $\bar{x}_2(\tilde{t}_f)$ will be greater than $\dot{q}_{max}(t_f)$. Since $\dot{q}_{max}$ is an increasing function, this implies that $\dot{q}_{max}(\bar{t}_f) > \dot{q}_{max}(t_f)$ will hold in contrary to (B.4.3).

Case 2 $\left(\lambda_a = 0\right)$ As we have shown in Prop. 11, the equality $\lambda_a = 0$ implies that there exists an integer $i \geq 0$ such that t_f is given by $t_{min}(i+1)$. Since the time $t_{min}(i+2)$ will always be greater than $t_{min}(i+1)$, see (4.2.11)-(4.2.12), we can then find a time $\tilde{t}_f \in (t_f, \bar{t}_f)$ which is smaller than $t_{min}(i+2)$. Moreover, by Prop. 6 and Prop. 7 there will again exist an extremal lift $\tilde{\Lambda} = (\tilde{\boldsymbol{x}}, \tilde{u}, \tilde{\boldsymbol{\lambda}}, \tilde{\lambda}_a)$ containing an optimally controlled trajectory $(\tilde{\boldsymbol{x}}, \tilde{u})$ defined on $\tilde{D} = [0, \tilde{t}_f]$. For this extremal lift, however, $\tilde{\lambda}_a$ will be equal to 1 since $\tilde{t}_f \in (t_{min}(i), t_{min}(i+1))$. Following the arguments we used for the first case above, we can then see that $\dot{q}_{max}(\bar{t}_f)$ must be greater than $\dot{q}_{max}(\tilde{t}_f) \geq \dot{q}_{max}(t_f)$ contradicting (B.4.3).

Our discussion of the two cases above shows that (B.4.3) can not be true. Consequently, $\dot{q}_{max}(\bar{t}_f)$ must be greater than $\dot{q}_{max}(t_f)$. Since our choice for $\bar{t}_f$ and t_f was arbitrary, we finally conclude that $\dot{q}_{max}$ is a strictly increasing function.

To conclude the proof of the proposition, it remains to show that (6.1.8) is true. Focusing first at the limit of $\dot{q}_{max}$ as t approaches 0 from the right, let us first note that the following relation holds for $\dot{q}_{max}$ according to Prop. 15:

$$\forall t \in (0, \infty) \left[0 < \dot{q}_{max}(t) < \sqrt{\frac{2E_{pot}(\dot{\theta}_{max}t)}{M}} \right]. \tag{B.4.5}$$

Since the upper bound for $\dot{q}_{max}$ above, i.e. $\sqrt{\frac{2E_{pot}(\dot{\theta}_{max}t)}{M}}$, goes to zero as t approaches zero from the right, we can conclude that $\lim_{t \to 0^+} \dot{q}_{max}(t) = 0$ indeed holds.

Focusing now on the second limit, we know from Prop. 11 that for each non-negative integer i there exists an abnormal extremal $(\boldsymbol{x}, u)$ with the final link velocity $x_2(t_f) = 2(i + 1)\dot{\theta}_{max}$. This means that the function $\dot{q}_{max}$ can never be bounded above by a positive constant. Since $\dot{q}_{max}$ is also an increasing function, we conclude that $\dot{q}_{max}(t)$ must go to infinity as x_2 goes to infinity. $\quad\square$

B.4.2 Parameter Dependence

In this second part, we will provide the proofs for Prop. 21 and Prop. 23-25 which are stated in Sec. 6.2. Moreover, we will provide two lemmas and a corollary which are made use of in these proofs as well as in our discussions in that section. We start with the lemma which will be essential in the proofs of Prop. 21 and Prop. 25.

Lemma 56. *Let $C_{dim} > 0$ be an arbitrary scalar. Moreover, let Σ be the control system corresponding to $\boldsymbol{p} = (M, \tau_J, \dot{\theta}_{max}) \in P_\Sigma$ and $\hat{\Sigma}$ the system corresponding to $\hat{\boldsymbol{p}} = (1, \hat{\tau}_J, 1) \in P_\Sigma$ such that the following relation holds between their TDP's:*

$$(\forall \phi \in \mathbb{R}) \left[\hat{\tau}_J(\phi) = \frac{\tau_J \left(\frac{\dot{\theta}_{max}}{C_{dim}}\phi \right)}{MC_{dim}\dot{\theta}_{max}} \right]. \tag{B.4.6}$$

In addition, let $u : [0, t_f] \to \mathbb{U}$ and $\hat{u} : [0, C_{dim}t_f] \to \hat{\mathbb{U}} = [-1, 1]$ be two piecewise continuous controls satisfying

$$(\forall t \in [0, t_f]) \left[u(t) = \dot{\theta}_{max}\hat{u}(C_{dim}t) \right]. \tag{B.4.7}$$

Finally, let $\boldsymbol{x}$ be a trajectory of the control system Σ which corresponds to the control u and $\hat{\boldsymbol{x}}$ a trajectory of $\hat{\Sigma}$ corresponding to $\hat{u}$. Then, we have

$$\boldsymbol{x}_0 = \begin{pmatrix} \frac{\dot{\theta}_{max}}{C_{dim}} & 0 \\ 0 & \dot{\theta}_{max} \end{pmatrix} \hat{\boldsymbol{x}}_0 \quad \Leftrightarrow$$

$$(\forall t \in [0, t_f]) \left[\boldsymbol{x}(t) = \begin{pmatrix} \frac{\dot{\theta}_{max}}{C_{dim}} & 0 \\ 0 & \dot{\theta}_{max} \end{pmatrix} \hat{\boldsymbol{x}}(C_{dim}t) \right]. \tag{B.4.8}$$

Proof. Let $C_{dim}, \boldsymbol{p}, \hat{\boldsymbol{p}}, \Sigma, \hat{\Sigma}, u, \hat{u}, \boldsymbol{x}$ and $\hat{\boldsymbol{x}}$ all satisfy the hypotheses of the lemma. Assume first that $\boldsymbol{x}_0$ and $\hat{\boldsymbol{x}}_0$ are related to each other as stated on the left hand side of (B.4.8). We want to show that in this case the right-hand side of (B.4.8) is true. For this, let us first introduce the function $\boldsymbol{y} : [0, t_f] \to \mathbb{R}^2$ defined by

$$(\forall t \in [0, t_f]) \left[\boldsymbol{y}(t) = \begin{pmatrix} \frac{\dot{\theta}_{max}}{C_{dim}} & 0 \\ 0 & \dot{\theta}_{max} \end{pmatrix} \hat{\boldsymbol{x}}(C_{dim} t) \right]. \tag{B.4.9}$$

Since $\hat{\boldsymbol{x}}$ is a trajectory of $\hat{\Sigma}$, the function $\boldsymbol{y}$ will be differentiable everywhere except at a finite number of times where $\hat{u}$ has a discontinuity. Denoting the set of these times as E and using the state dynamics in (2.1.4), we can then see that the following relation holds at each $t \in [0, t_f] \backslash E$:

$$
\begin{aligned}
\dot{\boldsymbol{y}}(t) \quad &= \quad \begin{pmatrix} \dot{\theta}_{max} \left(\hat{u}(C_{dim} t) - \hat{x}_2(C_{dim} t) \right) \\ C_{dim} \dot{\theta}_{max} \hat{\tau}_J \left(\hat{x}_1(C_{dim} t) \right) \end{pmatrix} \\[2mm]
&\overset{(B.4.6)}{=} \quad \begin{pmatrix} \dot{\theta}_{max} \hat{u}(C_{dim} t) - \dot{\theta}_{max} \hat{x}_2(C_{dim} t) \\ \frac{\tau_J \left(\frac{\dot{\theta}_{max}}{C_{dim}} \hat{x}_1(C_{dim} t) \right)}{M} \end{pmatrix} \\[2mm]
&\overset{(B.4.7),(B.4.9)}{=} \quad \begin{pmatrix} u(t) - y_2(t) \\ \frac{\tau_J(y_1(t))}{M} \end{pmatrix} = \boldsymbol{f}(\boldsymbol{y}(t), u(t)). \tag{B.4.10}
\end{aligned}
$$

Noting that (B.4.10) holds at almost everywhere in $[0, t_f]$, we can conclude that $\boldsymbol{y}$ is a trajectory of Σ which corresponds to the control u. Moreover, it follows from the definition of $\boldsymbol{y}$ in (B.4.9) and our assumption on the relation between $\boldsymbol{x}_0$ and $\hat{\boldsymbol{x}}_0$ that we have $\boldsymbol{y}_0 = \boldsymbol{x}_0$. This means that $\boldsymbol{y}$ and $\boldsymbol{x}$ must be equivalent trajectories and that the right-hand side of (B.4.8) holds as desired.

To conclude the proof of the proposition, we need to show that the right-hand side of (B.4.8) implies the relation between $\boldsymbol{x}_0$ and $\hat{\boldsymbol{x}}_0$ as stated on its left hand side. This can simply be done by evaluating the right-hand side at $t = 0$. $\qquad\square$

Lemma 56 shows how to relate trajectories of two different control systems, Σ and $\hat{\Sigma}$, if the parameters to which they correspond, i.e. $\boldsymbol{p}$ and $\hat{\boldsymbol{p}}$, satisfy a certain relationship that depends on an arbitrary scalar $C_{dim} > 0$. It is important to note here that the control system $\hat{\Sigma}$ in this lemma contains of dimensionless parameters if this scalar C_{dim} has the same dimension as $\dot{\theta}_{max}$. We next show how by appropriately choosing C_{dim} we can use this lemma to derive Prop. 21.

Proof of Prop. 21. Let $\boldsymbol{p}$ be an arbitrary element of P_Σ and Σ the control system corresponding to $\boldsymbol{p}$. Then, the TDP $\hat{\tau}_J : \mathbb{R} \to \mathbb{R}$ defined by (6.2.3) is clearly an element of $C^1_{\tau_J}$. Consequently, the parameter $\hat{\boldsymbol{p}} = (1, \hat{\tau}_J, 1)$ is an element of P_Σ and we can construct a control system $\hat{\Sigma}$ corresponding to $\hat{\boldsymbol{p}}$. Notice that Σ and $\hat{\Sigma}$ both satisfy the relation (B.4.6) in Lemma 56 with $C_{min} = \omega_0$. Moreover, the following equality holds for the SDP $\hat{K}_J$:

$$\hat{K}_J(\phi) = \frac{\mathrm{d}}{\mathrm{d}\phi} \left(\frac{\tau_J(\frac{\dot{\theta}_{max}}{\omega_0} \phi)}{M \omega_0 \dot{\theta}_{max}} \right) = \frac{K_J(\frac{\dot{\theta}_{max}}{\omega_0} \phi)}{K_J(0)},$$

which means that we have $\hat{\omega}_0 = \sqrt{\frac{\hat{K}_J(0)}{\hat{M}}} = 1$. We want to next use this last equality together with Lemma 56 and Prop. 3-4 to show that the equality $\omega_0 t_{min}(k; \boldsymbol{p}) = t_{min}(k; \hat{\boldsymbol{p}})$ holds for each $k \in \{1, 2, \ldots\}$. This will prove the proposition, as our choice for $\boldsymbol{p}$ was arbitrary.

Let k be an arbitrary positive integer and $(\boldsymbol{x}, u)$ an admissible controlled trajectory of Σ which is defined on $[0, t_f]$. Moreover, assume that $\boldsymbol{x}_0$ equals to $\boldsymbol{0}$, u is a switching control with $k-1$ switchings and all the three conditions (4.2.6), (4.2.7) and (4.2.9) are satisfied. By Prop. 3-4, we then know that t_f must be necessarily equal to $t_{min}(k; \boldsymbol{p})$. If we now construct a piecewise continuous control $\hat{u} : [0, \hat{t}_f] \to [-1, 1]$ such that $\hat{t}_f$ is equal to $\omega_0 t_f$ and (B.4.7) is satisfied, it follows from Lemma 56 that the trajectory $\hat{\boldsymbol{x}}$ of $\hat{\Sigma}$ which starts from the origin and which corresponds to $\hat{u}$ will be related to $\boldsymbol{x}$ by the right-hand side of (B.4.8) with $C_{min} = \omega_0$. Consequently, the three conditions (4.2.6), (4.2.7) and (4.2.9) will again be satisfied if we substitute there $u, \dot{\theta}_{max}, x_1$ and t_f with $\hat{u}, \hat{\dot{\theta}}_{max} = 1, \hat{x}_1$ and $\hat{t}_f$, respectively. Since Prop. 3-4 are also valid for $\hat{\Sigma}$, we can then see that $\hat{t}_f$ must be equal to $t_{min}(k; \hat{\boldsymbol{p}})$, i.e. $\omega_0 t_{min}(k; \boldsymbol{p}) = t_{min}(k; \hat{\boldsymbol{p}})$. Since our choice for the integer k was arbitrary, this concludes our proof. $\qquad \square$

Given a function $g \in C_{\tau_J}^1$, with $\frac{\mathrm{d}g}{\mathrm{d}\phi}(0) = 1$, we derive in the following lemma two closely related expressions for the dimensionless time function $\omega_0 t_{min}(.; \boldsymbol{p})$, which are valid for any $\boldsymbol{p} \in P_{\Sigma_g}$. One of these expressions is already used in Table 6.1 and they will both be important for the proof of Prop. 24 where we analyse the dependence of t_{min} on the eigenfrequency ω_0.

Lemma 57. *Let $g \in C_{\tau_J}^1$ with $\frac{\mathrm{d}g}{\mathrm{d}\phi}(0) = 1$. Then, for each positive integer k and each $\boldsymbol{p} \in P_{\Sigma_g}$ we have*

$$\omega_0 t_{min}(k; \boldsymbol{p}) = 2 \sum_{l=0}^{k-1} \left\{ \int_0^{a(l)} \frac{\mathrm{d}s}{\sqrt{(2l+1)^2 \dot{\Theta}_{max}^2 - 2E_{pot,g}(s)}} \right.$$

$$\left. + \int_0^{b(l)} \frac{\dot{\Theta}_{max} \mathrm{d}s}{g\left(E_{pot,g}^{-1}\left(\frac{\dot{\Theta}_{max}^2\left((2l+1)^2 - s^2\right)}{2}\right)\right)} \right\}, \qquad \text{(B.4.11)}$$

where for each $l \in S_{k-1}$ the pair $(a(l), b(l))$ is an arbitrary element of $(0, k_e{}^l \phi_{max}) \times (0, 2l+1)$ with

$$E_{pot,g}(k_e{}^l \phi_{max}) = \frac{(2l+1)^2}{2} \dot{\Theta}_{max}^2, \qquad \text{(B.4.12)}$$

and

$$2E_{pot,g}\left(a(l)\right) + \dot{\Theta}_{max}^2 b(l)^2 = \dot{\Theta}_{max}^2 (2l+1)^2. \qquad \text{(B.4.13)}$$

Moreover, the same product can also be expressed as

$$\omega_0 t_{min}(k; \boldsymbol{p}) =$$

$$\sum_{l=0}^{k-1} \int_0^{2l+1} \frac{2\dot{\Theta}_{max} \mathrm{d}s}{g \left(E_{pot,g}^{-1} \left(\frac{\dot{\Theta}_{max}^2 \left((2l+1)^2 - s^2 \right)}{2} \right) \right)}. \tag{B.4.14}$$

Proof. Let g be an element of $C_{\tau_J}^1$ with $\frac{\mathrm{d}g}{d\phi}(0) = 1$ and $\boldsymbol{p} = (M, \tau_J, \dot{\theta}_{max})$ an element of P_{Σ_g} such that we have

$$(\forall \phi \in \mathbb{R}) \left[\tau_J(\phi) = K_e g(k_e \phi) \right], \tag{B.4.15}$$

with $k_e > 0$ and $K_e > 0$. Moreover, let k be an arbitrary positive integer. Using the expression (B.4.15) for τ_J in (3.1.6) and (3.1.7), we can find the following relations for $E_{pot}, E_{MSS}, |\dot{\phi}|$ and $|\phi|$ which hold at each point of their respective domains:

$$E_{pot}(\phi) = \frac{K_e}{k_e} E_{pot,g}(k_e \phi), \tag{B.4.16}$$

$$E_{MSS}(\phi, \dot{\phi}) = \frac{K_e}{2k_e} \left[2E_{pot,g}(k_e \phi) + \dot{\Theta}_{max}^2 \frac{\dot{\phi}^2}{\dot{\theta}_{max}^2} \right], \tag{B.4.17}$$

$$|\dot{\phi}|(\phi, \phi_{max}) = \frac{\omega_0 \sqrt{2 \left(E_{pot,g}(k_e \phi_{max}) - E_{pot,g}(k_e \phi) \right)}}{k_e}, \tag{B.4.18}$$

and

$$|\phi|(\dot{\phi}, \dot{\phi}_{max}) = \frac{E_{pot,g}^{-1} \left(\frac{\dot{\Theta}_{max}^2}{2} \left(\frac{\dot{\phi}_{max}^2 - \dot{\phi}^2}{\dot{\theta}_{max}^2} \right) \right)}{k_e}. \tag{B.4.19}$$

In addition, using the definition of t_{min} in Prop. 4 and the definition of T_p in (3.2.11) we can arrive at the following equality:

$$\omega_0 t_{min}(k; \boldsymbol{p}) = \frac{1}{2} \omega_0 \sum_{l=0}^{k-1} T_p({}^l\phi_{max})$$

$$= 2\omega_0 \sum_{l=0}^{k-1} T_\phi({}^l\phi_s, \ {}^l\phi_{max}) + T_{\dot{\phi}}({}^l\dot{\phi}_s, \ {}^l\dot{\phi}_{max}), \tag{B.4.20}$$

where for each $l \in S_{k-1}$ we have according to (4.2.5), (4.2.12) and (B.4.16)-(B.4.19)

$$E_{pot,g}(k_e{}^l\phi_{max}) = \frac{(2l+1)^2}{2} \dot{\Theta}_{max}^2, \tag{B.4.21}$$

$${}^l\dot{\phi}_{max} = (2l+1)\dot{\theta}_{max}, \tag{B.4.22}$$

and

$$2E_{pot,g}(k_e{}^l\phi_s) + \dot{\Theta}_{max}^2 \frac{{}^l\dot{\phi}_s^2}{\dot{\theta}_{max}^2} = (2l+1)^2 \dot{\Theta}_{max}^2. \tag{B.4.23}$$

Notice that in the last equality the pair $({}^l\phi_s, {}^l\dot\phi_s)$ must belong to $(0, {}^l\phi_{max}) \times \left(0, (2l+1)\dot\theta_{max}\right)$ but is otherwise arbitrary, see Sec. 3.2.

With the equations summarized above, it is now possible to derive the two expressions for $\omega_0 t_{min}(k; \boldsymbol{p})$ in (B.4.11) and (B.4.14). Indeed, we can first use (B.4.15)-(B.4.16) and (B.4.18)-(B.4.19) in (3.2.2) and (3.2.4) to rewrite the two time functions T_ϕ and $T_{\dot\phi}$ in terms of $E_{pot,g}$ and $E_{pot,g}^{-1}$, respectively. This leads to

$$\omega_0 T_\phi(\phi, \phi_{max}) = \int_0^{k_e\phi} \frac{\mathrm{d}s}{\sqrt{2\left(E_{pot,g}(k_e\phi_{max}) - E_{pot,g}(s)\right)}},$$

which holds at each $(\phi, \phi_{max}) \in D_{T_\phi}$ and to

$$\omega_0 T_{\dot\phi}(\dot\phi, \dot\phi_{max}) = \int_0^{\frac{\dot\phi}{\dot\theta_{max}}} \frac{\dot\Theta_{max}\mathrm{d}s}{g\left(E_{pot,g}^{-1}\left(\frac{\dot\Theta_{max}^2\left(\frac{\dot\phi_{max}^2}{\dot\theta_{max}^2} - s^2\right)}{2}\right)\right)},$$

which holds at each $(\dot\phi, \dot\phi_{max}) \in D_{T_{\dot\phi}}$. By using these last two relations and (B.4.21)-(B.4.22) in (B.4.20), the expression for $\omega_0 t_{min}(k; \boldsymbol{p})$ in (B.4.11) is then directly obtained if we set for each $l \in S_{k-1}$ $a(l) = k_e{}^l\phi_s$ and $b(l) = \frac{{}^l\dot\phi}{\dot\theta_{max}}$. Note that the conditions on $a(l)$ and $b(l)$ as provided in the proposition follow from the conditions we have found on $({}^l\phi_s, {}^l\dot\phi_s)$. Finally, the expression in (B.4.14) can be derived from (B.4.11) using first the fact that for each term in the sum there the attained value does not change as long as $(a(l), b(l))$ remains an element of $(0, k_e{}^l\phi_{max}) \times (0, 2l+1)$ which satisfies (B.4.13). The desired expression then follows by noting that for each $l \in S_{k-1}$ $a(l)$ goes to zero as $b(l)$ goes to $2l+1$. $\qquad\square$

Using the equality (B.4.21) from Lemma 57 together with Prop. 1 and Prop. 21, we next show how to derive Prop. 23.

Proof of Prop. 23. Let $g, \boldsymbol{p}, \tilde{\boldsymbol{p}}, k$ and Φ_{max} all satisfy the hypotheses of the proposition and let $K = \mathrm{sgn}\left(\frac{\mathrm{d}^2 g}{\mathrm{d}\phi^2}(\Phi_{max})\right)$. Moreover, let l be an arbitrary positive integer which is less than or equal to k. It is important to first note that for each $\phi \in \mathbb{R}$, $\frac{\mathrm{d}^2\tau_J}{\mathrm{d}\phi^2}(\phi)$ and $\frac{\mathrm{d}^2\tilde\tau_J}{\mathrm{d}\phi^2}(\phi)$ are given by $K_e k_e^2 \frac{\mathrm{d}^2 g}{\mathrm{d}\phi^2}(k_e\phi)$ and $\tilde{K}_e \tilde{k}_e^2 \frac{\mathrm{d}^2 g}{\mathrm{d}\phi^2}(\tilde{k}_e\phi)$, respectively. Consequently, (6.2.8) implies the following two relations for the sign of $\frac{\mathrm{d}^2\tau_J}{\mathrm{d}\phi^2}$ and $\frac{\mathrm{d}^2\tilde\tau_J}{\mathrm{d}\phi^2}$:

$$\left(\forall\phi \in \left(0, \frac{2\Phi_{max}}{k_e}\right)\right)\left[\mathrm{sgn}\left(\frac{\mathrm{d}^2\tau_J}{\mathrm{d}\phi^2}(\phi)\right) = K\right], \qquad (\text{B.4.24})$$

and

$$\left(\forall\phi \in \left(0, \frac{2\Phi_{max}}{\tilde{k}_e}\right)\right)\left[\mathrm{sgn}\left(\frac{\mathrm{d}^2\tilde\tau_J}{\mathrm{d}\phi^2}(\phi)\right) = K\right]. \qquad (\text{B.4.25})$$

To prove the proposition, we will next consider three different possibilities regarding the sign of the difference $\frac{k_e \dot{\theta}_{max}}{\omega_0} - \frac{\tilde{k}_e \dot{\tilde{\theta}}_{max}}{\tilde{\omega}_0}$.

Let us first assume that $\dot{\Theta}_{max} = \frac{k_e \dot{\theta}_{max}}{\omega_0}$ and $\dot{\tilde{\Theta}}_{max} = \frac{\tilde{k}_e \dot{\tilde{\theta}}_{max}}{\tilde{\omega}_0}$ are equal to each other. It follows then from Prop. 22 that $\omega_0 t_{min}(l; \boldsymbol{p})$ and $\tilde{\omega}_0 t_{min}(l; \tilde{\boldsymbol{p}})$ are also equal to each other and (6.2.9) holds.

Let us next assume that $\dot{\Theta}_{max}$ is higher than $\dot{\tilde{\Theta}}_{max}$. Then, there exists a scalar $c \in (0, 1)$ such that $\dot{\tilde{\Theta}}_{max} = c\dot{\Theta}_{max}$ holds. Moreover, using this scalar we can construct a parameter $\hat{\boldsymbol{p}} = (\hat{M}, \hat{\tau}_J, \dot{\hat{\theta}}_{max}) \in P_\Sigma$ with $\hat{M} = M, \hat{\tau}_J = \tau_J$ and $\dot{\hat{\theta}}_{max} = c\dot{\theta}_{max}$ such that $\dot{\hat{\Theta}}_{max} = \frac{\hat{k}_e \dot{\hat{\theta}}_{max}}{\tilde{\omega}_0} = \frac{k_e c\dot{\theta}_{max}}{\omega_0}$ equals to $\dot{\tilde{\Theta}}_{max}$. Note that according to Prop. 22, $\tilde{\omega}_0 t_{min}(l; \tilde{\boldsymbol{p}})$ and $\hat{\omega}_0 t_{min}(l; \hat{\boldsymbol{p}})$ will then be equal to each other. Making use of the definition of t_{min}, this leads to

$$
\begin{aligned}
\omega_0 t_{min}(l; \boldsymbol{p}) - \tilde{\omega}_0 t_{min}(l; \tilde{\boldsymbol{p}}) &= \\
\omega_0 \left(t_{min}(l; \boldsymbol{p}) - t_{min}(l; \hat{\boldsymbol{p}}) \right) &= \\
\frac{\omega_0}{2} \sum_{i=0}^{l-1} T_p(^i\phi_{max}) - T_p(^i\hat{\phi}_{max}),
\end{aligned}
\tag{B.4.26}
$$

where for each $i \in S_{l-1}$ the following equalities will hold for $^i\phi_{max}$ and $^i\hat{\phi}_{max}$ according to (B.4.21):

$$
E_{pot,g}(k_e \, ^i\phi_{max}) = \frac{(2i+1)^2}{2}\dot{\Theta}_{max}^2,
\tag{B.4.27}
$$

and

$$
E_{pot,g}(k_e \, ^i\hat{\phi}_{max}) = \frac{(2i+1)^2}{2}c^2\dot{\Theta}_{max}^2.
\tag{B.4.28}
$$

With (B.4.27)-(B.4.28) and the inequality (6.2.7), we can now see that in the sum in (B.4.26) the following inequalities hold for each $i \in S_{l-1}$:

$$
^i\hat{\phi}_{max} < \, ^i\phi_{max} < \frac{2\Phi_{max}}{k_e}.
$$

Consequently, applying Prop. 1 with $\varphi_{max} = \frac{2\Phi_{max}}{k_e}$ we can see that according to (B.4.26) the difference $\omega_0 t_{min}(l; \boldsymbol{p}) - \tilde{\omega}_0 t_{min}(l; \tilde{\boldsymbol{p}})$ has in this case the opposite sign of K and thus of $\frac{\mathrm{d}^2 g}{\mathrm{d}\phi^2}(\Phi_{max})$. Consequently, (6.2.9) holds in this case as well.

Finally, if we assume that $\dot{\Theta}_{max}$ is less than $\dot{\tilde{\Theta}}_{max}$ we can again construct a parameter $\hat{\boldsymbol{p}}$ with $c = \frac{\dot{\Theta}_{max}}{\dot{\tilde{\Theta}}_{nax}} \in (0, 1)$ and $\hat{M} = \tilde{M}, \hat{\tau}_J = \tilde{\tau}_J$ and $\dot{\hat{\theta}}_{max} = c\dot{\tilde{\theta}}_{max}$. Noting that the difference $\omega_0 t_{min}(l; \boldsymbol{p}) - \tilde{\omega}_0 t_{min}(l; \tilde{\boldsymbol{p}})$ will this time be given by $\tilde{\omega}_0 t_{min}(l; \hat{\boldsymbol{p}}) - \tilde{\omega}_0 t_{min}(l; \tilde{\boldsymbol{p}})$, we can slightly adjust the arguments we used above to show that the sign of this difference will have the same sign as $\frac{\mathrm{d}^2 g}{\mathrm{d}\phi^2}(\Phi_{max})$. This means that (6.2.9) also holds in this last case. $\qquad \square$

As already mentioned, the expressions (B.4.11) and (B.4.14) from Lemma 57 will both be made use of in the proof of Prop. 24. To simplify this proof, we first state a corollary which directly follows from (B.4.11) and which shows that the two expressions are differentiable with respect to $\dot{\Theta}_{max}$.

Corollary 58. *Let g be an element of $C^1_{\tau_J}$ with $\frac{\mathrm{d}g}{\mathrm{d}\phi}(0) = 1$ and k an arbitrary positive integer. Moreover, let $t_{dim,k} : (0, \infty) \to (0, \infty)$ be the function determined by the formula*

$$t_{dim,k}(\dot{\Theta}_{max}) = t_{min}(k; \hat{\boldsymbol{p}}), \tag{B.4.29}$$

where $\hat{\boldsymbol{p}}$ is equal to $(1, \hat{\tau}_J, 1)$ with

$$(\forall \phi \in \mathbb{R}) \left[\hat{\tau}_J(\phi) = \frac{g(\dot{\Theta}_{max}\phi)}{\dot{\Theta}_{max}} \right]. \tag{B.4.30}$$

Then, for each $\dot{\Theta}_{max} \in (0, \infty)$ we have

$$\frac{\mathrm{d}t_{dim,k}}{\mathrm{d}\dot{\Theta}_{max}}(\dot{\Theta}_{max}) = \frac{t_{dim,k}(\dot{\Theta}_{max})}{\dot{\Theta}_{max}} +$$
$$(-4) \cdot \sum_{l=0}^{k-1} \int_0^{2l+1} \frac{K(l,s)\mathrm{d}s}{\frac{g^3\left(E^{-1}_{pot,g}(K(l,s))\right)}{\frac{\mathrm{d}g}{\mathrm{d}\phi}\left(E^{-1}_{pot,g}(K(l,s))\right)}}, \tag{B.4.31}$$

where $K(l,s)$ is equal to $\frac{\dot{\Theta}^2_{max}\left((2l+1)^2 - s^2\right)}{2}$.

Proof. For brevity, we will only sketch the proof. Let g, k and $t_{dim,k}$ satisfy the hypotheses of the lemma. For each $\dot{\Theta}_{max} > 0$, $t_{dim,k}(\dot{\Theta}_{max})$ is then given by the right-hand side of (B.4.11), see Lemma 57. By applying Leibniz rule and accounting for the conditions on the integration limits in the sum, we can differentiate this expression with respect to $\dot{\Theta}_{max}$. This then leads to the desired expression in (B.4.31) if we further exploit our freedom in our choice of the integration limits as done in the proof of Lemma 57 to derive (B.4.14). □

With Corollary 58, we can now prove Prop. 24 as follows.

Proof of Prop. 24. Let $g, \boldsymbol{p}, \tilde{\boldsymbol{p}}, k$ and Φ_{max} satisfy the hypotheses of the lemma and let l be a positive integer in S_k. Moreover, let $\dot{\Theta}_{max}$ denote the ratio $\frac{k_e \dot{\theta}_{max}}{\omega_0}$ and $\tilde{\Theta}_{max}$ the ratio $\frac{\tilde{k}_e \tilde{\dot{\theta}}_{max}}{\tilde{\omega}_0}$. Making use of the function $t_{dim,l} : (0, \infty) \to (0, \infty)$ as introduced in Lemma 58, with $k = l$, and Prop. 21 we can then arrive at the

following relation for the difference $\Delta t_{min,l} := t_{min}(l; \tilde{\boldsymbol{p}}) - t_{min}(l; \boldsymbol{p})$:

$$
\begin{aligned}
\Delta t_{min,l} &= \frac{t_{dim,l}(\tilde{\dot{\Theta}}_{max})}{\tilde{\omega}_0} - \frac{t_{dim,l}(\dot{\Theta}_{max})}{\omega_0} \\
&= -\int_{\omega_0}^{\tilde{\omega}_0} \frac{t_{dim,l}\left(\frac{k_e \dot{\theta}_{max}}{\omega}\right) + \frac{k_e \dot{\theta}_{max}}{\omega} \frac{\mathrm{d}t_{dim,l}}{\mathrm{d}\dot{\Theta}_{max}}\left(\frac{k_e \dot{\theta}_{max}}{\omega}\right)}{\omega^2} \mathrm{d}\omega \\
&= \frac{\int_{\dot{\Theta}_{max}}^{\tilde{\dot{\Theta}}_{max}} t_{dim,l}(\dot{\Theta}) + \dot{\Theta}\frac{\mathrm{d}t_{dim,l}}{\mathrm{d}\dot{\Theta}_{max}}\left(\dot{\Theta}\right) \mathrm{d}\dot{\Theta}}{k_e \dot{\theta}_{max}}, \quad \text{(B.4.32)}
\end{aligned}
$$

where we have also exploited the equality in (6.2.10) and the differentiability of the function $t_{dim,l}$. It is important to note here that the two conditions (6.2.10) and (6.2.11) imply that $\tilde{\dot{\Theta}}_{max}$ is greater than $\dot{\Theta}_{max}$. Consequently, in order to show that (6.2.14) is true and thus to prove the proposition, it is sufficient to show that the integrand in (B.4.32) is positive for each $\dot{\Theta} \in [\dot{\Theta}_{max}, \tilde{\dot{\Theta}}_{max}]$. We will conclude the proof of the proposition by showing that this is indeed the case.

Let $\dot{\Theta}$ be an arbitrary element of $[\dot{\Theta}_{max}, \tilde{\dot{\Theta}}_{max}]$ and let $I_\Delta(\dot{\Theta})$ denote the integrand in (B.4.32) evaluated at $\dot{\Theta}$. If we make use of the two expressions (B.4.14) and (B.4.31) from Lemma 57 and 58 together with Prop. 21, we can find the following equality for $I_\Delta(\dot{\Theta})$:

$$
\begin{aligned}
\frac{I_\Delta(\dot{\Theta})}{4\dot{\Theta}} &= \sum_{m=0}^{l-1} \int_0^{2m+1} \frac{1 - \frac{K(m,s)\frac{\mathrm{d}g}{\mathrm{d}\phi}\left(E_{pot,g}^{-1}(K(m,s))\right)}{g^2\left(E_{pot,g}^{-1}(K(m,s))\right)}}{g\left(E_{pot,g}^{-1}\left(K(m,s)\right)\right)} \mathrm{d}s \\
&= \sum_{m=0}^{l-1} \int_0^{a(m)} \frac{1 - \frac{E_{pot,g}(\bar{s})\frac{\mathrm{d}g}{\mathrm{d}\phi}(\bar{s})}{g^2(\bar{s})}}{\dot{\Theta}^2 s(m,\bar{s})} \mathrm{d}\bar{s}, \quad \text{(B.4.33)}
\end{aligned}
$$

where we have used $K(m,s)$ to denote the term $\frac{\dot{\Theta}^2\left((2m+1)^2-s^2\right)}{2}$, $s(m,\bar{s})$ to denote the term $\frac{\sqrt{(2m+1)^2\dot{\Theta}^2-2E_{pot,g}(\bar{s})}}{\dot{\Theta}}$ and finally $a(m)$ to denote the positive scalar given by

$$
a(m) = E_{pot,g}^{-1}\left(\frac{(2m+1)^2\dot{\Theta}^2}{2}\right). \quad \text{(B.4.34)}
$$

According to (6.2.12), the scalar $a(m)$ in (B.4.34) is less than $2\Phi_{max}$ for each $m \in S_{l-1}$. Consequently, using the inequality (6.2.13) we can now see that for each $m \in S_{l-1}$ the integrand in the right-hand side of (B.4.33) attains positive values when $\bar{s} \in (0, a(m))$. This means that $I_\Delta(\dot{\Theta})$ is positive as desired. $\quad\square$

It is important to note here that the proof of Prop. 24 can also be used to show the existence of a function g, a positive integer l and parameters $\boldsymbol{p}$ and $\tilde{\boldsymbol{p}}$ for which the difference $\Delta t_{min,l}$ in (B.4.32) takes a negative value. More

specifically, it follows from (B.4.32) and (B.4.33) that $\Delta t_{min,l}$ will be negative if the integrals in (B.4.33) can be made negative for $\dot{\Theta} = \dot{\Theta}_{max}$ and if $\tilde{\boldsymbol{p}}$ is sufficiently close to $\boldsymbol{p}$. This in turn requires the ratio $r := \frac{E_{pot,g}\frac{\mathrm{d}g}{\mathrm{d}\phi}}{g^2}$, which is uniquely determined by the function g, to be larger than 1 in a sufficiently large interval and constructing such a function g together with $l, \boldsymbol{p}$ and $\tilde{\boldsymbol{p}}$ is feasible. Indeed, the last condition on the ratio r describes a differential inequality for the energy $E_{pot,g}$ and this inequality has multiple solutions leading to a negative $\Delta t_{min,l}$. For brevity, we do not provide a detailed discussion on these solutions or the construction procedure. Nevertheless, we note that one possible solution for the mentioned inequality is given by the function $\frac{c}{d-\phi}$ with $c > 0$ and $d > 0$.

We conclude this part of the appendix by providing the proof of Prop. 25, which is based on the application of Lemma 56 with $C_{dim} = \frac{\hat{t}_f}{t_f}$.

Proof of Prop. 25. Let $\boldsymbol{p} = (M, \tau_J, \dot{\theta}_{max}) \in P_\Sigma$ and $t_f > 0$ be given. Moreover, let $\hat{t}_f > 0$ be an arbitrary scalar and $\hat{\boldsymbol{p}} = (1, \hat{\tau}_J, 1)$ the parameter with the function $\hat{\tau}_J : \mathbb{R} \to \mathbb{R}$ defined by (6.2.16). Then, $\hat{\boldsymbol{p}}$ is an element of P_Σ since $\hat{\tau}_J$ is an element of $C^1_{\tau_J}$. Let now $(\boldsymbol{x}, u)$ denote an optimally controlled trajectory which is defined on $[0, t_f]$ and which corresponds to $\boldsymbol{p}$. Similarly, let $(\hat{\boldsymbol{x}}, \hat{u})$ denote an optimally controlled trajectory which is defined on $[0, \hat{t}_f]$ and which corresponds to $\hat{\boldsymbol{p}}$. Finally, let Σ denote the control system corresponding to $\boldsymbol{p}$ and $\hat{\Sigma}$ the system corresponding to $\hat{\boldsymbol{p}}$. Notice that by setting C_{dim} to $\frac{\hat{t}_f}{t_f}$, we can apply Lemma 56 to see how trajectories of Σ, which are defined on $[0, t_f]$, are related to trajectories of $\hat{\Sigma}$, which are defined on $[0, \hat{t}_f]$. We will next exploit this relation to show that (6.2.17) holds.

First of all, it follows from Lemma 56 that the function $\boldsymbol{y} : [0, t_f] \to \mathbb{R}^2$ with $\boldsymbol{y}(t) = \dot{\theta}_{max} \left(\frac{t_f}{\hat{t}_f} \hat{x}_1(\frac{\hat{t}_f}{t_f}t) \quad \hat{x}_2(\frac{\hat{t}_f}{t_f}t) \right)^T$ is a trajectory of Σ which starts from the origin. Looking at the terminal link velocity of this trajectory, we can then arrive at the following inequality:

$$\dot{q}_{max}(t_f; \boldsymbol{p}) \geq \dot{\theta}_{max}\dot{q}_{max}(\hat{t}_f; \hat{\boldsymbol{p}}), \tag{B.4.35}$$

where we have used the optimality of $\hat{\boldsymbol{x}}$ and the definition of the function $\dot{q}_{max}$. Similarly, Lemma 56 implies that the function $\hat{\boldsymbol{y}} : [0, \hat{t}_f] \to \mathbb{R}^2$ with $\hat{\boldsymbol{y}}(t) = \frac{1}{\dot{\theta}_{max}} \left(\frac{\hat{t}_f}{t_f} x_1(\frac{t_f}{\hat{t}_f}t) \quad x_2(\frac{t_f}{\hat{t}_f}t) \right)^T$ is a trajectory of $\hat{\Sigma}$ which also starts from the origin. Consequently, by evaluating this function at $t = \hat{t}_f$ and noting the optimality of $\boldsymbol{x}$ we find the following inequality:

$$\dot{\theta}_{max}\dot{q}_{max}(\hat{t}_f; \hat{\boldsymbol{p}}) \geq \dot{q}_{max}(t_f; \boldsymbol{p}). \tag{B.4.36}$$

According to (B.4.35)-(B.4.36) and the definition of ϵ, we can now see that $\dot{q}_{max}(\hat{t}_f; \hat{\boldsymbol{p}})$ is equal to $\epsilon(t_f; \boldsymbol{p})$. Moreover, since $\hat{\dot{\theta}}_{max}$ is equal to 1 we have $\dot{q}_{max}(\hat{t}_f; \hat{\boldsymbol{p}}) = \epsilon(\hat{t}_f; \hat{\boldsymbol{p}})$ and this finally leads to the desired relation (6.2.17). $\quad\square$

Bibliography

[1] M. Abramowitz and I.A. Stegun. *Handbook of Mathematical Functions: With Formulas, Graphs, and Mathematical Tables.* Applied mathematics series. Dover Publications, 1964.

[2] Andrei A Agrachev and Yuri Sachkov. *Control theory from the geometric viewpoint*, volume 87. Springer Science & Business Media, 2013.

[3] Mohammed A Al-Gwaiz. *Sturm-Liouville theory and its applications.* Springer, 2008.

[4] R McNeill Alexander. Elastic energy stores in running vertebrates. *American Zoologist*, 24(1):85–94, 1984.

[5] Mokhtar S Bazaraa, Hanif D Sherali, and Chitharanjan M Shetty. *Nonlinear programming: theory and algorithms.* John Wiley & Sons, 2013.

[6] Ugo Boscain and Benedetto Piccoli. *Optimal syntheses for control systems on 2-D manifolds*, volume 43. Springer Science & Business Media, 2003.

[7] D. J. Braun, F. Petit, F. Huber, S. Haddadin, P. van der Smagt, A. Albu-Schäfer, and S. Vijayakumar. Robots driven by compliant actuators: Optimal control under actuation constraints. *IEEE Transactions on Robotics*, 29(5):1085–1101, Oct 2013.

[8] M. Braun. *Differential Equations and Their Applications: An Introduction to Applied Mathematics.* Texts in Applied Mathematics. Springer New York, 1993.

[9] Piermarco Cannarsa and Carlo Sinestrari. *Semiconcave functions, Hamilton-Jacobi equations, and optimal control*, volume 58. Springer Science & Business Media, 2004.

[10] Giovanni A Cavagna, Norman C Heglund, and C Richard Taylor. Mechanical work in terrestrial locomotion: two basic mechanisms for minimizing energy expenditure. *American Journal of Physiology-Regulatory, Integrative and Comparative Physiology*, 233(5):R243–R261, 1977.

[11] Lamberto Cesari. *Optimization-Theory and applications: problems with ordinary differential equations*, volume 17. Springer Science & Business Media, 2012.

[12] C.T. Chen. *Linear System Theory and Design*. Oxford University Press, 2009.

[13] A. Coddington and N. Levinson. *Theory of ordinary differential equations*. International series in pure and applied mathematics. McGraw-Hill, 1955.

[14] A.F. Filippov. On certain questions in the theory of optimal control. *Journal of the Society for Industrial and Applied Mathematics, Series A: Control*, 1(1):76–84, 1962.

[15] Hélene Frankowska. Value function in optimal control. Technical report, 2002.

[16] M. Garabini, A. Passaglia, F. Belo, P. Salaris, and A. Bicchi. Optimality principles in stiffness control: The vsa kick. In *Robotics and Automation (ICRA), 2012 IEEE International Conference on*, pages 3341–3346, May 2012.

[17] M. Garabini, A. Passaglia, F. A. W. Belo, P. Salaris, and A. Bicchi. Optimality principles in variable stiffness control: the vsa hammer. *2011 IEEE/RSJ International Conference on Intelligent Robots and Systems (IROS2011), San Francisco, USA*, pages 3770 − 3775, 2011.

[18] Markus Grebenstein, Alin Albu-Schäffer, Thomas Bahls, Maxime Chalon, Oliver Eiberger, Werner Friedl, Robin Gruber, Sami Haddadin, Ulrich Hagn, Robert Haslinger, Hannes Hoppner, Stefan Jörg, Mathias Nickl, Alexander Nothhelfer, Florian Petit, Josef Reill, Nikolaus Seitz, Thomas Wimböck, Sebastian Wolf, Tilo Wusthoff, and Gerd Hirzinger. The DLR hand arm system. pages 3175–3182, 2011.

[19] RI Griffiths. Shortening of muscle fibres during stretch of the active cat medial gastrocnemius muscle: the role of tendon compliance. *The Journal of Physiology*, 436:219, 1991.

[20] Giorgio Grioli, Sebastian Wolf, Manolo Garabini, Manuel Catalano, Etienne Burdet, Darwin Caldwell, Raffaella Carloni, Werner Friedl, Markus Grebenstein, Matteo Laffranchi, Dirk Lefeber, Stefano Stramigioli, Nikos Tsagarakis, Michael van Damme, Bram Vanderborght, Alin Albu-Schaeffer, and Antonio Bicchi. Variable stiffness actuators: The user's point of view. *The International Journal of Robotics Research*, 34(6):727–743, 2015.

[21] S. Haddadin, M. C. Özparpucu, and A. Albu-Schäffer. Optimal control for maximizing potential energy in a variable stiffness joint. In *Decision and Control (CDC), 2012 IEEE 51st Annual Conference on*, pages 1199–1206, 2012.

[22] S. Haddadin, F. Huber, and A. Albu-Schäffer. Optimal control for exploiting the natural dynamics of variable stiffness robots. In *Robotics and Automation (ICRA), 2012 IEEE International Conference on*, pages 3347–3354, 2012.

[23] Sami Haddadin, Felix Huber, Kai Krieger, Roman Weitschat, Alin Albu-Schäffer, Sebastian Wolf, Werner Friedl, Markus Grebenstein, Florian Petit, Jens Reinecke, et al. Intrinsically elastic robots: The key to human like performance. In *Intelligent Robots and Systems (IROS), 2012 IEEE/RSJ International Conference on*, pages 4270–4271, 2012.

[24] Sami Haddadin, Michael Weis, Alin Albu-Schäffer, and Sebastian Wolf. Optimal control for maximizing link velocity of robotic variable stiffness joints. *In: Proceedings. IFAC 2011,World Congress*, pages 3175–3182, 2011.

[25] Sami Haddadin, Roman Weitschat, Felix Huber, Mehmet Can Özparpucu, Nico Mansfeld, and Alin Albu-Schäffer. *Optimal Control for Viscoelastic Robots and Its Generalization in Real-Time*, pages 131–148. Springer International Publishing, Cham, 2016.

[26] Ian W Hunter, John M Hollerbach, and John Ballantyne. A comparative analysis of actuator technologies for robotics. *Robotics Review*, 2:299–342, 1991.

[27] K. Jittorntrum. An implicit function theorem. *Journal of Optimization Theory and Applications*, 25(4):575–577, Aug 1978.

[28] Arthur J Krener. The high order maximal principle and its application to singular extremals. *SIAM Journal on Control and Optimization*, 15(2):256–293, 1977.

[29] S. Kumagai. An implicit function theorem: Comment. *Journal of Optimization Theory and Applications*, 31(2):285–288, Jun 1980.

[30] E.B. Lee and L. Markus. *Foundations of optimal control theory*. SIAM series in applied mathematics. Wiley, 1967.

[31] Weiwei Li and Emanuel Todorov. Iterative linear quadratic regulator design for nonlinear biological movement systems. In *ICINCO (1)*, pages 222–229, 2004.

[32] D. Liberzon. *Calculus of Variations and Optimal Control Theory: A Concise Introduction*. Princeton University Press, 2011.

[33] Florian Loeffl, Alexander Werner, Dominic Lakatos, Jens Reinecke, Sebastian Wolf, Robert Burger, Thomas Gumpert, Florian Schmidt, Christian Ott, Markus Grebenstein, et al. The dlr c-runner: Concept, design and experiments. In *Humanoid Robots (Humanoids), 2016 IEEE-RAS 16th International Conference on*, pages 758–765, 2016.

[34] Hartmut Logemann and Eugene P Ryan. *Ordinary Differential Equations: Analysis, Qualitative Theory and Control.* Springer, 2014.

[35] L. Meirovitch. *Principles and techniques of vibrations.* Prentice Hall, 1997.

[36] Ali H Nayfeh and Dean T Mook. *Nonlinear oscillations.* John Wiley & Sons, 2008.

[37] John Noble and Heinz Schättler. Sufficient conditions for relative minima of broken extremals in optimal control theory. *Journal of Mathematical Analysis and Applications*, 269(1):98 − 128, 2002.

[38] Zdzisław Opial. Continuous parameter dependence in linear systems of differential equations. *Journal of Differential Equations*, 3(4):571–579, 1967.

[39] M. C. Özparpucu. *Optimal Control Concepts for Robots with Varying Stiffness Joints.* DLR and TU Darmstadt, Master Thesis, 2012.

[40] M. C. Özparpucu and S. Haddadin. Optimal control for maximizing link velocity of a visco-elastic joint. In *IEEE/RSJ Int. Conf. on Intelligent Robots and Systems*, 2013.

[41] M. C. Özparpucu and S. Haddadin. Optimal control of elastic joints with variable damping. In *2014 European Control Conference (ECC)*, pages 2526–2533, June 2014.

[42] M. C. Özparpucu, S. Haddadin, and A. Albu-Schäffer. Optimal control of variable stiffness actuators with nonlinear springs. *In: Proceedings. IFAC 2014, World Congress*, pages 8487–8495, 2014.

[43] M.C. Özparpucu and A. Albu-Schaffer. Optimal control strategies for maximizing the performance of variable stiffness joints with nonlinear springs. In *Decision and Control (CDC), 2014 IEEE 53rd Annual Conference on*, pages 1409–1416, Dec 2014.

[44] L.S. Pontryagin, V.G. Boltyanskii, R.V. Gamkrelidze, and E.F. Mischenko. *Mathematical Theory of Optimal Processes.* Wiley, 1962.

[45] Gill A Pratt and Matthew M Williamson. Series elastic actuators. In *Intelligent Robots and Systems 95.'Human Robot Interaction and Cooperative Robots', Proceedings. 1995 IEEE/RSJ International Conference on*, volume 1, pages 399–406. IEEE, 1995.

[46] Jerry Pratt, Peter Dilworth, and Gill Pratt. Virtual model control of a bipedal walking robot. In *Robotics and Automation, 1997. Proceedings., 1997 IEEE International Conference on*, volume 1, pages 193–198. IEEE, 1997.

[47] Andreea Radulescu, Matthew Howard, David J Braun, and Sethu Vijayakumar. Exploiting variable physical damping in rapid movement tasks. In *Advanced Intelligent Mechatronics (AIM), 2012 IEEE/ASME International Conference on*, pages 141–148. IEEE, 2012.

[48] Marc H. Raibert, Jr H. Benjamin Brown, and Michael Chepponis. Experiments in balance with a 3d one-legged hopping machine. *The International Journal of Robotics Research*, 3(2):75–92, 1984.

[49] Neil T Roach, Madhusudhan Venkadesan, Michael J Rainbow, and Daniel E Lieberman. Elastic energy storage in the shoulder and the evolution of high-speed throwing in homo. *Nature*, 498(7455):483–486, 2013.

[50] Thomas J Roberts and Emanuel Azizi. The series-elastic shock absorber: tendons attenuate muscle power during eccentric actions. *Journal of Applied Physiology*, 109(2):396–404, 2010.

[51] Thomas J Roberts and Nicolai Konow. How tendons buffer energy dissipation by muscle. *Exercise and sport sciences reviews*, 41(4), 2013.

[52] David Schaeffer and John Wesley Cain. *Ordinary Differential Equations: Basics and Beyond*, volume 65. Springer, 2016.

[53] H. Schättler and U. Ledzewicz. *Geometric Optimal Control: Theory, Methods and Examples*. Interdisciplinary Applied Mathematics. Springer, 2012.

[54] Bruno Siciliano and Oussama Khatib. *Springer handbook of robotics*. Springer, 2016.

[55] H. Sussmann. The structure of time-optimal trajectories for single-input systems in the plane: The c^∞ nonsingular case. *SIAM Journal on Control and Optimization*, 25(2):433–465, 1987.

[56] B. Vanderborght, A. Albu-Schaeffer, A. Bicchi, E. Burdet, D.G. Caldwell, R. Carloni, M. Catalano, O. Eiberger, W. Friedl, G. Ganesh, M. Garabini, M. Grebenstein, G. Grioli, S. Haddadin, H. Hoppner, A. Jafari, M. Laffranchi, D. Lefeber, F. Petit, S. Stramigioli, N. Tsagarakis, M. Van Damme, R. Van Ham, L.C. Visser, and S. Wolf. Variable impedance actuators: A review. *Robotics and Autonomous Systems*, 61(12):1601 − 1614, 2013.

[57] B. Vanderborght, B. Verrelst, R. Van Ham, M. Van Damme, D. Lefeber, B.M.Y. Duran, and P. Beyl. Exploiting natural dynamics to reduce energy consumption by controlling the compliance of soft actuators. *Int. Journal of Robotics Research*, 25(4):343–358, 2006.

[58] David A Winter. *Biomechanics and motor control of human movement*. John Wiley & Sons, 2009.

[59] S. Wolf, O. Eiberger, and G. Hirzinger. The dlr fsj: Energy based design of a variable stiffness joint. In *Robotics and Automation (ICRA), 2011 IEEE International Conference on*, pages 5082–5089, 2011.

[60] Sebastian Wolf, Giorgio Grioli, Oliver Eiberger, Werner Friedl, Markus Grebenstein, Hannes Höppner, Etienne Burdet, Darwin G Caldwell, Raffaella Carloni, Manuel G Catalano, et al. Variable stiffness actuators: Review on design and components. *IEEE/ASME transactions on mechatronics*, 21(5):2418–2430, 2016.

[61] V.A. Zorich, R. Cooke, and O. Paniagua. *Mathematical Analysis II*. Universitext. Springer Berlin Heidelberg, 2016.

[62] V.A. Zorich, R. Cooke, and O.P. Taboada. *Mathematical Analysis I*. Springer Berlin Heidelberg, 2016.

Özparpucu, Mehmet Can
Seumestr. 15
81379, München
Deutschland
+4915155503255
Mehmet.Oezparpucu@dlr.de

Born on 03.06.1985,
Istanbul, Turkey
Nationality: Turkish, French

Education

2010-2012	**Technical University Darmstadt (TUD), Master of Science** *"Mechanical and Process Engineering"* *GPA: 1.09 (passed with Honor, **VDI-Award**)*
2009-2010	**University of Illinois at Urbana-Champaign (UIUC)** Exchange Programme in *"Mechanical and Process Engineering"*
2007-2010	**Technical University Darmstadt (TUD), Bachelor of Science** *"Mechanical and Process Engineering"* *GPA: 1.46 (passed with Honor)*

Work Experience

2012-current	**Researcher in Institute of Robotics and Mechatronics, German Aerospace Center (DLR)**
2015-2018	**External PhD Student at Agile and Dexterous Robotics Lab (ETH Zurich)**

Teaching Experience

- Teaching Assistant in Technical University Munich (TUM)

    - Robotics (Fall 2013)

- Teaching Assistant (as a Student) in Technical University Darmstadt (TUD)

    - System Theory and Control (Fall 2010)
    - Structure Dynamics (Fall 2008)
    - Thermodynamics (Fall 2007)

Publications

1. **Optimal Control Strategies for Maximizing the Performance of Variable Stiffness Joints with Nonlinear Springs.**
   Mehmet Can Özparpucu and Alin Albu-Schäffer
   In Proc. 53st IEEE Conf. Decision and Control (CDC), Los Angeles, CA, USA, 2014.

2. **Optimal Control of Variable Stiffness Actuators with Nonlinear Springs.**
   Mehmet Can Özparpucu, Sami Haddadin and Alin Albu-Schäffer
   IFAC World Congress, Cape Town, South Africa, 2014.

3. **Optimal Control of Elastic Joints with Variable Damping.**
   Mehmet Can Özparpucu and Sami Haddadin
   13th European Control Conference (ECC), Strasbourg, France, 2014.

4. **Optimal Control for Maximizing Link Velocity of Visco-elastic joints.**
   Mehmet Can Özparpucu and Sami Haddadin
   Conference on Intelligent Robots and Systems (IROS), Tokyo, Japan, 2013.

5. **Optimal Control for Maximizing Potential Energy in Variable Stiffness Joints.**
   Sami Haddadin, **Mehmet Can Özparpucu** and Alin Albu-Schäffer
   In Proc. 51st IEEE Conf. Decision and Control (CDC), Maui, HI, USA, 2012.

6. **Legged Elastic Multibody Systems: Adjusting Limit Cycles to Close-To-Optimal Energy Efficiency.**
   Stratmann, Philipp; Lakatos, Dominic; **Özparpucu, Mehmet Can**; Albu-Schäffer, Alin
   IEEE Robotics and Automation Letters, Volume: 2, Issue: 2 Pages: 436-443, 2017.

Talks

- **Optimal Control of Elastic Joints with Nonlinear Springs.**
  Deutsche Gesellschaft für Robotik, DGR-Tage, Munich, 2013.

- **Time-optimal Braking of Torque-Controlled Series Elastic Actuators with Linear Springs**.
  Workshop on Human-Friendly Robotics, HFR 2015.

Projects (During Studies)

2011-2012   "Optimal Control Concepts for Cyclic Movements of Robot Joints with Varying Stiffness"
(Master Thesis at **Institute of Robotics and Mechatronics**, **German Aerospace Center (DLR)**
Supervisor: Prof. Sami Haddadin)

2010   "Modal Updating of a three-story shear-frame structure"
(Bachelor Thesis at **Linear and Nonlinear Dynamics and Vibrations Laboratory (UIUC),**
Supervisors: Prof. Alexander Vakakis, Prof. Lawrence A. Bergman)

2010   "Experimental Works on Identification of Cell and Cytoplasm Properties using
Ultrasonic Transducers" (Project at **Bioacoustics Research Lab (UIUC)**,
Supervisors: Dr. Lauren Wirtzfeld, Prof. William D. O'Brien)

Language Skills

FLUENT: English, German

INTERMEDIATE: French

MOTHER TONGUE: Turkish

Personal Interests

- Sports: Karate, Football, Jogging

- Music: Classical and Electric Guitar

References

- Prof. Alin Albu-Schäffer, email: alin.albu-schaeffer@dlr.de

- Dr. Christian Ott, email: christian.ott@dlr.de

- Prof. Alexander Vakakis, e-mail: avakakis@illinois.edu

- Prof. Lawrence A. Bergman, e-mail: lbergman@illinois.edu

- Prof. William D. O'Brien, Jr., e-mail: wdo@illinois.edu